Introducing Recent Electrical Engineering Developments into undErgraduate cuRriculum

Co-funded by the Erasmus+ Programme of the European Union

Reference No.:
IREEDER-D2.2
Date: June. 15, 2021
Version: v2.0

DELIVERABLE 2.2

Teaching Materials - Renewable Energy Lecture Notes

Written by	**Responsibility**
Andreas Kazantzidis (UPAT)	WP3 Leader
Efterpi Nikitidou (UPAT)	Member
Marios Raspopoulos (UCLAN)	WP2 Leader
Stelios Ioannou (UCLAN)	Member
Ziyad Al Tarawneh (MU)	Member
Khaled Al Awasa (MU)	Member
Abdallah Altahan Alnauimi (IU)	Member
Mohammad Zakariya Siam (IU)	Member
Eyad Almaita (TTU)	Member
Ahmad Aljaafreh (TTU)	Member
Edited by	
Andreas Kazantzidis (UPAT)	WP3 Leader
Approved by	
Saud Althunibat (AHU)	Project Coordinator

This publication was produced with the financial support of the European Union. Its contents are the sole responsibility of the partners of IREEDER project and do not necessarily reflect the views of the European Union

IREEDER

Introducing Recent Electrical Engineering Developments into undErgraduate cuRriculum

Introduction to Renewable Energy

Editor: Andreas Kazantzidis

University of Patras

June 2021

Co-funded by the Erasmus+ Programme of the European Union

This publication was produced with the financial support of the European Union. Its contents are the sole responsibility of the partners of IREEDER project and do not necessarily reflect the views of the European Union

Abstract

This document serves as a comprehensive handbook for a course named "***Introduction to Renewable Energy***". The course has been prepared within the scope of the iREEDER project which is funded by Erasmus+ (Call: Capacity Building in the field of Higher Education, Project No. 609971-EPP-1-2019-JO-EPPKA1-CBHE-JP (2019-1975/001-001)). The course aims to present the fundamental principles and architecture of Renewable Energy systems, discuss, examine, evaluate and review the key technological components of Renewable Energy.

The specific learning outcomes are:

1. Describe the challenges, problems and potential solutions associated with the use of various Renewable Energy sources

2. Understand the fundamental principles and technologies of renewable energy components and systems, and other related topics such energy storage systems, hybrid energy systems, and distribution (smart) grid.

3. Describe the use of renewables and the various components used in the energy production with respect to applications (e.g. heating, cooling, desalination, power generation)

4. Gain specific knowledge in special fields such solar, wind, fuel cell and battery storage.

5. Use different software/laboratory equipment for modelling/designing/analyzing a Renewable Energy system.

Chapters 1 and 2 serve as an introductory overview of the Renewable Energy resources. An overview of the energy use, the fossil fuels and their environmental impact is provided in order to highlight the need and importance of Renewable Energies. Then, the basic Renewable Energy types (Wind, Solar, Biomass, Hydropower, geothermal, wave/ocean current/tidal Power, storage devices) are presented is terms of their characteristics, operation principles/energy conversion and worldwide status as well the relevant social, economic/environmental aspects, standards and regulations.

Chapter 3 is about physics of sunlight and photovoltaics. It includes the basic information about the solar spectrum, effect of geometry, atmospheric attenuation and radiation on tilted surfaces. Moreover, the fundamentals of energy conversion in photovoltaic solar cells and the main photovoltaic technologies are presented. **Chapters 4 and 5** are devoted to photovoltaic systems where different types of PV systems are described. Relevant calculations (cost, performance) and aspects (social, environmental) are analysed. In addition, their performance as a function of angle, shading, load and atmospheric parameters are reported. **Chapter 6** refers to solar thermal systems. The general principles and the solar resource/forecasting needs are highlighted as well as the different technologies, designs and applications. Coming to wind now, the wind energy fundamentals are presented in **Chapter 7.** Further to that, **Chapters 8 and 9** are about wind energy operation and control including aspects like electrical components, alternator and power electronics, turbine monitoring, standards and specifications, diagnosis/prognosis of failures as well as resource/forecast of wind energy. **Chapters 10 and 11** cover all aspects related to energy storage including the principles of a bouquet of technologies like fuel cells, super capacitors and hydraulic systems. The off-grid/stand-alone systems in terms of operation, design, management and control are presented in **Chapter 12.** Finally, **Chapter 13** overviews some key topics related to Renewable Energies like energy management and smart grids. Moreover, some new/merging technologies in this fast changing field are highlighted.

Table of Contents

1 Introduction and Overview of Renewable Energy Resources (1/2)

Author(s): Dr Efterpi Nikitidou
Dr Andreas Kazantzidis

1.1 Overview of Energy Use

Energy is essential for all living organisms, everyday activities and economic progress. This ongoing progress, along with the continuous increase of Earth's population, makes the need for greater energy production crucial. Energy demands for residential, commercial and industrial needs, as well as transportation are high and will only keep growing. The energy resources are various, each one with its own advantages and disadvantages and their study and development are vital to secure our future safety in terms of energy demands.

The resources that are used for energy production are fossil fuels, nuclear fuel and renewable resources (solar energy, wind energy, biomass, geothermal, hydropower, wave/ ocean current/ tidal power).

The increase in our energy consumption over the years can be seen in Figure 1-1,**Error! Reference source not found.** from 1965 until 2015 and for various energy sources, whereas in

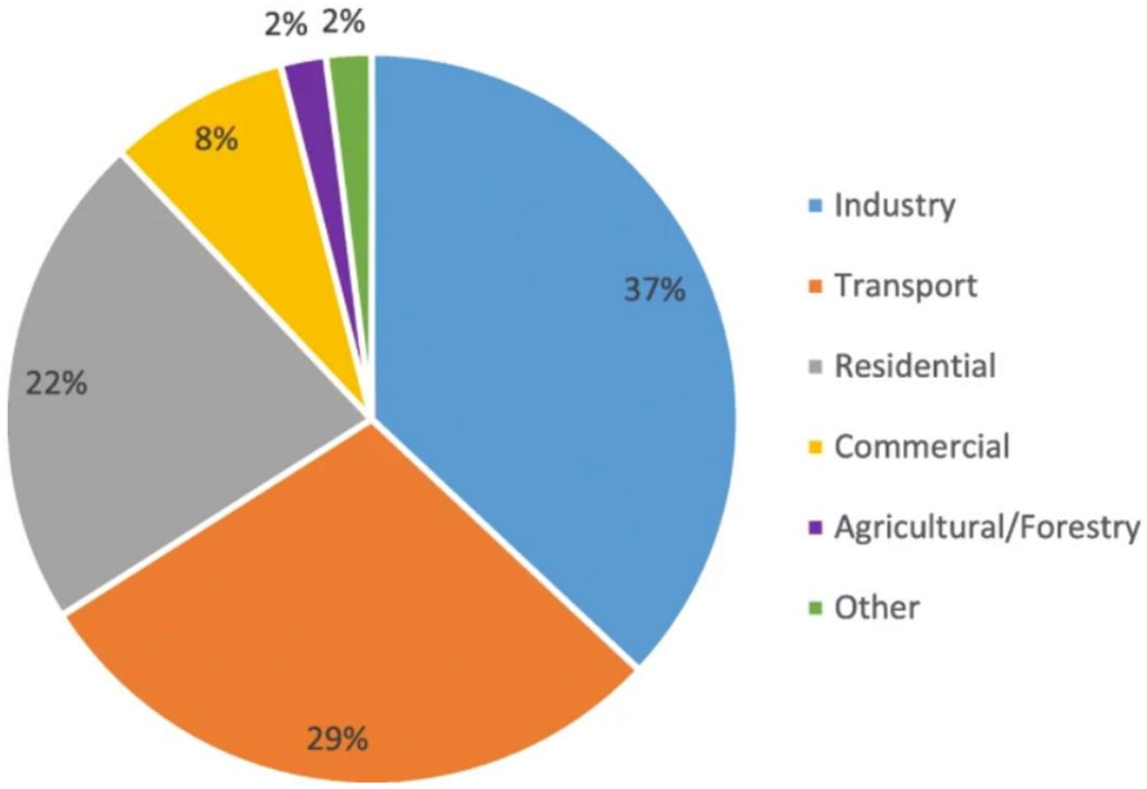

Figure 1-2 , the energy consumption for each sector, for 2015 and 2016, can be observed, with industry and transport having the highest percentages.

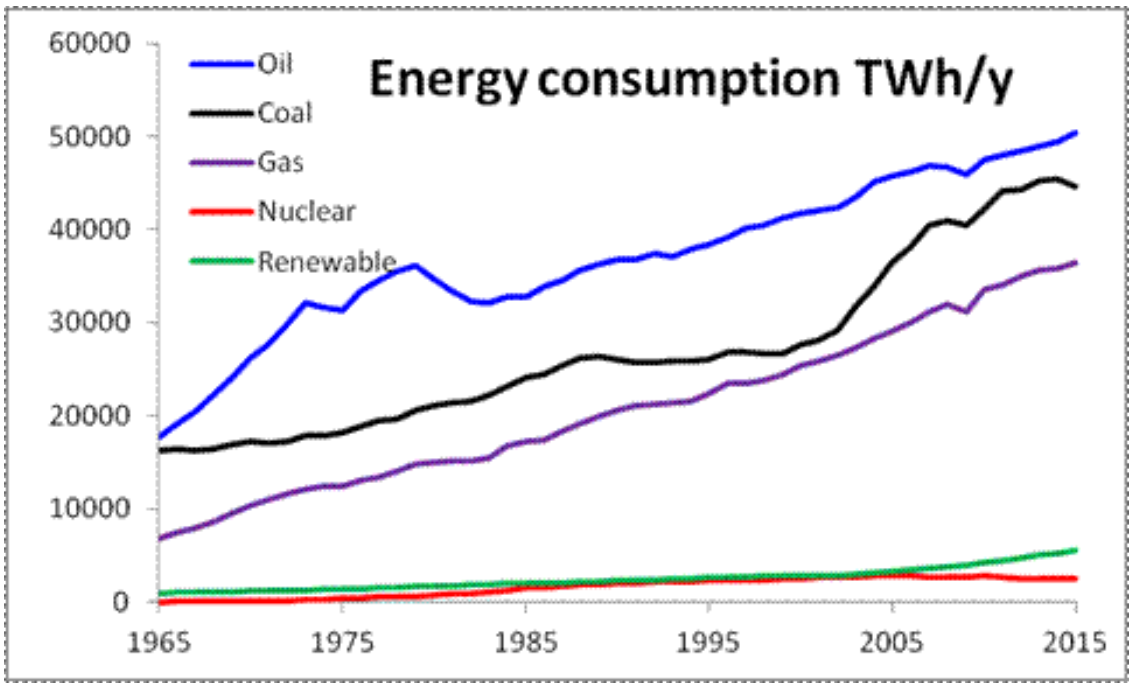

Figure 1-1: World's energy consumption based on data from 2015. [1] Licensed under CC BY-SA 4.0

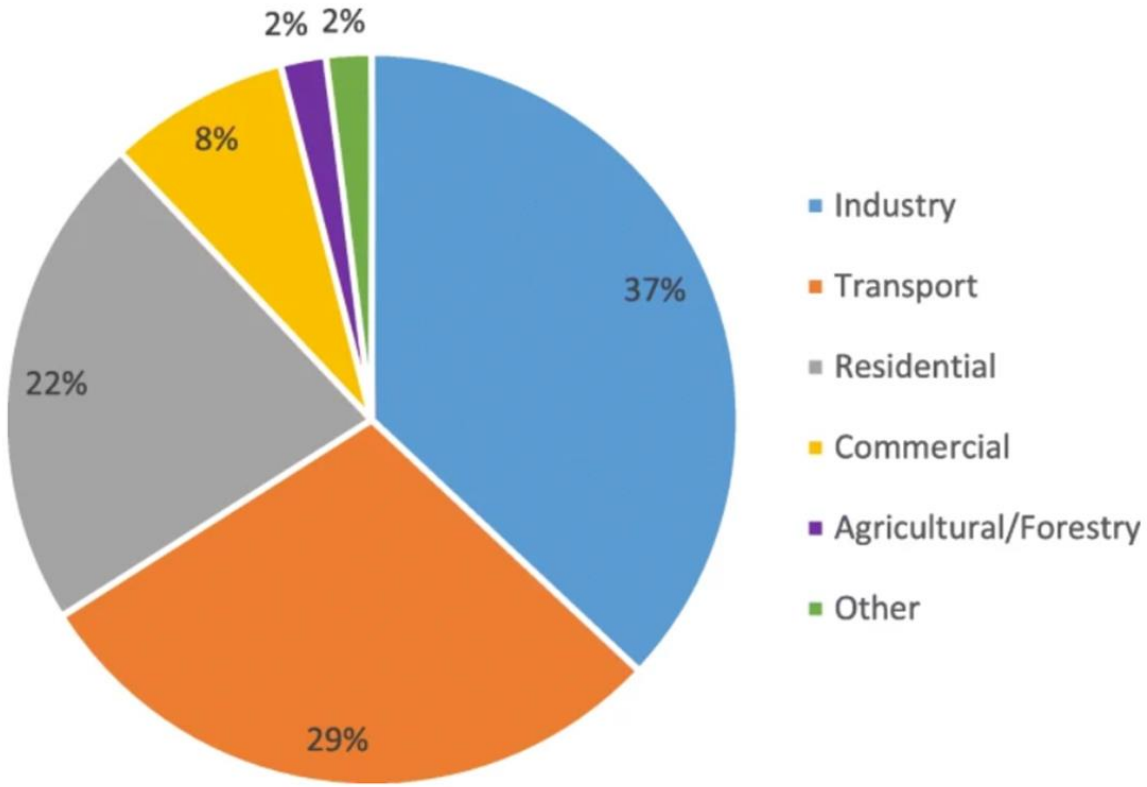

Figure 1-2: Total energy consumption by sector for 2015 and 2016. [2], [3] Licensed under CC BY 4.0

Figure 1-3 presents the primary energy consumption by region, for 2019, including fossil fuel, nuclear and renewable sources but not traditional biomass sources. The regions of Asia Pacific, which includes China as a major consumer, North America and Europe are the areas with the highest values in energy consumption, while the whole of Africa accounts for the smallest amount. It is obvious that energy consumption is not equally distributed among the world's nations. For example, the electricity consumption in the United States in 2018 was 13.1 MWh/capita, whereas in Bangladesh it was 0.5 MWh/capita, based on data from International Energy Agency (IEA).

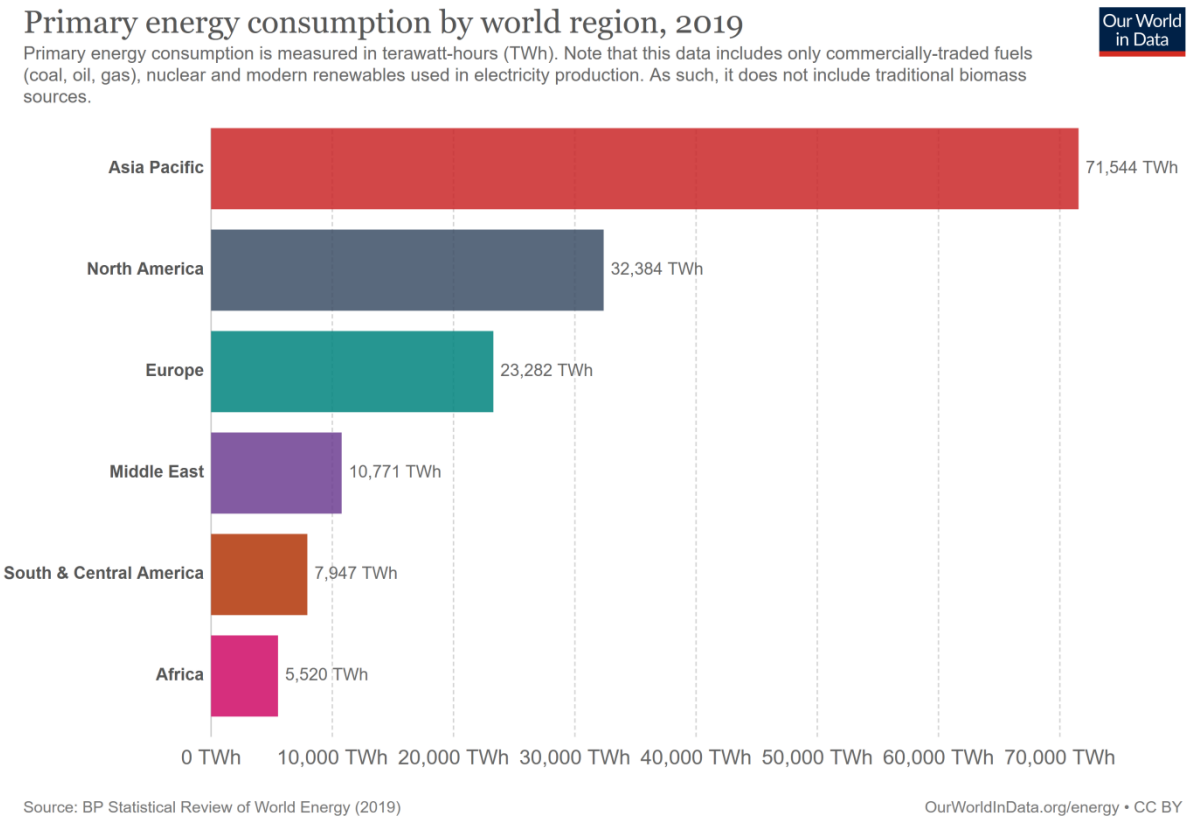

Figure 1-3: Primary energy consumption by region in 2019. [4] Licensed under CC BY 4.0

1.2 Fossil Fuels

It is obvious that the primary resource of energy is fossil fuels (oil, coal, natural gas), upon which the majority of human activity depends. Fossil fuels are formed from buried organic material during the course of millions of years, after which they become rich in carbon and

release energy when burned. They are responsible for more than 80% of the world's energy production. Fossil fuels are considered non-renewable resources due to the amount of time it takes for them to form and their depletion is much faster than their formation.

Global fossil fuel consumption has shown a rapid increase from its beginning in the 1800s until the present years, as can be seen in Figure 1-4. In 2019 it reached a total of over 136.000 TWh (gas+oil+coal). In 2018, the main resources of the global energy consumption consisted of oil (34%), coal (27%) and natural gas (24%) [5].

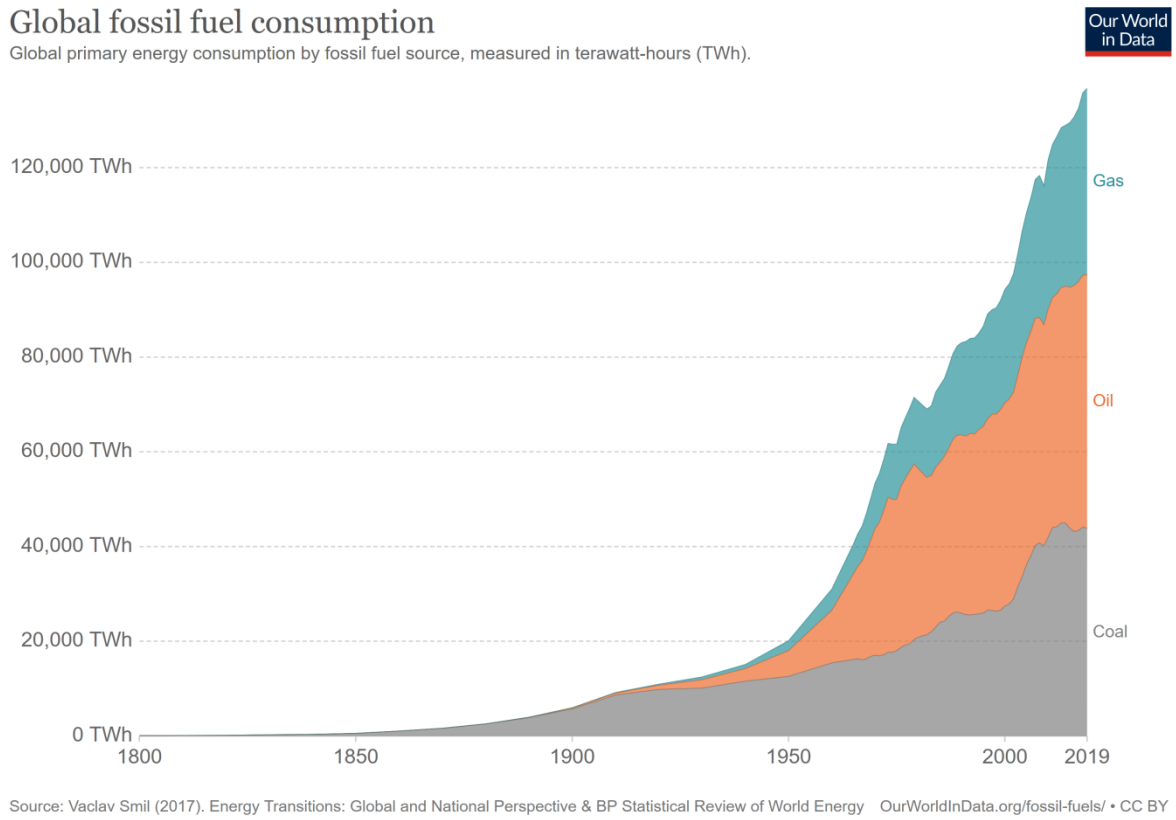

Figure 1-4: World's fossil fuel consumption for the period 1800-2019. [6] Licensed under CC BY 4.0

The use of fossil fuels as an energy source has a severe environmental impact. The burning of fossil fuels, for the production of energy, releases billions of tons of carbon dioxide (CO2) into the atmosphere, which results in an increase of the radiative forcing and adding to global warming. Based on the fifth assessment report of the Intergovernmental Panel on Climate Change (IPCC), the total annual anthropogenic greenhouse gases (GHGs) emissions from 1970

until 2010, per group of gases, can be seen in Figure 1-5. In 2010, it can be seen that a significant amount of 65% of the anthropogenic emissions of GHGs corresponds to CO2 from the combustion of fossil fuels and industrial processes.

Fossil fuels have a negative environmental impact even before they are burned, as there are emissions of air pollutants, such as benzene and formaldehyde, from oil and gas wells as well as transport and processing facilities. Furthermore, the burning of fossil fuels releases more than just CO2 into the atmosphere. There are also emissions of sulfur dioxide, mercury and particulate matter, as well as carbon monoxide and nitrogen oxide from fossil fuel-powered vehicles.

Fossil fuel industry affects more than just the atmosphere, as it has important impacts on water and oceans as well. The mining of coal, the technique of fracking and the extraction and transport of oil, which has serious risks of spills and leaks, pollute drinking water, rivers and lakes and pose a danger to freshwater and ocean ecosystems. Anthropogenic-emitted carbon is also absorbed by the ocean, which results in its acidification and affects marine organisms. Finally, fossil fuel industry with its infrastructure, such as wells and pipelines and its processing and waste facilities, changes entire landscapes and ecosystems.

Fossil fuels effects on the environment as well as the fact that they are not renewable energy sources are major disadvantages. Even though fossil fuels reserves don’t show any signs of depletion for the next decades, the fact remains that they are finite resources.

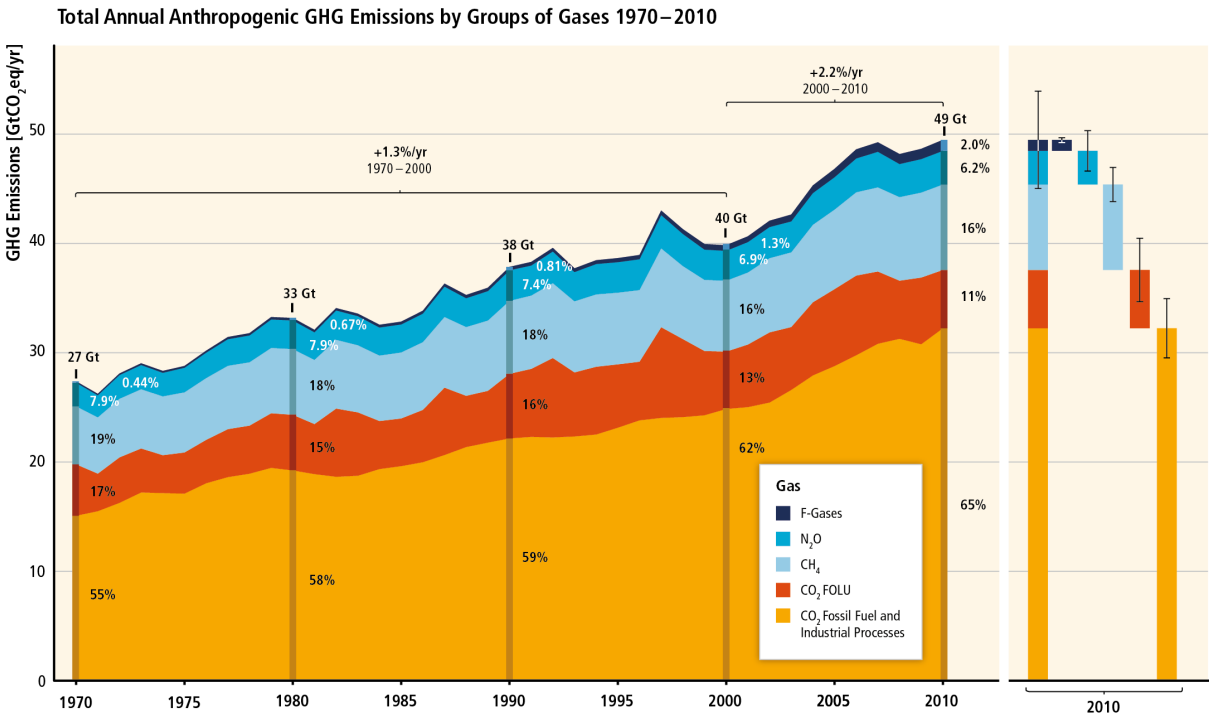

Figure 1-5: Total annual anthropogenic GHGs emissions by type 1970-2010. [7]

Based on current fossil fuels reserves, past productions and consumptions, predictions are made regarding the peak of fossil fuels production. Hubbert, back in 1956, predicted that the oil production peak in the United States would happen in the mid-seventies, based on a theory that the production follows a bell-shaped curve [8]. The theory was very close to the truth, as the peak occurred in 1970, after which the production showed signs of reduction. However, due to technology advances in the extraction of oil, the production started increasing again, as can be seen in Figure 1-6. Net imports are increasing during the time of production reduction to cover the difference and satisfy the demands. However, even though technology gives an extension to the lifetime of a fossil fuel reserve, whether this is oil, natural gas or coal, the production is bound to follow the same pattern eventually. Natural gas and coal are predicted to peak in 2035 and 2052, respectively [9]. As a result, the world is bound to turn to renewable energy, which has to increase its role in energy production and in time replace that of fossil fuels.

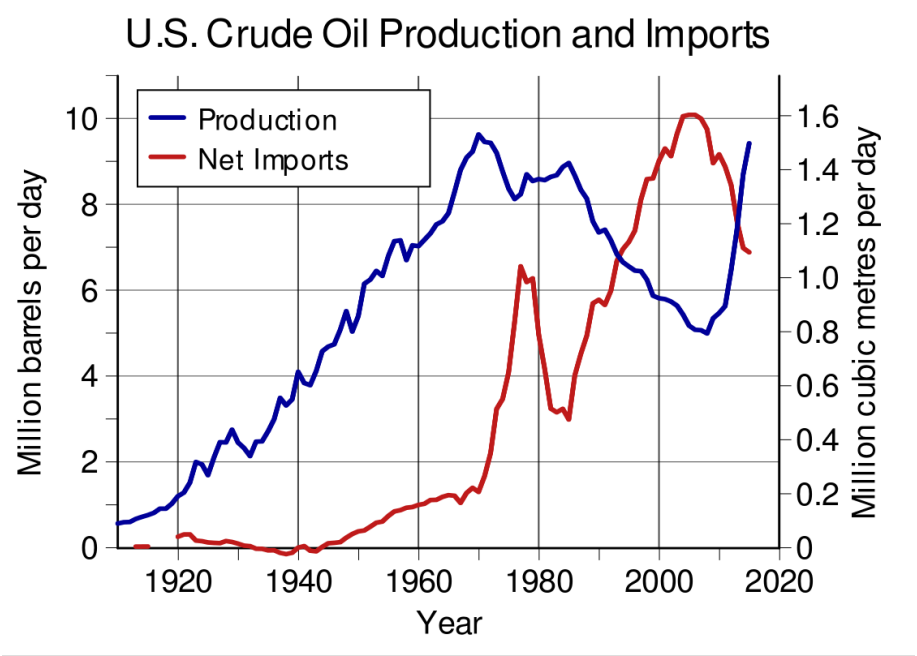

Figure 1-6: United States crude oil production and imports by year in millions of barrels per day. [10], [11] Licensed under CC BY-SA 3.0

1.3 Renewable Energy

The shift to renewable energy systems will help decrease the GHGs emissions, thus reducing the impact on global warming and in turn on extreme weather and climate effects. The term "renewable energy" covers various energy resources which are self-replenished and infinite, like solar energy, wind, geothermal, hydropower, energy from waves and tides or biomass. Technologies based on these renewable energies can produce electricity, fuels and heat.

Renewable energy has many important advantages compared to fossil fuels. The main one, as already mentioned, is of course the benefits for the environment, as they can help minimize the anthropogenic emissions of GHGs, making it a clean solution for energy production. They produce little if any at all pollutants which cause health issues and play a part in the formation of acid rain or urban air pollution and they do not require facilities for waste management and removal. It is infinite, meaning that they will be around for generations and generations, thus providing safety regarding the world's future energy needs and demands. Renewable energy is available everywhere in the world. Every country can develop an infrastructure based on the exploitation of a renewable resource, whether that is the sun, wind, water etc. That can provide each nation with safety and independence when it comes to energy

production, whereas the use of fossil fuels, which is more often than not imported, is subject to social, economic and political factors. Last but not least, renewable energy has an important economical impact, as their technology is continuously studied and improved, new jobs are created, boosting the nation's economy and costs are reduced, which will eventually make renewable energy the most viable solution in the energy production scheme.

1.4 Solar Energy

One of the main resources of renewable energy is the Sun. Solar energy can be used to generate electricity, as can be done with photovoltaic and concentrating solar power systems or it can be used for heating and cooling, as with solar thermal systems.

1.4.1 Photovoltaics

Solar photovoltaic (PV) systems convert solar energy directly into electricity. The main part of a PV system is the PV cell, which is primarily a semiconductor and specifically silicon. A PV module is formed by the interconnection of various PV cells, usually around 50 – 200 W. A PV module, connected with other components, such as batteries, electrical components, mounting systems etc., creates a PV system. PV systems can be linked together and they can produce power from a few watts to tens of megawatts.

Semiconductor is a material, where the band energy gap between the valance and conduction band is small, therefore electrons can obtain enough energy to leave the valance band and get to the conduction band, leaving a hole in the former (Figure 1-7). The current in a semiconductor is therefore the movement of electrons and holes, negative and positive, respectively. In order to increase the electrical conduction, the silicon can be doped with phosphorus (negative-type, n semiconductor) or with boron (positive-type, p semiconductor). Figure 1-8 provides the depiction of a solar cell, which has an n and a p layer. At the junction, the free electrons of the n-type layer are attracted to the holes in the p-type and in turn the positive holes of the p-type are attracted to the free electrons of the n-type and as a result an electric field is created. Due to the electric field, the electrons and holes move in the opposite direction creating an electric current and as solar energy (photons) is absorbed from the cell,

more electrons and holes are created, adding to the current flow. The photons should have energies equal to or higher than the band gap of the material. Therefore, as the majority of the photons from solar radiation are in the visible range, the materials should be modified in order for their band gap energies to be in that range. The excess energy, after the movement of the electron from the valance band to the conduction band, becomes heat.

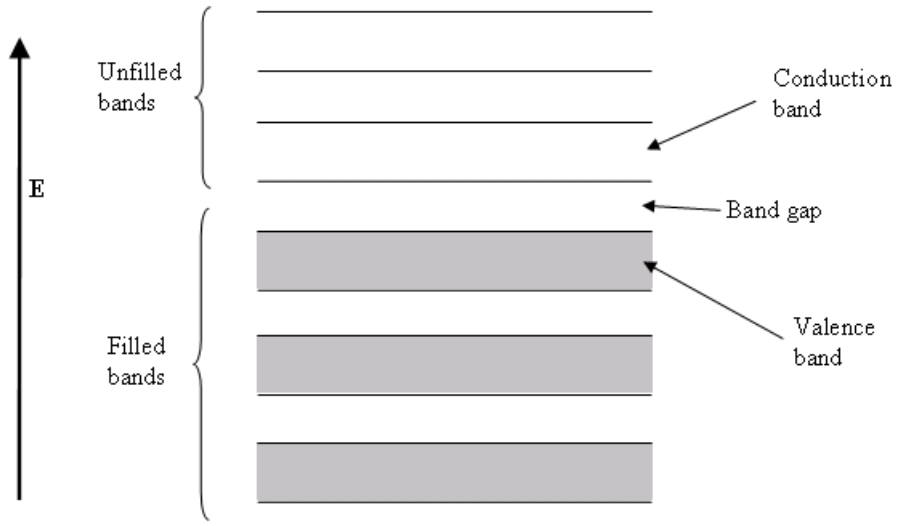

Figure 1-7: Energy band structure of a semiconductor. [12] Licensed under CC BY-SA 3.0

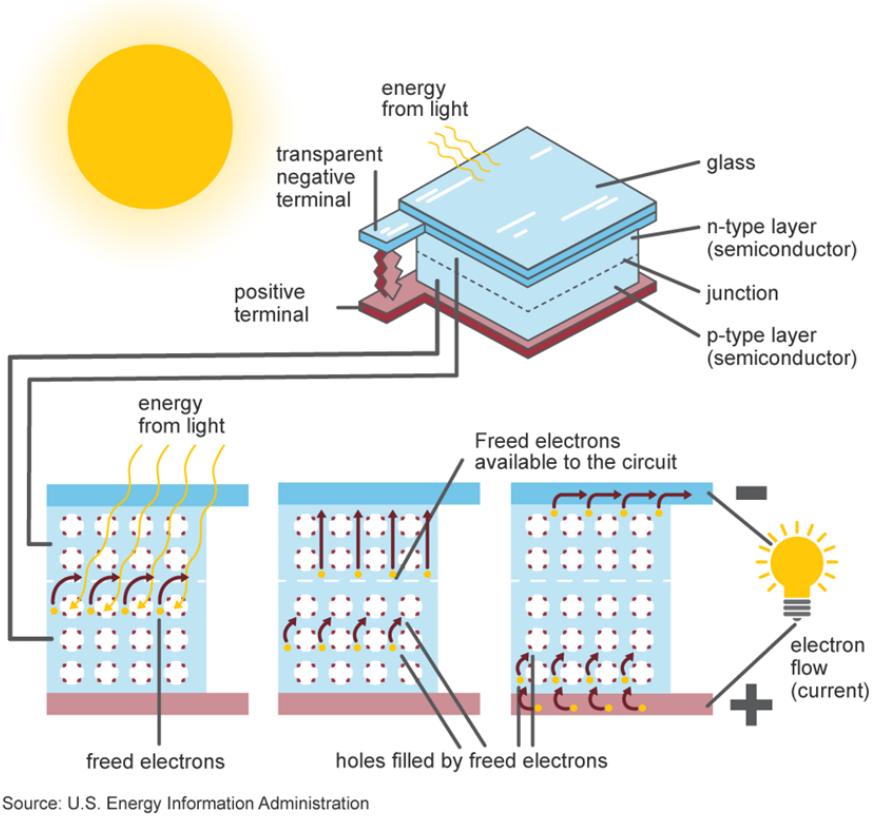

Figure 1-8: Depiction of a photovoltaic cell. [13] License: Public Domain

As a single solar cell produces little power, around 1-2 W, solar cells are integrated into a module, modules into a panel and panels into an array, depending on the desired power production. This is depicted in Figure 1-9, along with a list of all other possible components needed for the system to become operational.

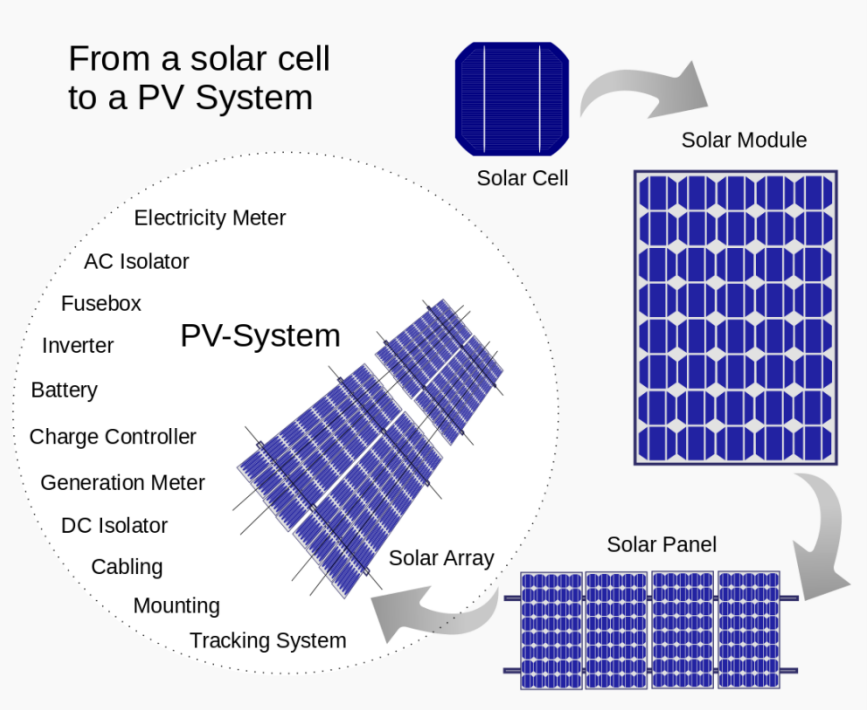

Figure 1-9: From a solar cell to a PV system. [14] License: Public Domain

The power conversion efficiency of a PV cell is the fraction of incident power which is converted into electricity. PV systems in operation yield an efficiency of 7-17% but higher percentages are obtained in the laboratory as improved devices are tried. The use of multiple p-n junctions and low temperatures of the PV cells improve the conversion efficiency.

There are several cell types, like single crystal, semicrystalline, thin film, amorphous and polycrystalline thin films. The efficiency of single crystal, which is the most expensive method, is around 10-12%, while it decreases for the other types.

Photovoltaic systems have the advantage that they use both direct and diffuse radiation, as opposed to CSP systems, so they produce power even on cloudy days, which makes them operational in more regions worldwide and not just areas with high solar resource. A PV system can be in a fixed position, in which case, for better efficiency, the azimuth angle is south (for the Northern hemisphere) and the tilt angle is the site latitude, or it can use a tracking system to follow the sun's position. Another option for a fixed PV system is to change the tilt angle with each season. Photovoltaic systems can be off-grid or grid-connected installations, which is the majority of installations in the developed world. Grid-connected PV systems can be for residential use, industrial use or even for utility power purposes. Off-grid

PV systems have the advantage that they can be used in developing countries, which have no access to the power grid, or remote areas, which are far away from power lines.

Photovoltaics have shown a significant worldwide growth in the past years and are now considered a conventional electricity source. Figure 1-10 and Figure 1-11 show the electricity generation (in GWh) from solar photovoltaic systems, as it has grown from 2000 until 2018 and the installed capacity (in MW) for the top 10 countries for the year 2019, respectively, based on data from the International Renewable Energy Agency (IRENA). This growth is expected to continue as more countries implement policies and incentives for the development of PV and other renewable energy systems, in their fight against global warming.

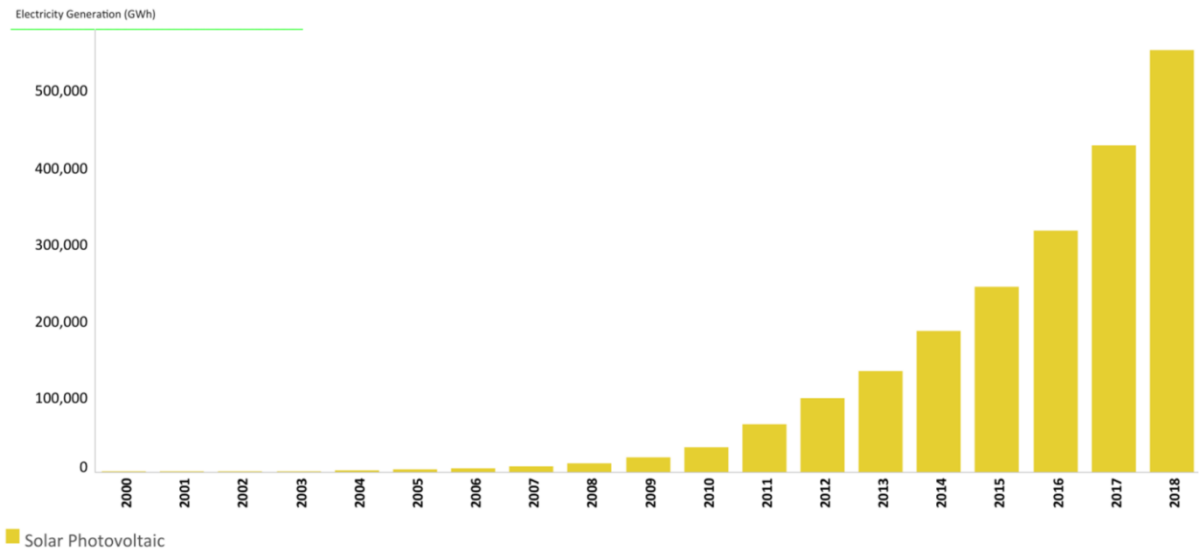

Figure 1-10: Worldwide electricity generation (GWh) from solar PV systems, from 2000 to 2018. [15]

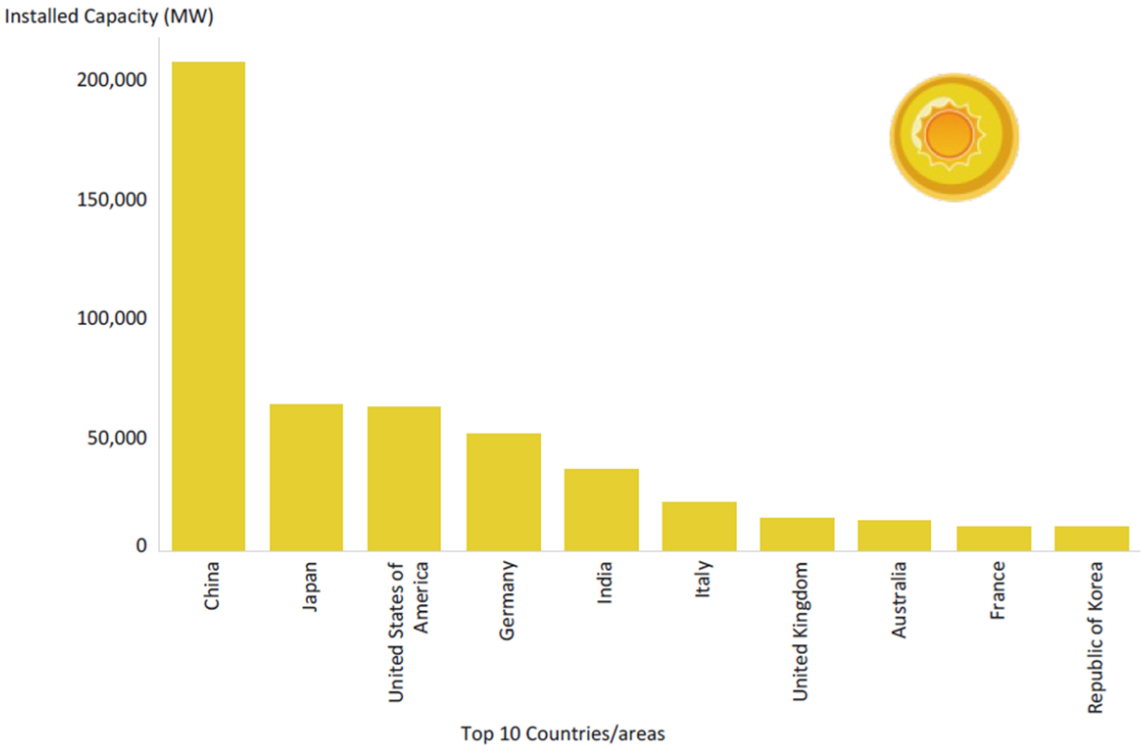

Figure 1-11: Installed PV capacity (MW) for the top 10 countries, for 2019. [15]

1.4.2 Concentrating Solar Power

Concentrating solar power (CSP) systems use direct solar radiation to produce electricity, thus they need to operate in areas with very high solar resource. They concentrate solar radiation onto a receiver with the use of mirrors or lenses. Radiation is then converted to thermal energy which is then used for electricity generation. These installations may have a thermal energy storage system in order to produce electricity in the evening or during cloudy days. For that purpose, some power plants may use other fuels, e.g. natural gas, to supplement energy, when the solar resource is not available.

The main types of CSP systems are power tower, which focuses light onto a collector on a tower with the help of tracking mirrors, linear focus, which focuses light on a linear collector tube with the help of parabolic troughs or Fresnel lenses and dish/engine, in which a parabolic dish and a receiver at the focal point are used (Figure 1-12).

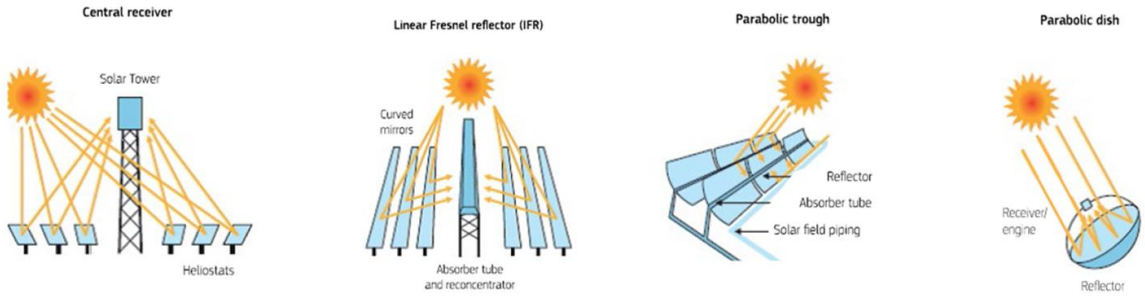

Figure 1-12: Concentrating solar power types: central receiver (solar power tower), linear Fresnel reflector, parabolic trough concentrator and parabolic dish concentrator. [16] Licensed under CC BY 4.0

1.4.2.1 Power Tower

Power tower systems use heliostats, which are mirrors distributed in a field, which track the sun and focus its light on a receiver located on top of a tower. This concentrated beam has very high energy, which is absorbed by a fluid (water, steam or molten salt), which is in turn used to generate steam to power a conventional turbine. These fluids have high heat capacity and can be used to store energy. Energy storage ability means that these systems can be operational even during cloudy days or at night. When there is no sunlight available, stored thermal energy is used to power the turbine. These installations usually cover large areas, of 1.500.000 m^2 up to 3.200.000 m^2.

Figure 1-13 depicts the National Solar Thermal Test Facility, operated by Sandia National Laboratories, in the USA, with a power tower of 61 m and 218 heliostats, established in 1978. Other operational power tower installations include the Abengoa towers in Spain of 11 and 20 MW installed maximum capacity, the Shouhang Dunhuang in China with 100 MW capacity, the Ashalim Power Station in Israel, 121 MW, which when completed in 2018 was the tallest power tower in the world (260 m) and the Crescent Dunes Solar Energy Project, USA, with installed capacity of 125 MW. The Ivanpah Solar Power Facility, in the Mojave Desert, USA, uses 3 power towers and is the second largest CSP facility in the world with a 392 MW electrical capacity. The Ouarzazate Solar Power Station, or Noor Power Station, in Morocco is currently the largest CSP facility with an electrical capacity of 510 MW (phase 3). The technology that the plant incorporates includes solar power tower and parabolic trough. The tower unit at 150 MW is the most powerful one built. An additional 72 MW PV power station

is planned to be added to the Noor Power Station, resulting in 582 MW capacity when finished. Finally Mohammed bin Rashid Al Maktoum Solar Park is a solar park near Dubai, UAE, which combines PV and CSP technologies and the solar power tower, completed during the project's fourth phase is currently the tallest power tower in the world at a height of 262.44 m.

Figure 1-13: National Solar Thermal Test Facility. [17] Licensed under CC BY-SA 3.0

1.4.2.2 Linear Focus

The line focus systems use parabolic troughs or linear Fresnel reflectors to focus the sunlight. A linear focus system is usually aligned on a north-south axis and it rotates to track the sun movement during the day.

A parabolic trough concentrator is a linear focus solar collector, which is straight in one dimension and has a parabolic shape in the other two. It is lined with mirrors of high

reflectivity. Solar radiation, parallel to the mirrors plane of symmetry, is concentrated along the focal line, where a fluid-containing tube is positioned. The fluid, which can be water, molten salt or synthetic thermal oil is heated as it absorbs the concentrated solar radiation and is then driven to a heat engine for the production of electricity (Figure 1-14). The power efficiency of a parabolic trough system is similar to that of photovoltaics. These systems can have heat storage facilities, usually using molten salt as the heat storage fluid. Among the largest parabolic trough solar thermal power systems in the world, are the Solar Energy Generating Systems (SEGS) in California, USA, with a combined capacity of 310 MW (Figure 1-15), the Solana Generating Station in Arizona, USA, with a capacity of 280 MW, the Genesis Solar Energy Project in California, USA (250 MW), the Solaben Solar Power Station (200 MW) and the Andasol Solar Power Station (150 MW), both in Spain.

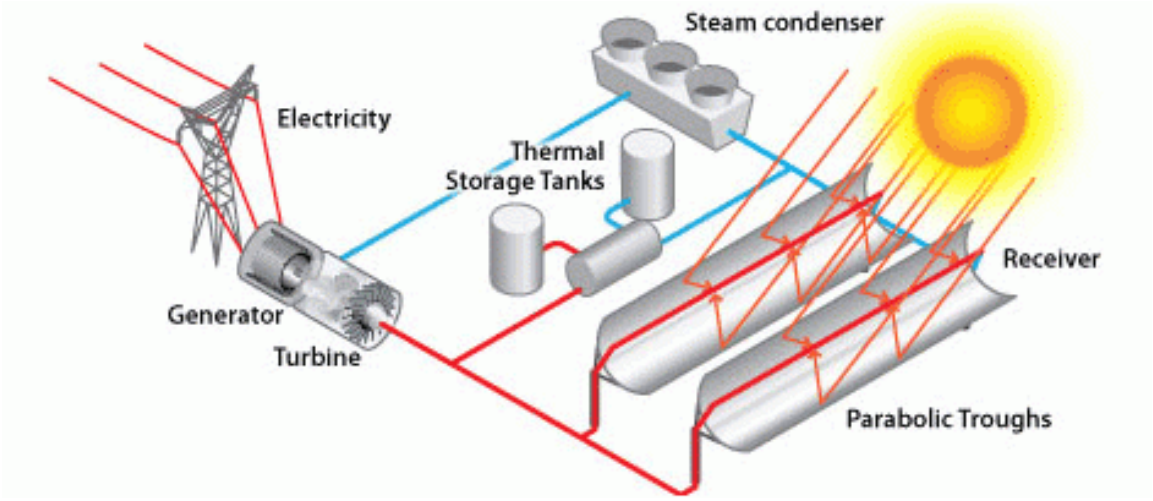

Figure 1-14: Diagram of a parabolic trough system. [18] License: Public Domain

Figure 1-15: Parabolic troughs at the SEGS plant, USA. [19] License: Public Domain

The linear Fresnel reflector takes its name from the Fresnel lens, which is a type of composite compact lens, in which the curved surface of a conventional optical lens is replaced by a series of concentric thinner and lighter lens fragments. In the same manner, linear Fresnel reflectors use long, thin rows of mirrors, with which the sunlight is focused onto a downward facing linear receiver. The receiver is in a fixed position above the reflectors, which can have a one or two-axis mechanical tracking system. The concentrated energy is then transferred into a thermal fluid, usually a synthetic oil and electricity is generated with the use of a steam turbine (Figure 1-16). The thermal fluid can also be used for heat storage.

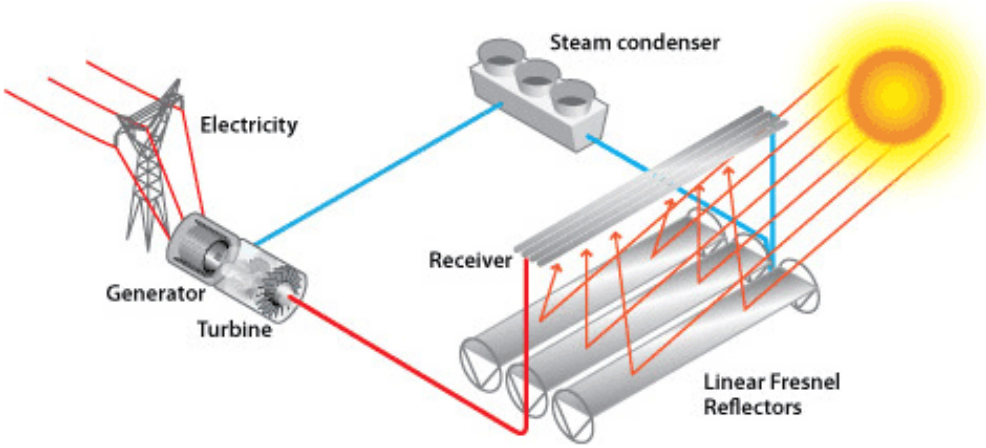

Figure 1-16: Diagram of a linear Fresnel reflector system. [18] License: Public Domain

The first commercial power plant, using linear Fresnel reflectors, in the USA, was the 5 MW Kimberlina Solar Thermal Energy Plant in Bakersfield, California. In 2009, the Puerto Errado 1 (PE 1) Fresnel solar power plant was constructed, in Spain, with an electrical capacity of 1.4 MW (Figure 1-17) to which 30 MW was added in 2012 with Puerto Errado 2, while the Reliance Power's plant in Dhursar, India is the largest CSP system that uses Fresnel reflector technology (125 MW).

Figure 1-17: Linear Fresnel reflector technology at Puerto Errado 1 solar thermal power plant, Spain. [20] Licensed under Free Art License

1.4.2.3 Dish / Engine

The dish/engine system consists of a parabolic dish, made from mirrors, that focuses sunlight on a thermal receiver, located at the focal point. The thermal receiver then transfers heat to the heat engine, which is usually a Stirling engine. A Stirling engine is operated by a cyclic compression and expansion of a gaseous working fluid at different temperatures, which results in the conversion of heat to mechanical power to run a generator. Dish Strirling systems are considered to have the highest efficiencies among solar technologies.

In 2008, Sandia National Laboratories and Stirling Energy Systems (SES) achieved a net efficiency of 31.25%, using a solar dish Stirling system at Sandia's National Solar Thermal Test Facility. In 2010, the 1.5 MW Maricopa Solar power plant, which uses Stirling technology, was commissioned in Arizona, USA. In Plataforma Solar de Almeria, in Spain, two dish Stirling

systems were designed and erected, under the Spanish-German EUROdish project (Figure 1-18).

Figure 1-18: EUROdishes at Plataforma Solar de Almeria. [21]

1.4.3 Solar Thermal Heating and Cooling

Solar heating and cooling technologies collect solar energy and use it to provide hot water, space heating and cooling and process the heat that is generated.

Active heating systems are the systems where the solar collector and storage component are usually separate from the building. In that way it consists of a system that can be added to any individual building. They have components that can convert solar energy to another form, e.g. hot water. Passive systems are those that are designed in such a way that maximizes the incoming solar heat or light in a building.

1.4.3.1 Active Heating

An active heating system needs pumps or fans in order to move the heat transfer fluid (liquid or air) and consists of the collector, storage unit and the controller, to turn on the pumps etc. In a solar hot water system, a space can be heated by radiant water heaters or air heating, where the air is heated as it goes over a heat exchanger. A structure can be heat sufficient with the use of these systems in warm periods, but during cooler periods, auxiliary heating is needed by another heating system that would work in parallel. In a solar hot air system, in order to provide the same heat with the hot water system, a larger volume of air than water needs to be transferred. Most active solar heating systems use flat-plate collectors and are positioned at an angle that produces the highest efficiency.

Flat-plate collectors are commonly used for space heating and domestic hot water. They include a collector surface, where solar radiation is absorbed, a glazing which prevents solar energy to be reradiated from the absorber, a heat transfer fluid, which is usually water or a propylene glycol mixture fluid, for cold climates so the fluid doesn't freeze and insulation, which is placed on the sides and back to avoid heat loss by conduction and convection (Figure 1-19). The heat transfer fluid transports heat from the solar collector to a separated reservoir. Glazing and insulation can be modified to fit each climate's needs. The absorbing surface is usually made of copper, iron or aluminum, whereas the glazing can be plastic or glass.

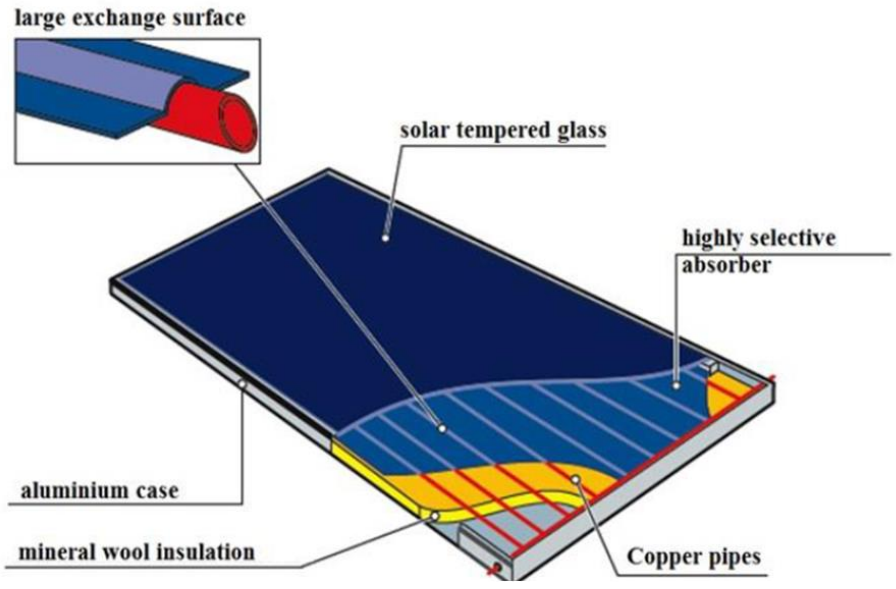

Figure 1-19: Diagram of a flat-plate collector. [22] Licensed under CC BY 4.0

An evacuated tube collector consists of single parallel glass tubes (Figure 1-20). These glass tubes surround the absorber and are evacuated in order to reduce heat loss. Their cylindrical shape means that the sun rays are always perpendicular to the tubes surface, increasing their efficiency. Each tube consists of an outer and inner glass tube, of transparent and selective absorbing surface, respectively, with the absorber placed inside the inner tube. The outer tube allows sunlight to enter with minimal reflection, while the inner tube also has minimal reflection properties. The air between the outer and inner tube is evacuated and as a result there is less heat loss, through conduction and convection, compared to flat plate collectors. Heat transfer fluid can flow in and out of the tubes or the tubes are connected to heat pipes, which transfer the heat to a fluid in a heat exchanger (Figure 1-21). The tubes are able to absorb infrared radiation, which is emitted even on cloudy conditions, while wind and lower temperatures also don't have much effect on their operational ability.

Figure 1-20: An evacuated tube collector. [22] Licensed under CC BY 4.0

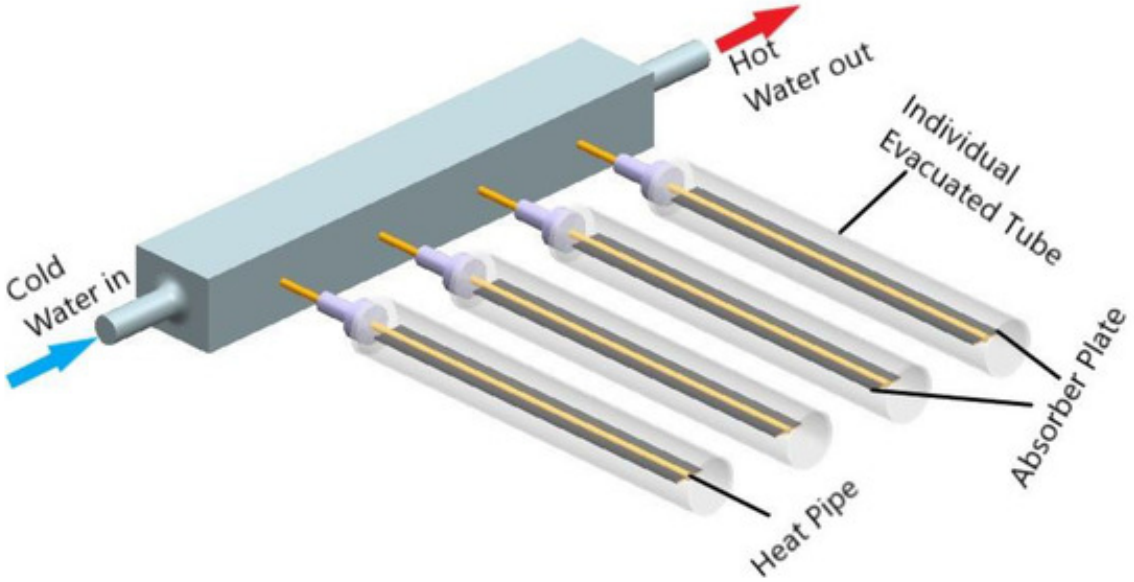

Figure 1-21: A heat pipe evacuated tube collector. [23] Licensed under CC BY 4.0

1.4.3.2 Active Cooling

Active solar systems can be used for cooling a building with the addition of an absorption cooling unit. This unit uses two fluids, an absorbent like water and a refrigerant like ammonia. The refrigerant performs evaporative cooling and is then absorbed by the absorbent. The energy needed for the cooling process is provided by the Sun. Concentrating and evacuated tube collectors can be used for cooling purposes but are more expensive.

1.4.3.3 Passive Heating and Cooling

In passive solar systems, buildings or parts of them are designed in such a way so as to collect, store and distribute solar energy, to provide heating in winter and discard it for cooling in the summer. They don't require additional mechanical or electrical parts to operate. The main factors that are considered in passive heating and cooling are the size and placement of the building's windows, their glazing, the shading and the thermal mass and insulation of the structure. There are other factors such as the orientation of the building, shape and colour (both inside and outside) and also vegetation, which can have shading effects and diminish the wind force on the building. Passive heating and cooling systems can be designed when building a structure or can be added in an existing one with modifications.

Windows are the most important factor in passive heating and cooling (their size, placement and glazing). Diffuse sunlight is important to have throughout the year as it provides internal lighting (daylighting). The direct component of sunlight is desirable in winter and the opposite in summer. When the windows are positioned vertically, there is less sunlight inside the building, unless the sun is low in the sky. In summer, shading is needed for windows facing south (for the Northern Hemisphere), to avoid direct sun radiation and for windows facing west during the afternoon. Double-pane windows are needed for cold climates, as they reduce heat loss. It's not desirable to have a building almost entirely made of glass, as it heats too much during the summer, therefore the glass in these situations should be very reflective. Large thermal mass of a structure reduces the temperature variations between summer and winter days.

In passive solar systems, there is direct and indirect solar gain. Direct gain is when the sunlight that enters a room is absorbed in it. Indirect gain is when there is absorption of sunlight and transport to the rest of the structure by convection, conduction or radiation (natural or forced), as it happens, for example, in a solarium, a greenhouse or a Trombe wall.

A Trombe wall is made of a masonry wall, which is thick and coated with a dark color material that absorbs solar thermal energy (Figure 1-22). It is covered with glass on the outside, with air insulation between the wall and the glaze. Solar radiation passes through the glaze and is absorbed by the dark coated outer surface of the wall, which emits very little radiation in the infrared range. Heat is trapped in the space between the glaze and the outer surface of the wall. It is then conducted through the masonry and distributed to the living space. Due to the thickness of the wall and the high heat capacity of the materials, it takes time for heat to flow from the warm outer surface to the inner surface. As a result, heat that is gained during the day, reaches the inner structure in the evening and the space receives amounts of heating even after sunset. Instead of masonry, water, placed in tubes or barrels, can be used to form the wall, due to its higher heat capacity.

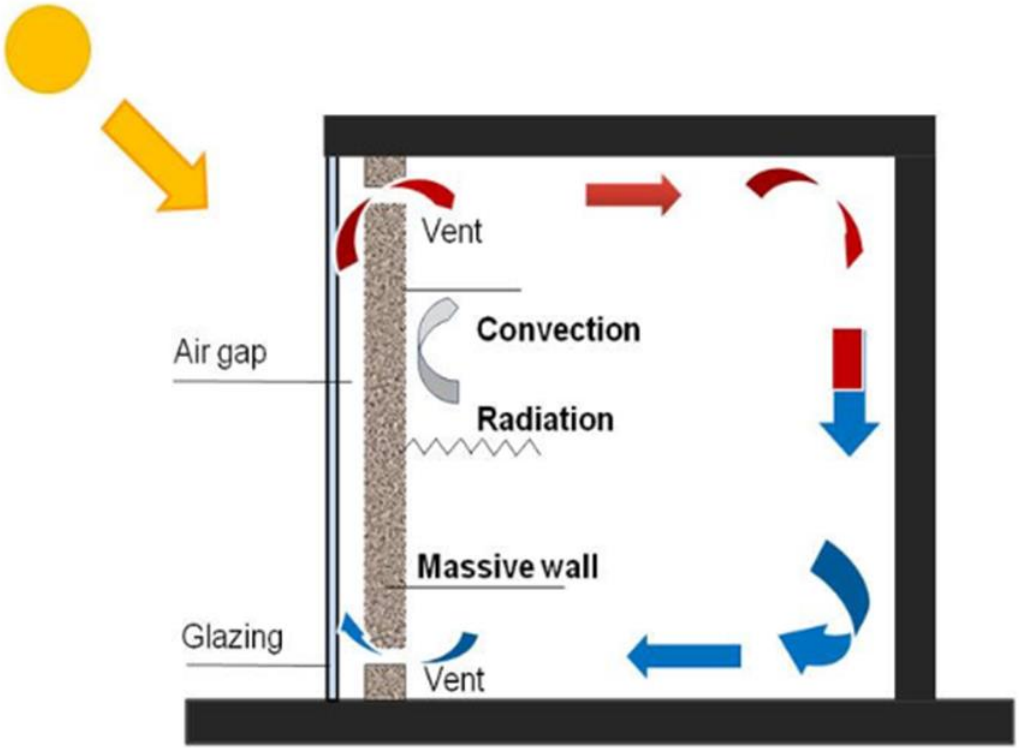

Figure 1-22: Diagram of a Trombe wall. [24] Licensed under CC BY 4.0

Passive cooling is the procedure of replacing hot air with cooler air, by convection, using natural ventilation. For example, a structure's thermal mass can be ventilated at night to reduce heat or thermal chimneys can be used. Also, a design with low windows facing south and high windows facing north can produce a current to cool the air inside the structure.

1.5 Wind Energy

Wind energy is provided from the wind with the use of wind turbines to produce mechanical power to turn electric generators. Wind energy is a renewable resource and it can be used in many areas worldwide. Also, like other renewable energy resources, it doesn't require water for the production of electricity. However, wind is a variable resource as it can't be provided continuously to generate electricity and its intensity is also variable with time. In order to provide a reliable supply of electricity, it needs to be used together with other power sources or energy storage.

Wind power has been used for centuries, as humans were using it to sail their ships, grind grain and pump water. Windmills were used extensively in the USA in the middle of the 20th century and during recent years there has been a major increase in wind power. That is mainly because of the construction of wind farms, which can reach a capacity of tens of gigawatts. The oil crisis of 1973 led Denmark and the USA to research and implement the construction of large wind generators with the purpose of connecting them to the grid. From 2009 onwards, many countries have developed wind power plants and the installed capacity in the USA reached 60 GW in 2012. Nowadays wind energy installations range from small, with the purpose, for example, of charging a battery, to extremely big wind farms, which produce electricity to supply national networks.

Figure 1-23 shows the increase in electricity generation from onshore and offshore wind power installations, from 2000 until 2018, while Figure 1-24 depicts the installed capacity for the top 10 countries for the year 2018.

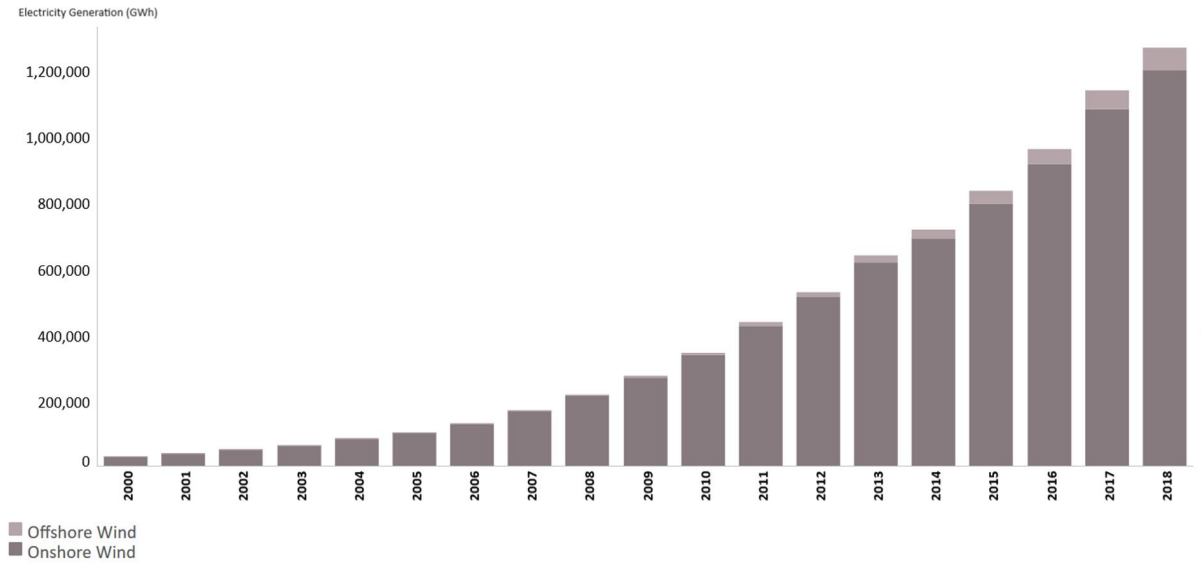

Figure 1-23: Electricity generation (GWh) from wind power, 2000 – 2018. [15]

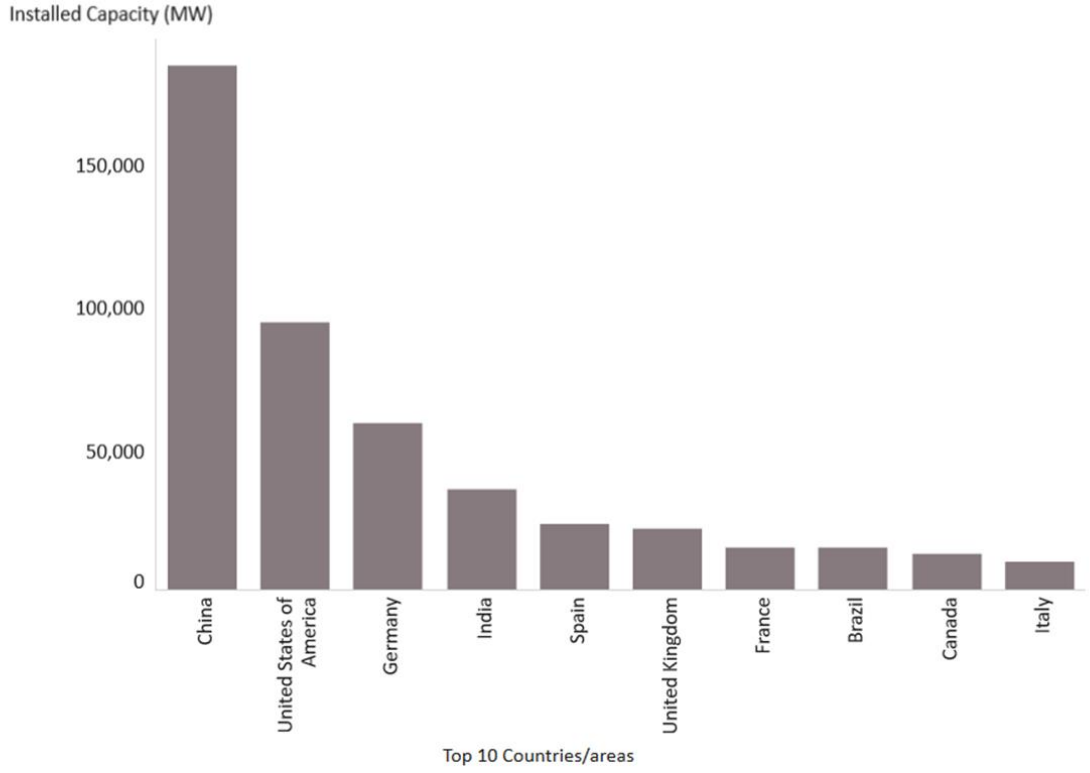

Figure 1-24: Installed wind power capacity (MW) for top 10 countries, for 2018. [15]

1.5.1 Wind Resource

The wind power density is the power P per unit area A, where power is the wind energy E per unit time t. The wind power density is calculated as:

$$\frac{P}{A} = 0.5 * \rho * v^3, \qquad W/m^2 \qquad \text{Equation 1-1}$$

where ρ and v are the air density and wind speed, respectively. That means that the wind power density is proportional to the third power of its speed and as the wind speed increases by two times, the wind power per unit area will increase by eight times. It is also proportional to air density, therefore the wind power will decrease with elevation. In order to determine the ability of a site to be used for wind power production, a frequency distribution of the wind speeds that are observed, during several years, needs to be provided and studied. As the wind

varies in strength, the average value of its speed is not enough to determine how much energy a wind turbine can produce at a specific site.

The change in wind speed with height is called vertical wind shear. Wind shear can have important effects on wind power installations and needs to be taken into account, as a small variation in wind speed will have a large one in wind power, as already seen from Equation 1-1. Significant wind shear means that there will be different wind speed at the top height of a turbine blade as it rotates than at the bottom, which will affect the power production performance. Wind shear can be calculated from the power law in Equation 1-2:

$$\frac{v}{v^0} = \left(\frac{H}{H_0}\right)^{\alpha} \qquad \textit{Equation 1-2}$$

Where v and v_0 are the wind speeds at heights H and H_0, respectively, with the latter speed being a known parameter, while α is the wind shear exponent, a parameter determined from measurements. Increase in the wind shear exponent means that the vertical gradient in wind speed increases too.

In order to develop a wind power installation, especially a large one like wind farms, a detailed wind resource assessment is needed. Wind power maps of high resolution are being produced for many countries and there are applications and databases with freely available data regarding the wind resource potential worldwide. Geographic Information System (GIS) data and software tools are also used to further assess wind power resources. Wind maps are essential for the preliminary selection of sites that are candidates for wind power installations. After that, further investigation of the site is needed, with high quality wind speed data from ground-based anemometers. Two examples of wind maps for the USA are shown in Figure 1-25 and Figure 1-26, for the mean wind speed and mean power density at 100m, respectively.

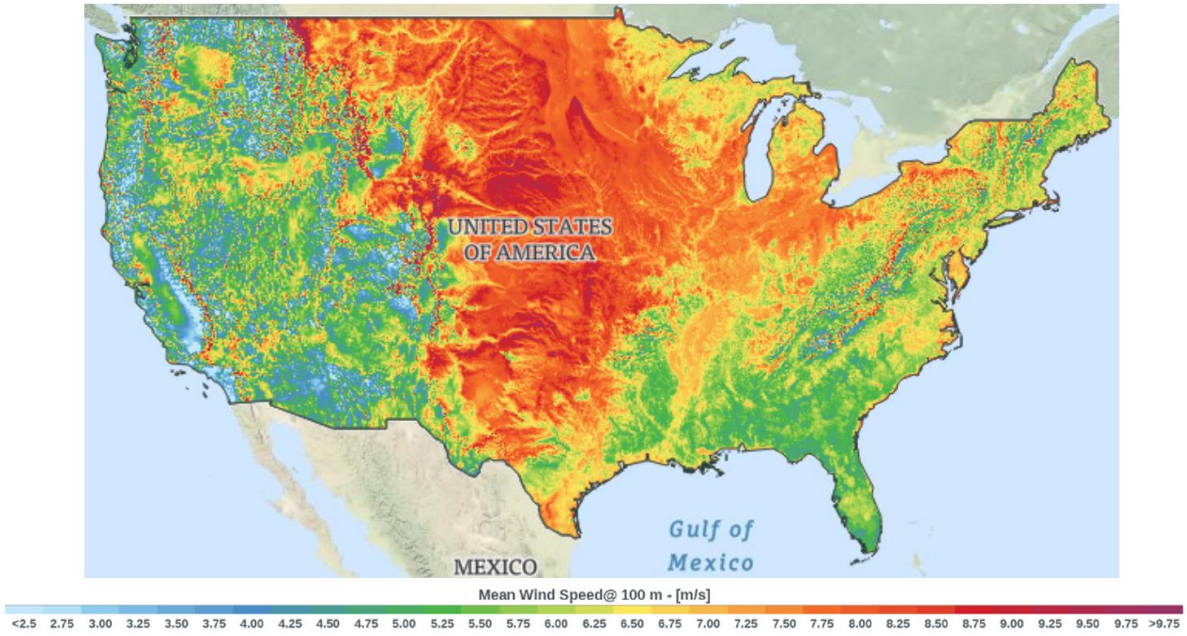

Figure 1-25: Wind map of mean wind speed (m/s) at 100m, for the USA. [25] Licensed under CC BY 4.0

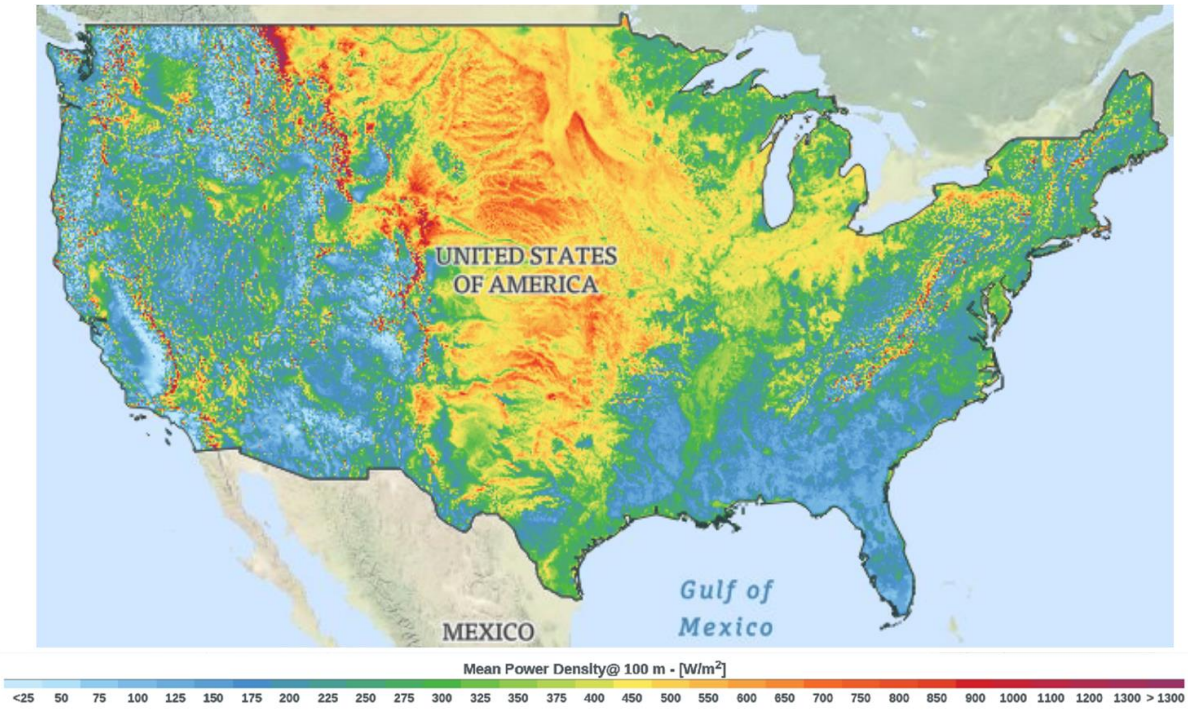

Figure 1-26: Wind map of mean power density (W/m^2) at 100m, for the USA. [25] Licensed under CC BY 4.0

1.5.2 Wind Turbines

The wind turbine converts kinetic energy (from the wind) into electrical energy. It can come in a variety of sizes, from small, for individual purposes up to bigger ones, for domestic power supply and arrays of large turbines, which are used to provide power to the grid.

Wind turbines are divided into two categories, regarding the aerodynamic force that is used to extract the wind energy. For that purpose, there are the lift-based and the drag-based turbines. In drag-based turbines, the rotor is made to turn on its axis as the wind pushes against the blade and as a result the blade speed can't exceed that of the wind, therefore drag-based turbines are less efficient. Lift-based turbines usually have airfoil surfaces for blades and the movement of the blades is perpendicular to the wind flow. As a result, the blades can reach speeds higher that the wind's and are more efficient.

Wind turbines are further categorized based on the orientation of their rotor axis with the ground. As a result, there are two categories, the horizontal axis wind turbines (HAWT) and the vertical axis wind turbines (VAWT), with the HAWT being the most common.

HAWTs (Figure 1-27) can be upwind or downwind. Upwind turbines have their rotor facing the wind, while downwind turbines have the rotor located on the lee side of the tower. Upwind turbines need a yaw mechanism in order to keep the rotor perpendicular to the wind. HAWTs with three blades rotating upwind are the majority of wind power installations worldwide.

Figure 1-27: Horizontal axis wind turbine. [26] Licensed under CC BY-SA 3.0

VAWTs have a vertical rotor axis and their main advantage is that they don't need to be placed to face the wind to be operational. Also the gearbox and generator can be placed at ground level which makes for easier maintenance. However their efficiency is lower than that of HAWTs and they are not used for large scale electricity generation. The two main types of VAWTs are the Darrieus and Savonius.

The Darrieus wind turbine is a lift-based turbine and has a number of aerofoil blades, which are curved, on a rotating axis (Figure 1-28). In order for the turbine to produce power, the Darrieus blades have to reach higher speed than the wind speed, which means that is doesn't

have the ability to self start. Savonius wind turbine is a drag-based turbine, which has a number of aerofoil blades, which have a semi-circular shape and are most commonly mounted on a rotating shaft (Figure 1-29). The main advantage of Savonius turbine is that it has the ability to self start, although it has a lower efficiency than Darrieus turbines. They are very effective though for applications, other than electricity production, such as water pumping or grain grinding. Another type of VAWTs is the Giromill or H-rotor, which is the same design as the Darrieus turbine, with the blades being replaced by straight vertical ones that use horizontal supports to connect with the turbine tower (Figure 1-30). Wind turbines can also be constructed from combinations of various designs, as seen in Figure 1-31, where the turbines are a combination of Darrieus and Savonius designs, located in Jinguashi, Taiwan.

Figure 1-28: Darrieus wind turbine. [27] Licensed under CC BY-SA 3.0

Figure 1-29: Savonius wind turbine. [28] Licensed under CC BY 2.0

Figure 1-30: Giromill or H-rotor wind turbine. [29] Licensed under CC BY-SA 3.0

Figure 1-31: Combination turbines of Darrieus and Savonius designs in Jinguashi, Taiwan. [30] Licensed under CC BY-SA 3.0

Apart from the rotor, other components of a large wind turbine are the gearbox, which increases the blades rotation, a conversion system (generator), controls and the installation's tower.

1.5.3 Wind Farms

An assembly of wind turbines in an area, with the purpose of generating electricity, is called a wind farm. There is a variety of sizes, as a wind farm can be small with several turbines or extensive with a few hundred or even thousand wind turbines. There are onshore and offshore wind farms. China, India and the USA are the countries with the largest onshore wind farms, with the largest being the Gansu Wind Farm in China, with a 7965 MW capacity and a target capacity of 20000 MW (Figure 1-32). The largest offshore wind farm in the world is the Hornsea 1 in the UK with a capacity of 1218 MW (Figure 1-33). It operates 174 turbines.

Figure 1-32: The onshore Gansu Wind Farm in China. [31] Licensed under CC BY-SA 3.0

Figure 1-33: The offshore Hornsea 1 wind farm, in the UK. [32] Licensed under CC BY-SA 4.0

For a wind farm to be successful in its operation it needs to be constructed to a site that has favourable wind conditions, it has access to electric transmission as well as physical access. Favourable wind conditions means that high wind speeds are needed, but wind needs to be consistent without high turbulence and it needs to come from one direction. Also, the altitude of the site and the distance between the turbines need to be determined.

The first onshore wind farm was built in New Hampshire, USA in 1980, with a capacity of 0.6 MW. Since then, other large onshore wind farms, besides the Gansu in China, include the Alta Wind Energy Center (or Mojave Wind Farm) in California, USA, which has a capacity of 1550 MW, the Muppandal Wind Farm and Jaisalmer Wind Park in India, with a capacity of 1500 and 1064 MW, respectively, the Los Vientos Wind Farm, Texas, USA with 912 MW capacity and the Shepherds Flat Wind Farm in the USA, with a 845 MW capacity. As far as offshore wind farms are concerned, Europe has the lead with the largest ones in the world. The first offshore wind farm was constructed in Denmark in 1991 and since then, besides Hornsea 1, the largest offshore wind farms include the recently commissioned Borssele 1&2 in the Netherlands with an installed capacity of 752 MW and the Borssele 3&4, ready for commission in 2021, with a 731.5 MW capacity, the East Anglia ONE with 714 MW capacity, the Walney and London Array in the UK, with capacities of 659 and 630 MW, respectively, the Gemini Wind Farm in the Netherlands at 600 MW and Hohe See in Germany at 497 MW. In 2010, the combined capacity of European offshore wind farms was calculated at 2396 MW and more massive projects are planned to be constructed in the future. When taking account all countries with wind power production, the total capacity reached 651 GW in 2019. There has been continuous increase in wind power plants in the last years, not only in the USA and Europe, but mainly in China and India.

Wind power installations don’t have an environmental impact like fossil fuels, as they don’t need fuel to operate and don’t emit pollutants in the atmosphere. However there is criticism regarding their effect on the landscape and wildlife. Big wind farms require extensive space to be built and they impact the habitat of many species, since they are built in rural areas. There is also criticism regarding the visual impact and the noise effects, although research hasn’t provided any evidence that there are health concerns.

Apart from large wind power plants, there are small wind power installations which can reach a capacity of 50 kW. These can be used by households in order to reduce their use of grid

electric power. The turbines can be connected to the grid and any surplus can be sold to the utility company. Small wind turbines can also be off-grid to be used in remote areas, which are not connected to the grid and usually use diesel generators or other sources of electric power. Small wind turbines can supplement these systems and there is a growing market for them, whether for on-grid or off-grid purposes.

1.6 Bioenergy

Bioenergy is a type of renewable energy that is produced from organic materials. Organic material which has stored the Sun's energy through photosynthesis is called biomass and this energy can be converted into other forms, such as heat, electricity or fuels (biofuels). Bioenergy can be produced from such organic materials as wood and crops, wastes whether municipal or from animals or algae and bacteria.

Biomass can be burned to produce energy directly or it can be converted to liquid or gas fuels, called biofuels, which can be transported and stored. In that way, energy can be produced on demand.

Biomass is a renewable source of energy that is based on the carbon cycle. Crop residues, manure and wood are important sources of biomass, as well as animal waste. Another source is the agricultural products that are manufactured for the production of biofuels, like corn or soybeans.

Figure 1-34 shows the gross energy consumption for 2017. The majority of energy consumption comes from fossil fuels, with oil, coal and gas having a share of around 40, 20 and 20%, respectively. When taking account the renewable resources, which account for around 18%, biomass is the largest source in energy consumption. In Figure 1-35, the electricity generation from biomass, the biopower, is presented for 2017 per continent. Europe and Asia are the two continents with the largest production of biomass power, most of which comes from solid biofuels, which include woodchips, pellets etc. Municipal waste and biogas are also major sources for electricity production in Europe, whereas in Asia industrial waste plays an important part.

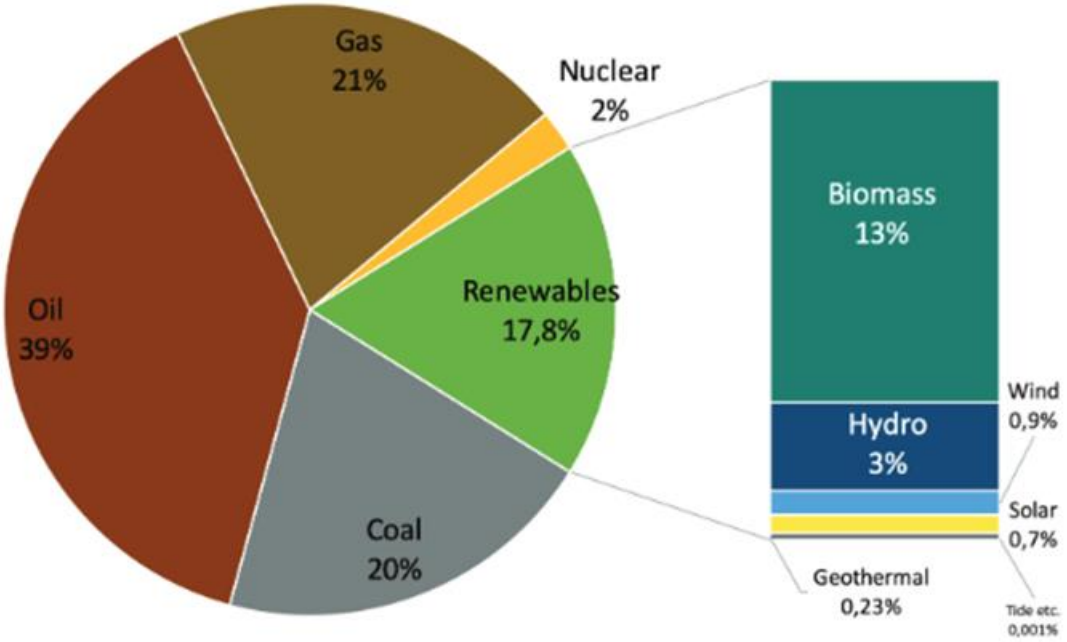

Figure 1-34: Total energy consumption for 2017. [33]

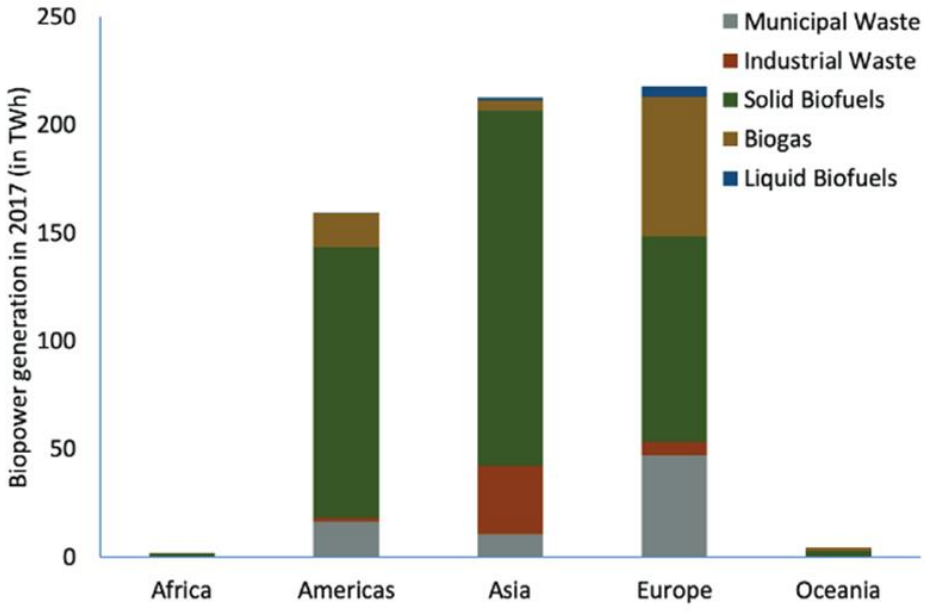

Figure 1-35: Biopower generation per continent for 2017. [33]

Wood had been the main source of energy in the past and it still constitutes a major source for energy production, especially in some developing countries which use mainly wood and

charcoal for their energy needs. Increase use of firewood though creates problems of deforestation. Wood is used directly or it can be processed to produce pellet (Figure 1-37) and other forms of fuel. Figure 1-36 shows the woodfuel production per continent for 2018. Africa and Asia are the top continents in wood fuel production, where many developing countries use it for cooking and heating.

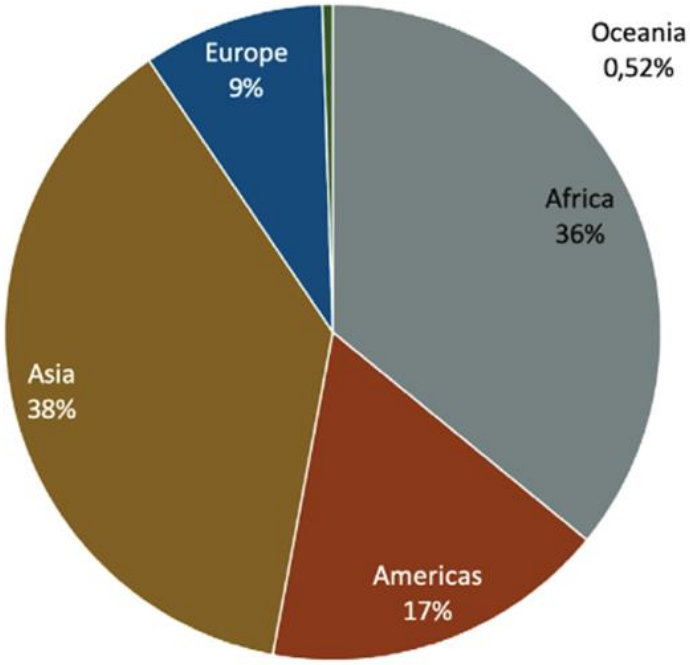

Figure 1-36: Woodfuel production per continent for 2018. [33]

Figure 1-37: Wood pellets. [34] Licensed under CC BY-SA 3.0

Municipal solid waste (MSW) is an important part of biomass. MSW is basically the trash that is discarded by the public, for example clothing, boxes, paper, food wastes etc., but not industrial and agricultural wastes or sewage products. MSW can be processed to produce energy through combustion and progress in technologies and new regulations have resulted in decreased emissions of pollutants during this process. Landfills, which are created for waste disposal and are basically huge holes filled with compacted garbage and sealed afterwards, can produce gas from the decomposition of MSW, called landfill gas, which contains mostly methane and carbon dioxide, both major greenhouse gases. Landfill gas can be used directly to produce heat through combustion or it can be used for electricity production with the use of steam turbines, microturbines or fuel cells. The Puente Hills Landfill in the USA (Figure 1-38) generates more than 40 MW of electricity while the Sudokwon landfill gas power plant in South Korea, produces 50 MW of electricity.

Figure 1-38: Aerial photo of the Puente Hills landfill in the USA. [35] Licensed under CC BY-SA 2.0

Sewage sludge is another source of biomass that is on the forefront of research for energy production, with focus on developing countries. The aim is to convert sewage waste water into drinking water and electricity by using solid sewage material as fuel. The main product from sewage is methane and by using sewage material, there is a reduction on landfill waste and on the atmospheric burden from produced gas.

1.6.1 Biofuels

Biofuels are the liquid or gas fuels that are produced from biomass processes and can be transported and stored. They are considered a renewable source of energy, since the biomass from which they are produced can be replenished. They can be produced from plants or agricultural, industrial and domestic organic waste. Plants that are grown for the mere purpose of being used for energy production are called energy crops. Examples of biofuels are biogas, ethanol and biodiesel.

1.6.1.1 Ethanol

Ethanol is produced mainly from the fermentation of sugars, from corn or sugarcane, or cellulose, which is a more difficult process. The production process includes the enzyme digestion, to release the sugars, fermentation of the sugars, distillation and drying. Figure 1-39 presents a diagram of the production of first and second generation bioethanol. First generation bioethanol is produced from sugars or edible biomass, while second generation bioethanol uses various lignocellulosic biomass sources. There are several steps before the materials enter the fermentation stage where ethanol is produced.

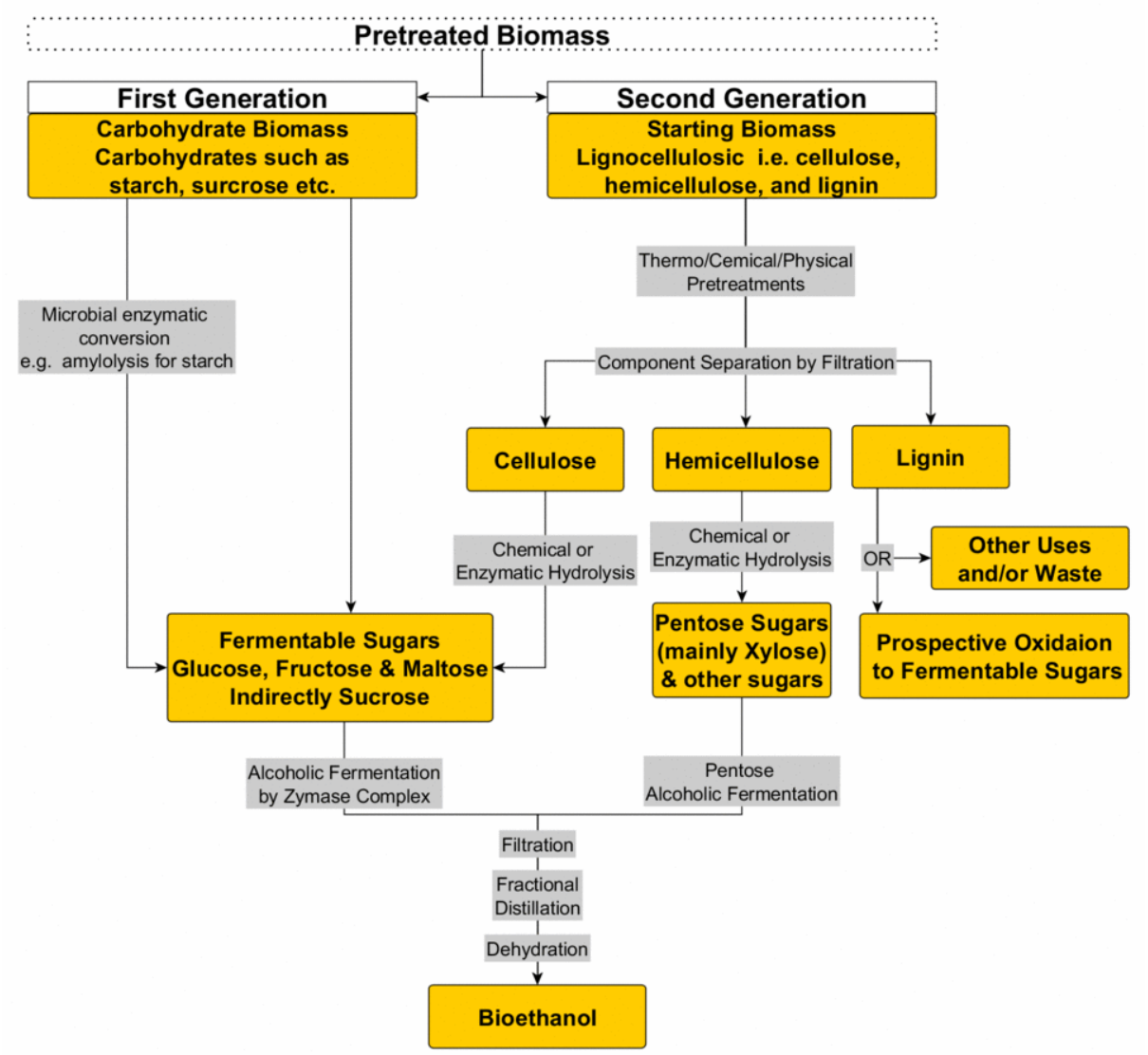

Figure 1-39: Production diagram of first and second generation bioethanol. [36] Licensed under CC BY-SA 3.0

Ethanol is the most known biofuel in the world and it's extensively used in Brazil. It can replace gasoline in petrol engines or it can be mixed with it. The production of bioethanol, from corn and sugarcane, reached 62% of total biofuel production worldwide, in 2017, with USA and Brazil being the top countries in its production. Figure 1-40 shows the global production of liquid biofuels, in billion litres, from 2000 until 2017, where the increase in worldwide production in recent years is evident, with ethanol holding the majority of production. Most cars in the USA use a mixture of gasoline with around 10% ethanol, while the mixture in Brazil contains around 25% ethanol. More ethanol is needed to replace the energy content of gasoline, as 1 volume of gasoline is equivalent to 1.5 volume of ethanol.

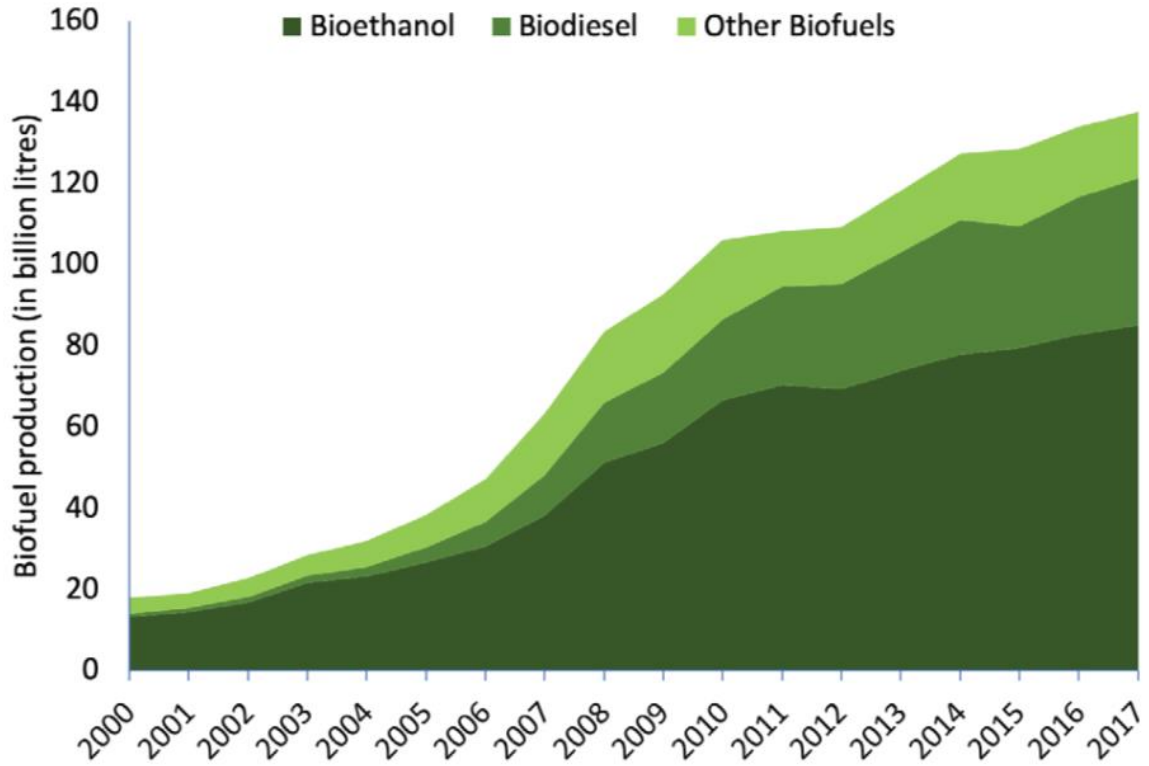

Figure 1-40: Global production of liquid biofuels. [33]

1.6.1.2 Biodiesel

Biodiesel can be produced from vegetable oils, animal fats or recycled grease or from fuel crops especially for its production, like palm oil. Production is achieved by transesterification, a process through which oils and fats are converted to biodiesel and glycerine, as shown in Figure 1-41.

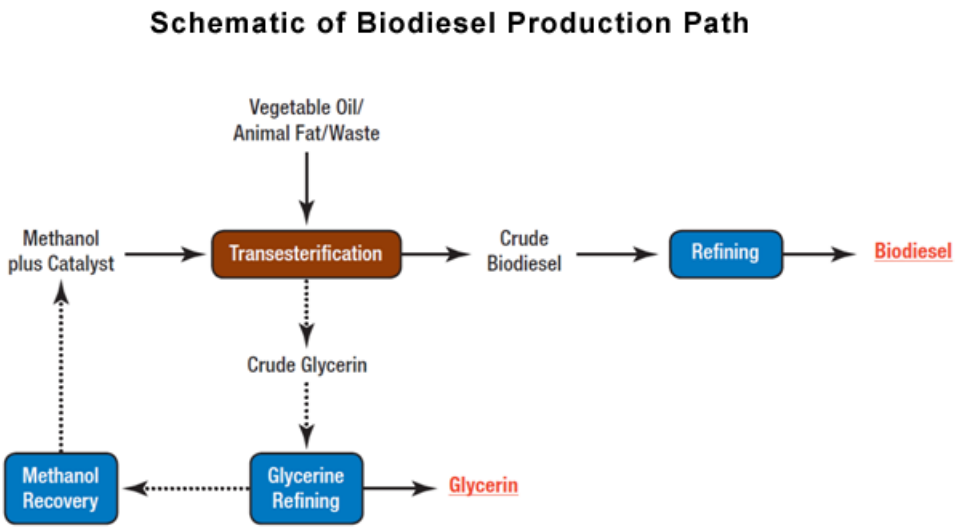

Figure 1-41: Diagram of biodiesel production process. [37] License: Public Domain

Biodiesel has similar properties to petroleum diesel and as a result it can be used in diesel engines alone or mixed with petrodiesel. Biodiesel is commonly used in Europe. It has a lower content in carbon and higher in hydrogen and oxygen, compared to petroleum diesel, therefore the particulate emissions are reduced. However higher emissions of nitrogen oxides may occur when pure biodiesel fuel is used. Figure 1-42Figure 1-42 presents the production of liquid biofuels, in billions of litres, per continent in 2017. Biodiesel is the major biofuel that is produced in Europe, with ethanol being the most common in the Americas.

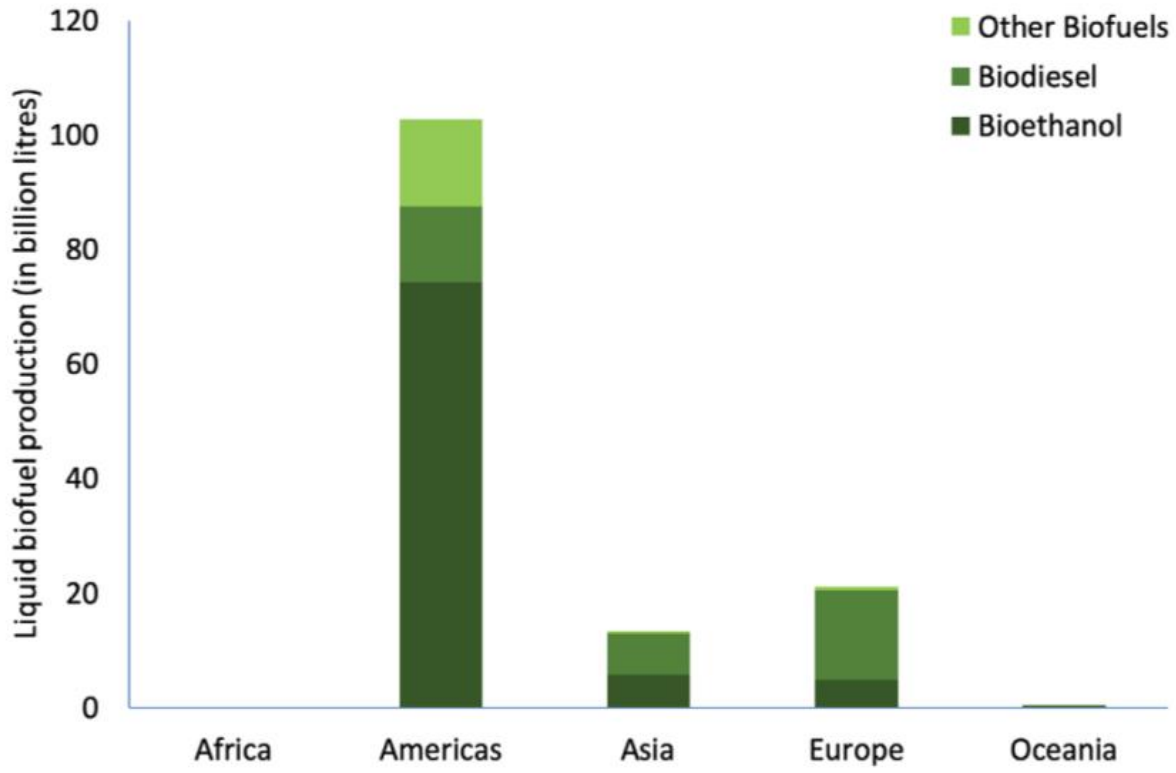

Figure 1-42: Liquid biofuels production per continent, in 2017. [33]

The amount of biodiesel in a fuel mix is usually identified with the B factor, where B100, B20, B5 and B2 refer to pure 100% biodiesel and a mix of 20, 5 and 2% biodiesel, respectively, with conventional petroleum diesel.

1.6.1.3 Biogas

Biogas is produced by anaerobic digestion or fermentation of biodegradable materials, such as manure, municipal waste, sewage, plants or energy crops. This closed system where the digestion process takes place is called an anaerobic digester or a biodigester. It is consisted mostly of methane and carbon dioxide, whose combustion results in energy production. Therefore biogas can be used as fuel, for the production of energy and heat. Industrial production of biogas includes production in landfills (landfill gas) and production in an anaerobic digester. Europe is the top continent in the production and use of biogas, as can be seen in Figure 1-43, with more than half of the world's supply in 2017.

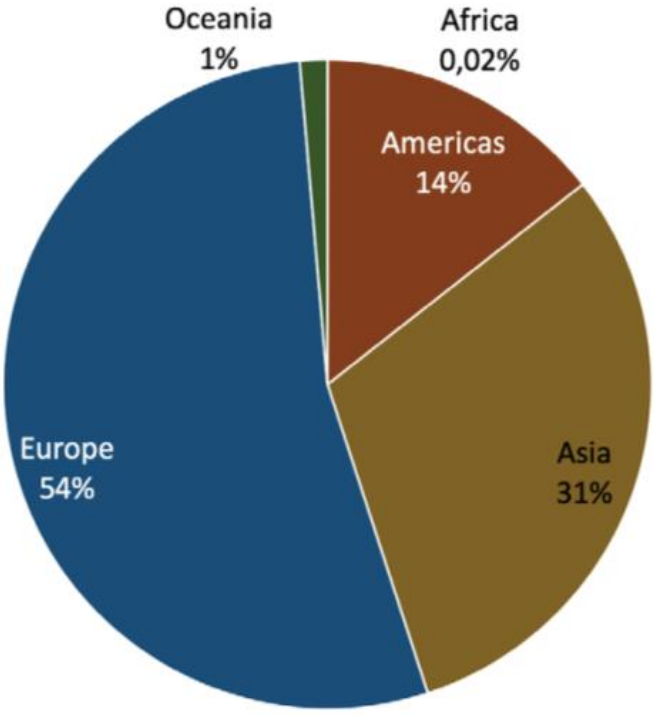

Figure 1-43: Biogas domestic supply per continent for 2017. [33]

Bioenergy is a growing industry in renewable energy production. The disadvantages are pretty much the same ones that concern most renewable resources, like low density and initial high cost. Biofuels also contribute to air pollution as their combustion releases pollutants, such as carbon monoxide and dioxide and particulate matter. The advantage in the case of bioenergy is the ability of transport and storage that is provided from the use of biofuels. The use of bioenergy for energy production will keep on growing and will remain the main resource for domestic use in developing countries.

2 Introduction and Overview of Renewable Energy Resources (2/2)

Author(s): Dr Efterpi Nikitidou
Dr Andreas Kazantzidis

2.1 Geothermal Energy

Geothermal energy is the heat derived from the subsurface of the Earth. This thermal energy of the Earth's crust comes from the formation of the planet and from the radioactive decay of matter. Due to the extremely high temperatures at the boundary between the Earth's core and mantle (Figure 2-1), there is melting of the rock and material from the mantle moves upward into the crust. This happens mainly along the edges of Earth's tectonic plates where volcanoes are formed (Figure 2-2). The rocks and the water that seeps into the cracks in the subsurface have very high temperatures, which increase with depth. This results in the formation of hot springs, geysers, fumaroles and mud pots. These formations are depicted in Figure 2-3 to Figure 2-6.

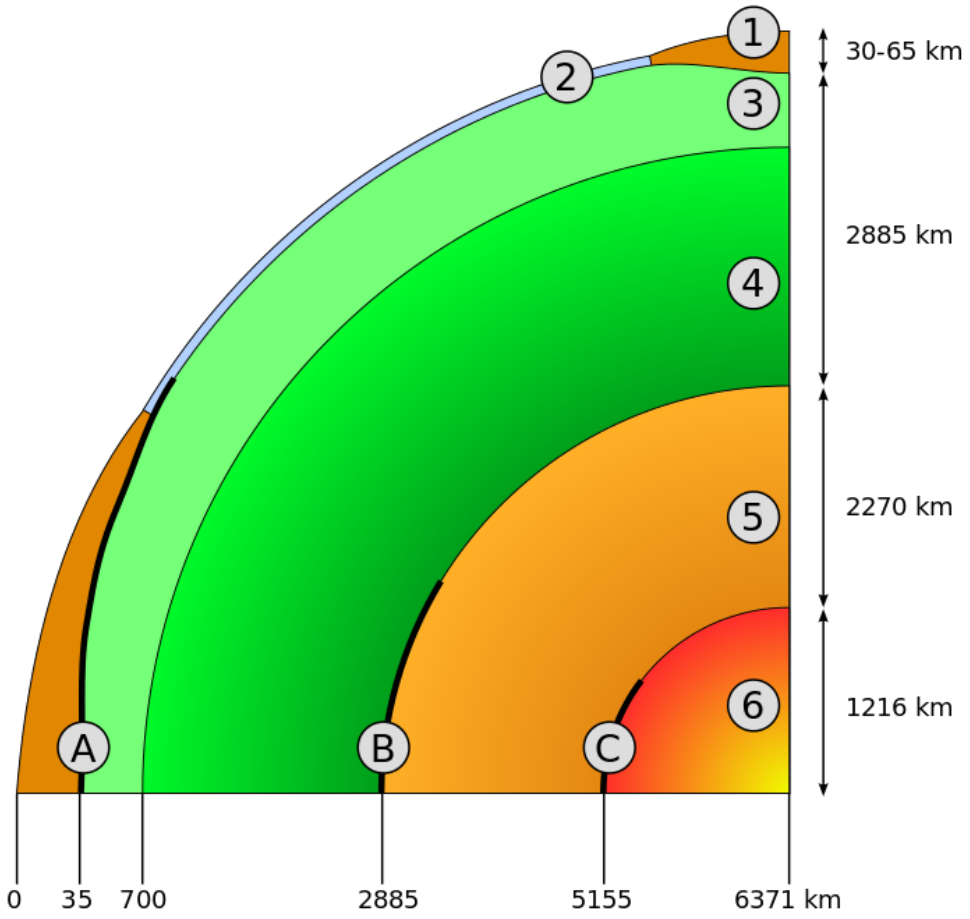

Figure 2-1: Earth's inner structure. (1.continental crust, 2.oceanic crust, 3.upper mantle, 4.lower mantle, 5.outer core, 6.inner core, A.crust-mantle boundary, B.core-mantle boundary, C.inner-outer core boundary). [38] Licensed under CC BY-SA 2.5

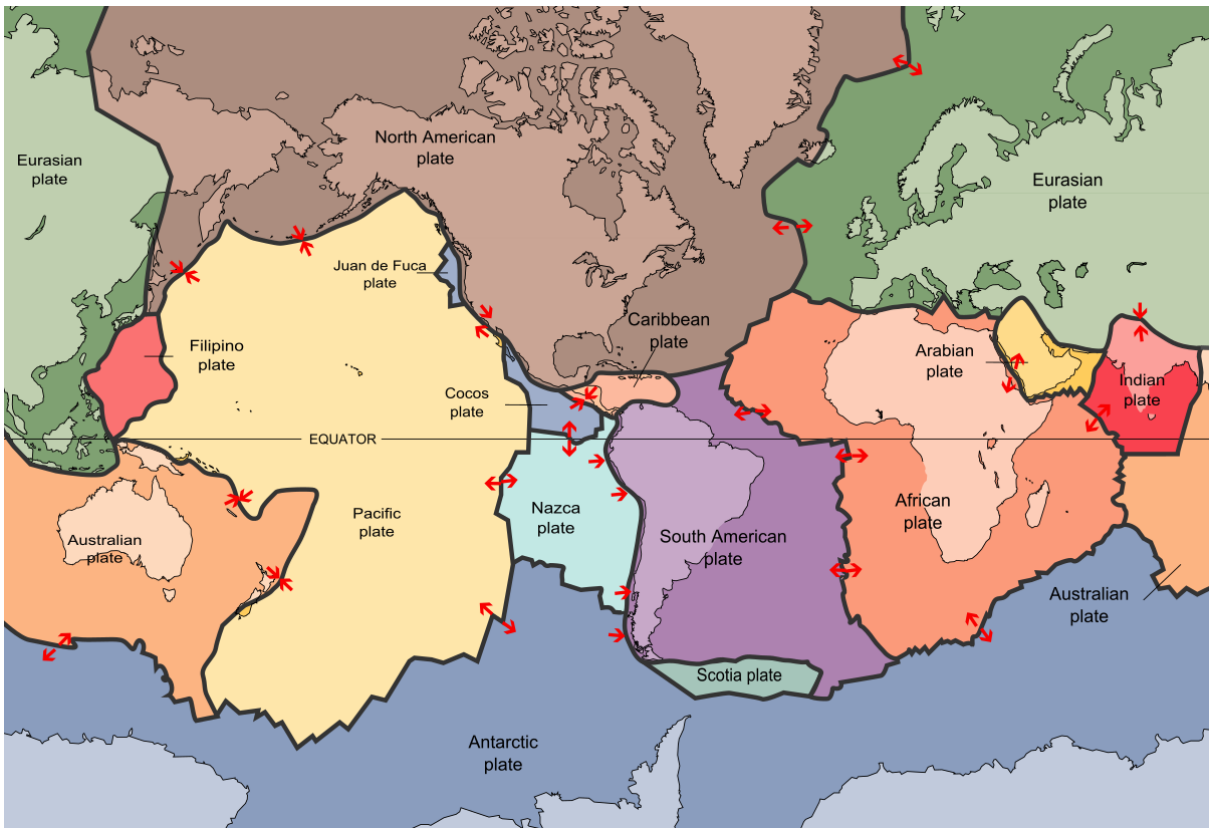

Figure 2-2: Earth's largest tectonic plates. [39] License: Public Domain

The increase in temperature with depth is around 25-30 °C/km. This is the average value worldwide, away from the boundaries of tectonic plates. The mean heat flow to the Earth's surface is around 60-65 mW/m^2 but it can reach much higher values in the regions of geothermal reservoirs. The majority of Earth's geothermal resources are around the boundaries between tectonic plates. Such areas include the so-called Ring of Fire around the Pacific Ocean, Hawaii, Yellowstone National Park in the USA etc. In Europe geothermal resources are found, for example, in Iceland, Italy and Turkey.

People have used hot springs and thermal pools since pre-historic times, for bathing and washing and healing purposes. Space heating with geothermal energy, started in Roman times and nowadays geothermal power is also being used for the production of electricity. Geothermal energy is not available everywhere in the world and is limited in locations near the boundaries of tectonic plates. Only a small portion of the world's geothermal resources is being exploited, as those that are deeper into the Earth's crust are more difficult and more expensive to be reached and used.

Figure 2-3: The Strokkur geyser in Iceland. [40] Licensed under CC BY-SA 3.0

Figure 2-4: The Grand Prismatic Spring, a hot spring in Yellowstone National Park, USA. [41] Licensed under CC BY-SA 3.0

Figure 2-5: Mud pots at Hverarönd in Iceland. [42] Licensed under CC BY 3.0

Figure 2-6: A fumarole at Námafjall, Iceland. [43] Licensed under CC BY 3.0

A geothermal reservoir has a heat content that depends on pressure, temperature and volume. A reservoir can be of high, medium or low temperature, where the temperature of water and steam is higher than 150 °C, between 100 and 150 °C and lower than 100 °C, respectively. In the last category there is basically no steam, just hot water. Reservoirs with lower temperature, which are at low depths, are used for space heating, greenhouses, spas etc., whereas reservoirs of high temperatures that are accessible with drilling are used for electricity generation in power plants. Systems like geothermal heat pumps or enhanced geothermal systems are used to extract heat from the subsurface reservoirs.

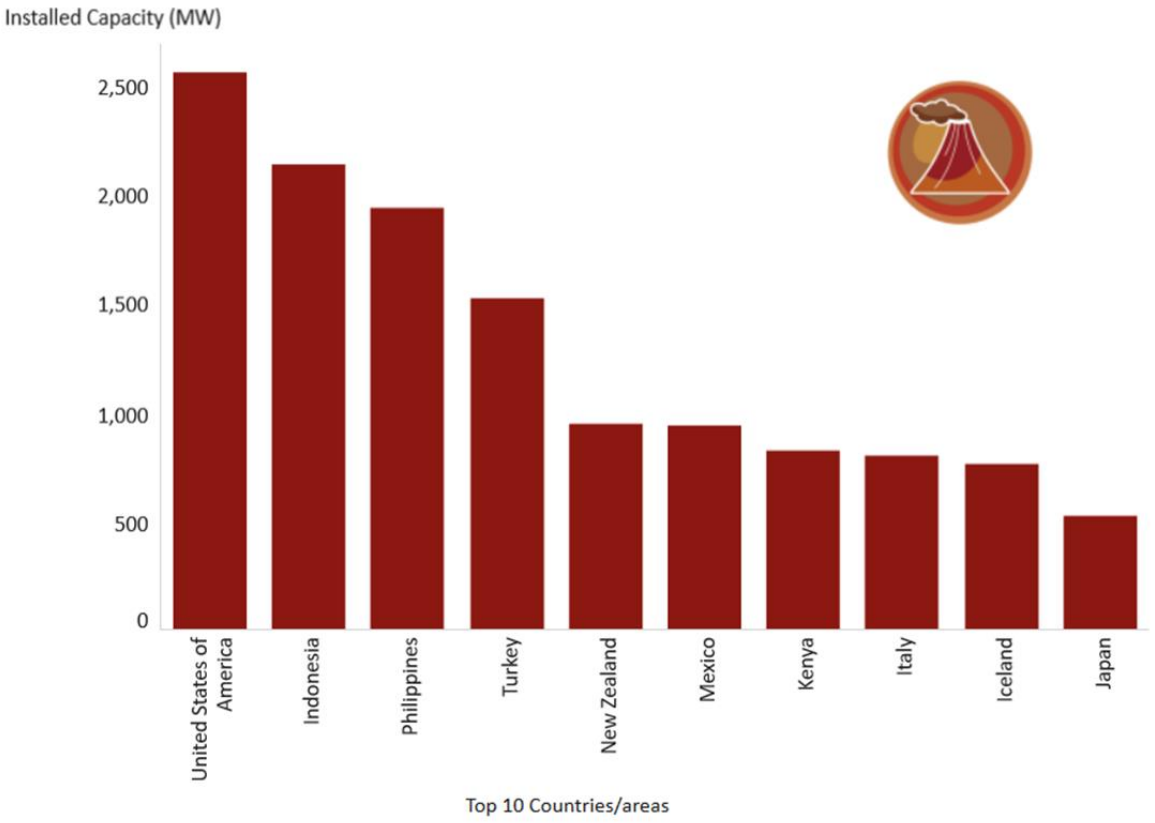

Figure 2-7: Installed capacity for geothermal energy, for the top 10 countries, in 2019. [15]

Figure 2-7 shows the installed capacity of geothermal energy in MW, for the top 10 countries in the world in 2019. USA, Indonesia and Philippines are the top three, located in the Ring of Fire, while the rest are countries well known for their geothermal reservoirs.

2.1.1 Geothermal Resources

Figure 2-8 shows the schematic of an ideal geothermal system.

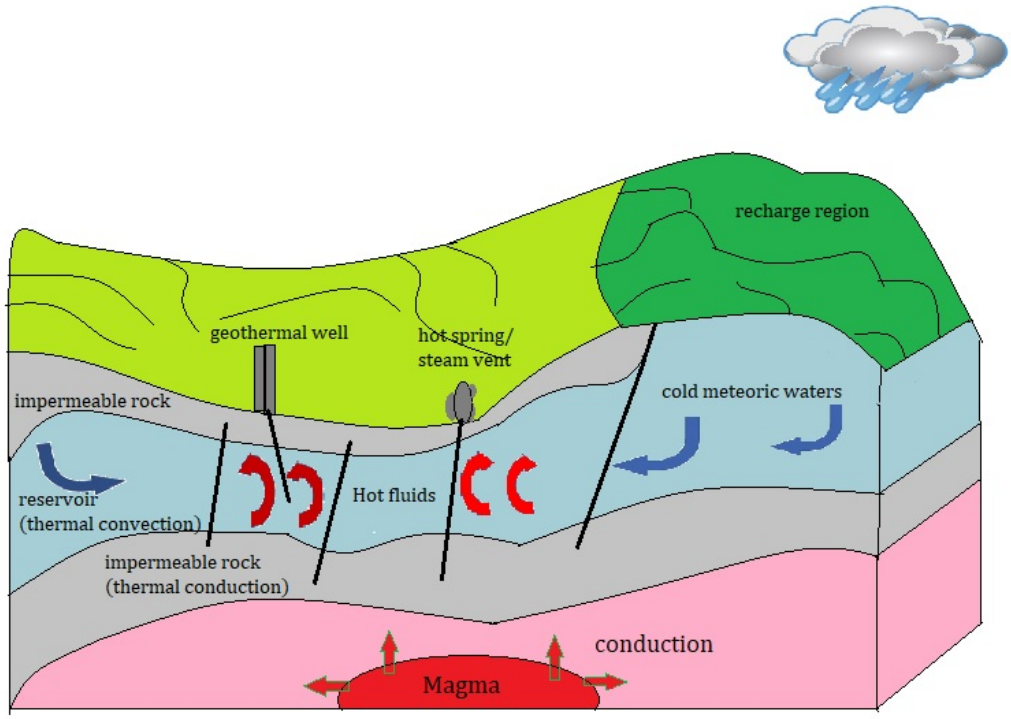

Figure 2-8: Schematic of a geothermal system. [44]

The most common geothermal reservoirs are liquid-dominated geothermal systems, where water can have temperatures higher than 200 °C. In vapor-dominated systems water boils to form steam which can have temperatures up to 300 °C. Both liquid-dominated and vapor-dominated systems are considered as hydrothermal convection systems. These systems permit fluid convection and the reservoirs have fractures to allow for recharge. Hydrothermal convection systems can be associated with hot springs and geysers.

Other geothermal resources are the hot igneous resources, which include hot dry rock and geologic magma systems and the conduction-dominated resources, which include sedimentary basin, geopressured and radiogenic resources.

Sedimentary basins have high heat flow and fracture is required, however exploitation of such a resource would require deep drilling. Geopressured resources are located in deep basins in which fluids within permeable sedimentary rocks are heated due to their high depth. Radiogenic resources are located in sites where there is an intrusion of granite near the

surface and there is heating of groundwater due to the decay of radioactive uranium, potassium and thorium.

Hot dry rock resources are systems with high temperatures up to 350 °C, where heat is stored in rocks that are deep in the ground and energy extraction is not possible through natural water or steam flow. For these systems, enhanced geothermal systems (EGS) are used for the extraction of energy. Finally, the magma resources reach even higher temperatures up to 1400°C and experimental systems are designed to extract heat from molten rock.

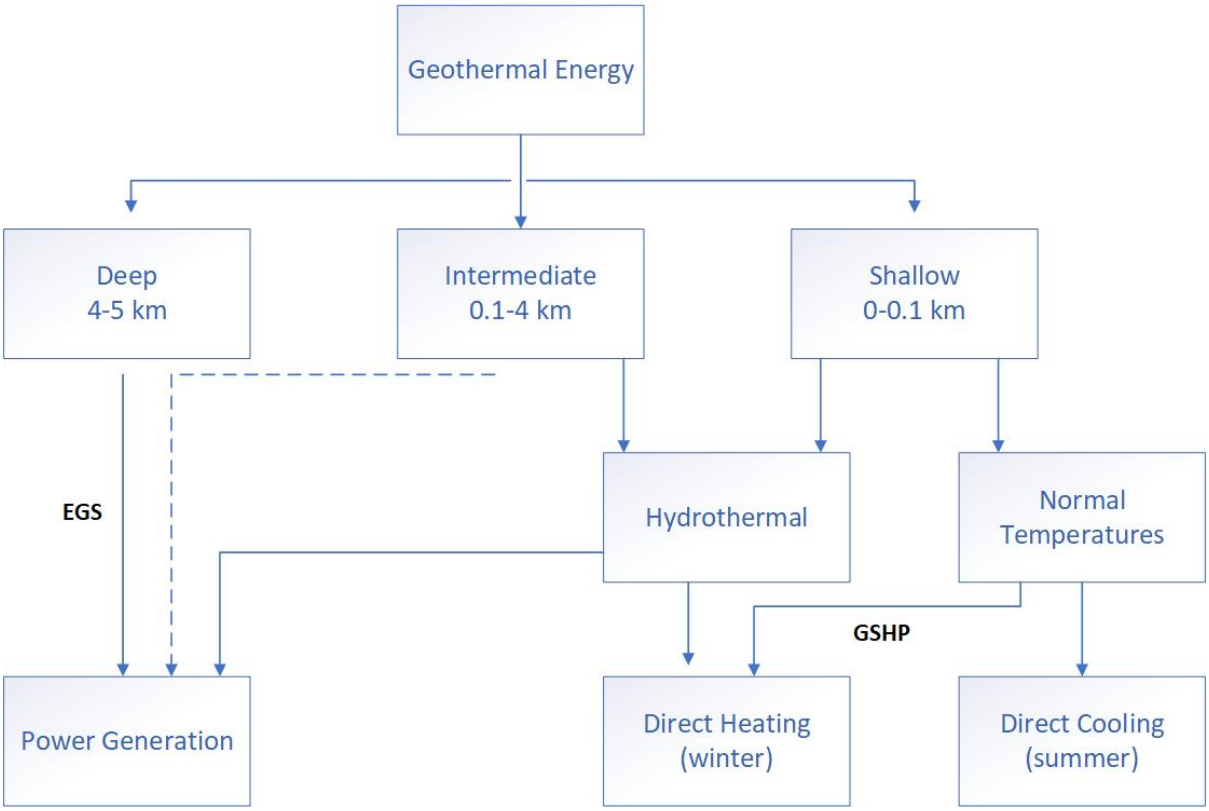

Figure 2-9: Forms of geothermal energy and utilization depending on depth. [45]

Figure 2-9 presents a simplified look at geothermal energy forms and their utilization, depending on their depth. Shallow or intermediate hydrothermal resources can be used for direct heating or power generation, whereas shallow resources found at normal temperatures can be used for direct heating and cooling with the use of geothermal heat pumps. Deep geothermal resources are used for power generation with the use of EGS

systems. The dashed line in Figure 2-9, refers to intermediate resources found at normal temperatures, which can in the future be used for power production.

2.1.2 Enhanced Geothermal Systems

An enhanced geothermal system generates electricity using geothermal resources in hot dry rock, with various stimulation methods, like hydraulic stimulation.

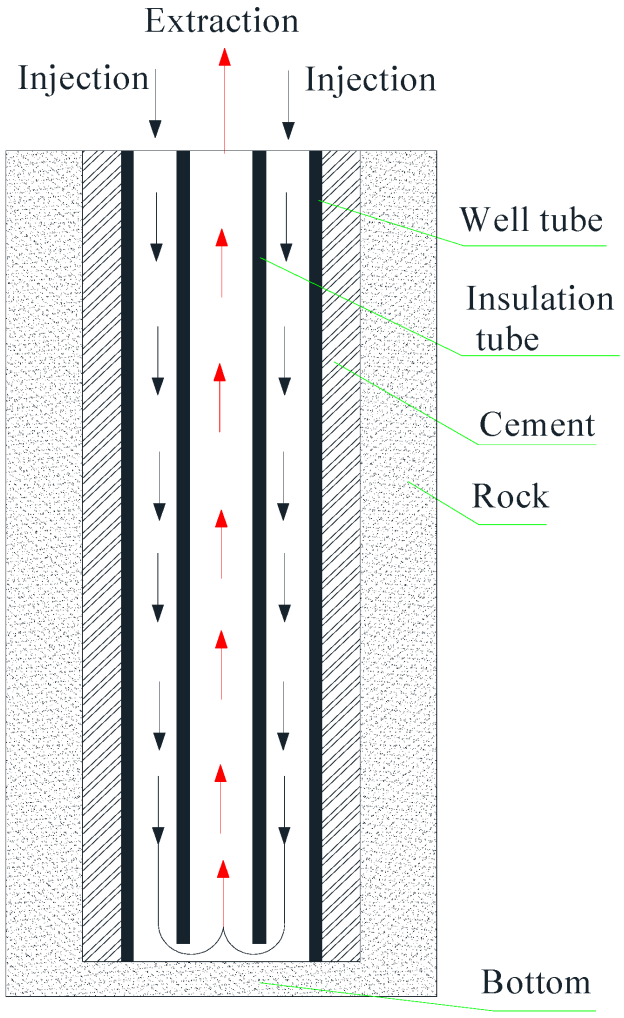

Figure 2-10: Schematic of an Enhanced Geothermal System. [46] Licensed under CC BY 4.0

The permeability of a rock layer can be enhanced by using high-pressure cold water, which is pumped down an injection well in the rock (Figure 2-10). The fluid pressure increases and the system's permeability is enhanced. A second borehole is made for the water, heated in the

rock, to be forced out. The heat from the water can then be converted to electricity in a steam turbine or power plant. The main constrain is to design the system in such a way, that high production rates are met without too rapid cooling of the reservoir, which would result in the reduction of its lifetime. Careful planning is also needed to reduce the risks of induced seismicity, which is inevitable in the application of such systems. There are no commercial systems of EGS technology, but several are designed for testing.

2.1.3 Geothermal Heat Pumps

A geothermal heat pump (GHP), also known as a ground source heat pump (GSHP) is a central heating/cooling system that operates by transferring heat from the ground, for space heating or to the ground, for space cooling. A circulating fluid is transferred through pipes, which are built in boreholes or trenches and a pump extracts heat at the surface for heating the space. The cool circulated fluid is injected back into the ground to absorb heat and complete the circle. In order to cool a space, the operation is reversed and heat is transferred out of the building and to the ground via the pump and the circulating fluid. The system can be a closed or an open-loop system, where wells are used as the heat exchange fluid (Figure 2-11).

GHP systems use around 25-50% less electricity when compared to conventional heating and cooling systems. They can be used essentially anywhere in the world so every country can use the heat of the earth for space cooling and heating. There are over a million such systems in operation in the USA and their number is increasing in Europe as well, with Germany being the lead market.

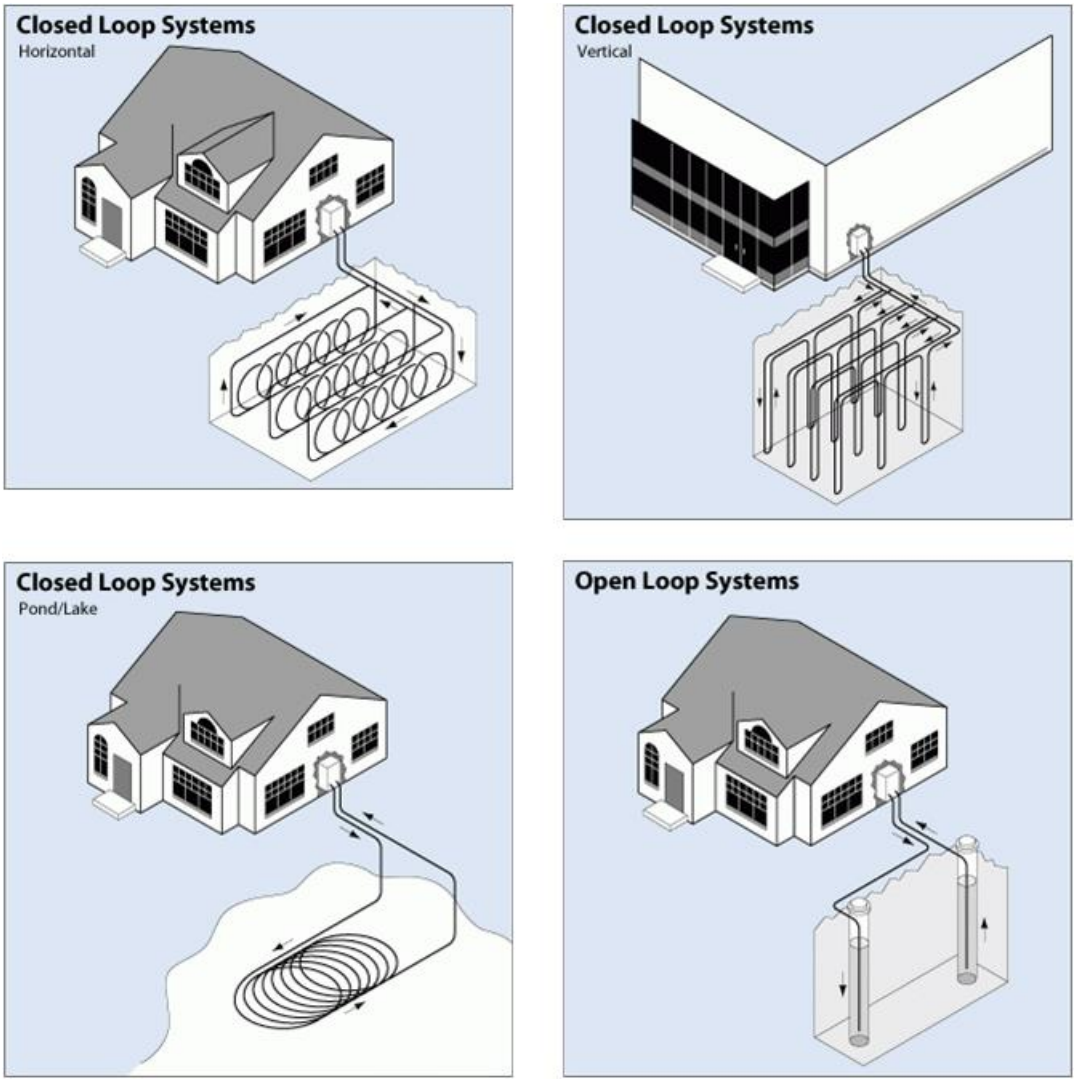

Figure 2-11: Examples of various types of geothermal heat pumps. [47] License: Public Domain

2.1.4 Direct use

Direct uses of geothermal energy include space heating and cooling, greenhouses, fish farming, bathing, swimming and health spas. Spas and bathing mainly use the heat from hot springs, so no pumps are required for their operation. Other direct use systems apply pumps to transfer hot water from the reservoir to the surface.

The top five countries with the largest direct use installed capacity (including geothermal heat pumps) are China, USA, Sweden, Germany and Turkey, at around 40.6, 20.7, 6.7, 4.8 and 3.5 MWt (megawatt thermal), respectively, while when considering the data in terms of

population, Iceland comes in first place, where most homes are heated with geothermal hot water [48].

Figure 2-12 shows the increase in direct use geothermal energy, worldwide, from 1995 until 2020, per category of use. Geothermal heat pumps have the highest use worldwide and have shown an incredible increase during the last years, followed by bathing and swimming.

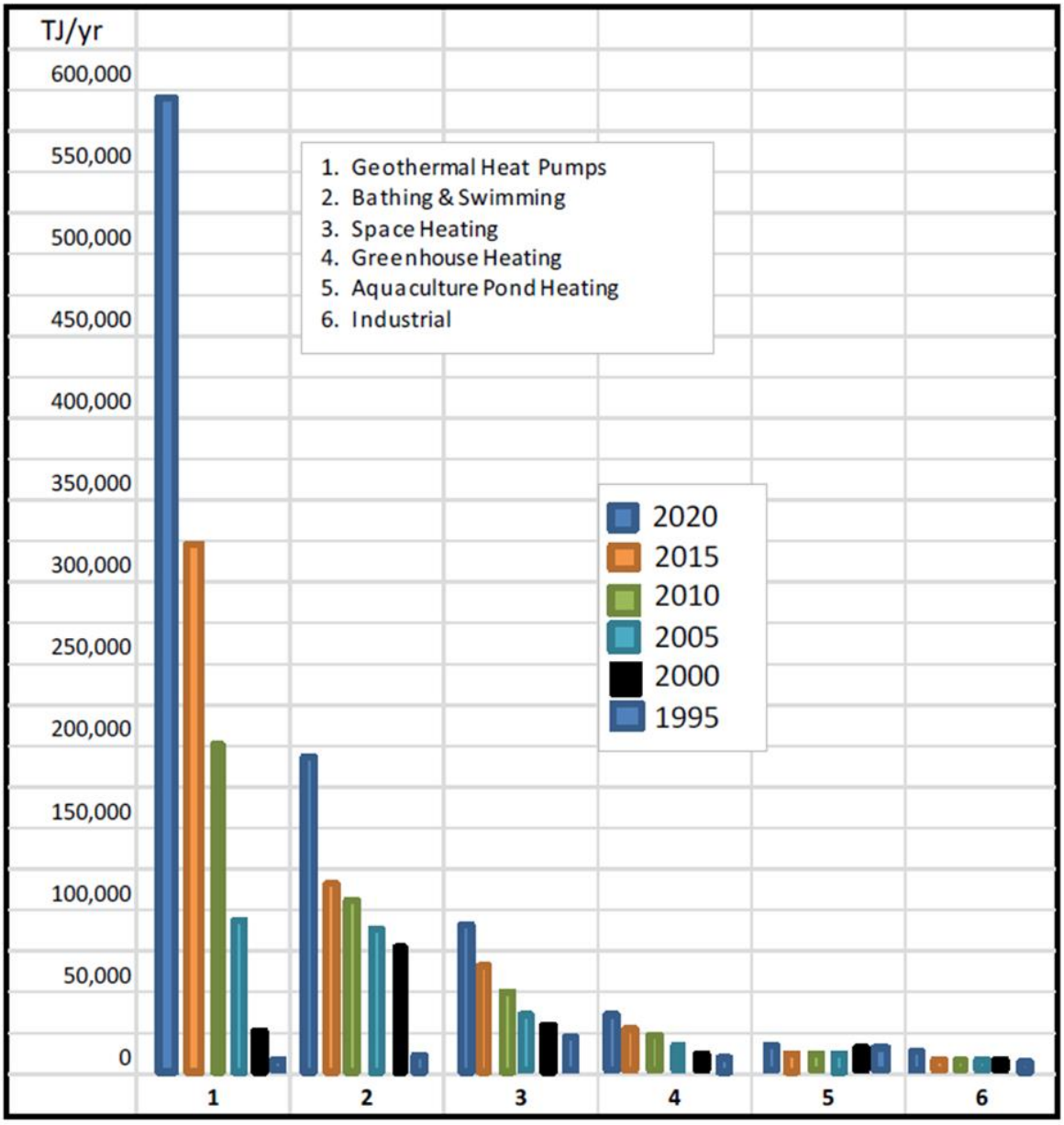

Figure 2-12: Worldwide direct use of geothermal energy (TJ/year) from 1995 to 2020 per category. [48]

Direct use of geothermal energy takes advantage of both high and low temperature geothermal resources, thus it is more common and widespread worldwide, compared to

electricity generation installations. Direct use can only be applied though to the site near the reservoir, since hot water and steam can't be transported much further away.

2.1.4.1 District Heating

District heating is a system for heat distribution for residential and commercial purposes, like space and water heating. District heating can be achieved with direct use of geothermal energy, which has been utilized in many countries worldwide. The first geothermal district heating system in the USA was created in 1892, in Boise, Idaho. Turkey uses 493 MWt for district heating. The largest district heating utility is in Reykjavik, Iceland, where geothermal energy is used from several low and high temperature reservoirs, inside and near the city. A total of 780 MWt geothermal power is utilized to heat the whole city and five communities nearby.

2.1.5 Electricity generation

Electricity can be generated from geothermal energy with the use of dry steam, flash steam and binary cycle power stations. For electricity production, medium and high temperature geothermal reservoirs are required. In 2015, total geothermal power capacity in the world was 12.8 GW, most of which was from installations in the USA.

2.1.5.1 Dry steam

Dry steam power stations are the oldest and simplest type for electricity production from geothermal power.

In dry steam power stations, steam from a geothermal reservoir, of a temperature of at least 150 °C, is used, which is routed through a turbine/generator in order to generate electricity (Figure 2-13Figure 2-13). After that the steam is lead to a condenser where it turns liquid and cools down. It is then lead back into the deep well to be reheated and continue the circle.

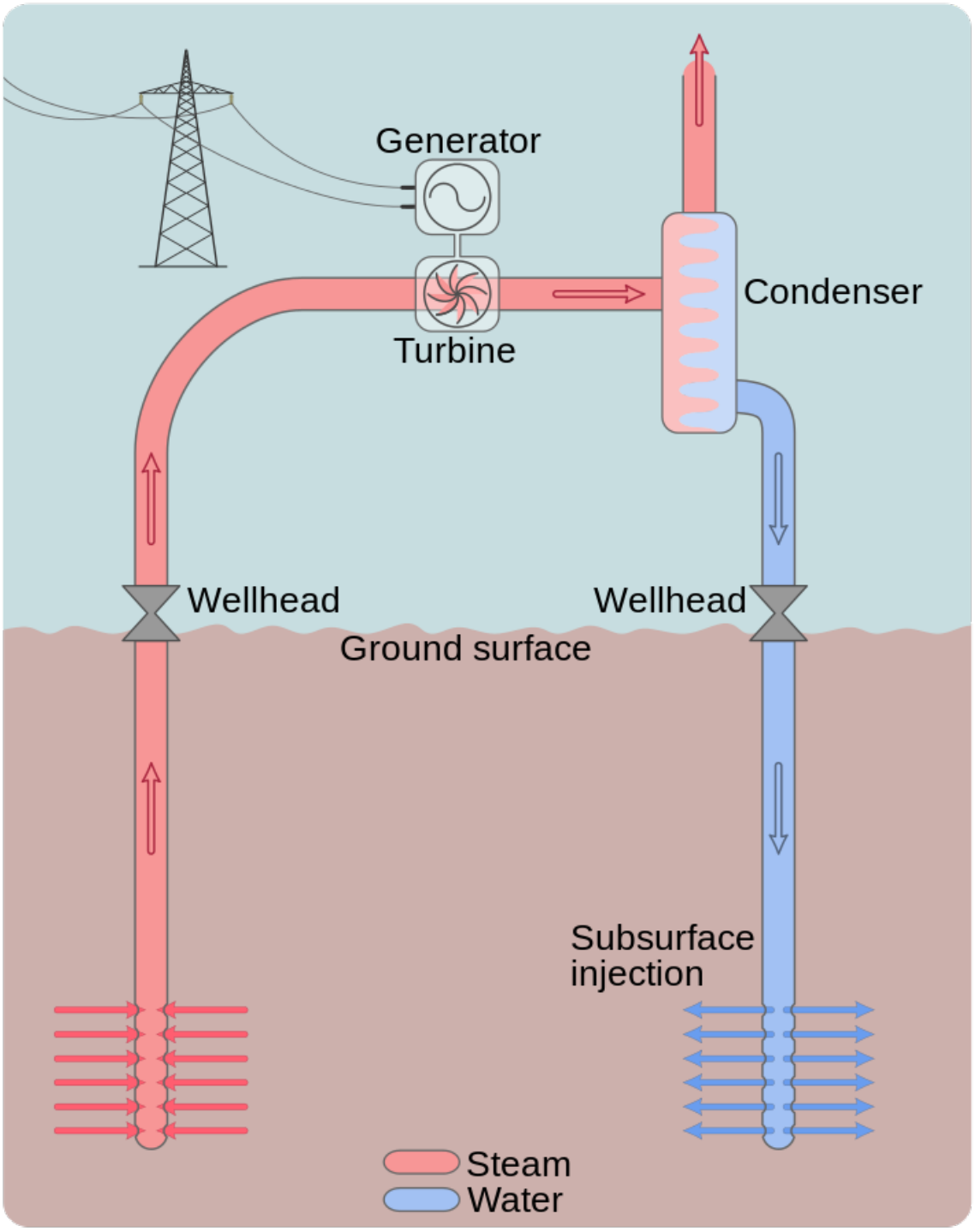

Figure 2-13: Schematic of a dry steam power station. [49] Licensed under CC BY-SA 4.0

The largest facility using dry steam power production is the Geysers in California, USA, a complex of 13 dry steam power plants with a net capacity of 725 MW, based on the facility's statistics for 2019.

2.1.5.2 Flash steam

Flash steam power plants are the most common used today. They use water from high temperature geothermal reservoirs, which has temperature of at least 180 °C. The high-pressure water enters a tank of lower pressure and the flashed steam that is formed is used to drive a turbine (Figure 2-14). The water that remains, that wasn't flashed into steam, and the water that is formed from the condensed steam, are pumped back into the ground.

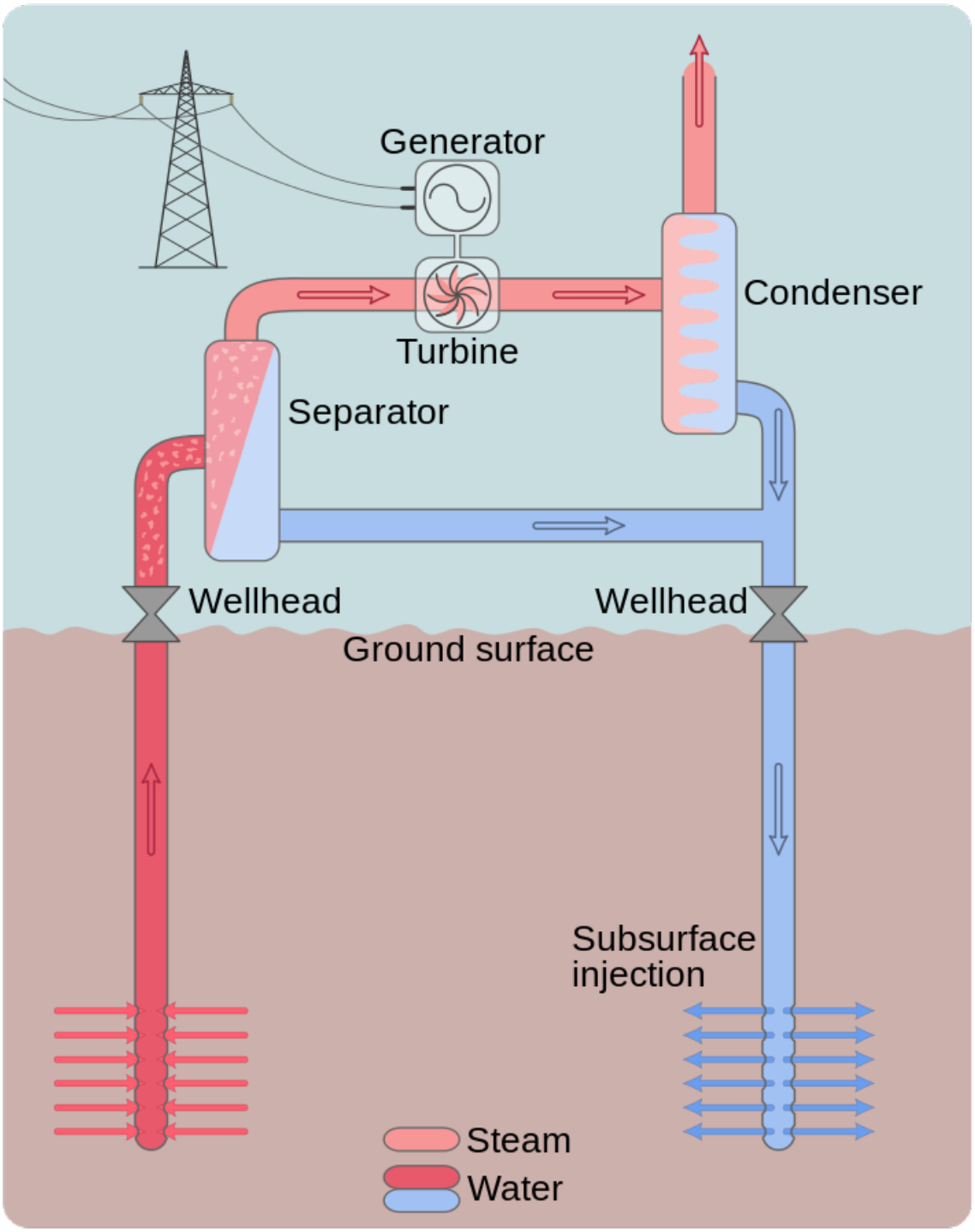

Figure 2-14: Schematic of a flash steam power station. [50] Licensed under CC BY-SA 4.0

An example of flash steam power station is the CalEnergy Navy I power plant at the Coso geothermal field in California, USA, which can produce as much as 270 MW of electricity. The Wairakei power station in New Zealand consists of a flash steam power plant of 140 MW, which was followed by a binary cycle power station to increase the total output to 181 MW.

2.1.5.3 Binary cycle

Binary cycle power stations are the newest that are being constructed. In this type of power stations, the fluid from the reservoir doesn't directly drive the turbine, like in the previous two types. In this type, water from the geothermal reservoir is used to heat a second working fluid, which in turn is vaporized and used to drive the turbine (Figure 2-15). The second working fluid has a boiling point lower than water, so with this type, lower temperature geothermal reservoirs can be exploited to generate electricity.

An example of binary cycle power stations is the McGinness Hills Geothermal Complex, in Nevada, USA, with 3 binary cycle plants and a total capacity of 138 MW.

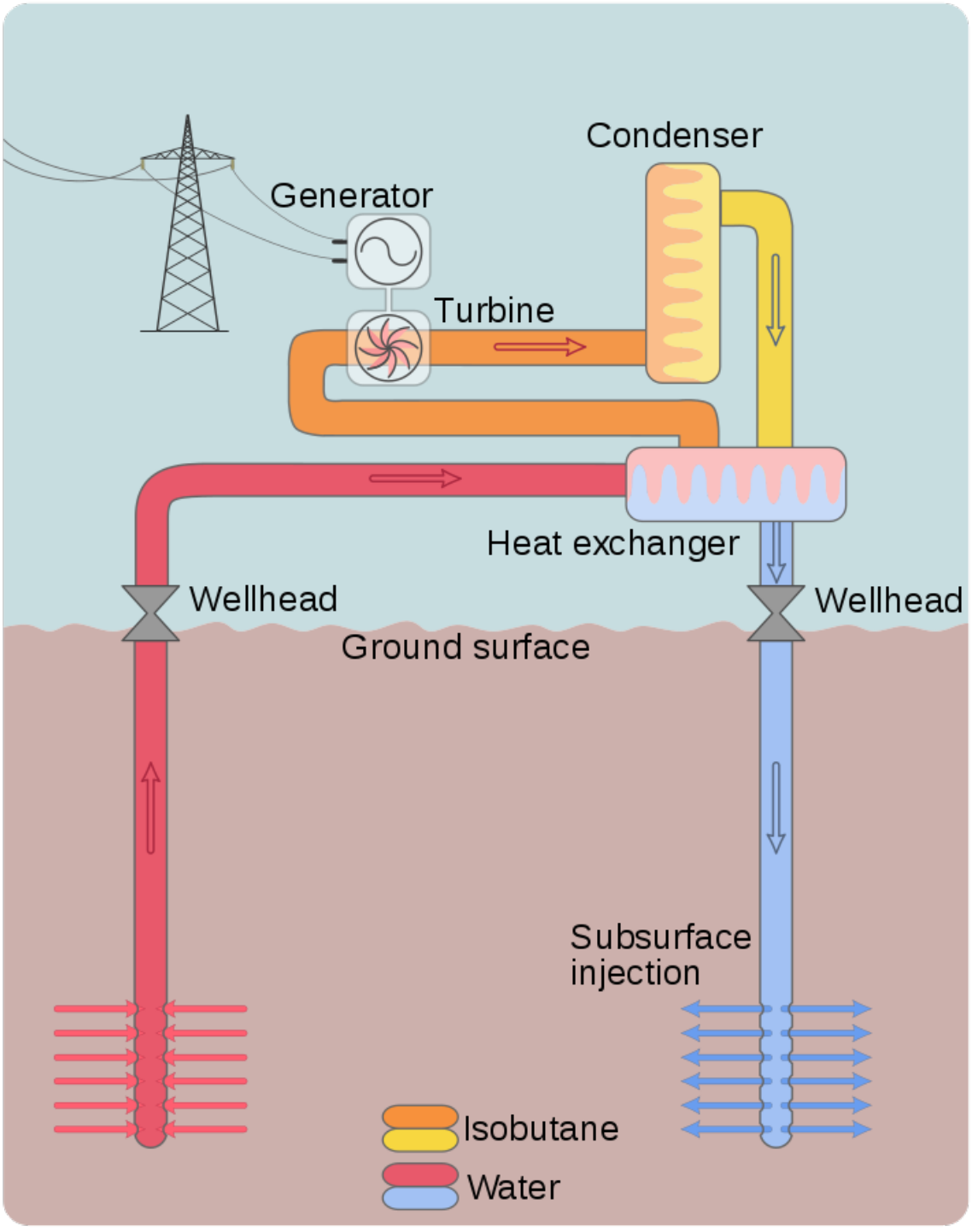

Figure 2-15: Schematic of a binary cycle power station. [51] Licensed under CC BY-SA 4.0

Geothermal energy is considered a renewable resource, because the amount that is being exploited is very small, compared to Earth's total thermal content. However, if not careful, uncontrolled exploitation of a local resource could lead to its depletion.

The exploitation of geothermal resources releases a mixture of gases, as fluids from deep in the ground are drawn in the surface. Some of these gases contribute to global warming, although the emissions are much lower than those from the combustion of fossil fuels. Apart from gases, there may be toxic elements in the hot water of geothermal sources, like mercury or arsenic, which if released into the environment can cause serious damage. However, most of geothermal energy installations have a mechanism to return the working fluids back to the ground, which minimizes the risks of environmental contamination and also the risks of the source depletion. Another important aspect that needs serious consideration is the effects on land stability. There are cases where a subsidence or an uplift of the ground has been observed in the area of a geothermal power plant and of course there is the risk of triggering earthquakes due to the deep drilling of enhanced geothermal systems.

2.2 Hydropower

Hydropower is power derived from the energy of moving water. It has been used since ancient times, as for example watermills which have been used for irrigation and the operation of mechanical devices. Many watermills are still in use for grinding grain in remote areas of the world, like the Himalayas or other elevated regions in developing countries. In the late 1800s water behind a dam was first used for the production of electricity. The first hydroelectric power plant was constructed in 1879, in the Niagara Falls, USA.

Water has potential energy due to height difference, as is the case in water stored in dams. This potential energy (PE) is calculated from Equation 1-1,

$$PE = F * d = m * g * H, \qquad J$$ *Equation 2-1*

where F is the force due to gravity, d is distance, m is the mass of water, g is the acceleration of gravity g=10 m/s^2 and H is the height. Since the mass of water is equal to its density ρ=1000 kg/m^3 times the volume V, the potential energy is given from Equation 2-2.

$$PE = 10000 * V * H, \qquad J$$ *Equation 2-2*

As the water falls from height H, its potential energy is converted to kinetic energy and the velocity of water is calculated from Equation 2-3.

$$KE = PE$$
$$0.5 * m * v^2 = m * g * H$$
$$v = (2 * g * H)^{0.5}, \text{ m/s}$$ *Equation 2-3*

By dividing energy with time, the power P is calculated, while volume divided with time gives the water flow Q. So the power, when taking into account the efficiency ε of the turbine as well, is given by Equation 2-4.

$$P = 10000 * \varepsilon * Q * H = 10 * \varepsilon * Q * H, \qquad kW$$ *Equation 2-4*

The structure of a hydropower installation requires extensive records of the water flow for its successful operation. The flow of water in a stream, for example, can have significant seasonal variations, while dams and reservoirs are more stable sources.

2.2.1 Hydropower resources

Hydropower relies on the water cycle, which in turn is caused by solar energy, as it heats water on the surface of oceans, lakes and rivers and lead to its evaporation. The vapors then condense in the atmosphere and return to the surface as precipitation (rain and snow) to close the cycle. This flow of water which is collected back to rivers and streams is the source for hydropower production.

In 2018, worldwide electricity production from hydropower, without taking into account pumped storage, reached 4150 TWh, according to Figure 2-16, while Figure 2-17 shows the contribution of hydropower in the electricity production of 2017, compared to the other renewable resources. Hydropower is the largest source of worldwide renewable electricity generation with a percentage of 65% in 2017.

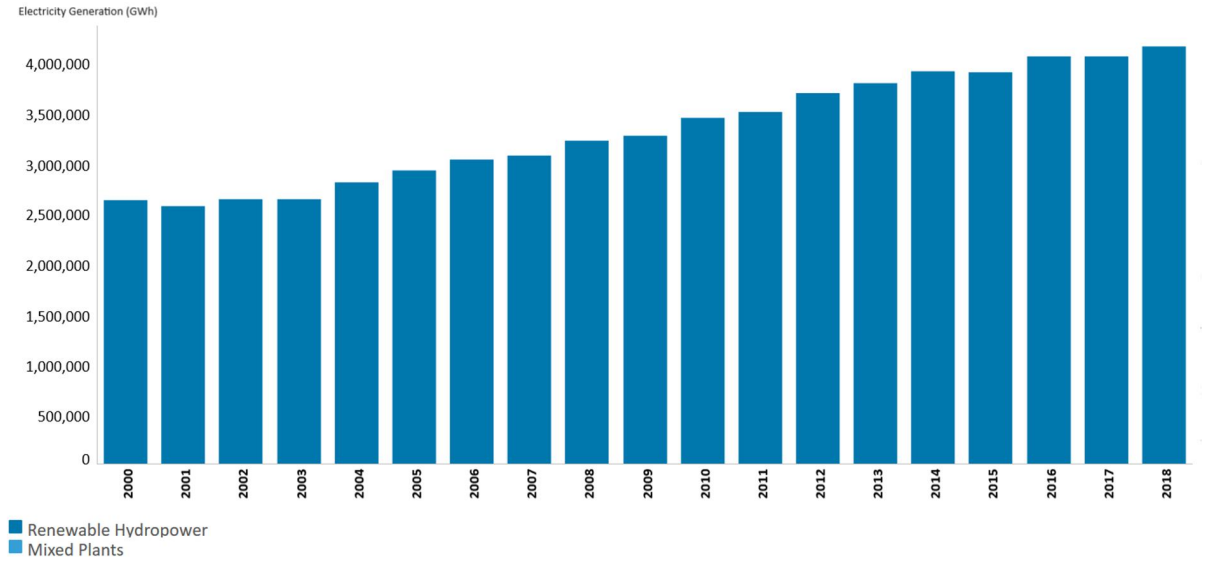

Figure 2-16: Total electricity generation (GWh) from hydropower, excluding pumped storage. [15]

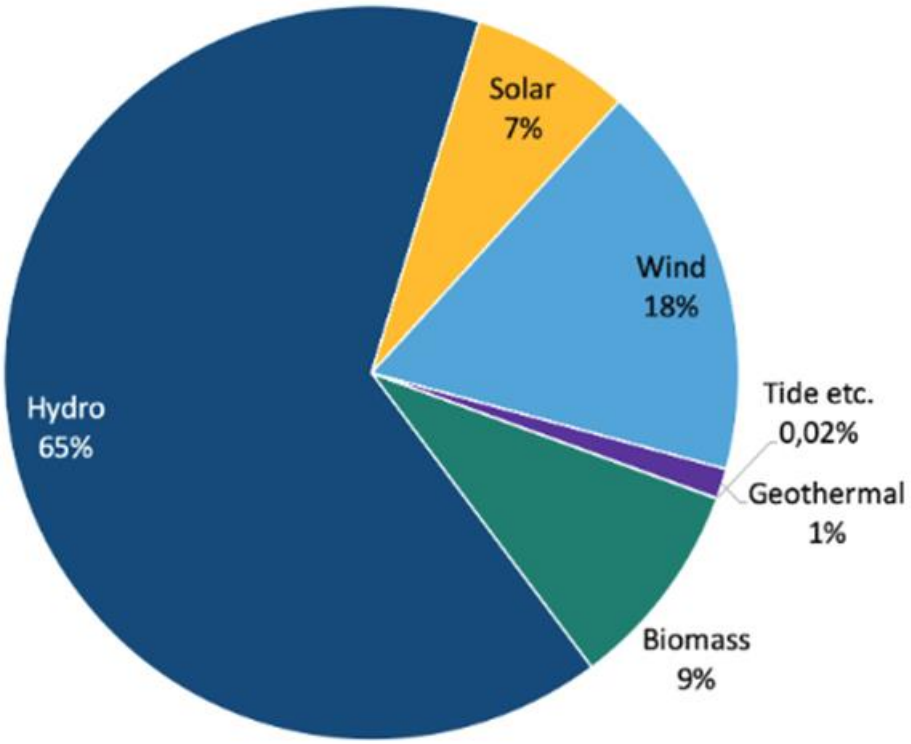

Figure 2-17: Electricity production from renewable resources for 2017. [33]

Hydropower can be used for the production of mechanical power, as in the case of water mills, where a water wheel or turbine is used for a mechanical process like grinding or

hammering etc. and trompes, which are water-powered air compressors. The main use of hydropower today is the generation of electricity, a process with a relative low cost, which makes hydropower very popular among other renewable forms of energy. Hydropower is site specific, meaning that it can't be available everywhere in the world.

2.2.2 Types of hydropower

Hydropower is usually classified according to the output amount of power, with large-scale hydropower installations, small, micro and pico.

Large-scale hydropower produces more than a few hundred megawatt power, with the largest plants in the world reaching a capacity of thousands of megawatts. China is the lead country in installed capacity and generated electricity, as can be seen in Figure 2-18, with Brazil, USA, Canada and Russia following. The largest hydropower plant is the Three Gorges Dam in China (Figure 2-19), with a 22.5 GW installed capacity, while the second largest hydro plant is the Itaipu Dam, on the border between Brazil and Paraguay, with a 14 GW capacity. The Xiluodu Dam in China and the Guri Dam in Venezuela are two other power plants with a capacity greater than 10 GW, at 13.8 and 10.2 GW, respectively.

Small hydropower is the definition used for installations producing up to 10 MW or 25-30 MW as is the upper limit in the USA and Canada. They can be connected to the electrical distribution network or they can operate alone in remote areas where there is no network connectivity.

Micro hydro describes hydropower installations with output lower than 100 kW, which can be used to power a home or a small community or even connect to the local network. There are many micro hydro installations in developing countries and usually they don't require dams or reservoirs.

Finally there are the pico hydro installations, with an output usually lower than 5 kW, which can be used to power a few devices in a small number of houses. Dams are not used, only pipes to divert some of the water flow.

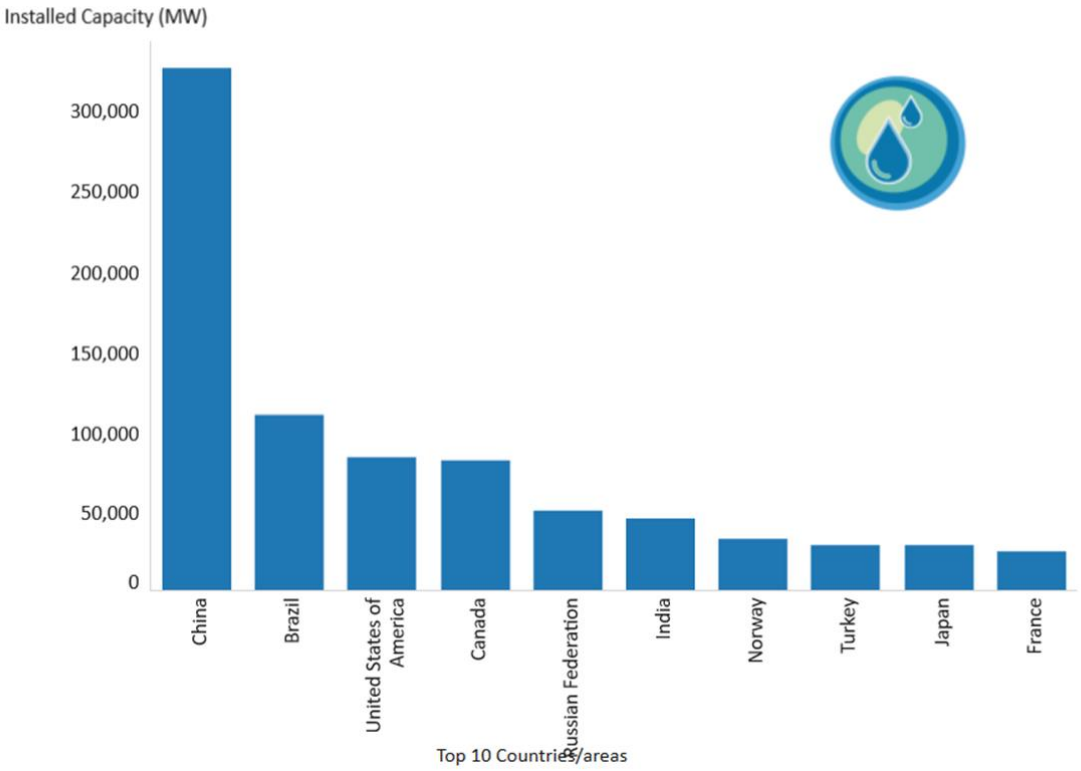

Figure 2-18: Installed capacity of hydropower (MW) exc. pumped storage, for the top 10 countries, for 2019. [15]

Figure 2-19: The Three Gorges Dam in China. [52] Licensed under CC BY 2.0

2.2.3 Hydroelectric stations

Hydropower facilities can be categorized into three types: impoundment (dam), diversion (run-of-the-river) and pumped storage.

2.2.3.1 Impoundment (dam)

An impoundment facility is the conventional dam hydropower plant (Figure 2-20). A dam is used to store the water from a river in a reservoir. The water is released from its elevated position to drive a turbine, which in turn activates a generator to produce electricity. The power that is produced depends on the volume of water and the head, which is the height difference between the water level of the reservoir and the tailwater level (downstream). The penstock is the pipe through which water is driven from the reservoir to the turbine. Water can be released in order to meet changes in electricity demands or to maintain a certain level in the reservoir.

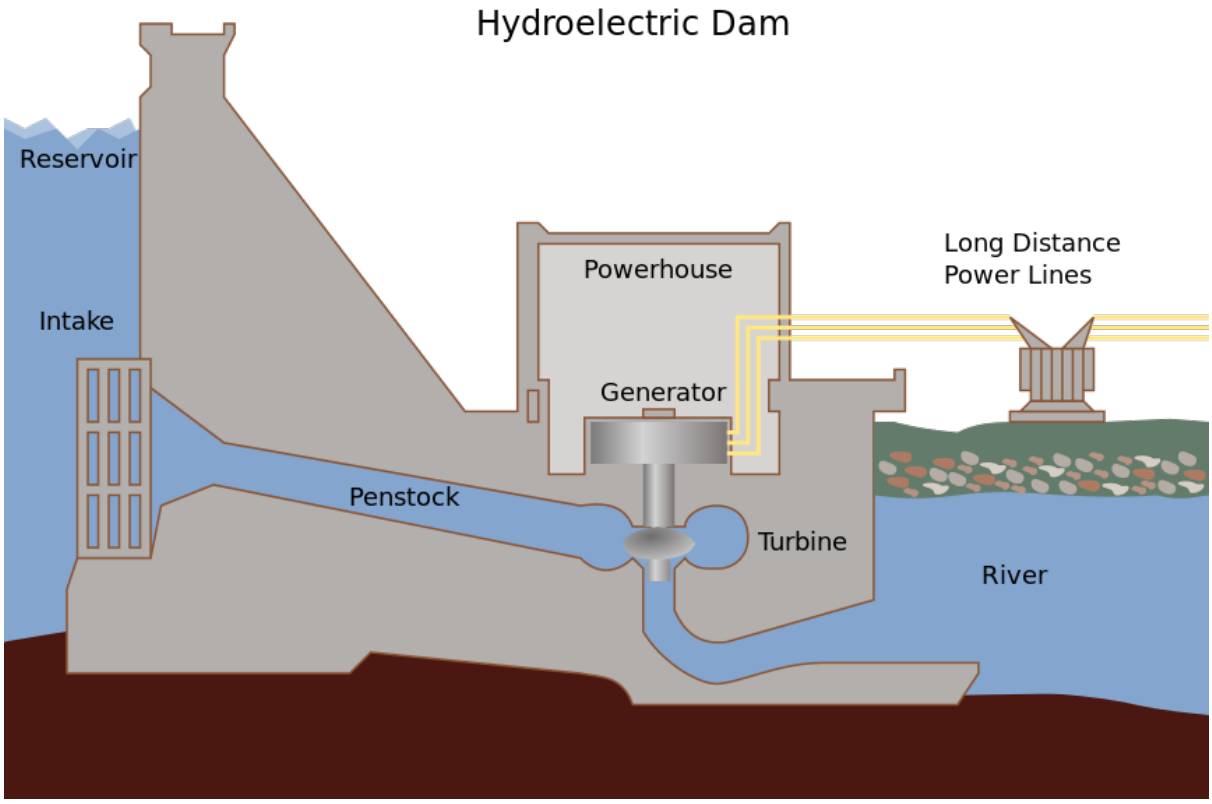

Figure 2-20: A conventional hydropower plant. [53] Licensed under CC BY-SA 3.0

One of the most famous impoundment facilities, although not among the largest in the world, is the Hoover Dam in the Nevada/Arizona border in the USA with a capacity of 2080 MW (Figure 2-21).

Figure 2-21: Hoover Dam in Nevada/Arizona, USA. [54] License: Public Domain

2.2.3.2 Pumped storage

In pumped storage facilities water is pumped uphill, from a low elevation to a higher elevation reservoir, so in that way energy is stored for later use. When there is electricity demand, water is released back to the lower reservoir to drive a turbine and produce electricity. Figure 2-22 shows the schematic of a pumped storage system, where red arrows indicate the route for pumping water and storing energy and blue arrows indicate the route for generating electricity. Pumped storage facilities have the role of a battery and they are the most important means of energy storage.

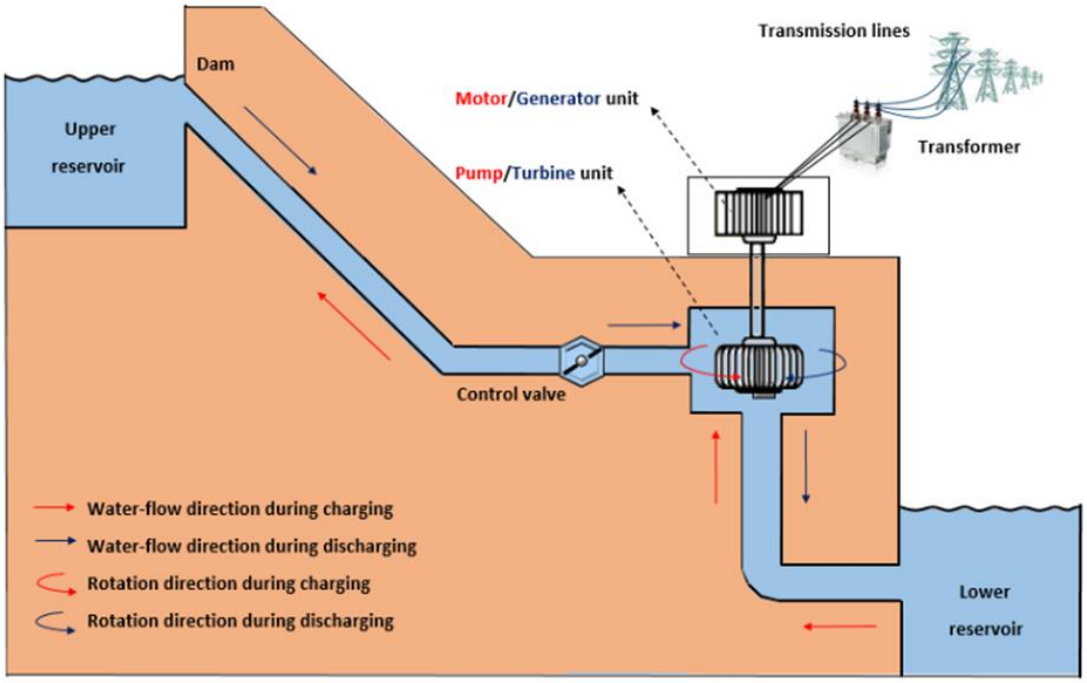

Figure 2-22: Pumped storage hydropower plant. [55] Licensed under CC BY 3.0

The largest pumped storage plants include the Bath County Pumped Storage Station, USA with a capacity of 3003 MW, the Guangdong and Huizhou Pumped Storage Power Stations in China, with capacities of 2400 MW each and the Okutataragi Pumped Storage Power Station in Japan, with a capacity of 1932 MW. Figure 2-23 shows the Castaic Pumped Storage Plant, in the USA, with a capacity of 1250 MW.

Figure 2-23: The Castaic Pumped Storage Plant, USA. [56] Licensed under CC BY-SA 3.0

2.2.3.3 Diversion (run-of-the-river)

Diversion facilities, also known as run-of-the-river hydroelectric stations, are facilities with no or small reservoir capacities. Water from a river is channelled through a canal or a penstock to drive a turbine (Figure 2-24). This facility has limited flexibility to follow peak variation in electricity demand, so it's mainly used for baseload capacity.

A run-of-the-river plant may have a small storage reservoir, in which case it's called a pondage, to meet daily energy demands. These plants divert some flow from the river (a part or most of it), which is lead through a pipe to the turbine, and it is then returned to the river downstream.

Figure 2-25 show the Chief Joseph Dam, a run-of-the-river plant in Washington, USA, with a capacity of 2620 MW.

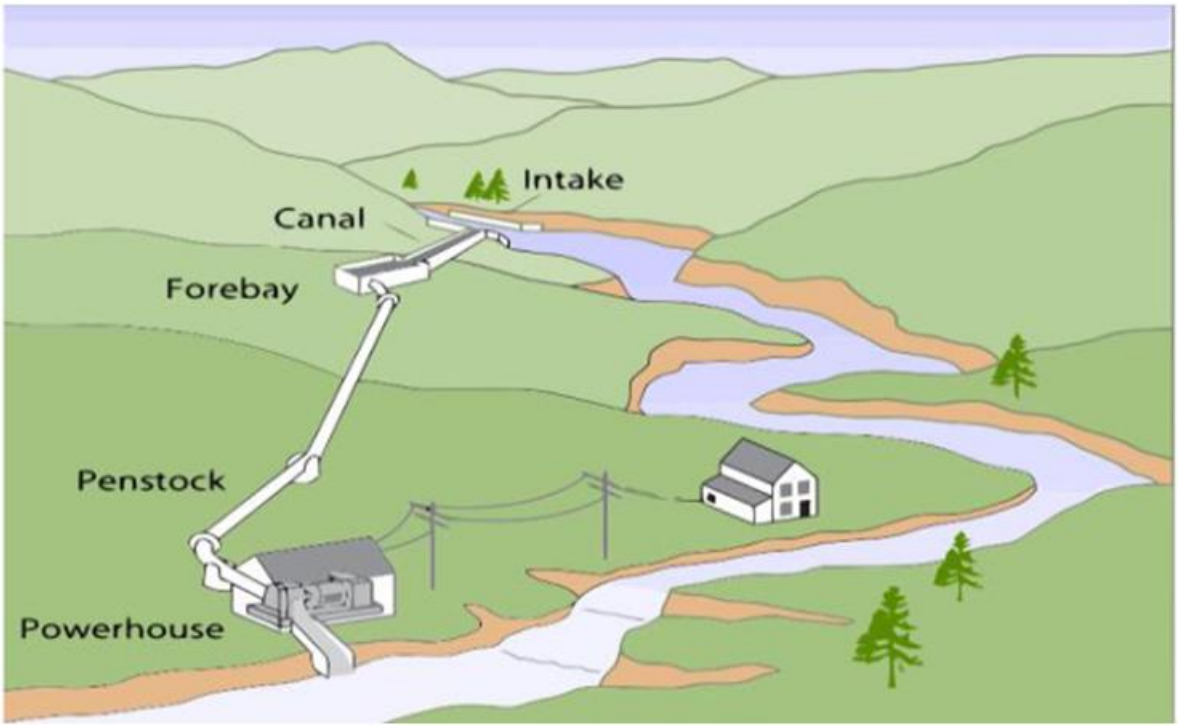

Figure 2-24: Run-of-the-river hydropower plant. [57] Licensed under CC BY 4.0

Figure 2-25: Chief Joseph Dam, a run-of-the-river plant in Washington, USA. [58] License: Public Domain

2.2.4 Water Turbines

The water turbines used in hydropower plants to convert the potential and kinetic energy of water to electricity, are of two main types, impulse and reaction turbines. The type that is selected for each power plant depends mostly on the head and the water flow, while the cost and efficiency are also factors to be taken into account.

2.2.4.1 Impulse turbines

In an impulse turbine, the turbine blades spin due to fast moving water fired through a nozzle. The blades usually have a bucket shape in order to catch the water and change the direction of its flow (Figure 2-26). The potential energy of water is converted to kinetic energy before heating the blades of the turbine. Newton's second law describes the energy transfer. Impulse turbines are used for high head and low flow applications.

An example of an impulse turbine is the Pelton turbine (Figure 2-27), which has one or more free water jets hitting the buckets of the runner (the rotating part). The Pelton turbine is considered on the most efficient types and it doesn't need to be contained inside a pipe or a housing.

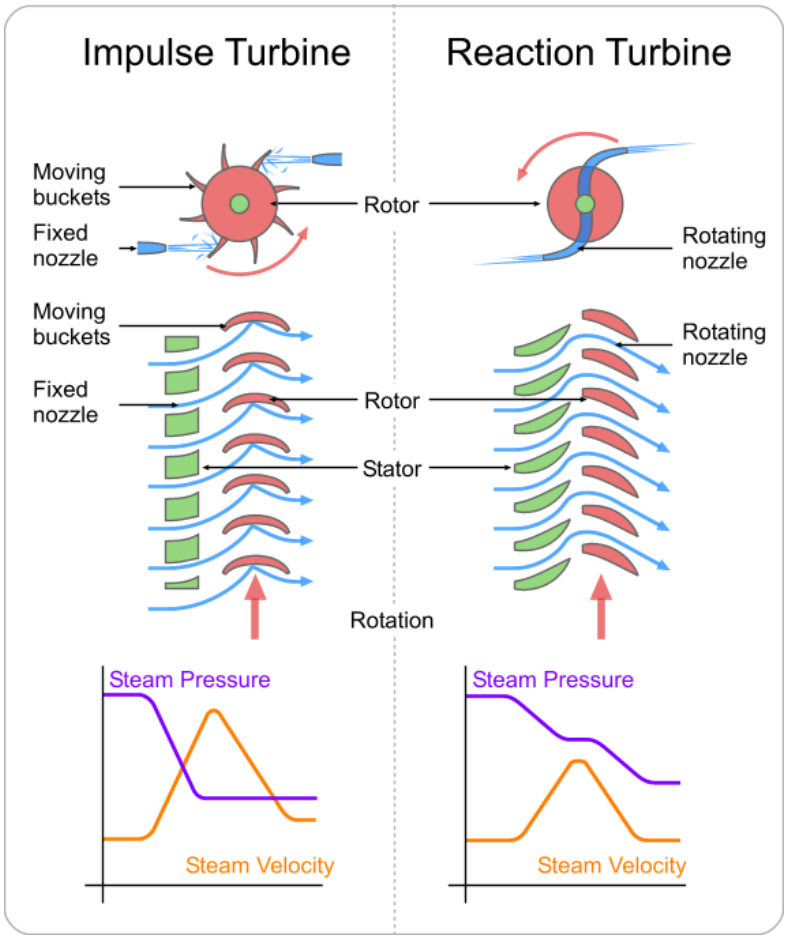

Figure 2-26: Difference between an impulse and a reaction turbine. [59] Licensed under CC BY-SA 3.0

Figure 2-27: A Pelton turbine. [60] Licensed under CC BY-SA 3.0

2.2.4.2 Reaction turbines

In a reaction turbine (Figure 2-26), power is developed from the combination of pressure and moving water (kinetic energy). Water changes pressure at it moves through the turbine and thus giving up its energy. Newton's third law describes the energy transfer. Reaction turbines must be inside a housing to contain the pressure of water or be fully submerged. They are usually used for lower head and higher flow.

An example of reaction turbines is the Francis turbine (Figure 2-28), the most common type used today. A Francis turbine is an inward flow turbine with a combination of radial and axis components. It consists of a spiral casing with openings to allow the water to impinge on the blades. Pressure is converted to kinetic energy before the water hits the blades. Other

components are the guide and stay vanes, the runner blades and the draft tube. Francis turbines usually operate in a water head between 40 and 600m.

Figure 2-28: A Francis turbine connected to a generator. [61] Licensed under CC BY-SA 3.0

2.2.5 Advantages and disadvantages of hydropower

Hydropower is a renewable source and it has flexibility, meaning it can easily adapt to changes in energy needs, to increase or decrease production very quickly and the reservoirs constitute power on demand. Power is stored with very little cost. Hydropower plants can have a very long life, up to a hundred years and they can also be used for flood control, irrigation, recreation etc. They also have low emissions of greenhouse gases.

The main disadvantage is that large hydropower plants have effects on the land, as it can be submerged or they can destroy forests and marshlands. Construction of large dams interrupts the river flow and sometimes displaces population and wildlife. Rivers with high siltation can cause damage to the dam. Another concern is the risks in case of a dam collapse, which is a possibility either due to poor construction or natural disasters.

2.3 Marine energy

Marine energy, also referred to as ocean energy or marine hydrokinetic energy, is a renewable energy resource and it comes from a variety of sources, like waves, currents, tides, ocean thermal energy conversion and salinity. The resource potential of ocean energy is huge however the technologies for the exploitation of the different sources are mostly in the early stages of development. As a result ocean power is the smallest contributor of all renewable energy resources.

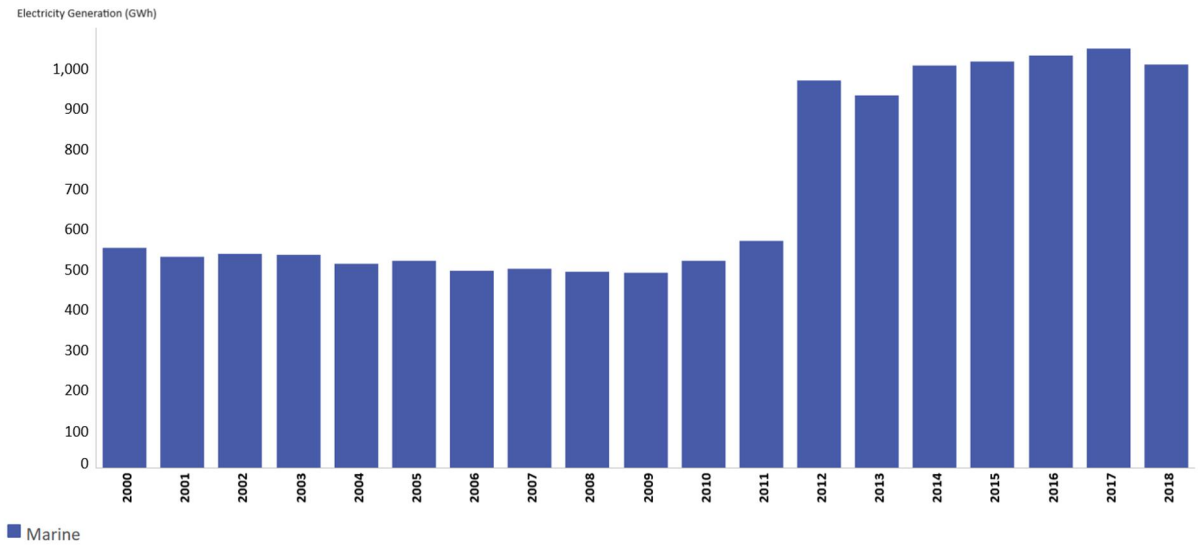

Figure 2-29: Electricity production from marine energy (GWh) from 2000 to 2018. [15]

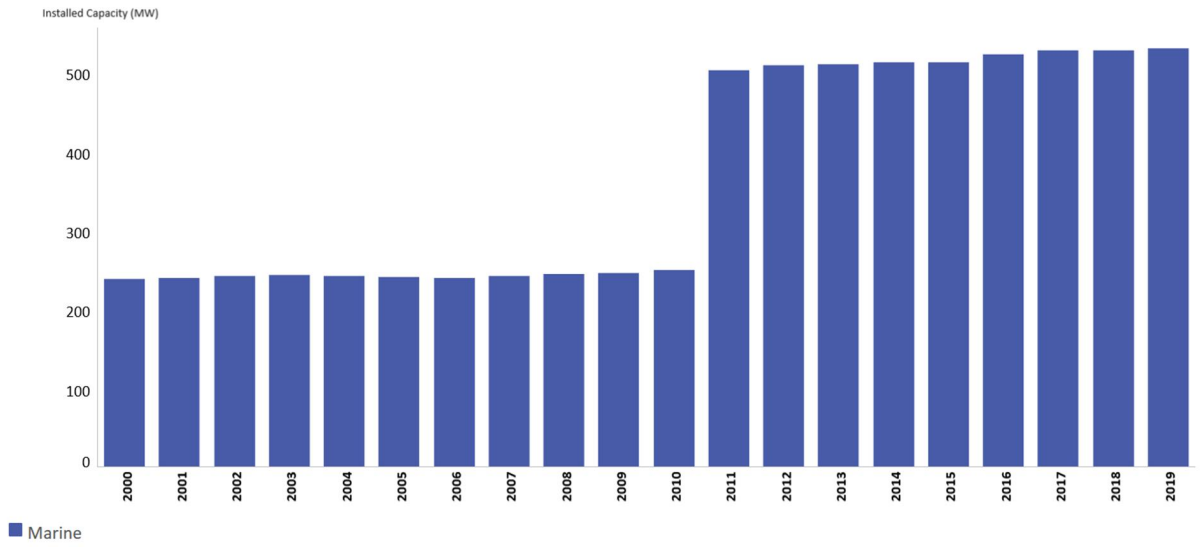

Figure 2-30: Installed capacity of marine energy (MW), from 2000 to 2019. [15]

Figure 2-29 shows the worldwide marine power electricity production, from 2000 to 2018, while Figure 2-30 is the world installed capacity, from 2000 to 2019. There has been an evident increase in the last decade but the total installed capacity in 2019 was just 530 MW.

The top 10 countries in installed capacity are shown in Figure 2-31, where Republic of Korea and France are basically the two countries responsible for over 90% of total installed capacity. The reason for that are their two tidal barrages, La Rance station in France with a capacity of 240 MW and the Sihwa plant in the Republic of Korea with a 254 MW capacity.

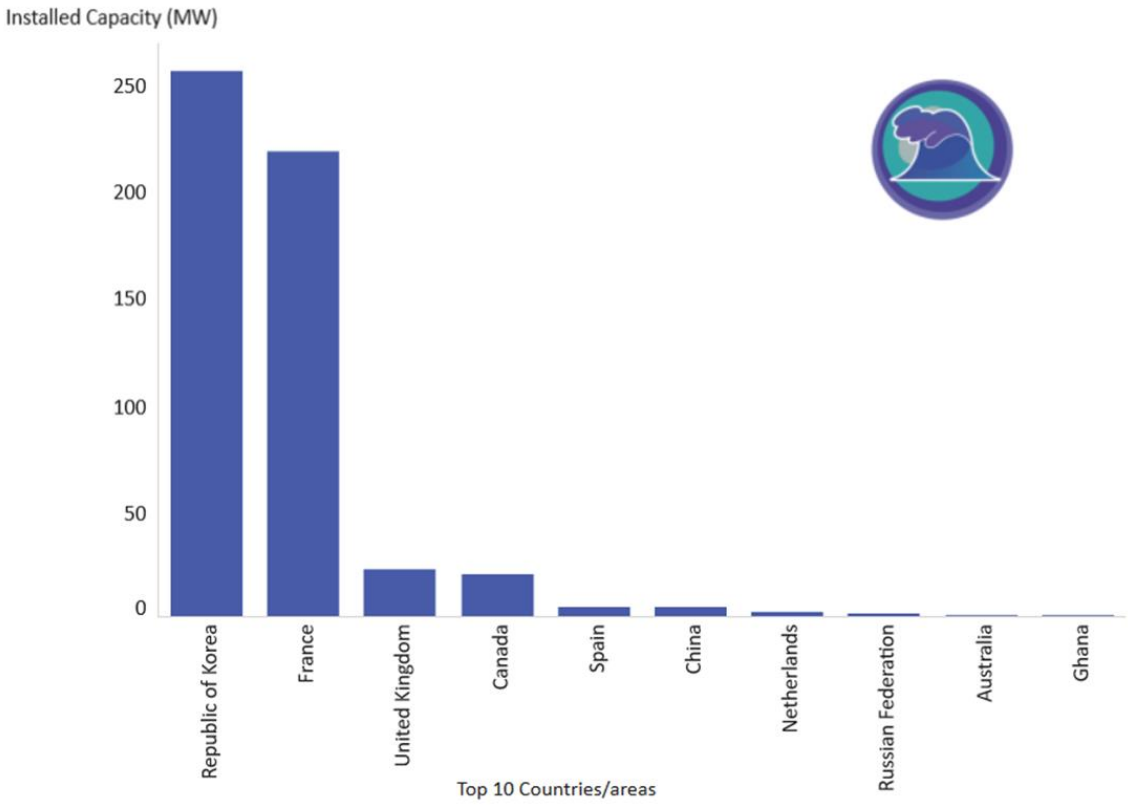

Figure 2-31: Installed capacity of marine energy (MW) for the top 10 countries, for 2019. [15]

2.3.1 Current power

Ocean currents carry large amounts of water and energy across Earth's oceans and their flow is relatively constant. The major ocean currents in the world can be seen in Figure 2-32, where blue arrows indicate the cold currents and red arrows the warm ones. One famous ocean current, for example, is the Gulf Stream, which transports warm water from the Gulf of Mexico to the North Atlantic and the west coasts of Europe. Ocean currents are created and controlled by various elements, like the wind, the Coriolis effect, topography of the ocean floor, temperature and salinity differences.

The ocean current power worldwide is estimated around 5000 GW, with power densities up to 15 kW/m^2.

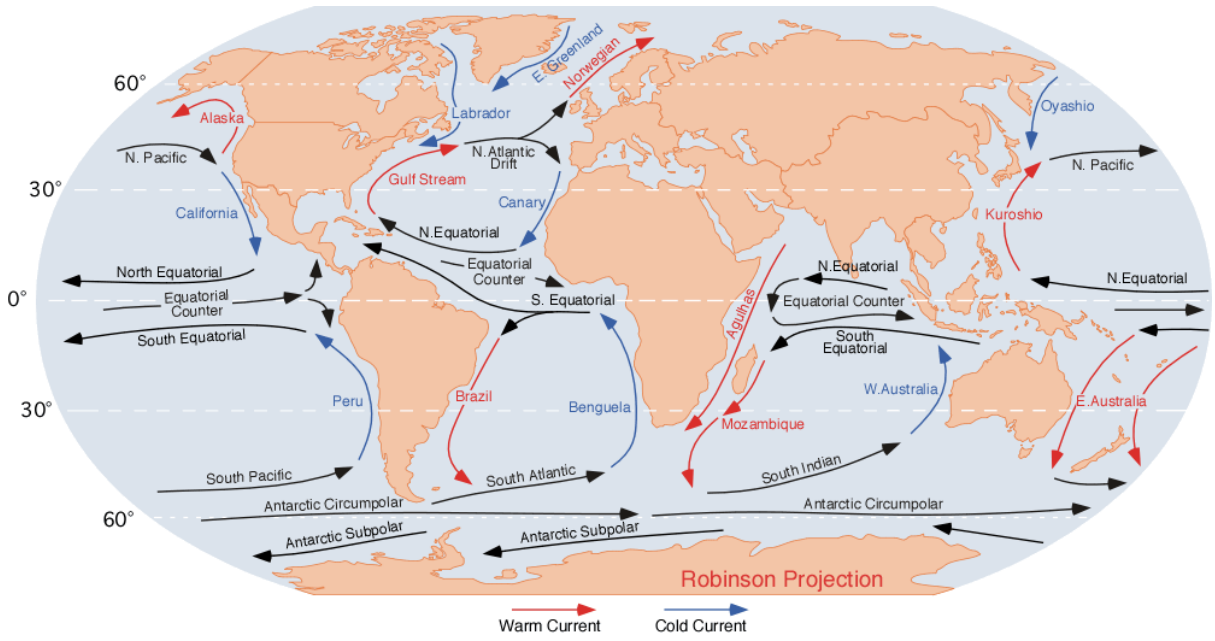

Figure 2-32: Major ocean currents worldwide. [62]

Electricity generation from ocean currents holds many advantages, as it is a very predictable resource, very large and its exploitation will have little impact on the atmosphere. There are no commercial applications for the generation of electricity from ocean current power, however research has been conducted in many countries for many years, as ocean current power is a promising resource for the near future. There are two types of turbines that are mostly being considered for ocean current exploitation, axial-flow horizontal-axis propellers and cross-flow Darrieus rotors. These turbines can be supported for example, in sea-bed mounted systems or floating moored systems.

2.3.2 Wave power

Waves on the water surface are created from the wind blowing over that surface. Energy is transferred from the wind to the waves, which can travel for very large distances without important energy loss.

Wave energy is calculated from Equation 2-5, where H is the wave height.

$$E = 0.5 * \rho * g * H^2/16, \qquad J$$

Equation 2-5

In the ocean though, the waves that are observed are superposition of waves instead of individual ones.

The wave speed, in terms of its period, is: speed = wavelength (λ) / period (T).

In deep water where the depth of water is larger than half the wavelength, the wave power per length, P/L is given in Equation 2-6.

$$\frac{P}{L} = \rho * g^2 * H^2 * \frac{T}{64 * \pi} \sim 0.5 * A^2 * T, \qquad kW/m$$

Equation 2-6

In a stormy weather, large waves can have a height around 15m and a period of 15sec. In that case there is 1.7 MW of wave power across each meter of wavefront. A wave power device is designed to capture most of that power and behind that device, waves will have lower heights.

Wave energy potential is very high worldwide, due to the large coastline length.

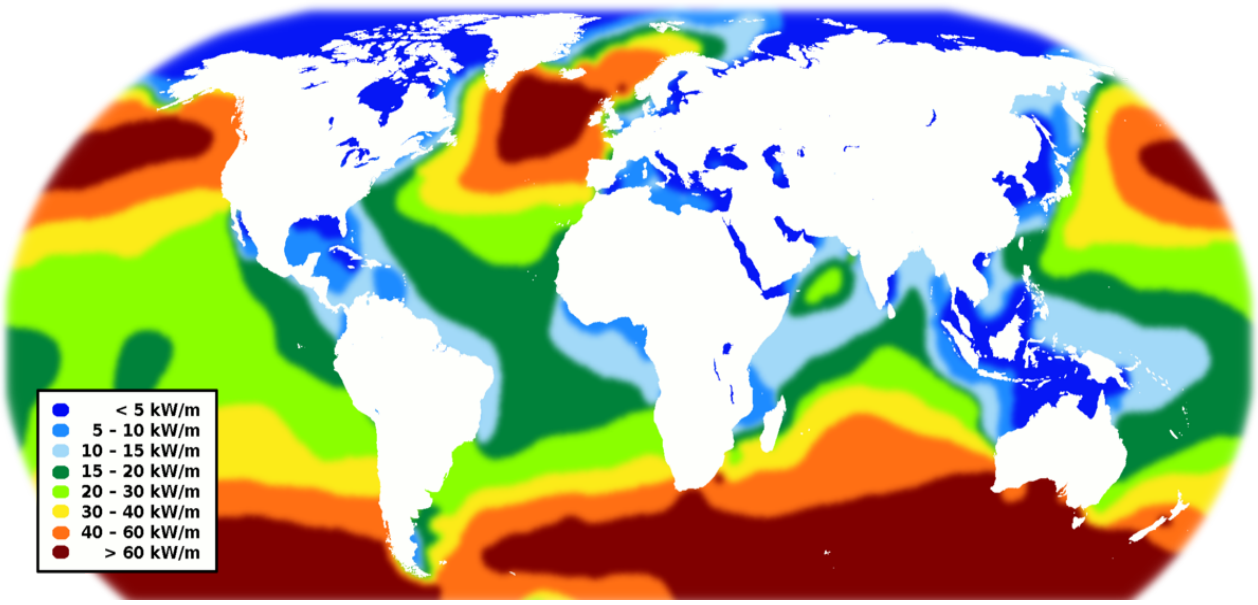

Figure 2-33: Global wave energy resources. [63] Licensed under CC0

Figure 2-33 shows the global wave energy resources, in terms of wave energy flux in kW per meter wave front. Areas with high potential are for example, the west coasts of Europe and northern coast of the UK, the pacific coasts on North and South America and the southern coasts of South Africa and Australia. The National Renewable Energy Laboratory (NREL) provides estimations for the wave power potential for the coastlines of various countries. For USA, for example, there is an estimation of 1170 TWh energy production per year.

2.3.2.1 Wave Energy Converters

Wave energy systems can be situated on the shoreline, near the shore or offshore. Shoreline devices are easier to install and maintain since they don't need moorings for deep waters or long cables underwater, but they receive less energy due to the fact that the wave energy decreases as the wave reaches the shore. Near-shore devices are situated a few hundred meters away from the shore, where the water depths are around 20-25m. The wave energy resource is higher and they share some advantages with shoreline devices since they are close to the shore. Offshore installations can exploit even higher wave energy resources and are situated it water depths higher than 25m.

Based on the method for capturing the wave energy, Figure 2-34 and Figure 2-35 present the main types of wave energy converter (WEC) devices.

An attenuator device (A) is a floating device, held by cables connected to the seabed, which operates parallel to the direction of the wave. It captures energy from the relative motion of the two parts as the wave passes by. An example of an attenuator WEC is the Pelamis Wave Energy Converter, shown in Figure 2-36.

A point absorber (B) is a floating device which has the ability to absorb energy from all directions through its movements near the surface of the water. The motion of the buoyant top relative to the device's base is converted into electricity.

An oscillating wave surge converter (C) uses wave surges and the movement of water particles within them to extract energy. The arm of the device oscillates, responding to the wave movement.

An oscillating water column device (D) is partially submerged and it's hollow. It encloses a column of air on top of a water column. As the water columns rises due to the waves, there is compression of the air in the column, which is forced through an air turbine to generate electricity.

An overtopping/terminator device (E) captures water from breaking waves to fill a reservoir to a level higher than the one surrounding it. A low-head turbine then captures the potential energy in the reservoir to generate power.

A submerged pressure differential device (F) is attached to the seabed. The device operates due to the pressure differential created by the wave motion above it. This difference in pressure is used to produce flow to drive a turbine and an electrical generator.

A bulge wave device (G) is a water filled rubber tube, which is moored to the seabed with one end facing the incoming waves. As the wave passes it causes pressure variations along the tube length, which result in the creation of a bulge. The bulge then grows as it travels through the tube and the energy that is gathered is used to drive a low-head turbine.

In a rotating mass device (H), there are two forms of rotation which are used to capture the wave energy, heaving and swaying in the waves. There is either an eccentric weight that is driven by the motion or a gyroscope that causes precession. Either way the movement is attached to a generator inside the device.

The most typical devices for shoreline applications are the oscillating water column devices, while common near-shore devices include the oscillating wave surge converters and the attenuator, point absorber and terminator devices are the most promising for offshore energy extraction.

WEC devices raise some environmental concerns, as there is high risk of fish and sea mammals being hit by turbine blades or being affected in general by the presence of these structures in their habitant. There is also underwater noise and electromagnetic fields due to the operation of some of these energy converters which should be taken into account.

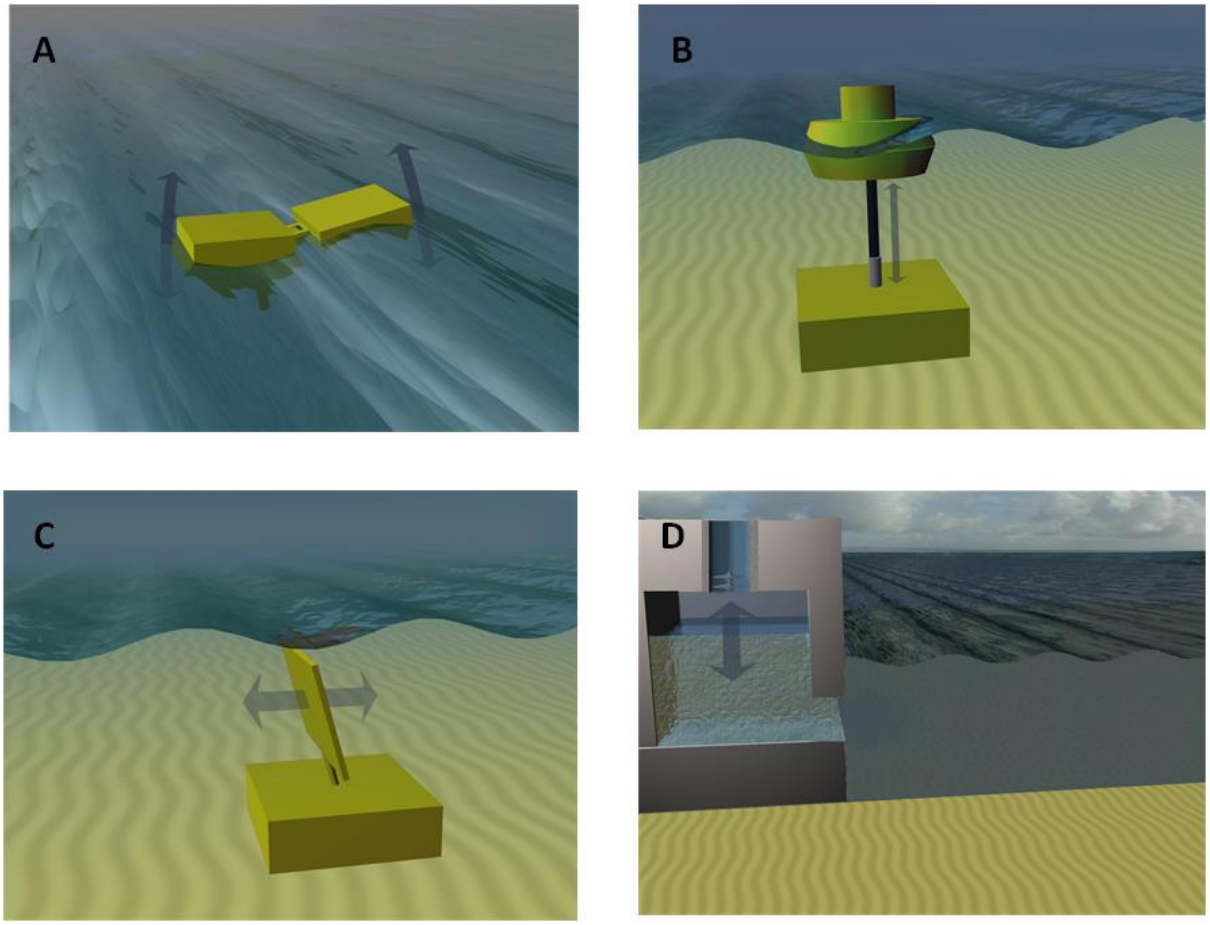

Figure 2-34: WEC devices: attenuator (A), point absorber (B), oscillating wave surge converter (C), oscillating water column (D). [64]

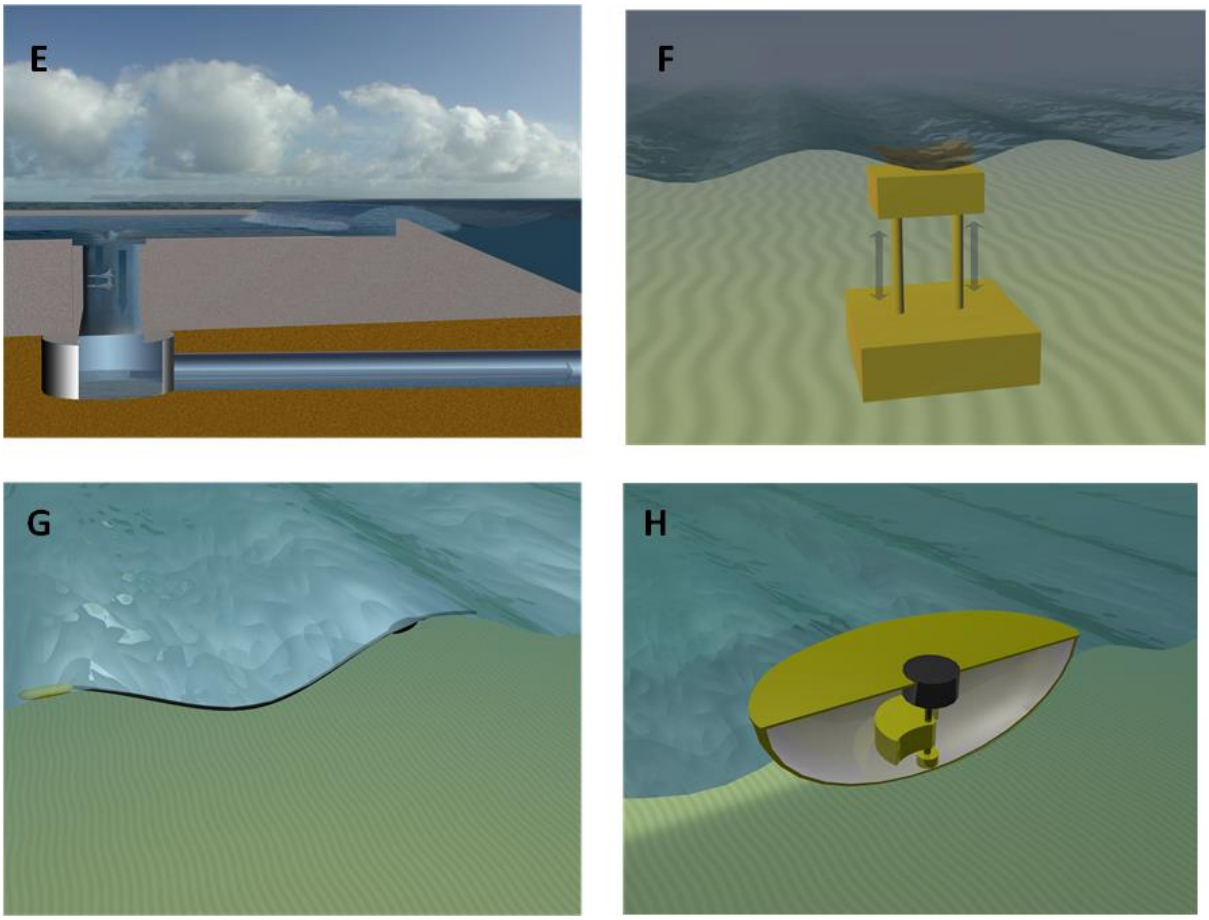

Figure 2-35: WEC devices: overtopping/terminator device (E), submerged pressure differential (F), bulge wave (G), rotating mass (H). [64]

Figure 2-36: The Pelamis Wave Energy Converter. [65] License: Public Domain

Many wave energy devices, operating together in the same area, form a wave farm. A wave farm project achieves larger production of electricity and there is a hydrodynamical and electrical interaction between the WEC devices. There have been wave farms operating in several sites, like the UK and Portugal, but they were shut down due to various financial reasons. Several wave farm projects are being studied and tested worldwide for future commercial operation.

2.3.3 Tidal power

Tidal power is the capture of energy from tides to convert to other forms, mainly electricity. Tides are the rise and fall of sea levels, due to the combined gravitational forces from the Moon and the Sun and Earth's rotation. Tides are very predictable and have a large potential for energy production but they are not widely used, mainly due to high installation costs and a limitation in the number of sites with high tidal ranges. Due to technological developments however, there are improvements in the design of tidal energy systems. The main contributors to worldwide marine energy production are the two large tidal power plants, the

254 MW Sihwa Lake Tidal Power Station in South Korea and the 240 MW Rance Tidal Power Station in France, which are shown in Figure 2-37 and Figure 2-38, respectively.

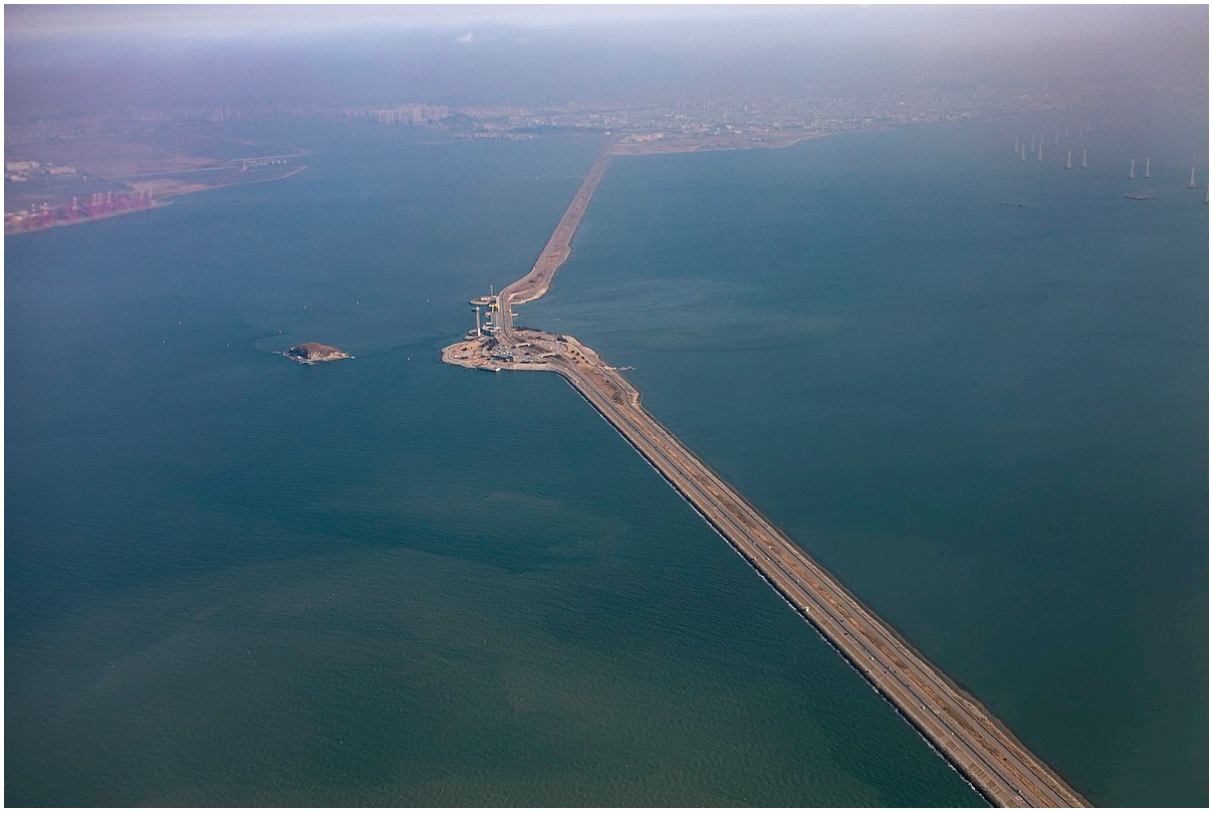

Figure 2-37: The Sihwa Lake Tidal Power Station in South Korea. [66] Licensed under CC BY-SA 3.0

Figure 2-38: The Rance Tidal Power Station in France. [67] License: Public Domain

Due to the tidal forces exerted on the surface of the oceans, a bulge in the water level is created which increases the sea level temporarily. This bulge moves towards the shoreline, due to the rotation of the Earth and a tide is created. A tidal generator is designed to convert the energy of tidal flows into electrical energy. The greater the tidal variation and the higher the tidal current velocities, the greater is the production of energy.

There are three main methods for tidal power production: tidal stream generator, tidal barrage and tidal lagoon.

2.3.3.1 Tidal stream generator

A tidal stream generator (Figure 2-39) has the basic concept of a wind turbine, meaning that it uses the moving water kinetic energy to drive a turbine, which can be horizontal, vertical, open or ducted. Seawater has a higher density than air, therefore energy can be collected with slower water currents and smaller turbines, compared to wind energy. Tidal stream

generators include axial turbines with blades facing the direction of the flow, crossflow turbines with spinning blades perpendicular to the flow direction, reciprocating devices which have a hydrofoil, instead of spinning blades, pushed back and forth transverse to the direction of the flow, venturi effect devices which have the turbines inside a cylindrical duct to create a second water flow and others.

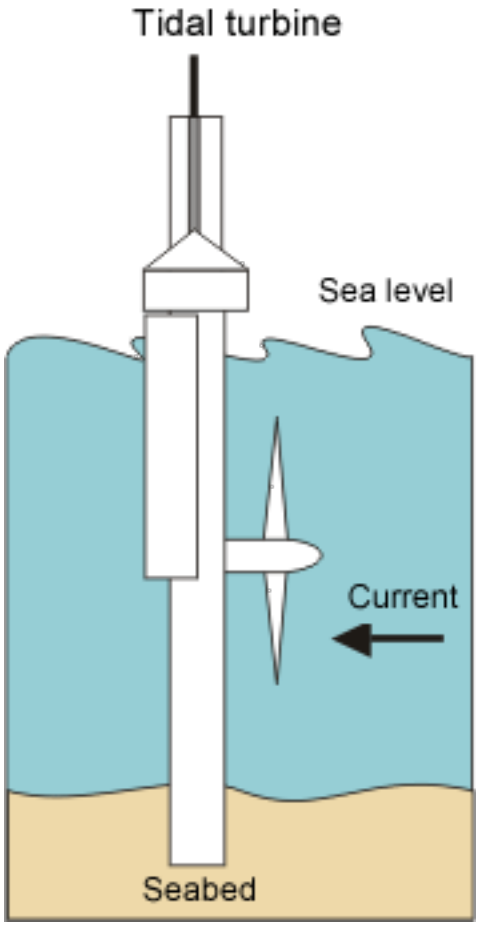

Figure 2-39: A tidal stream generator. [68] License: Public Domain

2.3.3.2 Tidal barrage

A tidal barrage system uses the potential energy due to the height difference between high and low tides, to generate energy. The system uses dams and sluice gates to capture this potential energy and store it. The dam is constructed across the entrance of a tidal inlet or basin, with its bottom located on the seabed. It allows water to flow in, during high tide and releases it during low tide, by controlling the sluice gates. The turbines, which are placed in

the barrage wall, generate power as the water flows in and out of the basin or bay. Both Rance and Sihwa Lake tidal power stations are tidal barrage systems. In these systems tidal power can be generated as the water enters the reservoir on the incoming flood tide, in which case it's called a tidal barrage flood generation system (Figure 2-40), or as the water leaves the reservoir on the ebb flow tide and it's called a tidal barrage ebb generation system (Figure 2-41). In a two-way generation system, power is generated as the water flows in both directions.

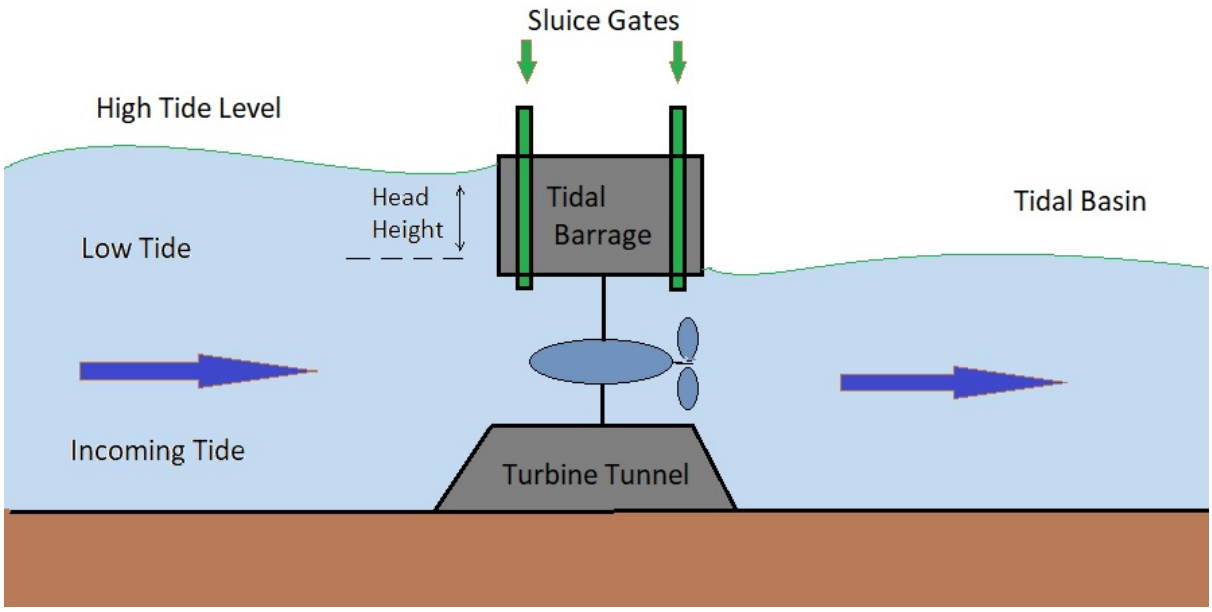

Figure 2-40: A tidal barrage flood generation system. [69]

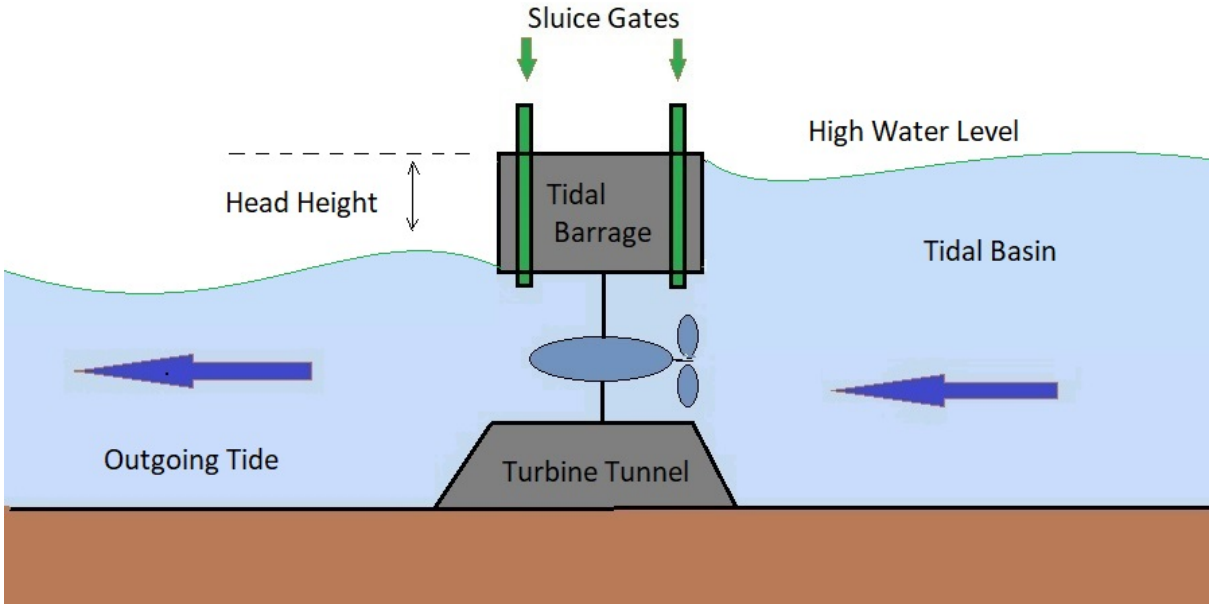

Figure 2-41: A tidal barrage ebb generation system. [69]

2.3.3.3 Tidal lagoon

A tidal lagoon is a more modern design and it consists of circular retaining walls, which are embedded with turbines to capture the tidal potential energy, with reservoirs similar to those in tidal barrage systems. There isn't a system of this type operating anywhere in the world yet, since the project Tidal Lagoon Swansea Bay in the UK was cancelled.

2.3.4 Ocean thermal energy conversion

Ocean Thermal Energy Conversion (OTEC) generates electricity by using the ocean thermal difference between warm surface and cooler deep water to drive a Rankine cycle.

There are many areas in the world with a temperature difference between surface ocean water and water at 1000m depth of at least 20°C, which is sufficient for an OTEC system to operate efficiently. These areas are shown in the map of Figure 2-42. The ocean temperature

difference is greatest in the tropics, where OTEC systems would have the most promising possibilities. OTEC could provide tens of times the energy that can be provided from other ocean energy systems and is an emerging technology with a lot of potential.

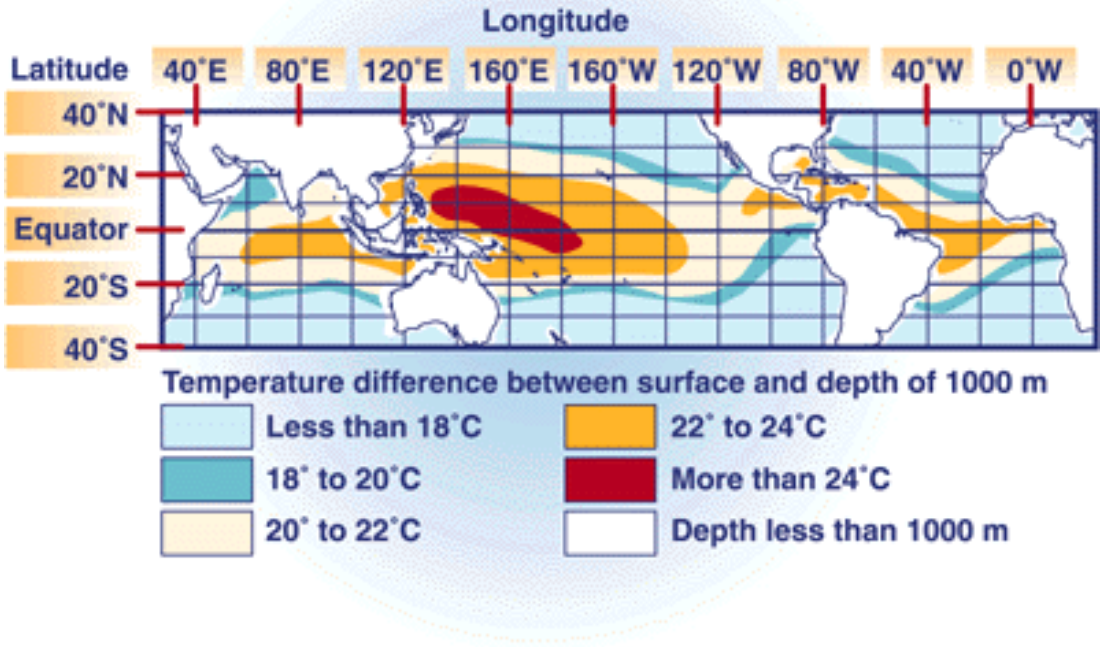

Figure 2-42: World map with the temperature difference between ocean surface water and depth of 1000m. [70] License: Public Domain

OTEC systems can be of three types, closed-cycle, open-cycle and hybrid.

In an OTEC closed-cycle system (Figure 2-43), a working fluid is used that is turned to vapour due to heat transferred from the warm seawater of the surface. The vapour expands and drives a turbine attached to an electric generator. The vapour, which is then contained inside a condenser, turns back into liquid as cold seawater passes through the condenser and the working fluid ends being recycled through the system. The working fluid that is used needs to have a low boiling point, like ammonia.

In an OTEC open-cycle system (Figure 2-44) the working fluid of the system is the warm surface water, which vaporizes at surface water temperatures in a near vacuum. The vapour,

which is basically pure freshwater, expands and drives a low-pressure turbine attached to a generator. It is then condensed as it is exposed to cooler temperatures from deep ocean water. The water can be used for drinking or irrigation, as long as the condenser doesn't allow direct contact with the cool seawater. In case of direct contact, there is more electricity that is produced and the mixture water is released into the ocean. An open-cycle

OTEC plant operated in 1993 experimentally, at Keyhole Point, Hawaii, USA and produced around 80 kW of electricity, more than the 40 kW which was produced by a system, tested in Japan in 1982.

Hybrid OTEC systems use parts of both closed and open-cycle systems with the purpose of increasing electricity production and producing freshwater. There is both seawater and ammonia used as working fluids.

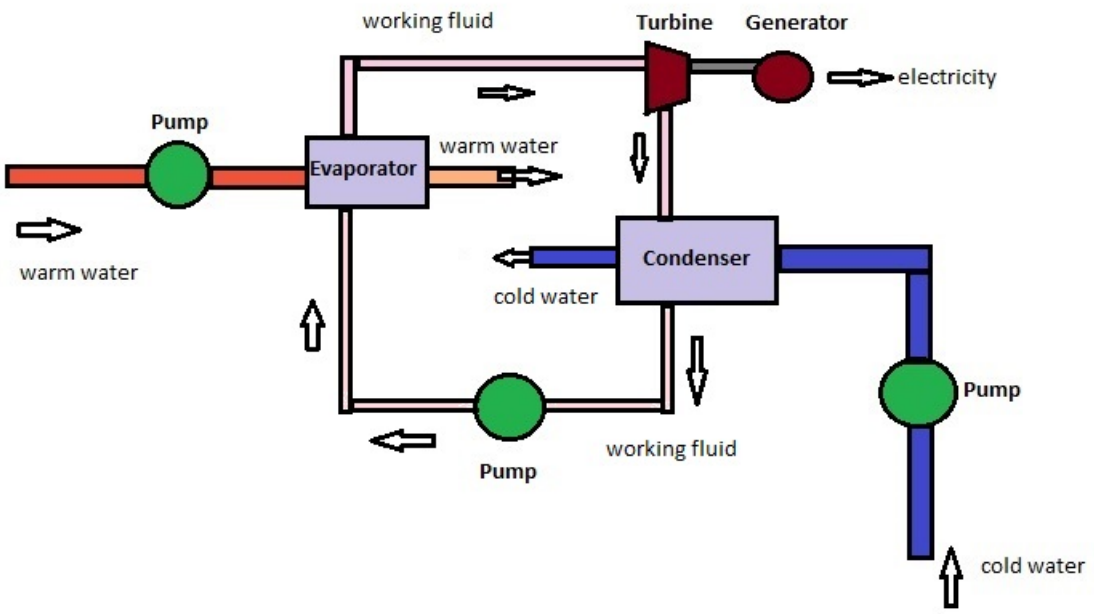

Figure 2-43: OTEC closed-cycle system. [71]

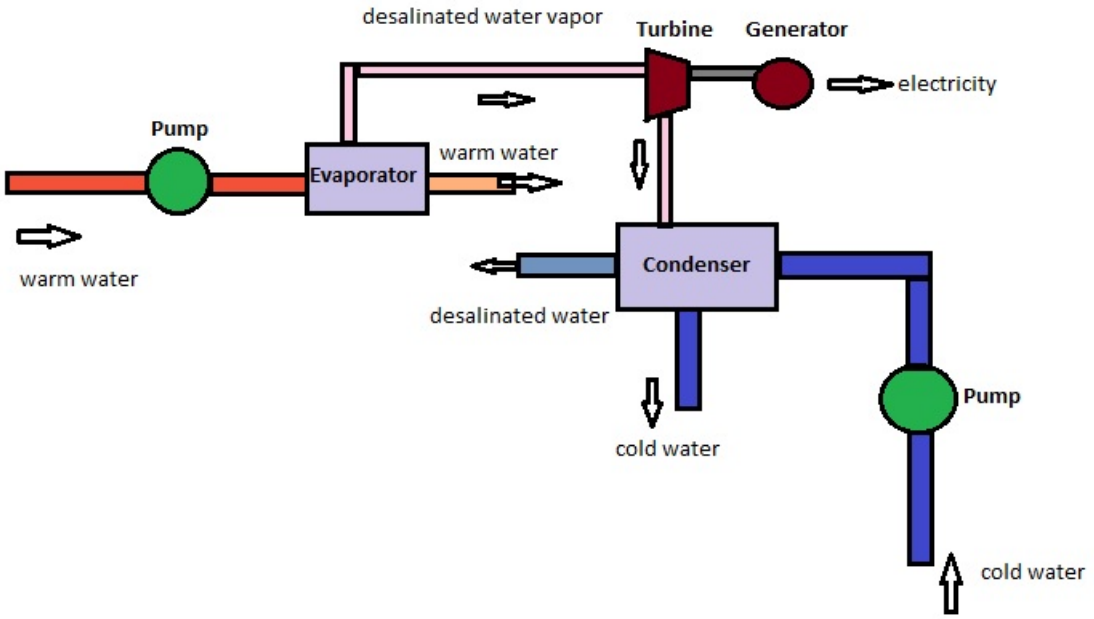

Figure 2-44: OTEC open-cycle system. [71]

2.3.5 Salinity gradient power

Salinity gradient power is the energy produced due to the difference in salt concentration between saltwater (sea) and freshwater (river), as it happens at the mouth of rivers, where freshwater mixes with saltwater. Two main methods for producing salinity gradient power is the reverse electrodialysis and the pressure retarded osmosis, which both rely on osmosis with membranes. These systems are currently being tested and they are developed for commercial use in Norway and in the Netherlands.

2.4 Storage

As more attention is concentrated on renewable forms of energy, another important issue is the storage of energy, in order to be able to have energy on demand. Energy storage systems are about transforming energy into a form that can be stored and can be converted into electricity when needed.

Energy storage systems can be classified as: mechanical, like pumped storage hydroelectricity, compressed air energy storage and flywheels, electrochemical, like batteries, electromagnetic, like capacitors and magnetic systems, thermal, like phase change materials or chemical, like biofuels and hydrogen storage. Energy density, efficiency and lifetime are important factors for energy storage systems. The efficiencies range between 50% and 80%, depending on the system and the lifetime could range from minutes, for non-rechargeable batteries for example, to a few years, for lead acid batteries for example or even 100 years in case of dams. Another important factor is the rate of charging and discharging of the storage system. The main energy storage systems are presented next.

2.4.1 Pumped storage hydroelectricity

Pumped storage systems store energy in the form of potential energy of water, which is pumped from a low elevation reservoir to a higher elevation reservoir. The stored water is released through turbines to produce electricity when energy demands require it.

Pumped storage is so far the most cost-effective type for storing large amounts of electrical energy. The energy density of these systems is low, which means that large flow is required or large height difference between the two reservoirs. The main disadvantage of these systems is the high initial cost because of the large reservoirs that are needed and the specific needs for an appropriate site for installation. Pumped storage plants can respond to load changes within seconds and can be used to provide peak-load power for fossil fuel and nuclear plants. They usually have 6 to 20 hours of hydraulic reservoir storage for operation.

Figure 2-45 shows the installed capacity of pumped storage systems, from 2000 to 2019, while in Figure 2-46 the top 10 countries are presented, with China having over 30 GW in installed capacity for 2019. The largest pumped storage plants, as mentioned before, are the Bath County in the USA, the Guangdong and Huizhou stations in China and the Okutataragi pumped storage power station in Japan.

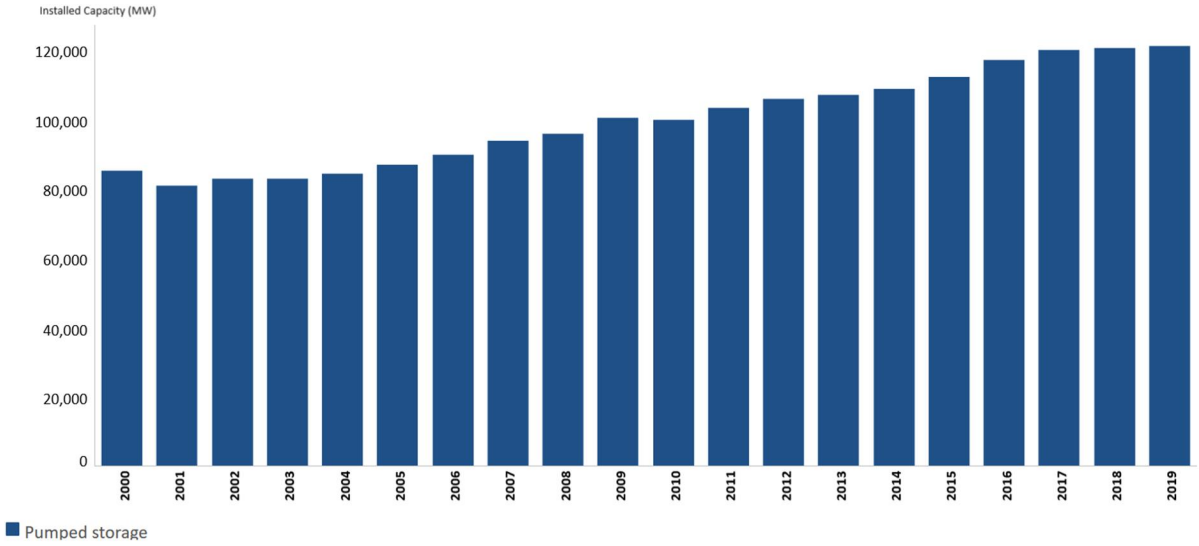

Figure 2-45: Pumped storage installed capacity (MW) from 2000 to 2019. [15]

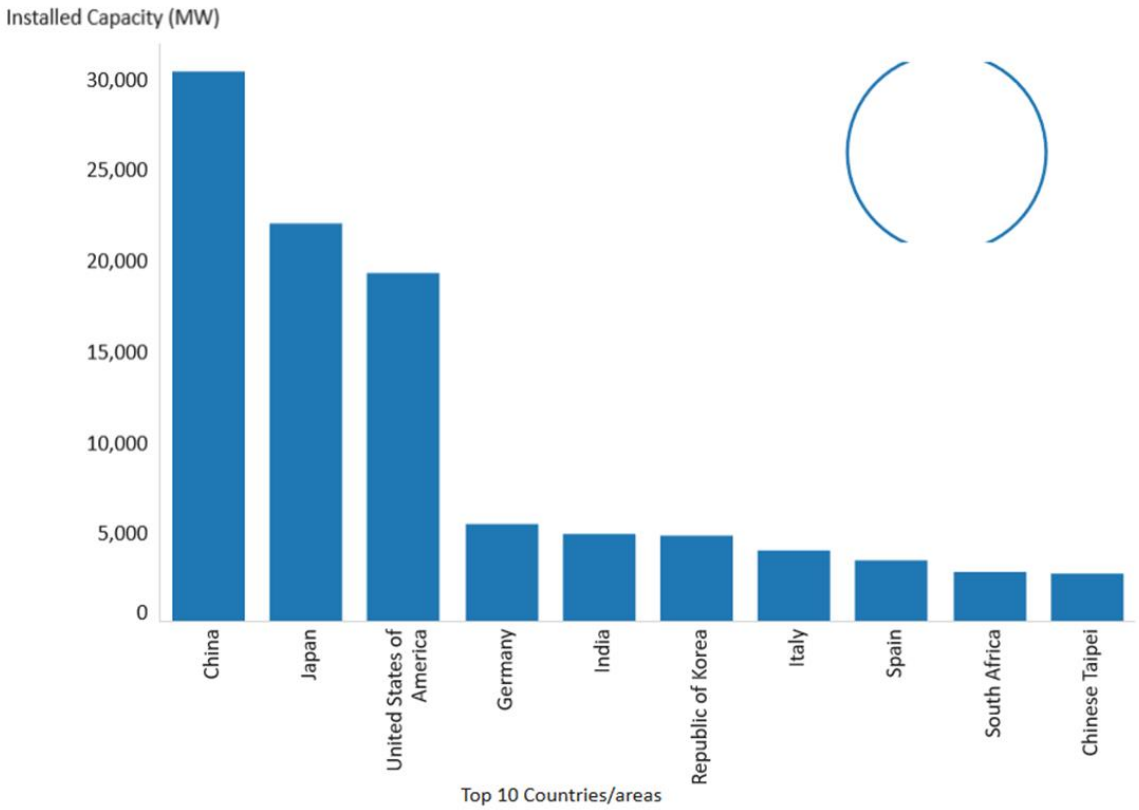

Figure 2-46: Pumped storage installed capacity (MW) for the top 10 countries for 2019. [15]

2.4.2 Compressed air energy storage

Compressed air energy storage (CAES) uses compressed air to store generated energy for use at another time. Air is compressed and stored under pressure in an underground cavern or mine and when electricity is needed it is expanded to drive a turbine connected to a generator. Heat is generated during compression and is removed during expansion. Depending on the way the system handles the heat generated during compression, the energy storage process can be diabatic, adiabatic, isothermal or near-isothermal.

In diabatic processes, much of the generated heat is dissipated into the atmosphere by using intercoolers. The stored energy is determined by the compressed air temperature. If the temperature is not high enough, then the air needs to be reheated before being expanded to drive the turbine. The reheating is usually done by using natural gas as fuel. The whole process decreases the efficiency of the energy storage system. Despite this fact, this type of compressed air energy storage system is the only one to have been used in a commercial way. Examples are the CAES plant in McIntosh, Alabama, USA, which was built in 1991 and the plant in Huntorf, Germany, built in 1978.

In an adiabatic process, the heat that is generated during compression is kept in the system and returned to the air to reheat it during expansion, to generate electricity. The efficiencies of this type are much higher and can reach up to 70%. No commercial applications though are in operation yet.

An isothermal process tries to maintain operating temperature by constant exchanging heat with the environment. However in reality there will always be some heat losses so the process can be characterized as near-isothermal. In this type, the compression is done near a large thermal mass in which the heat from the compression is transferred, in order to stabilise the temperature of the gas.

More projects are being studied and planned to be built in the near future.

2.4.3 Flywheel energy storage

A flywheel device is a rotating mechanical device, which is used to store energy in the form of rotational energy (Figure 2-47). It is connected to a motor-generator and they are sometimes enclosed in a vacuum chamber in order to limit friction and energy loss. The

flywheel spins to a high speed and rotational energy is generated. When energy is needed, rotational energy is converted to electricity by the generator, which results in the decrease of the rate of rotation. The device is recharged with the use of the motor, which increases the rotational speed. The amount of energy that can be stored is proportional to the device's moment of inertia and the square of its angular velocity.

The first flywheels were made of steel, however newer devices are made of carbon-fiber, which has higher tensile strength to withstand very high rotating speeds and more energy can be stored for the same mass in this way.

Most flywheel energy storage systems use electrical energy to accelerate and decelerate the rotor, but designs that use mechanical energy are also being developed. Flywheel systems have long lifetimes, they don't require a lot of maintenance and they have fast reaction times. Their energy efficiency can reach up to 90%.

Flywheels have been used in transportation, buses, trains and cars, mostly in an experimental way. They represent a field of continuous research since they present many advantages compared to batteries. They have longer lifetimes, they can operate at wider temperature ranges and are less damaging to the environment.

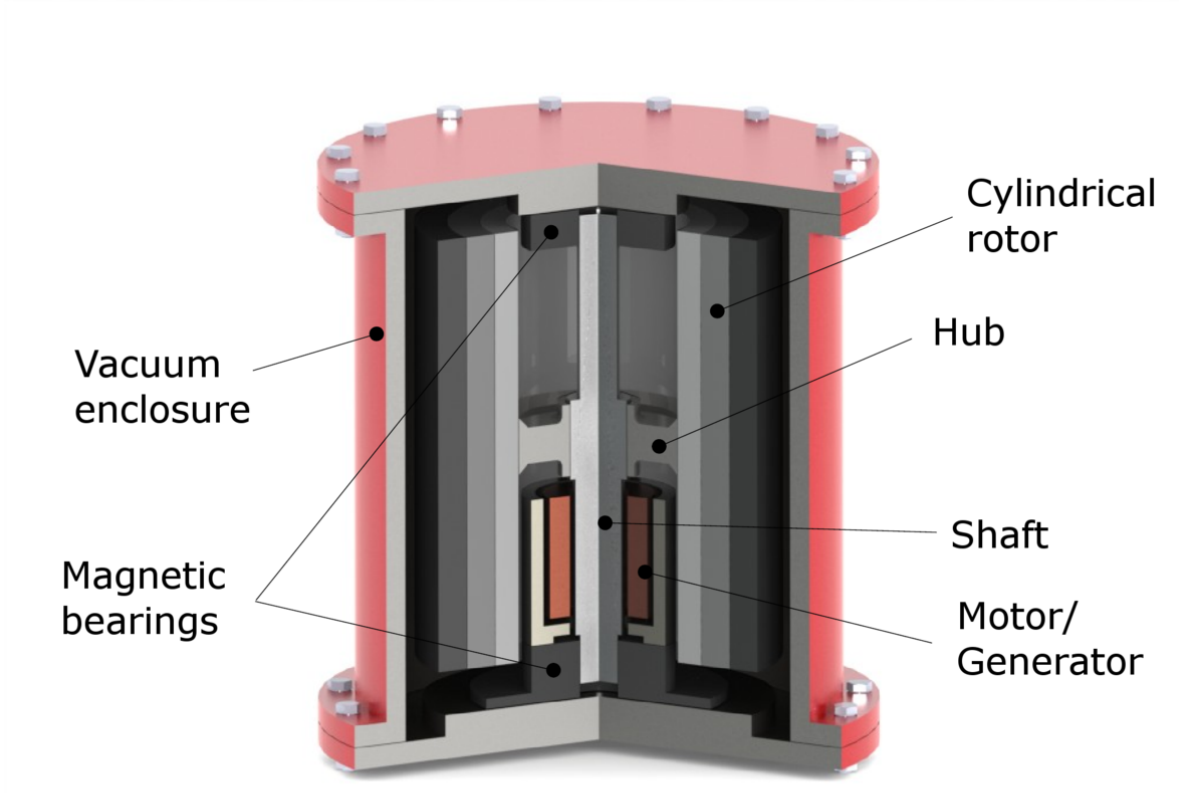

Figure 2-47: Diagram of a flywheel device. [72] Licensed under CC BY-SA 3.0

2.4.4 Batteries

Battery energy storage systems are devices that convert stored chemical energy into electrical energy and the opposite in the charge cycle. Batteries are very common worldwide as energy storage devices and are used in vehicles, electronic devices and many more applications. A battery consists of one or more electrochemical cells, each of which containing two electrodes immersed in an electrolyte, which allows the transport of ions, thus allowing current flow. There is always some energy loss during the charging and recharging, due to internal resistance. The storage capacity of a battery depends on the battery age, meaning the number of cycles that have been completed, temperature and the rate of discharge among other things. There are various types of batteries depending on the applications for which they are used.

Lead-acid batteries are a very common type of rechargeable batteries and they are used in many household and commercial applications. The negative side is pure lead and the positive

side is PbO_2, with the chemical energy being stored in the potential difference of the two, plus the aqueous sulphuric acid (Figure 2-48). Lead-acid batteries have low energy-to-weight and energy-to-volume ratios, but they can supply high surge currents, meaning that they have high power-to-weight ratio. They are low cost and are widely used for remote village power and stand-alone systems. Some examples of lead-acid energy storage systems are the 10 MW, 4-h system in Chino, California and the 20 MW, 40-min system in San Juan, Puerto Rico.

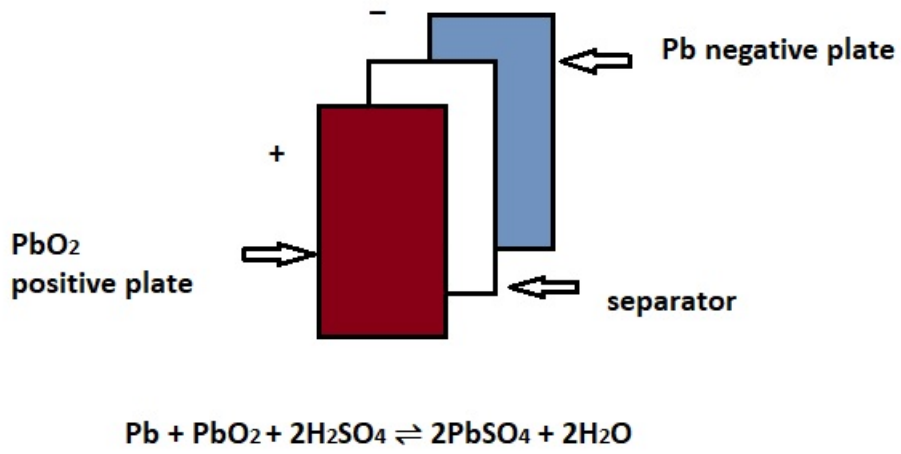

Figure 2-48: Lead-acid battery chemistry.

Lithium-ion batteries have high energy density and high efficiency, which is close to 100%. Another important advantage is their long cycle life with more than 3000 full discharge cycles. Their cost however is higher. The anode of a lithium-ion battery is carbon graphite and the cathode consists of lithiated metallic oxide, while the storage medium contains a mixture of lithium salts and organic carbonates. Lithium-ion batteries are used in a variety of energy storage applications, from residential applications of a few kilowatt-hours to grid services of multi-megawatt needs.

Sodium-sulfur batteries are constructed from liquid sodium and sulfur. They have high energy density and efficiency and long cycle life and they are inexpensive energy storage devices. A

sodium-sulfur battery operates at high temperatures, 300-350°C and it is more suitable for stationary applications. They can support stand-alone systems or the electric grid. They provide a good option for renewable energy systems like wind farms or solar power stations, in areas where there are no possibilities for other energy storage types. These energy storage systems have been demonstrated at various sites in Japan and a large system of 34 MW and 245 MWh is installed in a wind farm in northern Japan.

In a flow battery, there are two chemical components dissolved in liquids, which are pumped through the system on separate sides of a membrane to provide chemical energy (Figure 2-49). The two external electrolyte reservoirs are separated from the electricity converter unit. Three types of this category are the vanadium redox battery, the polysulfide bromide battery and the zinc bromide battery. Flow batteries can support off-grid village power, they can release energy for an extended time period and can support large power applications but they have high operating and maintenance costs. An example of a flow battery storage system is the 1.5 MW system in a semiconductor fabrication plant in Japan.

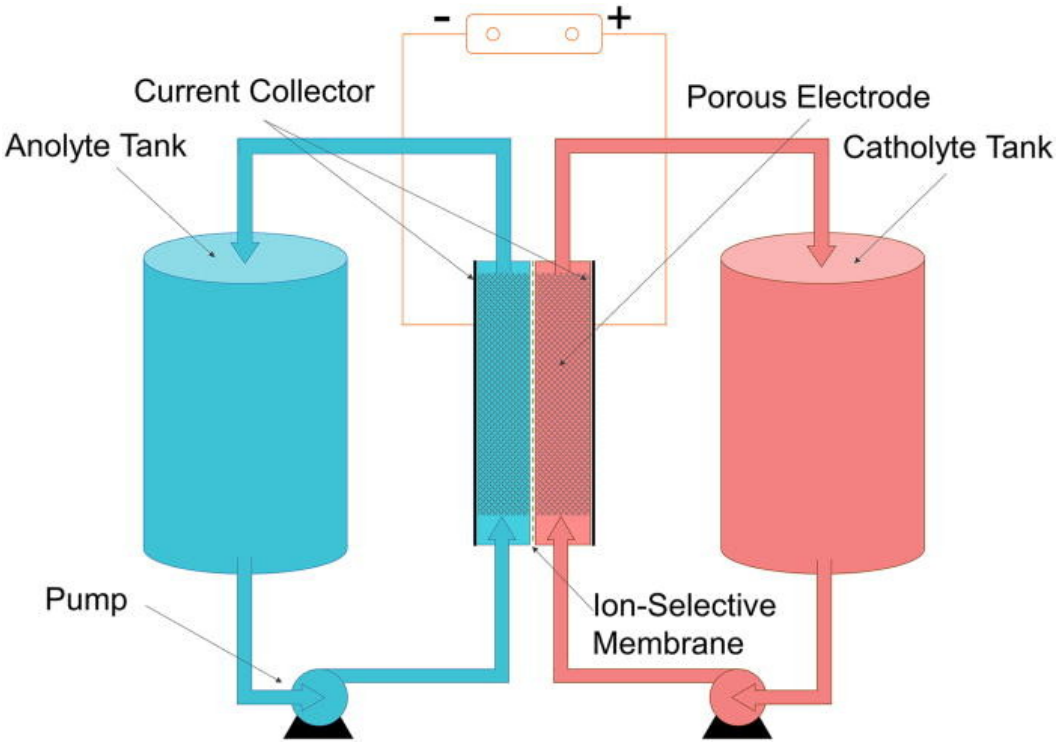

Figure 2-49: Diagram of a flow battery. [73] Licensed under CC BY 4.0

2.4.5 Superconducting magnetic energy storage

Superconducting magnetic energy storage (SMES) systems are systems that store energy in the magnetic field, which has been created by the direct current flow in a superconducting coil. The coil must have been cryogenically cooled to temperatures lower than its superconducting critical temperature. SMES systems have long lifetimes, very good response and their efficiency reaches up to 95%. There is practically no energy loss over time. The disadvantage is that due to the low temperatures required, there is a considerable cost for refrigeration and the superconductive coil. There are several 1 MWh systems in the world, which are used for clean power quality at manufacturing plants. They can also be used to provide grid stability or in utility applications. There are a number of SMES systems in Wisconsin, USA, used to enhance stability on a transmission loop.

2.4.6 Capacitors

Capacitors are energy storage devices, in which charge is stored on two conductors, which are separated by a non-conductive region. This region can be a vacuum or a dielectric, which is an electrical insulator material. The conductors hold equal opposite charges and the dielectric creates an electric field. A capacitor can store electric energy and can be used as a battery. They are very common in electronic devices with the purpose of maintaining power while there is a change is batteries. Electrochemical capacitors (ECs) or supercapacitors store electrical charge in the electric double layer, formed between each of the electrodes and the electrolyte ions (Figure 2-50). A supercapacitor has long life and fast response and is between the electrolytic capacitors and batteries, in terms of its energy density. Supercapacitors can be used for micro grid energy storage and they are usually used in conjunction with chemical batteries.

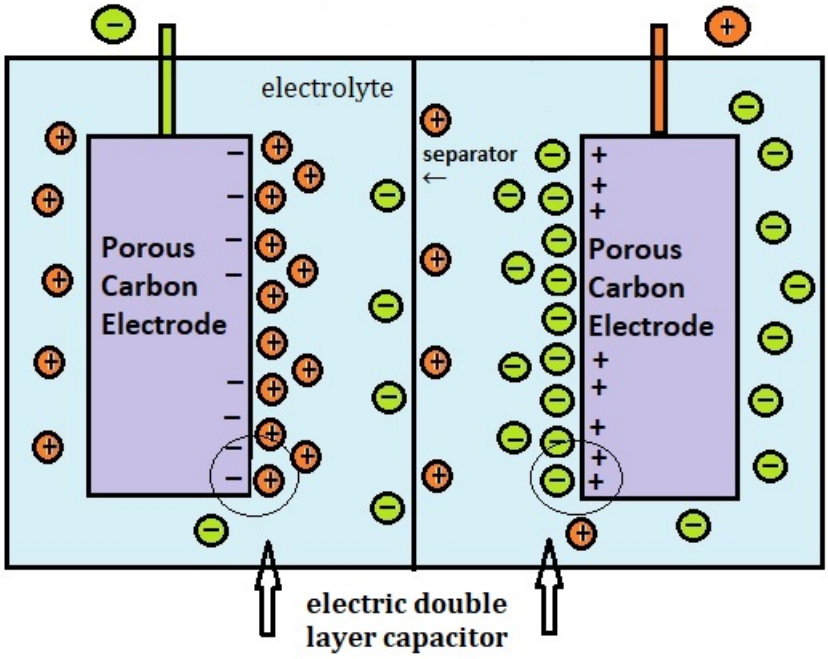

Figure 2-50: Illustration of a supercapacitor.

2.4.7 Phase change materials

A phase change material is a material that releases/absorbs energy, at almost constant temperature, as it changes phases to provide heating/cooling. For energy storage purposes, the liquid-solid phase change is used and the substance should have large latent heat and high thermal conductivity. Two main types of phase change materials are organic materials, which are derived from petroleum, plants or animals and salt hydrates, which use salts from the sea, mineral deposits or by-products. Phase change materials are used for commercial applications, like for example heating pads. Their biggest potential however is their use for building heating and cooling. For example, ice is stored in a building underground reservoir during winter and is used for cooling the building during summer.

2.4.8 Hydrogen storage

In hydrogen energy storage, hydrogen is produced from water by electrolysis. Electrolysis can be achieved by alkaline electrolysis or Proton Exchange Membrane (PEM) electrolyzers.

Hydrogen can then be stored in pressurized vessels or in underground salt caverns, in case of large hydrogen amounts. It can then be re-electrified in fuel cells or burned in gas power plants with efficiencies up to 60%. Hydrogen produced by electrolysis is a promising economic fuel choice. It can also be used as fuel for fuel cell cars or be injected into natural gas pipelines. The efficiency of electrolysis to fuel cell to electricity is around 50%. A 6 MW hydrogen storage plant using PEM technology was commissioned in Germany with the purpose of converting excess wind power to hydrogen to use in fuel cells or for natural gas supply. Another 2 MW PEM facility in Ontario was commissioned to produce hydrogen from water through electrolysis.

2.5 Renewable energy issues and aspects

There are various issues concerning the development and use of renewable energy applications, which have to do with political, economic and environmental factors, such as legislation and regulation, incentives, treaties, system standards etc.

2.5.1 Environmental concerns

The environmental issues are various and different for each renewable resource. In short, solar and concentrated solar power applications need large land areas to situate the collectors and this land can't really be used for any other purposes. Wind power applications create noise and visual concerns with their turbines, which can have serious effects on wildlife, particularly birds and bats. Large land areas are also needed for biomass production, for bioenergy applications, while the burning of biomass releases greenhouse gases into the atmosphere. For geothermal production, the concerns include the land subsidence which has been observed in various cases and the seismic activity due to deep drilling in the ground, while uncontrolled exploitation of the resources could lead to their depletion. Hydropower applications invoke concerns of their visual impact, as well as their impact on fish populations. There is the possibility of displacement of people and there's always the risk of failure or collapse of dams, which could have dramatic consequences. Finally marine power

applications come with issues as well, as they affect marine life and also raise concerns for ships.

2.5.2 Regulations

The regulations concerning renewable energy projects are different depending on the country. Small projects could follow a simple procedure, where they would need the approval of one or several corresponding agencies, while large projects could have more complicating processes with need for approval and permits from governmental departments. Large projects would also be under serious consideration regarding their environmental impact. Permits are required for construction and there are safety regulations regarding the issues of each installation, for example the height and noise level of wind turbines. Electricity production installations would need planning for restriction of access into the facility and warning for high voltage areas. The sum of permits and regulations that need to be followed by a renewable energy industry could become expensive and it is something that needs to be considered by any future project.

Environmental analysis should be conducted before any renewable energy project is approved. Projects with large areas needed for infrastructure should research the eligibility of the land. National parks and wild life protected areas should not be disturbed neither the populations of endangered species. Each country's regulations regarding such areas, as well as archeological and historic areas, should be taken into consideration. Detailed analysis of the project's impact on surrounding area and population should be provided.

2.5.3 Politics and incentives

Politics play an important role in the development and utilization of renewable energy projects. There is fierce competition in the energy industry and to implement new projects and ideas, there is a need for involvement of political authorities with the implement for example of subsidies, penalties and further regulations. There is need for research for technological development, which is funded by the government. In order to get people to invest in renewable energy technologies, there's need for incentives, such as tax reductions,

subsidies and regulations in favor of renewable energy advancement. Policies need to exist to demand the integration of renewable energy to the power grid. Renewable energy standards or renewable portfolio standards are regulations implemented by each country, to oblige electricity supply companies to generate a specific fraction of their electricity from renewable sources. Stricter policies regarding greenhouse emissions could further help the turn to renewable energy resources. The subsidies for conventional energy sources are so far much higher than those for renewable energy.

Tax incentives for renewable energy usually include investment and production tax deduction, property tax reduction, tax credits for research and development of equipment, taxes for use of conventional fuels etc. For USA for example, the policies and incentives for renewable energy for each state, can be found on the Database of State Incentives for Renewable Energy (DSIRE). Renewable energy is supported from both state and federal policies. In the European Union (EU) there has been continuous support for the development of renewable energy with the goal of reaching the amount of 20% of energy consumption from renewable by 2020 as a whole, while the percentages are even higher for individual countries. Major progress has been made especially on wind and ethanol farms and PV systems, with Japan, Germany and Spain being currently the biggest markets for the latter. Europe promoted wind energy by using two methods, the first was price support for kilowatt hour production and the second method was based on capacity. Germany is the top country in Europe in wind energy capacity. Its progress is mainly due to a law passed in 1990, which made utilities buy renewable energy from power producers at a minimum price, which was defined by the government. Investment grants and low-interest loans were also a possibility. China was the top country in 2018, in wind capacity, due to favorable policies implemented by the government for wind farm installations. It was also mandated that the majority of wind turbine components had to be manufactured within the country.

A similar process was conducted with PV installations. Spain and Germany lead the way in 2009 in PV installed capacity due to feed-in tariff systems that were implemented. In Israel, it was required in 1980 that there would be solar water heating in every new building being constructed. Incentives are also the reason for the increase in ethanol production.

2.5.4 Economics of renewable energy

For a renewable energy system to be built and run, it has to be determined that it will be profitable when taking account the cost of the installation and the net annual energy production. It will also need to be preferable, when costs and output are considered, to the competitive sources of energy that are available in each area. The development of renewable energy has been achieved due to the uncertainty that exists of future energy costs, the dependence on oil that is mostly imported and the goal of reducing harmful emissions.

There are many economic factors to be considered when deciding to buy a renewable energy system, whether it is for domestic use or commercial and industry purposes. The most important are the initial costs for installation, land costs, the value of produced power and the cost of energy from competitive sources. Regarding the system, there's the cost depending on the type, size and manufacturing company. The energy resource plays a vital part on the economics aspect, as the variations from year to year and within the year will determine the success of the operation of the installation. Operation, maintenance, insurances, inflation, legal costs and incentives are also among the many things that make up the economic aspect of a renewable energy production venture. In case of a large renewable project the most important things to consider are the land, which has to have a very good resource, the contract made to sell the generated electricity and the access to transmission lines, a factor vital to the overall successful operation of the project.

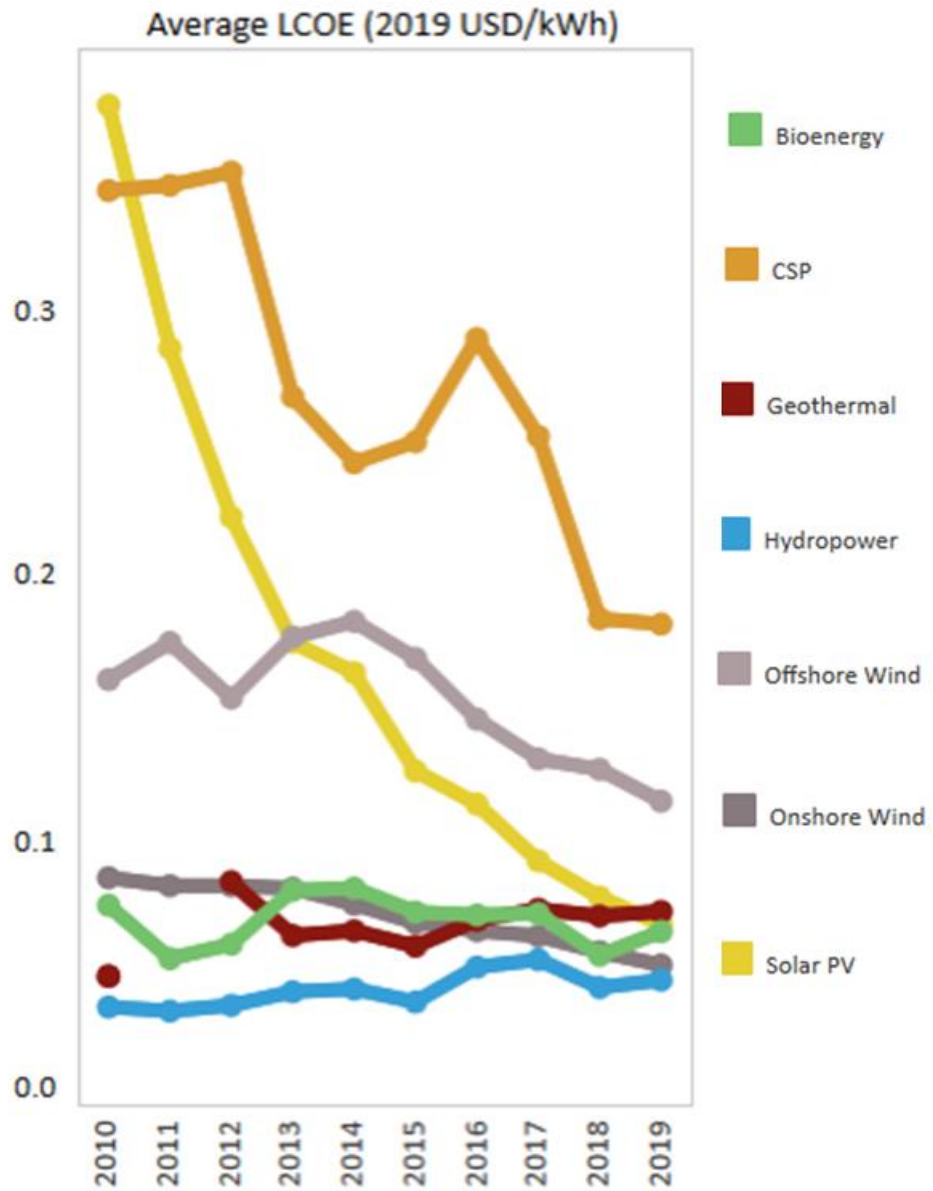

Figure 2-51: Average levelized cost of energy (LCOE) (2019 USD/kWh) trend for renewable technologies. [15]

Figure 2-51 shows the trend in the levelized cost of energy (LCOE) (2019 USD/kWh) for different renewable technologies. LCOE is roughly calculated by taking into account the sum of costs of the project over its lifetime and dividing it by the sum of electricity produced over its lifetime. LCOE values in Figure 2-51 are calculated based on project data for total installed costs and capacity factors. Renewable technologies, such as solar power and wind power technologies, show a decrease with time in their LCOE values. Since these technologies don't

include any fuel costs and if there are no major variations in their operation and maintenance costs, then their LCOE values are in proportion with their estimated capital costs. These costs mainly decrease due to technological improvements on equipment and capacities. For technologies with important fuel costs, their LCOE values are affected both by capital costs and fuel costs.

Renewable energy technologies have become cheaper due to technological progress, increased competition and provided incentives. The International Renewable Energy Agency (IRENA) predicts that their cost will be the same or even lower than the cost of conventional energy by fossil fuels, in a few years time. Solar and wind power are expected to produce half the world's energy needs by 2050. Renewable energy is considered the most economic option for new grid-connected capacity in locations with good resources.

3 Physics of sunlight and photovoltaics

Author(s): Dr Efterpi Nikitidou
Dr Andreas Kazantzidis

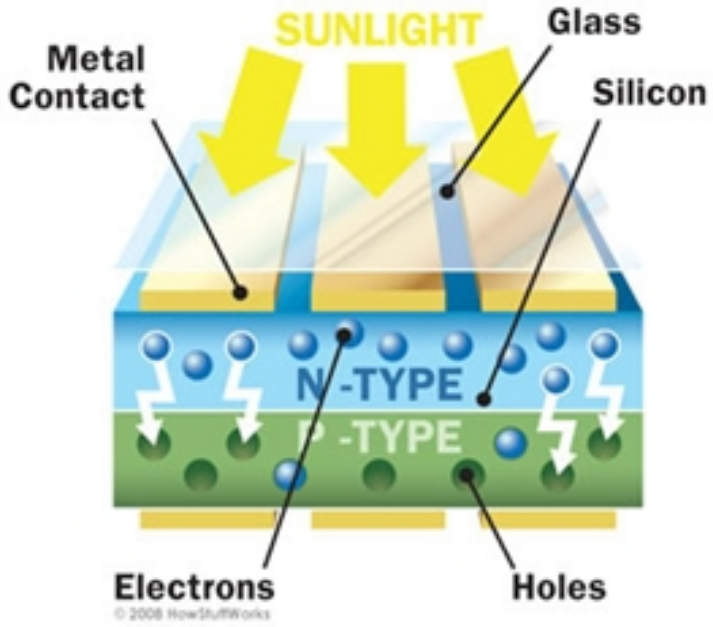

3.1 Solar Radiation

The Sun is a sphere of hot plasma that has a diameter of 1.39×10^9 m and a mass of 1.989×10^{30} kg. Its average distance from Earth is 1.496×10^8 km. It consists mainly of hydrogen (92%) and helium (8%), along with small amounts of other elements. In the plasma the electrons are separated from the nuclei due to their high kinetic energies, which result in high temperatures. The Sun is an approximate black body with an effective temperature of 5777 K, while the temperature at its center is estimated to be around 15.7×10^6 K. The Sun's energy is generated through nuclear fusion, where hydrogen (four protons) is converted to helium (one helium nucleus) with the difference in mass being converted to energy. This process will continue for another 5 billion years before the hydrogen is depleted and the burning of helium begins.

The energy that is produced in the core of the Sun is transferred to the surface by radiative and convective processes and is then radiated into space. Figure 3-1 shows the structure of the Sun and the zones of radiative and convective processes. Radiation in the Sun's core is in the x-ray and gamma ray part of the spectrum and as temperature decreases with distance from the core, the wavelengths of radiation increase. The photosphere, which is the upper layer of the convective zone, is the source of most emitted solar radiation, with an effective temperature of 5777 K. The Sun radiates an amount of power equal to 3.845×10^{26} W in all directions and Earth receives only a small part of that. In order to calculate this part that reaches Earth, Sun's power is divided with the area of a sphere with radius the average distance of Sun-Earth.

$$G_{SC} = \frac{Psun}{4\pi r^2} = \frac{3.845 * 10^{26} W}{4\pi (1.496 * 10^{11} m)^2} = 1367\ W/m^2 \qquad \textit{Equation 3-1}$$

G_{SC} is the solar constant, equal to 1367 W/m^2 and it's the energy received on a unit area of surface perpendicular to the direction of propagation of Sun's radiation, per unit of time, outside Earth's atmosphere.

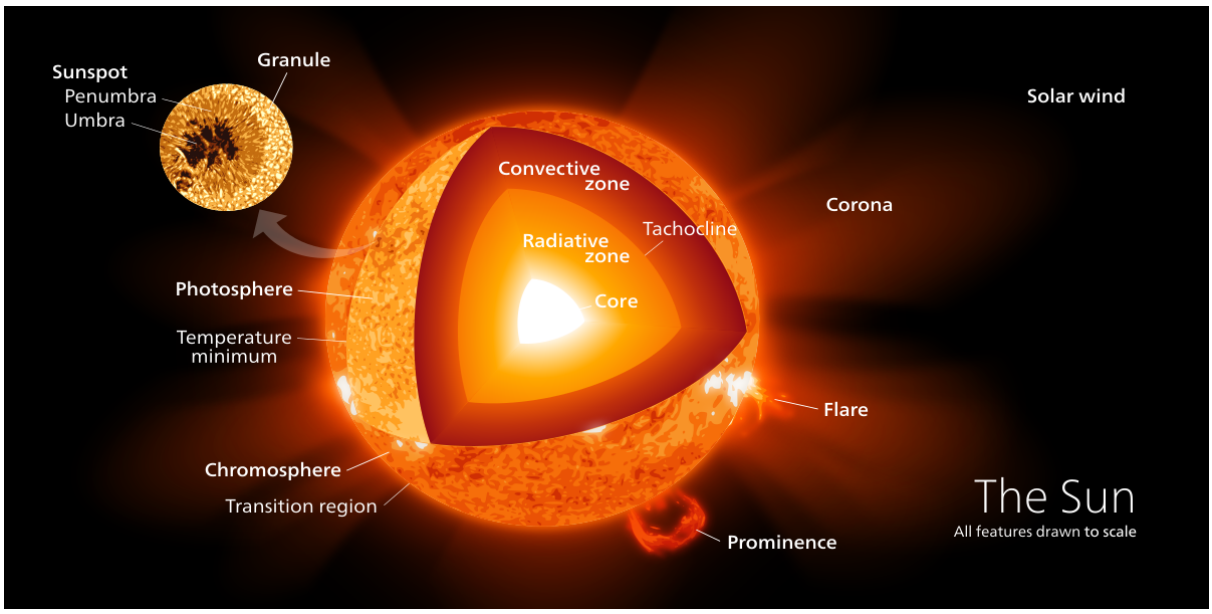

Figure 3-1: Structure and layers of the Sun. [74] Licensed under CC BY-SA 3.0

The spectral distribution of Sun's radiation is described by Planck's law, for a black body with effective temperature of 5777 K. Figure 3-2 shows the idealized black body spectrum (dashed line) and the actual spectrum as it is measured outside and inside Earth's atmosphere. The spectrum outside the atmosphere corresponds to an Air Mass (AM) of 0, meaning that light hasn't travelled through the atmosphere. For radiation at sea level, the spectrum for AM=1.5 is considered, which is the spectrum in spring and autumn and it represents the average year's spectrum. In the spectrum at sea level, the absorption zones and lines of the atmospheric gases are evident.

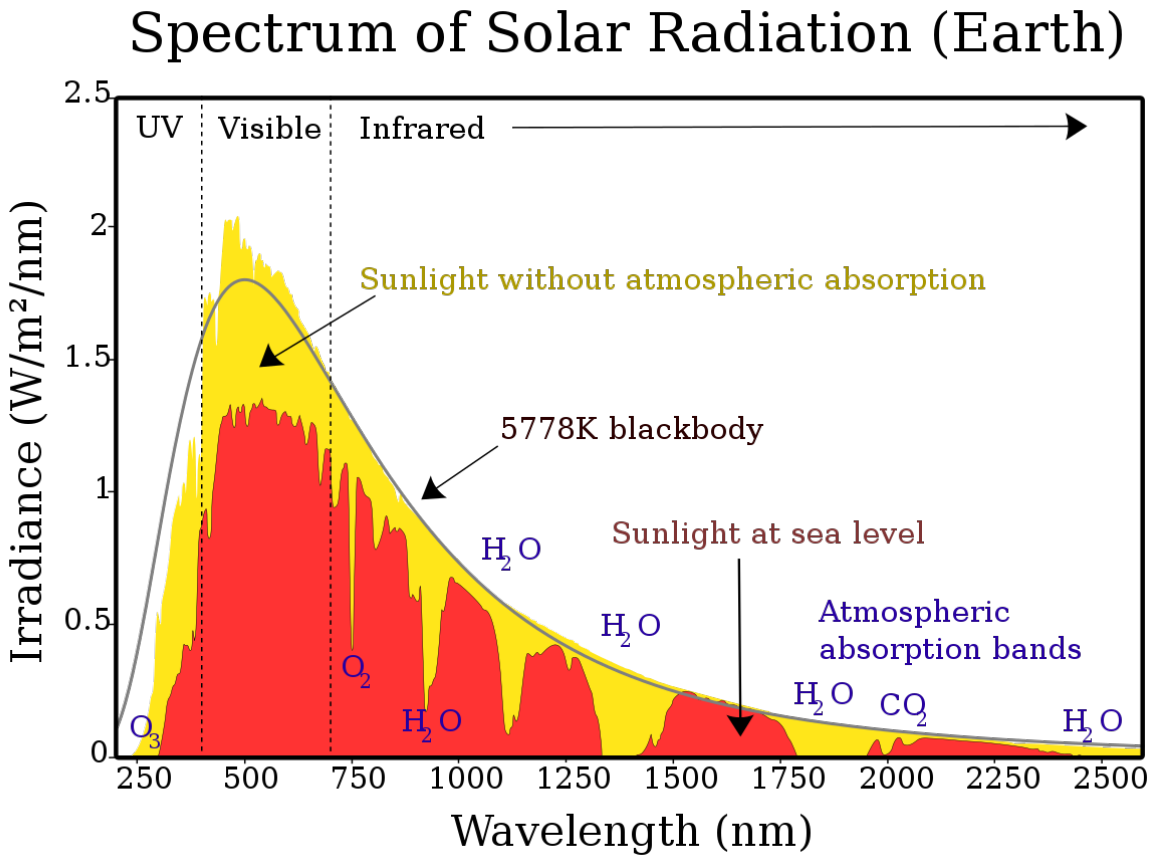

Figure 3-2: Solar spectrum outside the atmosphere and at sea level. [75] Licensed under CC BY-SA 3.0

As solar radiation travels through the atmosphere there are several processes that change it and the amount received on the surface is different. The absorption from molecules, as already mentioned, in a major factor. There are vast zones as well as specific wavelengths that are absorbed by oxygen molecules, ozone, water vapour, carbon dioxide, especially in the infrared part of the spectrum. Sunlight is also reflected in the atmosphere, reducing the received radiation on the surface. Finally there is Rayleigh scattering, from particles smaller that the incident wavelength, so this scattering is important mainly on shorter wavelengths and Mie scattering from particles larger than the incident wavelength, aerosols and dust particles.

3.1.1 Air Mass

The spectrum changes as it passes through the atmosphere and the way it changes depends on the path it travels. The longer the path through the atmosphere, the larger the amount of radiation being reflected, absorbed and scattered, thus the less the amount received on the surface. The term Air Mass (AM) is used to describe the ratio of the mass of atmosphere the direct radiation passes through to the mass of atmosphere it would pass through if it travelled in a vertical direction (Sun at zenith). The Air Mass is given by Equation 3-2, where θ_z is the zenith angle. AM is 1.5 for zenith angle 48.2° and 2 for a zenith angle of 60°. Figure 3-3 provides an illustration for understanding the Air Mass and its calculation.

$$AM = \frac{1}{cos\theta_z}$$ *Equation 3-2*

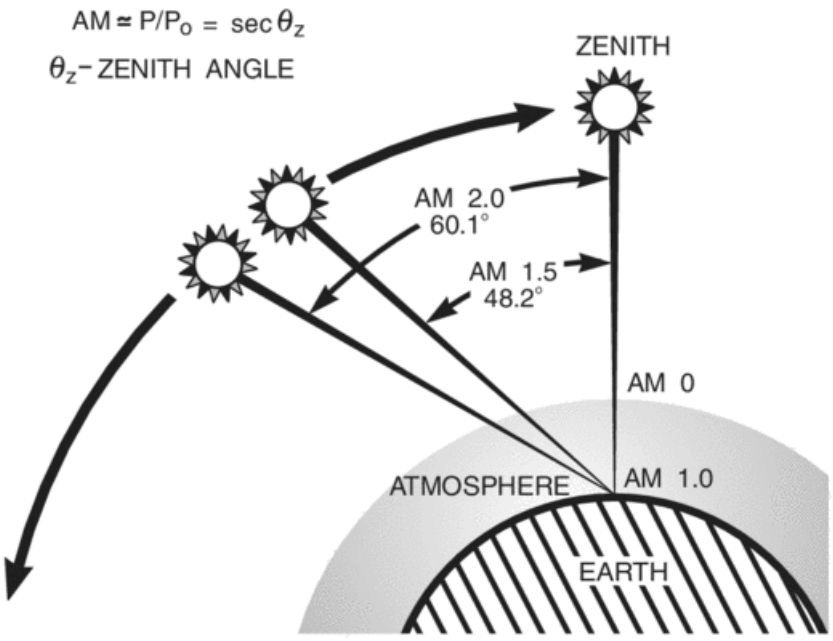

Figure 3-3: Illustration of Air Mass. [76] Licensed under CC BY 4.0

3.1.2 Direct and Diffuse Radiation

The radiation received on a surface is called global radiation and is the sum of two parts, the direct and diffuse radiation (Equation 3-3). Direct radiation is the component that is received from the Sun without having been scattered by the atmosphere and has a definite direction. Diffuse radiation is the radiation received on a surface after it has changed its direction due to scattering by the atmosphere.

$$E_G = E_{Direct} + E_{Diffuse} \qquad \textit{Equation 3-3}$$

Figure 3-4 shows an example of the daily variations of direct and diffuse radiation, received on a horizontal plane, along with their sum, global radiation, for a day with clear conditions. The most important variable for a photovoltaic installation is the global radiation received on a horizontal level.

$$E_{GH} = E_{Direct} * cos\theta_Z + E_{Diffuse} \qquad \textit{Equation 3-4}$$

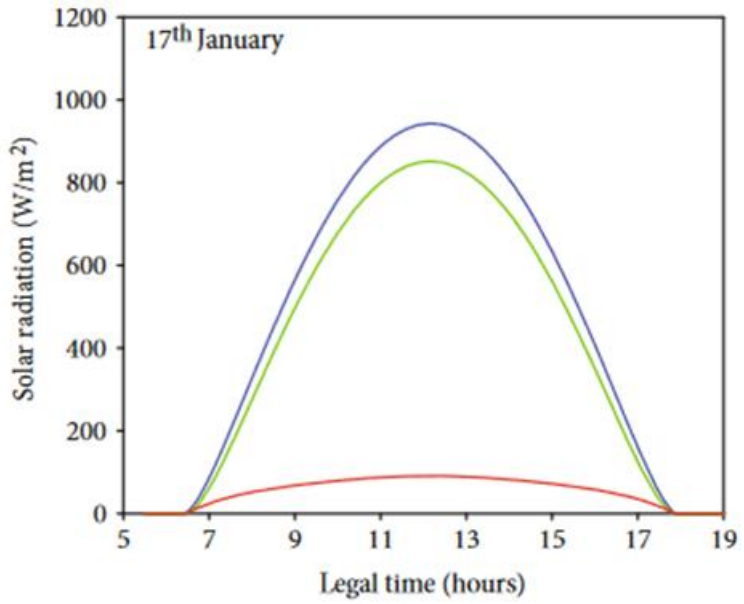

Figure 3-4: Example of modelled daily variations of direct (green), diffuse (red) and global (blue) radiation on a clear day. [77] Licensed under CC BY 4.0

3.1.3 Geometry of Sun-Earth system

Earth rotates around the Sun in an elliptical orbit, as it rotates around its own axis, in a 12-month periodic cycle. The amount of radiation received on the surface depends on the relevant position of Earth and Sun and several geometric parameters are needed for its calculation. Earth's rotational axis is tilted and it forms an angle with the axis of the orbital plane, equal to 23.45°. Due to this tilt, the Sun's rays form an angle with the equatorial plane, the declination angle δ, which ranges between -23.45° and 23.45° (Figure 3-5).

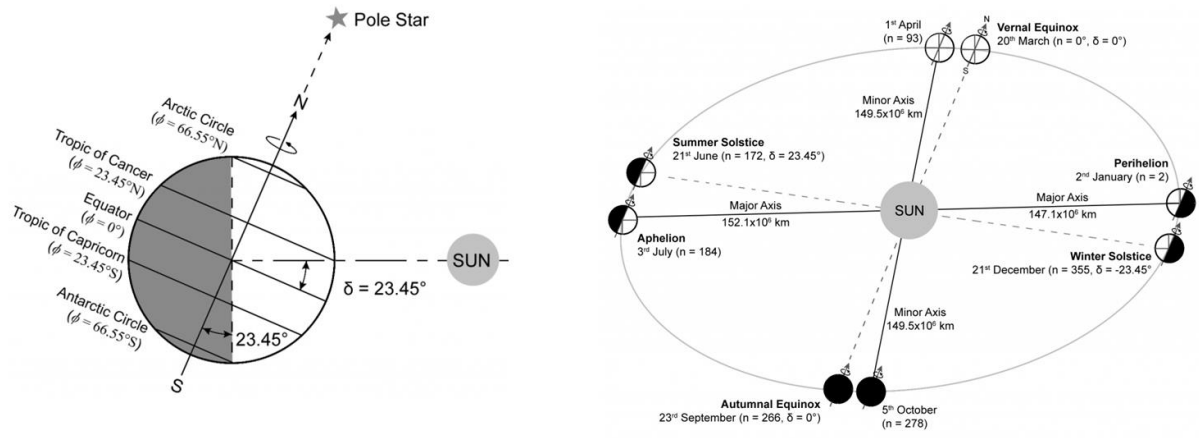

Figure 3-5: Declination angle and its variation during the year. [78]

On the horizontal plane, the angles that determine the position of the Sun in the sky are the zenith angle, the solar altitude and the azimuth angle (Figure 3-6). The zenith angle, θ_Z, is the angle that is formed between the line of sight of the Sun and the vertical axis. The solar altitude, α_S, is the angle between the horizontal axis and the Sun's position and is the complement of the zenith angle. The solar azimuth angle, γ_S, is the angular displacement from south of the projection of Sun's position.

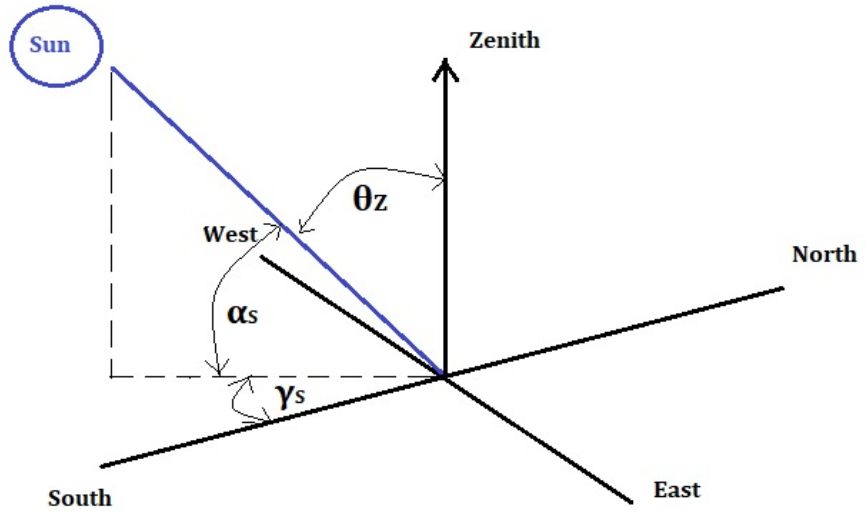

Figure 3-6: Solar angles on a horizontal plane. [79]

In summer, as the North Pole is tilted towards the Sun, the solar altitude at noon, at a site in the Northern Hemisphere, is higher than in winter. When planning a photovoltaic installation it is very important to consider the solar altitude of the winter solstice.

3.1.4 Sun path

For photovoltaic projects to be installed there's a need for detailed solar information. The path of the Sun in the sky is a useful parameter and is given by the local solar time (LST). Local solar time is time based on the apparent angular motion of the Sun across the sky with the solar noon being the time the Sun crosses the meridian of the site. Local standard time differs from local solar time due to man-made adjustments like time zones and daylight savings time, as well as the eccentricity of the Earth's orbit. The Coordinated Universal Time (UTC) is referred to the zero meridian at Greenwich, UK. In order to convert standard time to solar time there are corrections that need to be applied, based on the difference in longitude between the local meridian and the meridian that local standard time is based on (central meridian of the time zone) and the equation of time, due to the perturbations in Earth's rate of rotation. Equation 3-5 gives the difference in minutes between local solar time and local

standard time, with L_{st} the longitude of the standard meridian of the local time zone, L_{loc} the longitude of the site and E the equation of time.

$$solar\ time - standard\ time = 4(L_{st} - L_{loc}) + E \quad \textit{Equation 3-5}$$

The equation of time E (in minutes) is calculated as:

$$E = 229.2(0.000075 + 0.001868cosB - 0.032077sinB - 0.014615cos2B - 0.04089sinB) \quad \textit{Equation 3-6}$$

$$\text{where} \quad B = (n-1)\frac{360}{365} \quad \textit{Equation 3-7}$$

and n is the day of the year, 1≤n≤365.

In order to calculate the solar altitude α_S and solar azimuth γ_S, the site latitude ϕ, sun declination δ and the hour angle ω are needed. The hour angle is the angular displacement if the Sun east or west of the local meridian due to the Earth's rotation on its axis at 15° per hour.

$$\omega = (LST - 12) * 15° \quad \textit{Equation 3-8}$$

$$sin\alpha_S = sin\varphi * sin\delta + cos\varphi * cos\delta * cos\omega \quad \textit{Equation 3-9}$$

$$sin\gamma_S = \frac{cos\delta * sin\omega}{cos\alpha_S} \quad \textit{Equation 3-10}$$

3.1.5 Radiation on tilted surfaces

Photovoltaics are usually installed in a tilted position, forming an inclination angle β with the horizontal plane, for optimal operation. In this case, the radiation incident on the tilted surface (E_{tilt}) is the sum of three components, the direct radiation $E_{Dir,tilt}$, the diffuse radiation $E_{Dif,tilt}$ and the radiation that is reflected from the ground $E_{Ref,tilt}$ (Figure 3-7).

$$E_{tilt} = E_{Dir,tilt} + E_{Dif,tilt} + E_{Ref,tilt}$$ *Equation 3-11*

Each component will be calculated separately in order to estimate the total incident radiation on a tilted photovoltaic surface.

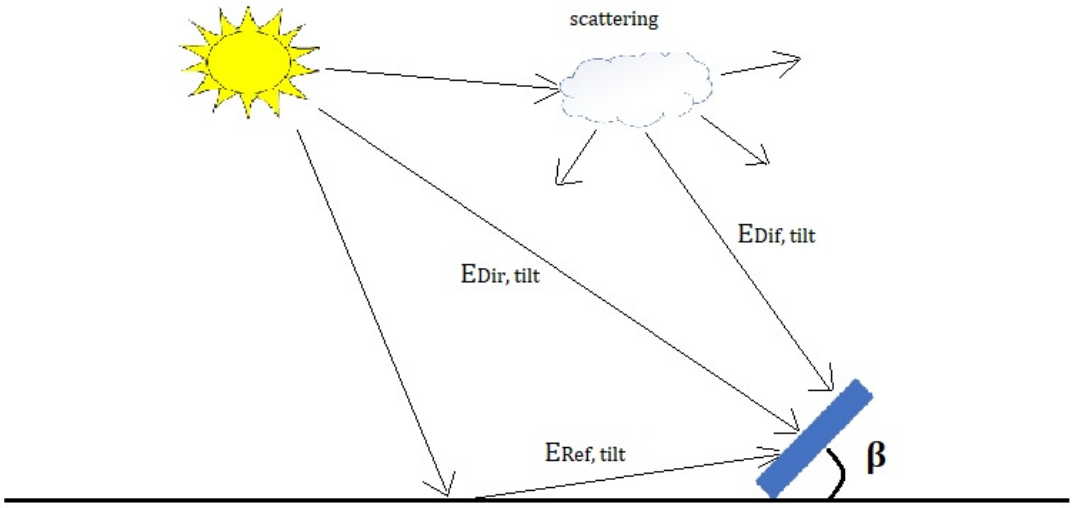

Figure 3-7: Components of incident radiation on a tilted surface. [80]

Figure 3-8 shows direct radiation incident on a horizontal surface of area A_{Hor} (left) and on a solar panel surface A_{Pan} at an inclination angle β (right). The power of the radiation on the horizontal surface is:

$$P = E_{Dir,H} * A_{Hor}$$ *Equation 3-12*

If there was a solar panel situated vertically to the sun rays direction, with area A_{Ver}, then it would take the same power on a smaller surface, that is:

$$P = E_{Dir,H} * A_{Hor} = E_{Dir,Vertical} * A_{Ver}$$ *Equation 3-13*

Looking at Figure 3-8, the three surfaces can be written with the following equations in terms of the angle χ, which is complementary to the inclination angle β and the angle α_S, which is the solar altitude.

$$A_{Ver} = A_{Hor} * sin\alpha_S \qquad \textit{Equation 3-14}$$

$$A_{Ver} = A_{Pan} * sin\chi \qquad \textit{Equation 3-15}$$

Since $\chi=\alpha_S+\beta$, then the direct radiation on a tilted surface of inclination β can be calculated from the direct radiation on a horizontal level and the solar altitude α_S.

$$E_{Dir,Gen} = E_{Dir,H} * \frac{sin(\alpha_S + \beta)}{sin\alpha_S} \qquad \textit{Equation 3-16}$$

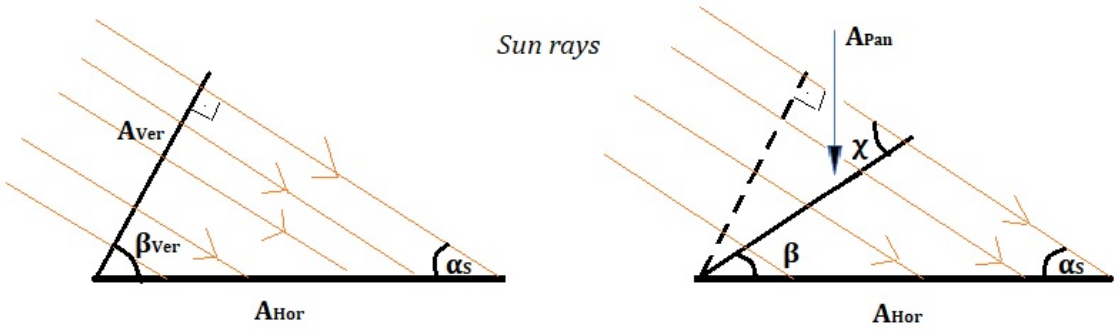

Figure 3-8: Direct radiation on a solar panel surface at two different tilt angles. [81]

In order to calculate the diffuse radiation on a tilted surface, the isotropic assumption is made, meaning that it is considered that the intensity of diffuse radiation is the same from any part of the sky. In that case, the diffuse component on a tilted surface can be calculated from the diffuse radiation on a horizontal surface and the inclination angle β.

$$E_{Dif,Gen} = E_{Dif,H} * \frac{1}{2}(1 + cos\beta) \quad \textit{Equation 3-17}$$

Finally, there is the radiation that is reflected from the ground and then received on the solar panel surface. An isotropic assumption is also made for the reflected radiation and it is calculated from Equation 3-18, where E_G the global radiation on the ground and ALB the ground albedo. The albedo depends on the material and there are values assigned to each type, e.g. grass, asphalt etc.

$$E_{Ref,Gen} = E_G * \frac{1}{2}(1 - cos\beta) * ALB \quad \textit{Equation 3-18}$$

3.2 Fundamentals of energy conversion in solar cells

Photovoltaic conversion of solar energy is a promising way to meet increasing energy demands. Solar energy is an infinite resource and the use of photovoltaic for its conversion is a process with no direct contamination of the environment. Photovoltaics (PV) is the direct conversion of solar energy to electric energy.

3.2.1 Physics of semiconductors

The basic part of a photovoltaic device is the solar cell, which consists of a semiconductor. To understand the operating principles of photovoltaics it is necessary to understand the physics that takes place in a semiconductor.

Every atom consists of a nucleus, which contains protons and neutrons and a shell, where electrons orbit around the nucleus (Bohr atomic model). Electrons can only orbit in specific

shells around the nucleus, with every shell describing the respective energy level. Thus in an atom there are the shells K, L, M, N and so on. Each shell has a specific number of electrons that are allowed to exist in that energy level. An electron needs to absorb energy, in the form of electromagnetic radiation (photons), to move to a higher shell and in an opposite manner radiation is emitted when an electron drops to a lower shell. With the absorption of enough energy, an electron can be free from the atom completely, in which case the atom becomes an ion (cation).

Figure 3-9 shows an illustration of Bohr's atomic model, with three shells described by their principal quantum number n (n=1 is the K shell, etc.). An electron jumps from the n=3 to the n=2 shell with the emission of a photon. The energy of the emitted or absorbed photon is given by Equation 3-19, where h is Planck's constant equal to $6.6*10^{-34}$ $Wsec^2$, ν is the radiation's frequency, λ the wavelength and c_0 is the light speed in a vacuum, equal to $3*10^8$ m/sec.

$$\Delta E = \left|E_{after} - E_{before}\right| = h * \nu = h * \frac{c_0}{\lambda} \qquad \textit{Equation 3-19}$$

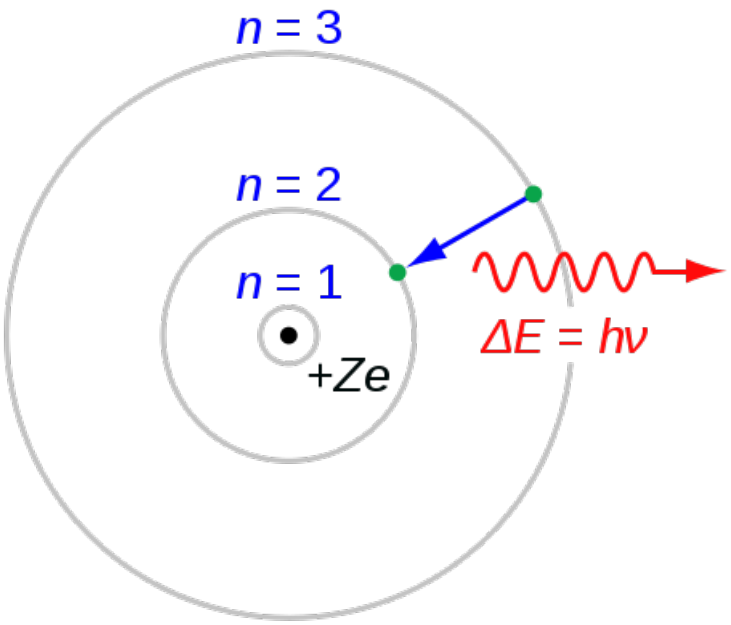

Figure 3-9: Bohr's atomic model. [82] Licensed under CC BY-SA 3.0

In a chemical element the electrons that occupy the outermost shell are called valence electrons. The predominant material in photovoltaic cells is silicon. Silicon has four valence electrons. In a silicon crystal, the valence electrons make connections with the corresponding electrons of a neighbouring atom. In general, in a semiconductor crystal there is an almost infinite number of atoms coupled together and the individual energy levels of each atom's electrons are not distinguishable. In this case the term energy bands is more appropriate. The highest band occupied by electrons is called the valence band and the first band that is empty of electrons is called the conduction band (Figure 3-10). In order for electrons to get from the valence to the conduction band they need enough energy to overcome the band gap. In a silicon crystal this band gap has energy equal to 1.12 eV. In absolute zero the electrons remain in the valence band. Temperature needs to be increased for electrons to overcome the band gap and jump to the conduction band, where they are considered free electrons and increase the crystal's conductivity.

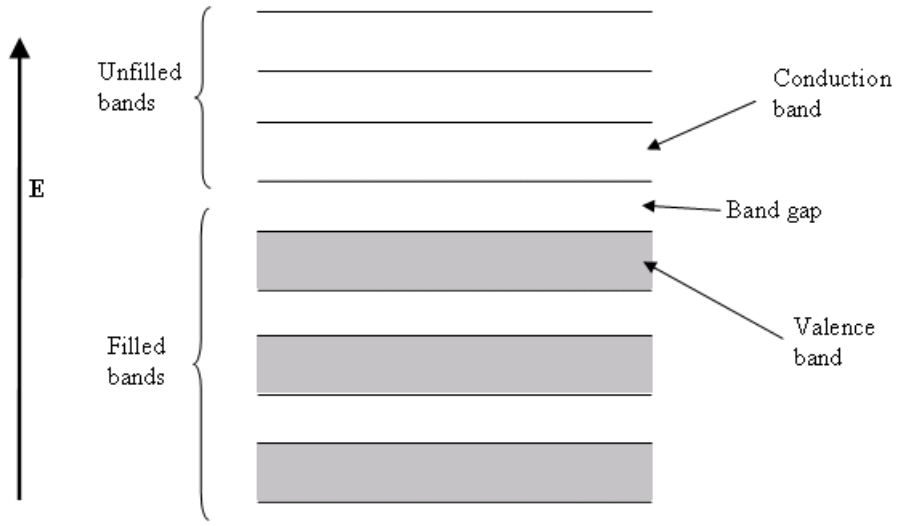

Figure 3-10: Band structure of a semiconductor. [12] Licensed under CC BY-SA 3.0

Semiconductors in general have band gaps with energies higher than 0 and up to 3 eV. At low temperatures they don't allow conduction, so they act as insulators. At medium temperatures conduction begins and increases at high temperatures where they act as good conductors.

Insulators have band gaps higher than 3 eV and in metals, the valence and conduction bands overlap, so they there is high conductivity even at low temperatures.

3.2.2 Doping of semiconductors

In a semiconductor electrons are freed continuously, generating a hole and at the same time electrons are captured by holes to recombine. At any time, there is an average number of free electrons and holes in the crystal, called the intrinsic carrier concentration, which depends on the material and the temperature. If an electric voltage is applied to the semiconductor, the electrons are accelerated in the direction of the positive pole and holes move in the opposite direction, creating a current.

Semiconductors are not the best electrical conductors but their conductivity can be increased and controlled. For that purpose the crystal is doped with foreign atoms. Negative-doping (n-doping) is done to increase the number of free electrons. Phosphorus is used for example for n-doping. Phosphorus has one electron more than silicon in the valance band, thus when four electrons bond with the neighbouring atom, the fifth is left with no bond and it serves as a free electron. The doping atom adds an energy level just below the conduction band so very little energy is required for the extra electron to jump to the conduction band (Figure 3-11). During positive-doping (p-doping), in which trivalent boron atoms are usually used, the number of holes is increased. Boron has three valance electrons so one bond is not completed and a neighbouring electron moves to complete that bond, resulting in the formation of a hole. Even though the densities of foreign atoms, in the doping process, are very low, the conductivity of the crystal can be greatly increased.

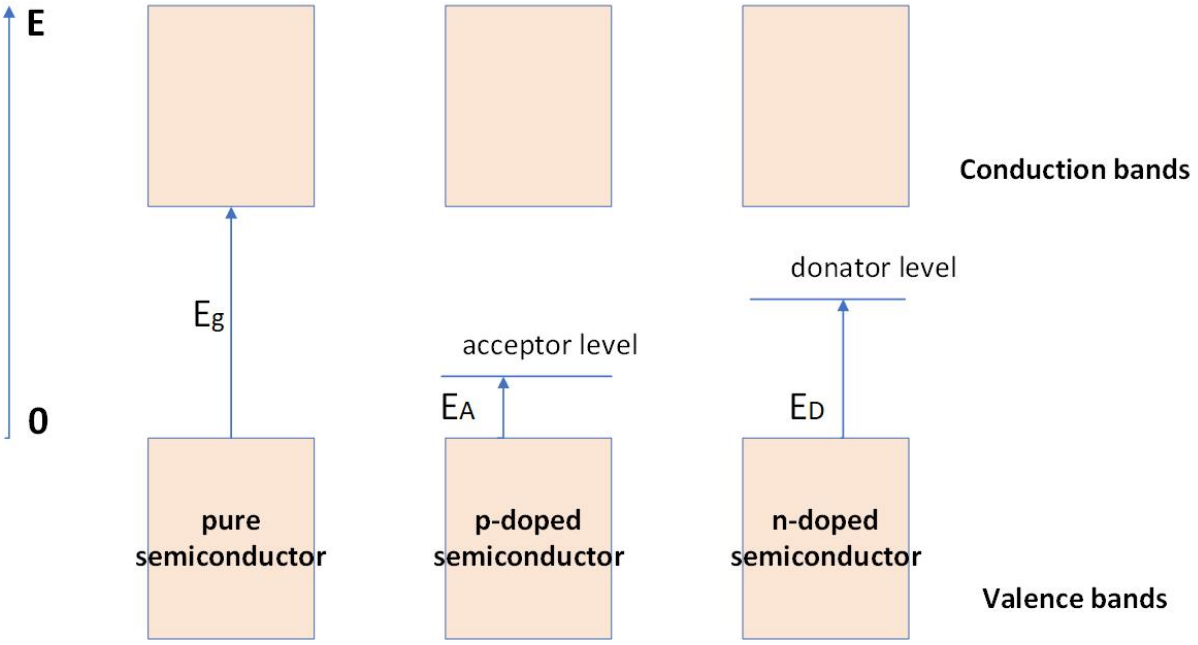

Figure 3-11: Energy bands in a pure, p-doped and n-doped semiconductor. [83]

3.2.3 The p-n junction in a semiconductor

Figure 3-12 shows the diagram of a p-n junction. A p-n junction is the boundary between two types of semiconductors, a p-type (left) and an n-type (right). The grey areas are electrically neutral. At the junction the surplus of free electrons of the n-type diffuse to the left into the p-type region to combine with the holes. At the same time the surplus of holes of the p-type diffuse to the right into the n-region to recombine with electrons. Thus in the n-type, a region near the junction becomes positively charged and vice versa in the p-type and an electric field is created. This field pushes electrons to the right and holes to the left and counteracts the diffusion process. When a balance is reached, there is a space charge region at the p-n junction, which causes a potential difference between the borders of that region.

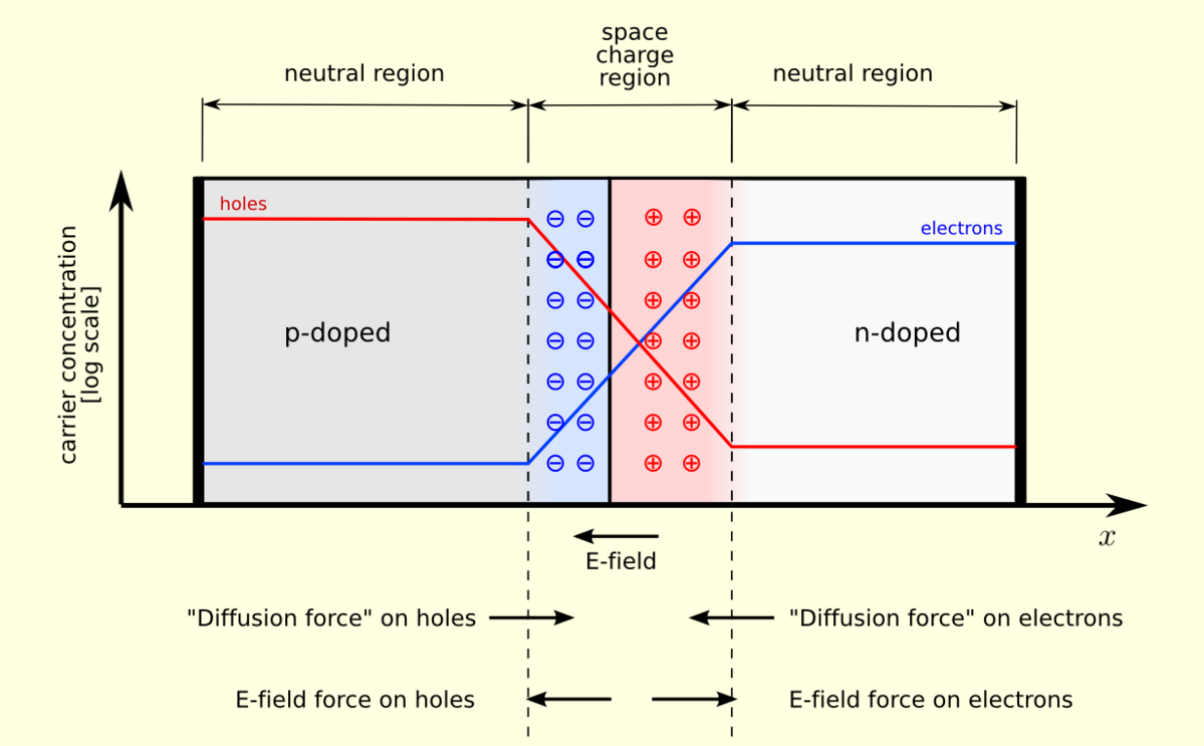

Figure 3-12: P-n junction diagram. [84] Licensed under CC BY-SA 3.0

A voltage can be applied, either in a forward bias, where the p-type is connected with the positive terminal or a reverse bias, where the p-type is connected to the negative terminal. In the forward bias, the electrons and holes are pushed towards the junction and the width of the space charge region decreases. Increase of the voltage leads to further reduction of the space charge region until it disappears and the current can now flow as the material becomes a conductor. In reverse bias, the width of the space charge region is enlarged and very little current flows through the junction. Increase of voltage leads to its breakdown and current begins to flow.

3.2.4 Light and semiconductors

When light is incident on a semiconductor, a photon can be absorbed to lift an electron from the valence to the conduction band. In order to do that, the energy of the photon must be higher or equal to the energy of the band gap. As radiation passes through the semiconductor, its energy decreases in an exponential way.

$$E(x) = E_0 * e^{-ax}$$ *Equation 3-20*

Equation 3-20 gives the energy at a depth x, E(x), as a function of the penetration depth x, the irradiance at depth x=0, E_0 and the absorption coefficient of the material, α.

Materials have different absorption coefficients, thus light interacts with them in a different way. Semiconductors are divided into two types, direct and indirect semiconductors. The difference is in their band gap, which can be a direct or indirect band gap. In a crystal, the lattice oscillations of the particles are allocated to a particle, called phonon. In the generation of an electron-hole pair both energy and momentum must be conserved. In an indirect semiconductor, the minimum energy state of the conduction band and the maximum energy state of the valence band are situated at different crystal momentums. As a result, an electron can't jump directly to the conduction band with the absorption of a photon but the participation of a phonon is also required. In a direct semiconductor however, the minimum energy state of the conduction band and the maximum energy state of the valence band are characterized by the same crystal momentum and the generation of an electron-hole pair can be achieved just with the participation of a photon. Figure 3-13 shows the opposite process, of an electron falling back to the valence band. In a direct band gap this is done with the emission of a photon (a), but in an indirect band gap an intermediate state is required where a phonon is also emitted (momentum is transferred to the crystal lattice) (b).

Indirect semiconductors have lower absorption coefficients that direct ones. Examples of indirect semiconductors are crystalline silicon, the most common material in photovoltaics and germanium. Thin-film solar cells are made of direct band materials, like amorphous silicon, cadmium telluride (CdTe) etc.

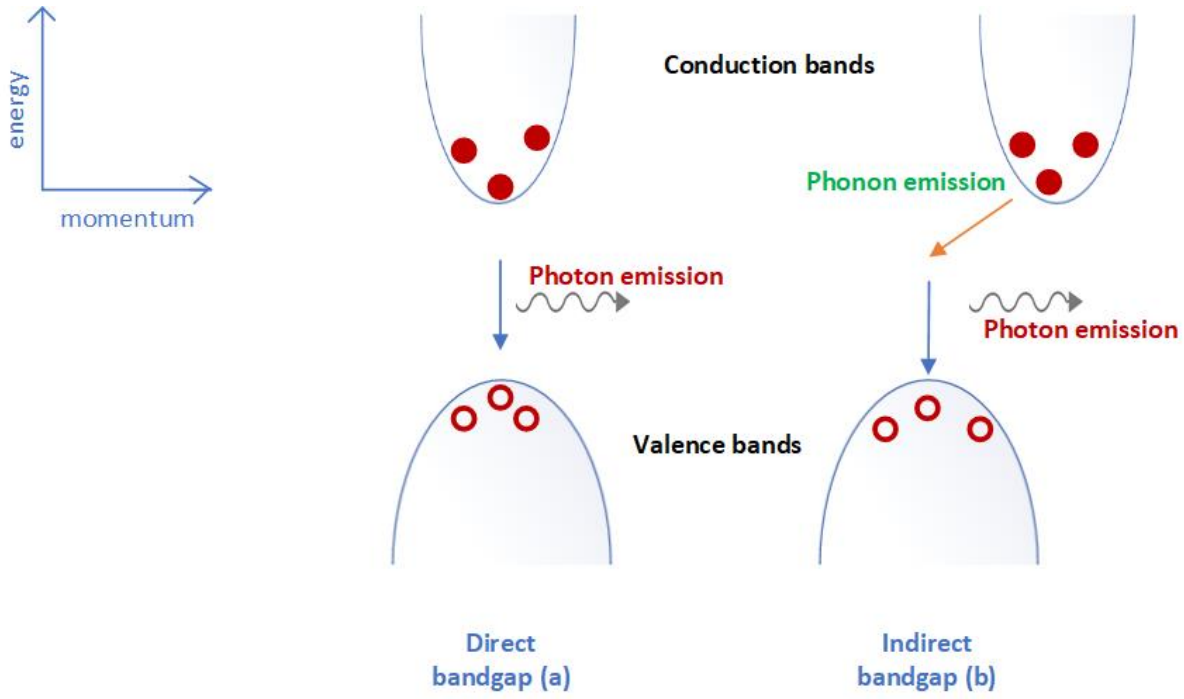

Figure 3-13: Photon emission in a direct and indirect semiconductor. [85]

3.3 Photovoltaic technologies

There are various photovoltaic technologies, depending on the material of the semiconductor that they use. Each material has distinct characteristics for sunlight absorption. Solar cells can be manufactured with one layer of the light absorbing material, single-junction cells or multiple layers, multi-junctions cells. The main photovoltaic technologies are divided into first, second and third generation cells. The first generation cells use crystalline silicon, the most common material in photovoltaic production, in both the monocrystalline and polycrystalline forms. Second generation cells are the thin film cells, which include amorphous silicon, cadmium telluride (CdTe) and copper indium gallium selenide (CIGS) cells. Third generation solar cells, which are not commercially used yet and are still under development, include organic materials for cell manufacturing.

3.3.1 Crystalline silicon

The production of a silicon solar cell begins with the conversion of quartz sand into silicon and is followed by the production of wafers.

Quartz sand is silicon oxide which reacts with carbon, in an electric arc furnace to a temperature of over 1900°C, to produce metallurgical silicon. Metallurgical silicon has around 2% impurities. In order to be used in solar cells it goes through a complex purification process. Metallurgical silicon is converted to trichlorosilane ($SiHCl_3$), in liquid form and hydrogen, in a reaction with hydrochloric acid, which typically takes place in a fluidized bed reactor at a temperature of about 300°C. Trichlorosilane has a boiling point of 31.8°C and is easily distilled repeatedly for further purification. After that, the liquid trichlorosilane is converted to solid polysilicon, commonly with the use of the Siemens process. In the Siemens process, trichlorosilane and hydrogen pass through a chemical vapor deposition reactor at a temperature of around 1000-1200°C. Trichlorosilane decomposes and silicon is deposited on thin silicon rods of high purity, which are placed inside the reactor and as a result highly purified polysilicon is produced. This process is relatively expensive and slow. An alternative method involves decomposition of silane (SiH_4) in a fluidized bed reactor. Silane and hydrogen gases are injected into the reactor bottom and a bed of small silicon seed granules become fluidized. As silane decomposes, silicon is deposited on the seeds, which grow in size. When they reach the desired size they are extracted and new seed granules are inserted to the reactor. This process is more energy efficient, less expensive and is a continuous process in contrast to the Siemens process. Figure 3-14 provides an illustration of the Siemens (a) and the Fluidized Bed Reactor (b) processes. The structure of the polysilicon is not good enough to be used in solar cells and there are further processes to improve the crystal's properties.

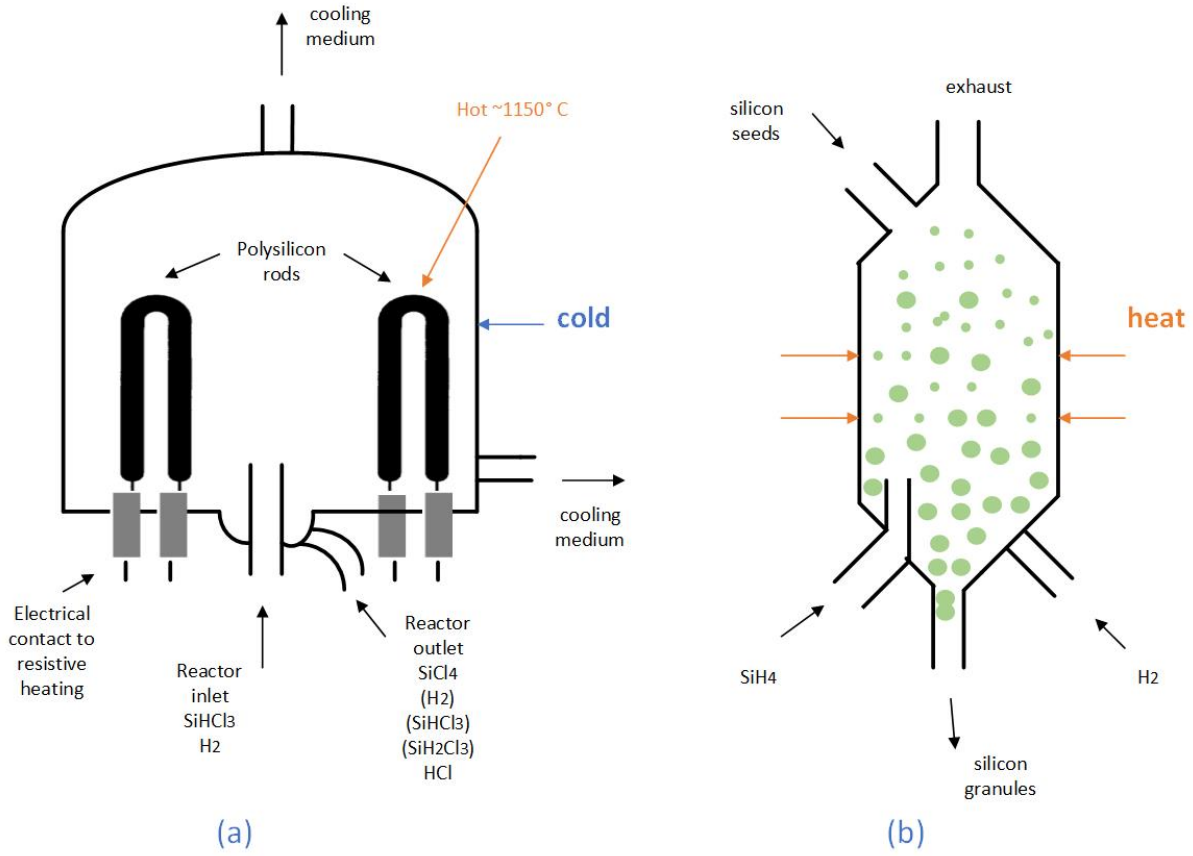

Figure 3-14: Illustration of the Siemens (a) and Fluidized Bed Reactor (b) processes for the purification of silicon. [86]

3.3.1.1 Monocrystalline silicon production

For the production of monocrystalline silicon from polysilicon, the Czochralski method is used (Figure 3-15). Highly purified silicon is melted in a crucible, usually made of quartz, at a temperature of a little over 1400°C. A rod-mounted seed crystal is dipped into the molten silicon with a specific orientation and is then slowly pulled upwards while it is rotated. Fluid silicon gets attached to the rod and crystallizes. The temperature, rate of pulling and speed of rotation can be controlled to adjust the thickness of the monocrystalline silicon rod. With this method the rods than can be produced have a diameter up to 30cm and a length up to 2m.

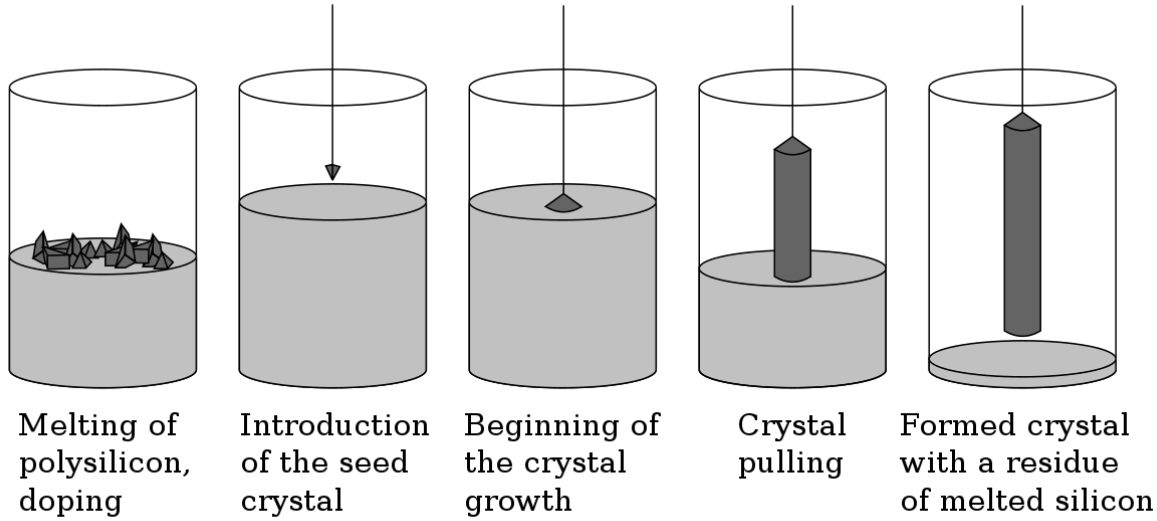

Figure 3-15: The Czochralski process. [87] License: Public Domain

For further improvement of the crystal quality, another method can be used instead of the Czochralski process, the Float Zone process (Figure 3-16). In this case, the seed crystal is placed under a vertical polysilicon rod. An induction coil is slowly pushed, beginning from the bottom, upwards over the rod, melting the silicon as it passes. The monocrystal is formed from the bottom upwards. In this method, any impurities are driven upwards during crystallization and a high crystal quality is achieved. The Float Zone process is more expensive than the Czochralski process therefore it is not commonly used.

Monocrystalline silicon systems have great conversion efficiency, with average values around 18-22% and even higher values achieved in laboratory conditions but they have high manufacturing costs and require pure materials and perfect crystal structure.

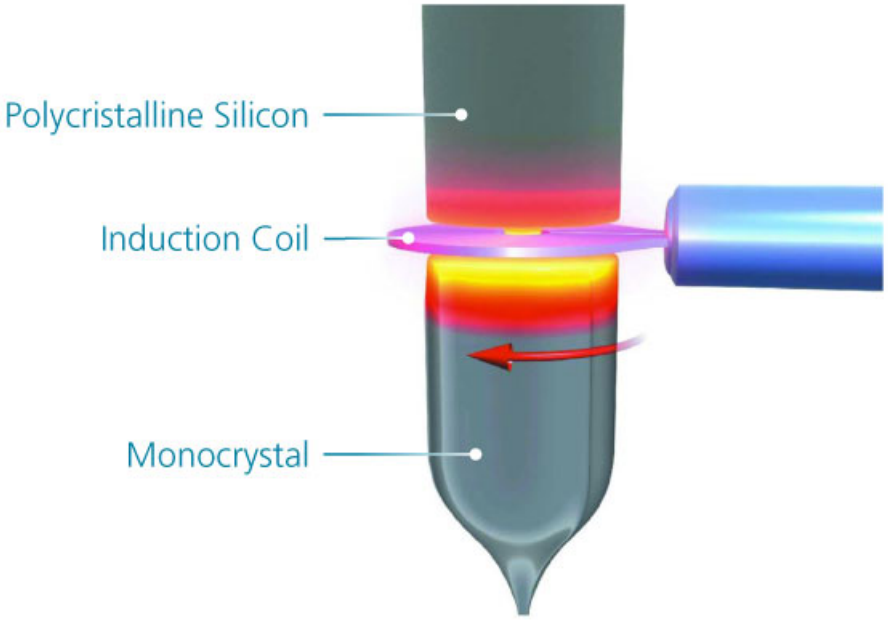

Figure 3-16: The Float Zone process. [88]

3.3.1.2 Multicrystalline silicon production

Multicrystalline silicon has typically 2-3% lower efficiency than monocrystalline silicon due to lower material quality but the production cost is lower and the crystal structure doesn't need to be perfect.

The process for the production of multicrystalline ingots is presented in Figure 3-17. Polysilicon pieces are put into a graphite crucible and they are melted using induction heating. The crucible is then let to cool from the bottom as the heating ring is being pulled upwards. On the bottom of the crucible small monocrystals begin to form and start growing sideways until they meet each other. Since the cooling takes place in a vertical direction, the crystals grow in a column. Crystal displacements which form at the boundary layers become centers of recombination in the cell. The monocrystals are allowed to grow as much as possible. After the melting completes, the silicon block that has formed is cut into ingots.

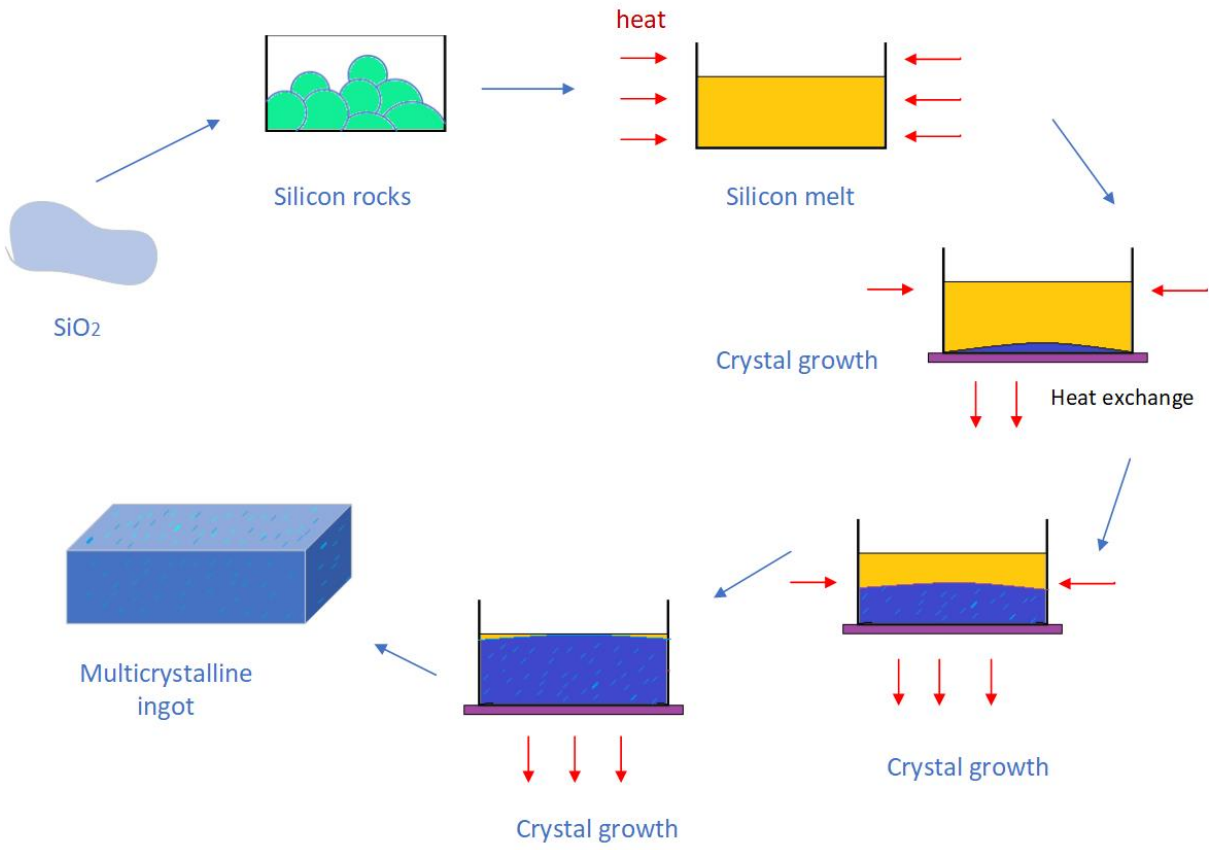

Figure 3-17: Multicrystalline ingot production. [89]

3.3.1.3 Wafer production

The next step, after the production of ingots is to saw them into wafers. This is usually done with the use of wire saws. The ingot is attached to a top plate and as it is lowered though the wire blades, it is cut into wafers (Figure 3-18). The saw consists of hundreds up to a thousand wires with a diameter of 0.2mm or less, which move at high speed. There are two slicing methods, the fixed abrasive slicing and the loose abrasive slicing (Figure 3-19). In fixed abrasive slicing, diamond abrasive particles are chemically bonded to the high speeding wire and the cut is made by pressing the ingot against the wire while coolant is applied. In loose abrasive slicing, slurry, which is a suspension of abrasive particles like water, oil or other materials, is applied to the wire which runs at high speed and the cut is made by the rolling motion of abrasive particles between the wire and the ingot. In the saw wire method there are saw losses which can be as large as the parts produced. In fixed abrasive slicing, with

diamond particles, there is the possibility of cleaning the silicon chips and using them again for wafer production.

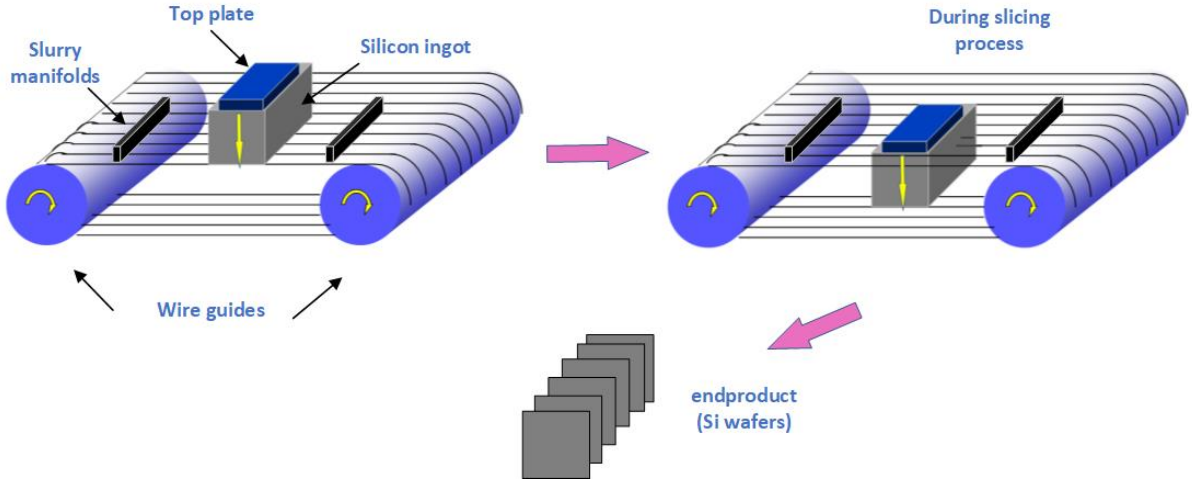

Figure 3-18: Wire saw wafer production. [90]

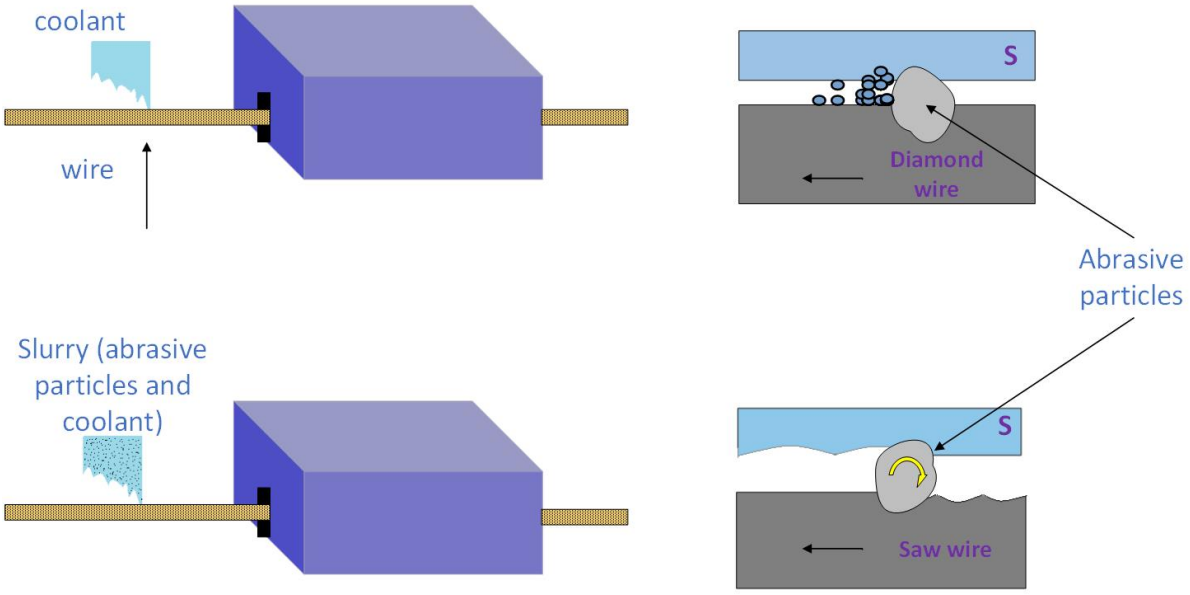

Figure 3-19: Fixed abrasive slicing (top) vs loose abrasive slicing (bottom). [90]

Another method is to produce silicon sheets directly without the need for sawing. This way the saw losses can be prevented. The method is based on the Edge-Defined Film-Fed Growth (EFG) process, where a thin sheet of silicon ribbon is pulled from a strip of molten silicon,

which is formed by means of capillary force at the top of a graphite dye. Another version is to pull the ribbon from an octagon-shaped gap. The wafers are then cut from the sides of the octagon, with the use of lasers. These two methods are depicted in Figure 3-20.

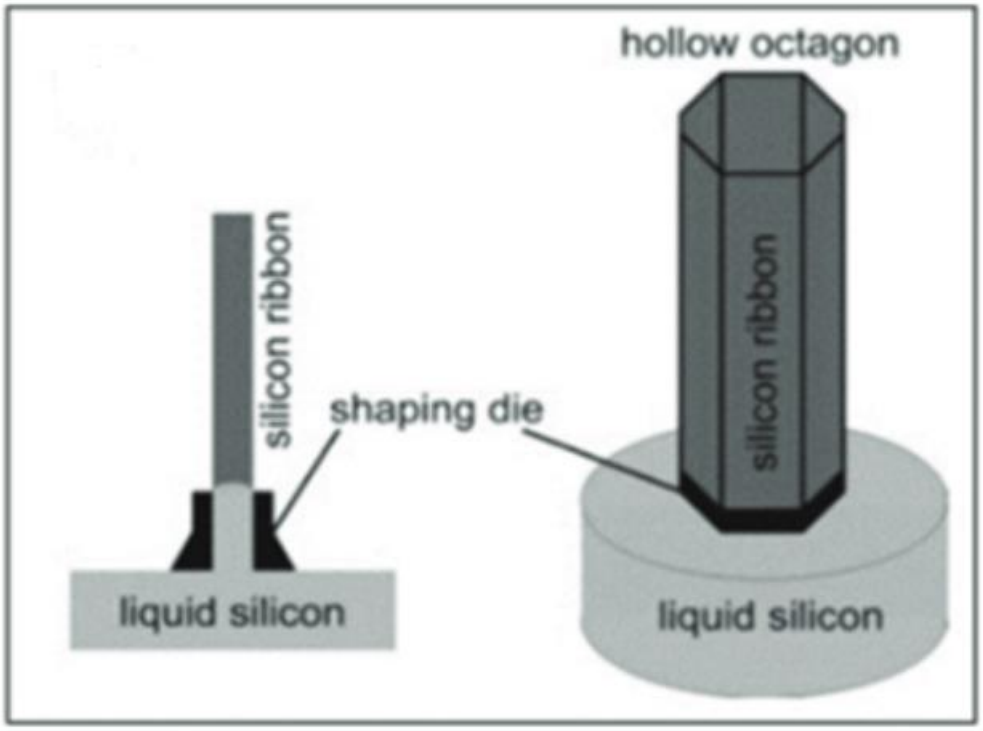

Figure 3-20: EFG method for wafer production (left) and growth of polygonal silicon ribbon based on EFG method (right). [91], adapted from [92].Licensed under CC BY 3.0

3.3.1.4 Solar cell production

The next step is the production of the standard crystalline silicon solar cell. This is achieved by following the process depicted in Figure 3-21. The wafers, which are already doped, are dipped into an etching bath with the purpose of removing contaminants or any damage to the crystal surface and after that is the texturizing of the surface, with is done for example with etching with potassium solvent. Then next step is the formation of the p-n junction. This is done with the method of emitter diffusion. The wafers, which are already doped with p-type material, are given a negative type surface by diffusing them with a phosphorus source at high temperatures. A phosphosilicate glass (PSG) is formed on the wafer surface, which is later removed. After the formation of the p-n junction, follows the anti-reflection coating,

which is done with the deposition of a silicon nitride coating. In the screen printing process next, the contacts are applied. A mask with slits gets placed on the cell and metal paste is brushed on, so it can be placed in particular positions of the wafer. For the rear side contacts, first the application of the soldering contact surfaces of silver paste is done and after that the rear side is covered with aluminum. After that follows the front side contacts application. The contact firing of the cells that follows is done at high temperatures to harden the pastes and for firing the anti-reflection layer between front contact and emitter. The aluminum atoms at the rear contact are diffused into the base so the p-layer for the back-surface field can be generated. An edge isolation step follows, with an etching or laser process, because during the phosphorus diffusion, the n-doping wasn't just done on the desired surface but also around the edges of the wafer, causing a short circuit at the p-n junction. The final step is to test the cell under simulated sunlight conditions and to classify it according to its efficiency. The solar cell can then be used in the assembly of solar modules.

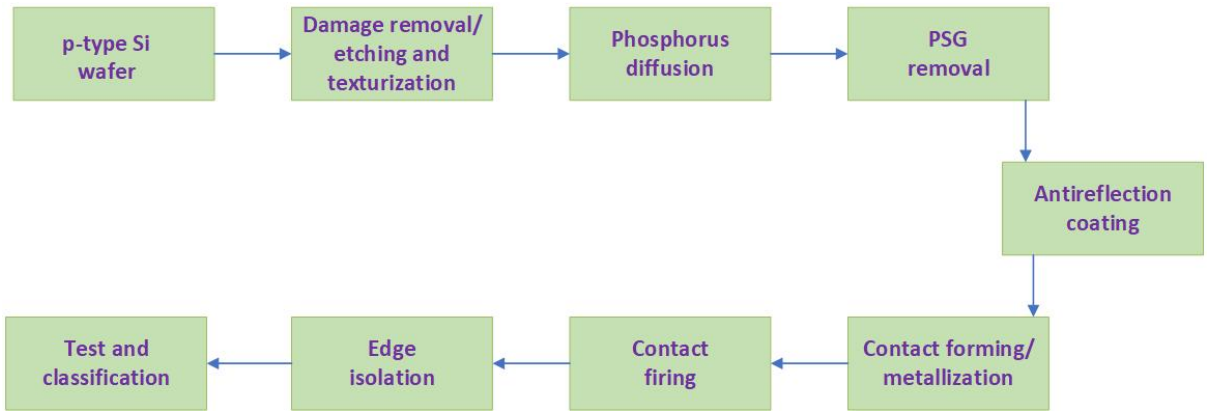

Figure 3-21: Standard crystalline silicon solar cell production steps.

3.3.1.5 Solar module production

Figure 3-22 shows a comparison of multicrystalline (left) and monocrystalline (right) silicon solar cells. After the production of solar cells, the next step is their integration into the solar module.

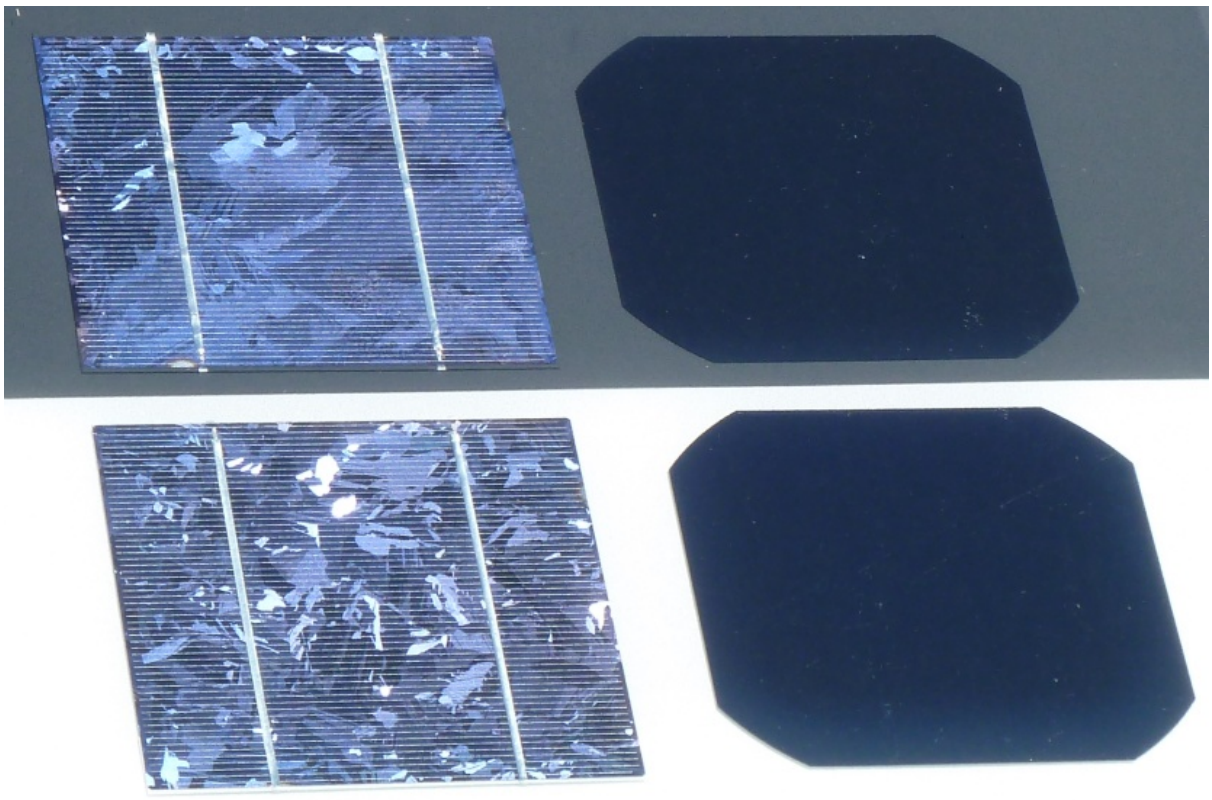

Figure 3-22: Comparison of multicrystalline (left) and monocrystalline silicon (right) solar cells. [93] Licensed under CC BY-SA 3.0

A solar module can have a glass-foil or a glass-glass structure (Figure 3-23). In a glass-foil module, the cells are electrically connected in series with galvanized copper strings, forming a cell string. The cell string is situated between two EVA (ethylene-vinyl-acetate) or POE (Polyolefin elastomer) transparent sheets. On the front side a glass sheet is placed and on the rear side a rear-side foil. It is all heated in a vacuum and the EVA (or POE) material softens and flows around the solar cells and afterwards hardens. The rear-side foil serves to protect from moisture and as an electric insulator and is usually a TPT back sheet, made of polyvinyl fluoride and polyester films. The module has its edges sealed before being put into the aluminum frame.

In a glass-glass module, the solar cells are sandwiched between glass on both front and back and the risk of cell breakage is reduced, cells are not so susceptible to shear stress. There is no metal module frame.

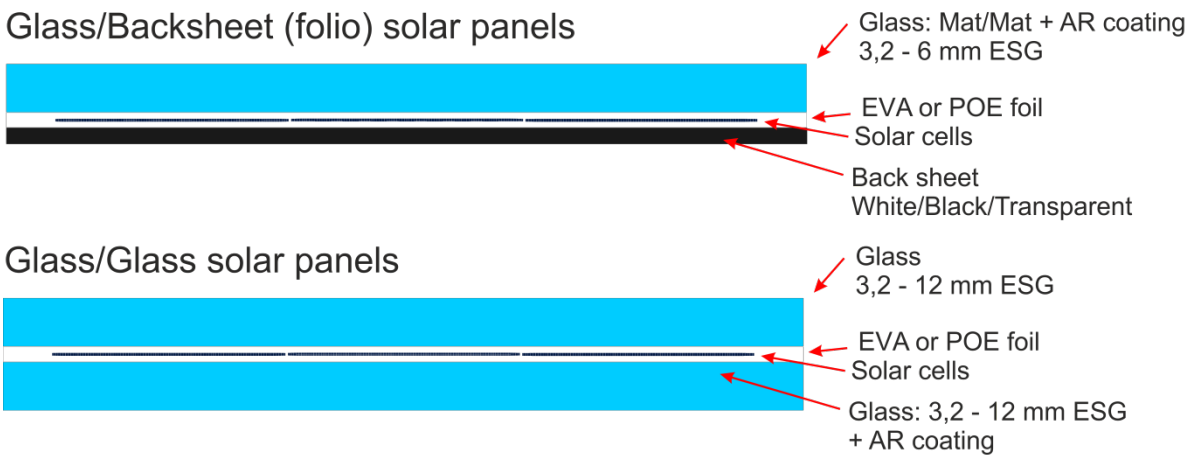

Figure 3-23: Glass-foil vs glass-glass solar module. [94]

3.3.2 Amorphous silicon

Thin film solar cells are the second generation cells, which include amorphous silicon, cadmium telluride (CdTe) and copper indium gallium selenide (CIGS) cells. A thin film cell is made by depositing one or more thin photovoltaic films on a substrate like glass, metal or plastic.

Amorphous silicon is the non-crystalline form of silicon and the most popular material in thin film technology. It has an irregular structure of silicon atoms, with multiple open bonds, called dangling bonds, which can cause anomalous electrical behaviour, thus it can't be used in photovoltaic technology. For that reason hydrogen is added, which bonds to the dangling bonds and passivates the material to a great degree. The material is then designated as a-Si:H. Figure 3-24 shows the structure of crystalline and amorphous silicon, after the addition of hydrogen.

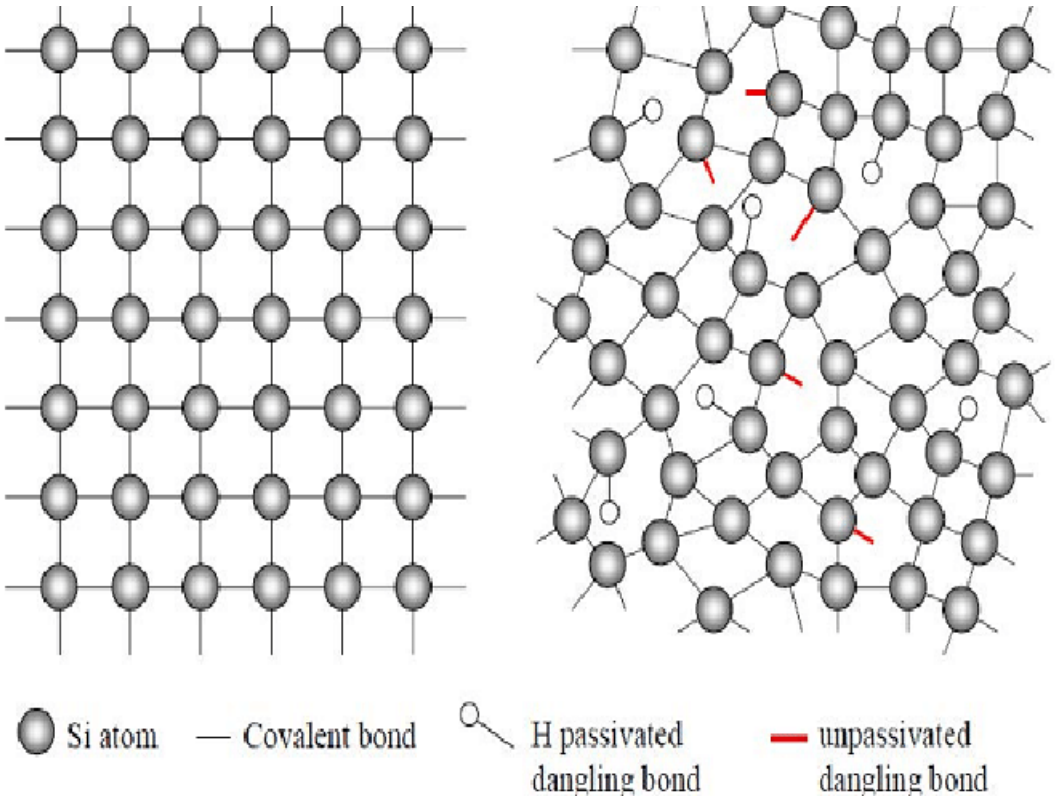

Figure 3-24: Structure of crystalline silicon (left) and hydrogenated amorphous silicon (right). [95] Licensed under CC BY-SA 4.0

The direct band gap of a-Si:H has an energy around 1.7-1.8 eV, depending on the percentage of hydrogen added. The absorption coefficient is one or two factors higher than that of crystalline silicon and with a cell thickness of 0.5µm, sufficient radiation can be absorbed.

For the production of amorphous silicon thin film cells there are two methods used, the chemical vapor deposition (CVD) and the plasma enhanced chemical vapor deposition (PECVD) processes, which are shown in Figure 3-25. In the PECVD process, the gases of silane and hydrogen flow into the process chamber, which is heated at around 200°C and enter a strong high frequency field. The field causes the acceleration of individual electrons, which cause the separation of silane and hydrogen molecules by impact ionization. Plasma is formed, which consists of highly reactive ions. These ions react with the substrate surface and settle on it. This way a layer of a-Si:H is formed and as the two gases, silane and hydrogen, continue to flow in, it continues to grow. In the CVD process, plasma is not used, therefore for the decomposition of the gases to happen the temperature needs to be much higher, more than 450°C. At these temperatures there's a limitation in the choice of substrate

materials. The deposition rate is normally around 0.2nm/sec, so it would take around 40min for an a-Si:H layer with thickness of 0.5μm to be produced. There are new processes, like the Very-High-Frequency-PECVD and the Hot-Wire-CVD, which promise to increase the deposition rates.

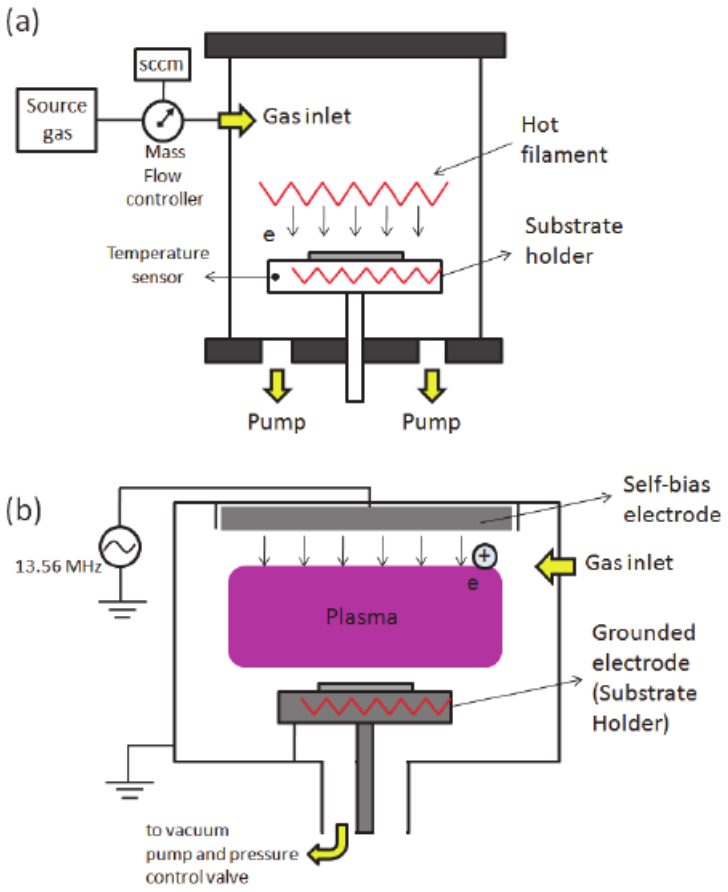

Figure 3-25: CVD (up) and PECVD (bottom) systems for thin film production. [96] Licensed under CC BY 3.0

The structure of the amorphous silicon thin film cell that is produced is shown in Figure 3-26. First there is a glass sheet, which has been coated with a transparent electrode of conducting oxide, the TCO, with the usual material being indium-tin oxide (ITO) or zinc oxide (ZnO). Next there are three layers of amorphous silicon, a p-doped layer, an undoped layer (intrinsic) and an n-doped layer. The final layer is a thin rear contact of silver or aluminum. The total thickness of the thin film cell is less than 2μm. This particular cell is called a superstrate cell

because the glass layer is the first one that sunlight meets. In the substrate cell, sunlight first meets the TCO layer and the glass layer is the last one.

The intrinsic layer is where the photon absorption should happen mostly, since the electron-hole pairs that are generated in the doped layers are paired again very shortly after. To achieve that, carbon is added to the p-doped layer to increase its band gap so light passes through it as if it is transparent. The absorption happens in the intrinsic layer and a strong electric field, generated by building up p-i-n cells, separates the generated particles and transports them to their designated areas so they don't have time to recombine.

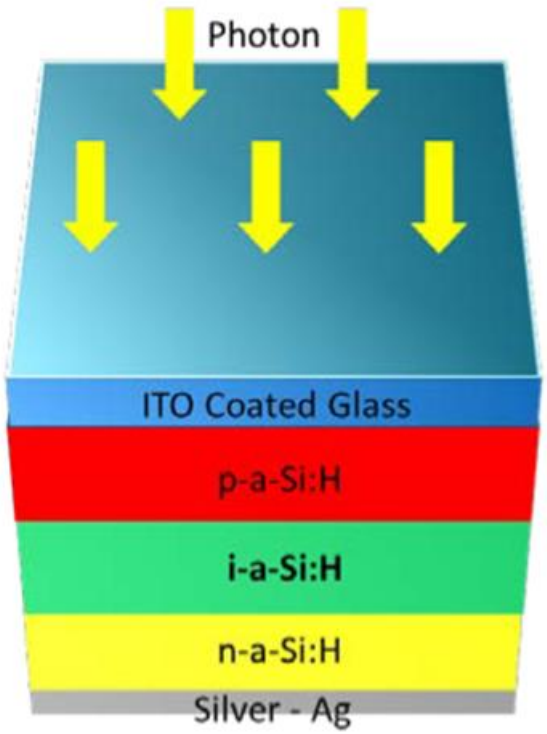

Figure 3-26: Structure of amorphous silicon thin film cell. [95] Licensed under CC BY-SA 4.0

Amorphous silicon cells have lower efficiencies than crystalline silicon and their major drawback is that they suffer from light induced degradation, due to the Staebler-Wronski effect. Staebler and Wronski discovered that the photoconductivity of hydrogenated amorphous silicon is reduced significantly under prolonged illumination. The cause of this effect is still not known, although it is widely accepted that it is due to the disorder of the structure of amorphous silicon, since crystalline silicon doesn't seem to be affected in the

same degree. The Staebler-Wronski effect can be reduced with increasing temperature or making the intrinsic layers thinner.

3.3.2.1 Multi junction cells

In order to increase the efficiency, two p-i-n cells with materials of different band gaps are stacked together, in a tandem cell. This design has the advantage of a more efficient absorption of solar radiation, since a composite absorbing layer is formed with multiple band gaps. The light separation is even better when triple cells are used. Figure 3-27 shows an example of a triple cell, in particular it presents the structure of a triple-junction a-Si:H/a-SiGe:H/a-SiGe:H cell, in which the various cells are connected with each other by electrically tunnel junctions. As light passes, the higher energy photons are absorbed by the wide band gap material, a-Si:H with band gap 1.8 eV and the lower energy photons carry on to generate electron-hole pairs in the lower levels that have narrower band gaps. These are a-SiGe:H cells with band gaps usually at 1.6 and 1.4 eV. The band gap decreases from top to bottom layer. The thickness of the layers needs to be selected to achieve current matching, so that the current is the same through all the cells.

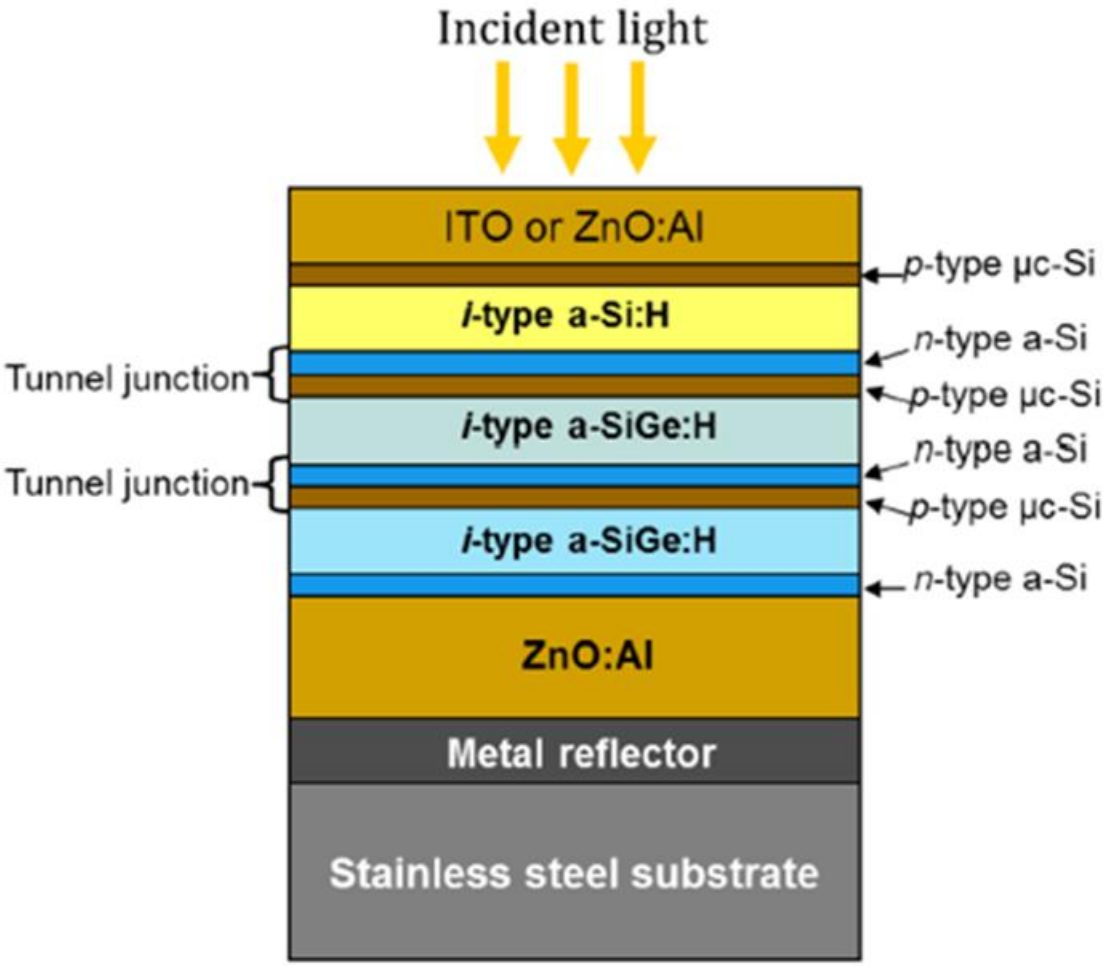

Figure 3-27: Structure of a triple-junction a-Si:H/a-SiGe:H/a-SiGe:H solar cell. [97] Licensed under CC BY 4.0

3.3.2.2 Micromorphous cells

Micromorphous silicon cell technology uses the combination of two different silicon types, amorphous silicon and microcrystalline silicon. Microcrystalline silicon is amorphous silicon that also contains small crystals. It has similar behaviour to crystalline silicon and a band gap of 1.12 eV. The combination with amorphous silicon covers a large part of the spectrum. Microcrystalline silicon doesn't show any degradation but has low absorption coefficient, like crystalline silicon, so thick layers need to be used. Figure 3-28 shows the structure of a micromorphous tandem cell.

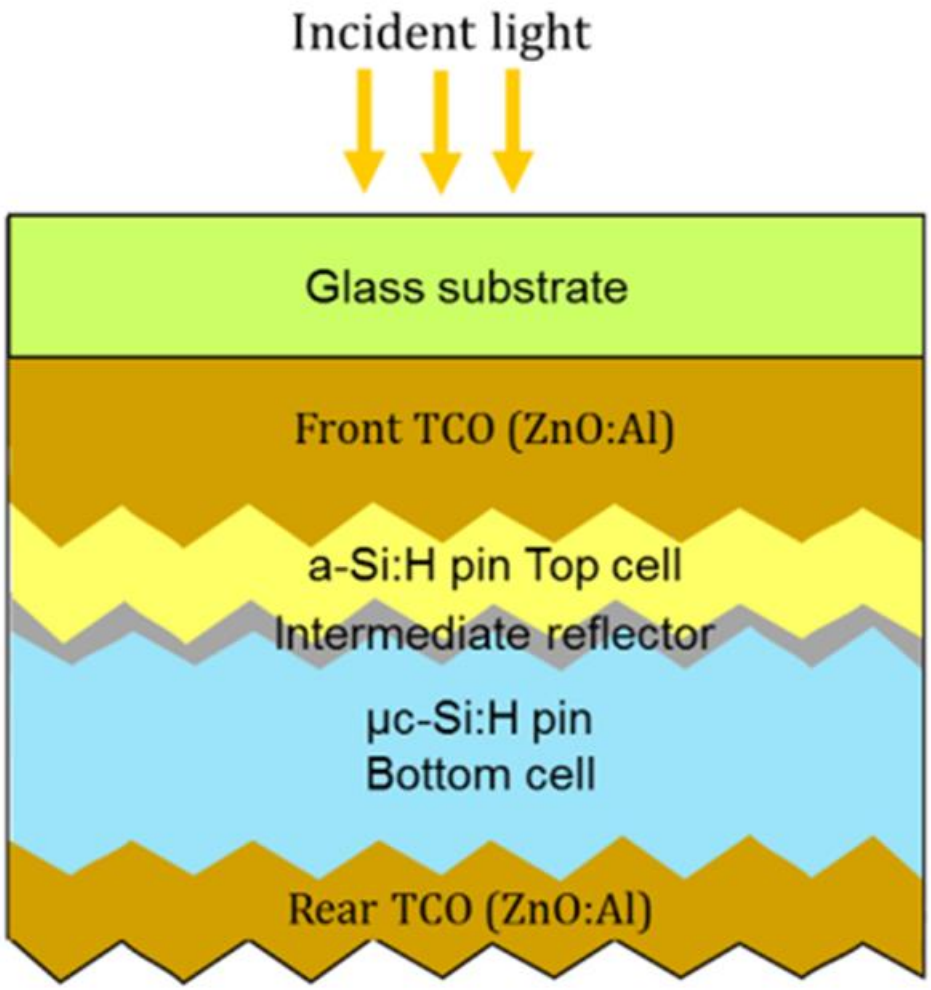

Figure 3-28: Structure of a micromorphous silicon solar cell. [97] Licensed under CC BY 4.0

Thin film solar cells can be connected to a whole module during production. This integrated series connection, the interconnection process of individual cell stripes, is embedded in the cell manufacturing, whereas in wafer technology, the cell manufacturing and series connection are separated processes.

3.3.3 Cadmium-Telluride Cells

Cadmium telluride (CdTe) accounts for more than half of the thin film market. Its efficiency has increased in recent years and competes than of multicrystalline silicon. It is the only thin film technology that has lower costs than crystalline silicon technology. CdTe is a direct

semiconductor with a band gap of 1.45 eV. The usual deposition method is thermal evaporation over a short distance (Close-Spaced Sublimation, CSS), in which the semiconductor vaporizes at 500°C and deposits on a lower temperature substrate. A conventional structure of a CdTe solar cell is shown in Figure 3-29. A thin layer of n-doped cadmium sulphide (CdS) is followed by the thicker absorbing layer of CdTe, while the two layers have different band gaps. Manufacturing includes a thin coating with cadmium chloride ($CdCl_2$) to increase efficiency. There are concerns for this technology, due to the toxicity of cadmium and its environmental effects but also due to the availability of telluride.

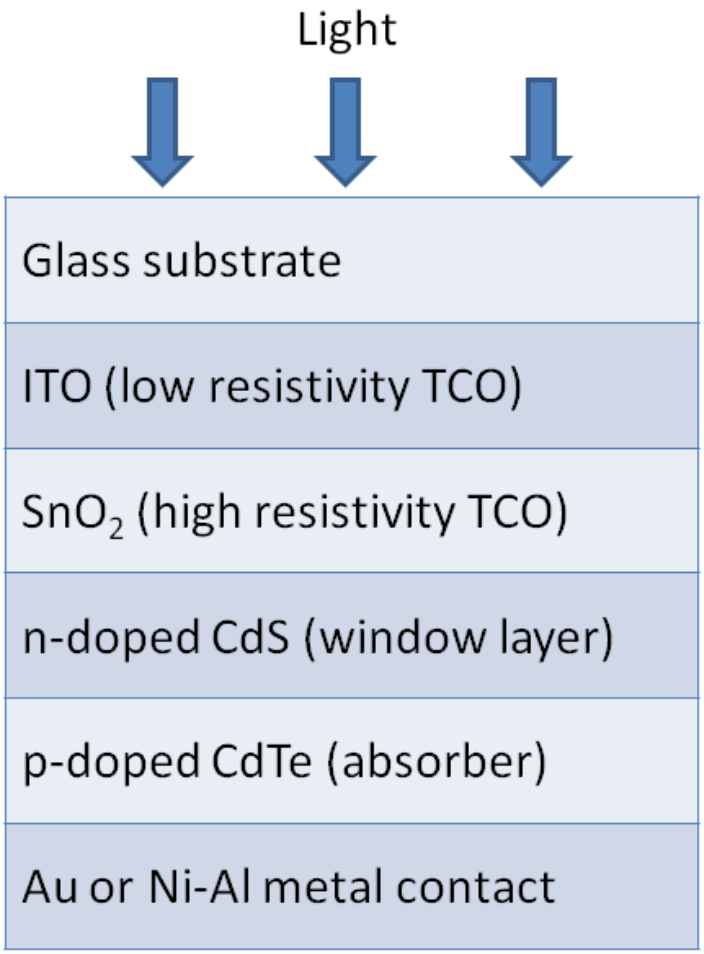

Figure 3-29: Structure of a CdTe solar cell. [98] Licensed under CC BY-SA 3.0

3.3.4 CIGS Cells

CIGS is a direct band gap semiconductor. The CIGS cell uses an absorber made of copper, indium, gallium and selenide, while there are also absorbers without gallium, abbreviated CIS. The structure of a typical CIGS cell is shown in Figure 3-30. Molybdenum acts as the rear electrode. The p-n junction is formed with a thin CdS layer and the thicker absorbing layer of CIGS. The method of deposition usually is the co-vaporization, where the individual elements vaporize at 500°C and are deposited on the substrate. CIGS has a higher absorption coefficient than CdTe and has shown the highest potential with produced efficiencies that compare to those of multicrystalline silicon cells.

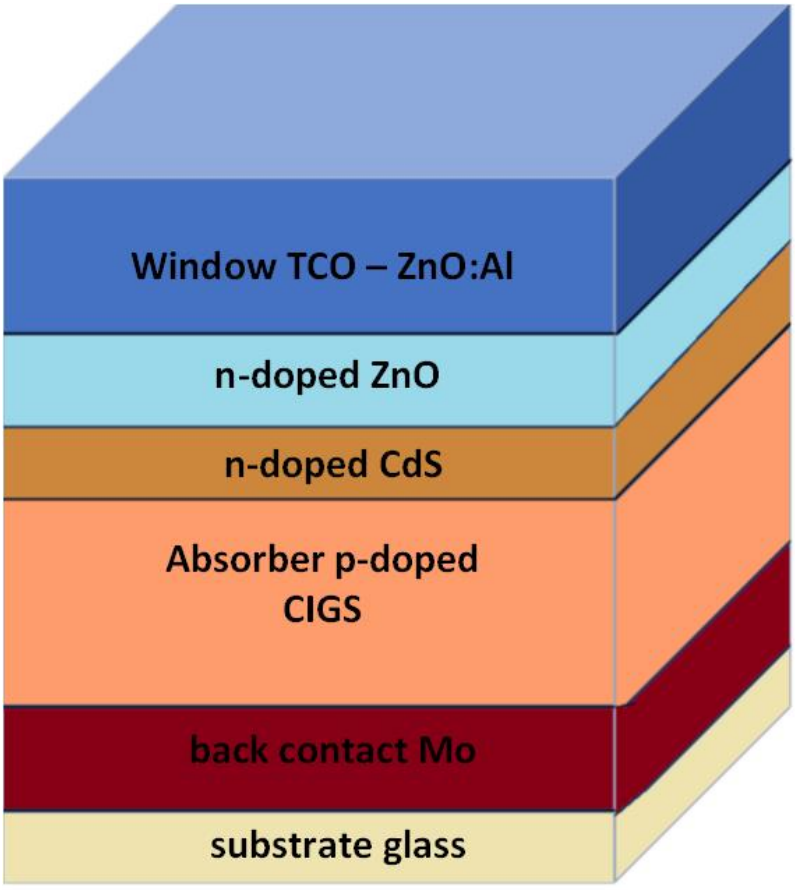

Figure 3-30: Structure of a CIGS substrate solar cell. [99]

3.3.5 Hybrid Cells

Hybrid solar cells combine different materials on the basis of wafer cells with the purpose of achieving higher efficiencies.

The company Sanyo developed the HIT cell (Heterojunction with Intrinsic Thin-Layer), a hybrid of crystalline and amorphous silicon, whose structure can be seen in Figure 3-31. The wafer is n-doped on both sides and an intrinsic layer with a doped (n and p, respectively) amorphous silicon layer are deposited on each side. A TCO layer is also deposited on each side along with metal contact strings. The amorphous silicon layers act as effective surface passivation layers for the crystalline silicon wafer. Another advantage is that the amorphous silicon deposition is done at lower temperatures compared to those of conventional crystalline silicon technology. The HIT cell is considered as a low cost alternative to traditional crystalline silicon cells.

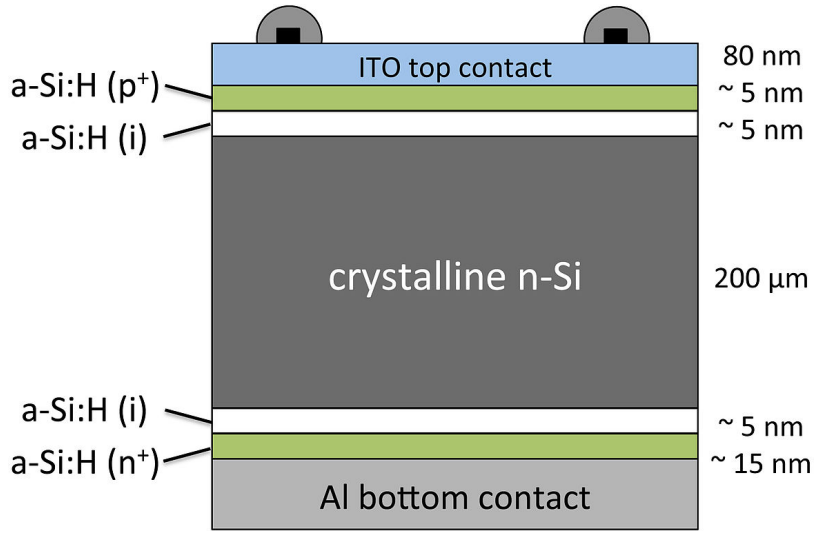

Figure 3-31: Structure of a HIT solar cell. [100] Licensed under CC BY-SA 4.0

Gallium arsenide (GaAs) is a direct band gap semiconductor with a crystal structure. It's a material used for high cost but high efficiency solar cell manufacturing. GaAs cells have achieved an efficiency of 29%. Figure 3-32 shows a monolithic (left) and a mechanically stacked (right) triple-junction cell with GaInP and GaAs as the upper and middle cell, respectively. In monolithic stacking, the upper and middle cells grow onto the bottom cell so the lattice constants of these materials must be very close to each other. These cell types

have achieved efficiencies of over 30%. Mechanically stacked cells are an alternative multi-junction technology in which different cells are stacked mechanically on top of each other and the different materials used can have different lattice constants. The cells don't have to be connected in series and high efficiencies can be achieved.

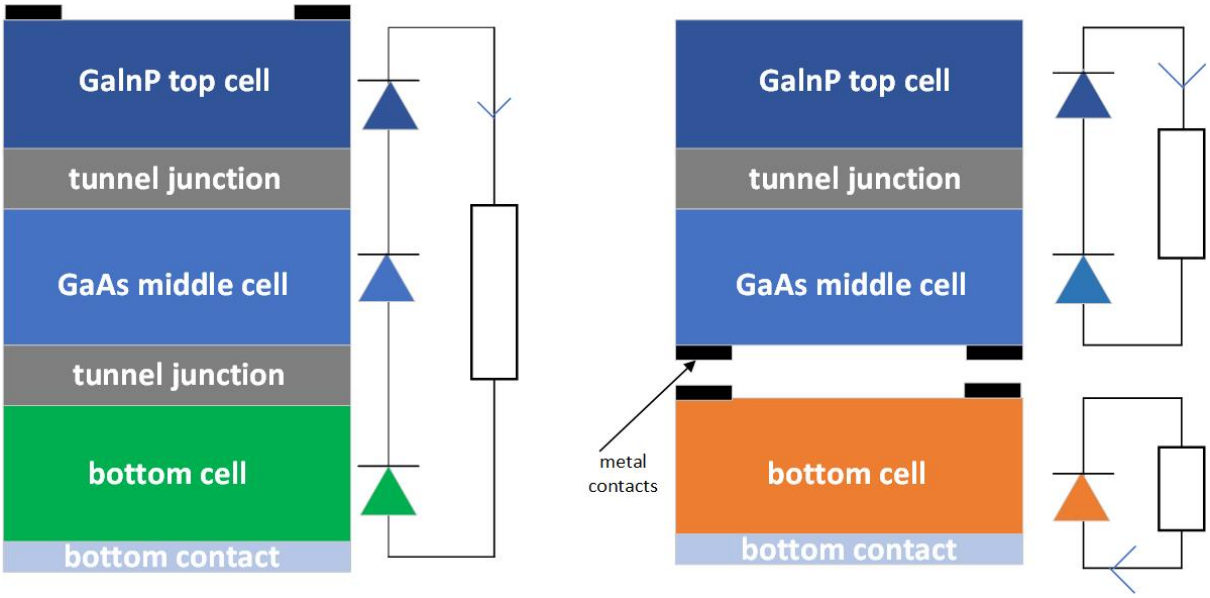

Figure 3-32: Structure of a monolithic (left) and a mechanically stacked (right) triple-junction cell. [101]

3.3.6 Other cell technologies

Third generation solar cells include the dye sensitized solar cell (DSC) and organic cells.

An n-type DSC cell, which is the most common type, is composed of a layer of titanium dioxide nanoparticles, which is covered with molecular dye that absorbs sunlight. The titanium dioxide is submerged in an electrolyte solution, which has a catalyst above based on platinum. DSC cells are low cost and stable over time.

Another type is the organic solar cell, which uses polymers for the role of semiconductor materials. These are composed of small molecules like pentacene, polyphenylene vinylene, carbon based nanostructures etc. Organic cell manufacturing is less expensive than conventional crystalline silicon but the absorption coefficient is lower because organic cells have a large band gap.

4 Photovoltaic system components

Author(s): Dr Efterpi Nikitidou
Dr Andreas Kazantzidis

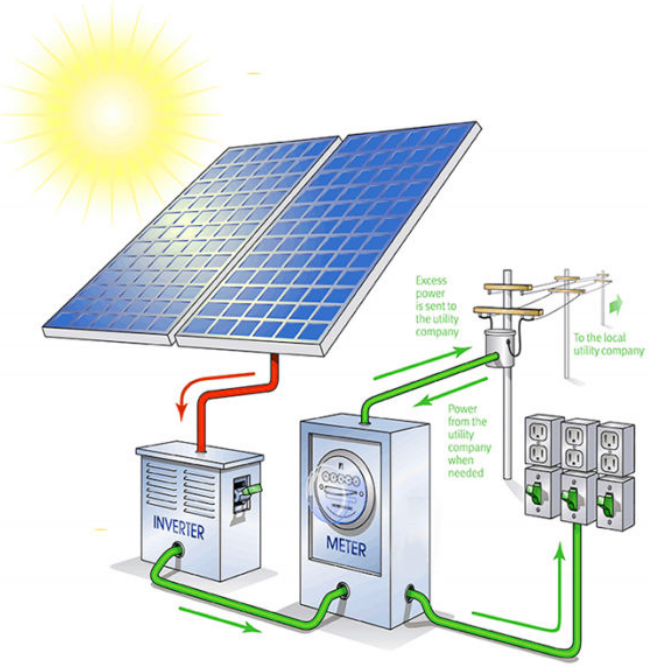

4.1 Photovoltaic circuit

4.1.1 The photodiode

In order to understand the function of a solar cell, it is important to understand the function of the photodiode, a p-n junction semiconductor that converts photons into electrical current. The symbol for the photodiode is shown in Figure 4-1 with the arrows representing the incident sunlight and the triangle the p-region.

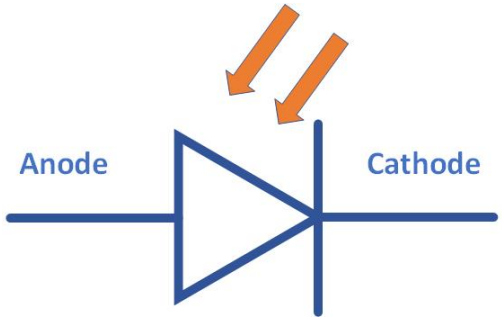

Figure 4-1: Photodiode symbol.

Electron-hole pairs are generated as photons are absorbed when sunlight hits the semiconductor. Figure 4-2 shows the p-n junction, with the diffusion force, due to concentration gradient, on holes and electrons, which move to the opposite side to recombine and the force from the electric field that is created near the junction. Electron-hole pairs that are created from photon absorption far from the space charge region will quickly recombine. Photons absorbed near the space charge region will create electron-hole pairs that will move to opposite directions due to the electric field and will not have time to recombine. These moving charge carriers form the photocurrent, I_{Ph}, which is proportional to the irradiance E. When no light is incident on the photodiode and with a reverse voltage, there is only a small reverse current flow, the dark current. Dark current is basically formed due to the random electron-hole pair generation that takes place in the depletion region (space charge region). The moment light is incident on the photodiode, there is also the photocurrent flowing in the opposite direction.

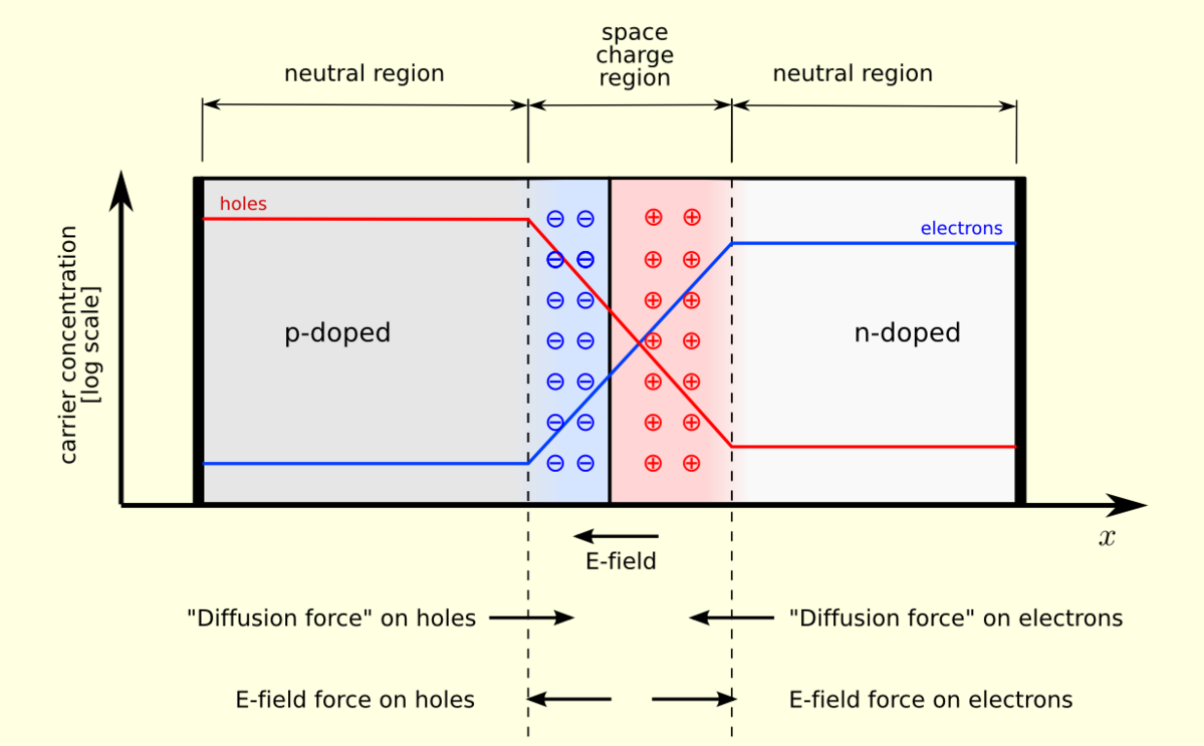

Figure 4-2: P-n junction diagram. [84] Licensed under CC BY-SA 3.0

Figure 4-3 shows the graph of the photodiode modes of operation, where I_0 is the dark current, I_{Ph} is the photocurrent, and P shows the different light levels with P_0 being the no incident light situation. When there is zero bias or in photovoltaic mode, the flow of photocurrent is restricted and a voltage builds up. The diode is then forward biased and dark current starts to flow in an opposite direction to the photocurrent. The photovoltaic mode is the basis for solar cells. It's preferred in low frequency or low light applications. The photocurrent in the photovoltaic mode shows little variation with temperature.

In the photoconductive mode, the photodiode is usually reverse biased, which causes the width of the depletion region, creating a larger area to absorb photons. The reverse bias induces a small amount of current, the saturation current, along its direction. The photocurrent basically remains the same and is linearly proportional to the irradiance. This mode provides faster response times but also increased noise. When the applied reverse bias increases after a certain point, there's a sharp increase in the current and this is the breakdown voltage. Photodiodes should not be operated beyond this point.

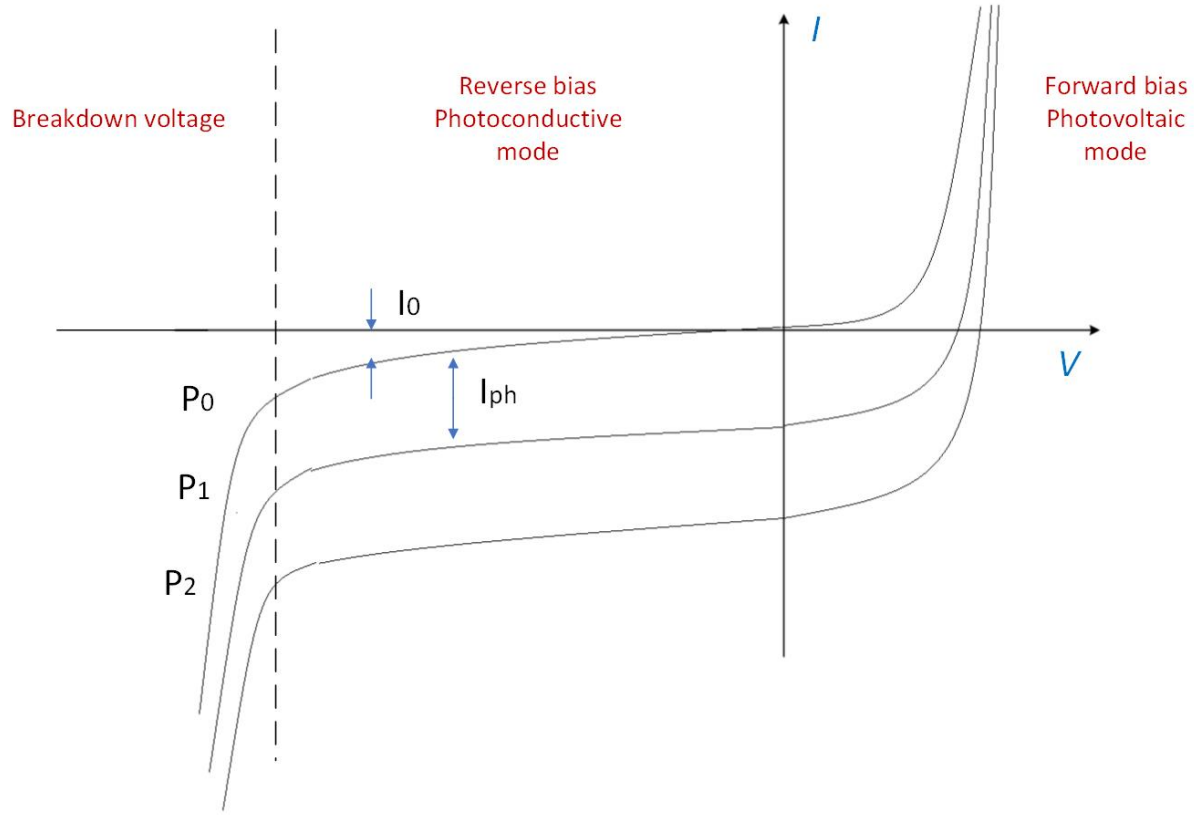

Figure 4-3: Photodiode mode of operation graph. [102]

4.1.2 Equivalent circuit

A solar cell can be represented by a current source in parallel with a diode, where the current source represents the generated current from incident radiation and the diode represents the p-n junction. Resistances are added to represent losses. The series resistance R_S is represents the losses in the contacts of the cell and the metal-semiconductor contact surface. The parallel resistance, called the shunt resistance R_{sh} represents the leak currents at the cell edges and short circuits of the junction. This equivalent circuit is depicted in Figure 4-4. The shunt resistance is the slope of the photodiode current-voltage curve for V=0. The current I is given by Equation 3-2.

$$I = I_{Ph} - I_D - I_{sh} = I_{Ph} - I_S\left[exp\left(\frac{V_D}{m * V_T}\right) - 1\right] - \frac{V_D}{R_{sh}}$$
$$= I_{Ph} - I_S\left[exp\left(\frac{V + I * R_S}{m * V_T}\right) - 1\right] - \frac{V + I * R_S}{R_{sh}}$$

Equation 4-1

The parameters of this equation are:

I_{Ph}: the photocurrent

I_D: the diode current

I_{sh}: the current flowing through the shunt resistance

I_S: the reverse bias saturation current of the diode

V_D: the voltage across the diode

m: the ideality factor that accounts for the deviation of the diodes from the Shockley diffusion theory that calculates the diode current and is usually between 1 and 2

V_T: the thermal voltage of the diode, which depends on temperature T, the Boltzmann constant k, the number n of cells in series and the electron charge q.

$$V_T = \frac{n * k * T}{q}$$

Equation 4-2

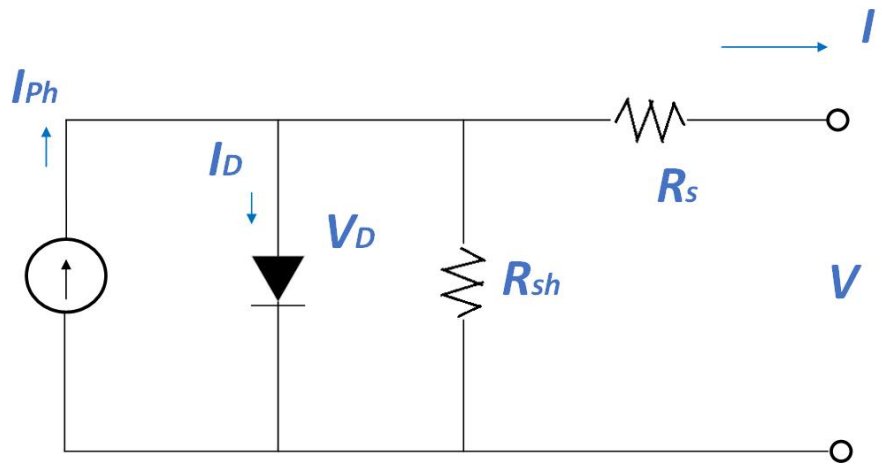

Figure 4-4: Solar cell equivalent circuit. [103]

Figure 4-5 shows the characteristic curves of a typical solar cell, the blue current-voltage curve and the purple power-voltage curve.

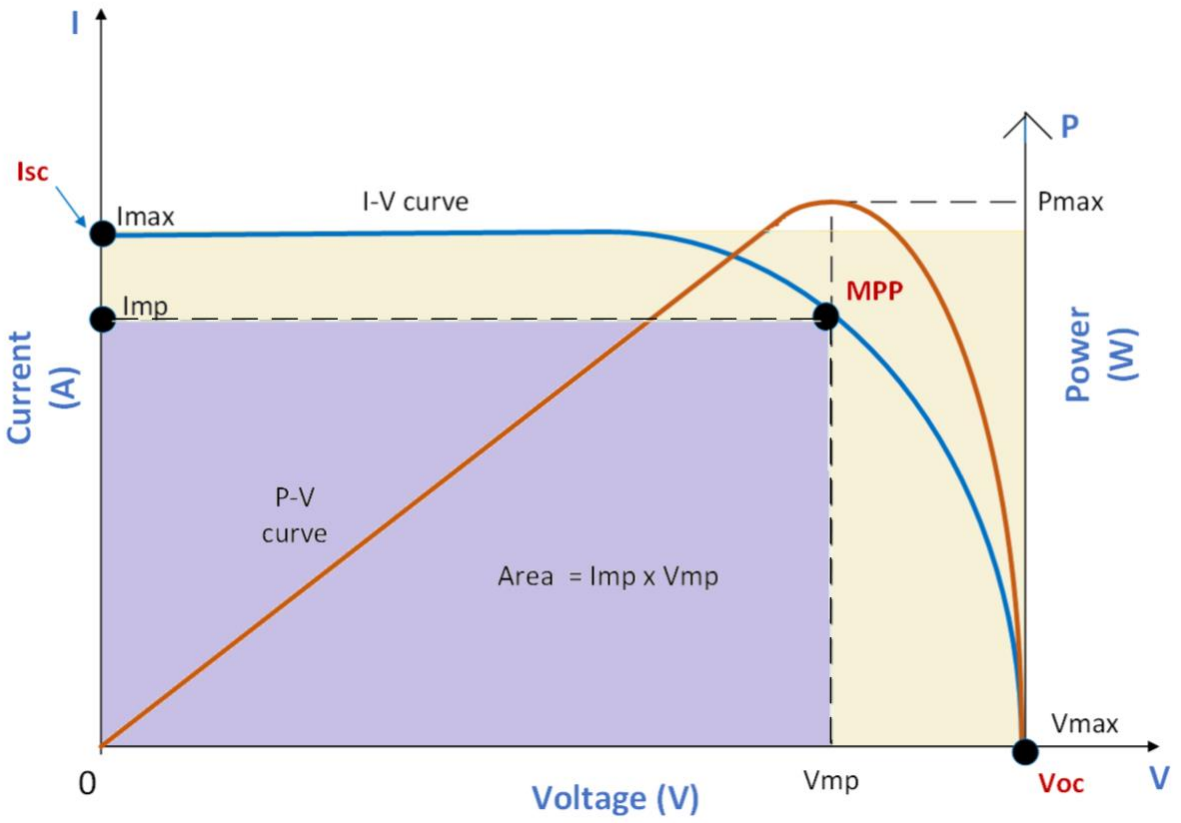

Figure 4-5: Characteristic current-voltage and power-voltage curves of a solar cell. [104]

There are three characteristic points, the short circuit current, the open circuit voltage and the maximum power point.

The **short circuit current, I_{SC}** is the current provided by the cell when it is short circuited, the voltage is zero. In this case Equation 3-2 becomes

$$I(V = 0) = I_{SC} = I_{Ph} \qquad \textit{Equation 4-3}$$

meaning that in an ideal solar cell the short circuit current is equal to the photocurrent, hence the short circuit current is proportional to the irradiance E.

The **open circuit voltage, V_{OC}** is the voltage when the current is zero and represents the maximum voltage available from a solar cell. Open circuit voltage is calculated from Equation 3-2 by setting I=0 and solving according to V, while taking into account Equation 4-3.

$$V_{OC} = V(I = 0) = m * V_T * ln\left(\frac{I_{SC}}{I_S} + 1\right) \qquad \textit{Equation 4-4}$$

The open circuit voltage has lower dependency on the irradiance than short circuit current.

The **Maximum Power Point, MPP** is the operating point at which the solar cell provides the maximum power and corresponds to current I_{mp} and voltage V_{mp}. The maximum power corresponds to the surface area I_{mp}*V_{mp} (Figure 4-5). MPP varies depending on parameters like the irradiance and temperature and photovoltaic systems use methods to track it, for the purpose of achieving maximum net power output.

The **fill factor, FF** is a parameter to determine the maximum power of a cell with the help of open circuit voltage and short circuit current. It is defined as the ratio of the maximum power P_{MPP} (light blue surface area in Figure 4-5) to the product of V_{OC} and I_{SC}.

$$FF = \frac{P_{MPP}}{V_{OC} * I_{SC}} = \frac{V_{MPP} * I_{MPP}}{V_{OC} * I_{SC}}$$ *Equation 4-5*

The fill factor describes the quality of a solar cell. Silicon solar cells usually have values between 0.75 and 0.85, while thin film solar cells have fill factors between 0.6 and 0.75. An approximation equation can be used for the calculation of the fill factor.

$$FF = \frac{1 + ln\left(\frac{V_{OC}}{V_T} + 0.72\right)}{\frac{V_{OC}}{V_T} + 1}$$ *Equation 4-6*

The **efficiency, η**, of the solar cell represents the part of the optical power P_{opt} incident on the cell that is available as output electrical energy P_{MPP}.

$$\eta = \frac{P_{MPP}}{P_{opt}} = \frac{P_{MPP}}{E * A} = \frac{FF * V_{OC} * I_{SC}}{E * A}$$ *Equation 4-7*

In Equation 4-7, E and A are the irradiance and cell area, respectively. Crystalline silicon cells usually have efficiencies between 15 and 22%.

The following figures, Figure 4-6 - Figure 4-8, show the effect that temperature, series resistance and shunt resistance have respectively on the I-V curve of the solar cell. Temperature increase of the solar cell leads to an increase in intrinsic carrier concentration, which in turn increases the saturation current. From Equation 4-4 it is evident that this leads to a reduction in open circuit voltage, as it is depicted in Figure 4-6. Due to the reduction of the band gap with temperature however, the effect on short circuit current is the opposite and there is a slight increase with increasing temperature.

Increase of the series resistance leads to flattening of the I-V curve and sinking of the fill factor. Similar is the effect that the reduction of shunt resistance has on the I-V curve. As the shunt resistance is reduced, the current flowing through it increases and very low values of shunt resistance lead to a slight reduction in the open circuit voltage.

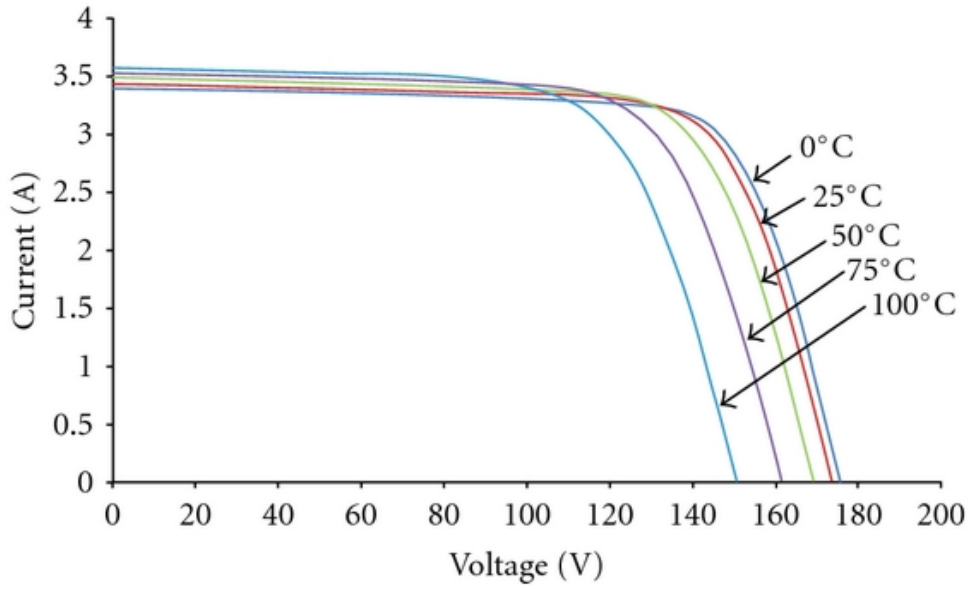

Figure 4-6: Temperature effect on I-V curve of solar cell. [105] Licensed under CC BY 3.0

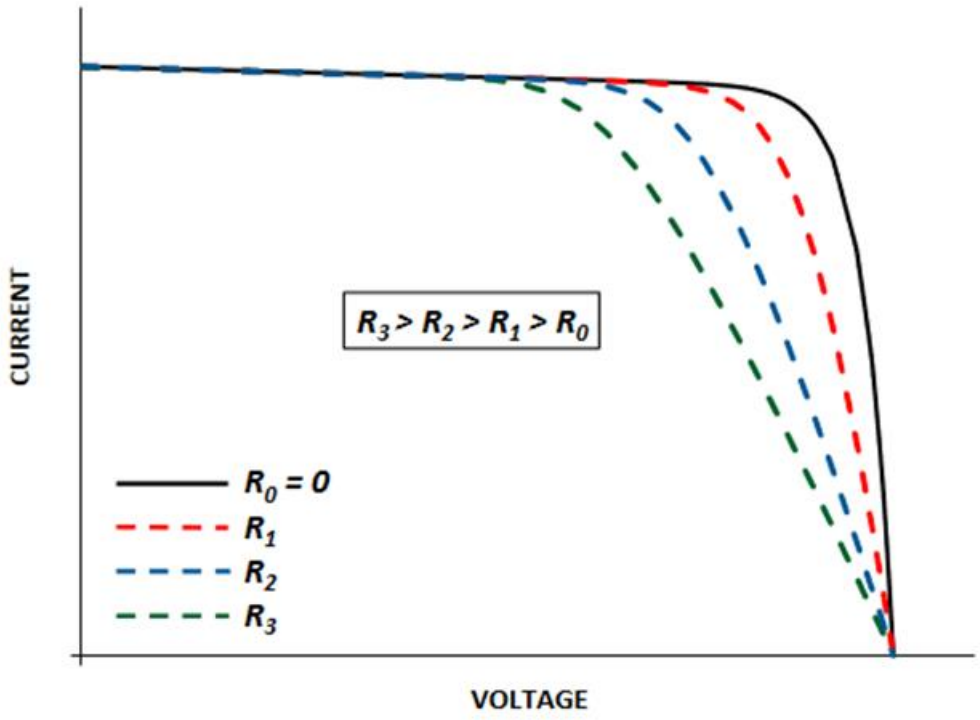

Figure 4-7: Effect of series resistance on I-V curve of solar cell. [106] Licensed under CC BY 4.0

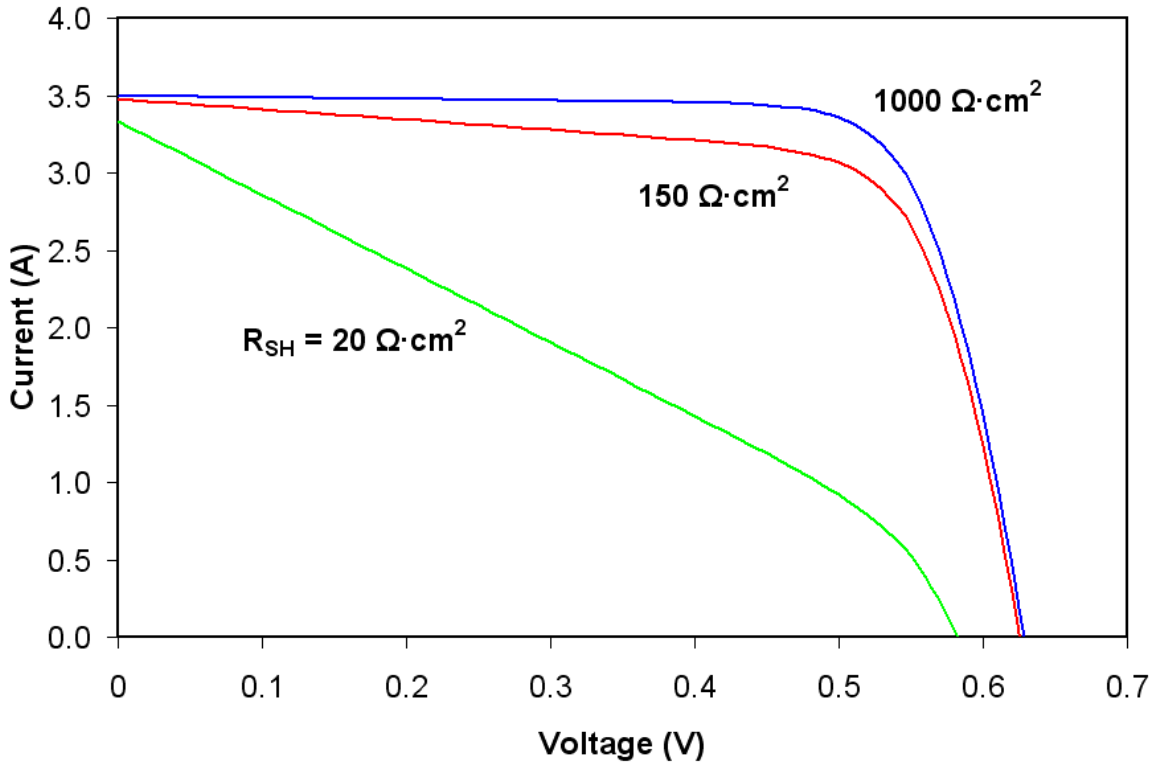

Figure 4-8: Effect of shunt resistance on I-V curve of solar cell. [107] Licensed under CC BY-SA 3.0

4.1.3 Optical characteristics

Other parameters of importance in the operation of a solar cell are the spectral responsivity and the quantum efficiency.

The spectral responsivity, R_λ of a solar cell measures the sensitivity to light and is the ratio of the photocurrent to the incident light power P at a specific wavelength. The responsivity shows the effectiveness of the cell in converting light power to electrical current. It depends on wavelength, reverse bias and temperature.

$$R_\lambda = \frac{I_{Ph}}{P}$$ *Equation 4-8*

The quantum efficiency, QE is the fraction of incident photons that make a contribution to the photocurrent. The external quantum efficiency, QE_{ext} is the ratio of electron-hole pairs contributing to the photocurrent, N_{EHP}, to the number of photons incident on the cell, N_{Ph}.

$$QE_{ext} = \frac{N_{EHP}}{N_{Ph}}$$ *Equation 4-9*

The internal quantum efficiency, QE_{int} is similar but it takes into account the number of photons, not incident on the cell, but absorbed by the cell. In this case the losses due to reflection are not taken into account. It is defined by the external quantum efficiency and the reflection factor, R.

$$QE_{int} = \frac{Q_{ext}}{1 - R}$$ *Equation 4-10*

The quantum efficiency is related to responsivity with the following equation,

$$QE(\lambda) = \frac{R_\lambda}{\lambda} * \frac{hc}{q} = 1240 * \frac{R_\lambda}{\lambda}, \quad W * nm/A$$ *Equation 4-11*

where h,c,q are the Planck constant, the speed of light and the electron charge respectively.

Figure 4-9 shows the spectral responsivity of a measured solar cell and the ideal spectral responsivity. The spectral responsivity at low wavelengths is poor because these high energy photons are absorbed close to the surface and many holes generated there recombine and don't contribute to the photocurrent. For intermediate wavelengths the spectral responsivity increases and approaches that of the ideal. In the infrared wavelengths the responsivity is reduced again since the absorption only takes place in the lower layer of the cell. After a certain wavelength the energy of the photons can't overcome the band gap of the cell material and the curve collapses.

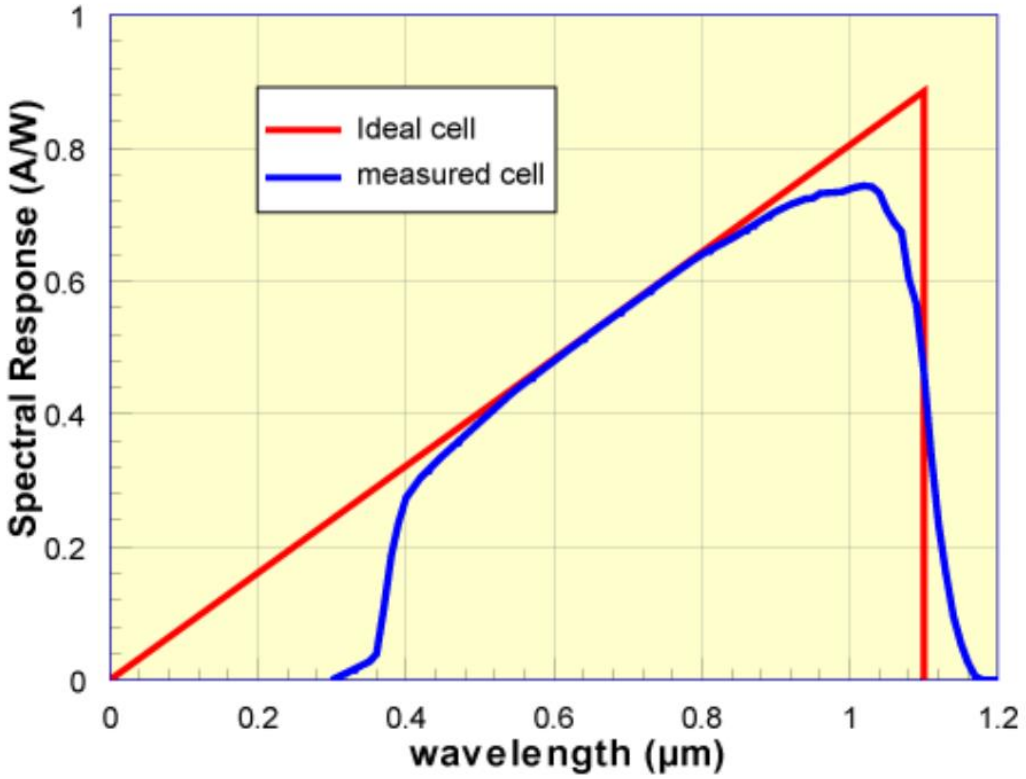

Figure 4-9: The spectral responsivity of an ideal and a measured solar cell. [108]

4.1.4 The two-diode model

In real solar cells, the one diode equivalent circuit of Figure 4-4 is not enough to describe the recombination that takes place in the space charge region. For that reason the two diode model is used, to represent the equivalent circuit (Figure 4-10), which has two diodes, an ideal one with ideality factor equal to 1 (representing the diffusion current) and a non-ideal one with ideality factor equal to 2 (representing the recombination current).

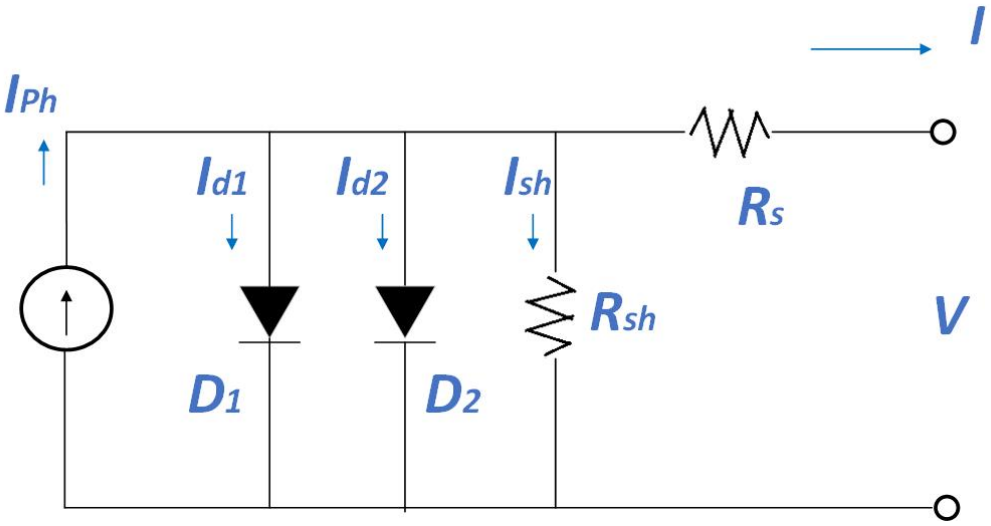

Figure 4-10: The two diode equivalent circuit. [109]

The characteristic curve equation is similar to Equation 3-2 and is now given by Equation 4-12, where I_{S1} and I_{S2} are the saturation currents of the two diodes.

$$I = I_{Ph} - I_{S1}\left[exp\left(\frac{V + I * R_S}{V_T}\right) - 1\right] - I_{S2}\left[exp\left(\frac{V + I * R_S}{2 * V_T}\right) - 1\right] - \frac{V + I * R_S}{R_{sh}}$$

Equation 4-12

4.2 PV power electronics

In order to use electricity from solar power for practical installations, solar cells are connected together to form a photovoltaic (PV) module. In large scale installations, PV modules are connected together to form PV arrays. A PV system consists of more than solar panels. There are many components required for the operation of a PV system, which are together called balance of system (BOS). The number and type of components that each system needs depends on whether it's a grid-connected or a stand-alone system. These components include mounting structures, energy storage which is vital for stand-alone systems, DC-DC converters, inverters, charge controllers, MPP tracking, cables etc. (Figure 4-11).

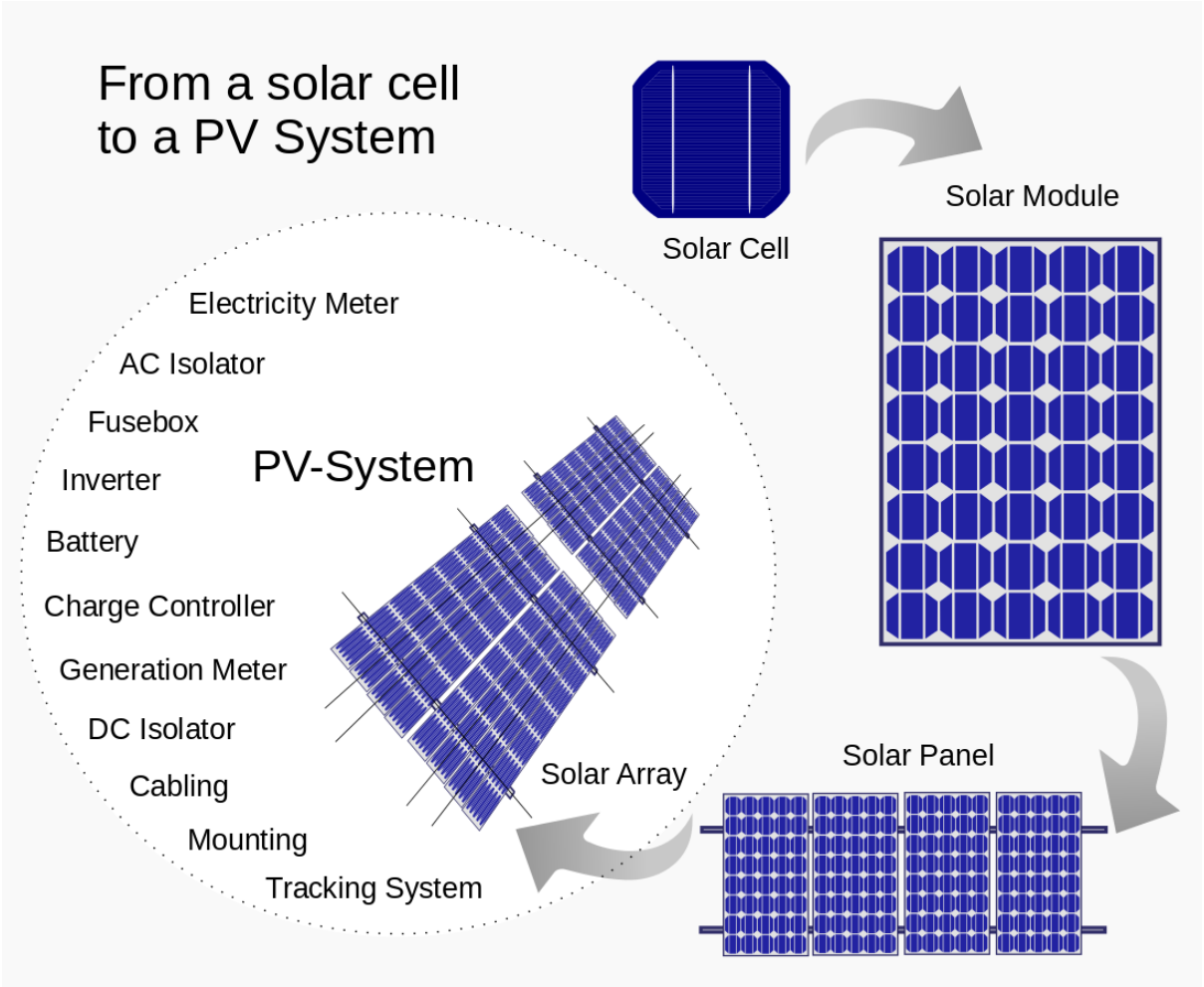

Figure 4-11: From solar cell to PV system. [14] License: Public Domain

The electronic components of PV systems handle large amounts of power and are usually classified as power electronics. The most important components of the power electronics of a PV system will be presented in this section.

4.2.1 DC-DC converter

A DC-DC converter is used for multiple purposes. It transforms the voltage from the solar panels that is variable into a constant voltage, which will be then used by the DC-AC inverter. Another function is to set the operating point of the modules, which is controlled by the MPP tracker. Further more in stand-alone systems the MPP voltage from the solar modules might not be the same with the one required by batteries and the electric load (connected electric appliances).

A simple load using the produced power of a PV generator will have an ohmic resistance R and in the I-V curve of the PV generator it will be depicted as a linear load line, where I=V/R. The intercept of the load line with the I-V curve of the module gives the operating point of the load. Due to varying irradiance and temperature conditions the I-V curve changes and the operating point moves along the load line. As it can be seen in Figure 4-12 the operating point is not always near the MPP of the module. For example in the cases of 40 or 60% insolation, the operating point is far away from the MPP meaning that the PV module will contribute only a part of the available power to the load. For this reason the DC-DC converter is used.

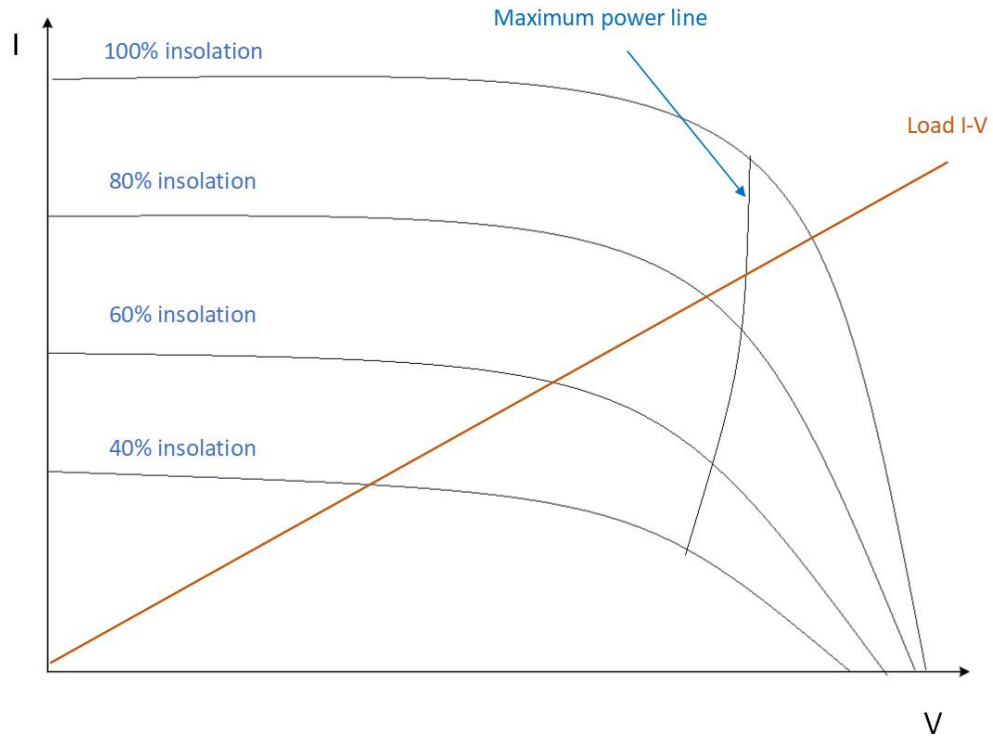

Figure 4-12: Load line with various I-V curves for different insolation levels. [110]

The DC-DC converter is used to convert an input voltage of V_1 to an output voltage of V_2. In this way the PV module voltage can be selected independently of the load voltage. When using a DC-DC converter there is always some loss even if it's a small one, which is converted to heat. An ideal converter has 100% efficiency and in this case the output power is equal to input power.

$$P_1 = I_1 * V_1 = I_2 * V_2 = P_2$$ *Equation 4-13*

The DC-DC converter can be a buck converter, a boost converter or a buck-boost converter.

4.2.1.1 Buck converter

A buck converter is used to reduce the output voltage. The principle is to switch through the input voltage V_d for a specific time period T_{on} to the output voltage V_0 (pulse width modulation, PWM). When the switch is on, the input voltage is applied to the load. When the switch is off, then the load voltage is zero. This results in a pulsed voltage at the output with mean value:

$$V_0 = \frac{T_{on}}{T} * V_d = D * V_d$$ *Equation 4-14*

In Equation 4-14, T_{on} is the time period the switch is on, T is the total time period and D, which is their ratio, is called duty cycle. Practically a pulsed output is not acceptable so other elements are added to the circuit to smooth the current and voltage and the buck converter circuit is that depicted in Figure 4-13. The inductor L is used for the purpose of maintaining a continuous current I_L and the capacitor C is used to smooth the output voltage. In the continuous mode operation, the time integral of the voltage across the inductor during one switching cycle is zero. It is obvious that output voltage V_0 will be lower or equal at most to input voltage V_d.

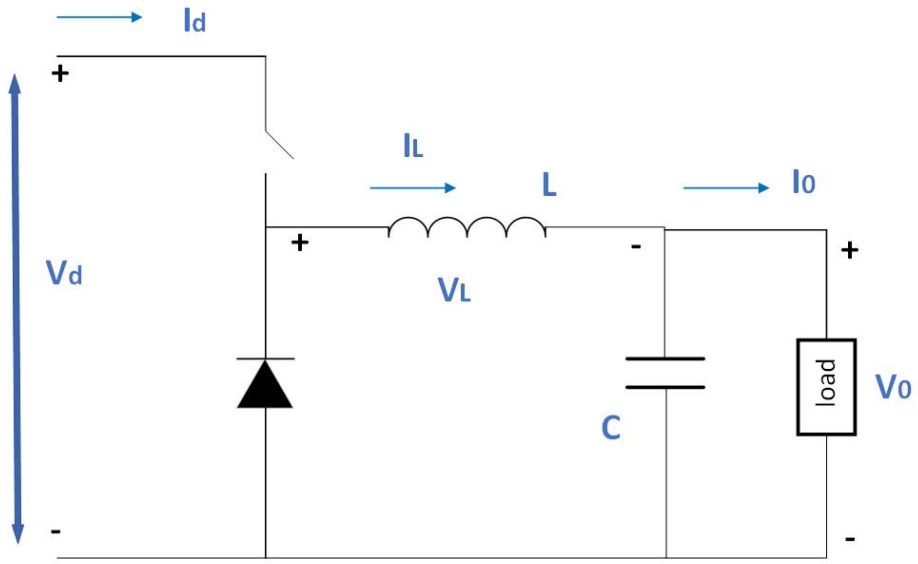

Figure 4-13: Buck converter circuit. [111]

4.2.1.2 Boost converter

A boost converter is used when a small voltage is needed to be converted to a higher voltage. The boost converter circuit is depicted in Figure 4-14. The time integral of the voltage across the inductor for the switching cycle is zero, for the operation to be in continuous mode and the output voltage is given by Equation 4-15.

$$V_0 = \frac{1}{1-D} * V_d \qquad \textit{Equation 4-15}$$

When the switch is on, energy is stored in the inductor and is later released against higher voltage V_0. As a result energy is transferred from the lower PV module voltage to the higher load voltage.

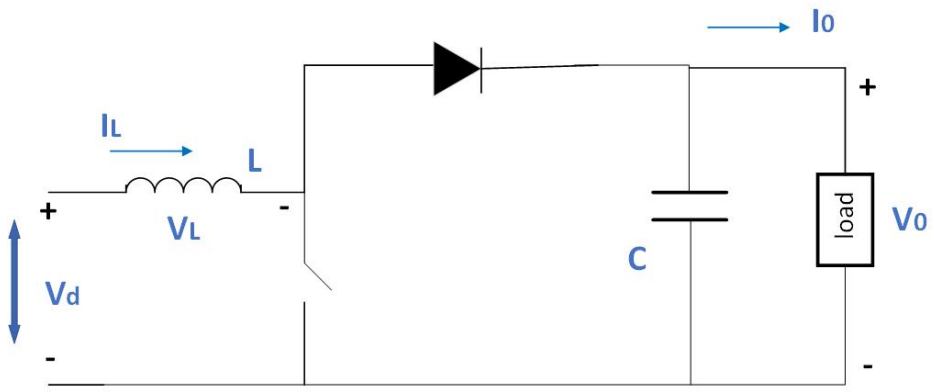

Figure 4-14: Boost converter circuit. [111]

4.2.1.3 Buck-Boost converter

In the buck-boost converter, the output voltage can be higher or lower than the input voltage. The buck-boost converter circuit is shown in Figure 4-15. Given that again for the operation to be in continuous mode, the time integral of the voltage across the inductor for the switching cycle must be zero, the output voltage is given by Equation 4-16.

$$V_0 = \frac{D}{1-D} * V_d \qquad \textit{Equation 4-16}$$

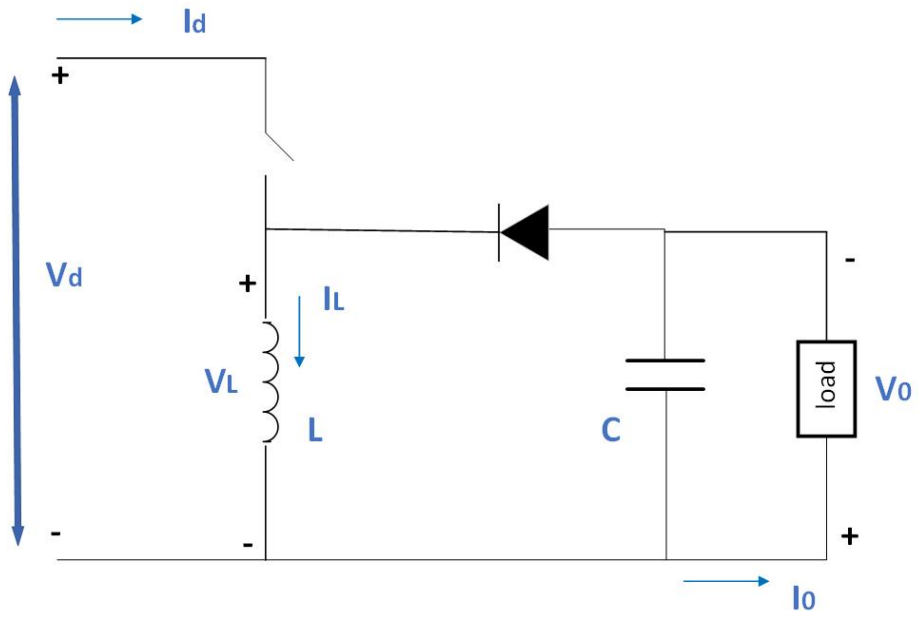

Figure 4-15: Buck-boost converter circuit. [111]

4.2.2 Maximum power point tracking

The DC-DC converter can be used for MPP tracking. The equivalent circuit is depicted in Figure 4-16. The power at the input or output of the DC-DC converter can be found by measuring the current and voltage. By varying the duty factor D, the operating point can be varied. There are several MMP algorithms, including the Perturb and Observe method. Here the MPP tracker starts at the open circuit voltage point in the I-V curve. The actual power is determined and then the duty factor is increased. The tracking is considered to be correct if the new power in greater than the previous one and the duty factor is increased again. In case that the MPP is exceeded then the measured power is decreased and the duty factor is then decreased as well. As a result, the operating point varies a little around the MPP.

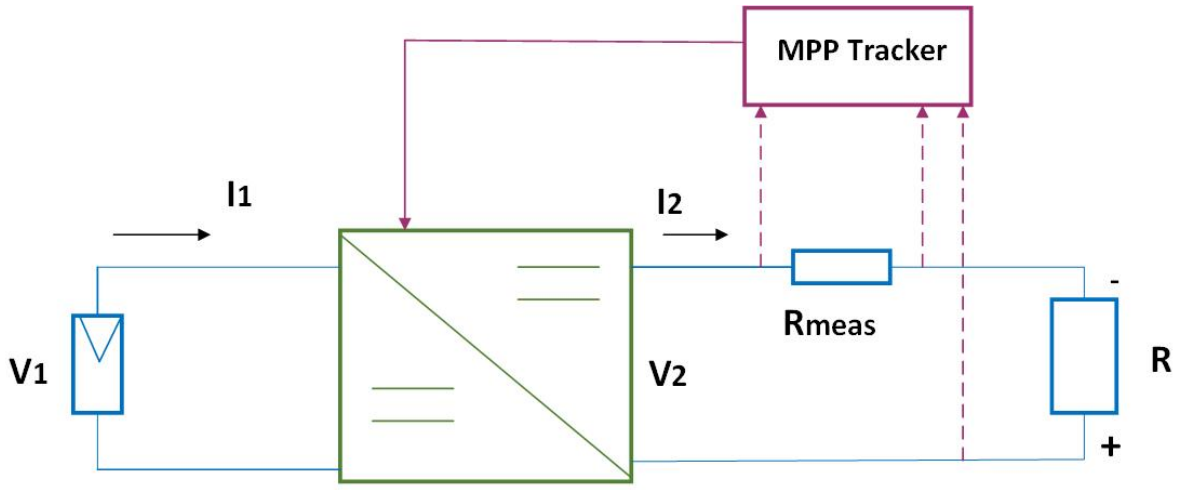

Figure 4-16: Circuit with DC-DC converter and MPP tracker. [111]

4.2.3 Inverters

PV systems that are designed to deliver alternating current (AC), as is the case with grid-connected systems, need an inverter in order to convert the direct current (DC) that the module provides to AC. The AC electricity provided by the inverter, must be in sinusoidal form and synchronized to the frequency of the grid. The feed-in voltage (feed-in: given to the grid)

must not exceed the voltage of the grid and the inverter must disconnect from the grid if the voltage of the latter is turned off.

Figure 4-17 shows the different architectures of connecting inverters to PV systems. The simplest architecture is the central inverter (left). PV modules are connected in strings, which results in increased system voltage. The strings are connected in parallel to form a PV array, which is connected to a central inverter. The central inverter feed the generated power into the grid. This type has the advantage that there's need for only one inverter. However if the strings are shaded in a non uniform way, then the parallel connection will cause mismatching losses. The system layout means that power is carried over significant distances with DC wires which can cause several issues. Another important disadvantage is that this architecture has no flexibility, meaning that it will be difficult to expand the system if needed.

Another type is the string inverter (Figure 4-17, middle). Here each string of PV modules is connected to a separate inverter. Each string can have its own MPP tracking system and be operated independently at its MPP. The cabling system is also simpler than in the case of central inverter, although safety requirements are still needed. However there are still expected to be unequal current and power sharing within the individual string.

In the concept of micro inverters, each module is connected to its own inverter (Figure 4-17, right). That means that each module can be monitored separately and operated at its MPP. An important disadvantage of this architecture is that due to the fact that each inverter is attached directly to the module, which can be located for example in a roof, they are subject to variable wind, temperature and weather conditions in general. This takes its toll on the lifetime of the electronic components. Micro inverters are also the most expensive type of inverter topologies.

Figure 4-18 shows another type of installation, the central inverter with optimizers. This type is a hybrid of central and micro inverters. There's an optimizer box connected to each module that contains an MPP tracker and a DC-DC converter. The optimizer boxes are connected in series with each other and then they are all connected to a central inverter. Every module can operate at its own MPP and all optimizers can operate at voltages which are near the PV module voltage, so the DC-DC conversion is very efficient.

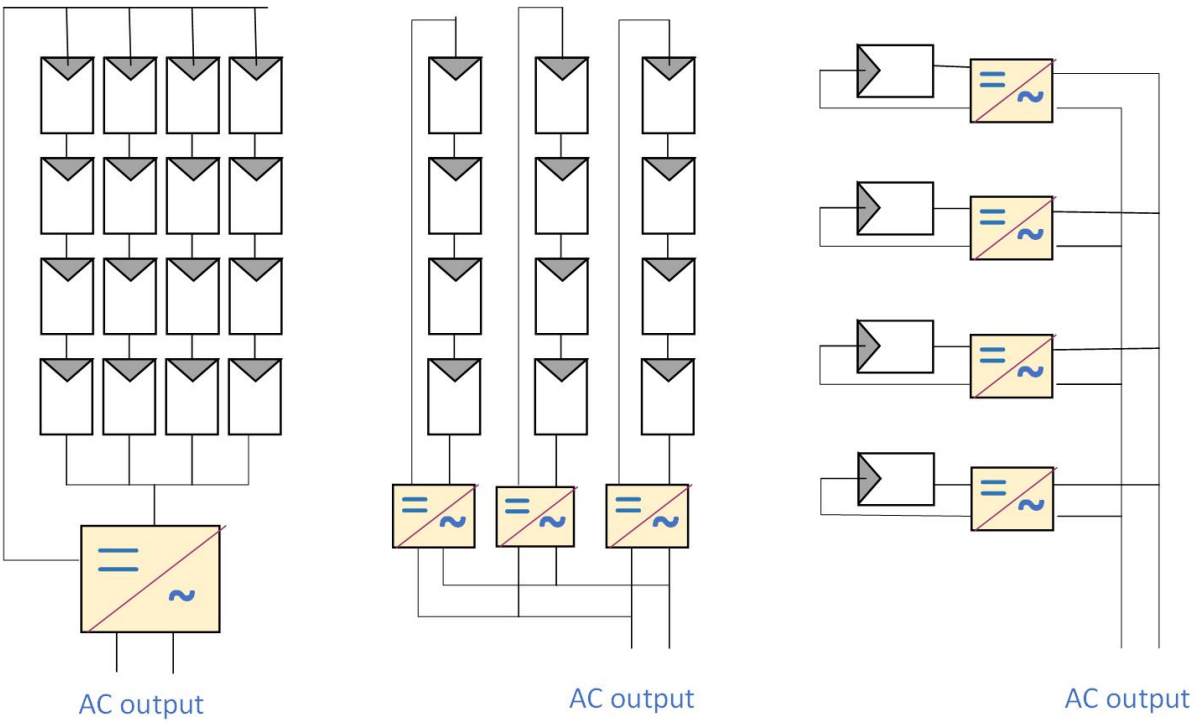

Figure 4-17: Inverter topologies: central inverter (left), string inverter (middle), micro inverter (right). [112]

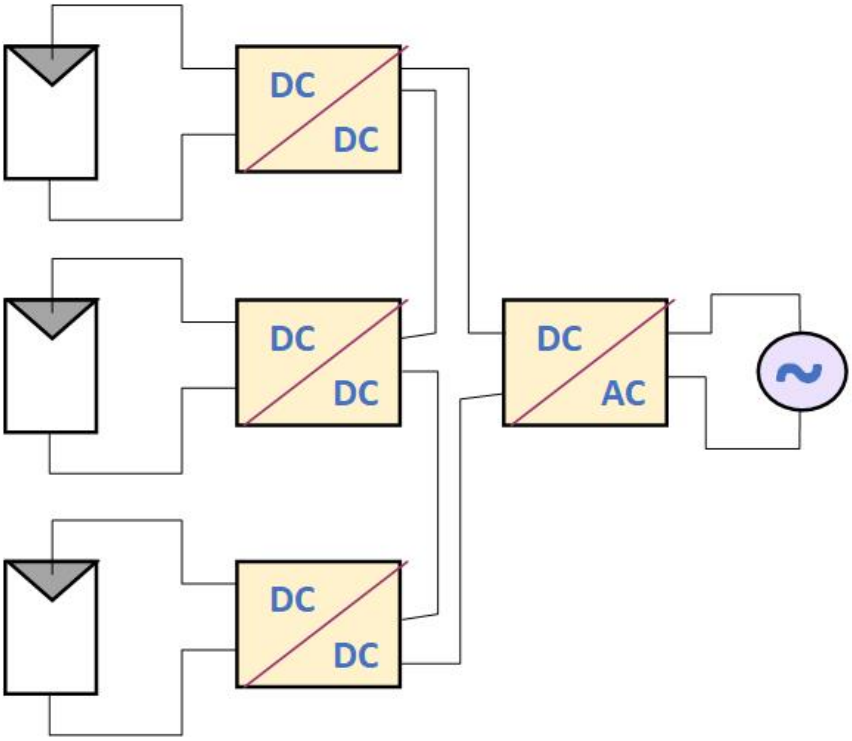

Figure 4-18: Inverter with optimizers. [113]

4.2.3.1 H-bridge inverter

For PV systems connecting to the grid, a DC-AC converter is required. Figure 4-19 shows the diagram of a simple H-bridge inverter (full bridge inverter), where the DC input is connected to the load (AC output), which is placed between four switches. The operation of this system is done under three different conditions:

1. All switches are open: no current flows across the load
2. Only switches S1 and S4 are closed: current flows across the load from left to right (+ to the left side of load, - to the right side of load)
3. Only switches S2 and S3 are closed: current flows across the load from right to left (+ to the right side of load, - to the left side of load)

In this type, the voltage across the load can be $+V_S$, 0 or $-V_S$. AC current switches between positive and negative voltages and in the simplest operation mode the H-bridge inverter switches between the 2nd and 3rd condition continuously, providing a square wave.

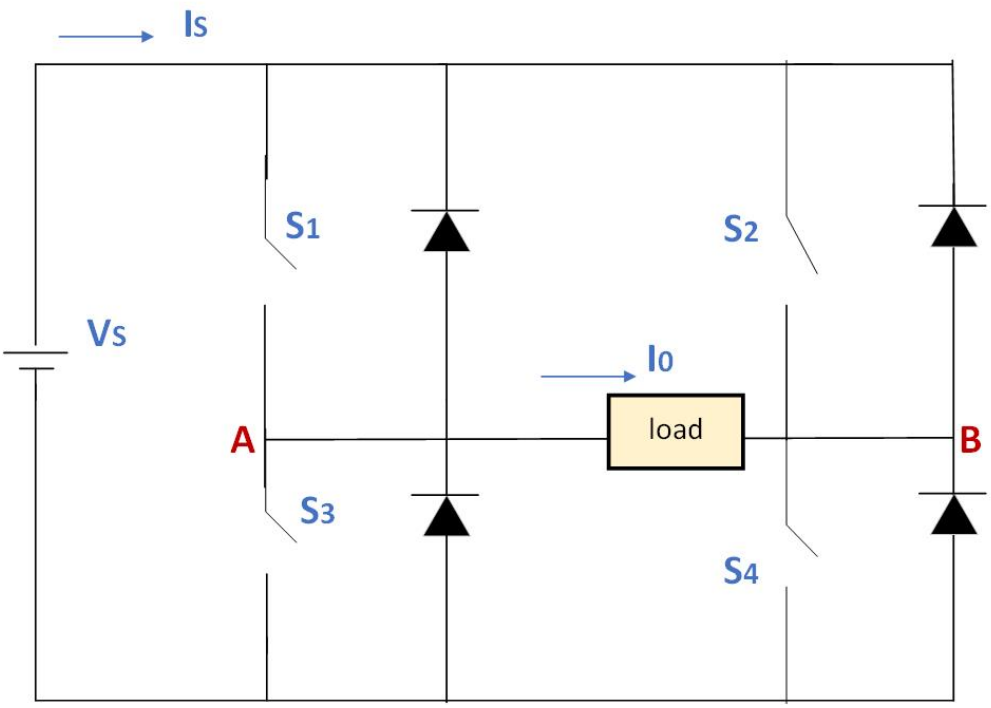

Figure 4-19: H-Bridge inverter diagram. [114]

There are some applications however, where a square wave is not suitable for meeting the harmonic distortion that the load requires. These harmonic distortions can be reduced with various methods, so a sine wave can be produced. One such method is with pulse width modulation, PWM, where each situation (S1 and S4 or S2 and S3) has the role of a buck converter. Figure 4-20 shows the circuit (left) with a low pass filter of inductors and capacitors. Here the high frequency components will be filtered and the produced wave will be that of a smooth sine curve (right) which will be suitable for grid-connected applications. The diodes are in parallel connection with the switches, so if the switch goes from close to open condition fast, there will still be current flowing and there won't be any high induced voltages.

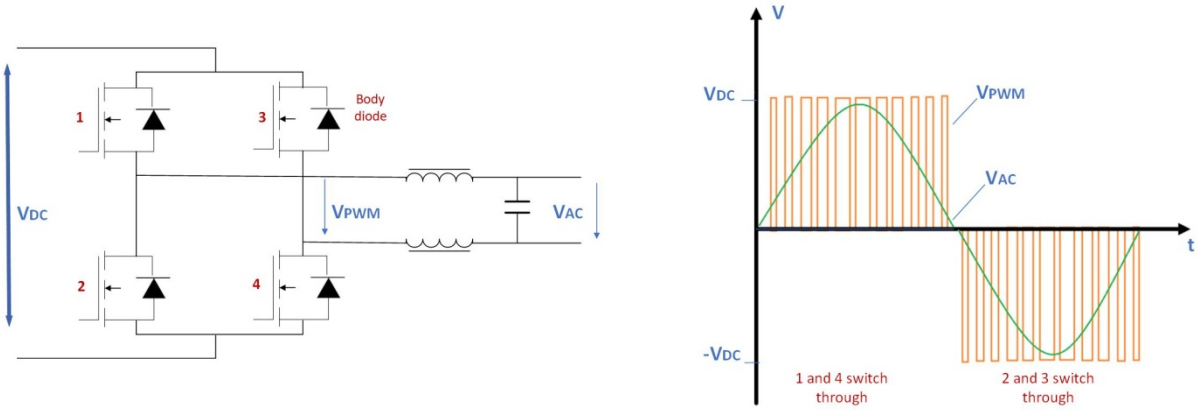

Figure 4-20: H-bridge with low pass filter (left) and output sine signal (right). [81]

If the voltage from the PV array is low, then a boost converter is used to increase it before passing to the inverter. Another way is to use a transformer which can transform a low AC voltage to the desired AC voltage of the grid. Figure 4-21 shows an example of an inverter circuit without transformer which is used frequently in a string inverter topology. The boost converter increases the DC input voltage to a higher level, based on the MPP tracking needs. The DC voltage is then converter by the PMW bridge into a sinusoidal voltage which can be fed into the grid. When no transformer is used, there is no galvanic isolation, so a residual current protective device (RCD) is used to protect from sudden current changes. After that, the grid monitoring makes sure that both voltage and frequency are within suitable ranges so that feed-in can occur when grid is available.

When a transformer is used, there is the advantage of galvanic isolation but the overall efficiency is reduced.

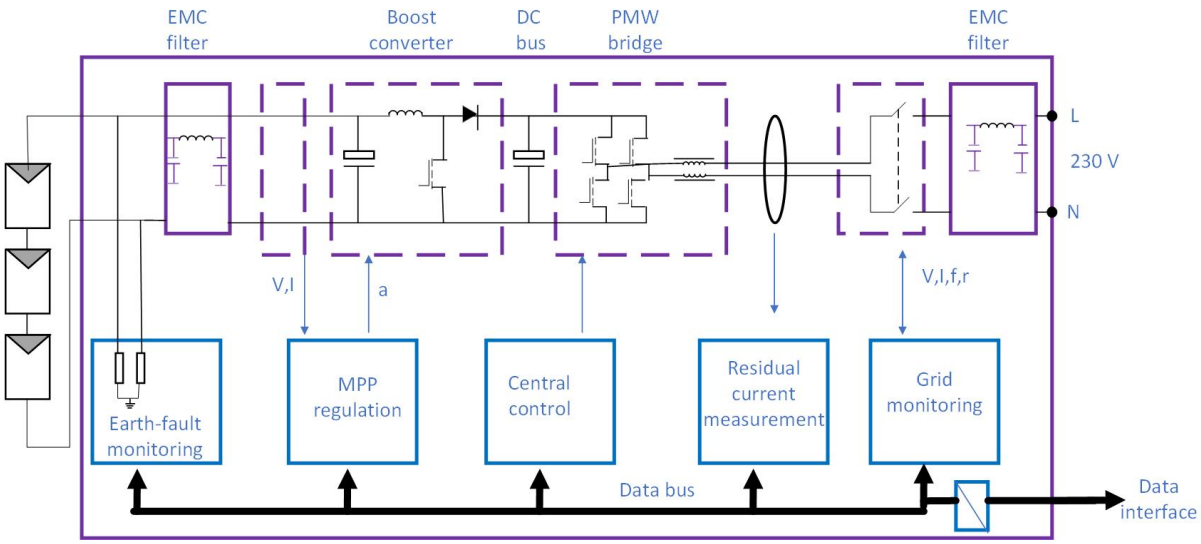

Figure 4-21: Inverter arrangement without transformer. [81]

4.2.3.2 Three-phase inverter

Due to the higher power inverters required for large installations, there are inverters which feed three-phase power to the grid. Figure 4-22 shows a simple circuit of a three-phase inverter. It is similar to the single phase inverter but it consists of three legs, each one creating a sinewave output with a phase shift of 120° between them.

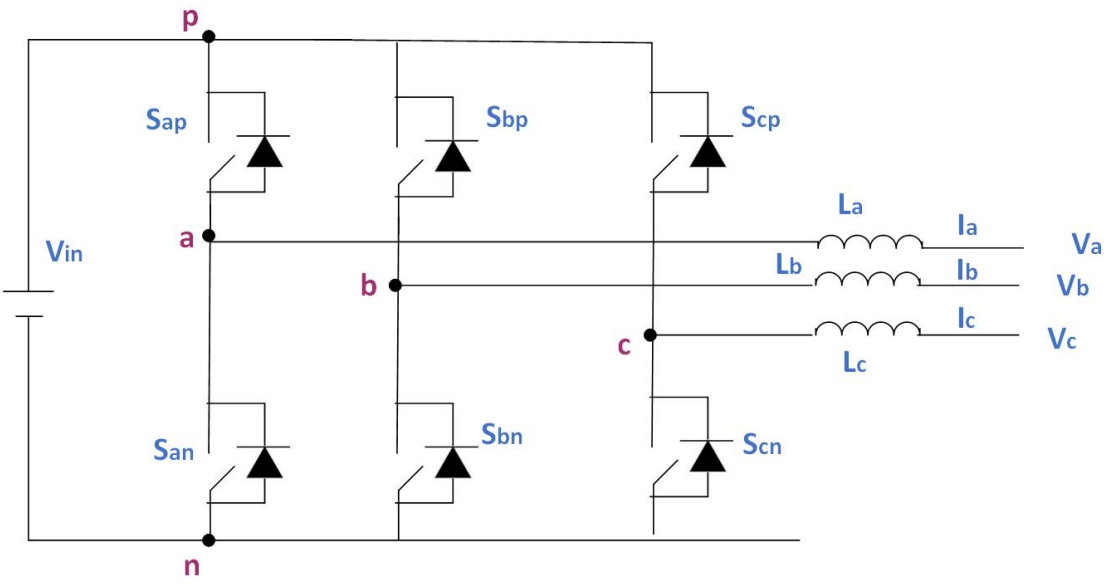

Figure 4-22: Three-phase inverter. [115]

4.2.3.3 Half-bridge inverter

Figure 4-23 shows the half-bridge inverter circuit, a simpler topology, where there are two switches and the other two from the H bridge inverter have been replaced by capacitors. The midpoint between the two capacitors is grounded. Although it is a simpler configuration, the main disadvantage is that it requires high DC voltage. In half-bridge inverter the peak output voltage is half of the DC supply voltage, while in H-bridge it is the same.

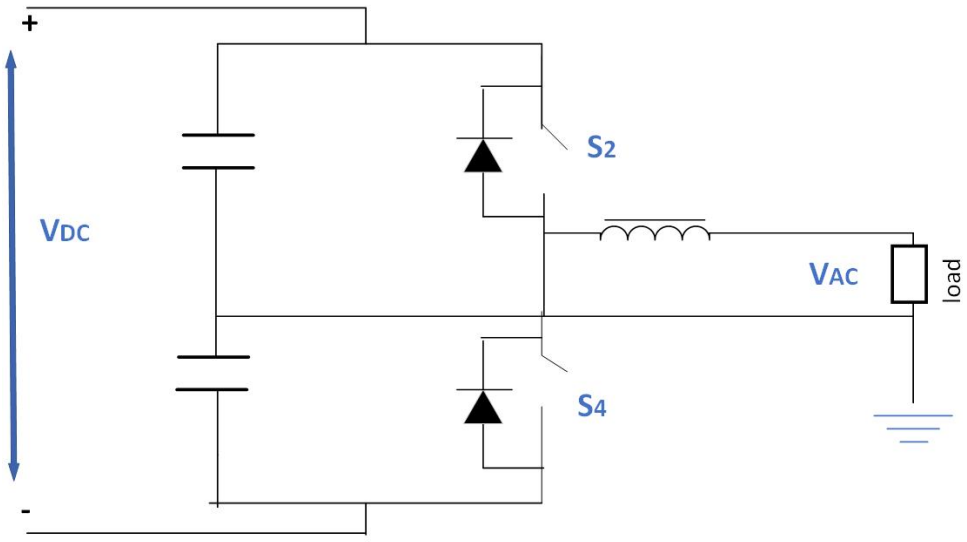

Figure 4-23: Half-bridge inverter. [111]

4.2.4 Power converter efficiency

The efficiency of a DC-DC or a DC-AC converter is given as:

$$\eta = \frac{P_0}{P_0 + P_d} \qquad \textit{Equation 4-17}$$

where P_0 is the output power and P_d is the dissipated power. The dissipated power is the sum of various parts, representing the power lost at various components of the electric circuit and is given as:

$$P_d = P_L + P_{switch} + P_{other} \qquad \textit{Equation 4-18}$$

where P_L is the power lost in the inductor, P_{switch} is the power lost in the switch and P_{other} are the other power losses in the circuit.

In the case of a complete inverter unit, the efficiency is given as the ratio of output AC power to input DC power.

$$\eta_{inv} = \frac{P_{AC}}{P_{DC}} \qquad \textit{Equation 4-19}$$

The maximum efficiency that is achieved depends on the applied input voltage.

4.2.5 Batteries

Batteries are an essential part of the PV system, especially in stand-alone systems, for energy storage. Types of batteries used in PV applications include lead-acid, nickel-metal hydride, nickel-cadmium, lithium-ion and lithium-polymer batteries. Lead-acid battery is the most popular type for stand-alone systems and has the lowest cost.

Nickel-metal hydride (NiMH) batteries have high energy density but they have a high rate of discharge. Nickel-cadmium (NiCd) batteries have lower energy density and their major disadvantage is the toxicity of cadmium. Lithium-ion (Li-ion) and lithium-ion polymer (LiPo) batteries have high energy density but also high costs and their technology is still new compared to lead-acid batteries.

Another type of batteries is the redox flow batteries, which is a combination of batteries and fuel cells. Figure 4-24 shows the schematic of a redox flow battery. It this structure, there are two liquids, a positive and a negative electrolyte, which are separated by a membrane. Only protons can pass through the membrane. The charging and discharging of the cell can happen without the reactants mixing. This prevents the liquids from ageing. By increasing the size of the tanks, where the electrolytes are kept, the chemical energy that is stored can be increased. The maximum output power can also be increased by increasing the membrane area. The most important disadvantage of this type is that the structure is more complicated, it requires pumps and other components compared to the conventional types of batteries.

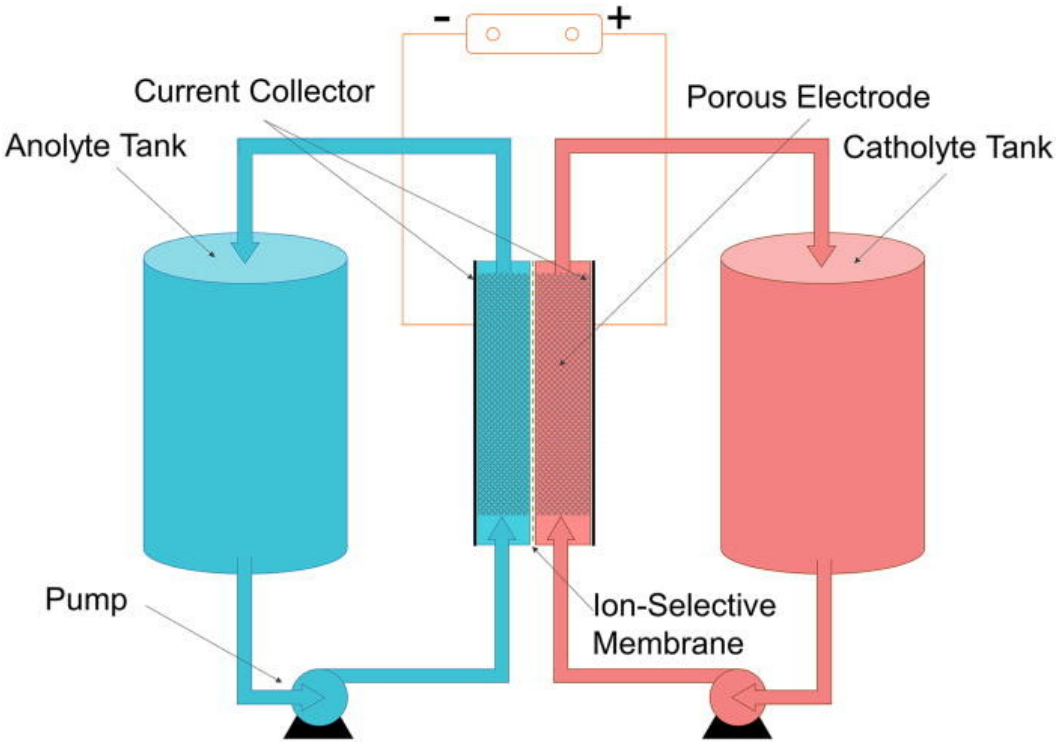

Figure 4-24: Diagram of a redox flow battery. [73] Licensed under CC BY 4.0

Figure 4-25 shows the diagram of a lead-acid battery during its charge and discharge cycle. Lead-acid battery has diluted sulphuric acid (H2SO4) as an electrolyte and lead and lead oxide (PbO2) are respectively the constituents of the negative and positive electrode. During the discharging process, there's a flow of electrons from the negative to the positive electrode via an external circuit, which causes a chemical reaction between plates and electrolyte. The charging of the battery takes place when a higher voltage source, compared to the battery voltage, is connected. The flow of electrons is then reversed. The energy storage takes place in the electrolyte, whose density increases during charging. The voltage source is the PV module. In grid-connected systems, that use batteries, the inverter can charge the battery.

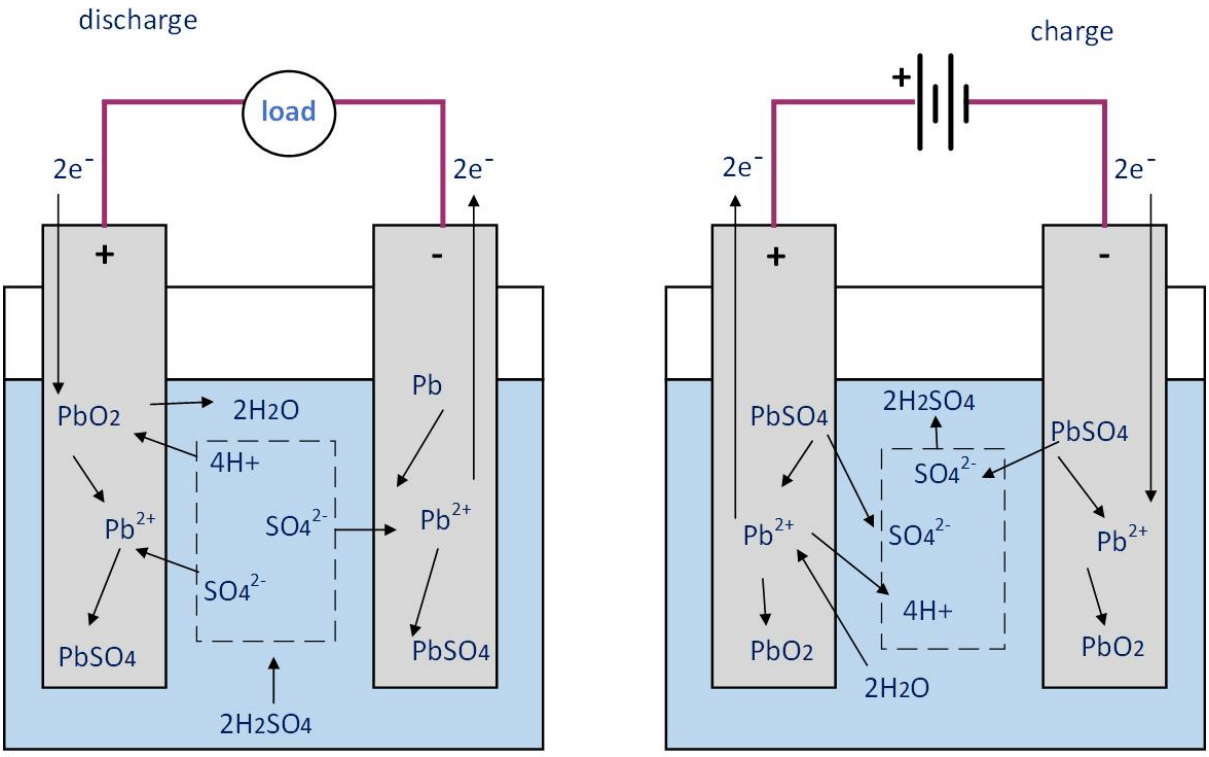

Figure 4-25: Lead-acid battery discharge and charge cycle. [116]

4.2.5.1 Battery parameters

The voltage of the battery operation is called the nominal voltage. The lead-acid batteries used in PV systems usually have nominal voltages of 12, 24 or 48 V.

The battery capacity, C_{bat} describes the amount of charge delivered by the battery at the nominal voltage. This is proportional to the electrode material amount. Capacity is measured in ampere-hours (Ah). The energy capacity of the battery is the product of nominal voltage and battery capacity.

The efficiency of the battery is described by the round-trip efficiency, which is the ratio of total storage output to total storage input.

$$\eta_{bat} = \frac{E_{out}}{E_{in}} \qquad \textit{Equation 4-20}$$

This can also be calculated as the product of two individual efficiencies, the voltaic efficiency, η_V and the coulombic efficiency, η_C.

$$\eta_V = \frac{V_{discharge}}{V_{charge}} \qquad \textit{Equation 4-21}$$

Voltaic efficiency is the ratio of average discharging voltage to average charging voltage and the coulombic efficiency is the ratio of total charge extracted from battery to total charge put in battery in a full charge cycle.

$$\eta_C = \frac{Q_{discharge}}{Q_{charge}} \qquad \textit{Equation 4-22}$$

This way the battery round-trip efficiency becomes:

$$\eta_{bat} = \eta_V * \eta_C = \frac{V_{discharge}}{V_{charge}} * \frac{Q_{discharge}}{Q_{charge}} \qquad \textit{Equation 4-23}$$

The battery state of charge (SoC) describes the percentage of battery capacity available for discharge,

$$SoC = \frac{E_{bat}}{C_{bat} * V}$$ *Equation 4-24*

and the depth of discharge (DoD) describes the percentage of battery having being discharged.

$$DoD = \frac{C_{bat} * V - E_{bat}}{C_{bat} * V}$$ *Equation 4-25*

The battery's cycle lifetime is the number of charging and discharging cycles that are available before the capacity drops below 80% of its nominal value. This lifetime increases in colder operating temperatures. Temperature also has an effect on the battery capacity. Capacity decreases with temperature decrease.

4.2.6 Charge controllers

In PV systems that use batteries, charge controllers are an essential component. A charge controller controls the current that flows between the battery, the PV module and the load. Its job is to keep the battery electrical parameters within the manufacturing limits. The charge controller tasks include protection from overload and deep-discharge, prevention of discharging when it's not wanted, monitoring of the state of charge and sometimes voltage conversion and MPP tracking. Figure 4-26 shows the position of a charge controller in a PV system.

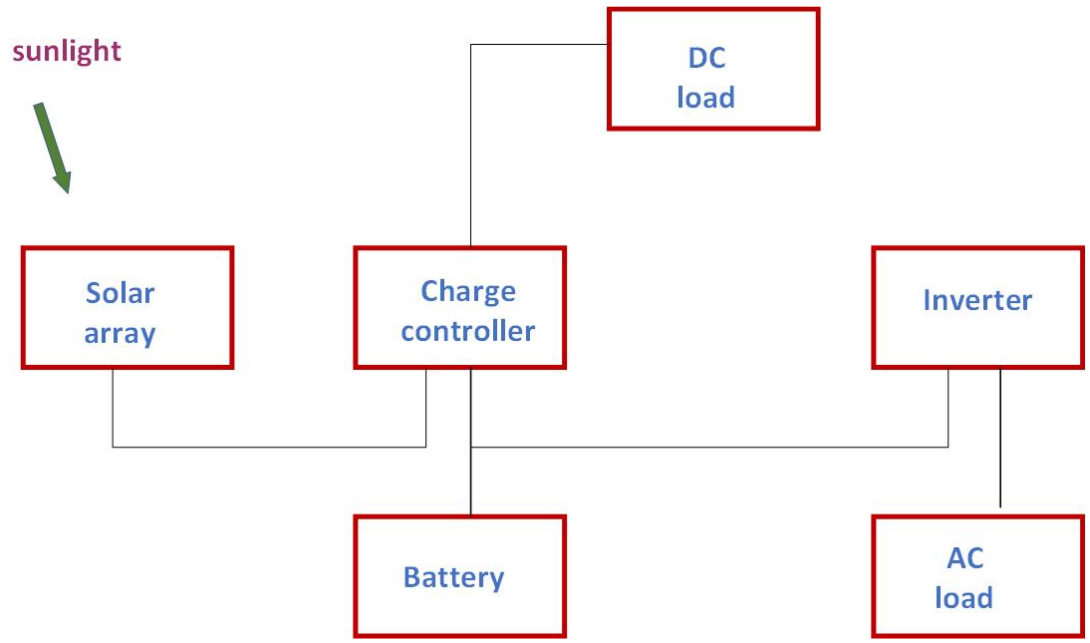

Figure 4-26: Position of charge controller in a PV system.

A charge controller can be a series controller or a shunt controller. The basic equivalent circuits can be seen in Figure 4-27 and Figure 4-28, respectively. A series controller prevents overcharging by disconnecting the PV panel, turning the switch 1 off. The switch 2, between battery and load, is turned off when there's a need to protect from deep-discharge.

In the shunt controller, the controller is connected in parallel to the PV panel. Here overcharging is prevented by short-circuiting the PV panel. The module operates under short circuit mode and there's no current to the battery. Deep-discharge protection is ensured by disconnecting the load via the switch 2.

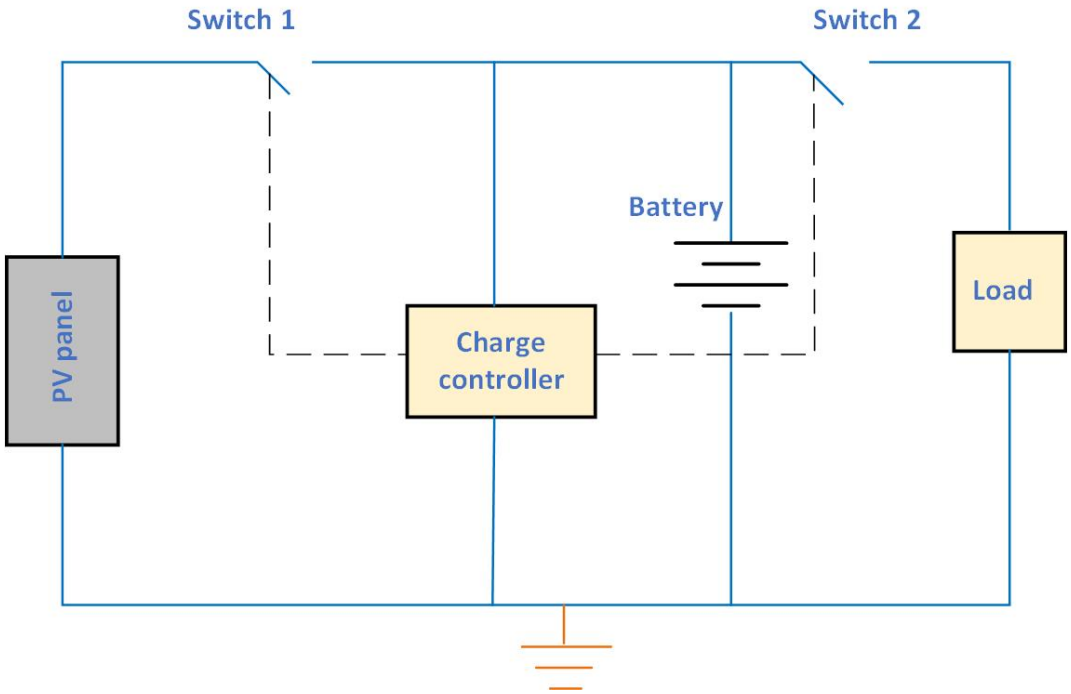

Figure 4-27: Series charge controller. [117]

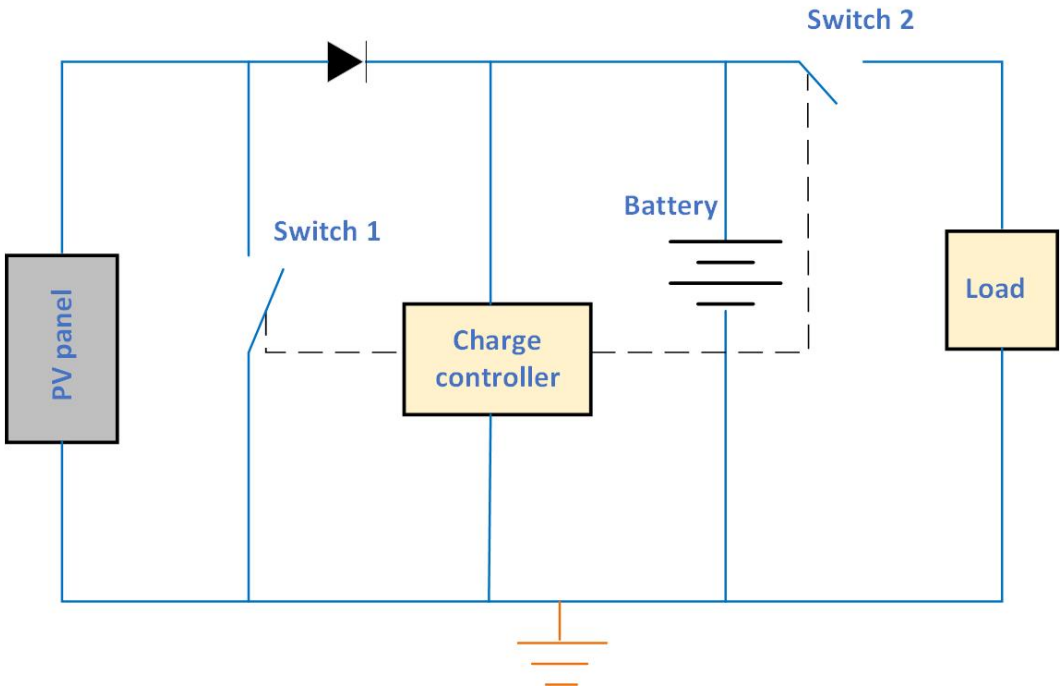

Figure 4-28: Shunt charge controller. [117]

Since temperature effects the operation of the battery, modern charge controllers have temperature sensors, which allow them to adjust the battery electrical parameters to the temperature.

4.3 Design of PV system

4.3.1 Types of PV systems

Photovoltaic systems vary in size and design. They can be small, consisting simply of a module and a load, for example to power a water pump, or they can be large power plants with the purpose of providing power to the grid. There are systems for residential use that need to be operational continuously when the houses are not connected to the grid. PV systems can be designed to provide power to both DC and AC loads, may include reserve power or a backup generator. The three main types that PV systems can be distinguished in are the stand-alone, the grid-connected and the hybrid systems.

Stand-alone or off-grid PV systems are independent of the utility grid. They can include only the PV module and the load or they can also include batteries for energy storage. In the latter these systems also include charge controllers. Batteries should have sufficient capacity to store energy which is produced in the day and can be used at night or days with cloudy conditions.

Grid-connected PV systems are connected to the utility grid with the help of inverters, which are used to convert the DC power from the module to AC power to feed the grid. These systems range from small, for residential and commercial use, to large scale power plants. They don't usually include batteries, to lower the overall cost and oversupply of produced electricity (when talking about residential installations) is transported to the utility grid. In turn, when more energy is needed than the one provided by the PV system, the house is powered by the grid. Lately though more grid-connected systems include batteries with the purpose of increasing self consumption. PV power plants transport all produced electricity to the utility grid.

Finally, hybrid PV systems consist of a combination of PV modules with another source for generating electricity, like for example a wind, gas or diesel generator. Due to the different

methods for electricity generation, this structure requires more sophisticated controls. Hybrid systems include batteries to store excess generated energy, along with charge controllers.

Both stand-alone and hybrid PV systems can also include inverters, depending on their use, if they are for example connected to both DC and AC loads.

A PV system can be designed on an energy balance basis. That means that the energy that is generated will match the energy that is consumed via the loads. Another basis of the design of PV systems is economics.

There are several steps involved in the process of designing a PV system. These steps include an overall planning, assessment of load and solar irradiation information, determination of the solar array requirements, arrangement of modules, selection of suitable system components.

4.3.2 Stand-alone PV system

Figure 4-29 shows a simple design of a stand-alone PV system with DC and AC loads.

4.3.2.1 Energy requirement assessment

First step is to select the nominal operational voltage of the system, usually 12, 24 or 48 V. Next, the requirements of the loads in daily energy need to be determined, based on current and average operational time, expressed in ampere-hours (Ah). The daily energy (Wh) requirement of a DC load is calculated by multiplying the power rating (W) of each appliance with the average daily operational time (h). The division of Wh with the nominal operational voltage, provides the Ah of the appliance. In AC loads, the equivalent DC energy use is calculated, by dividing the AC load energy use with the inverter's efficiency. Next follows the division with the nominal PV system voltage to determine the Ah. The energy requirements of the loads need to be increased by 20 or 30% in order to account for the energy required by components such as charge controllers and batteries.

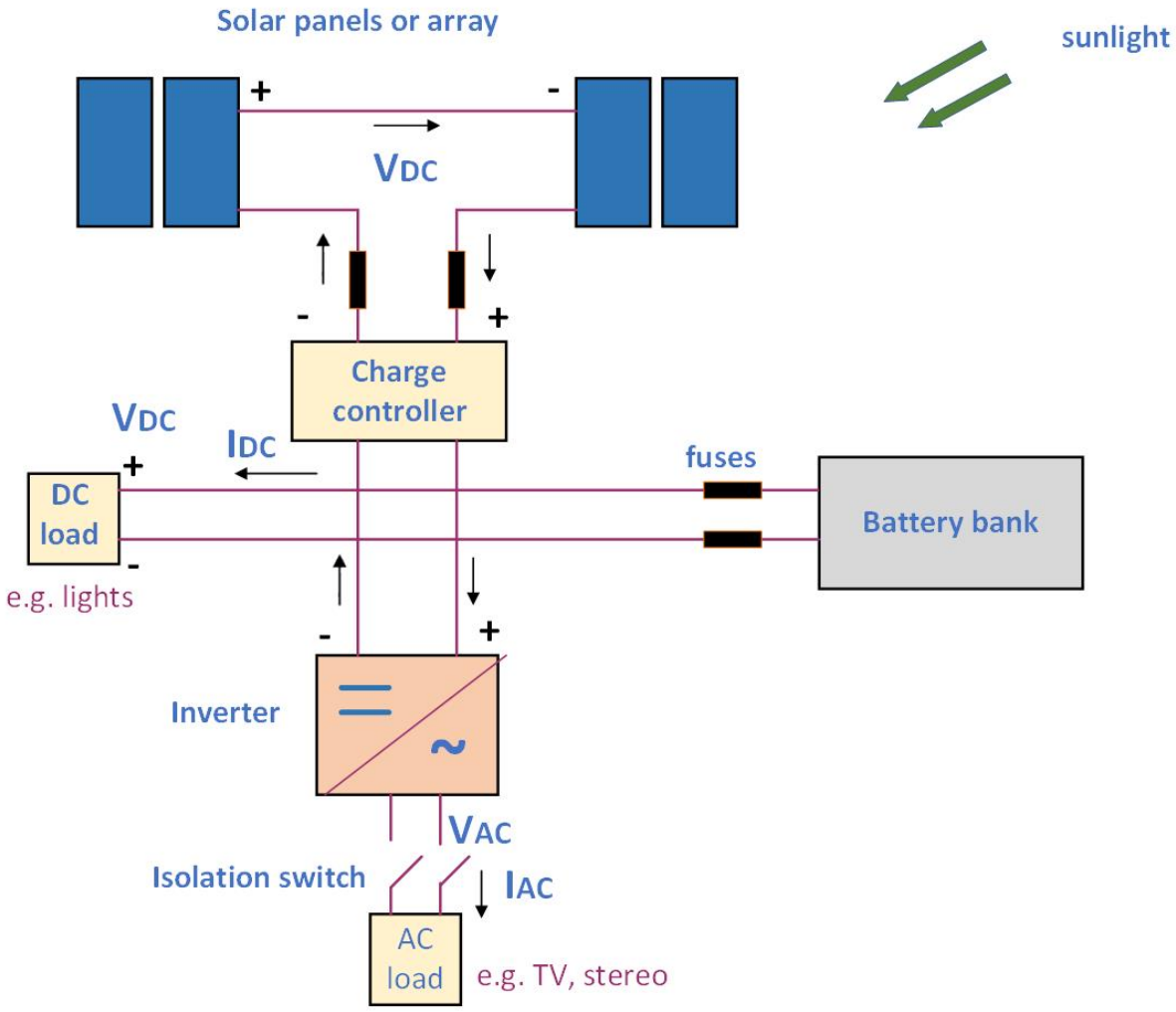

Figure 4-29: Simple design of a stand-alone PV system. [118]

4.3.2.2 Solar energy resource assessment

The next step is to determine the solar energy resource. The energy that will be received by the PV module depends on weather conditions and its variations with time, as well as the orientation of the module. The spectrum corresponding to Air Mass equal to 1.5 is usually used, which normalized has a total irradiance equal to 1000 W/m^2. This corresponds to 1 equivalent sun hour (ESH). If a site, for example, receives an average annual solar irradiation of 1000 kWh/m^2, on a horizontal plane, then that equals to 1000 ESH and divided by 365 is around 2.7 average daily sun hours. When the module is in a tilted position, this number is slightly higher. For the purpose of examining the design of a PV system, an average value of 3 ESH per day will be assumed.

4.3.2.3 Solar array requirements

The total current that the solar array must generate is determined by dividing the DC energy requirement that has already been calculated including the losses, which is expressed in Ah, by the daily equivalent sun hours (e.g. 3 ESH that has been assumed).

The next step is to determine the suitable arrangement for the solar array. This is done by figuring the minimum number of modules that will produce the calculated energy requirement. If the modules are connected is series then the nominal system voltage is increased and if they are connected in parallel then this leads to higher current. To determine the number of modules that will be connected in parallel, the total required current must be divided with the produced current of each module at maximum power. To determine the number of modules that will be connected in series, the nominal PV system voltage must be divided with the voltage at maximum power. The total number of modules required is determined by multiplying the number in series with the number in parallel connection. The output voltage of the modules should fit the voltage of the battery in order to achieve optimal operation of the system. It should also be within the range of the MPP tracking system of the inverter.

Other important issues regarding the PV modules are the efficiency and the effects of temperature and irradiance on the module performance that need to be determined.

4.3.2.4 Battery requirements

Batteries are an essential component of stand-alone PV systems and an important step in their design is to determine the size of the batteries, in order to have the desirable for each application reserve time. The reserve capacity of batteries is to be used at night or during days with no or little sunlight. The battery capacity will provide the required energy for a number of days, called days of autonomy. Depending on the load, days of autonomy differ. For residential systems it's usually around five days. For other loads, more essential, for example telecommunications, the autonomy is higher, around ten days or more. The batteries capacity (Ah) is calculated by multiplying the daily DC energy requirement, calculated in the beginning,

including losses, with the number of days of reserve time that is recommended. Lead-acid batteries are the most common used in stand-alone PV systems and they should be discharged at around 80% maximum, in order to prolong the lifetime.

4.3.2.5 Load profiling

Next step is the load profiling, in order to determine the maximum load and the average daytime and night time energy requirement. Different loads have different priorities. One load may need to draw a constant amount of power for a specific time period. Another load may show peaks in power consumption, corresponding to turning an appliance on and off. These different loads are drawing power from the PV modules at the same time or at different times. It is best to look at load profiles in an annual fashion, given that loads have different time variations: others are used every day, others several times a month and others have a seasonal usage, like for example air conditioners. For that reason the total energy consumed is calculated for the whole year and is given by Equation 4-26, where $P_L(t)$ is the load power at time t. The consumed energy is expressed in kWh per year.

$$E_L^Y = \int_{year} P_L(t)dt \qquad \textit{Equation 4-26}$$

4.3.2.6 Charge controller selection

Stand-alone PV systems with batteries need charge controllers to protect the batteries from overcharge or deep-discharge. The main purpose of a charge controller is to disconnect the battery from the array when it is fully charged and the load from the battery when the latter is in danger of deep-discharge. Due to the act that each type of battery has a different charging routine, the charge controller needs to be selected for the specific battery type of the PV system. The charge controller consumes power which as a result leads to a typical efficiency of 85 to 95% in the transfer of power.

4.3.2.7 Inverter selection

An inverter is part of the system when output AC power is required. The inverter should have the same nominal input voltage as the battery voltage and in stand-alone systems it should be large enough to deal with the total amount of power which will be used at one time. The size of the inverter should be 20 to 30% larger than the total power of the appliances. The inverter must be able to supply continuous power to AC loads and provide sufficient surge capability, in order to start loads which may surge when they are turned off, especially in the case that they are turned on at the same time. The typical efficiency of an inverter is 80 to 90% with a good inverter reaching efficiencies up to 95%.

4.3.2.8 Mounting and tracking

The next step is to select the mounting of the modules, which should be oriented to face the Sun. The mounting system can be classified as ground mount, roof mount or pole mount and the mounting structure is usually made of galvanized iron, aluminum or mild steel.

The modules should be placed in a way that they receive maximum amount of sunlight. In the northern hemisphere they should be placed facing true south and vice versa in the southern hemisphere. The PV system can have a tracking system to increase the power received. This increase can be around 20 to 25% for single axis tracking systems and around 30% for double axis tracking systems.

4.3.2.9 Wiring selection

Another important task is to select the correct size and type of the wire that will be used, in order to enhance the system performance. The wire should be large enough to carry maximum current without significant voltage losses. Due to the wire resistance there will be voltage drop from source to load, so the minimum wire length should be used. The specifications of the wire should be based on the calculated output current and voltage of the system. The number and type of switches, circuit breakers, fuses etc. also needs to be determined.

4.3.2.10 Shadowing

Finally, a shadowing analysis is very important for the operation of a PV system, so that possible shading can be recognized and if inevitable, taken into account. The number of modules in series must be determined accordingly, because shadowing in parts of the array can lead to having the maximum power voltage, at high temperatures, below the inverter's minimum operating voltage.

4.3.3 Grid-connected PV system

PV systems that are grid-connected use the PV generated energy during the day and the grid power during the night. Any excess generated power can be fed into the utility grid or stored in batteries if the system is connected to them.

Batteries are not necessary, since the grid-connected systems feed their excess energy directly into the grid, so the system is simpler and less expensive. The system is connected to the grid on a permanent basis, so solar energy consumption and panel sizing calculations are not necessary, allowing a range of options to be chosen in the design of these systems.

Net metering is the mechanism by which when the PV system generates more power than is consumed, the excess amount is fed into the utility grid and the electric meter is rotated backwards. This means that the producer is given credits from the utility company depending on the amount of power that is delivered to the grid. The billing is done for the net amount of electricity, which could result in a reduction on the bill or even direct payment. A new electrical meter is usually installed which measures the energy leaving and entering the system to calculate the net energy consumption.

Figure 4-30 shows a simple design of a grid-connected PV system without batteries. The most important component is of course the inverter, since the PV DC output can't be fed into the grid without being converted to AC with the help of an inverter. The inverter converts DC power to AC to feed into the grid at suitable voltage and frequency. The choice of inverter is important, taking into account the maximum high and low voltage power that the inverter can handle, as well as its efficiency.

Apart from the components already presented in the design of a stand-alone PV system, the grid-connected system has a kWh electric meter, as mentioned before, measuring the electricity flow from and to the utility grid. This can be achieved with twin meters, where one measures the energy consumption and the other the energy fed into the grid or with a bidirectional meter, measuring the net electricity received from the grid. Depending on the fed-in power, the PV system can slow down or stop the disc of the electric meter and spin it backwards, which is the net metering process mentioned before.

The grid-connected PV system has an AC breaker panel or fuse box, like the typical fuse box that comes with domestic electricity supply and installation, but there are extra breakers for the inverter and filter connections that the system may have. Other components include isolator and safety switches, so the system can be safely disconnected if needed.

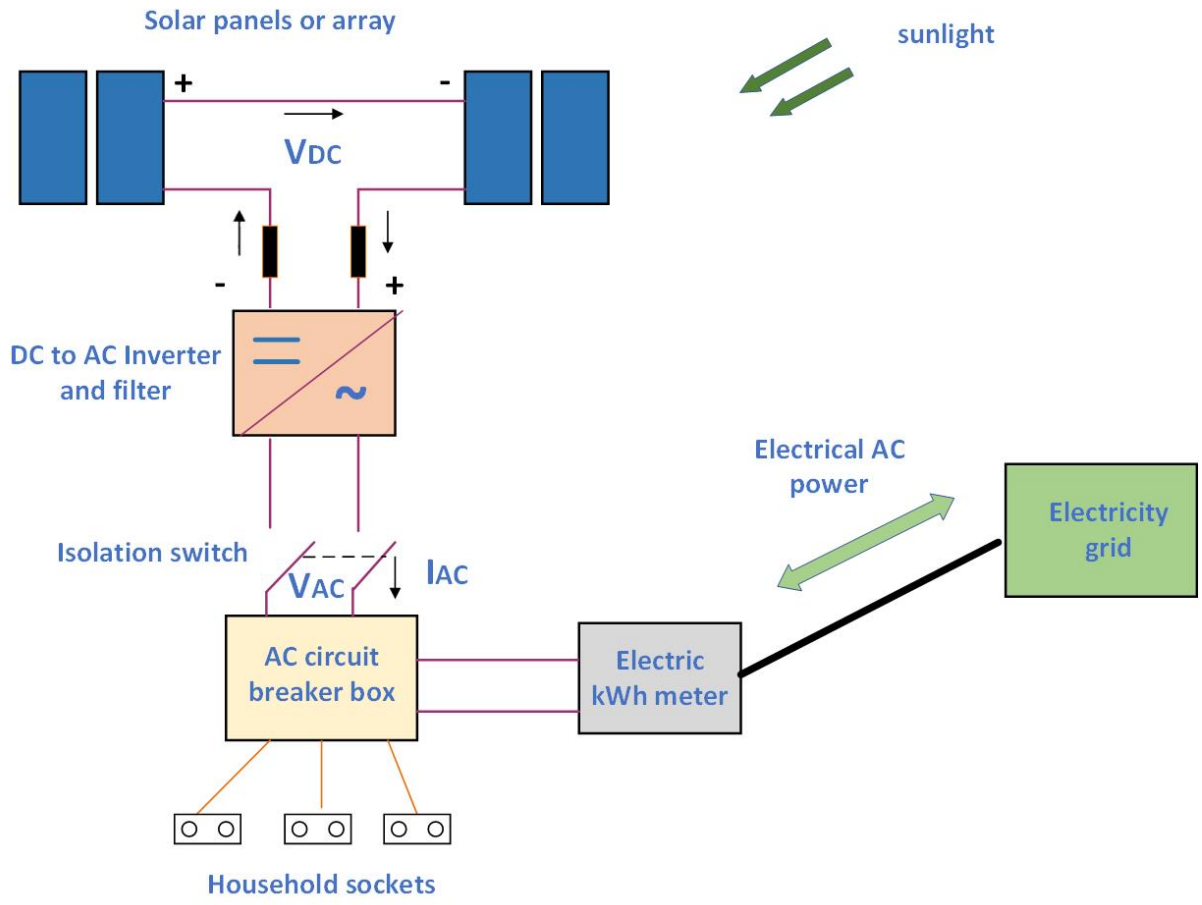

Figure 4-30: Simple design of a grid-connected PV system without batteries. [118]

The grid-connected PV system can also include batteries, in order to be independent. A simple design of this system can be seen in Figure 4-31. Energy can be drawn from the storage of the battery instead of the utility grid. In grid-connected systems, batteries can be utilized for short term storage, few hours or days or long term storage, few weeks, depending on the needs. The cost increases when batteries are included into the system and charge controllers must also be selected.

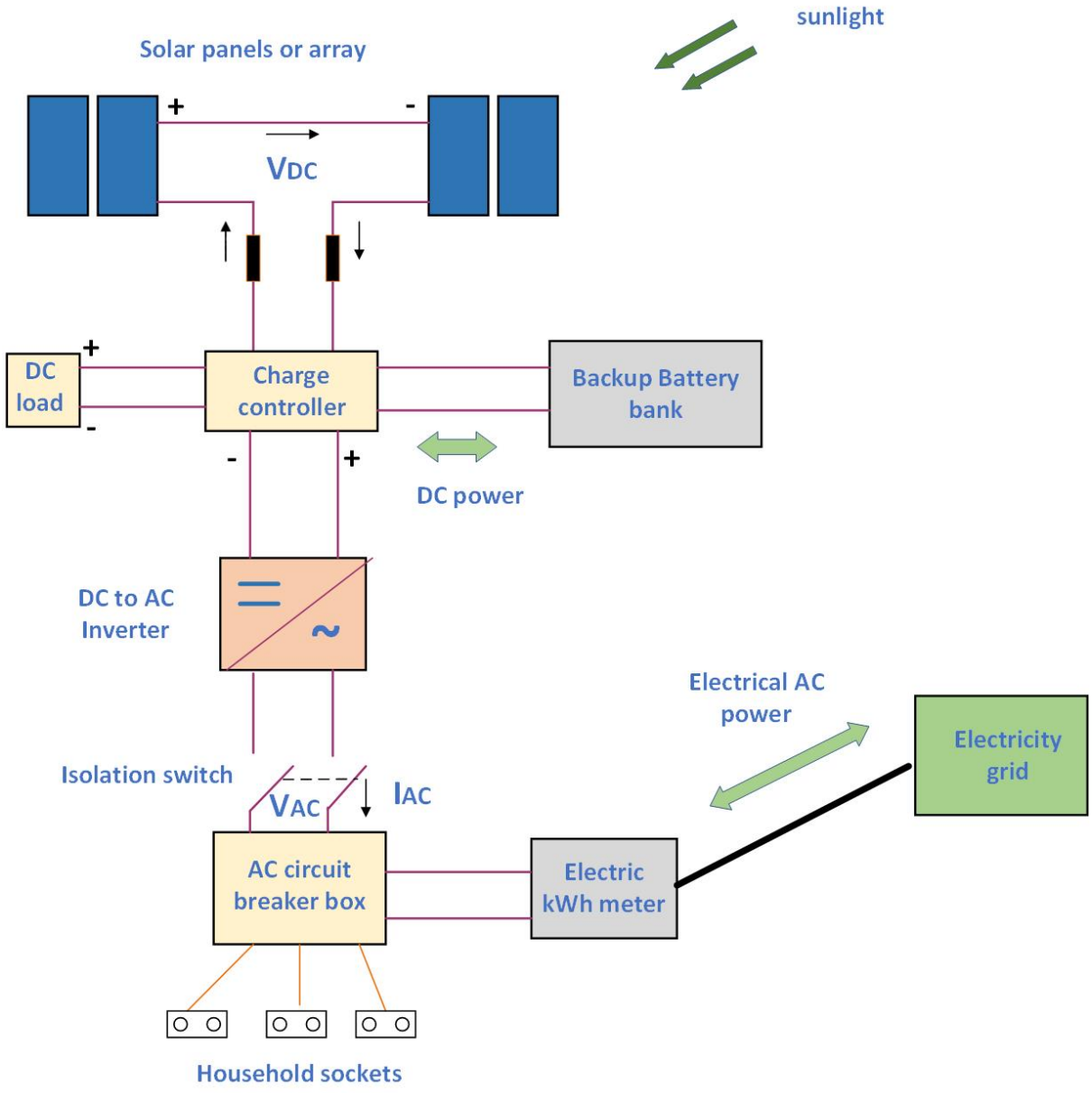

Figure 4-31: Simple design of a grid-connected PV system with batteries. [118]

4.3.4 Hybrid PV system

In hybrid PV systems there are two or maybe more energy sources that are joined in their operation to generate energy. The system may include storage unit and be connected to an AC distribution network. The component that is essential in a hybrid system is the multifunctional inverter, which is used to convert DC to AC current, control the power generation, storage units, voltage and frequency. Along with PV modules, a hybrid system can most commonly incorporate a diesel generator or a wind turbine. The common designs of a hybrid PV-diesel and a hybrid PV-wind system are shown in Figure 4-32 and Figure 4-33, respectively.

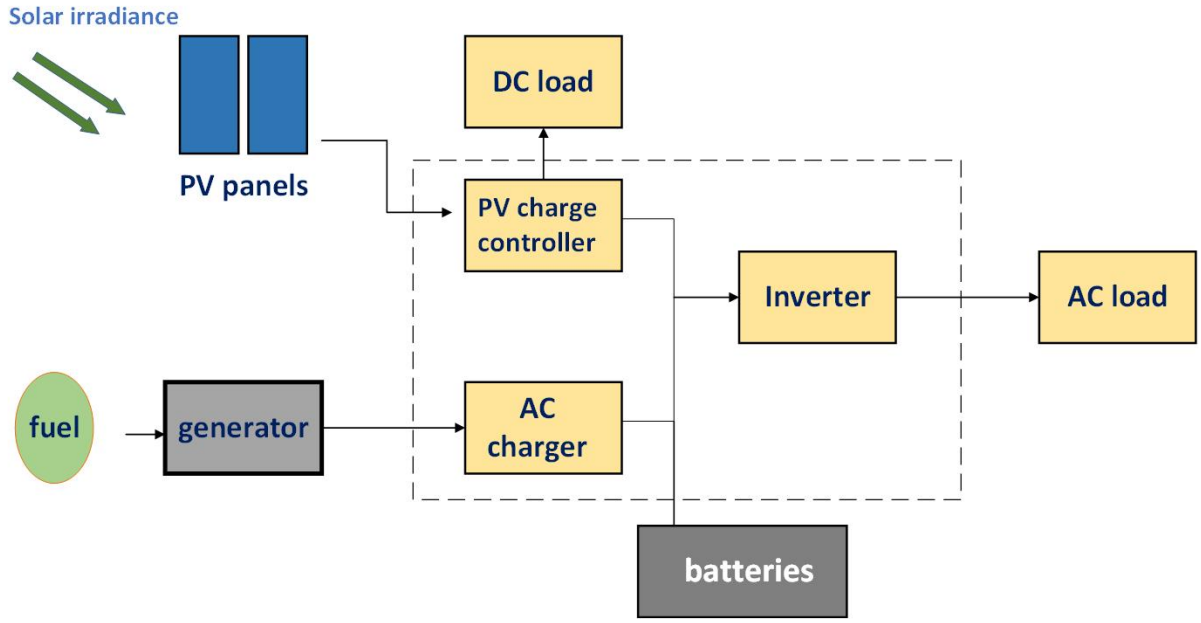

Figure 4-32: Design of a hybrid PV-diesel system. [119]

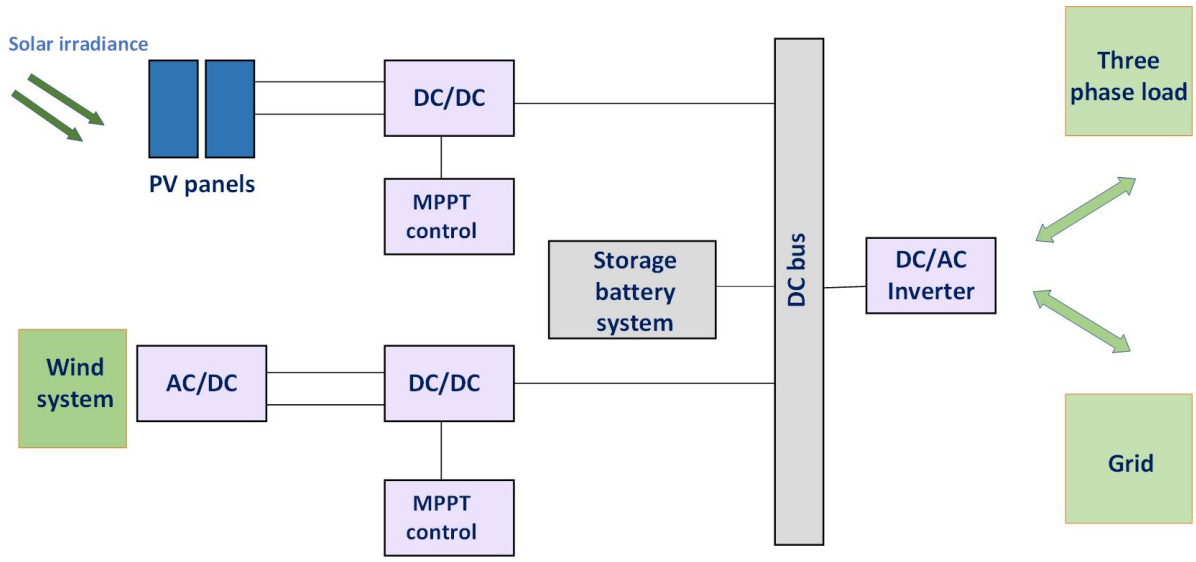

Figure 4-33: Design of a hybrid PV-wind system. [120]

The hybrid PV-diesel system will be used as an example to present the design of a hybrid PV system. Except from the main components that have been described in both stand-alone and grid-connected PV systems, the hybrid system also has a generator, which produces electricity with the use of liquid fuel. The fuel can also be gasoline or propane, instead of diesel.

To achieve optimal performance of the generator, it should be used for loads at around 80% of its rated capacity and not for small loads. The generator consumes more fuel in the beginning of its operation and if it's turned on and off for small time periods, it degrades much faster. Each generator has specifications regarding the minimum running-time that is suggested for its operation.

The excess energy that is generated from the PV modules and the generator is stored in batteries for later use. The batteries are accompanied by charge controllers for their protection from overcharge and deep-discharge.

The loads may be of both DC and AC power, so an inverter is needed to convert DC power from the PV modules into AC to power the loads. In the hybrid PV-diesel system, and AC charger is also required, which transforms AC power that is produced from the generator into DC power to charge the batteries, which store DC power. The charge controller, the inverter and the AC charger can be three individual devices or there is the option of using a bi-directional inverter, which combines the operation of the inverter and the AC charger. The

devices should be chosen so that both the PV modules and the generator can charge the battery and the rated charging current must match the maximum charge current of the battery.

In order to choose a hybrid PV-diesel system, there are certain factors that need to be considered. There should be an assessment of the PV output and if it is sufficient to consider the solution of a hybrid system instead of a pure diesel generator. The load forecast is also essential in designing a hybrid system, since more information is needed in this type of system. The average daily total energy requirement, the average daily peak power and its time, the maximum peak power in high season, the average and maximum demand levels in the time period that the PV modules operate and the amount of energy that is used during the night, are all variables that need to be determined.

This type of system has the advantage of being able to supply a low load for a large time period during the night, by using the battery storage, while the generator can be used to cover evening peak demand and contribute to the battery charge if needed.

4.3.5 PV simulation tools

The design of a PV system is aided with the use of software designing tools offered by various manufacturers. These can be dimensioning tools, which calculate the dimensions of the PV system in regards to input data, like load data, climate data and system components. Simulation tools are used to simulate the behaviour of the PV system in a given time period, based on the input data. Research tools are used to simulate different systems for research purposes and mini-grid design tools help in the design of mini-grid electrical distribution network.

A dimensioning or sizing tool has the role of determining the optimal size of the various system components, when given the desired energy output. Some tools, depending on their design, provide the system dimensioning having as a focus the life-cycle cost of the system, while others base their outcome on a proper function of the system. These tools are usually easy to use and are favoured by PV installers.

Simulation tools differ from dimensioning tools in the way that the user must specify the type and size of the system components. This is done in order for the tool to give a detailed description of the behaviour of the system under the given circumstances. Time resolution of the simulation analysis depends on the each tool itself as well as the resolution of input data, like weather data. Hourly resolution is common and provides the performance of the system under various conditions, the impact of changes in the components operation etc. Life-cycle cost and emissions information can also be provided. Some simulation tools provide system dimensioning as well.

Research tools allow for flexibility in modifying algorithms, in order to study the behaviour and interactions of the various components in the system. They are used by research organisations.

Mini-grid design tools are used in order to choose the most suitable type of system (e.g. stand-alone) to power a house in a village. These tools can also help in minimizing power losses with the correct selection of voltage and wiring.

Examples of software tools are RETScreen with focus on preliminary study and general dimensioning, HOMER which allows comparison between DC and AC coupled systems and can focus on economic aspects, PV-SPS, PV*SOL and PVsyst which provide detailed configuration, Hybrid2 and PV-DesignPro for system analysis and TRNSYS and MATLAB/Simulink for detailed research focus.

Results of these software tools depend on the quality of input data and rely a lot on the experience and knowledge of the user.

5 Photovoltaic system calculation and aspects

Author(s): Dr Efterpi Nikitidou
Dr Andreas Kazantzidis

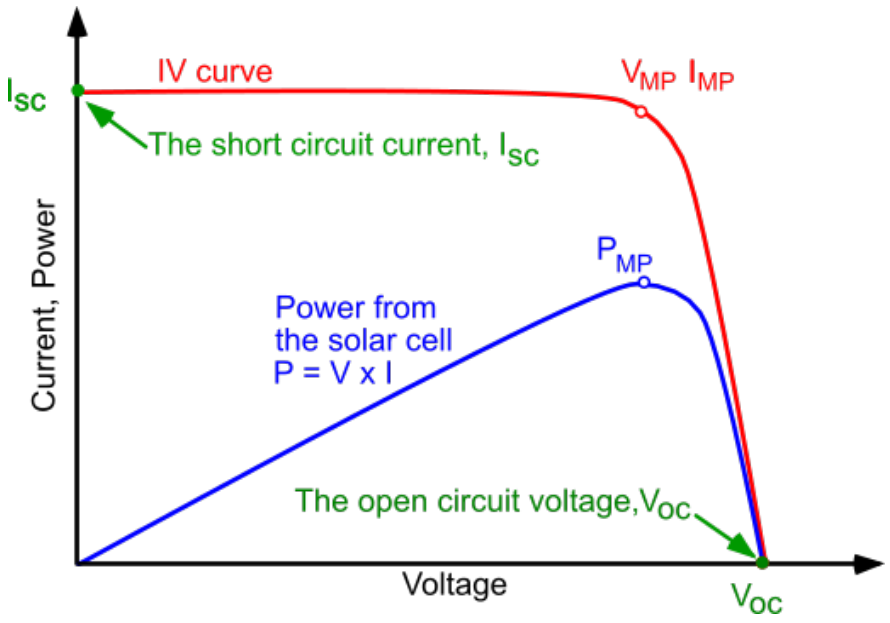

5.1 PV applications examples

The continuous demand for energy has resulted in the ever increasing use of renewable energy resources. Photovoltaic applications are used worldwide to cover the energy needs and they vary from large scale installations, which are connected to the utility grid, to smaller installations for various energy purposes. Some examples of PV applications are described in the following.

5.1.1 Solar home systems

Solar home systems (SHS) are stand-alone PV systems that provide power to houses in remote areas, not connected to the utility grid. They are commonly used in developing countries to power rural areas, where conventional fuels are not a viable solution. These systems usually operate at a rated voltage of 12 V DC and power appliances like radios, TVs, lights etc. for a few hours a day. SHS cal also power AC loads with the use of an inverter.

Figure 5-1 shows a SHS situated in a house in Peru, while Figure 5-2 and Figure 5-3 show the schematics of a SHS with DC and AC loads.

Figure 5-1: Solar home system in a house in Peru. [121] Licensed under CC BY-SA 3.0

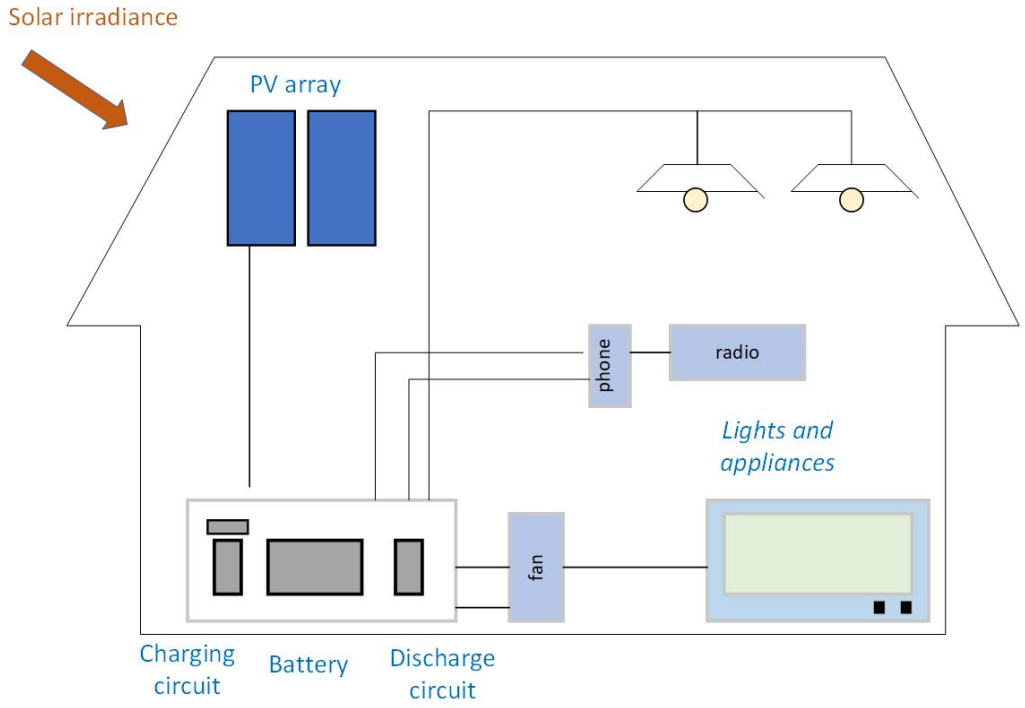

Figure 5-2: Schematic of a typical DC solar home system. [122]

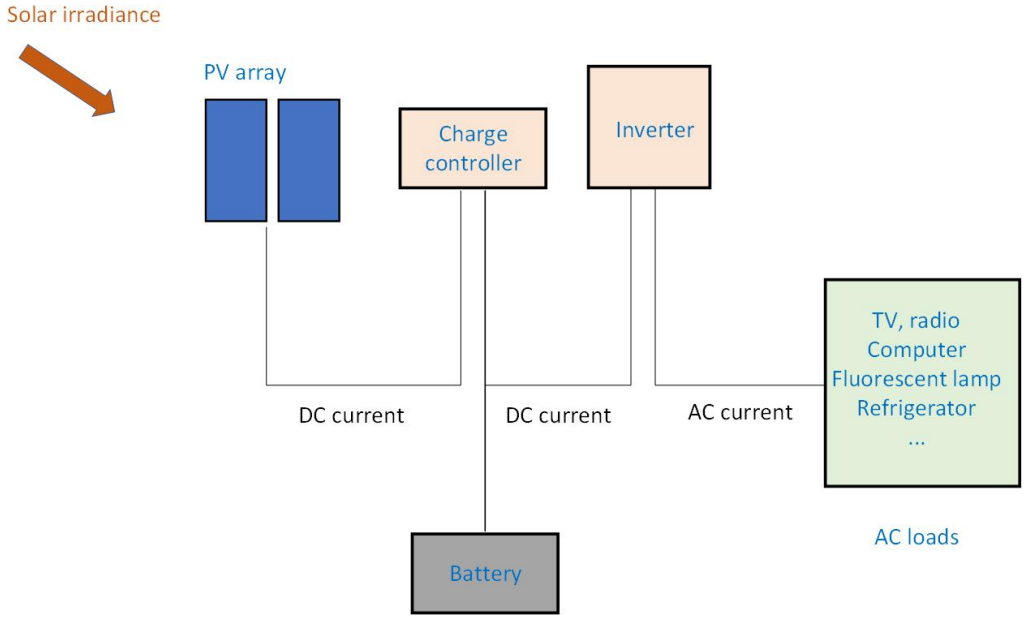

Figure 5-3: Solar home system with AC loads. [123]

Solar home systems consist of one or more PV modules, one or more batteries for energy storage, charge controller and inverter when AC loads require it.

The size of the system is to be determined by engineers while technicians can educate the users about the basic characteristics. The PV panels are installed on rooftops or poles with a tilt angle to increase received radiation. Shading analysis should be performed so that the panel is not subject to shades from trees or other buildings. The batteries should be connected close to the panel, in a location that is cool, dry and ventilated. The operation of a SHS, once installed properly, doesn't require a lot of supervision and maintenance. The users should be educated on properly using the system and manage loads.

The main problem of solar home systems is the high initial cost, with the battery being the most expensive component. The prices are usually high for the end-users. There are however projects, depending on the country, for funding solar home systems or there is the possibility of offering a down-payment and continue with monthly payments or microleasing projects.

SHS replace previously used energy sources, like kerosene, candles, dry batteries and thus reduce indoor air pollution as well as fire hazards. The quality of lighting is improved in the room. The particulate emissions and the use of natural resources are reduced.

5.1.1.1 Example of sizing a solar home system

Let's consider an example of a solar home system that is used to power a few appliances for a few hours every day. First the load is calculated. A load consisting of a few light bulbs, a TV, a radio and a phone charger, operating for 4-5 hours per day would consume around 200 Wh per day. After that the peak sun hours (PSH) is estimated, which is the number of hours in a day where the average solar irradiance is 1000 W/m^2. Let's consider that the site has PSH equal to 5 for the worst month of the year, e.g. December.

The desired output energy of 200 Wh/day is the product of the PV system output multiplied with PSH and the performance ratio of the PV module. If the performance ratio is 55%, then the desired PV system output is calculated at 72.7 W, so a PV module of 75W should be selected to support the desired load.

In order to select a battery, the energy stored in it is calculated by multiplying the desired number of days of autonomy with the energy load per day and divide with the depth of discharge (DOD) of the battery. So if the number of days of autonomy is 4, the energy load

per day is 200 Wh and DOD is 70%, then the battery stored energy is calculated at 1142.8 Wh. The stored energy in Wh is the product of the battery capacity in ampere-hours (Ah) with the battery terminal voltage. Given the voltage at 12 V, the capacity is calculated at 95.2 Ah, so a 12 V, 100 Ah battery should be selected for the system.

Through various initiatives solar home systems have been installed in countries, like Peru and Bangladesh, where many houses are cut off from the grid, in order to improve life quality.

5.1.2 PV-powered water-pumping system

The pumping of water in rural areas with no connection to the utility grid can be done by using solar power. A PV water-pumping system can be used for such a purpose providing a solution in many remote villages. Such a system consists of a PV panel and pumps. It may include batteries for energy storage in which case it also contains a charge controller (Figure 5-4). The DC current from the PV panels is either supplied to a DC pump, to pump water or stored in batteries for use in conditions with no sunlight.

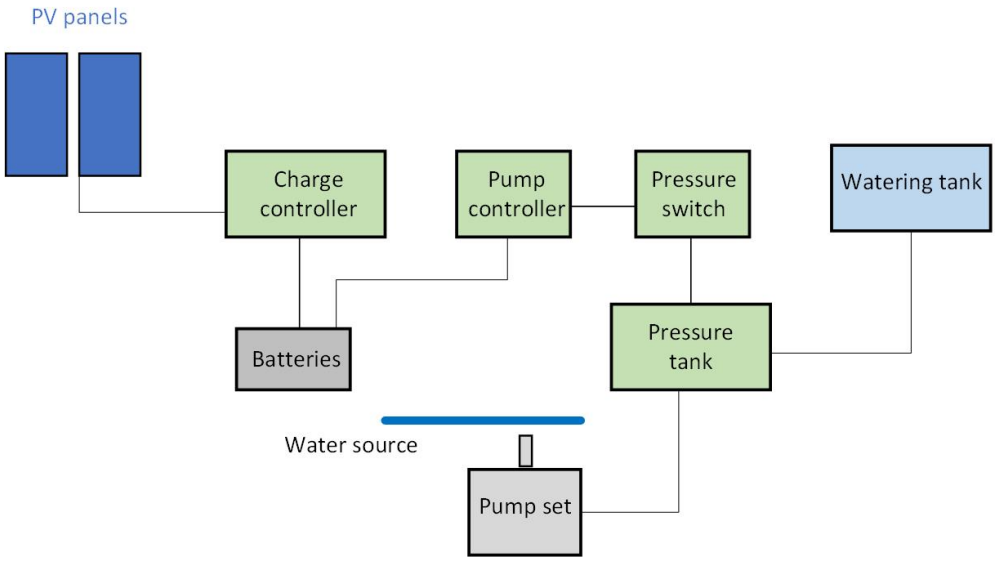

Figure 5-4: Schematic of a PV-powered water-pumping system. [124]

In particular, the generated electricity from the PV system is used to drive a usually submersible motor pump, which pumps water to an elevated water tank. Due to gravity, the

water flows from the tank to water taps used by the public or to places for feeding livestock or the irrigation system. Solar water pumps are specially designed to use DC current from PV panels or batteries, as opposed to conventional pumps using AC current. Their design also makes them suitable to be used at low light conditions at reduced voltage. Most systems can store water for later use, when no sunlight is available, so the use of batteries is not required, which reduces the overall cost of the system.

In systems with batteries, batteries are charged during the day and provide power to the pump to extend the period during which the pump operates. They provide a steady voltage to the motor of the pump. Batteries however reduce the system's efficiency because the voltage supplied by them can be lower than the one produced by the PV panels. For this reason a pump controller is used to boost the voltage of the battery that is then supplied to the pump.

In systems without batteries, electricity is sent directly from the PV panels to the pump, which operates only during sunlight hours. The water that is pumped depends on the amount of sunlight that is received, which changes during the day. As a result, the amount of water that is pumped also changes during the day. To account for these variations in the flow rate, a good match is required between the PV panels and the pump so the system can operate efficiently. These systems are designed to store more water during sunlight hours to use in cloudy conditions or at night. They have larger water tanks or a separate tank that then feeds smaller water tanks.

5.1.2.1 Designing a PV water-pumping system

In order to design a PV-powered water-pumping system there are certain things that need to be determined, first of which is the need in water supply. Depending on the application the domestic water supply (water needs per person per day) and the irrigation water supply are to be determined. Next the pumping head needs to be calculated. The pumping head is determined by adding the elevation head (distance between the water source surface level and the outlet pipe level), the major losses head (which depend on the rate of water flow, type and dimensions of the pipe) and the minor losses head (which depend on pipe components such as valve, elbow etc.).

The next step is estimating the solar resource, which can be done by taking solar radiation measurements in the site throughout the year or to limit the cost, by using global databases of solar radiation. After that the solar pump needs to be selected. The pump chosen must be adequate to both daily water flow and pumping head requirements. Three types of pumps are usually used in PV water-pumping systems: the centrifugal pump, which has characteristics similar to a conventional pump, the helical rotor pump with one turning part and the piston (diaphragm) pump with more moving parts. It is usually preferable to choose a pump head specification higher than the pumping head that is required.

Last the PV panel needs to be selected. The size of the PV panel that is required depends on the pumping head, the amount of water that is required and the solar resource available.

The advantages of a PV water-pumping system are various. There are no costs for fuel and it's an installation with long lifetime. The system can operate unattended and its maintenance needs are low. However the main disadvantage is the high initial cost. Systems without batteries have lower costs.

5.1.3 PV-powered refrigeration system

PV modules can be used to power refrigeration systems (Figure 5-5), which are usually used in off-grid locations to keep food or medicine, like vaccines, which will perish if not refrigerated. These systems have thick insulation and use DC vapour compression cooling systems.

At first, PV-powered refrigerators used batteries for energy storage, so that they could be used at night or in cloudy conditions. These systems with batteries are expensive and the batteries deteriorate in hot temperatures. They also require maintenance. During the 1990s, the NASA Johnson Space Center designed a solar-powered refrigeration system that doesn't require batteries, which store chemical energy, but instead it uses phase change material to store thermal energy for later use. This design is now commercial and used in freezers, vaccine coolers or household refrigerators.

Figure 5-5: PV-powered refrigeration system. [125]

For the operation of the system, the DC power generated by the PV panel is used to drive the compressor and the refrigerant is circulated through a vapour refrigeration loop, which extracts heat from an enclosure that is insulated. In this enclosure there are the thermal reservoir and the phase change material, which freezes when there is heat extraction from the enclosure. In that way, temperature is maintained inside the enclosure when sunlight is not available.

The system uses a variable speed DC compressor, in order to operate longer during the day and take better advantage of the variable solar resource. The speed of the compressor is controlled by a microprocessor, which has the role of maximizing the speed of the compressor for the available solar power. The PV panel is kept at its peak power point during the operation of the compressor. Load testing of the panel is also done by the microprocessor, before turning on the compressor, as well as cabinet temperature control and speed control of the compressor. Capacitors are incorporated into the system to smooth the power voltage so additional current is provided during the start-up of the compressor.

PV-powered refrigeration systems are used in off-grid locations, where utility grid is not available. These systems don’t depend on fossil fuels to provide power.

5.2 Economics of PV systems

Over the years a lot has changed in the costs and market prices of photovoltaic technology. This is a result of various factors like the manufacturing processes, the supply chain of PV, the installation costs, distribution channels, regional markets and many more. Policies have been implemented in many countries in order to support the increase in PV energy production, with financial incentives that encourage PV industry and make it a competitive alternative in the industry of energy production. Advancements in technology and improvements in the manufacturing process have also contributed in the overall decrease of photovoltaic costs.

Figure 5-6 shows the decline in the costs of renewable energy technologies that have occurred from 2010 to 2019. Solar PV technology has shown the highest decline in cost, at 82%. This has occurred mainly due to reduction in module prices and balance-of-system costs.

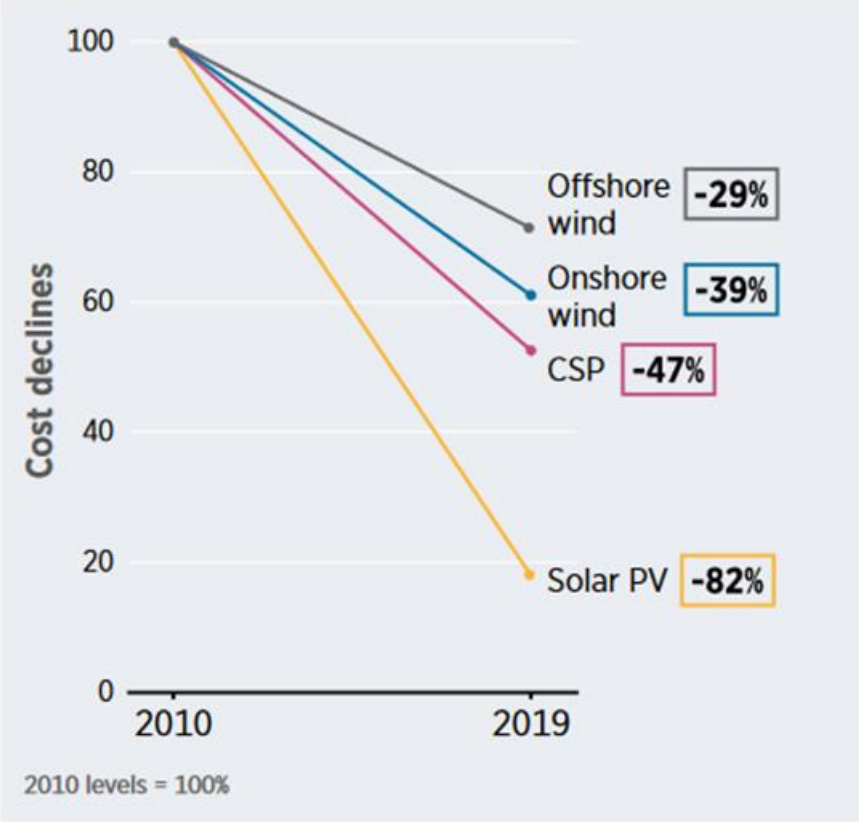

Figure 5-6: Cost decline in renewable energy technologies from 2010 to 2019. [126]

There are various topics regarding the economics of PV systems which can be discussed, in order to get a better understanding of them.

5.2.1 Payback time

An important factor in the PV economics is the payback time, which is defined as the time it takes to recover the investment cost. It can be calculated as the ratio of the cost of initial investment to the annual return. This describes the financial payback time.

$$payback\ time = \frac{initial\ investment}{annual\ return} \qquad \textit{Equation 5-1}$$

Payback time depends on various factors. One of them is the annual solar radiation that the PV system receives, which in turn is influenced by the location and orientation of the system. Sites with good solar resource will give shorter payback times for the installed PV systems. Utility electricity costs also influence payback time, which decreases with utility costs increase. Another factor that plays a role is of course the initial costs of the PV system. Other factors that are of importance, especially when viewed for long time periods, are the variations that occur in the value of money, as a result of inflation, and policies that are implemented, which affect the costs of PV systems.

5.2.2 Financial compensation

PV systems owners who feed power into the utility grid are compensated in various ways, the most important of which are the schemes of net metering and feed-in tariffs.

PV systems produce power that is used by the user for personal consumption. Power that is produced though may exceed the needs of the user, so the excess amount is fed into the utility grid. Conventional analogue electricity meters can measure both the electricity that is consumed from the grid and the one that is delivered to the grid. The user in the end must

pay only the net electricity consumption. Nowadays, there are smart digital electricity meters that can distinguish between the consumed and the delivered electricity, can monitor both and can allow the utility grid to adapt the tariff system depending on which type is measured.

Feed-in tariffs are a system by which the generated PV electricity is sold to the utility grid at a fixed price. The electricity consumed from the grid and the electricity fed into the grid can be measured by two analogue electricity meters or one smart digital meter. There are gross feed-in tariffs and net feed-in tariffs. In gross feed-in tariffs, all the generated electricity from the PV system is sold to the utility grid and in turn all the electricity consumed from the grid is bought from it. In net feed-in tariffs, as the name suggests, the electricity consumption is subtracted from the electricity generation and only the excess electricity is sold to the utility grid. The installation of PV systems is encouraged, when feed-in tariffs are higher than the electricity price, otherwise self consumption is encouraged, which is discussed in the following.

5.2.3 Self consumption

Self consumption of photovoltaic energy is the economic model where the user uses the generated PV electricity for his own electrical needs, therefore is producer and consumer at the same time. In this scheme, the generated PV energy is consumed instantaneously as it is being produced. The electricity that is produced from PV systems has variations due to the unpredictable nature of its resource. The peaks of this generated electricity are difficult to be predicted by the utility companies and sometimes the electricity fed into the grid may be higher than the demands of the grid. For this reason, the users of PV systems are encouraged to directly consume the electricity that they produce, so that the grid doesn't have to deal with instability issues.

In order to achieve self consumption, the size of the PV system can be reduced so that peak generated power is always lower than the peak power consumed by the user. A more preferable way is to incorporate storage devices so excess power can be stored for later use. Net metering doesn't promote self consumption as it treats generated and consumed electricity in the same manner, so the user doesn't have any incentives to consume his own power. Feed-in tariffs however, when they are lower than retail energy, promote self

consumption, as it is economically preferable for the user to consume all generated electricity than feed it into the grid.

5.2.4 Levelized cost of electricity

An important term in PV economics is the levelized cost of electricity (LCoE), which defines the cost of electricity, per kWh, which is produced from a power generation facility. LCoE can be used to compare lifetime costs of different technologies that produce electricity. It is calculated as the ratio of all costs during the lifetime of the electricity generating facility to all energy produced over the lifetime of the facility.

$$LCoE = \frac{\sum_{t=1}^{n} \frac{I_t + M_t + F_t}{(1+r)^t}}{\sum_{t=1}^{n} \frac{E_t}{(1+r)^t}}$$ *Equation 5-2*

In Equation 5-2, I_t are the investment expenditures in year t, M_t the operations and maintenance expenditures in year t, F_t the fuel expenditures in year t, E_t the electrical energy generated in year t, while n and r are the expected lifetime of the facility and the discount rate, respectively. The discount rate is used to discount future costs so that they can be translated into present value. For PV systems F_t is basically equal to zero. As it can be deduced by looking at Equation 5-2, the LCoE value for a PV system will vary between different locations and countries. LCoE can be a good indicator of where an energy technology stands in terms of cost competitiveness. Profit is made when LCoE is lower than the electricity price.

Figure 5-7 shows the LCoE for various technologies of energy production in Germany in 2018. Solar PV has slightly higher LCoE from fossil fuel technologies, while wind offshore has one of the highest LCoE.

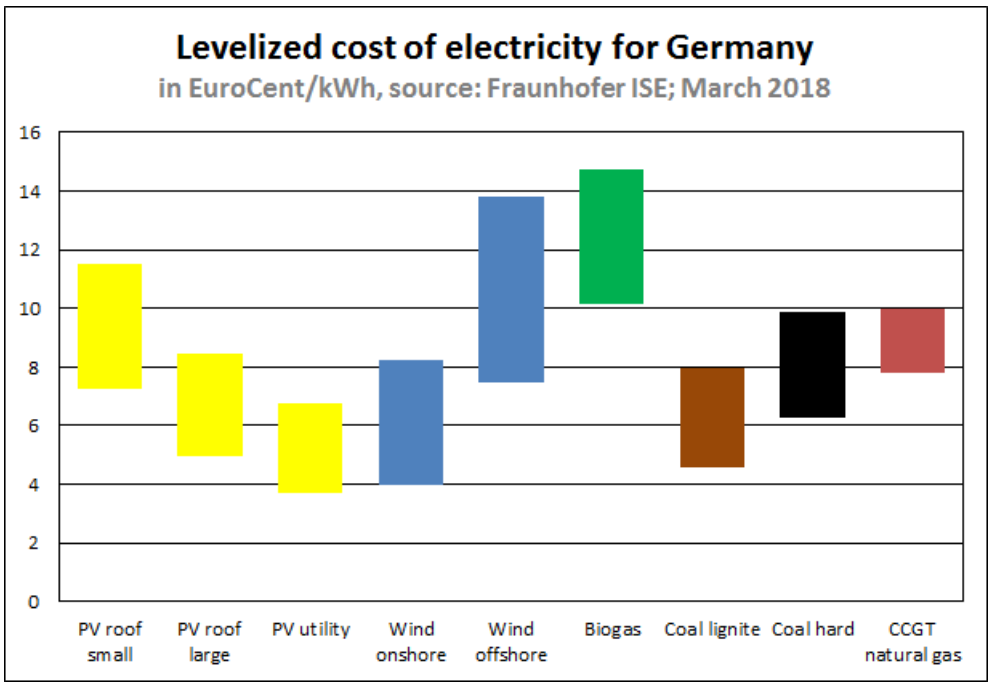

Figure 5-7: LCoE per energy technology, for Germany 2018. [127] Licensed under CC BY-SA 4.0

Other terms that are useful in determining whether or not PV generated electricity is competitive to electricity produced from other technologies are the grid parity and socket parity. When the LCoE of PV electricity is equal to that of other technologies that produce electricity, without taking into account subsidies and incentives, then that point is called grid parity. When the LCoE of a PV system is equal to the price paid by the consumer for grid electricity then that point is called socket parity. Basically grid parity will occur when the PV power producer will sell electricity to the utility company at the same price the company is paying other power generators, using other technologies and socket parity will occur when the PV power is the same price as electricity that a consumer buys from the utility company. These terms are useful in indicating the feasibility of a technology using renewable energy sources. When the technology is close enough to grid parity, it's easier to be included in the electricity mix.

5.2.5 Life-cycle cost

The costs of a PV system are various and include installation costs, operating and maintenance costs as well as replacement costs. When the system is no longer operational, it could have a

salvage value or an additional decommissioning cost. Life-cycle costing is the method by which all costs, which are associated with the PV system throughout its lifetime, are accounted for, while the time value of money is taken into account. The design of a PV system takes into account the life-cycle cost in order to evaluate it. The PV system owner can use life-time cost to have a sense of when the system will pay off its installation costs or have an overall idea of the expectations he can have from the system.

Depending on each situation, life-time cost can also take into account the incentives that could be available as well as the cost of a loan, in cases when one is taken by the owner for the system purchase. Some costs of the PV system refer to installation and operation of the system and are paid in the beginning of the project, while others are paid at later times. The value of money over time is affected by the inflation rate and the discount rate.

The inflation rate, i, describes the decline in the value of money that occurs with time. For example, if the inflation rate is 2% per year, the same object will be 2% more expensive the next year, so the value of money is decreased. Different objects or services don't follow the exact inflation rate and their costs may exceed the inflation rate or the opposite.

The discount rate, d, describes the interest that is earned on saved principal. Money that has been invested can be increased the next year due to a positive interest rate. For example, if the amount of N_0 is invested at a rate of d% per year, then after n years the increased amount N(n) will be:

$$N(n) = N_0(1 + d)^n. \qquad \textit{Equation 5-3}$$

In order to take inflation into account, if an investment is made at the cost of C_0 and the inflation rate is i%, then after n years the cost of the same investment will be:

$$C(n) = C_0(1 + i)^n. \qquad \textit{Equation 5-4}$$

Both the inflation and discount rate fluctuate over time.

Assuming C_0=N_0, then the ratio of C(n) to N(n) is the dimensionless quantity Pr, which describes the present worth factor of an item which will be bought in n years time.

$$Pr = (\frac{1+i}{1+d})^n.$$ *Equation 5-5*

The present worth, PW, of an item, is the amount of money that should be invested in the present at a rate of d% so that the item can be purchased in n years, assuming an inflation rate of i%.

$$PW = (Pr)C_0$$ *Equation 5-6*

Present worth is important is one is to determine it for recurring expenses, for example the cost of fuel.

When the PW has been determined for all aspects of the costs of the project, like purchase of the system, operation, maintenance, replacement of components etc., then the life-cycle cost (LCC) can be defined as the sum of all individual PWs. The LCC of a PV system provides important information for deciding between various choices in order to select the most economical.

5.3 Environmental aspects

Apart from the economical aspects of PV systems, it is also important to consider the environmental aspects. The purpose of PV systems is to produce electricity without having serious effects on the environment like conventional fuels. Therefore the environmental aspects of a PV system are an issue that should be checked. There are various terms which deal with PV environmental impact.

Carbon footprint is a concept that is used to estimate the emissions of CO2 due to the manufacturing of PV panels and compares these emissions with the CO2 reduction that is achieved because the PV system is used instead of fossil fuels for electricity production. A more detailed approach would be to study the total energy that is required in order for the PV panel with all its components to be manufactured. Life-cycle analysis (LCA), which is different from life-cycle cost, is a method for assessing the environmental impacts during the

lifetime of a project. As a result with the help of LCA the energy and carbon footprints of a PV system for the duration of its lifetime can be studied.

The energy yield ratio is a concept, used to address the ecological aspects of PV systems. It is defined as the ratio of the total energy yield of a PV system during its lifetime to the total amount of energy that is invested in the system during that time. The latter includes the energy used for manufacturing the system components, energy for transportation and installation of the components as well as the energy for recycling them after they are no longer operational. The energy yield ratio depends on the technology used for the PV system and the quality of the components.

Another concept that is important for the environmental impacts of PV technologies is the energy payback time, which is different from the economic payback time described previously when discussing the economics of a PV system. The energy payback time is described as the ratio of the total energy investment that is required over the project's lifetime to the average annual energy yield of the project.

$$energy\ payback\ time = \frac{total\ invested\ energy}{average\ annual\ energy\ yield} \qquad \textit{Equation 5-7}$$

Usually PV systems have an energy payback time between 1 and 7 years and this depends mainly on the available solar resource throughout the year as well as the position of the PV system. Different PV technologies have different energies that are required for the production of the respective modules. Producing thin-film modules from amorphous silicon, CdTe or CIGS requires less energy than in the case of modules from polycrystalline and monocrystalline silicon. The amounts of energy for the production of PV modules reduce with time as technology improves. Also, the energy payback time differs between various parts of the system, such as the module, the module frame and the balance of system, because the technologies and manufacturing processes can vary between them. Due to technology improvements the energy payback time reduces with time for both crystalline silicon and thin film technologies. Also, rooftop installations have lower energy payback times, mainly because the balance of system for ground mounted systems is more energy extensive. The energy payback times are usually quite lower than the lifetime of the systems which is usually

between 25 and 30 years, therefore energy invested in PV systems can be paid back multiple times during their lifetimes. Technology improvements will continue to reduce the required energy for PV systems production, while recycling of components is also very important.

Finally, a significant issue regarding the environmental impact of PV systems is the pollution caused by their production. The chemicals involved in the production of PV panels can sometimes be toxic therefore serious consideration is needed along with legislation to prevent their release into the environment.

5.3.1 Other aspects of PV systems

Apart from environmental impact, PV systems also have social impact with both positive and negative effects. For example, the land use involved in the installation of PV systems is usually smaller than the one required from conventional energy resources and land areas, previously unused, like deserts can now be used for energy production. At the same time land can be unavailable due to other uses, the most common being agriculture. PV systems take advantage of structures already made, like the roof and façades of buildings. They can however have negative visual effects. Regarding infrastructure, there's a reduction in transmission lines with the use of PV technologies. PV systems can be used to power areas where connection to the grid is not possible, especially in developing countries. The downside is that energy storage is needed in order for the power supply to be continuous.

The use of PV technologies and renewable energy resources in general, leads to the reduction of the dependency on oil and its import, which in turn depends on geopolitical parameters and conflicts. Finally PV technologies lead to the creation of job openings and act towards the increase in development and education levels, as well as environmental consciousness.

5.4 Effects on PV performance

The performance of a PV system can be affected by various external parameters, which have to do with the environment or position of the system.

5.4.1 Solar irradiance

Solar irradiance affects the power output of a PV system and it can be seen in Figure 5-8. Increase in irradiance brings an increase in the output power of a PV module, as it is expected, so PV systems can be more effective in locations with good solar resource.

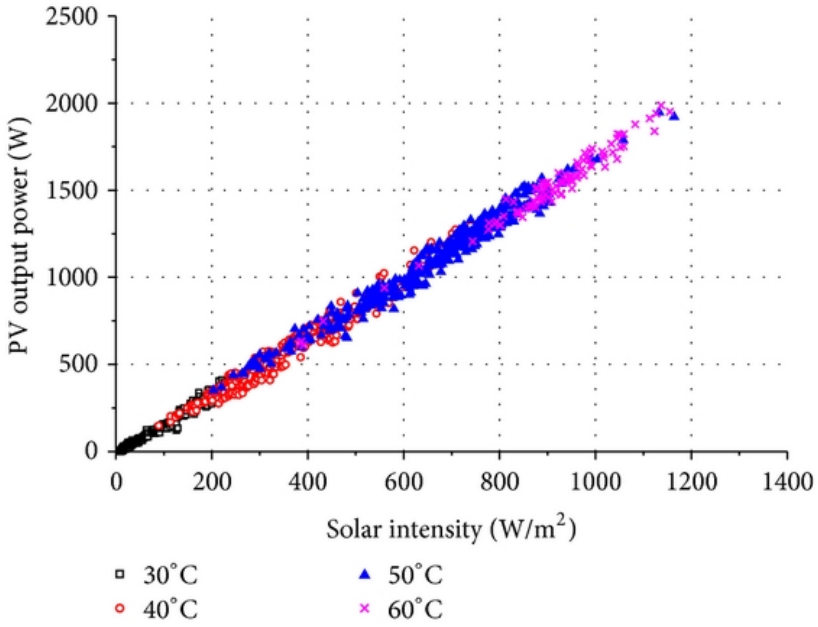

Figure 5-8: Power of PV module as a function of irradiation. [128] Licensed under CC BY 3.0

5.4.2 Temperature

The performance of a PV module depends also on temperature. The PV cell is a semiconductor and is sensitive to temperature variations. Increase in temperature results in the reduction of the power output, as can be seen in Figure 5-9. The normalized values of maximum power and open circuit voltage present a linear decrease with temperature increase, while short circuit current shows a slight increase. The reduction in voltage is much higher than the increase in current, which results in a reduction in the power output. Figure 5-10 shows the decrease of the cell's efficiency with temperature mainly because of the increase in the rate of internal carrier recombination due to increased carrier concentration.

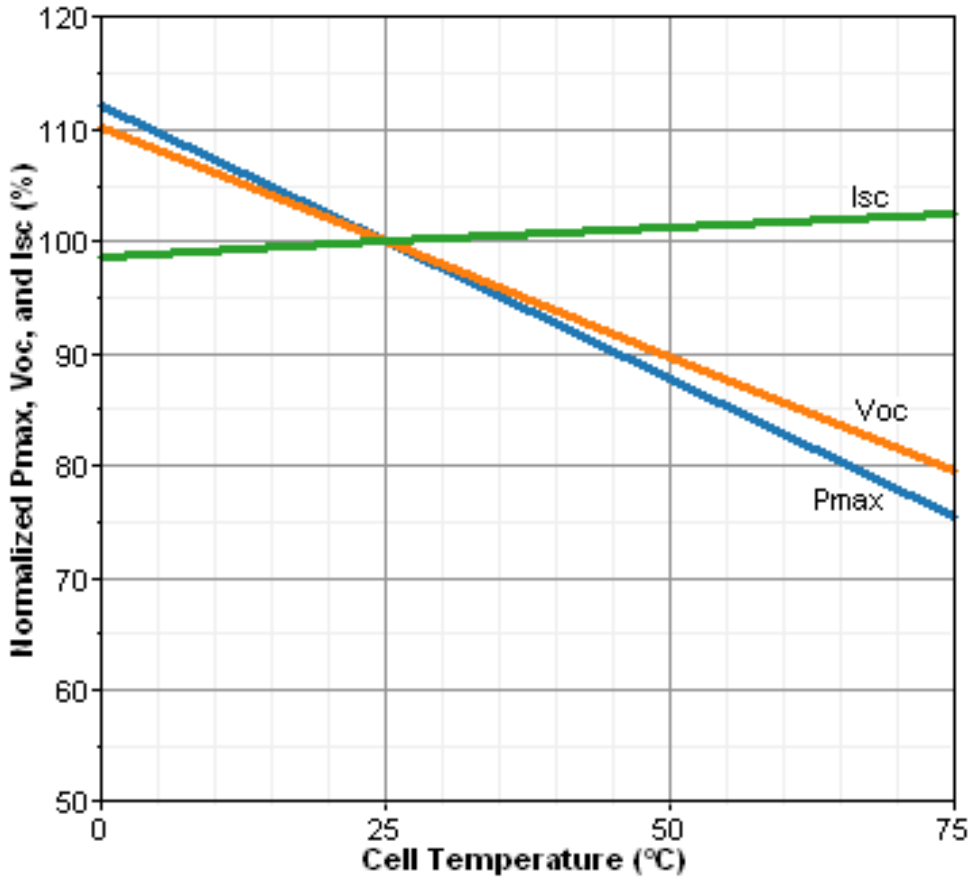

Figure 5-9: Normalized P_{max}, I_{SC} and V_{OC} as a function of temperature. [129]

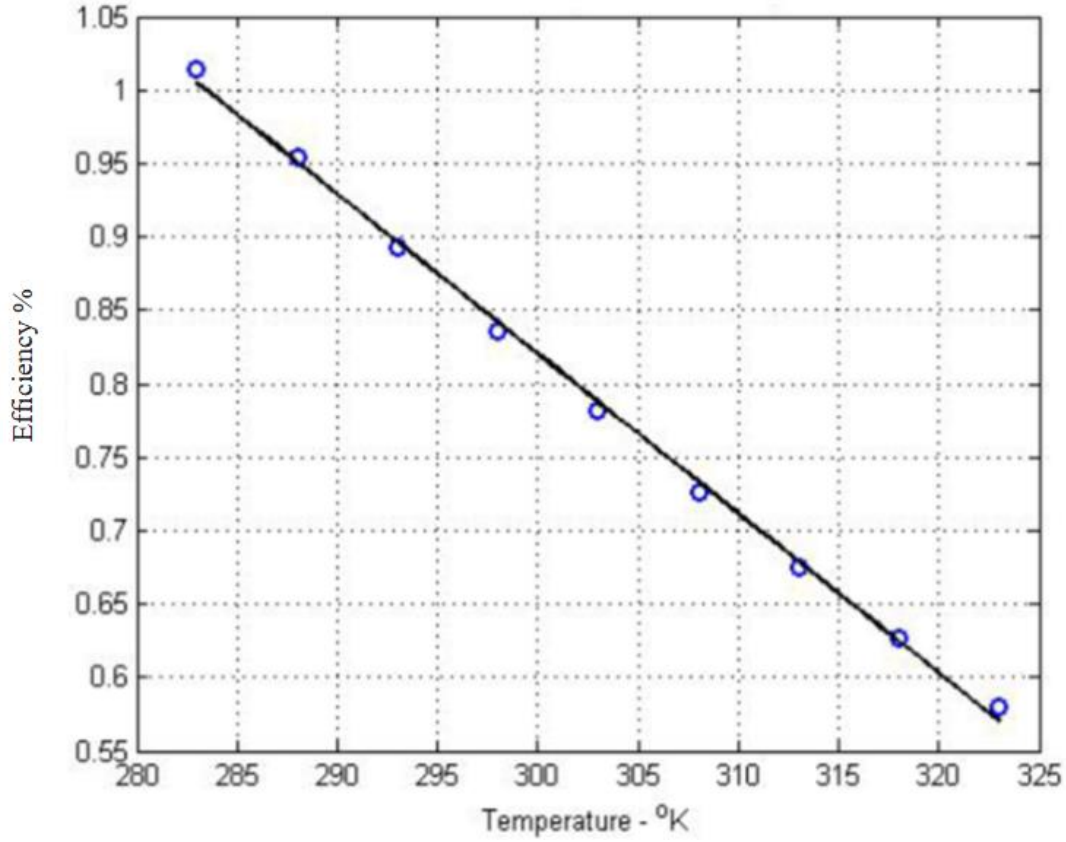

Figure 5-10: Conversion efficiency of a silicon cell as a function of temperature. [130]

The temperature of the PV module will increase as solar radiation increases as well as the temperature of air, but it will be reduced with increase in wind speed. There are various ways to protect the PV system from the effects of increased temperature, like allowing air to circulate between the module and the roof or ground where it is situated or having light coloured panels and supports in order to reduce heat absorption. Another option is to use cooling fans.

5.4.3 Shading

The output of a PV system is very sensitive to shading. Shading can occur because of clouds, trees, buildings, dirt etc. and can cause mismatches in the current that is generated from the individual solar cells of a PV module. Even if a single solar cell is partially shaded then the power output of the entire system can be reduced. When a cell is shaded then it generates less current than one with no shade upon it. As the cells are connected in series in a module,

the same current must flow through all of them. If current that is higher than the capability of the shaded cell passes through it, then the shaded cell will be overheated and probably damaged. If on the other hand, the current that flows through it is less than its capability, then the shaded cell will not be damaged but the overall current and power of the string will be limited.

In order to avoid heating of individual solar cells within the array due to shading and the resulting effects on generated power, bypass diodes are commonly used. The bypass diode is connected in parallel to a sub-string of the PV module and the common types of PV modules with 60 or 72 cells usually have three bypass diodes (Figure 5-11). The bypass diode acts like an open switch when there's no shading and the light received by each cell is uniform. When there is shading however and as a result there are current mismatches, then the bypass diode that is connected to the sub-string, where the shading occurs, acts like a closed switch and bypasses that sub-string.

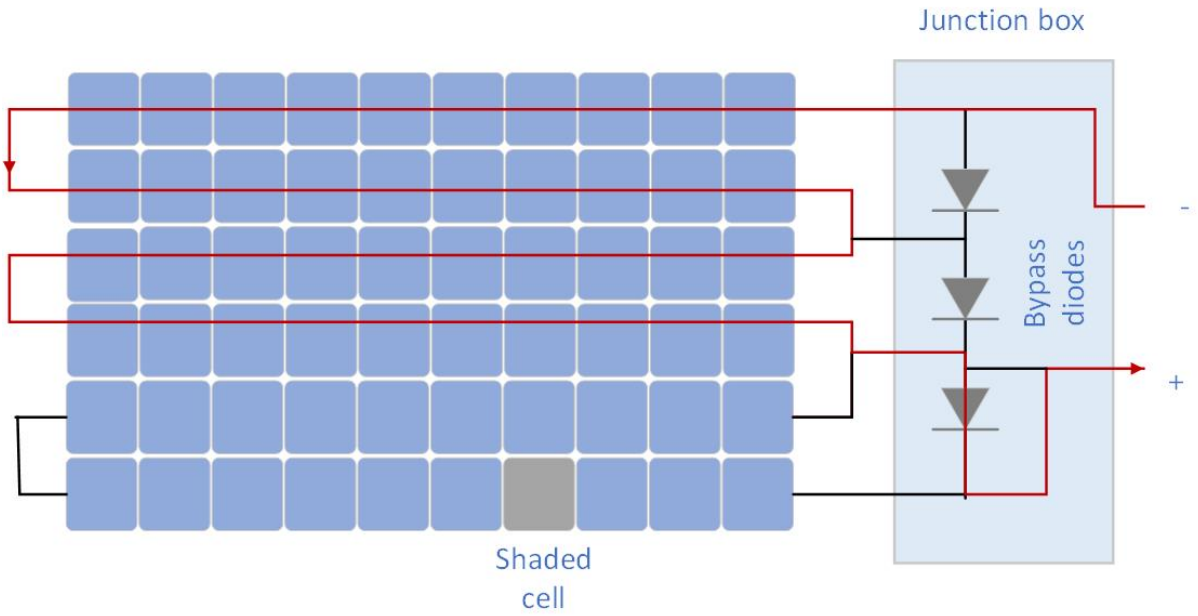

Figure 5-11: PV module with bypass diodes. [131]

The characteristic I-V and P-V curves of the PV system also change due to partial shading conditions. The shaded cells will overheat, if no bypass diode is used, because they will operate with a reverse bias voltage in order to provide the same current as the illuminated cells. This causes a reverse power polarity which results in power consumption and a

reduction in the maximum power that the PV module generates. When bypass diodes are included, there's an alternate current path, so the cells don't carry the same current anymore when shading occurs. As a result the curve in the P-V graph of the PV module presents multiple maxima. This can be seen in Figure 5-12, where the module consists of two 18-cell groups, connected in series. The curve under uniform insolation is presented (red), as well as the one under partial shading without bypass diodes being used (blue), where the reduction in power is evident. When bypass diodes are used the reduction in output power is less and there are multiple maxima of power (green curve). However most of the conventional MPPT algorithms can't always distinguish between a local and a global maxima. There are various techniques to track MPP under shading conditions.

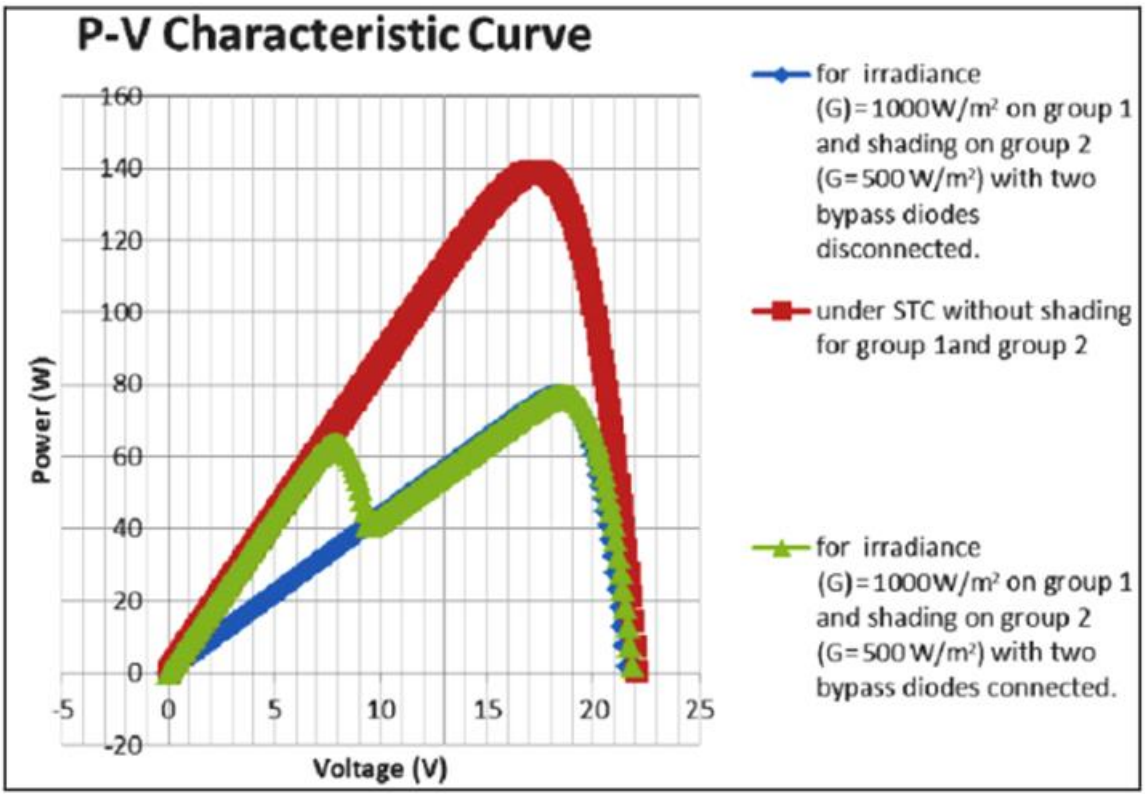

Figure 5-12: P-V curve of a PV module under various conditions. [132]

In the arrangement of string inverters, each inverter is connected to a series of modules which are being treated as a single unit. This is depicted on the left image in Figure 5-13. The MPPT controller is therefore at the string level and responds to the module of the string that is least

efficient. As a result, several modules will operate below their MPP and the overall efficiency will be reduced. To account for this issue, the MPPT algorithm must consider the entire range of the string voltage so that it can detect the global maxima instead of a local one. These are called the Shade-Tolerant String Inverters.

Another way to account for the issue of partial shading is the micro inverter (right image in Figure 5-13). In this arrangement every module is connected to its own inverter, which is connected in parallel to the AC bus. Because of the parallel connection, any mismatches in currents that occur between different modules will not cause any issue. Each inverter features an MPPT algorithm. The only disadvantage in this situation is the cost of micro-inverters, which is higher than in the case of a string inverter arrangement.

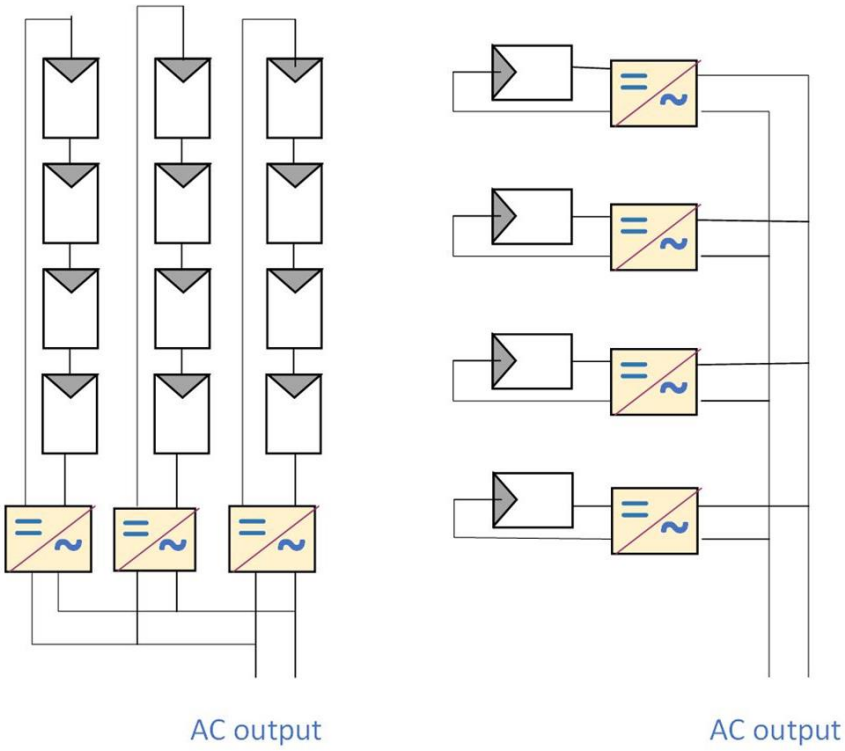

Figure 5-13: Arrangement of string (left) and micro-inverters (right). [112]

5.4.4 Soiling

Soiling refers to the accumulation of dust, dirt, snow and other particles which cover the PV module surface. A thin layer is formed on the module surface and the sunlight received by

one or more solar cells is reduced. Dust particles are minute solid particles with diameters less than 500 μm. The deposition of dust depends on various parameters, like the size and weight of the particles, the weather conditions, the tilt angle of the module, the surface finish of the module, the wind speed etc. Another factor that is of significance is the location of the PV system, whether it is located in a coastal or dusty area. Horizontal surfaces have a tendency of accumulating more dust than surfaces with an inclination. Low wind speeds act in favour of dust settlement and also the geometry of the module in relation to the wind direction plays a part. A PV system installed on a rooftop will receive less dust than one mounted on the ground.

Soiling in a PV module can decrease the annual power output by 5-17% or even more depending on the conditions. Figure 5-14 shows the reduction in solar intensity as a function of dust deposition density, for various dust particles diameters. Dust particles with smaller diameters seem to cause higher losses in the performance of the module than larger particles. In dust particles of the same type, the finer particles have greater effect than coarse particles, due to their higher ability to decrease the interparticle gap. As a result they are more effective in blocking the light path compared to coarse particles.

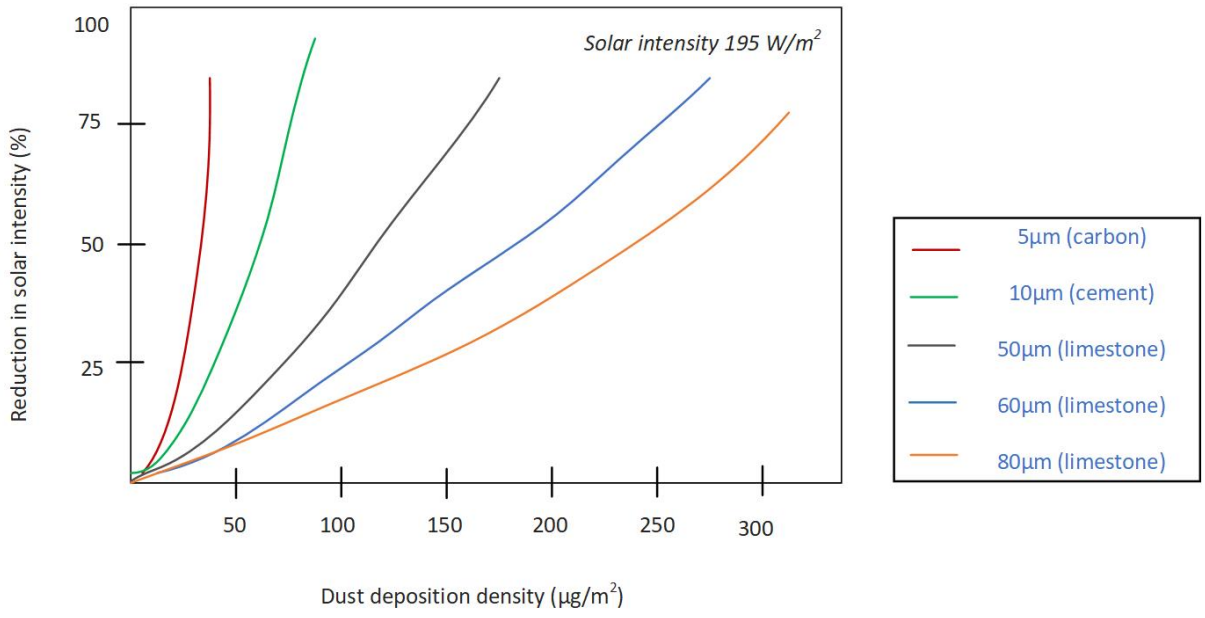

Figure 5-14: Reduction in solar intensity due to dust deposition. [133]

In order to diminish the effect of soiling on output power, the PV modules should be cleaned regularly. The cleaning can be done manually or there are other methods such as self-cleaning glass, electrostatic curtain and others.

5.4.5 Tilt angle

The orientation of the PV panels is very important in order to achieve maximum output power. The tilt angle of the module affects the PV performance. Figure 5-15 shows the basic angles of the geometry between the Sun and the PV module, where θ_z, α_s, γ_s and β are the zenith angle, the solar altitude, the solar azimuth and the tilt angle of the module, respectively.

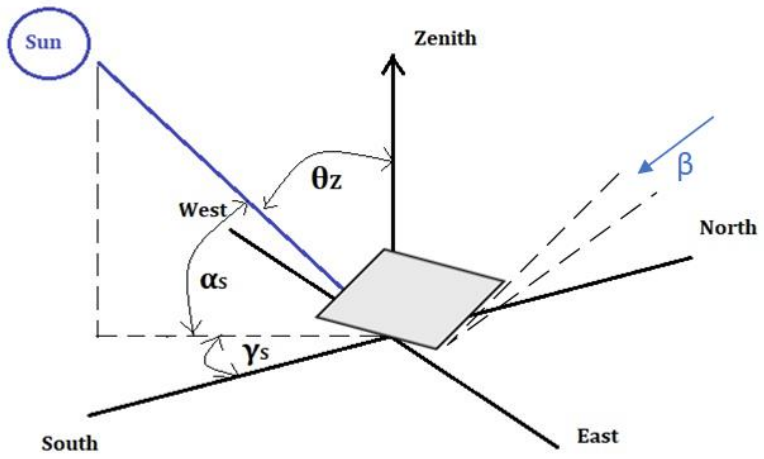

Figure 5-15: The angles of the Sun-panel geometry. [79]

The direction in which the module faces is important and in the northern hemisphere, the modules are oriented towards the true south. If they are oriented towards another direction, there will be blocking by shade, with the worst orientation being towards the north where there will always be some shade. For optimum power output a PV module should always point to the direction of the Sun, but this is not always possible because there are daily and seasonal

variations in the position of the Sun. Trackers are used to account for these issues. Single-axis tracking improves the PV performance against daily variations, from morning until evening, while dual-axis tracking improves the performance against both daily and seasonal variations.

The tilt angle of the PV module is usually fixed at a certain inclination, especially in the case of small scale installations. The calculation of the optimum tilt angle can be done with various algorithms. The general rule is to have a tilt angle of $\phi \pm 15°$, where ϕ is the latitude of the location. The "+" is used for the winter period and the "-" during summer. For March and September, the tilt angle should be the same as the location's latitude. The adjustment of the tilt angle twice or even four times a year would provide better results.

5.5 Tracking systems

Solar tracking systems are used in order to tilt a solar panel during the day. By tracking the Sun, the total power produced by a PV system can be increased by around 20-25% in the case of a single-axis tracker or 30% and more in the case of a dual-axis tracker, depending on the location's latitude. The method of tracking can enhance the performance of the PV system during early morning or late evening and it is effective in locations which receive a lot of direct sunlight, as tracking doesn't have any serious effect in diffuse light conditions. Tracking systems make sure that the surface of the PV module is perpendicular to the incoming solar radiation. Figure 5-16 shows a simple design of a PV panel with a tracking system.

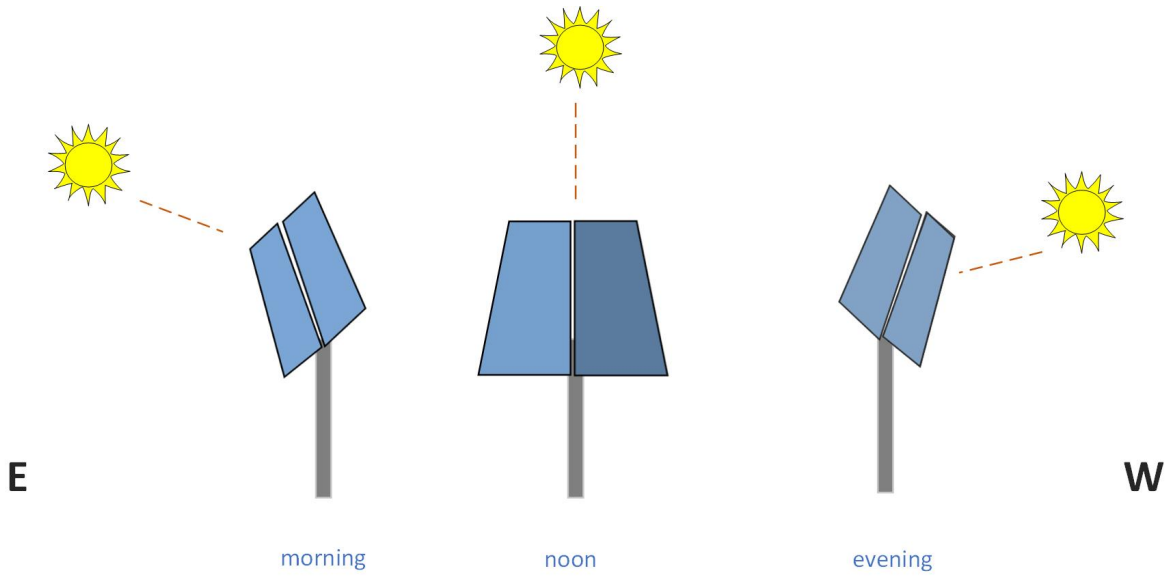

Figure 5-16: A simple design of a solar panel with a tracking system. [134]

Tracking systems can be categorized according to the degrees of freedom. This way, there are the single-axis and the dual-axis PV tracking systems. Single-axis tracking systems follow the Sun's trajectories by moving around one axis, which is usually from east to west. Dual-axis tracking systems move around two axes, east to west and north to south. The control systems of tracking systems can be of closed-loop or open-loop. Closed-loop control systems use a photosensor which sends a signal to the control unit and open-loop systems use an algorithm which is loaded in the controller's processor. A combination of both open-loop and closed-loop results in the hybrid control tracking system. Finally the classification can be based on the driving system, where there are the passive and active tracking systems.

5.5.1 Driving system

A common distinction between tracking systems is based on their driving systems, in which case there are the passive and active tracking systems, depicted in Figure 5-17. In passive tracking systems, the axes move due to pressure difference of certain liquids or gases with low boiling point. The pressure difference is the result of thermal differences created by the shaded and illuminated sides of the tracking system. When a side is under shade, pressure difference is created and the tracking system moves until that difference is eliminated. This

type of tracking doesn't have a lot of precision and is not used very often, especially in large scale applications.

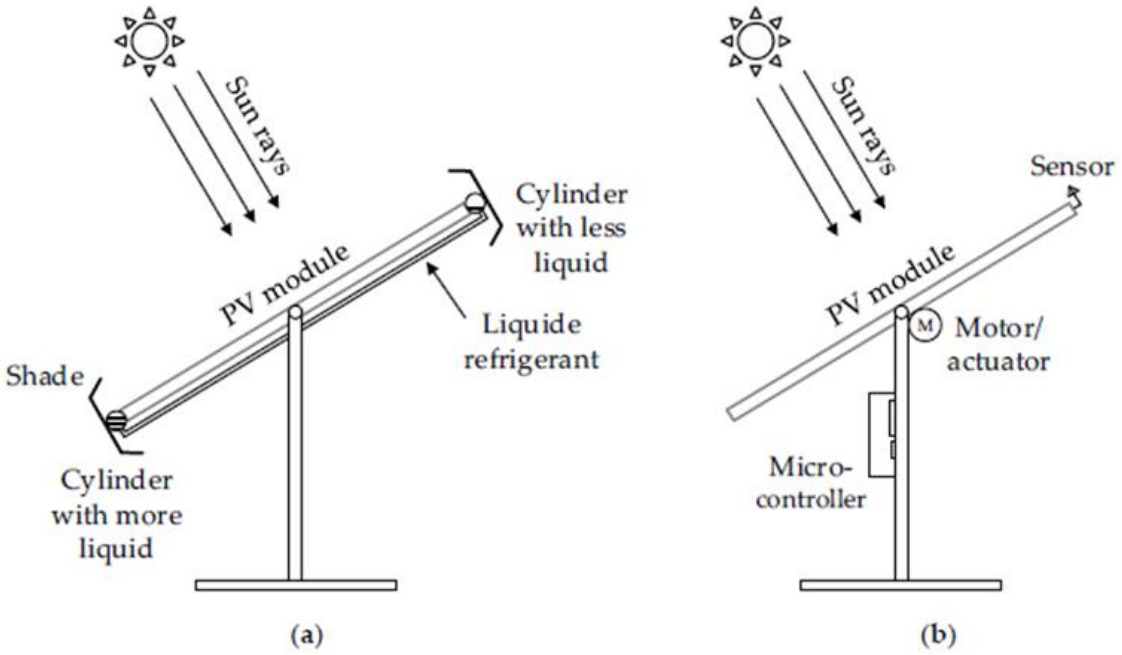

Figure 5-17: Classification based on the driving system: passive (a) and active (b) tracking system. [135] Licensed under CC BY 4.0

Active tracking systems use motors and gear trains for their operation. The components included are a microprocessor, an electric motor, sensors and gearboxes. They detect the Sun's position and track it. Based on their control drive, they can be active closed-loop, open-loop or hybrid tracking systems. Further more active tracking systems can be classified into intelligent control, microprocessor control and sensor-based control systems. Intelligent control systems take advantage of artificial intelligence or neural network algorithms to control the tracking. Microprocessor control systems use Programmable Interface Controllers (PIC) and digital signal microcontrollers. Finally sensor-based control systems use electro-optical sensors and light-dependent resistors (LDR).

5.5.2 Degrees of freedom

Based on the number of degrees of freedom, there are single-axis and dual-axis tracking systems. The different types of each class can be seen in Figure 5-18.

The single-axis tracking system types are: the horizontal single-axis tracker (HSAT) where the rotating axis is horizontal to the ground and moves in the north-south direction, the vertical single-axis tracker (VSAT) where the rotating axis is vertical to the ground and rotates from east to west, the tilted single-axis tracker (TSAT) with the axis of rotation between the horizontal and vertical and the polar aligned single-axis tracker (PASAT) which is aligned to the polar star. The tilt angle in the PASAT is equal to the location's latitude and the rotating axis of the system is aligned with Earth's rotating axis.

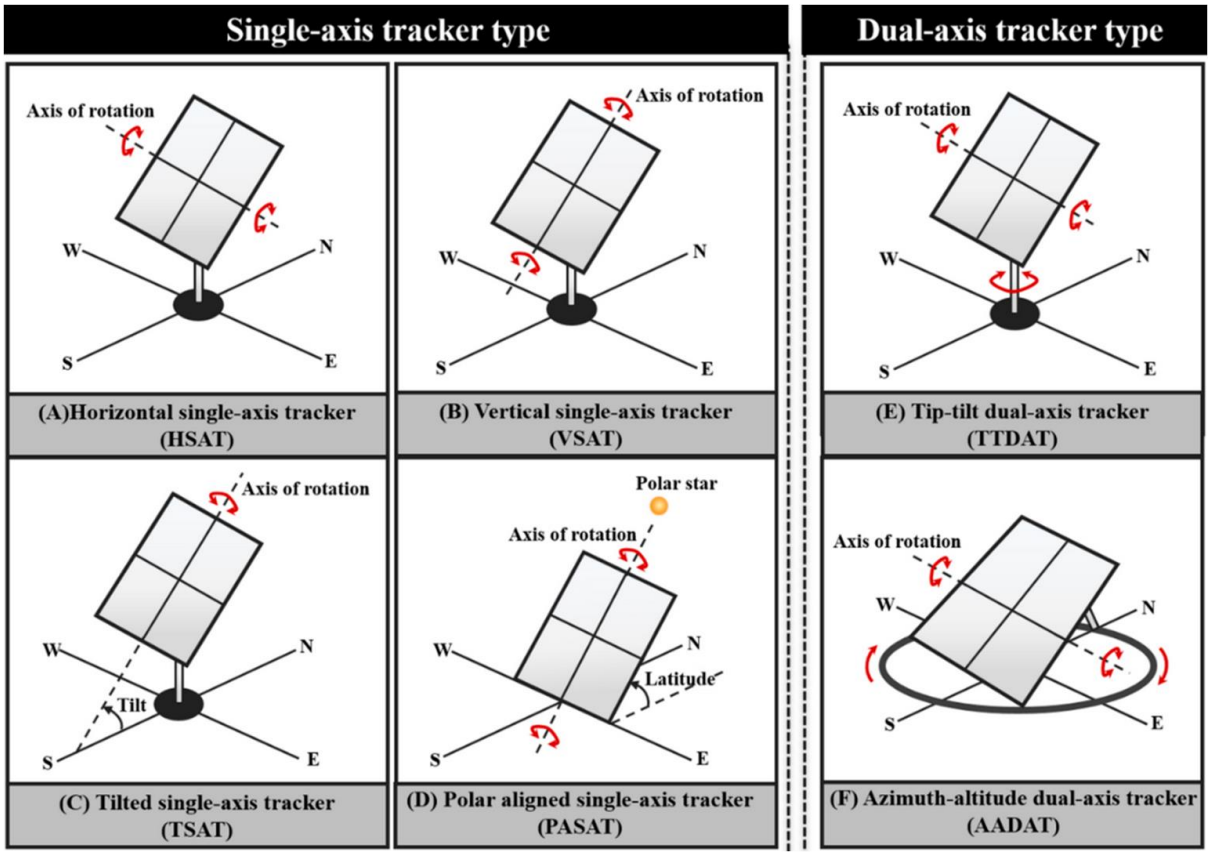

Figure 5-18: Single-axis and dual-axis tracking system types. [136] Licensed under CC BY 4.0

The dual-axis tracking systems are divided into two types: the tip-tilt dual-axis tracker (TTDAT) and the azimuth-altitude dual-axis tracker (AADAT). In the TTDAT, the primary axis is horizontal to the ground and the secondary axis is normal to the primary axis, tracking the

Sun in the east-west and north-south direction. In the AADAT, the primary axis is vertical to the ground and the secondary axis is normal to the primary axis. It can track the east-west and north-south motion of the Sun with the use of a ring mounted on the ground with a series of rollers.

5.5.3 Control system

Active tracking systems can be classified into three types: open-loop control systems, closed-loop control systems and hybrid control systems. In open-loop control systems (Figure 5-19, top), the determination of the Sun's position is achieved with a mathematical algorithm, which is loaded into the microprocessor. By controlling the input data, like date and time, the Sun's position can be calculated from the algorithm for any location.

The closed-loop control system (Figure 5-19, bottom) uses sensors to find the direction with maximum incident energy, therefore detect the position of the Sun. According to the sensors data, the axes move to track the Sun. The closed-loop control system is thus based on a feedback control system from the sensors. Due to the addition of sensors, this type is more expensive but more precise.

A hybrid control system uses a combination of both open-loop and closed-loop control systems to take advantage of the benefits of each type.

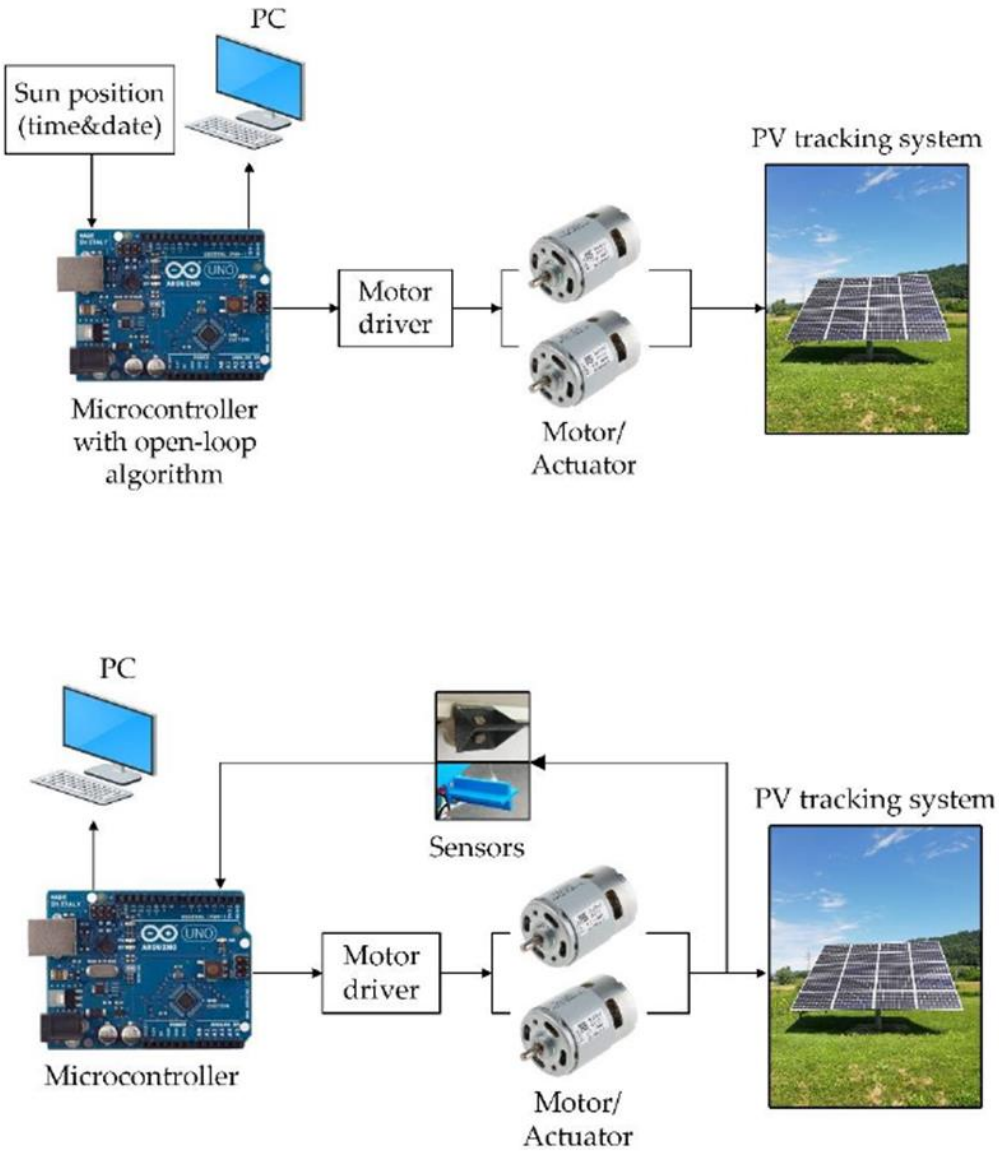

Figure 5-19: Designs of an open-loop (top) and a closed-loop (bottom) tracking system. [135] Licensed under CC BY 4.0

Fixed photovoltaic systems are more common and less expensive however constant technological improvements are used in order to increase the yield of electrical energy. Photovoltaic tracking systems can be used in that direction. The extra costs and maintenance due to the addition of tracking systems should be taken into account along with the increase in power output, as well as the applicability of the tracking system depending on the photovoltaic installation.

6 Solar thermal systems

Author(s): Dr Efterpi Nikitidou
Dr Andreas Kazantzidis

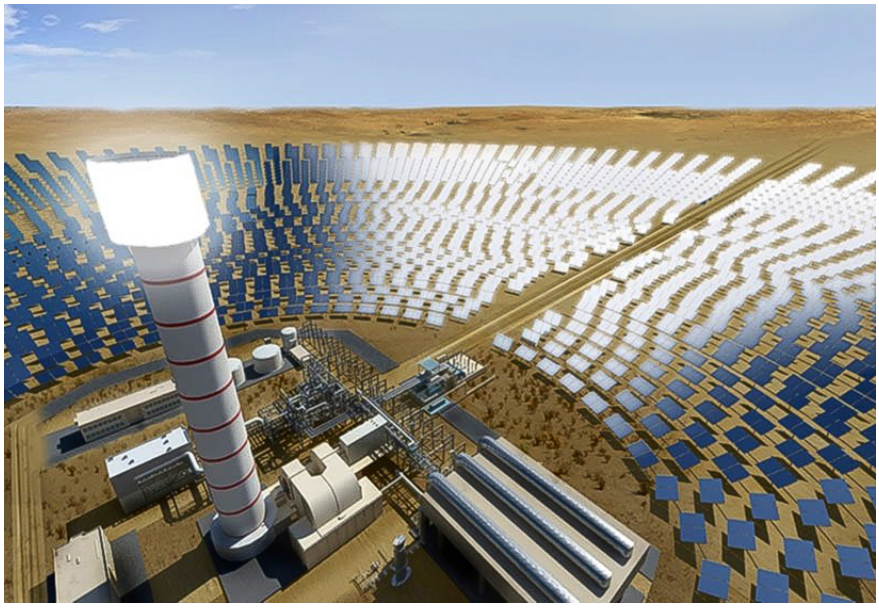

6.1 Concentrated solar power technologies

Concentrated solar power (CSP) (otherwise known as concentrated solar thermal power (CSTP)) technologies are based on the use of mirrors or lenses to concentrate sunlight onto a receiver in order to generate power. The concentrated light is converted to heat, which is used to drive a heat engine connected to a power generator to produce electricity. CSP systems utilise direct solar irradiance, therefore their operation is effective in areas with strong sunlight conditions and clear skies, e.g. arid or semi-arid areas. CSP systems first began to be utilised as small scale applications, e.g. for pumping water but have since then been developed and there are now large scale CSP power plants in operation.

Figure 6-1 presents the basic process that takes place in a solar thermal power system. The first component of the system is the concentrator with various configurations as they will be presented in the following. Other system components include a collector (receiver), a storage system which is usually water or a phase change material, a boiler which acts as the heat exchanger between the collector's operational fluids and the heat engine, the heat engine which converts thermal energy into mechanical energy and the electrical generator to generate electricity. Usually the heat engine is a steam turbine. Energy is stored in hot steam and as the steam expands in the turbine, it is partially converted to mechanical energy in a process known as the Rankine cycle.

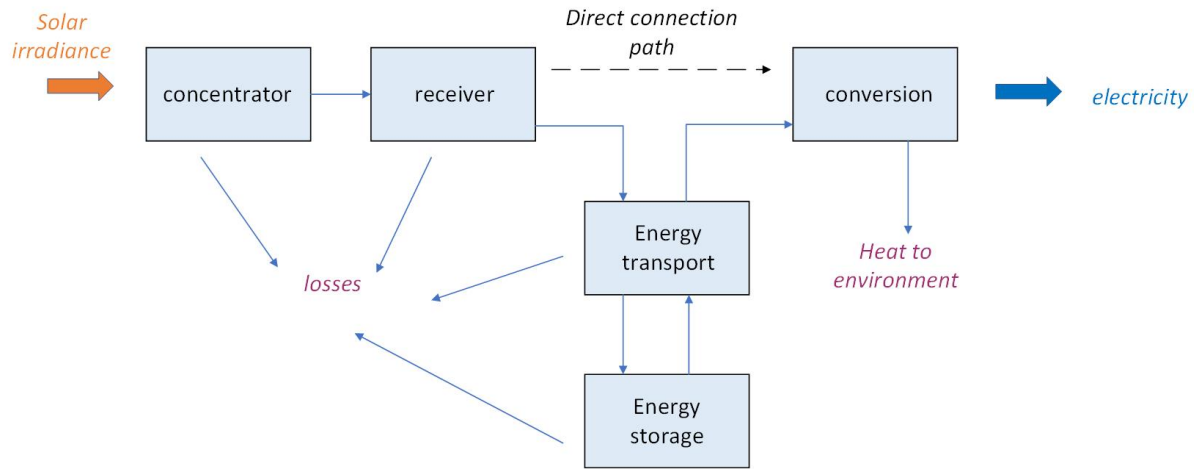

Figure 6-1: Basic process in a solar thermal power system. [137]

There are four main CSP technologies which are used for electricity generation: the parabolic trough, the solar tower, the linear Fresnel reflector and the parabolic dish concentrator (Figure 6-2). Each type of concentrators produces a different peak temperature and therefore has a different thermodynamic efficiency, due to the various ways of tracking the Sun and focusing sunlight. Line-focusing systems (parabolic trough, Fresnel reflector) can concentrate solar radiation by 50-100 times, while point-focus systems (solar tower, parabolic dish) can concentrate it by 500 to several thousand times.

In CSP systems the collector efficiency decreases with temperature, while the heat engine's efficiency increases with temperature. For that reason the operating temperature must be chosen in order to compromise between these two facts and maximize the system's efficiency. CSP efficiencies are around 30%, depending on the technology.

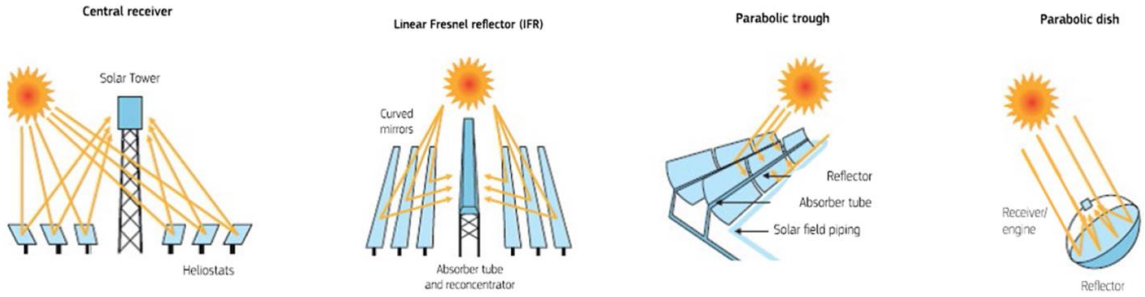

Figure 6-2: Concentrating solar power types: central receiver (solar power tower), linear Fresnel reflector, parabolic trough concentrator and parabolic dish concentrator. [16] Licensed under CC BY 4.0

6.1.1 Parabolic trough

A parabolic trough system consists of a linear parabolic reflector which concentrates light onto an absorber tube located in the focal line of the parabolic mirror (Figure 6-3). Inside the absorber tube is the working fluid.

The basic design of a parabolic trough system is shown in Figure 6-4. The working fluid inside the absorber tube is heated and then pumped into the steam generator (heat exchanger), which is connected to a steam turbine generator in order to produce electricity. The working

fluid is then cycled back through the solar collector field so it can collect more heat and continue the cycle.

Figure 6-3: Parabolic troughs. [19] License: Public Domain

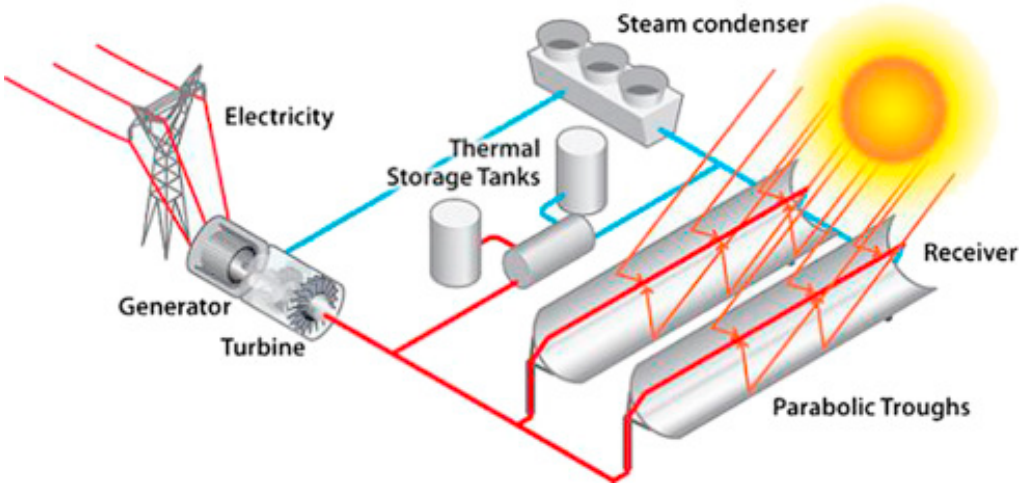

Figure 6-4: Parabolic trough system design. [18] License: Public Domain

The working fluid that is used as heat transfer fluid is usually synthetic oil or molten salt and during operation its temperature can reach up to 400 °C. The absorber tube is designed to withstand high temperatures since it absorbs most of the solar energy that is focused on it. The tube is usually made of steel with a black coating and a protective glass cover surrounds it. The space between the glass and the tube is evacuated in order to reduce heat loss. The parabolic reflector surface can be coated glass mirrors or it can be made of polished aluminium.

The parabolic trough system consists of several solar collector modules which move together as one solar collector assembly. Each module can have length up to 15 meters while the assembly can reach up to 150 or 200 meters in length. The parabolic troughs are usually aligned on a north-south axis and are mounted on supports in order to track the Sun in the east-west direction. A parabolic trough system that incorporates thermal energy storage can transfer heat from the working fluid to a storage medium, usually a blend of nitrate salts, which is stored in insulated tanks.

The thermal efficiency of a parabolic trough system, when the working fluid is used to heat steam to drive the turbine generator, can range between 60 and 80%. The overall efficiency however, from the solar collector to the grid, is similar to that of photovoltaic cells, around 15%.

6.1.2 Linear Fresnel reflector

The linear Fresnel reflector (LFR) system approximates the parabolic shape of the trough systems but instead uses long rows of flat or slightly curved mirrors, which rotate to track the Sun and reflect direct sunlight onto a linear receiver, which faces downward (Figure 6-5). The LFR takes its name from the Fresnel lens, where thin lens fragments are used in combination in order to simulate the effect of a thicker conventional lens. The linear receiver is situated at the common focal point of the reflectors and is at a fixed position. Heat is transferred to the working fluid in an absorber pipe at the receiver and it is converted to steam to drive a turbine to generate electricity (Figure 6-6). The working fluid is usually water or oil. The receiver usually has a secondary parabolic reflector on top, to further focus the sunlight. The receiver

can consist of one or several tubes with the heat transfer fluid and they can be contained in a vacuum glass tube enclosure.

Figure 6-5: Linear Fresnel reflectors. [20] Licensed under Free Art License

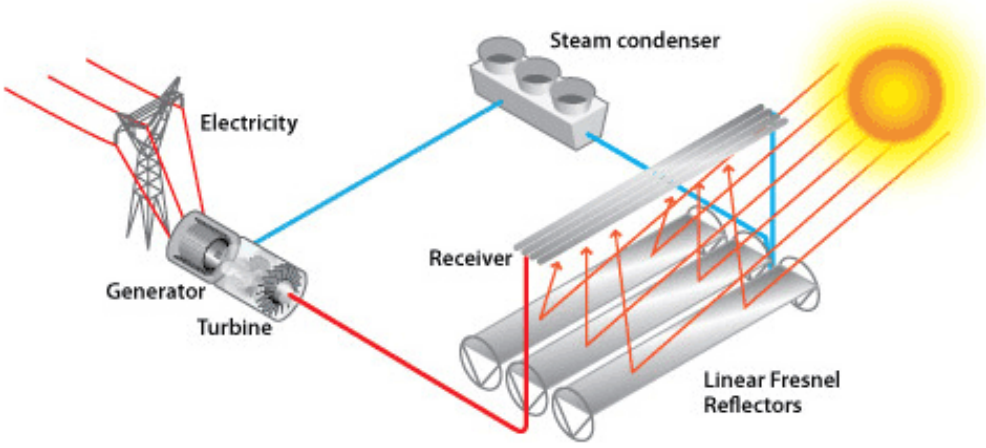

Figure 6-6: Linear Fresnel reflector system design. [18] License: Public Domain

The optical efficiency of a LFR system (fraction of incident solar radiation on the receiver tube that is transferred to the working fluid) can reach up to 70%, which is lower than that of a parabolic trough system, reaching up to 80%. The advantage of an LFR system is that the Fresnel reflectors it uses have lower costs than the curved glass parabolic reflectors. Also a Fresnel system requires less land for its structure, around 1/3 of the land area that a parabolic trough system with the same installed power would use. An important disadvantage is that several rows of mirrors use the same receiver row to focus direct solar radiation. There may be shading effects or blocking of the reflected radiation by nearby reflectors. An improved design, the compact linear Fresnel reflector (CLFR), uses multiple parallel receivers that are located in the vicinity of the mirrors (Figure 6-7). The receivers are elevated on towers and the individual mirror rows can direct the reflected solar radiation at two alternative linear receivers, located at separate nearby towers.

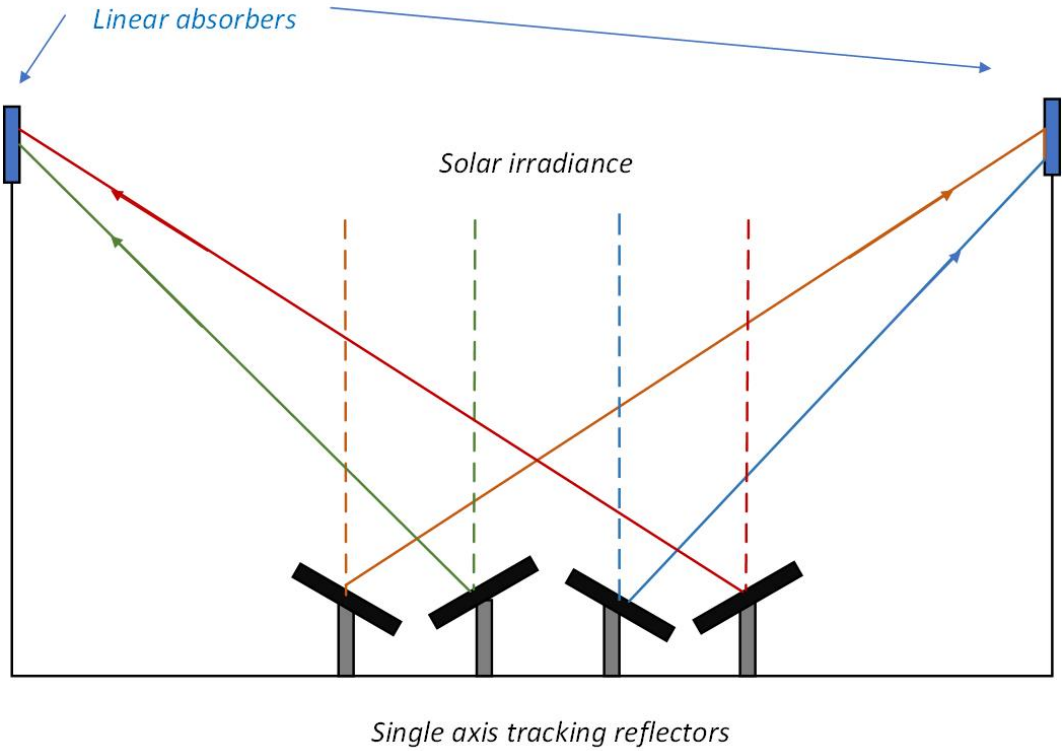

Figure 6-7: Compact linear Fresnel reflector. [138]

6.1.3 Parabolic dish/engine

Parabolic dish/engine systems use mirrored parabolas in order to concentrate sunlight onto a receiver, which is located at the focal point of the dish (Figure 6-8). The dish can track the Sun in two axes to capture maximum direct solar radiation.

The working fluid in the receiver can be heated up to 700 °C and is then used to drive a heat engine to generate electricity. The heat engine is usually a Stirling cycle engine, which is the reason why these systems are also known as dish Stirling systems. The Stirling engine is externally heated. It has a receiver with thin tubes that contain hydrogen or helium gas, which run on the outside of the four piston cylinders of the engine and open into them. The gas is heated by the concentrated sunlight at very high temperatures and it expands inside the cylinders, driving the pistons as a result, which in turn drive the electric generator. These components, the receiver, the engine and the generator, are all mounted as an assembly at the focal point of the parabolic dish.

Figure 6-8: Dish Stirling system. [21]

Dish/engine systems are the most efficient, among all solar power technologies, with efficiencies around 30% while photovoltaic technologies show efficiencies around 15%. They have high optical efficiency and small area for thermal losses. Their modularity is another advantage as well as the fact that there's no water requirement for cooling. When many dishes are incorporated in a power plant however, they require larger land areas, compared to other CSP technologies, to avoid shading effects.

6.1.4 Solar power tower

A solar power tower system, also known as a central receiver system, uses heliostats in order to track the Sun. Heliostats track the elevation and azimuth of the Sun and reflect the sunlight onto a central receiver, which is installed at the top of a tower (Figure 6-9). In the receiver, the working fluid is heated, from the concentrated solar energy, at 500-1000 °C and it is lead to storage or a power conversion system, in order to convert thermal energy to electricity (Figure 6-10). The heat transfer fluid can consist of water/steam or molten salt.

The advantages of solar power tower systems are the high efficiencies in energy collection and conversion to electricity and the capability of energy storage with the use of molten salt tanks. When using water/steam as heat transfer fluid, the tower can produce steam directly and the thermal-to-electricity conversion efficiency is higher. When using molten salt for heat transfer fluid there's efficient thermal energy storage for several hours.

Figure 6-9: Solar power tower. [17] Licensed under CC BY-SA 3.0

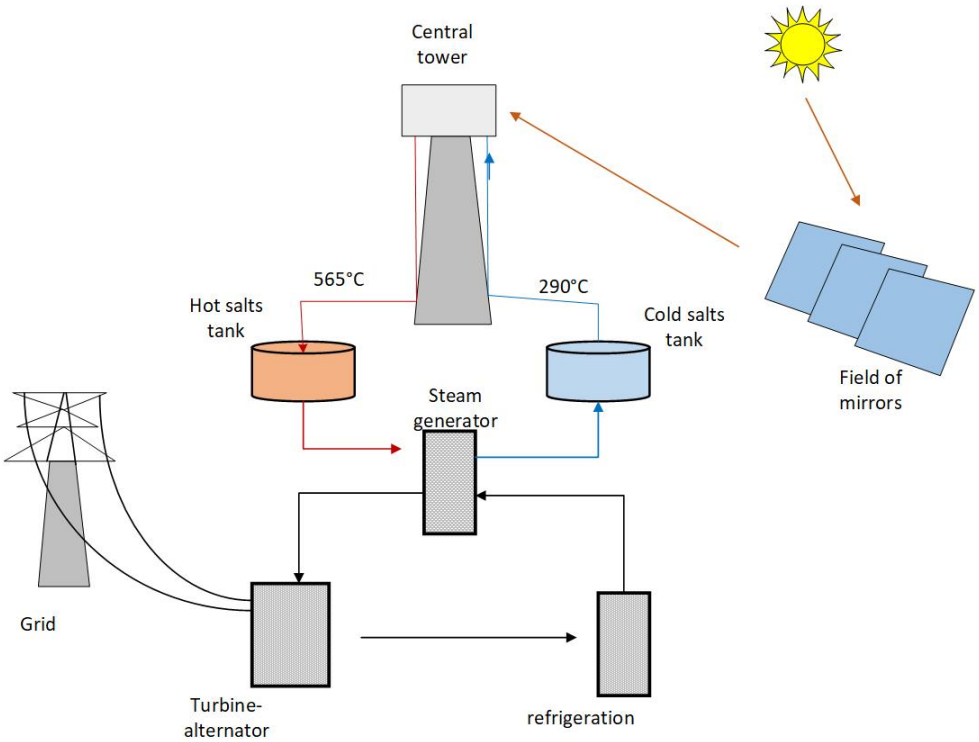

Figure 6-10: Solar tower system design with energy storage. [139]

6.2 Thermal energy storage

Thermal energy storage (TES) is very important in CSP systems, as it allows thermal energy to be stored for later use. CSP systems can provide continuous power during cloudy conditions or at night with the incorporation of TES systems. A CSP system, depending on the technology of its receiver, can store energy in thermal storage media like molten salt, phase-change materials, concrete and others, and use it at a later time to produce electricity.

In general, TES systems are divided in three types, sensible heat, latent heat and thermochemical storage. A TES system is characterized by its storage capacity, the rates of heat input and output during the charging and discharging processes and the storage efficiency, which is the ratio of energy that is provided to the energy required to charge the system. Other important parameters are the storage period and the overall cost of the storage system.

6.2.1 Sensible heat storage

Sensible heat storage (SHS) is the simplest way of storing thermal energy and it is achieved by heating or cooling a liquid or solid storage medium. This medium can be water, molten salt, rock or others. When the material is solid, heat is stored and extracted by means of gas or liquid flow through the pores or voids of the material. The amount of heat that is stored depends on the medium's specific heat, the change in temperature and the amount of storage medium.

The heat amount that is stored in the storage medium is given by Equation 6-1, where Q_s is the heat stored (J), m is the medium's mass (kg), c_p is the specific heat of the medium (J/kg*K) and t_i and t_f are the initial and final temperatures (°C), respectively.

$$Q_s = m * c_p * (t_f - t_i) \qquad \textit{Equation 6-1}$$

6.2.1.1 Water tank storage

Water is an inexpensive medium with high specific heat, therefore is popular as a heat storage material. The majority of solar water heating and space heating systems incorporate hot water tanks for storage, with sizes from a few hundred liters to several cubic meters. For seasonal storage, large hot water tanks are used, which can have a size up to several thousand cubic meters. The final temperatures of water (charging temperatures) are around 80-90 °C. The difference in temperature can be enhanced by using heat pumps for discharging. A water tank storage system can be seen in Figure 6-11.

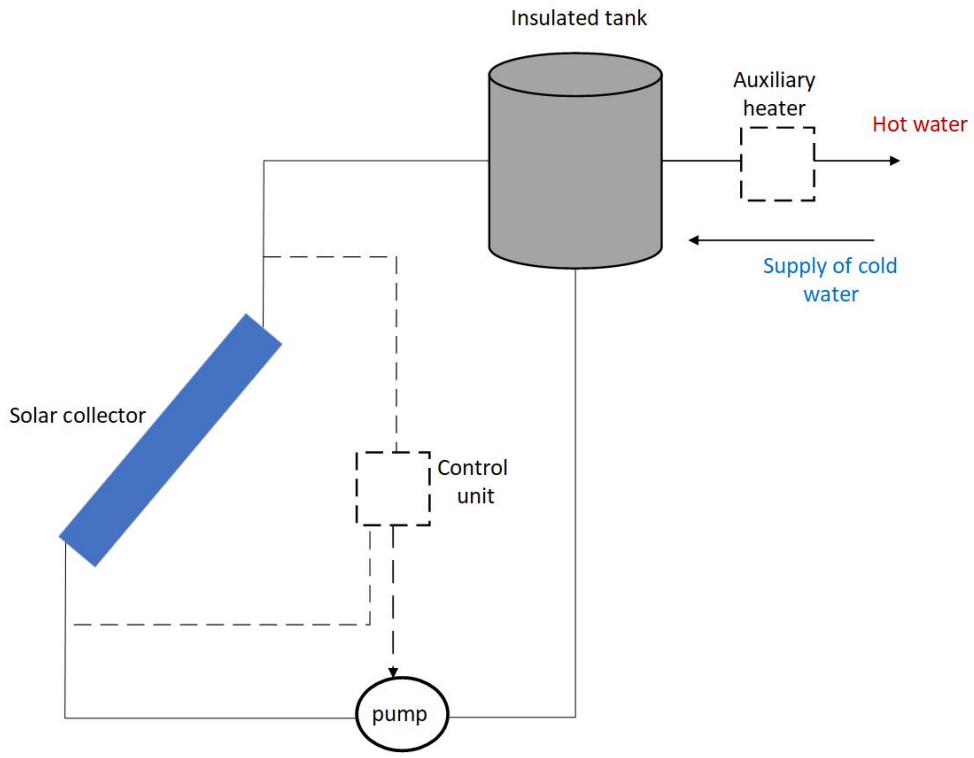

Figure 6-11: A water tank storage system. [140]

6.2.1.2 Underground storage

Underground thermal energy storage uses the ground, e.g. rocks, sand, soil, as a storage medium. A heat transfer fluid is pumped in the ground through pipes, which can be buried in trenches in a horizontal plane or they can be inserted vertically in boreholes (wells). Charging and discharging depends on the length of the pipes and the heat transfer rate through the ground.

In aquifer storage, water is the storage medium and it flows underground in a naturally occurring aquifer (Figure 6-12). Hot water is pumped into the aquifer for storage, displacing the cold ground water that already exists. The aquifers that can be used for that purpose must have low natural flow rate.

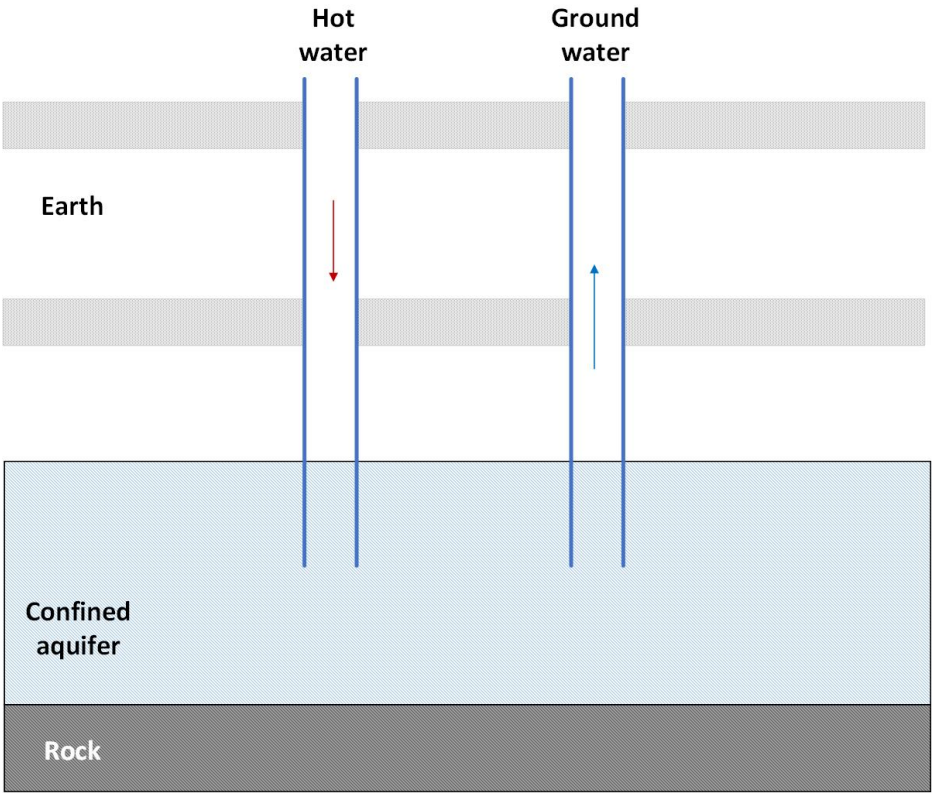

Figure 6-12: An underground aquifer storage system. [141]

Other underground storage systems are the cavern and pit storage, which are based on large underground reservoirs of water. These are located in the subsoil and can be used as TES systems. Water is pumped into or out of the storage unit in order to add or remove energy. These systems have high costs which is why there are not many applications in operation.

Water can be used as the storage medium for temperatures up to 100 °C. When temperatures are higher than 100 °C, oils and molten salts are commonly used as heat storage materials. For very high temperatures, solid materials, like ceramics or concrete, are better candidates as storage mediums.

6.2.1.3 Pebble-bed storage

A pebble-bed storage system is based on heat storage in solids. The system uses the heat capacity of a bed of loosely packed particulate material in order to store heat (Figure 6-13). A fluid, which is usually air, circulates through the bed so that energy is added or removed. The solid material that is used is usually rocks and pebbles. Heat is added with the flow through the bed in one direction, usually downward, and it is removed with the flow in the opposite direction. The two processes can't take place at the same time.

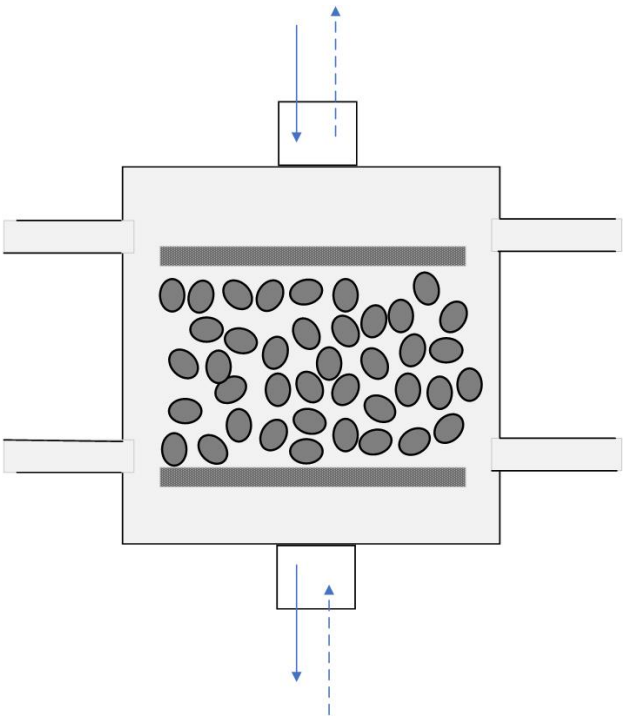

Figure 6-13: A pebble-bed storage system. [142]

An important advantage of the pebble-bed storage system is that it has a high degree of stratification. As the pebbles close to the entrance begin to get heated, the ones close to the exit remain in the same initial temperature. As the heating progresses, the temperature increases passes through the bed and when the medium is fully charged, the temperature is uniform. The pebble-bed is generally heated during the day with hot air from the collector and in the evening and at night, there's energy removal.

6.2.2 Latent heat storage

Latent heat storage (LHS) systems are based on the principle that a material changes its phase when heat is applied to it. It can be changed from solid to liquid when storing the heat as latent heat of fusion or it can be changed from liquid to vapour when storing the heat as latent heat of vapourization. When the stored heat is extracted, the material will change its phase again, from liquid to solid or from vapour to liquid. These materials are called phase change materials (PCM). The latent heat is used for the change in the material phase without any change in the temperature of the material. A LHS system is an effective manner to store thermal energy and has high energy storage density.

The storage capacity Q_s (J) of a LHS system using a PCM medium is given by Equation 6-2, where m is the PCM mass (kg), c_{ps} is the average specific heat of the solid phase between t_i and t_m (J/kg*K), c_{pl} is the average specific heat of the liquid phase between t_m and t_f (J/kg*K), t_m is the melting temperature (°C), f is the melt fraction and Δq is the latent heat of fusion (J/kg).

$$Q_s = m * \left[c_{ps}(t_m - t_i) + f\Delta q + c_{pl}(t_f - t_m)\right] \qquad \textit{Equation 6-2}$$

The latent heat for change from a solid phase to another solid phase (where the crystallization form changes) is small. The solid-vapour and liquid-vapour transitions have large amounts of latent heat but there are also large changes in volume, which makes the storage system impractical. The solid-liquid transition has high latent heat and small volume changes, which makes it the most widespread process in LHS systems. The process of melting can have energy densities up to 100 kWh/m^3 (e.g. ice), while the equivalent for a SHS system is typically around 25 kWh/m^3. Phase change materials can be used for daily or seasonal energy storage. These systems however have higher investment costs.

A LHS system should have three main components: a suitable PCM in the desired temperature range, a container for the storage material and a suitable heat transfer fluid which will transfer heat from the heat source to the storage. The PCMs that are more widely used for

thermal energy storage are organic, e.g. paraffin compounds, fatty acids and inorganic materials, e.g. hydrated salts. For cold storage applications water/ice is used as well.

6.2.2.1 Containment of PCMs

Containment of PCMs can be achieved with bulk storage in tank heat exchangers, macro-encapsulation or micro-encapsulation. Bulk systems need more extensive heat transfer than conventional tanks due to the higher heat storage density of PCMs.

Macro-encapsulating is the most common type of containment and it consists of keeping PCMs in a tube, sphere, cylinder or other container, which can be plastic or metal. Micro-encapsulating consists of micro-spheres of PCM which are encapsulated in a thin polymer with high molecular weight.

The capsules can be incorporated in a one tank TES system, where heat is transferred to/from a heat transfer fluid as it flows in the space between the capsules. The fluid that is heated from the solar collector circulates through the tank and the PCM in the capsules absorbs latent heat and turns into liquid. This is the charging process. In the discharging process, cool heat transfer fluid circulates through the tank and absorbs heat from the PCM, which in turn freezes. This can be seen in Figure 6-14.

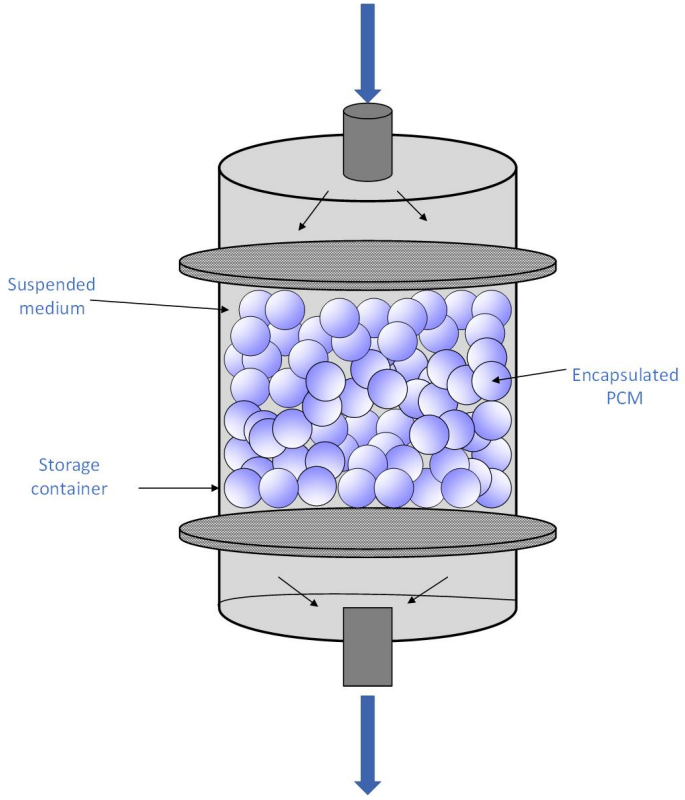

Figure 6-14: A direct contact TES system. [143]

6.2.3 Thermochemical storage

Thermochemical storage is the thermal energy storage by means of chemical reactions. Experimental storage systems based on endothermic/exothermic chemical reactions, like the salt hydrate technology are being tested for development. Salt hydrate technology takes advantage of the reaction energy that is created when salts are hydrated and dehydrated. Heat storage is achieved by using the heat from a solar collector to evaporate the water in sodium hydroxide, in an endothermic reaction. Addition of water releases back heat in an exothermic reaction. The storage of dried salt for prolonged time periods makes the system suitable for seasonal thermal energy storage. Another advantage is the possibility of transport of the stored dried salt. Suitable storage materials and various applications are being tested in laboratory conditions for further improvement of the technology.

Thermochemical energy storage can provide high storage densities with minor thermal losses.

6.2.4 Thermal energy storage for CSP systems

TES systems can be coupled with CSP technologies in order to provide energy in the absence of sunlight. During the night or cloudy conditions, the flow of the heat transfer fluid in the TES system can be reversed, so the fluid can be heated and used to drive the steam generator to produce electricity. This way the power production can be continued after sunset and be provided on demand.

The TES system incorporated in a CSP installation should have high energy density or heat storage capacity. It should consist of a stable storage medium that won't present any signs of degradation after several cycles. There must be good heat transfer between the heat transfer fluid and the storage medium and also good compatibility between these two and the heat exchanger. The process must be completely reversible so that energy can be stored, used and the system can return to the initial state. Finally the thermal losses in the system must be kept at a minimum.

The TES systems that are used in CSP installations are mainly two-tank and single-tank systems.

6.2.4.1 Two-tank storage system

In a two-tank storage system, the fluid is stored in two tanks, where one is at a high temperature and the other at a low temperature (Figure 6-15). The fluid from the low temperature tank flows through the solar collector and is heated at a high temperature, after which it flows to the high temperature tank to be stored. When needed, fluid from the high temperature tank flows through a heat exchanger in order to generate steam for electricity production. The fluid that exits the heat exchanger is at a low temperature and flows back to the low temperature tank. This is the two-tank direct system.

In the two-tank indirect system, the difference is that there are two fluids used, one for heat transfer and the other for storage. An indirect system is suitable for CSP installations where the heat transfer fluid is expensive or not suitable to be used as the storage fluid. The process in a two-tank indirect system is that the storage fluid in the low temperature tank flows through an extra heat exchanger, where it is heated with the help of the high temperature heat transfer fluid. The storage fluid, which is now at high temperature, flows to the high

temperature tank. The heat transfer fluid exits the heat exchanger at a low temperature and flows back to the solar collector where it is heated again. The storage fluid which is stored in the high temperature tank can be used to generate steam for electricity production.

A two-tank indirect system can use oil as the heat transfer fluid and molten salt as the storage fluid, while a two-tank direct storage system can use molten salt for both the heat transfer and the storage fluid.

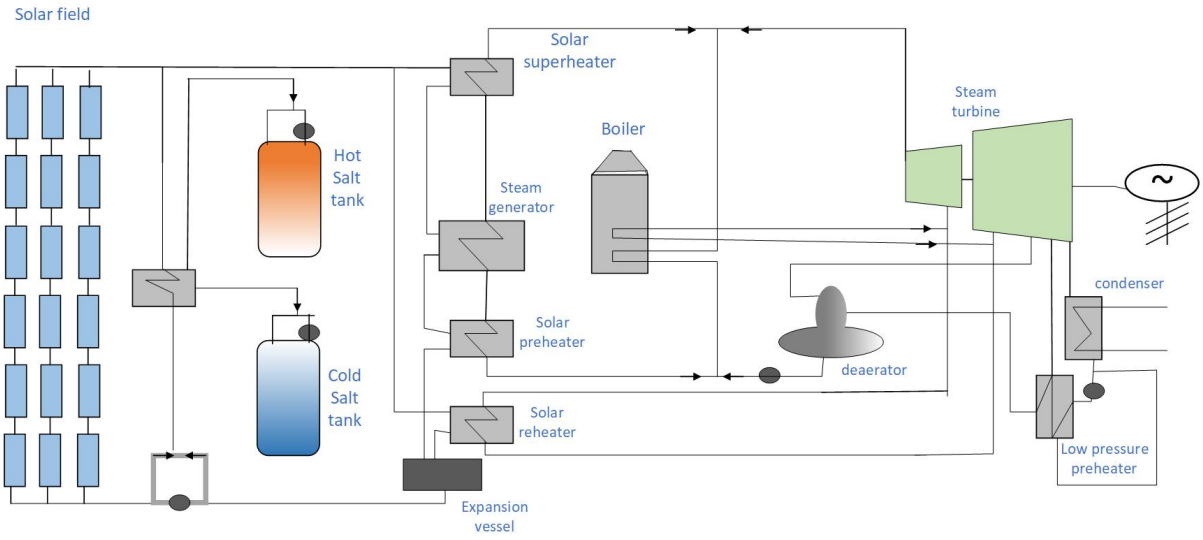

Figure 6-15: A two-tank molten salt thermal storage system. [144]

6.2.4.2 Single-tank storage system

A single-tank system, mainly a thermocline system, is used to store energy in a solid medium in a single tank (Figure 6-16). The solid medium is usually silica sand. In a thermocline system, the top part of the medium is always at high temperature while the bottom part is at low temperature. These two parts are separated by a thermocline or temperature gradient (Figure 6-17). Heat transfer fluid of high temperature enters the thermocline at the top and leaves at the bottom at low temperature. This process results in moving the thermocline downwards and thermal energy is added to the system for storage. When the flow is reversed, the thermocline moves upwards and thermal energy is removed from the system to generate steam for electricity production. Thermal stratification of the fluid in the tank is created due to buoyancy effects and this way the thermocline is stabilized and maintained. In this system,

the use of just one tank and a solid medium, results in costs reduction, compared to the two-tank storage system.

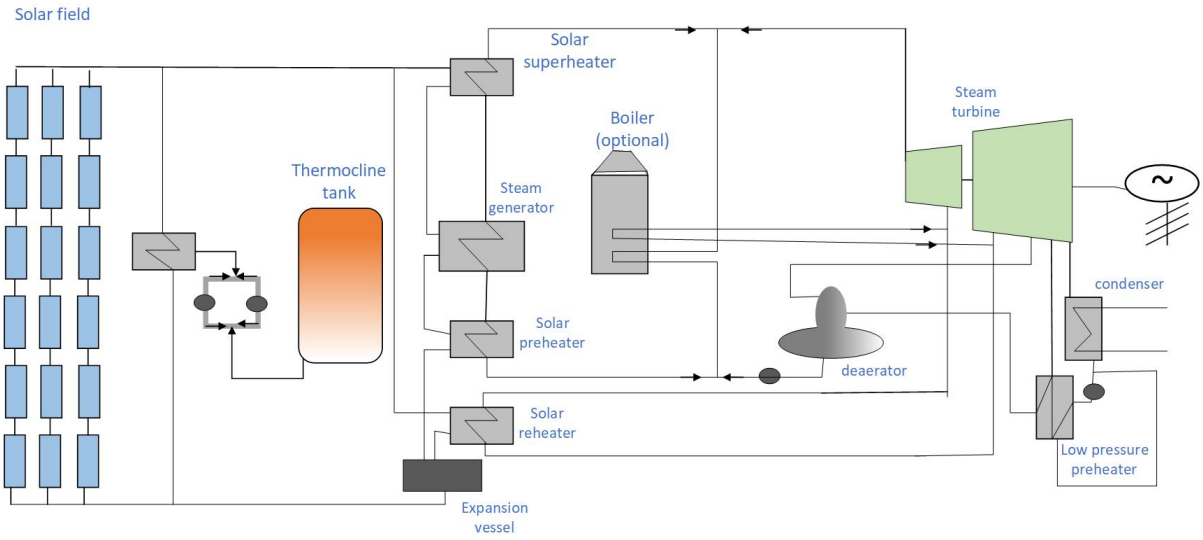

Figure 6-16: A single-tank (thermocline) thermal energy storage system. [143]

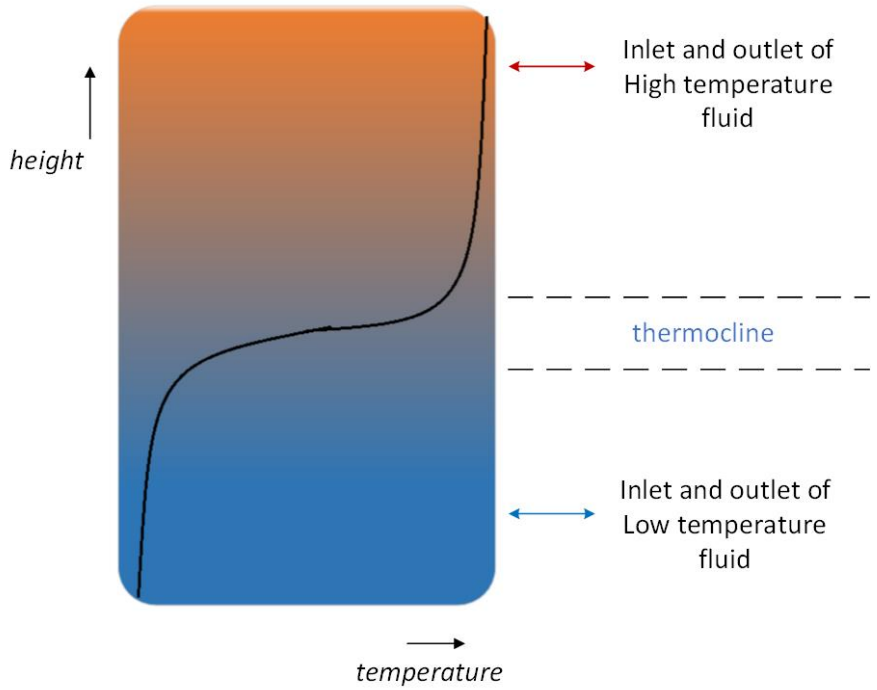

Figure 6-17: Schematic of thermocline energy storage. [145]

Present CSP installations that incorporate thermal energy storage use two-tank sensible heat storage systems with synthetic oil or molten salts.

6.3 Solar water heating

Solar water heating (SWH) is the process of heating water with the use of a solar thermal collector. There are various configurations for SWH systems. They can be active or passive systems, using water or water and another fluid as working fluid. They can be heated in a direct manner or with light-concentrating mirrors.

Regarding the propulsion, SWH systems can be passive or active. In passive systems, the working fluid circulation is based on convection or heat pipes while active systems make use of pumps in order to circulate the working fluid. A passive or active SWH system can be direct or indirect based on the manner of heat transfer. In direct or open loop systems, the potable water circulates through the collectors. Indirect or closed loop systems use a heat exchanger in order for heat to be transferred from the heat transfer fluid to the potable water.

Active SWH systems are in general more efficient, complex and expensive. They can be used for industrial applications or applications with high load demand. Passive SWH systems have lower costs and are easier in their construction and installation. They are commonly used in domestic applications or applications with low load demand.

6.3.1 Passive water heater

The passive water heater or natural circulation system doesn't use pumps to circulate water from the collector to storage but instead the water circulation is achieved by means of gravity and convection, as hot water tends to rise above cooler water.

Passive SWH systems can be direct or indirect in their operation. Direct systems circulate the water through the collector. In indirect systems, a heat transfer fluid is used to transfer energy from the solar collector to the storage tank that contains the water. The thermosyphon and integrated collector storage (ICS) systems are passive SWH systems.

A passive water heater (thermosyphon) is depicted in Figure 6-18. The tank is located above the collector and the circulation of water is achieved by natural convection. The medium, after being heated in the collector, rises to the tank top, cools down and flows back to the bottom of the solar collector. Hot water can be taken directly from the tank or indirectly via a heat exchanger in the tank. The design is simple and cost effective as it doesn't require pumps. Auxiliary power can be added to the water in the top of the tank in order to maintain an efficient hot water supply.

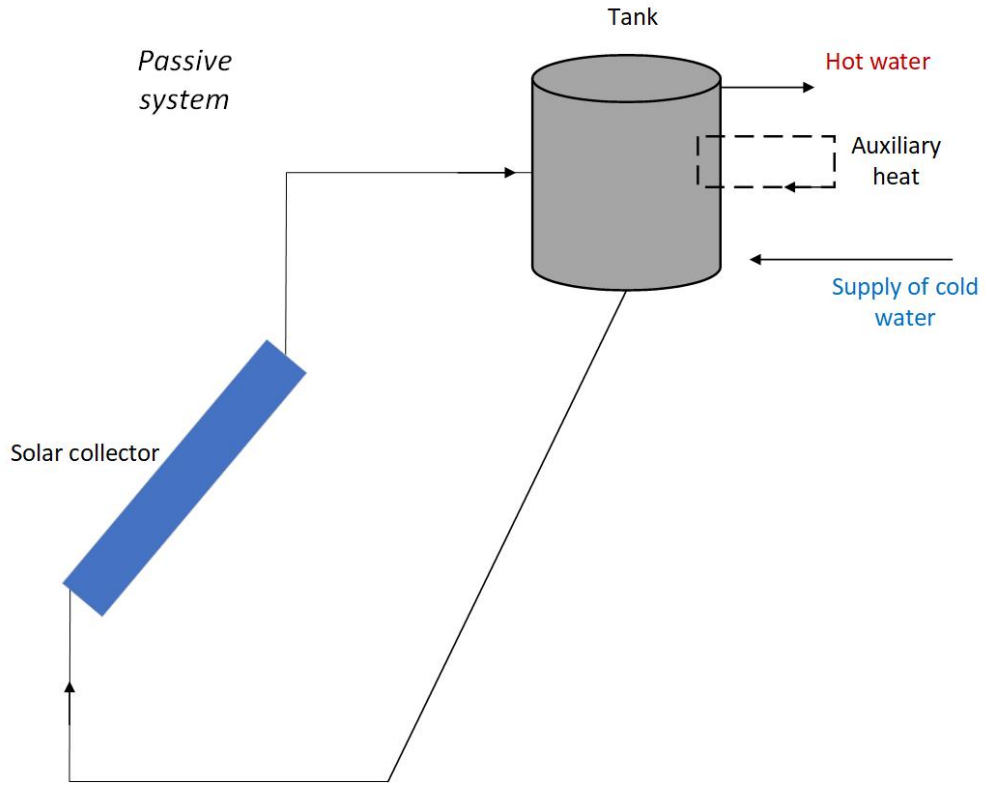

Figure 6-18: A passive SWH system. [146]

An ICS system or a batch heater system uses a tank as both a collector and a storage device (Figure 6-19). The system consists of a thin rectilinear tank with a glass side that is situated to face the Sun at noon. It's a simple, cost effective system since it doesn't require pumps, heat exchangers etc. ICS systems are often preferred for domestic installations. However they are more efficient in locations with favourable weather conditions as they have high heat losses.

Modern versions have the storage tank enclosed in an insulated box with layers of glazing in order to minimize heat losses.

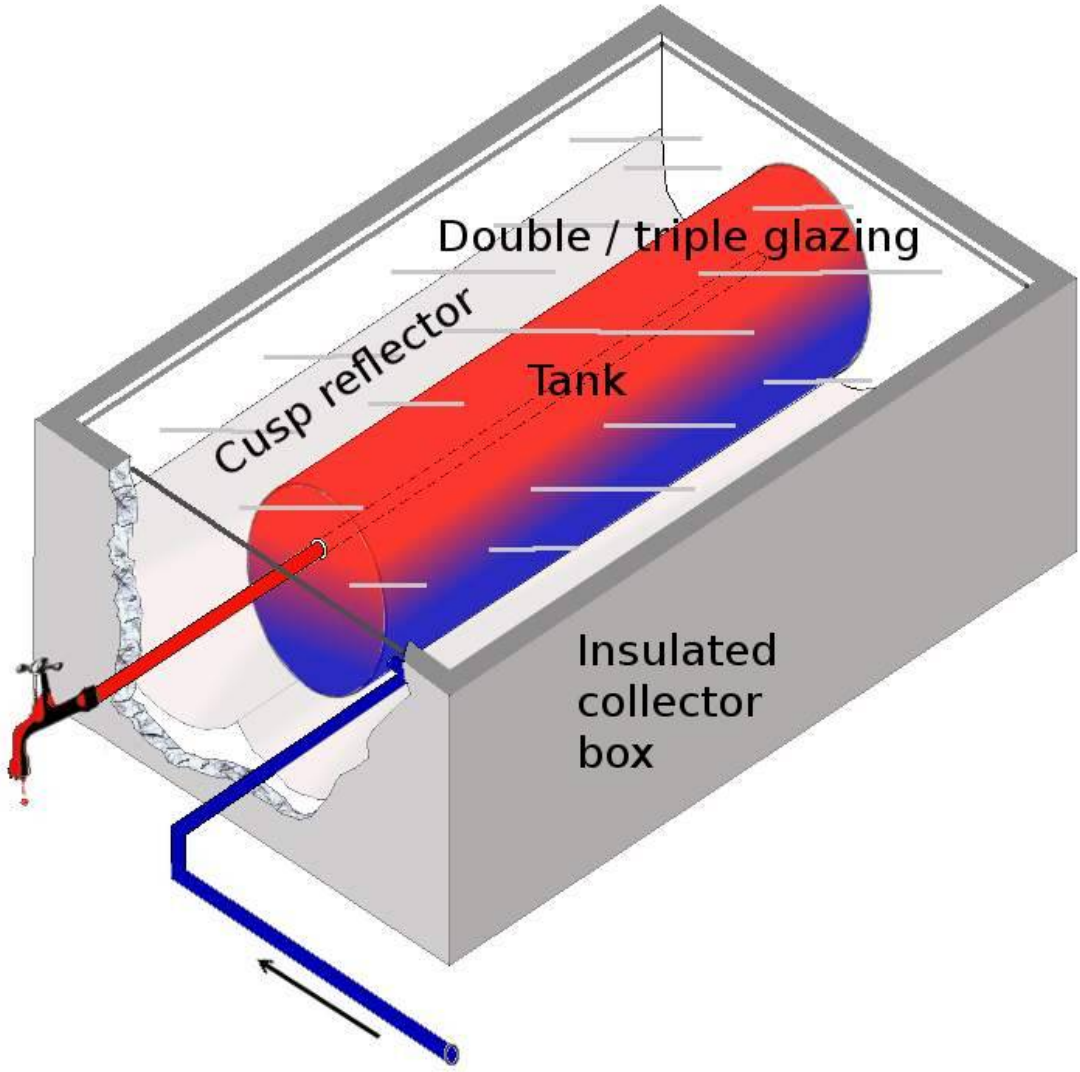

Figure 6-19: An ICS system. [147] License: Public Domain

6.3.2 Active water heater

Figure 6-20 shows a simple design of an active SWH system or a forced-circulation system. The difference with the passive system is that an active SWH system requires the use of a pump. Control is usually achieved with a differential thermostat that turns on the pump when the temperature at the top header reaches higher values than the water temperature at the bottom of the tank. The difference in temperature must have a sufficient margin in order to

achieve control stability. A check valve is used in order to prevent reverse circulation and thermal losses from the collector during the night. Auxiliary energy can be added here also to ensure hot water supply.

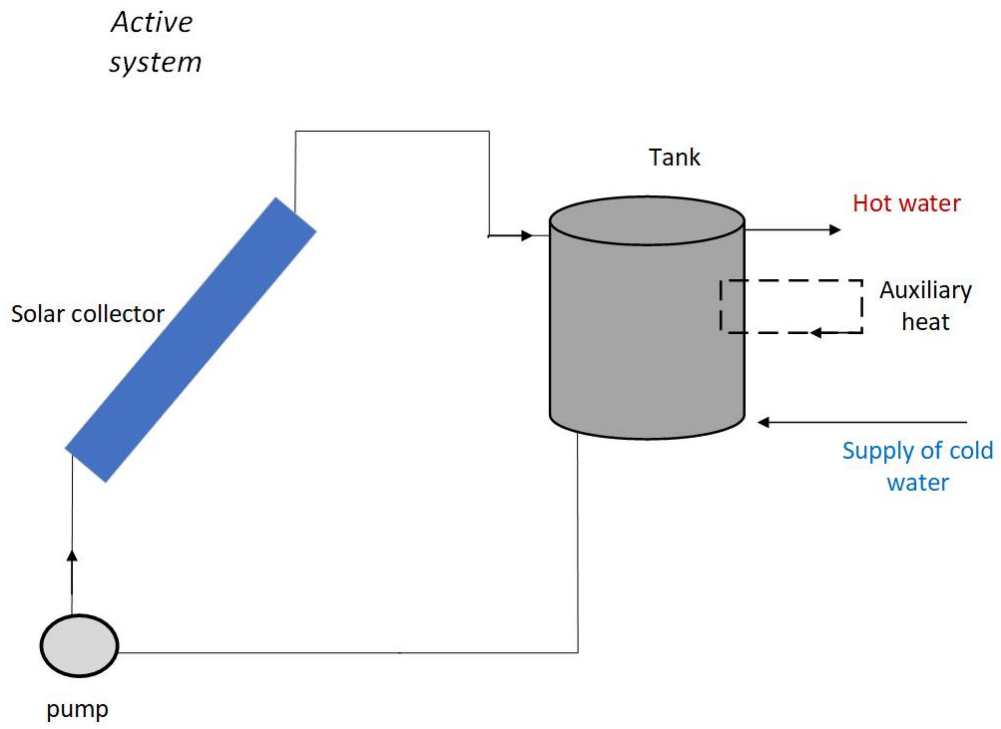

Figure 6-20: An active SWH system. [146]

Figure 6-21 shows the designs of an active direct (a) and an indirect (b) SWH system. In a direct system, the water runs directly through the solar collector. This system is fit for domestic hot water applications and it is suitable in locations that don't have extended freezing conditions or where water is not hard or acidic. The system's design and use is simple and this type has the lower costs among active SWH systems. The use of a heat exchanger is not required and heat is transferred directly to the water. The operating performance is high since there are no heat losses during the night, as is the case with stored water in a passive system or losses through a heat exchanger, as is the case in indirect systems. Some stored heat though can be lost due to the recirculation of the system.

The operation of direct systems in freezing conditions can result in pipe damage. For that purpose a drain-down system can be used, which is a modification of the direct circulation

(Figure 6-22). In this type, the collector is filled with domestic water under supply pressure when there are no freezing conditions. After the system is filled, a differential controller is used to operate a pump to move water from the tank through the collector. A drain-down valve helps protecting from the freeze. When the valve is activated, the collector's inlet and outlet are isolated from the tank and water in the collector is drained away. Installation of a vacuum breaker at the collector top ensures that air is allowed to enter the collector in order for water to be drained at the bottom.

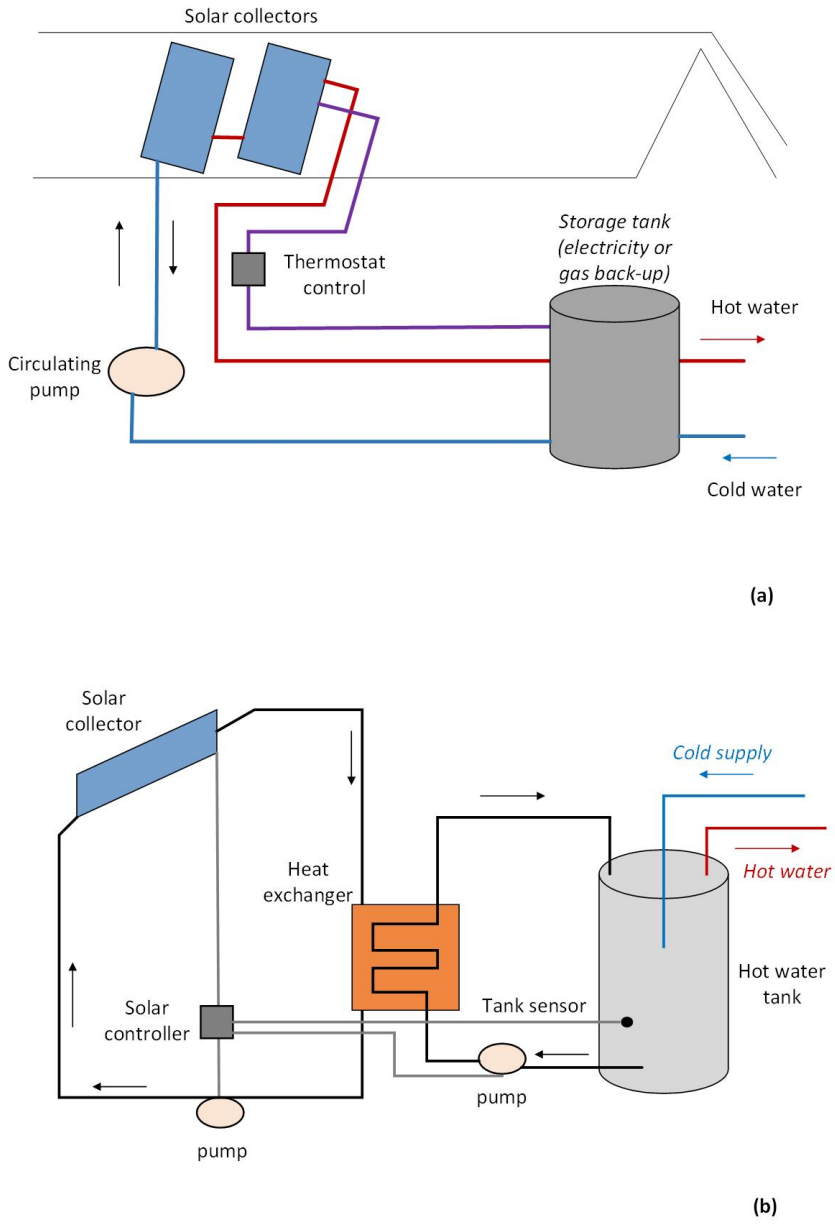

Figure 6-21: (a) An active direct [148] and (b) an active indirect [149] SWH system.

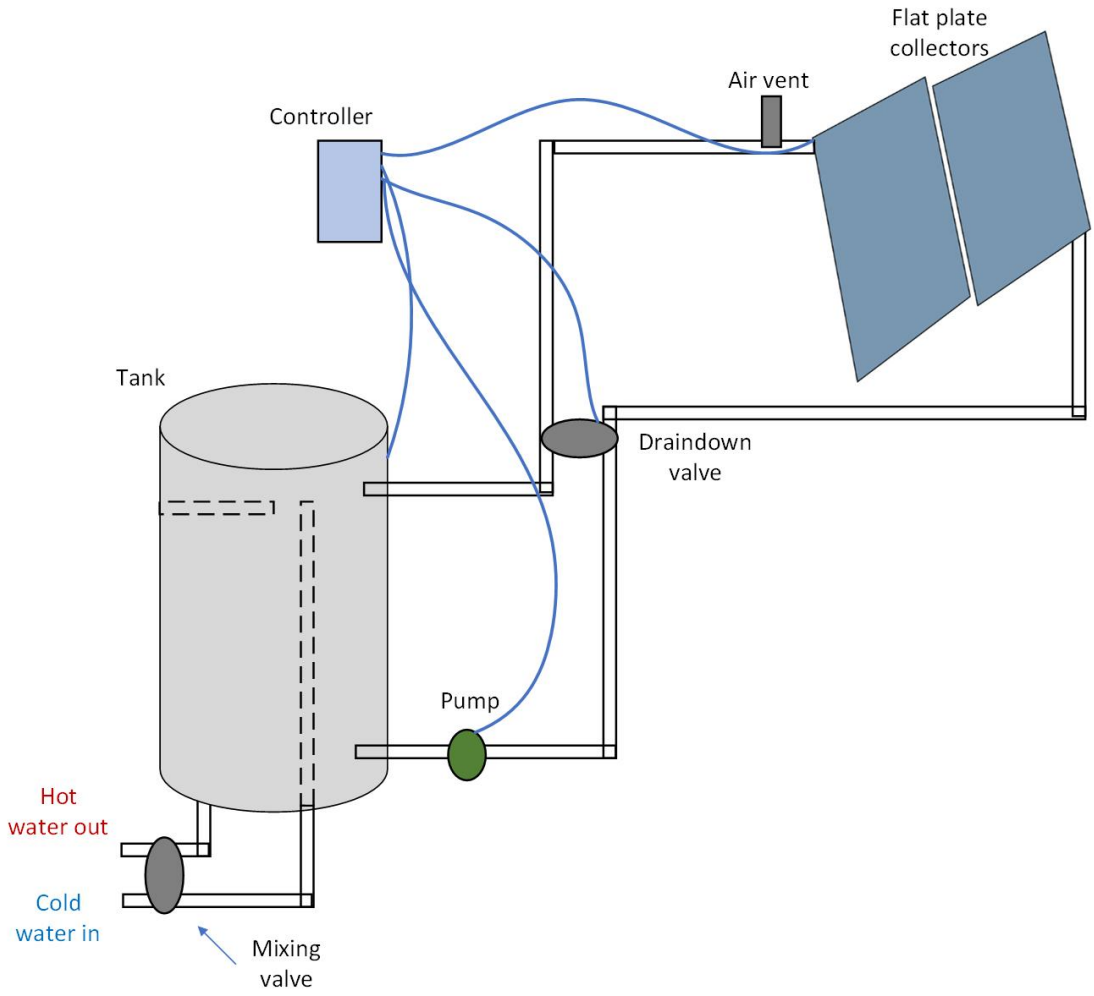

Figure 6-22: Design of a drain-down SWH system. [150]

In an indirect system, water or another heat transfer fluid flows through the collector and passes through a heat exchanger in order to heat the water in the tank (Figure 6-21b). This configuration with the heat exchanger requires more piping. Indirect active SWH systems use a mixture of glycol and water antifreeze as a heat transfer fluid to prevent damage under freezing conditions. This non-freezing fluid is circulated with pumps through the collector and heat exchanger. These systems are commonly used in cold climates. In order for the system to operate properly, the antifreeze should be recharged every 3-5 years. An indirect system is more complicated than a direct one because it requires a tank with a heat exchanger coil or an external heat exchanger.

A drain-back system is a modified active indirect system that is not pressurized and makes use of pumps to circulate water, used as heat transfer fluid, through the collector. When the pumps are not activated, the water in the collector loop is drained into a reservoir. The heat exchanger transfers heat from the collected water to the domestic water. Since the heat transfer fluid is water, it doesn't need to be changed like in the case of pressurized antifreeze systems. A drain-back system is not in danger of freezing or overheating, making it efficient for cold climates.

Another version of an active indirect system is the air system, where air is used as the working fluid. This way freezing and overheating are avoided. In this system, a fan circulates air through the tubes and the heat exchanger that transfers heat from the air to the water, which is located in a horizontal tank. It's a noncorrosive and low maintenance system that can be used in very cold conditions. It takes up a larger area though because of the use of the air unit.

6.3.3 Solar thermal collectors

The solar thermal collector is the main component of a SWH system. It absorbs sunlight and transfers heat directly or indirectly to the water in the storage tank. The type and size of the collector is important to the overall efficiency of the system. The types of solar collectors that are mostly used in SWH systems are the flat-plate collectors (FPC), the evacuated tube collectors (ETC) and the concentrating collectors. The collector is selected based on the heating requirements of the system and the conditions concerning the location.

6.3.3.1 Flat-plate collector

The flat-plate collector is most commonly used in solar thermal applications. It consists of an absorber plate, located inside an enclosure, along with transparent cover sheets to allow solar energy transmission (Figure 6-23). The absorber material is usually one with high thermal conductivity, like copper or aluminum and it incorporates tubes for fluid circulation. Heat loss is limited from the sides and the back of the enclosure due to insulation. A heat transfer fluid circulates through the tubes in order to remove heat from the absorber. The heat transfer

fluid can be water or an antifreeze mixture which is suitable for cold climates. When a heat transfer fluid is used, a heat exchanger is incorporated in the system in order to transfer heat from the collector fluid to the water in the storage tank. The absorber is coated with a selective material so energy absorption can be maximized while minimizing emission.

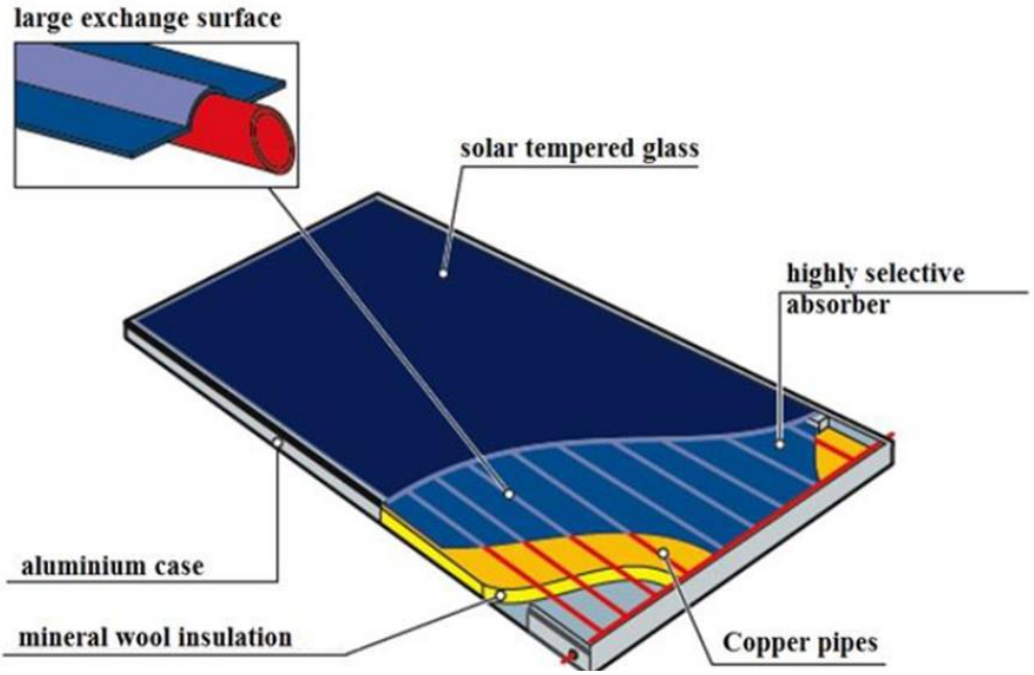

Figure 6-23: Flat-plate collector. [22] Licensed under CC BY 4.0

The usual tube layout is parallel with bottom pipe risers and top collection pipe however there are various disadvantages with this design. The distribution of temperature is not uniform in the surface of the absorber, there's not equal distribution of the working fluid in the collector risers and there's increased heat loss in the collector due to the higher temperature of the absorber plate when the flow rate is low. For these reasons a serpentine configuration is used for the piping layout, where there's a continuous s-shaped pipe. This design allows total mass flow rate to pass through the tube which results in the increase in the heat transfer coefficient and a better thermal performance.

6.3.3.2 Evacuated tube collector

The evacuated tube collector is made of a number of rows of transparent glass tubes, which are connected together in parallel. The glass tube surrounds the absorber with high vacuum in order to reduce heat losses via convection and conduction. This results in increased energy conversion efficiency. The absorber can be metallic or it can be a second concentric glass tube. The heat transfer fluid flows in and out of the tube or it is in contact with a heat pipe inside the tube. The heat pipe transfers heat to the fluid in a heat exchanger (manifold) which is placed transverse in regards to the tubes. The design of the evacuated tube collector is depicted in Figure 6-24.

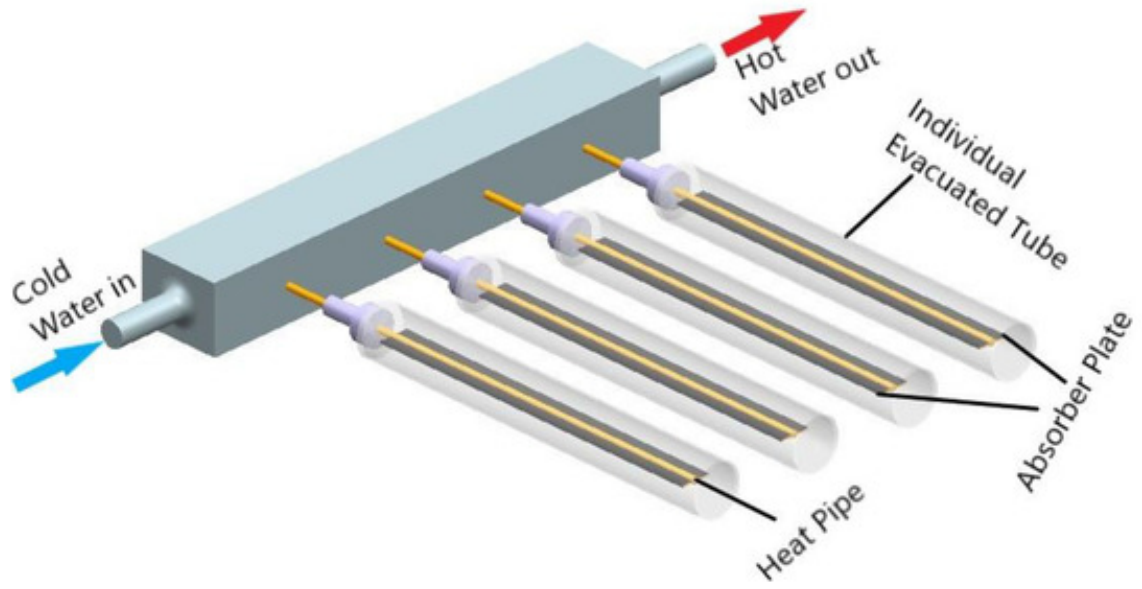

Figure 6-24: Evacuated tube collector. [23] Licensed under CC BY 4.0

The cylindrical shape of the glass tubes allows the angle of sunlight to always be perpendicular to the tube resulting in good performance of the collector even in early morning or late afternoon. Each tube consists of a thick glass outer tube and a thinner glass inner tube. The tubes are made of borosilicate and a vacuum is formed in the space between the inner and outer tube.

Inside the glass tube there's an aluminum or copper fin, which can be flat or curved and it is connected to a metal heat pipe that runs the length of the inner tube. The absorber fin is covered with a selective coating to transfer heat to the fluid circulating through the heat pipe.

The heat is subsequently transferred to the manifold, which is connected to the storage tank and heats the water inside. The vacuum offers very good insulation and evacuated tube collectors can heat water at high temperatures even in cold weather conditions when flat-plate collectors don't perform so well. The disadvantage of evacuated tube collectors is their higher cost but they are more suitable for cold climates.

Another design of evacuated tube collectors is the U-tube design or direct flow evacuated tube collector seen in Figure 6-25. In this design there are two heat pipes that run through the tube center. One pipe is responsible for the flow and the other for the return. Their connection at the bottom of the tube forms the shape of a U, from where the name derives. This design is more energy efficient due to the direct flow and the absence of a heat exchanger between fluids. However, fluid flows into and out of each tube and if there's any damage to the tubes it's not easy to replace them.

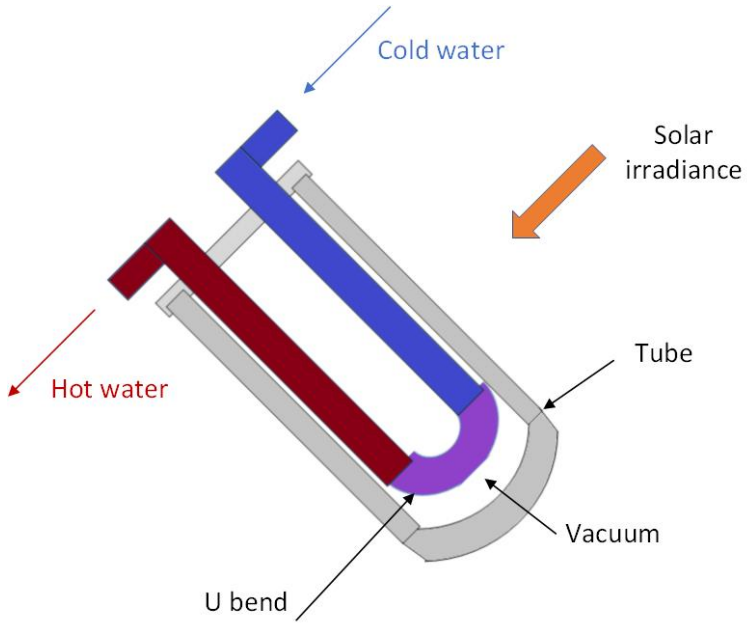

Figure 6-25: Direct flow evacuated tube collector. [151]

6.3.3.3 Concentrating collector

Flat-plate and evacuated tube collectors are commonly used in solar thermal installations and can provide temperatures up to 120 °C. If higher temperatures are required then the

collectors used are concentrating collectors. Concentrating collectors can be parabolic or paraboloidal collectors or Fresnel reflectors. These concentrating collectors maximize incident solar radiation and can produce high temperatures. They are usually used when the temperatures required are higher than 100 or 150 °C. The temperature level of the concentrating collector depends on the concentration ratio which is given in Equation 6-3.

$$C = \frac{total\ concentrator\ aperture}{receiver\ surface} \qquad \textit{Equation 6-3}$$

When the concentration ratio is lower than 5, the concentrating collectors are characterized as non-imaging collectors and are usually used in applications with temperatures up to 200 °C. Higher concentration ratios, usually higher than 10, correspond to imaging concentrating collectors that are used in applications with temperatures up to 500 °C.

The most commonly used types of concentrating collectors are the compound parabolic collector, the parabolic trough concentrator, the linear Fresnel reflector and the solar dish concentrator. The parabolic trough concentrator, linear Fresnel reflector and solar dish concentrator have been discussed previously. Parabolic trough concentrators can be used for temperatures up to 400 °C and the usual values of concentration ratio are between 15 and 45. The linear Fresnel reflector has concentration ratio from 10 up to 40. The solar dish concentrator has the highest concentration ratio, over 100 and it is used for very high temperature applications.

The compound parabolic concentrator is a non-imaging collector and its concentration ratio is between 1 and 5. Figure 6-26 shows a comparison between a non-imaging compound parabolic concentrator and a parabolic concentrator. The compound parabolic concentrator can receive higher amount of light. Due to the design of the mirror, this collector can collect and focus direct as well as diffuse solar radiation without requiring tracking of the Sun. The tilt angle may periodically be adjusted. It consists of a tubular receiver and when the system operates without tracking, it is a cost effective solution.

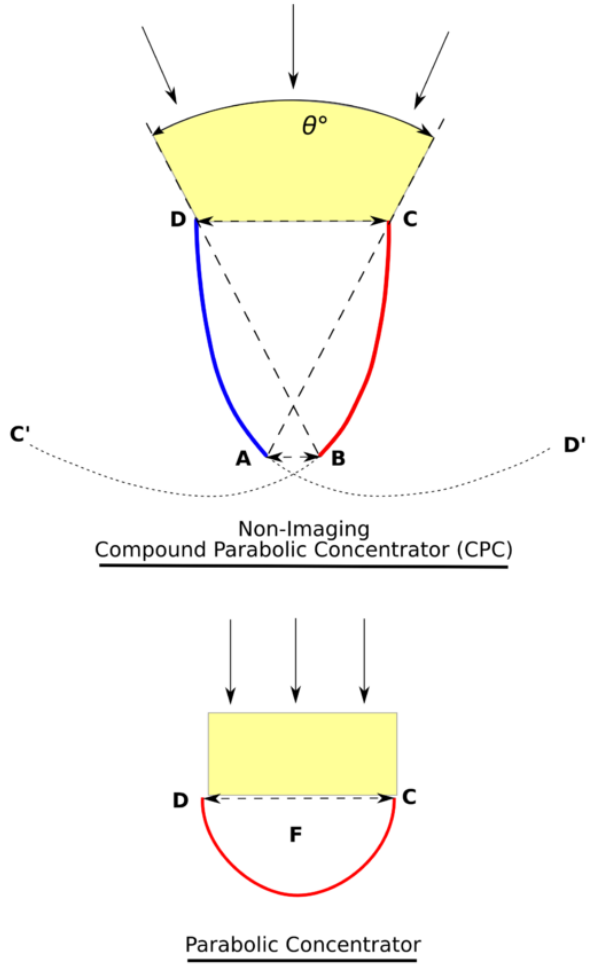

Figure 6-26: Comparison between a non-imaging compound parabolic concentrator (top) and a parabolic concentrator (bottom). [152] Licensed under CC BY-SA 3.0

6.4 CSP system

6.4.1 Solar resource and forecast

CSP systems require a strong solar resource for their effective operation. The potential for incorporating a CSP installation in any given location largely depends on the location's solar radiation characteristics. Since CSP technologies utilize mainly the direct component of solar radiation, these data are important in selecting the suitable locations. Direct Normal Irradiance (DNI) is the solar irradiance incident on a normal plane directly from the Sun. DNI is the parameter that determines the suitability of a location for a CSP installation. Figure 6-27 presents the distribution map of DNI for the year 2019, in daily and yearly totals (kWh/m^2).

The most suitable areas are located in south-western USA, north Mexico, Chile, North Africa, Middle-East, western Australia and other parts as it can be seen from the map.

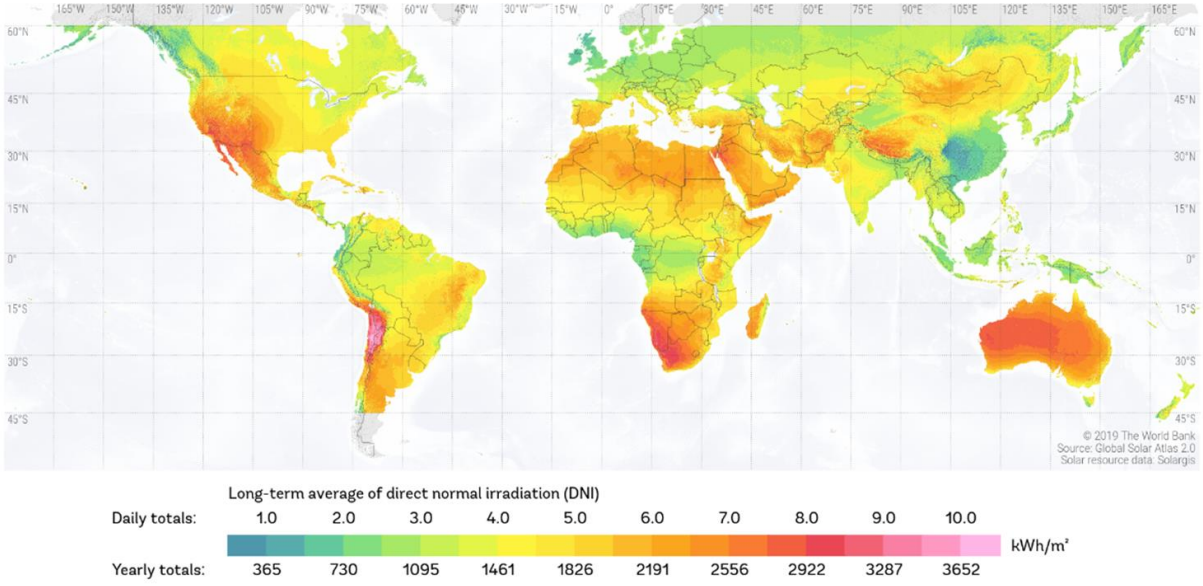

Figure 6-27: Distribution map of direct normal irradiation. [153] Licensed under CC BY 4.0

Since DNI is important for the operation of CSP plants, its forecast is vital. The efficient operation of CSP installations rely on good and accurate forecasts of DNI. Different forecast methods should be used depending on the forecast horizon, since the forecast accuracy depends on the accuracy of forecasting the atmospheric conditions that affect DNI and thus depends on the time scale of the forecast horizon. This way, time series analysis models have a forecast horizon of a few minutes to one hour, while satellite-based cloud motion vectors have a forecast horizon of a few hours and numerical weather prediction models have a forecast horizon of several days. Forecasts of global horizontal irradiance (GHI) perform well and have been well researched and DNI can be calculated for GHI values. However the DNI forecast should not be based on the derivation from GHI forecasts, since atmospheric conditions have a greater effect on DNI than GHI. The main factors that affect DNI are clouds and in cloudless skies, aerosols have the most important effect.

Clear Sky Models (CSMs) can be used to forecast DNI. These are based on the annual cycle that solar irradiance follows at a particular location and model it using variables to determine

the position of the Sun and the irradiance. CSMs of more complexity can model the solar irradiance attenuation as it travels through the atmosphere as they include aerosol optical depth and ozone data.

Numerical Weather Prediction models (NWP) use the atmosphere description at a certain time as a starting point. Based on that and on equations describing horizontal and vertical momentum, energy conservation etc., they calculate changes that occur in the atmospheric conditions at fixed time steps and thus produce the desired forecast. NWP models can be global models that cover the entire Earth or mesoscale/regional models that cover regions of the globe.

Time Series Analysis (TSA) methods deliver forecasts by performing statistical analysis of historical time series trends in the forecast variable or parameters that affect the forecast variable. A simple version is the persistence model, which, as the name indicates, makes the assumption that future conditions will be the same as those previously. Artificial Intelligence (AI) TSA models have the ability to identify patterns in the time series that recur and make more accurate forecasts. These types can be produced with the use of an artificial neural network (ANN).

Finally, the cloud motion vector (CMV) method is based on data from satellites or ground-based images in order to track the cloud motion. Solar irradiance forecasting can make use of CMVs in order to describe advection of present clouds and make predictions of future cloud cover images. The cloud imaging is converted to solar irradiance forecast with the use of statistical and physical models.

6.4.2 Land and water

A CSP system needs a significant land area for its installation and operation. This land can't be used for other applications at the same time and it needs to be relatively flat. The collectors of the CSP system must be arranged in such a way so as to maximize concentrated solar energy and have enough space between them to avoid shading effects. The land should be located near transmission lines and roads and not be in a protective area. It also needs to be

basically arid, so sunny deserts present very desirable solutions for CSP installations manufacture.

Another important issue for the CSP system is the water resource. CSP systems require large amounts of water for cooling and cleaning of the mirrors. This comes in contrast with the arid and desert regions that are most suitable for CSP installations, since these regions have low water resources, so that issue also needs to be taken into account when constructing a CSP plant. There are alternative cooling systems, like dry cooling, but these are more expensive and add to the overall cost of the installation.

6.4.3 Performance

The efficiency of a CSP system depends on the type of technology that is used for the energy conversion, the operating temperature, the thermal losses in the system and other parameters. The overall efficiency of the system, η is given by Equation 6-4.

$$\eta = \eta_{optical} * \eta_{receiver} * \eta_{transport} * \eta_{storage} * \eta_{conversion} \qquad \textit{Equation 6-4}$$

In this equation, optical efficiency, $\eta_{optical}$ includes all reflectivity losses and flux spillage losses that take place until the radiation reaches the receiver. Receiver efficiency, $\eta_{receiver}$ includes reflective losses from the receiver, as well as convective, conductive and radiative losses. Transport efficiency, $\eta_{transport}$ includes thermal losses from the pipes network that lead the heat transfer fluid to storage or through the power cycle, as well as losses in the heat exchangers between the heat transfer fluid and working fluid. Storage efficiency, $\eta_{storage}$ includes thermal losses due to the storage device and losses in the heat exchangers between the heat transfer fluid and storage medium and between storage medium and working fluid. Conversion efficiency, $\eta_{conversion}$ includes thermal, electrical and friction losses that take place in the power cycle.

The value of the conversion efficiency of a heat engine between isothermal reservoirs has an upper limit, due to the second law of thermodynamics and it is given by the Carnot efficiency:

$$\eta = 1 - \frac{T_L}{T_H}$$

Equation 6-5

In Equation 6-5, T_L is the heat sink temperature and T_H is the receiver temperature. In reality, typical engines reach up to 50-70% of the Carnot efficiency because of various losses that are unavoidable, like heat losses.

6.4.4 Wet/dry cooling

The majority of CSP plants (parabolic trough, linear Fresnel, power tower) use the steam Rankine thermal power cycle. This process consists of pressurized water that is boiled, whether directly from solar heat or through a heat transfer fluid and the steam that is generated is used to drive a steam engine to produce electricity. After completion of the cycle, it starts again with the steam being condensed and the water being re-pressurized. The steam is usually condensed with the use of external cooling water and an evaporative cooling tower. Wet cooling (Figure 6-28) is the method most commonly used in CSP plants because it is the most efficient and with the lowest cost. Concerns regarding this cooling method include the water supply in arid and semi-arid regions, where most CSP plants are installed and the fact that it can consume more water per unit of produced electricity than conventional fossil fuel plants that also incorporate wet cooling.

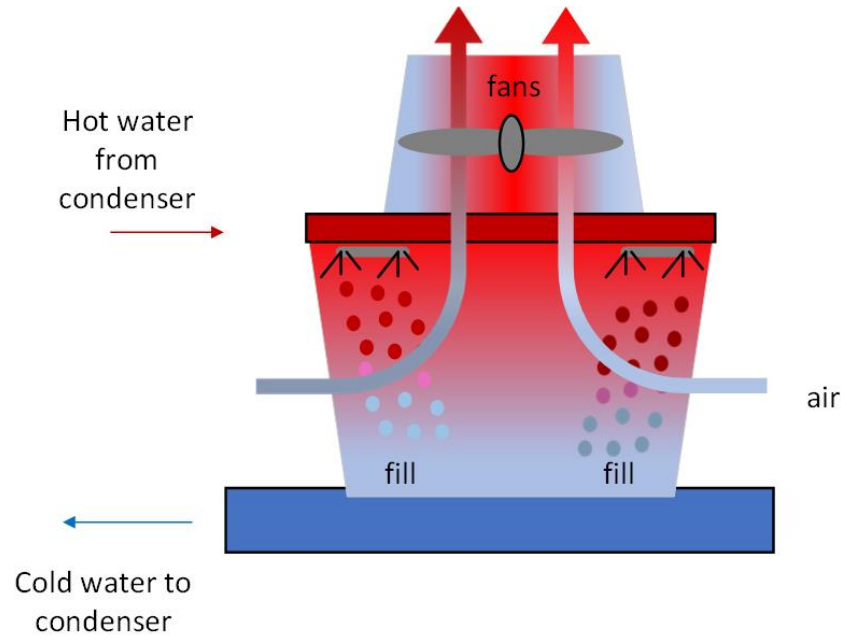

Figure 6-28: Wet cooling system. [154]

The dry cooling method can eliminate 90% of the water requirement. In this process, the heat from the condenser is rejected by means of fans and ambient air (Figure 6-29). In order for the heat exchange to be adequate there should be a large enough difference in temperature between the outside air and the exhaust steam, that's why this method doesn't perform so well on hot days of the summer. The disadvantages of dry cooling systems are the higher costs, compared to wet cooling and the overall lower performance of the CSP system. However they reduce significantly the water consumption.

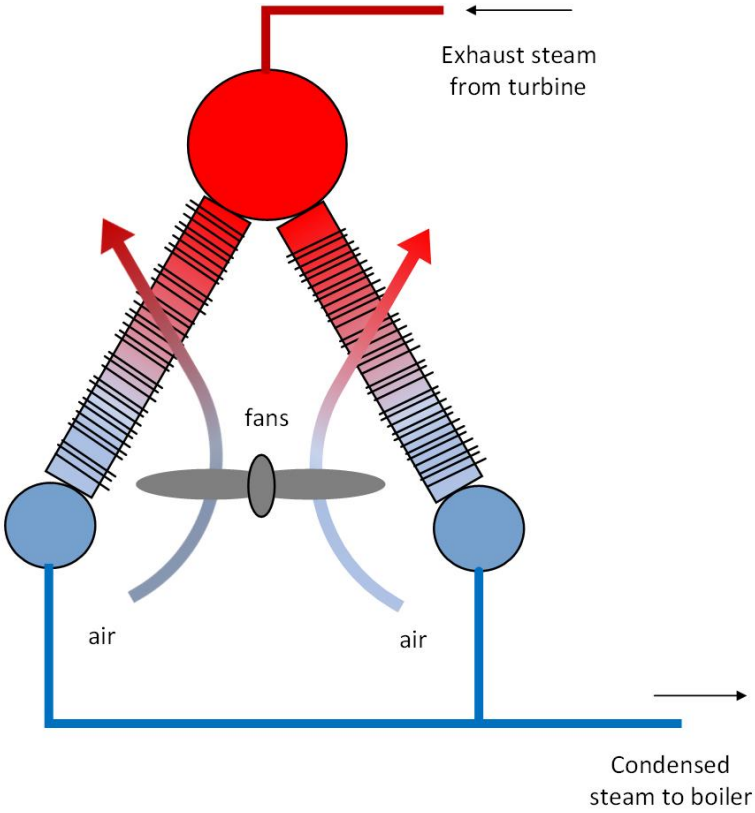

Figure 6-29: Dry cooling system. [154]

Another method is the hybrid wet-dry cooling system which allows maintaining a system performance close to that achieved when wet cooling is used and decrease the water consumption at the same time. The system incorporates both wet and dry cooling systems, which can be used in parallel or the operation can be switched from one system to the other, depending on the conditions and the system that they favour. The costs are potentially lower than dry cooling but it's a system with more complexity.

6.5 Hybridization

While photovoltaics (PV) represent the largest solar power systems capacity in the world, CSP technologies exploit solar energy's thermal capacity to drive a power cycle, like a steam Rankine cycle. CSP technologies are a promising source that can be integrated into established power production systems. Integration of TES systems in CSP installations is able to address reliability issues that arise, in the power dispatch process, during times of absent solar energy.

TES systems store energy in a thermal state as opposed to batteries that store it in a chemical state and are commonly incorporated in PV systems. TES systems are simpler and have lower costs. Another option in increasing CSP reliability is hybridization, which refers to the coupling of CSP technologies with another energy source to produce power.

6.5.1 PV-CSP hybrid system

There are ongoing efforts to increase CSP efficiencies and decrease the overall costs. Photovoltaic (PV) systems directly convert solar energy into electricity with the use of solar cells. Only the photons that have energies near the band gap of the cell material are converted to power, since the majority of solar irradiance is converted to heat. Another issue of PV systems is the difficulty in large scale electric energy storage.

Based on the above, it can be considered that CSP and PV technologies are complementary to each other. They can be combined in a PV-CSP hybrid power system. One such design is depicted in Figure 6-30. Hybridization can be achieved with various approaches. The PV system can provide power to the CSP plant as a station-service power or they can be combined to provide stable power output for the duration of a whole day. Another option is for the PV system to be operational at high efficiency and the CSP system to operate at the same time with the energy that is not exploited by the PV system. This is achieved with the spectral beam splitting (SBS) technology.

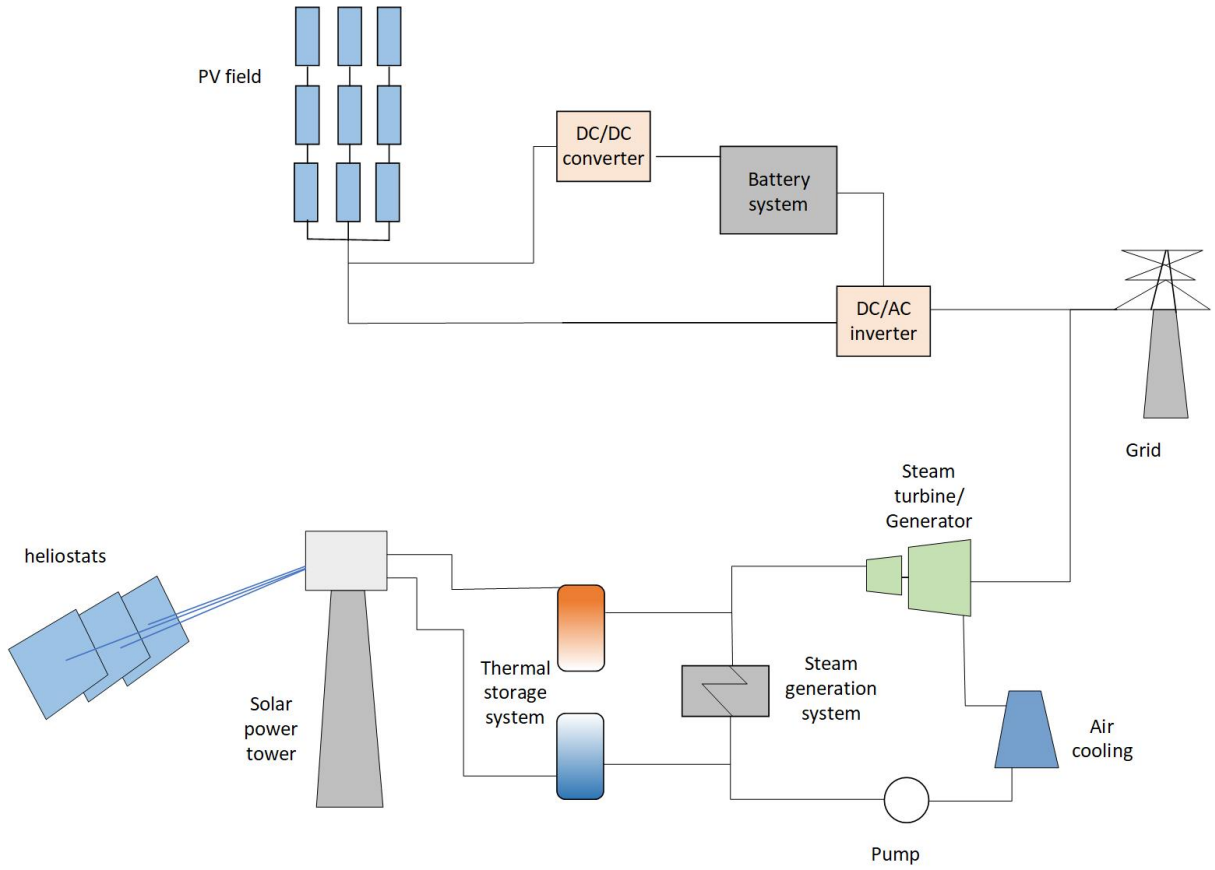

Figure 6-30: Design of a hybrid PV-CSP plant with energy storage. [155]

The hybridization of CSP and PV technologies has gained a lot of attention and is continuously examined for further development. The main advantage of this technology is that the characteristics of the power generated by a CSP system can offer stability to this new hybrid system and the impact of the PV system on the grid can be reduced. Solar energy can be fully exploited, thus increasing the efficiency of the power generating system, while reducing the levelized cost of electricity of the system at the same time. The technology of a PV-CSP hybrid system can be of two types: non-compact, which includes the flat PV-CSP system and the CPV-CSP system and compact, which includes the PV-topping and the SBS technology, as well as their combination.

In non-compact hybrid systems, the PV and the CSP systems operate independently. The system is integrated together by the electric power dispatching system or the control system. The PV system is responsible for part of the station-service power for the CSP system and in this way the electricity cost of the latter can be reduced. This type of hybrid system is

expected to provide a stable power output for grid or off-grid power demands and it can have a high capacity factor which can be over 80%. Several commercial non-compact PV-CSP hybrid systems are under development and construction.

Compact hybrid technology tries to take advantage of the different methods of energy conversion of PV and CSP technologies. With this concept, photons that have lower energies than the band gaps of PV cells are transmitted and converted into heat in the cells substrate. Photons that have energies higher than the band gaps, are partly converted into electricity in the PV process and the rest of the energy is used as heat. Compact hybrid systems take full advantage of the incident solar energy and the overall conversion efficiency is increased. In the compact PV-topping hybrid system, the dissipated heat of the PV cells is used to produce power through the CSP system, thus solar cells are here used as thermal receiver and PV converter at the same time. The PV system is used as the topping cycle and the CSP system as the bottoming cycle. In the SBS hybrid system, the spectral beam of solar radiation is split, so visible light can be converted to electricity in the PV cells and near-infrared/ultra-violet light is converted to heat in the CSP system. A higher conversion efficiency is achieved for the solar cells and the temperature of the CSP system's working fluid is not limited by them. PV-topping and SBS technologies can be combined with the purpose of achieving lower PV temperatures and higher working fluid temperatures. This method is under research and aims at further increasing the overall efficiency of the system.

6.5.2 CSP-fossil fuel hybrid system

CSP technologies can also be coupled with sources such as fossil fuels that can dispatch energy in times of unavailability of solar energy. In that way, a power plant can have consistent operation with improved capacity and increased efficiency.

The most common concept is the integration of solar collectors with the steam cycle of a combined cycle gas turbine (CCGT) plant or a coal plant. The principle in the operation of a CCGT plant is that after the completion of the first engine's cycle, the working fluid/exhaust has high enough temperature to be used in a second heat engine, after passing through a heat exchanger. Depending on the type of solar collector and fossil fuel plant, the integration with the steam cycle can be achieved in various ways. Parabolic troughs that can operate at

around 400 °C, can be used to evaporate steam in Rankine cycle or a CCGT plant. Linear Fresnel reflectors that usually operate below 300 °C, can use concentrated heat to replace the auxiliary steam in feed water preheating in coal plants.

In order to retrofit a fossil fuel plant with solar collectors, the age of the plant needs to be taken into account along with the availability of land and the solar resource of the area. The fossil fuel plant should have many years remaining in its operation, otherwise the procedure of retrofitting solar collectors will not be worth it. Land availability is important since there should be large enough area near the fossil plant, where solar collectors can be installed. Finally the location of the plant should be characterized with high solar resource in order for solar collectors to provide adequate energy. Hybridization of CSP and fossil fuel systems can increase power capacity, decrease costs and reduce the effect of fossil fuel plants on the environment.

7 Wind Energy Fundamentals

Author(s): Dr. Ziyad Al Tarawneh
Dr. Khaled Al Awasa

7.1 Introduction

7.1.1 Wind Power Statistic worldwide

The development of wind generation, which dates back to the beginning of this century, has made energy from renewable resources important in power systems. Figure 7-1 shows the wind power global capacity and annual additions for years 2009-2019. In 2009, the total installed capacity worldwide was 159 GW, and this capacity has been dramatically increasing since then. In 2019, the global market for wind power expanded with approximately 20 % with totally installed capacity 651 GW, with around 60 GW of new capacity added to the world's electric grids. Figure 7-2 depicts the capacity distribution of wind power and additions, for the top 10 countries, where largest percentage being installed in China followed by United States and among the EUs, Germany has the largest share.

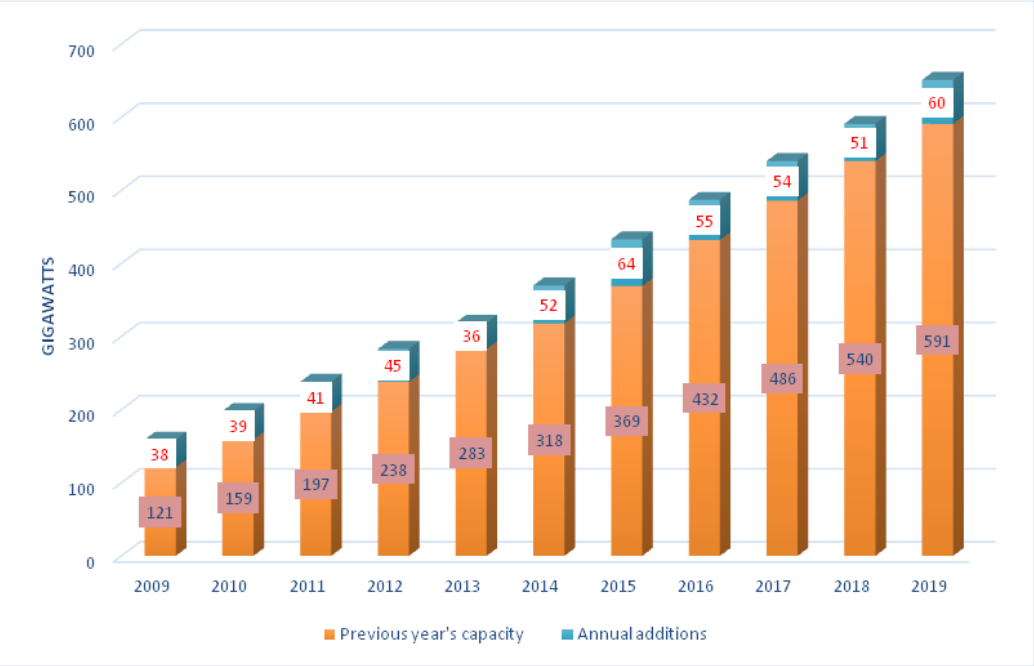

Figure 7-1: Wind power global capacity and annual additions, 2009-2019 [156].

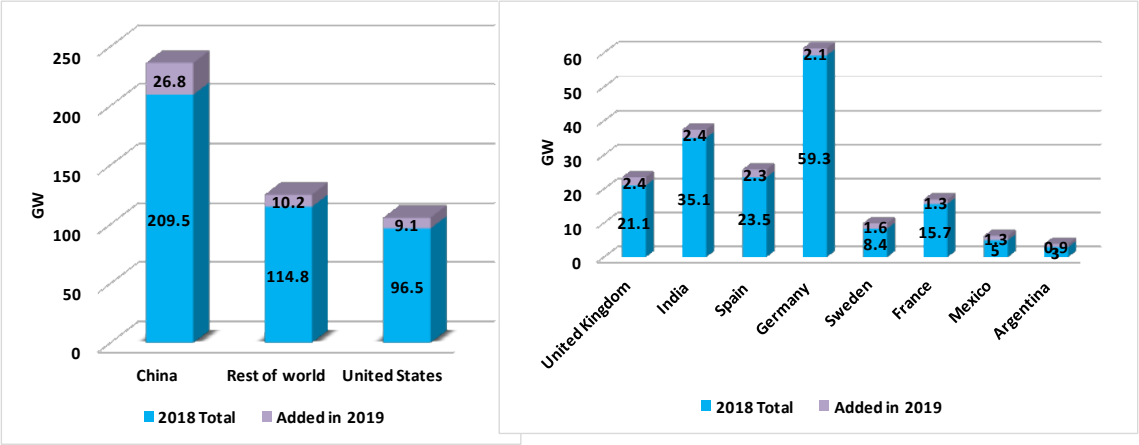

Figure 7-2: Wind power capacity and additions, Top 10 Countries, 2019 [156].

7.1.2 Wind Power in Jordan

Jordan is one of the leading countries in the region in integrating RESs. Since 2010, renewable energy regulations have in been place in Jordan. According to Jordanian's renewable electricity road map 2019, the Jordanian government has a target of installing 1600 MW of RES (wind and PVs) in the national grid, which represents around 20% of the installed capacity, and to reach 30% of the installed capacity by the year 2022 [157], [158].

Figure 7-3 below shows the map of the average wind speed in Jordan at 50 m height. As indicated in figure several areas in the east and west regions have fresh to strong winds with an average wind speed of about 8.0-10.0 m /s.

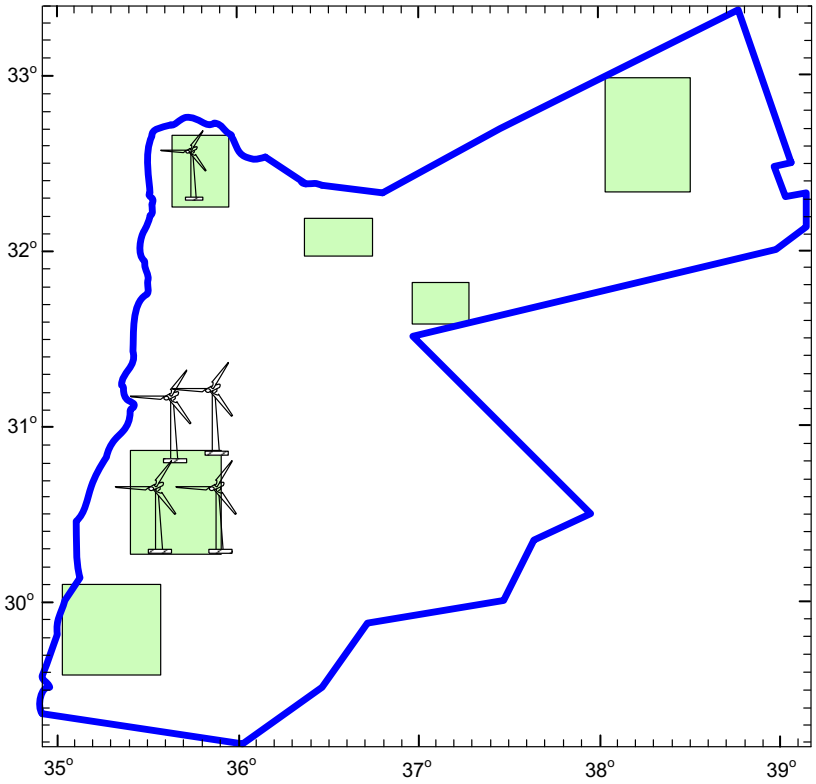

Figure 7-3: Wind map of Jordan and promising Locations [159].

7.1.3 Wind Turbine Types and Classifications

According to axis of rotation, wind turbines can be classified into two types: Horizontal axis wind turbine (HAWT) and Vertical axis wind turbine (VAWT). Figure 7-4 shows these types. Figure 7-5 shows the Wind Turbine mechanical structure and components for HAWT. The general mechanical components for are: Foundation, Tower, Nacelle, and Hub & Rotor.

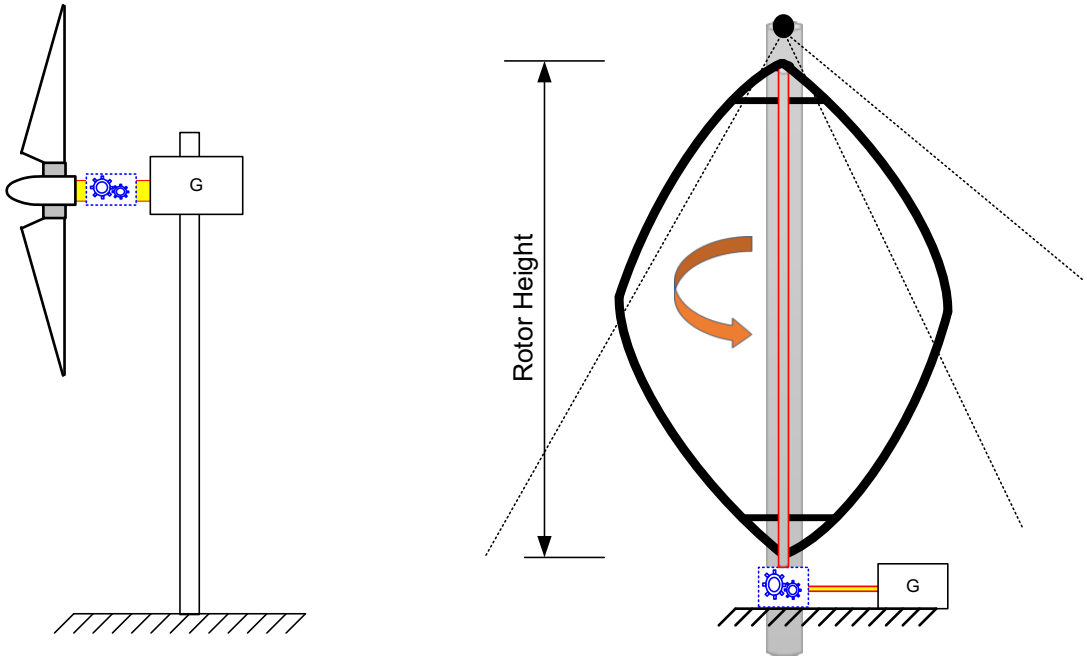

Figure 7-4: Horizontal axis wind turbine (HAWT) and Vertical axis wind turbine (VAWT) [160]

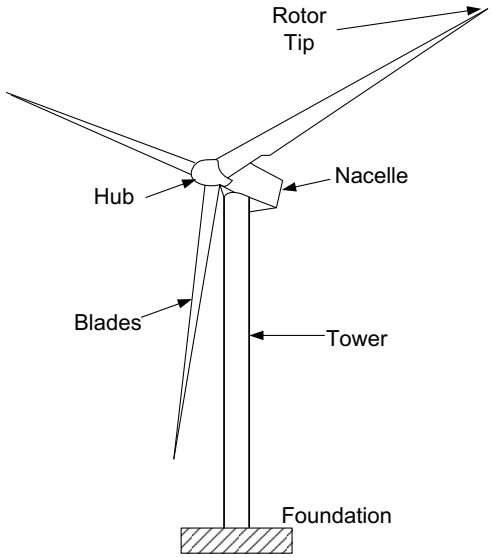

Figure 7-5: Wind Turbine mechanical structure for HAWT.

As wind energy consumption has increased, wind turbine concepts and generator types have been developed and improved. Various wind turbines (WTs) and generator systems have been built for the market. Figure 7-6 depicts the available wind generation configurations in the current market. These types are known in the literature as, Types A, B, C, and D. Type A is

a fixed speed wind turbine using a squirrel-cage induction generator (SCIG) with capacitor bank for magnetization. This type is manufactured mainly by Vistas. The demand for this type is decreasing, and it is being phased out of the market. Type B is known as a limited variable speed wind turbine; it is based on wound-rotor induction generator (WRIG) with variable resistance connected at the rotor. This type is also rarely used. Types C and D are both categorized as variable speed wind turbines (VSWTs). The former is a double-fed induction generator (DFIG) with a partial power converter and the latter is a full-scale wind turbine (FSWT).

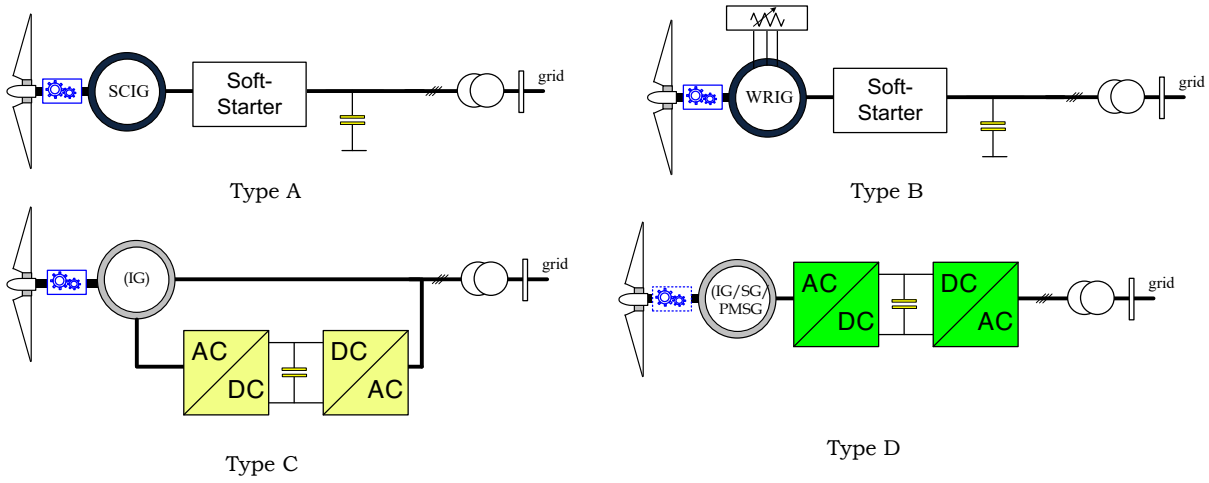

Figure 7-6: Wind turbine types according to generator configurations. [161]

7.1.4 Variable Speed Wind Turbine; Technology and Comparison

Variable-speed wind turbines have attained popularity in the last decade and are quickly becoming the most common type of wind turbine (accounting for 90 percent of available WTs). Variable-speed wind turbines are implemented to produce highest efficiency by capturing the most power possible from the available wind even through wind speed variations. Variable speed wind turbines need power electronics (a converter) able to manage the rotor speed (to accomplish MPPT) and to synchronise the generator frequency and voltage with the network. The two main topologies of variable speed are variable speed with a partial power converter (well-known as DFIG or Type C) and variable speed with a full scale power converter (FSWT or Type D).

The doubly fed induction generator is a multiphase wound rotor induction machine. The stator is connected to the network directly, and the rotor windings are connected to the grid via a back-to-back IGBT-based voltage source converter. The power converter handles only approximately 30 % of the generated power passing to/from the system. The typical operational speed range is around ± 30 % of the synchronous speed. The second topology is the FSWT, which employs induction or synchronous generator. This concept is completely independent of the grid. The size of the converter is larger than that of DFIG because the entire generated power is required to be transmitted through the converter. Commercially, the DFIG is the dominant wind turbine and accounts for about 70 % of the turbines installed in 2010. The size of the converter makes this type more attractive in terms of the cost. Because of the low rating of the converter, the converter cost and the converter losses can be reduced. Nevertheless, full-scale converters (with different topologies) are increasingly being used because of their better performance and capability in terms of the grid and its requirements. The current trend is to use wind turbines that are based on full scale power converter (FSWTs) due to their elevated capabilities and comparative advantages above doubly-fed induction generators (DFIGs). In comparison to partial scale power converters, full scale power converters can provide a smooth grid link over the entire speed range and reactive power support even when there is no wind (i.e. STATCOM operation). With this topology, the FSWT, the turbine and the generator dynamics are decupled from the grid, leading to better fault-ride through (FRT) capability. The features of the converter controllability provide a better turbine performance for the grid requirements in terms of voltage and frequency control.

Technically, DFIG topology requires a gearbox and slip rings, which might be a source of failure, reliability reduction, and high maintenance requirements, especially at high power ratings. Moreover, the DFIG is very sensitive to grid disturbance which needs high FRT requirements which increases the control complexity. Because of the torsional feature of the drive train, the output power of the DFIG has been reported to be vulnerable to oscillation, which could result in power system instability. Main wind turbine manufacturers (such as Vistas, GE, and Siemens) are beginning to produce full scale wind turbines (Type D) in response to the stated drawbacks of DFIGs. Although the converter is large in this topology, moreover, the cost of the converter has considerably decreased throughout the last ten years.

The number of stages in the gearbox can be decreased or removed entirely with this type, which is a desirable feature. This advantage benefits the turbine's maintenance and longevity and has added to its popularity. At the end of 2010, FSWTs accounted for approximately 28% of the world's wind turbines. Currently, different ratings are available in the market; for example, 1.2, 2.5, 3, 4, 5 MW are being used. Recently Enercon launched a 7.5 MW. Figure 7-7 summarizes the available topologies of full-scale wind turbines.

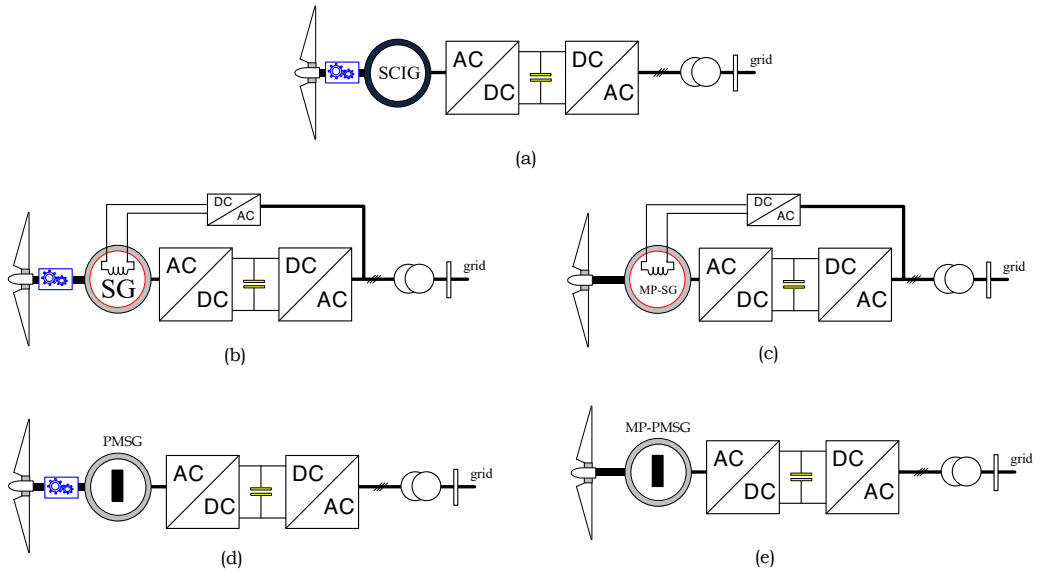

Figure 7-7: Available configurations of full-scale variable speed wind turbine: (a) full scale with a squirrel cage induction generator, (b) full scale with a synchronous generator, (c) full scale with a multi-pole synchronous generator,(d) full scale with permanent magnet synchronous generator and (e)full scale with a multi-pole permanent magnet synchronous generator. [161]

Recently, the utilisation of permanent magnets synchronous generators (PMSGs) has been increasing as the cost of PM materials has decreased, and the performance of PMs has been improved. Furthermore, a permanent magnet synchronous generator does not need separate rotor excitation since the excitation is provided by the permanent magnets, resulting in a high power factor and efficient operation. This feature significantly decreases excitation losses while increasing torque density. The generator requires less maintenance and less downtime than other generators because of the elimination of the rotor slip rings. These advantages make PM more attractive for wind turbine applications and very beneficial for offshore wind

applications. This high degree of growth, performance enhancement, and lower costs in both PMs and power electronics has resulted in a promising future for the adoption of a new turbine concept: direct-drive wind turbine concept with PMSG. Simplified linkage between the generator and the turbine would accelerate the growth of wind-power generation by discarding the gearbox (the direct drive). In this concept many advantages can be achieved: a simplistic drive train, better overall performance, and better reliability and availability, resulting in lower periodic maintenance. However, direct drive generators have the following disadvantages: huge weight and large diameters. This concept was used in 18% of installed turbines in 2010; the three major vendors are Enercon, Goldwin, and Hara XEMC. Two wind turbines based on direct-drive concepts were released in 2012. (Vistas 7.0 MVA with PMSG and Enercon 7.5 MW with EESG). In variable-speed high-power direct-drive wind turbines, low-speed high-torque permanent-magnet synchronous generators (PMSGs) are the preferred option. The world's largest turbine to date, GE's 12 MW, began producing electricity in November, with serial production set to begin in 2021. At 107 meters in length, the turbine blades are the longest ever built.

7.1.5 Wind Origin

As Figure 7-8 shows, the actual primary energy sources of the renewable energies are the movements of the planets, the heat of the Earth and solar radiation. In Fact, solar radiation is the basis for a surprising range of energies. In particular, atmospheric movement originates mostly due to solar radiation, which is the basis for the use of wind power, as illustrated in Figure 7-9.

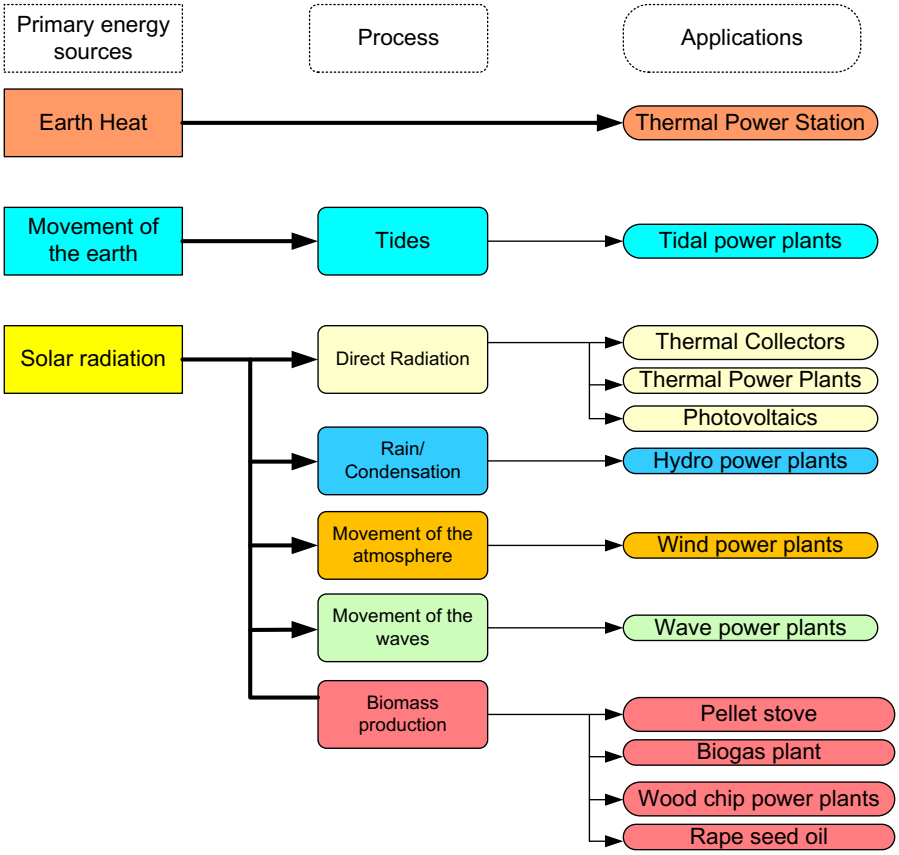

Figure 7-8: Primary energy sources and wind origin. [162]

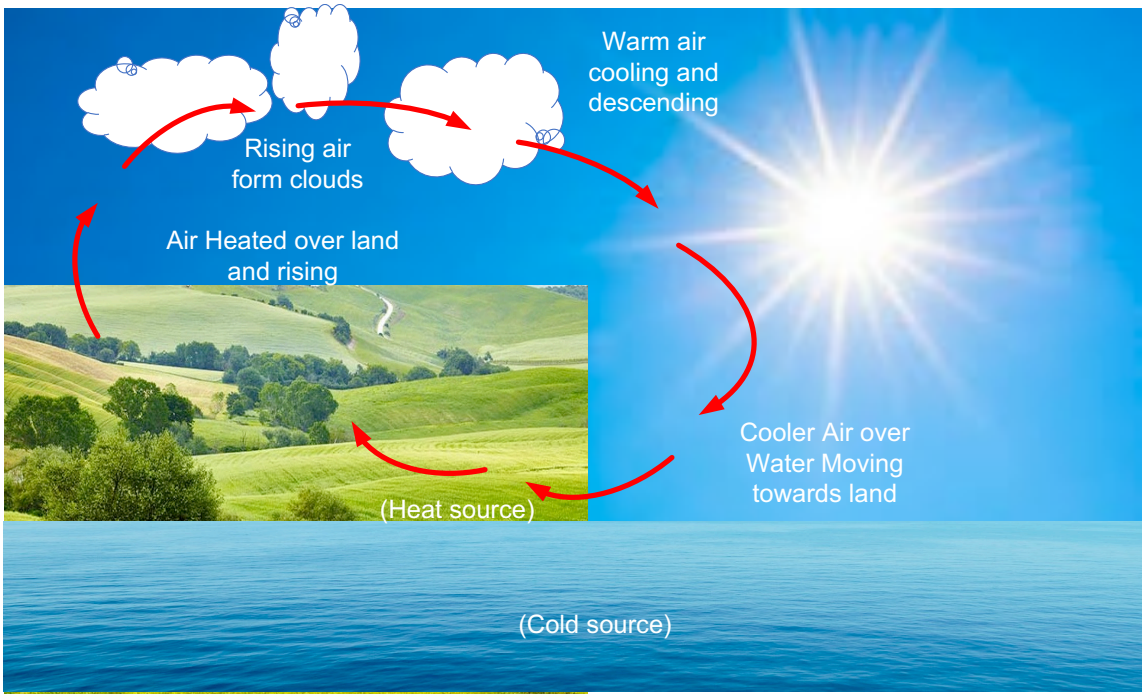

Figure 7-9: Wind power generation [162]

7.2 Aerodynamics of Wind Turbines

7.2.1 Wind's Kinetic Energy

Wind turbines are designed to absorb the kinetic energy of the wind and transform it to electrical energy. Newton's second law states that the kinetic energy of a packet of air of mass m travelling at a speed of v.

$$K.E. = \frac{1}{2} mv^2$$ *Equation 7-1*

Where K.E. denotes the kinetic energy of the air packet (Ws), m denotes the mass of the air (kg), and v denotes the wind velocity (m/s).

Figure 7-10: The kinetic energy of a packet of air with a mass of m moving at a speed of v. [160]

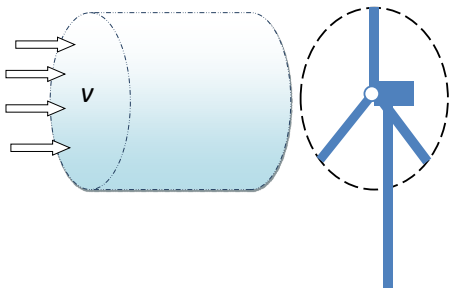

The mass of air flowing through a given region (A) is measured as the product of the area (A), wind speed (v), air density (ρ), and time (t):

$$m = A.\rho.v.t$$ *Equation 7-2*

The wind power (P_{wind}) *in watt can be expressed as*

$$P_{wind} = \frac{K.E}{t} = \frac{1}{2} A.\rho.v^3$$ *Equation 7-3*

The specific power or power density which represents the wind power per square meter of cross sectional area (A).

$$p = \frac{P_{wind}}{A} = \frac{1}{2}\,\rho . v^3 \qquad \textit{Equation 7-4}$$

Wind power density is mostly used to investigate the feasibility of power generation sites. For dry, thin air of 1 kg/m^3, the wind power density is approximately 3.0 kW /m^2 when the speed of wind is 18 m/s. This is an enormous amount of energy for moderate wind speeds; for storm, at 35 m/s, the wind power density is about 21.5kW/m^2 and can be destructive [160]. **Error! Reference source not found.** shows a map of the average wind speed in Jordan at 50 m height. Several areas in the east and west regions have fresh to strong winds with an average wind speed of about 8.0- 10.0m/s. These locations have an average annual power density of approximately 500W/m^2.

7.2.1.1 Air Density (ρ)

Several factors affecting the Air density, and hence power in the wind, such as atmospheric pressure, temperature, humidity, elevation and gravitational acceleration. As evident from the following equation:

$$\rho = \frac{P_r}{\mu \mathrm{T}} e^{\left(-\frac{gh}{\mu \mathrm{T}}\right)} \qquad \textit{Equation 7-5}$$

where P_r is the normal ambient pressure at sea level, T is the air temperature (Kelvin), μ is the specific gas constant (Ws/ (kg Kelvin)), it equals 287 for air, g is the gravitational acceleration,

h is the height above the sea level (m) and ρ is air density (kg/m^3). It can be noticed that the air density increases when the temperature drops. Also, air at higher altitudes the air density reduces. This equation can be represented as (by substituting the previous values)

$$\rho = \frac{353}{\mathrm{T} + 273} e^{\left(-\frac{h}{29.3\ (\mathrm{T}+273)}\right)} \qquad \textit{Equation 7-6}$$

Note: the temperature (T) in the above equation is in Celsius (°C)

Problem 7-1

If Al karak city is 900 meters above the sea level and its average wind speed is about 13 meters per second at 50 meters above ground level. The city's average temperature is 17°C. Determine the wind power density based on these average values.

Solution

The power density is given by:

$$\text{Power density} = \frac{1}{2}\,\rho . v^3$$

The air density, then need to be calculated by:

$$\rho = \frac{353}{\mathrm{T} + 273} e^{\left(-\frac{h}{29.3\ (\mathrm{T}+273)}\right)} = 1.089\ kg/m^3$$

$$\rho = \frac{353}{17 + 273} e^{\left(-\frac{950}{29.3\ (17+273)}\right)} = 1.089\ kg/m^3$$

The power density is obtained as:

$$\text{Power density} = \frac{1}{2}\ 1.089 . 13^3 = 1.196\ kW/m^2$$

Problem 7-2

Determine the wind power density when the wind speed of 12 m/s and air temperature reaches to 30°C. if the area is 350 m above sea level.

Solution

$$\rho = \frac{353}{30 + 273} e^{\left(-\frac{350}{29.3\ (30+273)}\right)} = 1.12\ kg/m^3$$

$$\text{Power density} = \frac{1}{2}\,\rho.v^3 = \frac{1}{2}\,1.12.12^3 = 0.9677\ kW/m^2$$

Problem 7-3

Considering the previous example (*Problem *7-1), compute the wind power passing through a sweep area of 30 m blade.

Solution

The area of the sweep area of wind turbine can be determined as:

$$A = \pi r^2 = \pi\,(30)^2 = 2827.43\ m^2$$

Then, the power of wind in the specific sweep area is given as

$$P_{wind} = \ Area.Power\ density = 1196\ \text{x}2827.43 = 3.381\ MW$$

7.2.1.2 Tower Design

One of main aspect of wind plant design is the tower design. Several factors contribute to design criteria such as cost, safety, aesthetics, or a combination of all these factors. The installed capacity of the towers and their height has to be between the tower energy production and the maintenance cost of the tower. From the overall project investment, the approximate 15-20% is accounted for the tower cost steel is the fundamental materials that being used in wind turbines fabrication. In recent years, concrete towers have been used and promoted, however, due to some circumstances and applications where production costs are competitive, their use is limited. Several steel tower designs are used such as steel tubular tower, lattice tower, hybrid tower, and guyed tower. Figure 7-11 shows the general appearance of these designs.

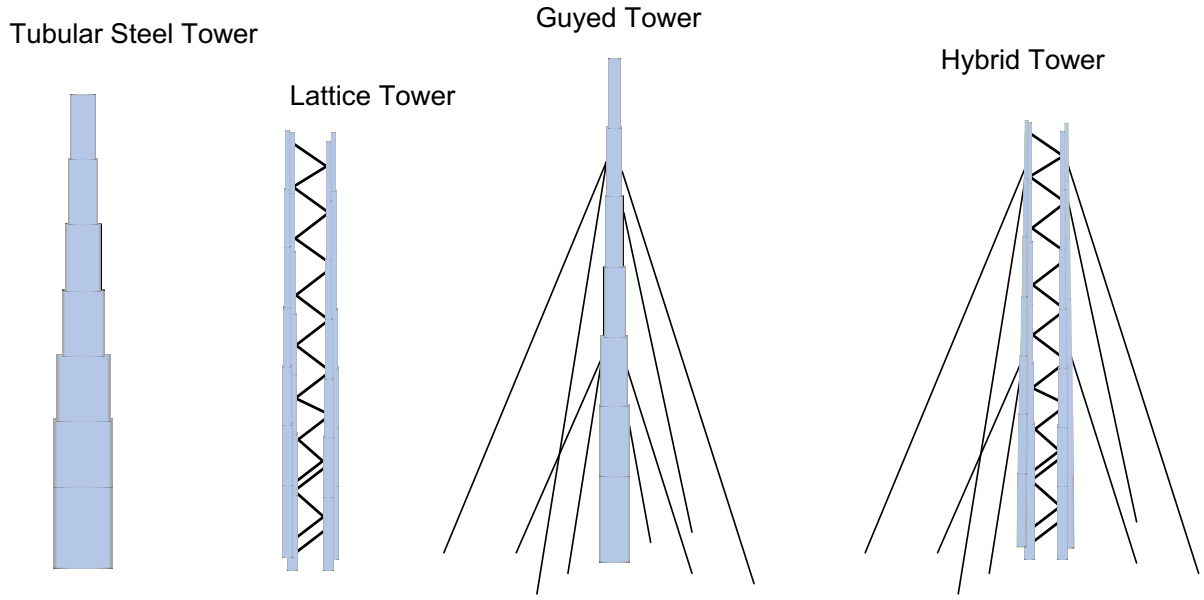

Figure 7-11: Wind tower designs [163]

The tower structure and all of its elements must endure substantial load forces induced by rotational torque, wind thrust, and gravitational loads. Such loads may have various profiles, such as static, quasi-static cyclic, dynamic cyclic or stochastic turbulence dependent loads.
One of common terminology in wind power is wind shear which relates the variation in wind speed with height. This factor has a major influence in tower cost design. With high wind shear, i.e., a taller tower, Wind speed increases dramatically with height, resulting in a more energy-efficient but more expensive tower. Taller towers are often necessary to handle larger diameter rotors. Recently, the largest wind turbine is released by GE with 14 MW with rotor diameter and height, 220 m and 260 m respectively [164] .

7.2.1.3 Impact of Friction and Height on Wind Speed

Considering that wind power is directly proportionate with the cube of the wind speed, even small wind speed changes can have a major economic effect. One possible solution is to install the wind turbine into a higher tower. However, wind speed at the first few hundred meters above the ground is significantly influenced by the friction that the air encounters when it travels over the surface of the earth. Smooth surfaces, such as the lakes, offer very little resistance, and the speed variation with elevation is modest. On the other end, the surface winds are considerably hampered by strong disturbances, such as trees and houses. This

means area topography as well as several meteorological parameters are highly needed to be considered when designing wind farms [165, 166]. An estimate for characterizing the influence of roughness of the earth's surface and height on wind speed is given as follows

$$\frac{v}{v_0} = \left(\frac{H}{H_0}\right)^{\alpha} \qquad \textit{Equation 7-7}$$

Where α is a coefficient of friction, *v* donates the wind speed at height of H and v_o is the wind speed at height of H_o.

It is worth noticing that α is function of terrain and topology of the area; typical values are α= 0.143 for an open terrain; α = 0.4 for a large city; and α = 0.1 for calm water.

Problem 7-4

Compute the wind power density at 50 m in an open terrain if the wind power density at 100 m is 2.5 kW/m² when wind speed is 10 m/s.

Solution

For an open terrain, α = 0.143

$$\frac{\text{Wind power density}}{\text{Wind power density}_0} = \frac{\text{P}_{wind}}{\text{P}_{wind\_0}} = \left(\frac{v}{v_0}\right)^3 = \left(\frac{H}{H_0}\right)^{3\alpha}$$

$$\text{Wind power density} = \text{Wind power density}_0 . \left(\frac{H}{H_0}\right)^{3\alpha} = 2.5\text{x}\left(\frac{50}{100}\right)^{3\text{x}.0.143}$$

$$= 1.86 kW/m^2$$

$$\text{Wind power density} = 2.5 . \left(\frac{50}{100}\right)^{3\text{x}.0.143} = 1.86 kW/m^2$$

Problem 7-5

A wind turbine with a 30 meter rotor diameter and a friction coefficient of 0.2 is installed with its hub 50 meter above the ground surface. Calculate the ratio of specific power in the wind at the peak point reached by a rotor blade tip to the lowest point reached by it.

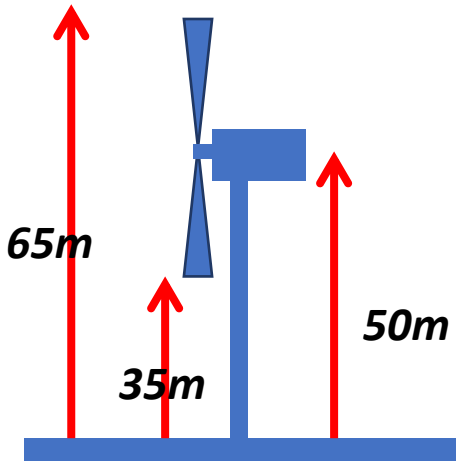

Figure 7-12: Example 7-5

Solution

The power ratio at the height of the blade's swing (65 m) to the power ratio at the bottom of the blade's swing (35m) would be

$$\frac{P_{wind}}{P_{wind0}} = \left(\frac{H}{H_0}\right)^{3\,\alpha} = \left(\frac{65}{35}\right)^{3x\ 0.2} = 1.45$$

Wind power is 45 percent greater at the highest tip of the blade than it is at the lowest position.

7.2.2 Wind Turbine Blades

Figure 7-13 shows a cross sectional view wind turbine blade, known as “airfoil”. The blade consists of two upper and lower cambers. The upper side is longer than the lower one, with a leading edge that faces the wind and a trailing edge that faces away from it.

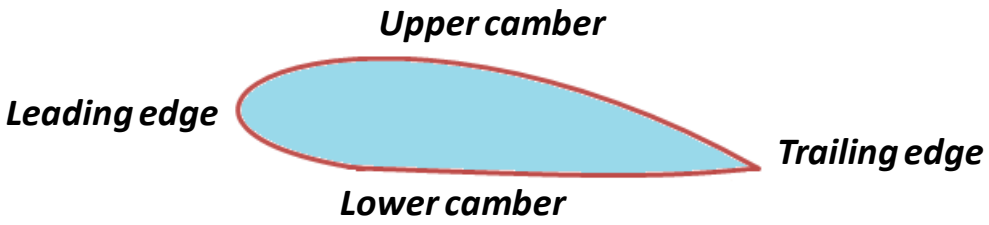

Figure 7-13: a cross sectional view wind turbine blade [160]

According to the airlift principle known as "Bernoulli's Principle", wind air above the top side of the airfoil travels more distance until it reunites with the air under the airfoil that travels a shorter distance. As a result, a lower air pressure will be developed on top of the airfoil creating a lifting force which ultimately rotates the wind turbine blade in a circular motion.

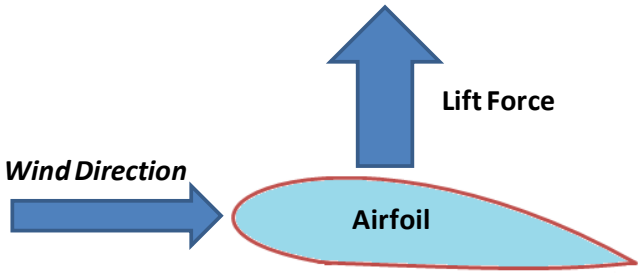

Figure 7-14: The lift force due to the pressure difference (airlift principle). [160]

Mathematically speaking, the net pressure of the lift can be expressed as

$$P_{net} = P_{r2} - P_{r1}$$ *Equation 7-8*

And the aerodynamic force *F caused by t*he net pressure causes

$$F = P_{net}A$$ *Equation 7-9*

Where P_{net} *denotes the net pressure exerted on an object, F denotes the aerodynamic force created by the net pressure and A denotes the surface area.*

7.2.2.1 Angle of Attack

One possible approach to control the aerodynamic force of the blade is by using the angle of attack (α) which is the angle between the wind direction and the cord line of the airfoil (blade).

- If the angle of attack α=0, the aerodynamic force will be lift force.

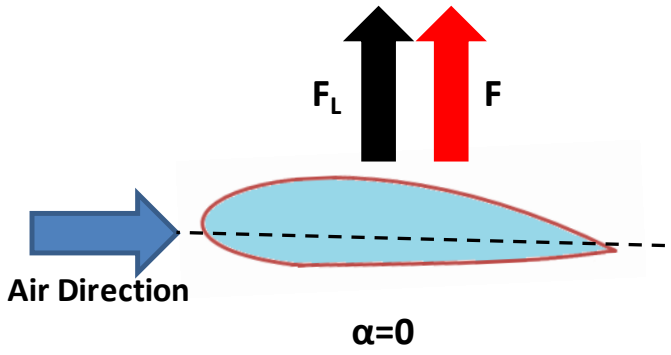

Figure 7-15: The aerodynamic forces at α=0 [160]

- If the angle of attack α>0, the aerodynamic force at the centre of gravity is divided into two components. The "lift force," F_L, is a component that is perpendicular to the relative wind speed in front of the blade. The component in the direction to relative wind speed is known as "drag force," or F_D.

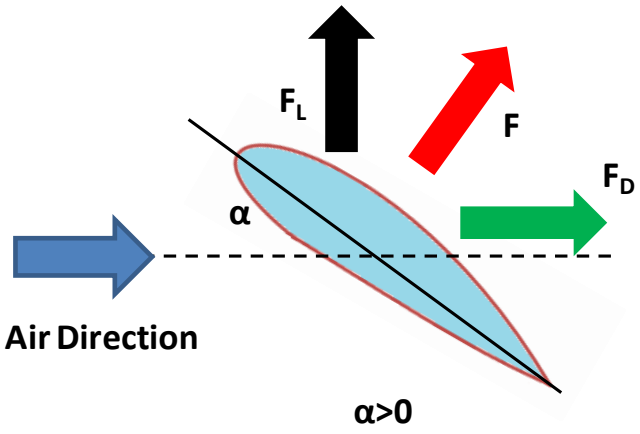

Figure 7-16: The aerodynamic forces at α>0 [160]

The lift coefficient C_L and the drag coefficient C_D are defined as

$$C_L = \frac{F_L}{F}$$ *Equation 7-10*

$$C_D = \frac{F_D}{F}$$ *Equation 7-11*

Both C_L and C_D are function of the blade design (shape) and its angle of attack (α). To absorb more energy from the wind, we need to raise C_L and reduce C_D.

- If the angle of attack α<0, the lift force (F_L) is reversed while the direction of the drag force (F_D) is maintained.

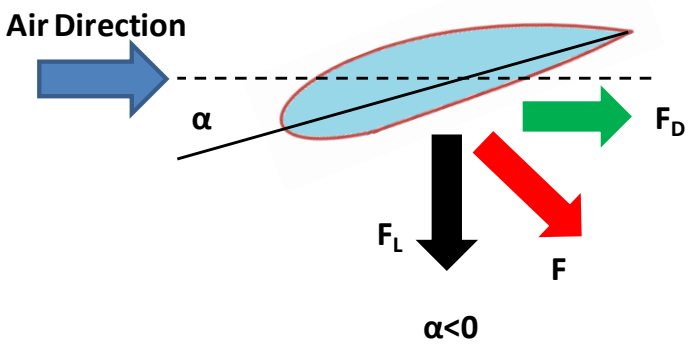

Figure 7-17: The aerodynamic forces at α<0 [160]

- If the angle of attack $\alpha = \alpha_o$, F_L is equal to zero and the entire aerodynamic force is F_D.

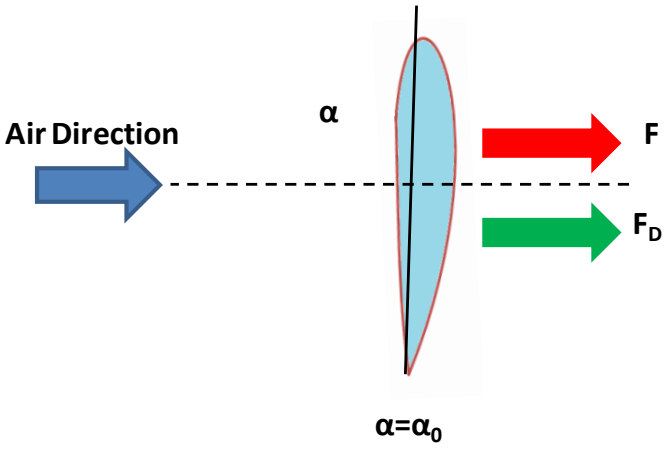

Figure 7-18: The aerodynamic forces at α= αo [160]

Figure 7-19 shows the lift force versus angle of attack (α). For a negative angle α o, the lift force is zero. This is the feathering position of WTs (a position where the lift force is minimized). A greater negative angle will cause the lift force to be reversed. At α = 0, the blade provides some lift. The lift increases when the angle of attack increases up to a limit. Beyond the optimum lift level, raising α decreases lift whilst increasing drag. Bear in mind that raising the angle of attack raises air turbulence away from the wind turbine. When the air is unstable,

the lift force is greatly decreased. As a consequence, WT downstream of the turbine containing turbulent air gathers less wind energy.

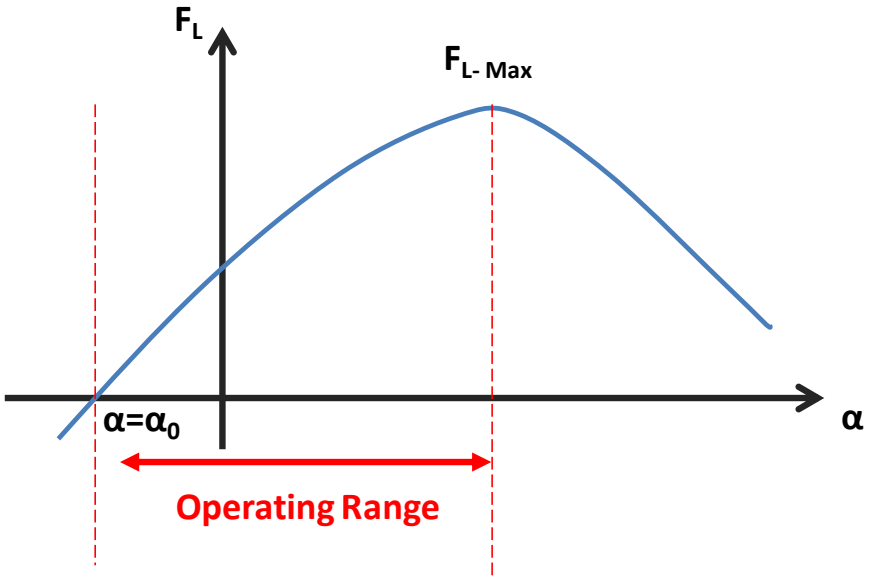

Figure 7-19: The lift force (FL) versus α. [160]

In extreme weather conditions such as storms, the blades of wind turbine are feathered to oblation a zero lift force. This usually is done with a negative α. In particular, when α is changed from positive to negative hence the lift force goes to zero before it reverses.

Problem 7-6

A wind turbine with three-blades is operating at a given α and the aerodynamic force applied by wind on each blade is 2000 N and C_L is 0.95 at the given α. If the distance from the centre of gravity of the blade and the hub is 30 meters.

- ***Calculate the torque produced by the turbine***
- ***Calculate the mechanical power produced by the blades if they rotate at 30r/min.***

Solution

The lift force of a single blade can be computed as

$$F_L = C_L F = 0.95 \text{ x } 2000 = 1.9 \text{ kN}$$

The total torque of three blades is

$$T = 3F_L r = 3x\ 1.9x\ 30 = 171\ \text{kN.m}$$

Where r is the distance from the hub to the centre of gravity of the blade

The total generated power is

$$P = T\omega = 171\left(\frac{2\pi.S}{60}\right) = 171\left(\frac{2\pi x30}{60}\right) = 537.2\ \text{kW}$$

Where ω and S are the angular and the rotation speed of the blades

7.2.2.2 Pitch Angle

The pitch angle (β) is angle is the angle formed by the blade's cord line and the vertical line showing the center of gravity's linear motion. It is obvious that raising the pitch angle decreases the angle of attack and vice versa. This is the primary technique used in advanced wind energy systems to adjust the lift and drag levels in order to regulate the strength absorbed from the wind. Each blade's pitching operation is accomplished independently by geared electric motors installed on each blade bearing or it is accomplished by controlling the blades by hydraulically operated leverage mechanisms. [161].

The blades must be positioned at a suitable angle to the wind to achieve the highest amount of lift force (F_L). The angle of the wind ‘seen' by the blade varies with the radius when the tips of the blades move farther than points near the axes. If the angle ‘seen' by the blade is as large as possible without allowing the rotor to stall, the rotor would be most productive. It is enough to rotate the blade to make the angle wide all the way along. The blades of a fast-rotating rotor, such as a two- or three-bladed wind turbine, are set at a slight pitch for the same purpose.

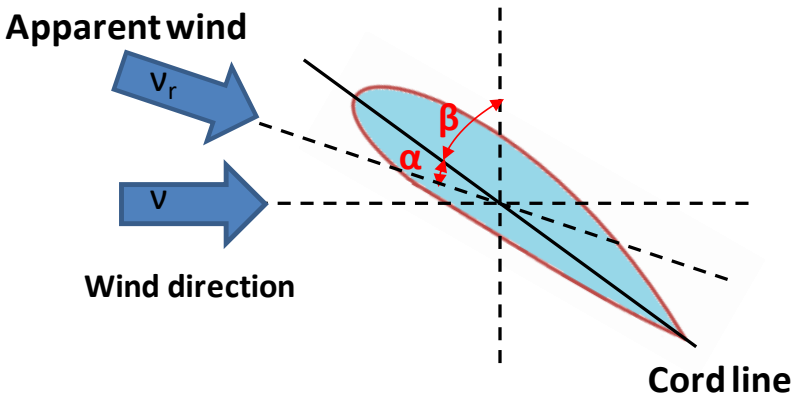

Figure 7-20: The Pitch angle (β) and its relation to angle of attack (α). [160]

Problem 7-7

Compute the angle of attack if the pitch angle is 5°, if the relative winds speed is 49 m/s with an angle of −73.31

Solution

The angle of the apparent wind speed is −73.31°.

$$\alpha + \beta = 90° - 69.02° = 20.98°$$
$$\alpha = 20.98° - 5° = 15.98°$$

7.2.3 Coefficient of Performance

Wind energy is transformed to electrical energy in two stages: first, kinetic energy in the wind is transformed to mechanical energy, which is used to move the shaft of a wind generator. Wind blades are the most important transforming devices at this point. Wind blades must be specifically built to optimize the absorption of wind energy. The power coefficient Cp corresponds with the converting efficiency in the first stage, also called the coefficient of performance of a wind turbine, is determined by the ratio of the wind power collected by the blade of the wind turbine, P_{blade}, over the total power in the wind reaching the sweep area of the blades, P_{wind}, just before it interacted with the blade of the turbine.

$$C_p = \frac{P_{blade}}{P_{wind}}$$ *Equation 7-12*

The coefficient of performance depended on many key parameters such as the wind speed, the revolving speed of the blade, α and β. The coefficient of performance, CP can be represented in terms of wind speed γ, and is given as

$$C_p = \frac{1}{2}(1+\gamma)(1-\gamma^2)$$ *Equation 7-13*

Where γ represents the ratio of the downstream to the far upstream wind speed as shown from Figure 7-21 and defined as

$$\gamma = \frac{\mathrm{v_d}}{\mathrm{v_u}}$$ *Equation 7-14*

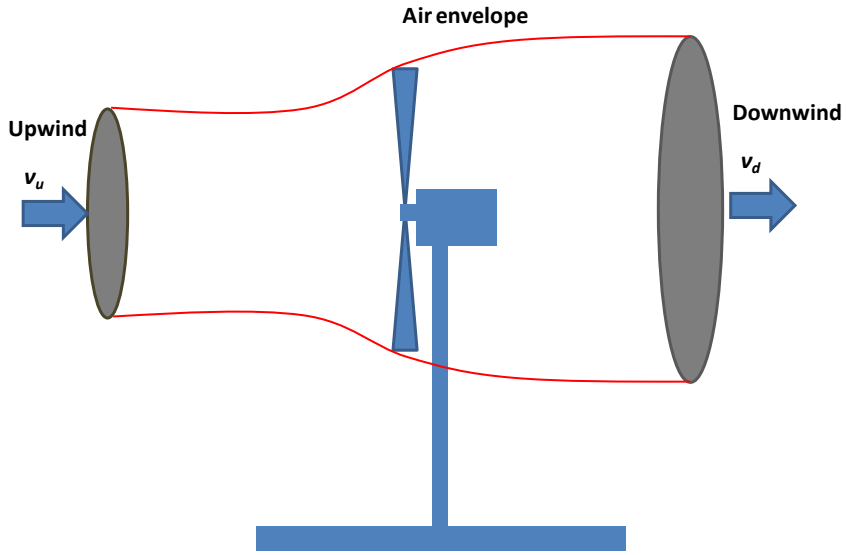

Figure 7-21: The variation of wind speed (the downstream and the upstream) due to the presence of a WT. [160]

To compute the maximum value of C_p, we need to equate the derivative to zero

$$\frac{dC_p}{d\gamma} = 0 \qquad \textit{Equation 7-15}$$

$$\frac{\mathrm{dC_p}}{\mathrm{d}\,\gamma} = \frac{1}{2}.[(1+\gamma)(-2\gamma) + (1+\gamma)(1-\gamma)] = 0$$

$$\frac{\mathrm{dC_p}}{\mathrm{d}\,\gamma} = \frac{1}{2}.(1+\gamma)(1-3\gamma)] = 0$$

The solution is

$$\gamma = 1/3$$

The resulted $\gamma_{\,\mathrm{best}} = 1/3$ and the corresponding Cp-max =0.593 as depicted in Figure 7-22. The maximum Cp is also known as the "Betz Limit," which was theoretically established by Albert Betz in 1920. It indicates that the maximum extracted power that can be produced from wind power is 59.3 percent. That is only when the down-wind speed is one third of the far up-wind speed. In fact, today there is no wind turbine capable of achieving this maximum value due to numerous aerodynamic losses in wind turbine systems. The actual power coefficient Cp is usually between 30 and 45 percent of its theoretical maximum.

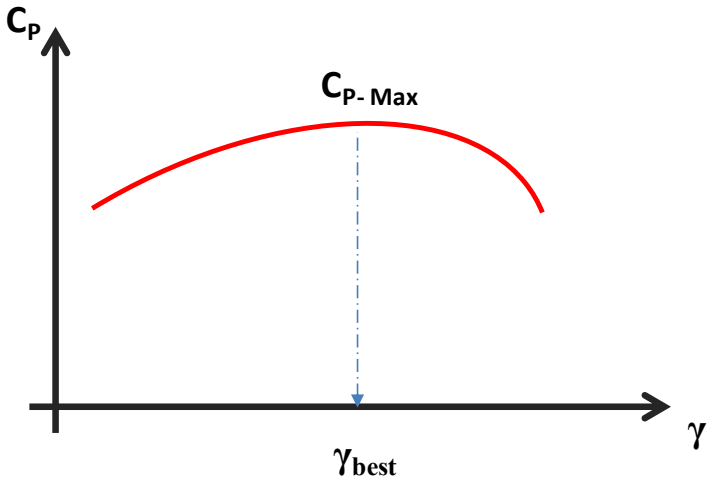

Figure 7-22: Cp as a function of γ . [160]

For a given wind speed, Cp is dependant on the speed at which the blade is rotated. when the wind turbine is turning very slowly, the effectiveness drops as the blades allow too much wind to flow unaffected. when the wind turbine is spinning so fast, the efficiency is decreased as the turbulence generated by one blade gradually influnces the next blade. The common to describe Cp is to represent it as a function of the Tip Speed Ratio (TSR). As will be discussed in the following section.

7.2.3.1 Tip Speed Ratio (TRS)

In wind energy systems, the tip speed ratio (TSR) is a critical parameter. It is characterized as the ratio of the blade tip speed to the incoming wind speed.

$$\mathrm{TSR} = \frac{\upsilon_{\mathrm{tip}}}{\upsilon_{\mathrm{wind}}} \qquad \textit{Equation 7-16}$$

Where tip speed (vtip) denotes the linear velocity of the blade's tip and can be measured as follows:

$$\upsilon_{\mathrm{tip}} = \omega \mathrm{r} = \frac{2\pi \mathrm{nr}}{60} \qquad \textit{Equation 7-17}$$

Where ω denotes the angular speed of the blade (rad/s) , n denotes the number of revolutions of the blade in a minute , r denotes the radius of the turbine rotor (blade lenght) (m)

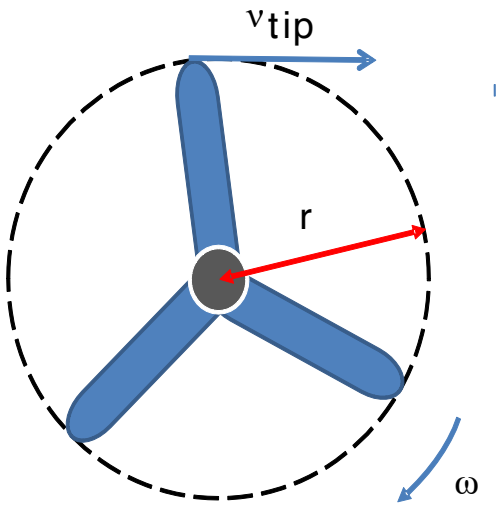

Figure 7-23: representation of the linear velocity of the blade's tip. [160]

Problem 7-8

If the tip of a wind blade is travelling at 45 m/s (161 km/h) and the wind speed is 9 m/s (32 km/h), obtain the tip-speed ratio.

Solution

$$\mathrm{TSR} = \frac{\upsilon_{\mathrm{tip}}}{\upsilon_{\mathrm{wind}}} = \frac{161}{32} = 5$$

This means that the tip of the blade is traveling five times faster than the speed of the wind.

Problem 7-9

Consider a wind turbine with 3 m radius blade is rotating at 30 rpm, and the wind speed is 6 m/s, obtain the tip speed ratio of the blade.

Solution

$$\mathrm{TSR} = \frac{\pi . \frac{6.30}{60}}{6} = 1.6$$

7.2.3.2 Performance Coefficient (Cp)

Figure 7-24 shows the effect of TRS on the output coefficient. This can be shown that it is practically difficult to draw all the energy from the wind without bringing the air behind the turbine to a complete stop (the air will move at no pace across the blades). As a consequence, there is a maximum value of Cp of 59.3%. When the blade set rotates steadily, much of the wind moves through the turbine without it being caught by the blades. When the turbine rapdily rotates , the blades will often pass through used or turbulent winds. That's because the blades will move across a region where the leading blade in front of it just passed through (and used up all the wind in that region).

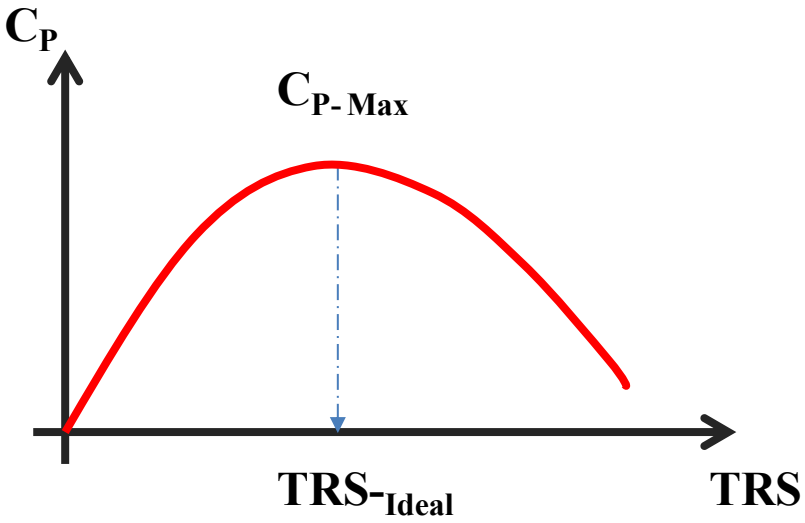

Figure 7-24: Performance Coefficient versus TSR. [160]

Problem 7-10

Consider a wind turbine with *a sweep radius of 5 m and* a *tip speed ratio of 7. Assuming that wind turbine is designed to start producing power when the generator speed is above 905 r/min, which corresponds to a wind speed of 5 m/s. Find the ratio of the gear system.*

Solution

The tip speed can be calculated as

$$\upsilon_{\text{tip}} = \text{TSR}.\,\upsilon_{\text{wind}} = 7\text{x}5 = 35\frac{\text{m}}{\text{s}}$$

The shaft speed at the gearbox side can be determined as

$$\text{n} = \frac{\upsilon_{\text{tip}}}{2\pi.r} = \frac{35}{2\pi.5}x60 = 67\frac{\text{r}}{min}$$

The gear ratio

$$\frac{\text{n}_{\text{gear}}}{\text{n}} = \frac{905}{67} = 13.5$$

Problem 7-11

Calculate the tip speed ration for a 90-meter-diameter turbine rotating at 15 rpm with wind speed of 8 m/s?

Solution

$$\text{r} = \frac{\text{D}}{2} = \frac{90}{2} = 45\ \text{m}$$

$$\omega = \frac{2\pi n}{60} = \frac{2\pi x\ 15}{60} = 1.57\ rad/s$$

$$\text{TSR} = \frac{\upsilon_{\text{tip}}}{\upsilon_{\text{wind}}} = \frac{\omega\text{r}}{\upsilon_{\text{wind}}} = \frac{1.57\ \text{x}\ 45}{8} = 8.8375$$

7.2.4 Tracking the optimal Cp

In advanced wind turbines the maximum coefficient of performance can be tracked by adjusting the speed of the generator (TRS) and the pitch angle (β) of the turbine blades.

7.2.4.1 Tracking optimal Cp by blade speed regulating

The Tip-Speed Ratio (TSR) must be regulated to track the maximum performance coefficient as shown in Figure 7-25. If wind speed varies, the speed of the generator must be adjusted to achieve optimum TSR. This is accomplished by altering the injected voltage to create a temporary change in electrical torque until the required speed is reached.

- For the case that the wind speed is stronger than TSR, the generator speed needs to be increased to track the ideal TRS value.
- For the case that the wind speed is weaker than TSR, The generator speed needs to be reduced to track the ideal TRS value.

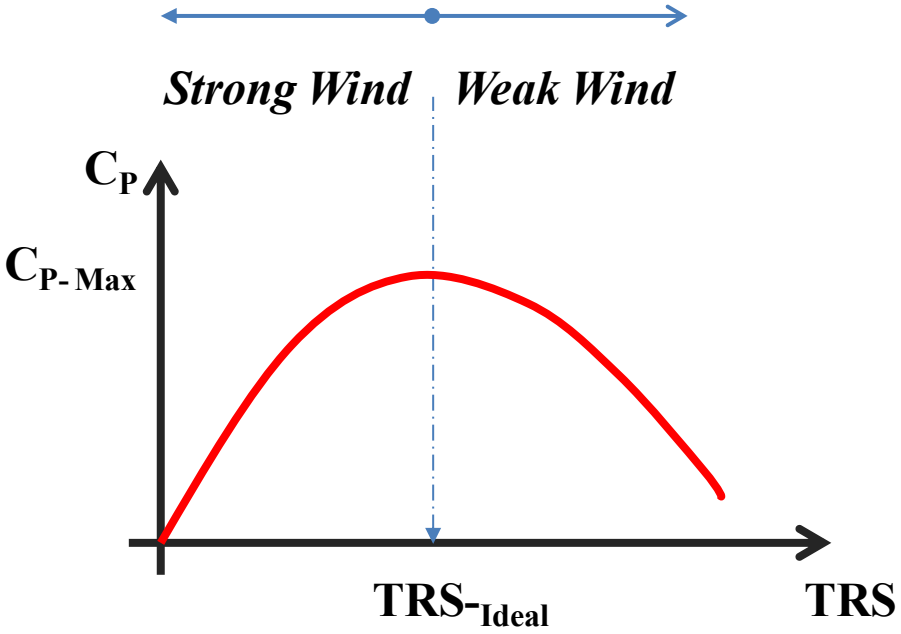

Figure 7-25: Tracking optimal Cp by adjusting the speed of the blade. [160]

7.2.4.2 Track the optimal Cp by changing the pitch angle.

The blade pitch angle of the wind turbine has been implemented in modern wind turbine technology to ensure the effectiveness of wind energy conversion and power generation reliability and also provides as a protection option in the event of higher wind speeds or extreme circumstances. It ensures that even in the case of power failure, the blades can be

directed into their feathered positions by using external backup systems such as the backup batteries, capacitors and mechanical energy storage devices. Figure 7-26 demonstrates the concept of tracking the optimal Cp by adjusting the pitch angle (β). If we assume that the wind speed is decreased and that the operating point is moved from A to B in which the TSR is changed to TSR_B. Consequently, the power coefficient is reduced and hence lesser energy is extracted from the incoming wind. However, if the pitch angle (β) is reduced to β_2 (by increasing the angle of attack), then it's possible to operate with maximum Cp where C point is located.

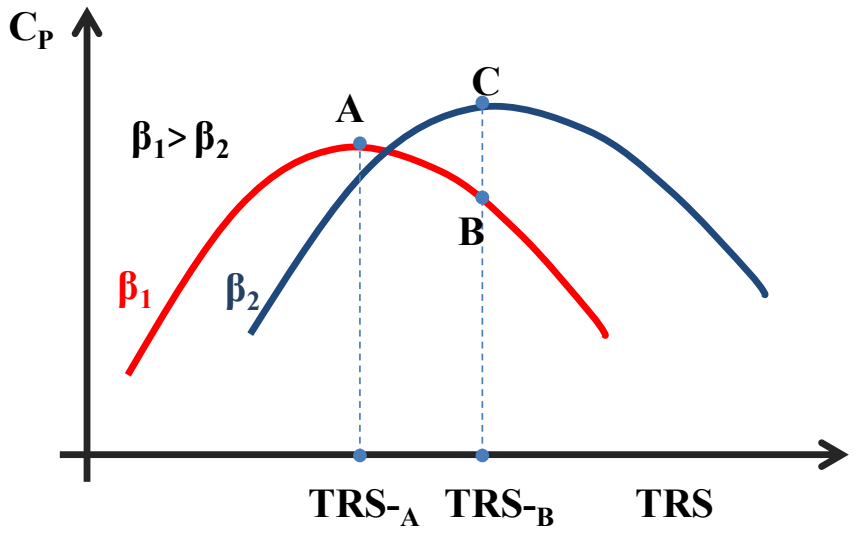

Figure 7-26: Changing the pitch angle to track the optimal Cp. [160]

A wind turbine can extract the highest power from the wind if the turbine is operating at the optimal power coefficient. Figure 7-27 presents the generated mechanical power as a function of the generator speed at different wind speeds. It is clear that over the entire rotor speed range, one speed can generate the maximum power (the circles in the figure show where the maximum power is extracted from the wind). Therefore, the maximum power point can be achieved by adjusting the rotor speed according to the change in the wind speed. In variable speed wind turbines, the rotor speed is regulated by the power converter, which is the operational basis of variable speed wind turbines.

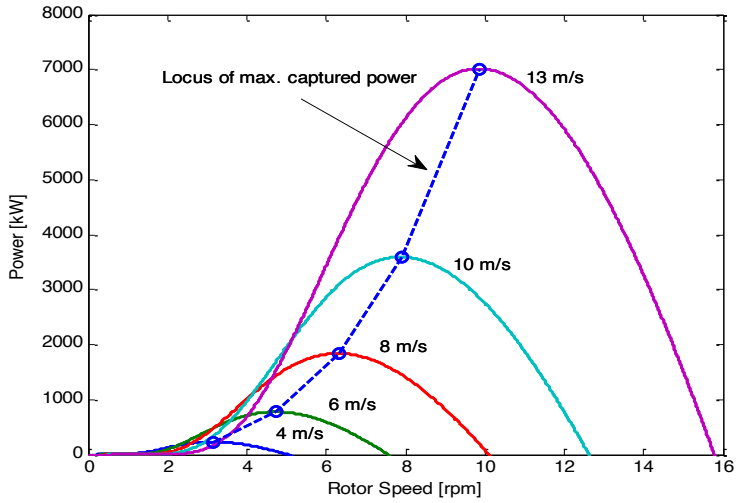

Figure 7-27: Power-speed characteristics with maximum power point tracking [166]

7.2.4.3 Blade Configurations

Blade's design and its configuration, as the prime mover for the generator, play important role in maximum extracted power from the wind and energy conversion efficiency. Question can rise what is the optimal number of blades, Figure 7-28 shows wind turbine with different blades configurations; one blade, two-blades, three blade wind turbines.

From the basic wind power conversion, aerodynamic efficiency can be increased by increasing the number of blades in the wind turbine. However, the achieved efficiency is not promising. For example, moving from two to three blades, the efficiency increase is only by 3% and moving from three to four blades, the gained efficiency is incremental. One important note needs to be understood that, as number of blades increase, the mechanical design of blades becomes more difficult. For this reason, three blades design become the standard blades model as ideal compromise between high energy yield and greater stability and durability of the turbine itself. Even through, researchers are still working on wind turbine development and improvement for more efficient and reliable designs for wind energy harvesting.

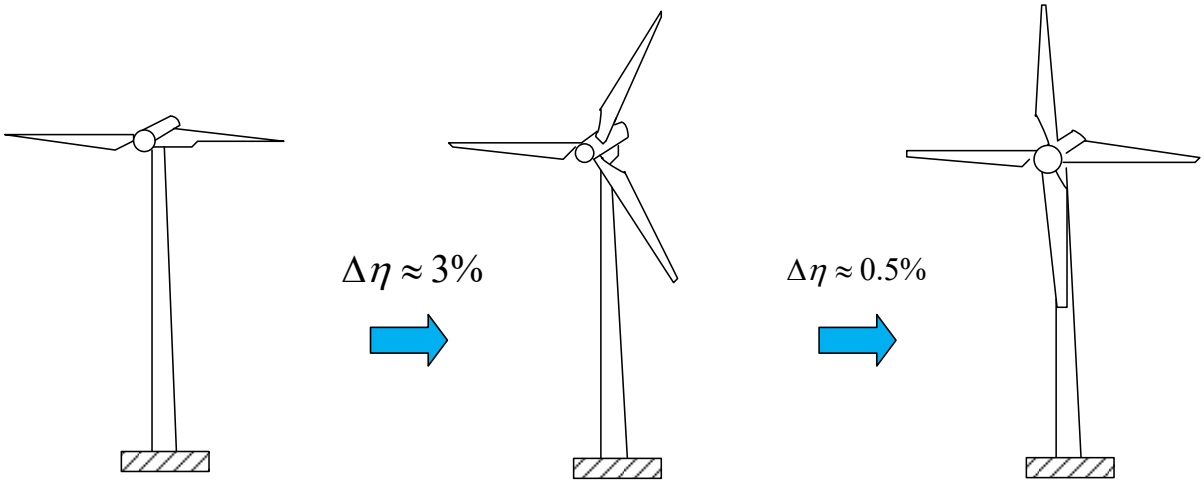

Figure 7-28: Blade configurations

7.2.5 Operating characteristic of a wind turbine

Figure 7-29, depicts the typical operating characteristics and operating zones of the wind turbine. The generated power is plotted as a function of the wind speed, the operational regions are divided into four operating zones. In both *zones 1 and 4,* there is no generated power. In the former, the available wind speed, below the minimum speed (ω_{min}) which is also known as cut-in speed, is insufficient to generate power from the wind. (The wind power is insufficient to overcome the power losses in the turbines.). In the latter, the wind speed exceeds the rated speed level (the maximum permissible wind speed (ω_{max})) which is also known as cut-out speed. This speed is determined by the wind turbine structural size and rating. Once reached, the turbine initiates to feather its blades. When the wind speed exceeds the highest design limit of the turbine, the turbine is stalled aerodynamically (known as feathering). This is controlled by regulating the pitch angle to make Cp close to zero, and thereafter blades rotation is completely stopped by applying mechanical brakes. The turbine must be shut down to protect the generator and the converter from overloading. In zone 2, the turbine operates between the minimum speed (ω_{min}) and the rated speed (ω_B), (points A and B). the generated output of the turbine is proportional to the cube of wind speed.

Within this zone, the pitch angle is continuously adjusted to drive the turbine close to its peak Cp to capture as much wind power as possible. In reality, most wind turbine operation lies in zone 2. In *zone 3,* the wind speed is between the rated speed and the cut-out speed. In this region, the generator delivers its rated power, and the pitch control is activated to maintain the rated power. When the wind speed exceeds the rated speed (ω_B), path A-C-D, the wind system must expel part of the wind power to maintain the safe turbine operation within its rated capacity. Such action is achieved by regulating the pitch angle (angle of attack) to produce less lift force. This is controlled by regulating the pitch angle to make Cp close to zero, and thereafter blades rotation is completely stopped by applying mechanical brakes. [167, 160, 161]

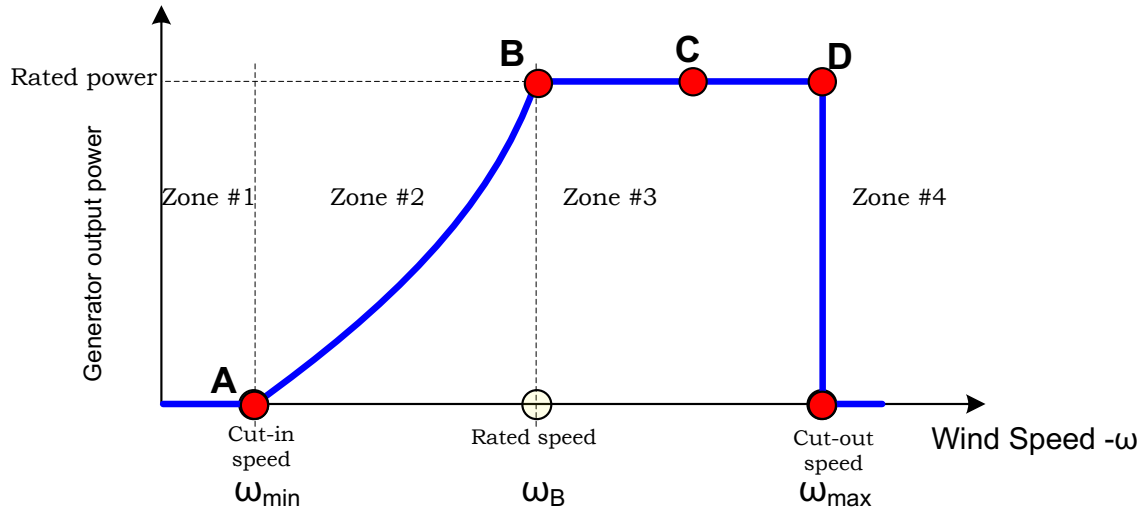

Figure 7-29: Wind power and turbine power curves versus wind speed. [160]

7.2.6 Separation of Wind Turbines

A wind farm is a group of WTs producing electricity in a single location. To have a successful wind farm, selecting a proper location is key. The most important item is selecting a site with the desired wind resource. The winds must be consistent and have a sufficient speed to generate the desired energy. Wind resource maps are a typical starting point. Meteorological data from "met" towers erected by companies interested in a site give a detailed view of the wind resource at a specific site. Potential impacts of WT farms also need to be considered. As

noted earlier, bird/bat activity and avian migration need to be considered to prevent negative effects on the environment. Noise effects can also have an impact in the area local to a proposed wind farm site. In addition, larger questions are also studied, for example: Will the turbines create interference for local air traffic? These additional factors must be weighed in addition to the wind resource when selecting a WT site. Besides wind resource and environmental effects, other factors that must be considered include land access (lease or purchase, zoning, and permits must be obtained) and sufficient capital to fund the project (approximately $1 million per megawatt of installed generating capacity). The wind farm would ideally be located near existing transmission lines to limit the cost (up to $1 million/mile) of installing large lengths of new transmission lines that drive the BOS costs up. In addition, there has to be a market available and an agreement in place to buy the electric power produced. Assuming that other factors are favorable, based on wind resource and turbine costs, the wind farm developer selects a WT model. Additional steps include checking with the manufacturer for availability and considering a service provider for annual maintenance.

Clustering wind turbines within wind farms has several advantages:

- Reduces the installation costs
- Reduces operation costs
- Reduces maintenance costs
- Simplifies grid connection

In addition to the strong influence of wind instability, the downside of the clusters is as follows:

- The speed of wind is reduced as it passes through the blades.
- The air turbulences which created when it passes through blades, Therefore, Close turbines located will not be able to capture energy efficiently from the turbulent wind.

Figure 7-30 shows an illustrative example for wind turbines arrangement for square area configuration. The distribution of the wind turbines depends on distance between the turbines. The separation between the two turbines is calculated as the minimum distance between the tips the two adjacent turbine blades, the separation factor S

$$S = \frac{D}{2r}$$ *Equation 7-18*

Where D denotes the distance between adjacent towers, r is the length of the blade.

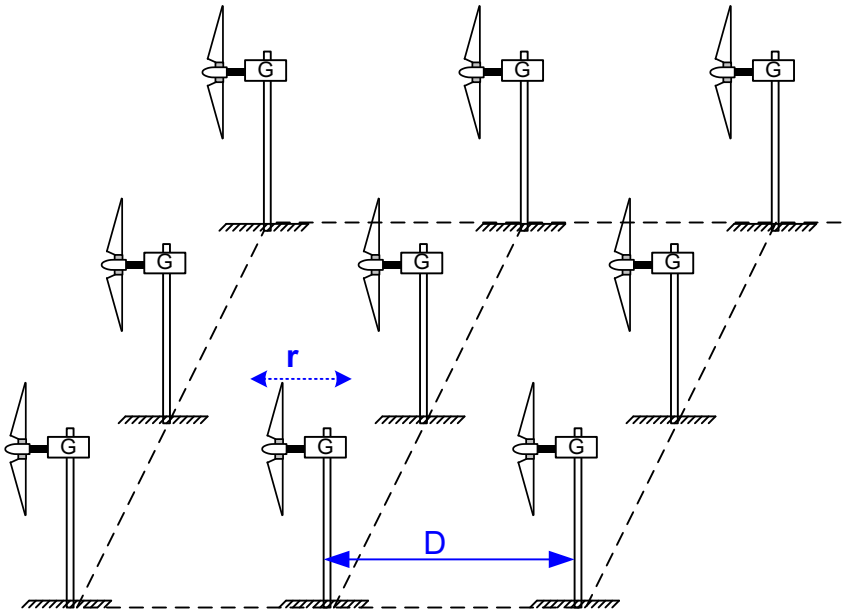

Figure 7-30: The square arrangement of wind turbines.

The array efficiency can be computed empirically by a curve fitting formula such as

$$\eta_{array} = 100\,(1 - ae^{-bS})$$ *Equation 7-19*

Where *a and b are constants values that depend on the number of turbines in the array.*
The acquired land depends on the number of turbines, the length of the blade, and the separation factor.

The minimum land area can be determined as

$$A_{land} = (xD - D + 2r)^2$$

Equation 7-20

Where *x* is the number of turbines in one row

Problem 7-12

How many Wind turbines of 50 m blade length can be installed at the site of 10 × 10 km while achieving a separation factor of 800?

Solution

The distance between towers:

$$D = 2rS = 100\text{x}800 = 800\ m$$

The number of WTs in each row or column can be computed form

$$A_{land} = (800x - 800 + 2\text{x}50)^2 = 10^8$$

Resulting, the number of wind turbines in each row/column is $x = 13$ turbines

For the whole site, the number of turbines is

$$N_{Total} = 13x13 = 169$$

Problem 7-13

For the wind farm in the previous example, compute the power production per land area when the wind power density at the hub is 400 W/m^2, the performance coefficient of is 0.3, and the overall efficiency of the turbine generator system is 85%. Assume the array efficiency is 74%.

Solution

The wind power,

$$P_{wind} = \rho A_{blade} = 400(\pi\ \text{x}\ 50^2) = 3.14MW$$

The output power of is

$$P_{out} = \eta . P_{blade} = \eta . C_P . P_{Wind} = 800kW$$

The total power of the turbines in the farm is

$$P_{Total} = n . P_{out} = 800 \text{ x}169 = 135.2\ MW$$

The output power of the farm is

$$P_{Farm} = \eta_{array} . P_{Total} = 135.2 \text{ x } 0.74 = 100.05\ MW$$

The power production per land area

$$\frac{P_{Farm}}{land\ area} = \frac{100.05\ MW}{10kmx10\ km} \approx 1 \frac{MW}{Km^2}$$

8 Wind Turbines operation and Control (1/2)

Author(s): Dr. Ziyad Al Tarawneh
Dr. Khaled Al Awasa

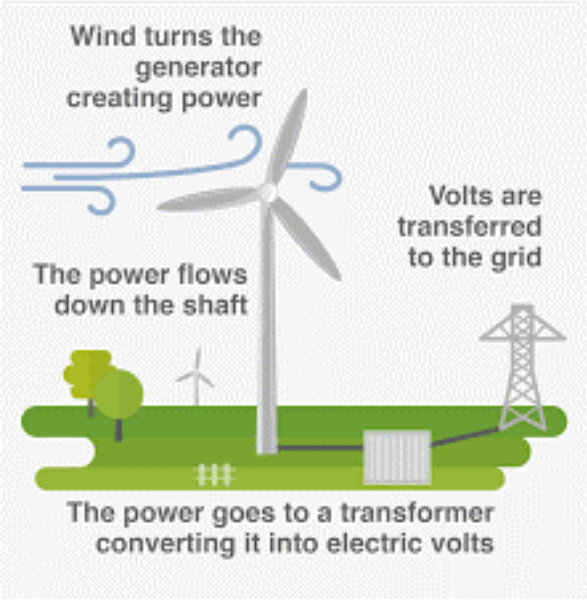

8.1 Introduction

8.1.1 Wind Turbines Components

Wind turbines harvest wind power by aerodynamically engineered wind blades and transform it from a mechanical power to electrical power. Normally, the rotational speed for multi-MW wind turbines is 10-15 rpm. The most powerful way to convert low-speed, high-torque power to electrical power is to use a gearbox and a conventional fixed-speed generator as shown in Figure 8-1 . It is worth noting that using the multi-pole generator systems are potential solutions for replacing gearbox transmission system. In addition, a power converter can be mounted between the grid and the generator.

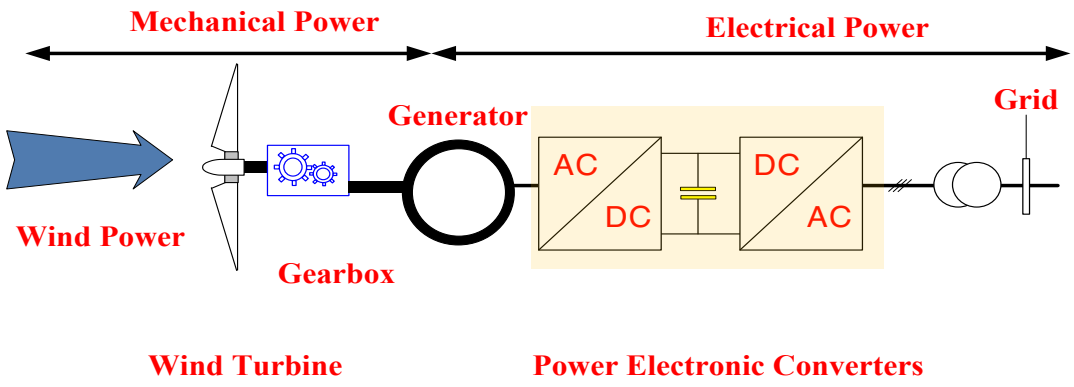

Figure 8-1: The conversion of wind power to electrical power using wind turbine [168].

Figure 8-2 provides a roadmap for technology that starts with wind and transforms the mechanical power to electricity. It includes solutions with or without transmission box (gearbox) and solutions with or without power electronic conversion systems. Additionally, the output power may be ac or dc.

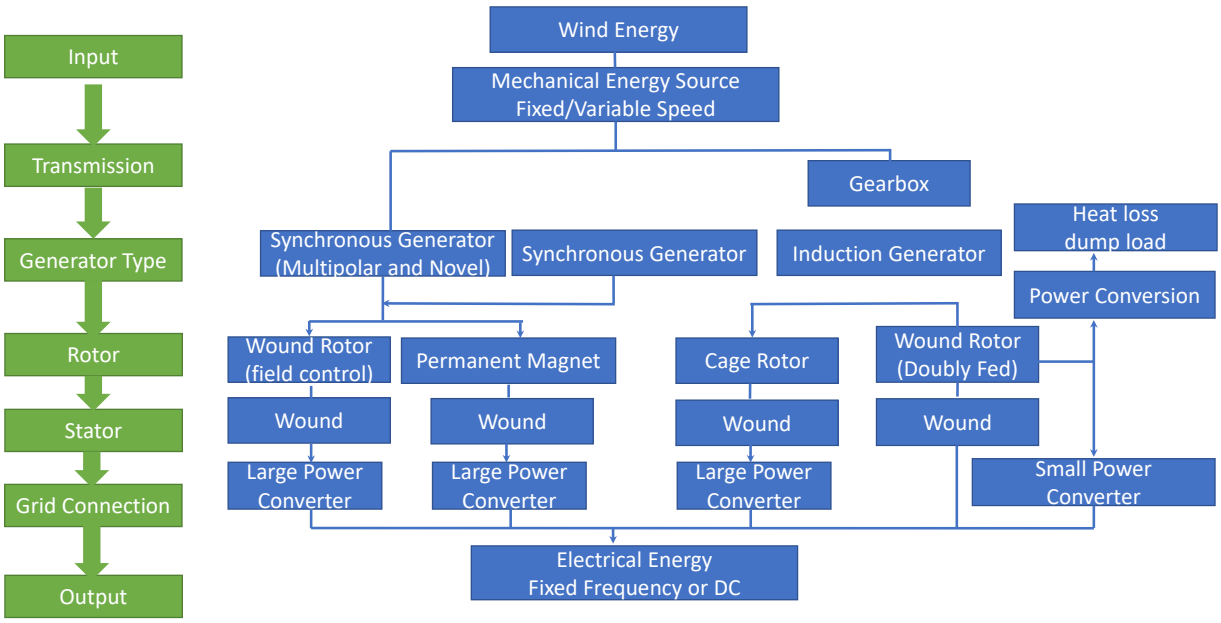

Figure 8-2: Possible solutions for converting wind energy into electrical energy [169]*and* [170].

8.2 Wind Turbine Generators

In many wind turbine configurations, asynchronous and synchronous generators are normally used. The typical generator used today in wind turbines is the induction generator (asynchronous), which also has different forms including: squirrel cage and wound rotor (slip ring) based generator. The squirrel-cage generator has no access to the rotor winding. This is both the cheapest and the most durable machine. Nevertheless, there is no control that can be carried out on these devices. The induction generator with the wound rotor has access to its rotor windings by means of a configuration of brushes and slip rings. It enables one to conduct two key control functions such as injecting a voltage signal into the rotor as well as adding an external resistance into the rotor side.

8.2.1 Induction Generator

Two key designs of the induction generator: squirrel cage and wound rotor. The squirrel cage design has its rotor windings made of short-circuited heavy bars which cannot be accessed. The wound-rotor (also known as the "slip-ring") consists of three phase windings which can be reached by a mechanism of brushes and slip rings from a stationary frame. This means, the rotor can be excited, or external circuits may change its windings. The induction system

consists of 3-phase stator windings and 3-phase rotor windings. Inaccessible rotor (squirrel-cage) machines are primarily used in type 1 turbines. For types 2 and 3 schemes, the machines with open rotor circuit (slip-ring or wound-rotor) are used. The stator windings of either machine are attached to a 3-phase source to create a spinning magnetic field in the air gap between the stator and the rotor, which transfers the energy from the stator to the rotor in the situation of motor operation, or from the rotor to the stator for generator operation.

8.2.1.1 Squirrel Cage Induction Generators (SCIG)

Squirrel cage induction generators (SCIGs) are most widely found in the topology of type 1 wind turbine as shown in Figure 8-3. These are wired directly to the power grid without the need of using power electronic converter systems so that the stator provides an ac voltage of constant frequency (50 Hz in the Europe and Jordan). In this configuration, a gearbox is required to link the low-speed shaft which is attached to the blades with the high speed shaft attached to the SCIGs generator. The Squirrel cage induction generator (SCIG) rotates at nearly its synchronous speed. Therefore, this type of wind turbine is known as a fixed speed wind turbine.

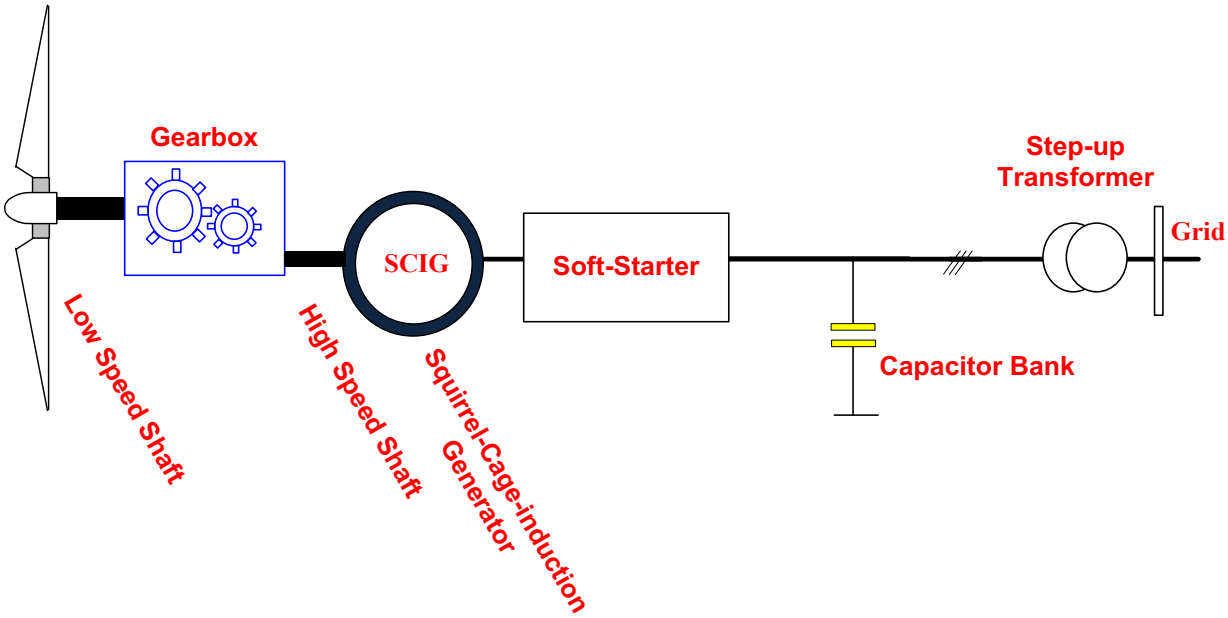

Figure 8-3: Type-1 wind generator topology [171]

8.2.1.2 Wound Rotor Induction Generators (WRIGs)

A wound rotor induction generator (WRIG) is used in type 2 wind turbine. The distinction from Type 1 turbine is that it does not have short-circuited windings on the rotor side. As shown in Figure 8-4, it can be reached through slip rings and brushes. The rotor windings are then attached to the outer 3-phase resistor bank which includes variable resistors that can be operated from 0 to maximum resistance per single phase. To achieve higher system reliability, the mechanically varying resistors are completely avoided. Instead, the control of resistor bank is achieved by an appropriate power electronic system. This removes the need for slip rings and brushes requiring frequent maintenance, however the control signals need to be wirelessly transmitted to the rotor side for adjusting the external resistances. However, this will increase the heat dissipation at the rotor side leading to difficulties in designing such machine.

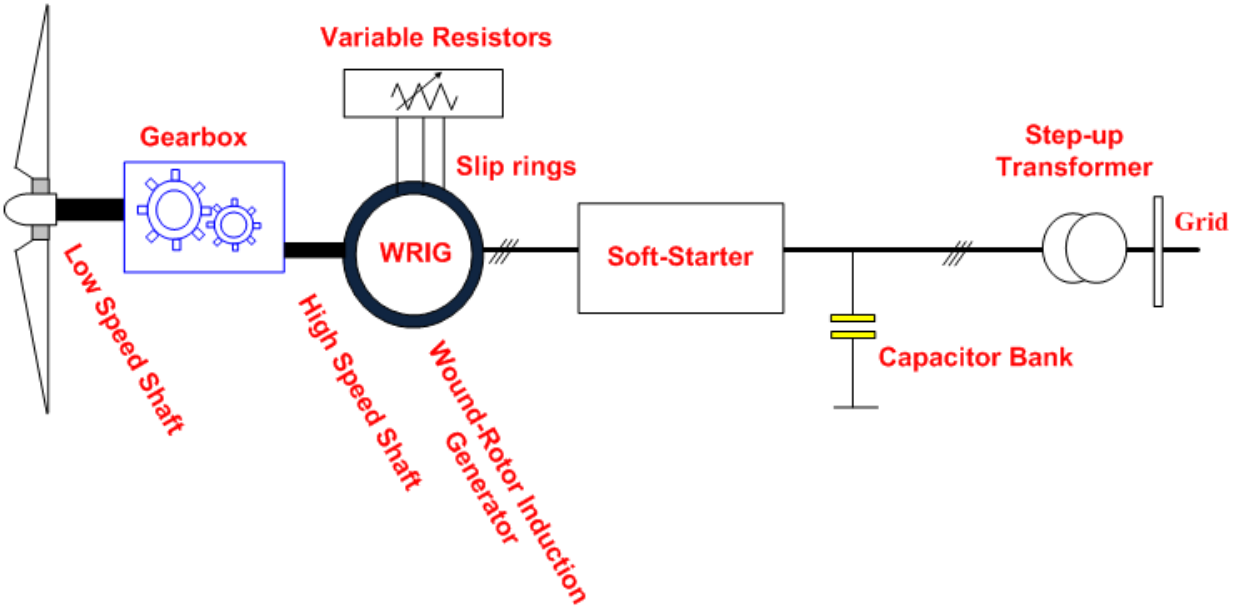

Figure 8-4: Type-2 wind generator topology [171]

8.2.1.3 Doubly-Fed Induction Generators (DIFGs)

Figure 8-5 shows the configuration of a doubly-fed induction generator (DFIG), known as a type 3 wind turbine, Analogous to type-2 WT, this configuration utilises a wound-rotor induction generator (WRIG), however, the key distinction is that the rotor of the doubly fed

induction generator (DIFG) is simply connected to the power grid using a suitable power electronic converter such as back to back ac-dc-ac converter, which is composed of two different bi-directional converter topologies attached with a dc link as shown in Figure 8-5. Considering the generator side converter, it relies on advanced control system that

1. Controls the frequency of the currents in the windings of the rotor to maintain the synchronization of the magnetic fields between the stator and the rotor at all times.

2. Controls the amplitude and the phase shift of the currents in the windings of the rotor which ultimately means that both real and reactive powers provided to the power system are also controlled by such type of converters.

It should be noted that the step-up transformer shown in Figure 8-5 is a 3-phase transformer which is composed of two low-voltage windings for the stator and rotor, and a medium-voltage winding at the power grid side

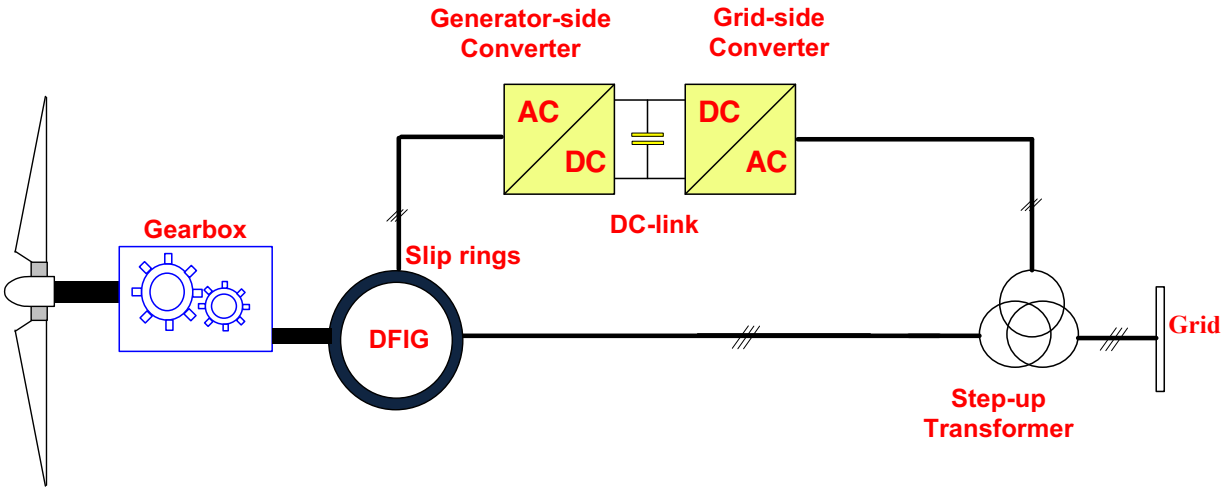

Figure 8-5: Type-3 wind generator topology [171].

In general, the induction generator (IG) runs at a slip such that its rotating speed is not precisely constant. Consequently, the generator itself without rotor injection cannot produce

electricity unless it rotates at a speed higher than that of its synchronous speed n_s which is given as:

$$n_S = 120\frac{f}{p} \qquad \textit{Equation 8-1}$$

where n_s is the synchronous speed, f is the operating frequency of the power system (i.e., the grid), p is the number of poles, and s is the slip of the generator which is given as follows:

$$s = \frac{n_S - n}{n_S} \qquad \textit{Equation 8-2}$$

The slip of the induction generator, without rotor injection, is often small (2%–10%), and the generator needs to be a negative slip to generate electricity.

8.2.2 Synchronous Generators (SGs)

The synchronous generator (SG) is the mainly common generator used at power plants to produce electricity. The synchronous generators produce over 98 percent of all electrical power worldwide. The machine has the rotor attached to the excitation circuit. For small-sized generators, ferrite permanent magnetic material provides the excitation. It is the most economical configuration for fractional horsepower generators that do not undergo frequent increases in stator currents (the rotor can be demagnetized by frequent surges).

For better designs, the rotor is fabricated using permanent magnetic material like the samarium cobalt (SmCo) to create larger magnetic fields. Their high power / volume ratios make the generators compact in size and weight which enables designers to create generators as large as 1.0 MW. Another benefit the permanent magnetic synchronous generator (made from rare earth magnets) is that they cannot be easily demagnetized so that it can be used for applications where strong currents and current surges are expected such as in wind turbine systems. In the case of high power generation (in traditional power plants and in some powerful wind turbines), the generator field is electrical in order to generate a flux intensity; this also enables the operator to adjust/modify the terminal voltage and the reactive power produced by the generator. For both types (electric magnet and permanent magnet synchronous generators), the frequency of the generated power is directly linked to its

rotational speed. In fact, there is no slip in these types. Moreover, a power converter between the generator and the grid sides is needed to deliver electricity at the grid frequency since the output frequency of such machines is not constant due to the significant fluctuations in wind speed.

Considering the electric magnet based generator, it gives access to its field circuit. By modifying the field current, the voltage and reactive power at the terminals of the generator can be controlled.

On the other hand, the permanent magnet generators do not provide an access to field current of the machine and are often fabricated from scarce earth magnetic material with stronger magnetic fields.

Recently, a newer type of wind turbines utilizes the synchronous machine without gearbox. This type of generator requires large number of poles in order to reduce the generator's synchronous speed and allow for power generation at low blade speed. It is worth noting that the diameter of such generator is normally large because of the large number of poles requirement, making the nacelle very wide.

8.2.2.1 Permanent-Magnet Synchronous Generators (PMSGs)

Figure 8-6 shows the topology of type 4 wind turbine which is relies on permanent magnet synchronous generators (PMSGs). In this configuration, a fully rated power electronics converter is used to link the generator with the power system and hence handle the maximum electrical power generated by the generator. The converter allows the rotational speed of the system to be decoupled from the steady electrical frequency of the grid. In the case of variable speed operation (VS), the converter at the stator side produces alternating currents and voltages of the required frequency to accommodate the speed of the rotor because the rotor must synchronize with the stator's magnetic field in synchronous machines. The converters can also control the generator's electromagnetic torque, by modifying the stator current's magnitude and phase. This allows the approach of rotor speed to be adopted where the speed value is changed to achieve the maximum tip-speed ratio. The topology of power electronics is usually identical to the one seen in Figure 8-13, which utilises two IGBT-based back to back converters coupled with a dc link. Another common power converter topology could be used, instead of a completely controllable converter; an unregulated diode rectifier is attached at

the stator side. It helps to minimise the cost and hardware complexity of power electronics, but it suffers from the reduced flexibility of controlling the currents of the stator.

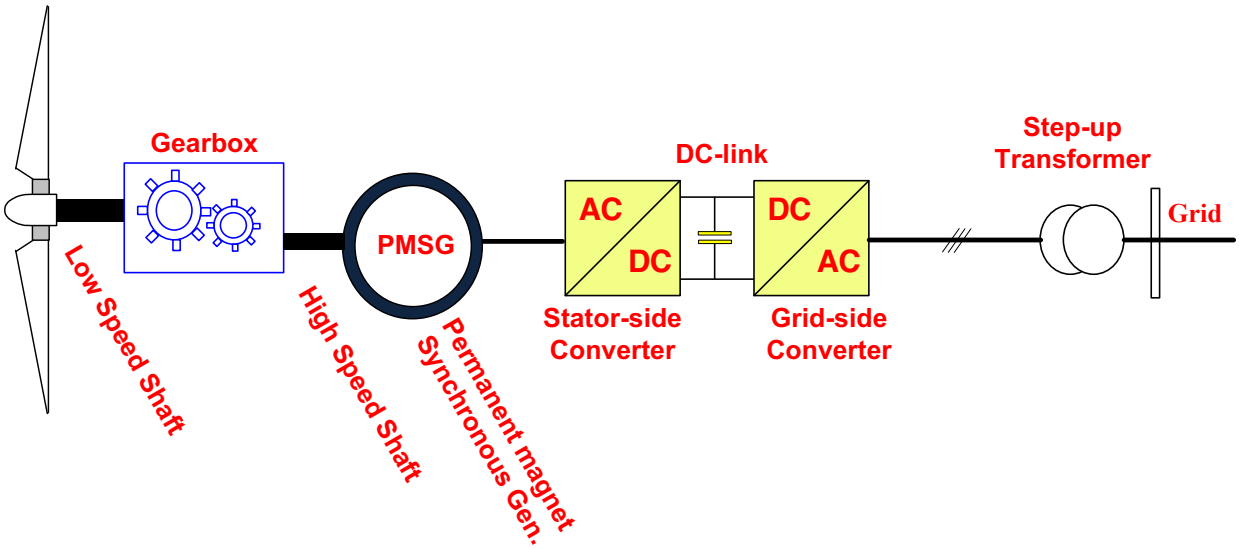

Figure 8-6: Type-4 wind generator topology [171].

8.3 Types of wind turbine generator systems

Wind turbines can be categorized into two main categories: a fixed speed wind turbine (FSWT) and a variable speed wind turbine (VSWT). Older models were mostly of a fixed speed type, since they are cheaper to construct and operate as compared with variable-speed types. Electricity is generated only when the wind speed is sufficient to cause the generator shaft to rotate faster than its synchronous speed. While it is cheaper and requires less maintenance than the variable speed types, its power generation is limited. The torque-speed characteristic of the FSWT is shown in Figure 8-7. It can be seen that the generator operates in nearly linear range (point 1 to point 2). The speed of the turbine is below the cut in speed before the point 1. When the speed exceeds that at point 2, the machine enters into its unstable nonlinear region. Since the steep slope of the FSWT torque-speed characteristic, the speed range is very narrow, thus it is called “fixed-speed turbine.” The range of the developed power (shaft power of the generator) in this system can be given:

$$\Delta Pcs = \mathrm{P}_2 - \mathrm{P}_1 = \mathrm{T}_2\omega_2 - \mathrm{T}_1\omega_1 \qquad \textit{Equation 8-3}$$

Where ΔPcs is the range of the developed power of constant speed generator, P_1 is the developed power at point 1, P_2 is the developed power at point 2, T_1 is the developed torque at point 1, T_2 is the developed torque at point 2, ω_1 is the speed of the generator at point 1, ω_2 is the speed of the generator at point 2. Finally, as $\omega_2 \cong \omega_1$, the equation can be rewritten as be

$$\Delta Pcs = P_2 - P_1 = (T_2 - T_1)\omega_1 \qquad \textit{Equation 8-4}$$

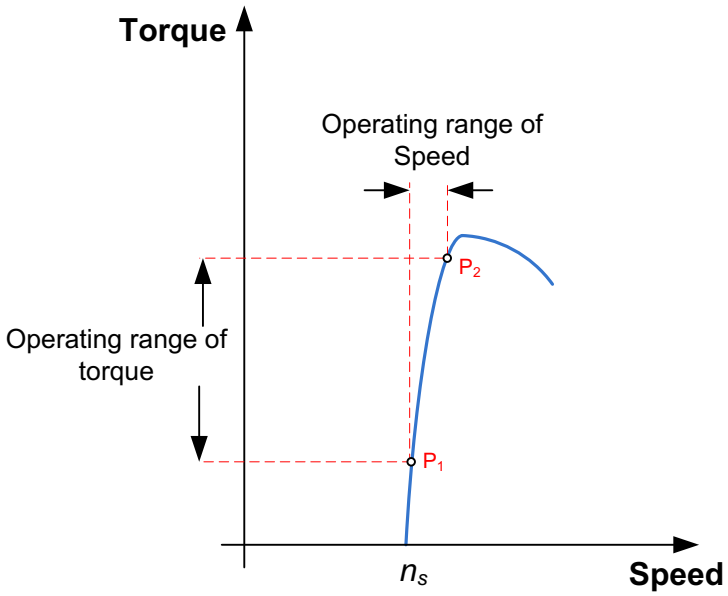

Figure 8-7: Torque-speed characteristics of a fixed-speed wind turbine [160].

Because the FSWT speed is relatively constant, the output power is regulated using the pitch angle control by changing the lifting force.

VSWTs can generate electricity at a wide range of speeds even at less than synchronous speeds. Their range of operations is therefore much wider than the FSWT. But they suffer from the increasing complexity of the system as power converters are needed. Figure 8-8 shows the torque-speed characteristics of the VSWT. As shown, a voltage is introduced into the rotor circuit of the generator to achieve these characteristics. The speed of the generator is $P_2 > P_1$ when the operating torque is between T_1 and T_2. This machine has a range of power:

$$\Delta Pvs = T_2\omega_2 - T_1\omega_1 \qquad \textit{Equation 8-5}$$

where ΔP_{VS} is the developed power of the variable speed generator. It can be concluded that the $\Delta P_{VS} > \Delta P_{CS}$ because of the wider variation of operating speed.

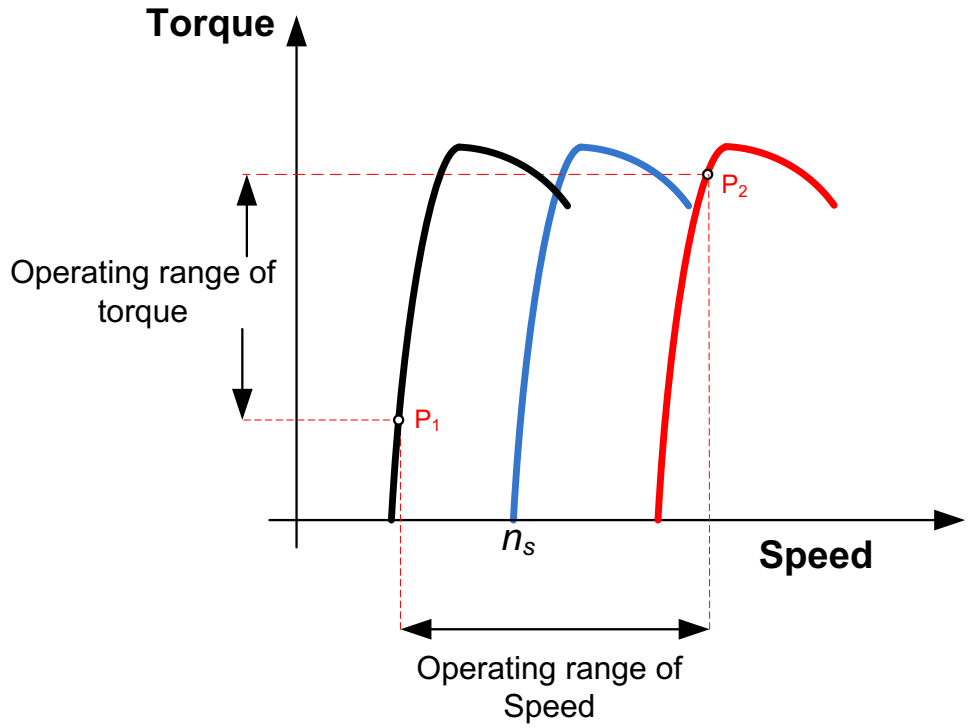

Figure 8-8: Torque-speed characteristics of variable-speed wind turbine [160].

Problem 8-1

If the torque of a fixed speed generator is ranging from 500 NM to 3000 NM and its synchronous speed is 1200 rpm. Assume that the slip is –0.02; estimate the range of the established generator power.

Solution

The speed of the generator can be computed as follows.

$\omega_2 \cong \omega_1 = \omega_S(1 - S) = 128.18\, rad/s$

The range of the developed power is

$$\Delta Pcs = \mathrm{P}_2 - \mathrm{P}_1 = \mathrm{T}_2\omega_2 - \mathrm{T}_1\omega_1 = 320.45\, kW$$

Problem 8-2

From the previous example, assume that the generator is equipped with a power converter which can operate the generator at a speed range of 900–1500 r/min. Estimate the range of the established power.

Solution

The range of the established power using Equation 4.6 is

$$\Delta Pvs = \mathrm{P}_2 - \mathrm{P}_1 = \mathrm{T}_2\omega_2 - \mathrm{T}_1\omega_2 = 424.12\ kW$$

It is an improvement in power range of about 32 per cent over the fixed-speed system.

8.3.1 Assessment of FSWT and VSWT

For FSWTs, the cut in speed (minimum wind speed needed to produce electrical power) is higher than the synchronous speed of the VSWT generator, and it's cut out speed which is determined by the maximum speed of the turbine at point 2 as shown in Figure 8-8. For VSWT, the cut in speed is below the synchronous speed. In addition, the cut out speed is higher than that of FSWT, as illustrated in Figure 8-9. For FSWT, the rated power is less than that for VSWT which is delivered by its stator windings. For VSWTs, the stator and rotor both deliver the output power.

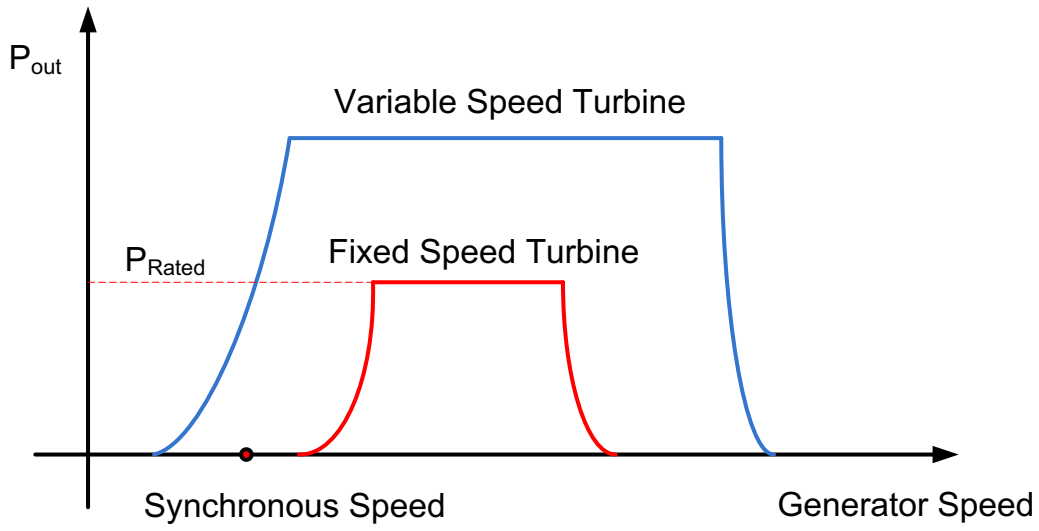

Figure 8-9: Power generation for fixed- and variable-speed wind turbines [160].

Despite the fact that FSWT has a relatively primitive design, it is still used for small size systems because of several reasons:

• No need for brushes or slip rings.

• Low maintenance.

• Rugged generator.

• Low cost.

• Simple to operate.

However, the FSWT has many drawbacks, including:

- Wind speed variations result in continuous and abrupt tensional torques, which stress the drive shaft and gearbox, due to a fixed-speed operation.
- Rotation speeds are high, because they need to exceed the synchronous speed to produce power. For this to happen the gear needs to be designed with high ratios or the blades needs to rotate at high speed. The tower is needs to be designed for higher structural loads in either case.
- The FSWT may be noisy and cause more bird collisions because of its high speed.

On the other hand, VSWT is much more popular these days due to its overwhelming advantages:

- Can generate power at low speeds (less than the synchronous speed).
- Even though the turbine speed varies widely, it is possible to control the output power. Generator speed can be adjusted so that aerodynamic efficiency is increased (Enhance the performance coefficient).
- Reduction of the torque of the drive train due to lower mechanical stress.
- Noise and collision problems with bird are significantly minimized as the turbine rotates at low speed.

However, the VSWT's main disadvantages are:

- High costs.
- More complex system (more system components).
- Increased maintenance costs.

8.4 Power Electronic in Wind Turbines

The Power electronic components are capable of accommodating high power and voltage levels, and provide lower power losses and more reliable systems. Furthermore, as the price/power ratio continues to decline, the power converters are becoming increasingly attractive solutions for increasing the efficiency of wind turbine (WT) systems. In the following section, the power converters most commonly used in the wind turbine (WT) systems are presented including their both their strengths and pitfalls.

8.4.1 Power Electronics for Wind Turbine Type 1

8.4.1.1 Soft-starter

Soft-starter is a simple and cheap electrical power component that is mostly used in FSWTs to connect the generator to the grid side (types 1 and 2). The main function of the soft-starter is to reduce the inrush current (reduce the effects of the start-up situation) and thus prevent voltage / current disturbances in the grid. The inrush current can be up to 7–8 times the rated current without a soft starter, which can cause significant voltage disruptions on the grid.

Figure 8-10 shows the configuration of an active controlled soft starter. The soft-starter contains two thyristors as commutation devices in each phase. They are connected in parallel with back-to-back connected thyristor pairs for each phase to eliminate the power losses in the thyristors due to the voltage drop across the thyristors during conduction.

The smooth connection of the generator to the grid, during a predefined number of grid periods, is achieved by adjusting the firing angle of the thyristors. After the in-rush, the thyristors are bypassed in order to reduce the losses of the overall system.

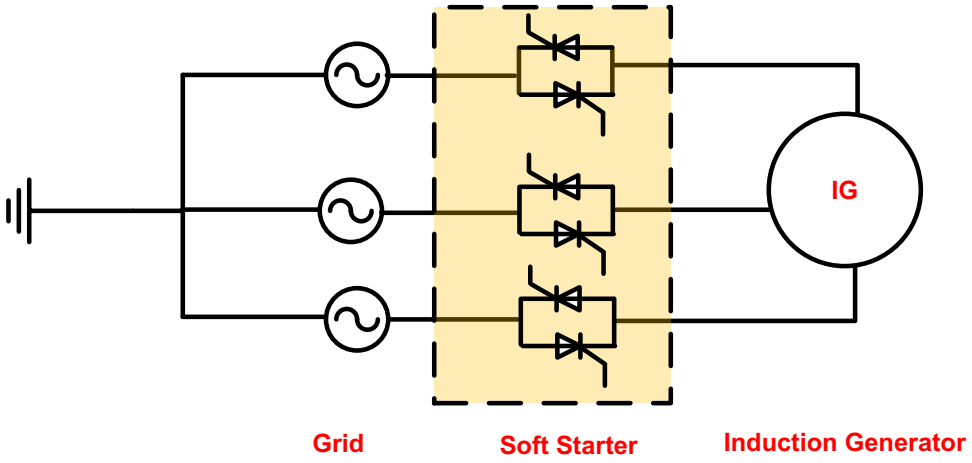

Figure 8-10: the configuration of an active controlled soft starter [172].

8.4.1.2 Capacitor bank

The capacitor bank is used in fixed speed or limited variable speed wind turbines (types 1 and 2). It is an electrical component that supplies reactive power to the induction generator. Thus, the reactive power absorbed by the generator from the grid is minimized. The generators of wind turbines can have a full load dynamic compensation, where a certain number of capacitors are connected or disconnected continuously, depending on the average reactive power demand of the generator over a predefined period of time. The capacitor banks are usually mounted at the bottom of the tower or to the nacelle (i.e. at the top of the wind turbine). They may be heavy loaded and damaged in the case of over voltage on the grid and thereby may increase the maintenance cost of the system.

Finally, during the start-up phase, it is preferable to attach the capacitor banks. However, since the soft starter generates harmonic currents that can harm capacitors, the capacitor banks will not be connected until the grid connection process of the squirrel-cage induction generator (SCIG) is completed.

8.4.2 Power Electronics for Wind Turbine Type 2

Type 2 wind turbine consists of a variable resistor bank external to rotor side. The external variable resistor bank is achieved through connecting the external 3-phase resistors in parallel

to the power electronic converter which is composed of a B6 diode bridge and an insulated bipolar transistor (IGBT) as shown in Figure 8-11. The external resistors and the associated electronic power circuit are both linked to the rotor windings through slip rings and brushes. The duty ratio of insulated bipolar transistor is usually adjusted in away that the effective value of external resistance to the rotor of the wound-rotor induction generator (WRIG) is modified dynamically. The generated electrical power, P_e, is given as:

$$P_e = n_p {I_2}^2 (\frac{R_2}{s}) \cong n_p {V_1}^2 (\frac{s}{R_2}) \; for \; s \leq 0.02 \qquad \textit{Equation 8-6}$$

where n_p is the number of phases, V_1 is the terminal voltage of the stator windings. I_2 the rotor current, R_2 is the resistance at the stator side, and s is the slip.

If the speed of the rotor is increased above its synchronous speed, the generator starts to produce electrical power. When the wind speed increases above this point, the slip of the rotor increases hence the output power increases. However, If the generated electrical power has become below its rated value, then the external rotor resistors will be short circuited by making the duty ratio of the IGBT module to be 1. Furthermore, when the generated output power reaches the rated value, the resistance of the external rotor is modified to maintain a constant output power. This is accomplished by fixing the ratio of the overall rotor resistance to the slip to be constant as given in the following equation [172]:

$$\frac{R_{2-Total}}{s} = \frac{R_2}{s_{rated}} \qquad \textit{Equation 8-7}$$

where R_{2_Total} s_{rated} are the overall resistance of R_2 and the effective resistance of the external rotor and the rated slip when the rotor resistance is R_2, respectively.

In this configuration, the generator can function at a wider speed range by modifying the external rotor resistance of the generator.

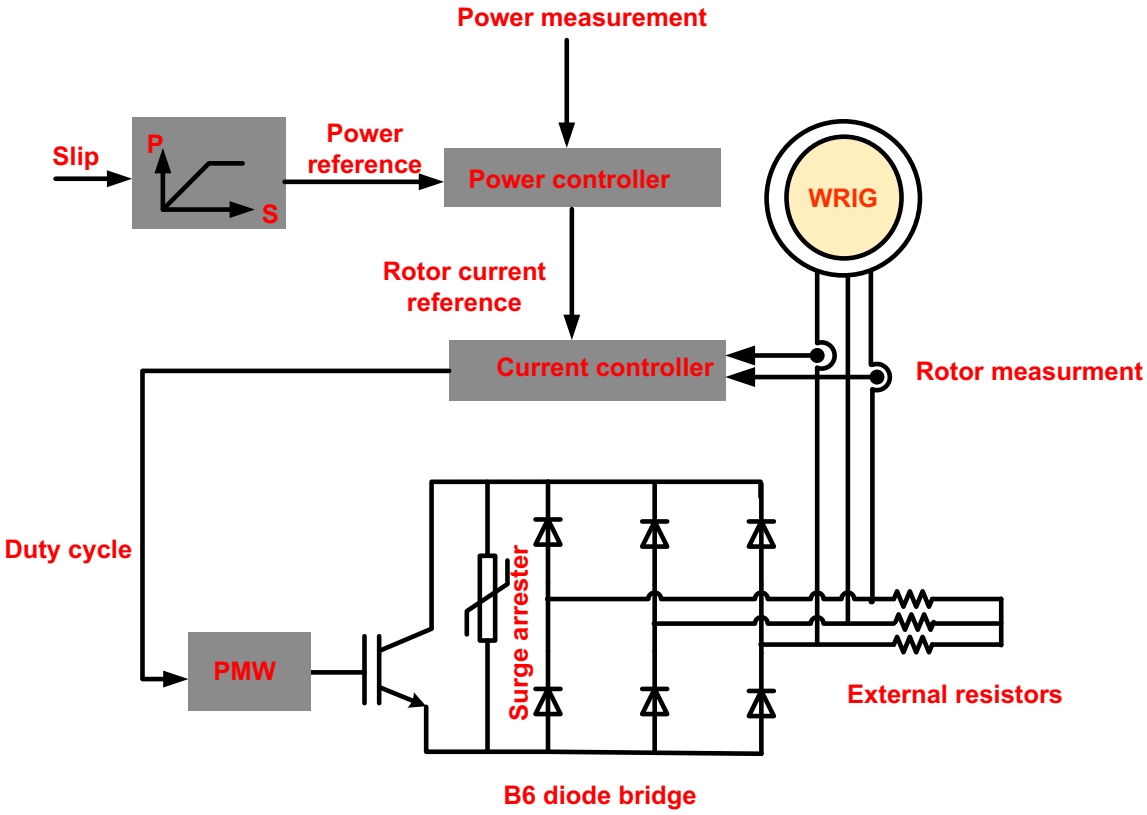

Figure 8-11: Power electronic circuit used to regulate the external resistance of rotor of the wound-rotor induction generator (WRIG) [172].

As seen in Figure 8-4 above, the generators used in the type 2 wind turbines also need a soft starter to reduce the inrush currents during the start-up phase. In addition, they need switched capacitor banks to compensate for reactive power.

The type 2 has several strengths over type 1.

- Increasing the system efficiency by adopting partial variable speed operation using a lightweight power converter.
- Reducing the structural loads at high wind speeds;
- Enhancing the quality of the generated output power;
- Reducing noise levels as the turbine is spinning at a lower speed.

However, slip rings and brushes are usually used to connect the external resistors to the rotor terminal, which is a disadvantage compared to the squirrel cage induction generator (SCIG) because it requires more components and requires more maintenance.

8.4.3 Power Electronics for Wind Turbine Type 3

Figure 8-12 shows the typical arrangement of a type 3 wind turbine generator, which comprises of a low speed wind turbine (WT), attached to a high speed wound-rotor induction generator (WRIG) through a gearbox. As shown, the stator is linked directly to the power grid and a variable frequency electronic converter connects the rotor to the grid via slip rings. This generator is usually referred as a doubly-fed induction generator (DFIG). In this configuration, the converters at both sides are coupled back to back by a common DC link.

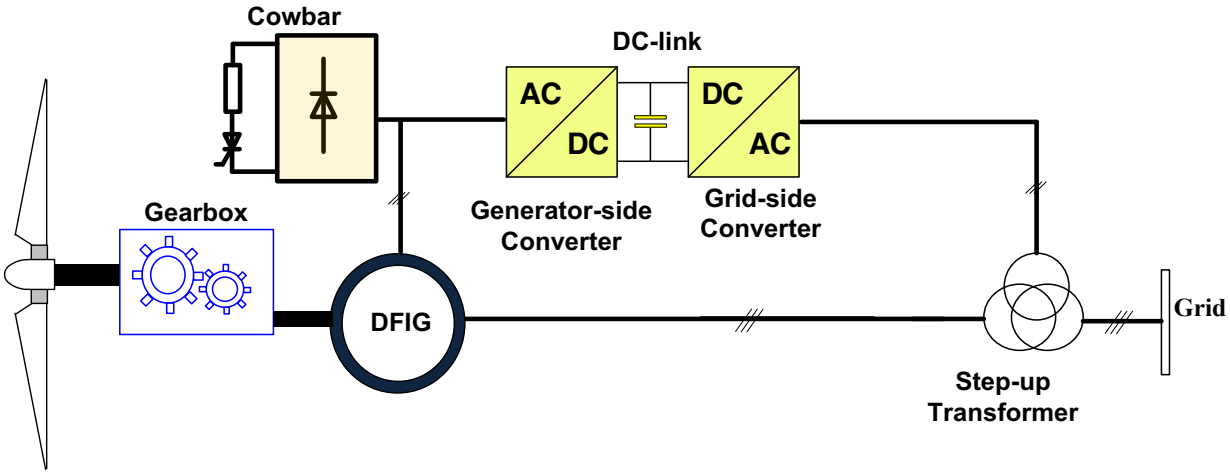

Figure 8-12: Configuration of wind turbine type 3 [172].

In order to maintain the electrical power on grid at constant voltage and frequency over a wide range of wind speeds. Both electronic converters at generator and the grid sides are generally rated at a fraction of the nominal generator power (approximately 30%) to carry the slip power. Accordingly, the generator can function at a spinning speed around ±30 percent of its synchronous speed.

If the spinning speed is lower than the synchronous speed, then the power flows from the power grid to the rotor windings. On the other hand; if the spinning speed is larger than its synchronous speed, the power flows from the rotor windings to the power grid.

In such arrangement, both active and reactive power components of the generator and the converter can be separately regulated.

The active power of the power converter can be used to adjust the generator's spinning speed, and hence the rotor's speed of the wind turbine. Moreover, at weak wind condition, this configuration has a reduced noise level as it operates at a lower speed. Compared to type 1 and 2 wind turbine topologies, Type 3 wind turbine proved better dynamic response and controllability. Furthermore, this type of wind turbine does not need either a soft starter or capacitors bank for reactive power compensation.

Power electronic converters can be classified into two types namely naturally commutated and forced-commutated power converters. The naturally commutated converters are typically based on thyristor devices. In fact, this type of converter is not capable of regulating the reactive power in a system as it consumes the inductive reactive power; consequently, thyristor based converters are normally utilized in high voltage and power applications.

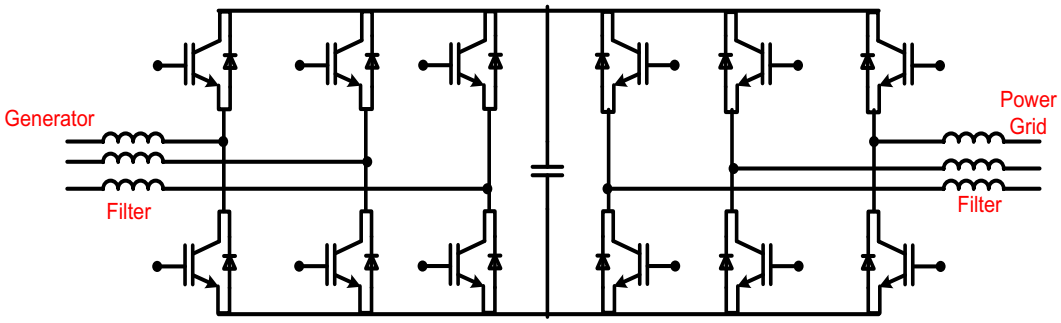

Figure 8-13: back to-back PWM-VSCs typically used in type 3 *wind power systems* [172].

On the other hand, forced commutated power converters are typically used in type 3 wind turbine generators such as back to back PWM VSCs based on IGBT which is presented in Figure 8-13. The double fed induction generator (DFIG) configuration employs a pair of bidirectional back to back PWM-VSCs coupled with a shared DC link.

The active and reactive power supplied to the grid can be controlled by this form of power converter. Under the converter's rating limit, the reactive power (from the DFIG and converter to the grid) can be changed to a value needed by the power grid. This helps the grid integration to be enhanced with regard to active and reactive power control, power quality, and angular stability. Additionally, the high switching frequencies of a PWM based VSC suggest that harmonic frequencies can be quickly removed utilizing lightweight filters.

In the last years the nominal power of wind turbines has gradually increased to reduce costs per megawatt and also enhance the overall efficiency of such systems. As a result, multi-level power converters are becoming increasingly important, particularly for medium and high power wind turbine (WT) systems. The resulting improvement in voltage rating permits the wind turbine converters to be linked directly to the power grid, thus eliminating the need of using of a massive transformer. The principle involved in multi-level converter technology is to create a sinusoidal voltage of steps, typically from a variety of power semiconductor devices and capacitor based voltage sources.

The widely used arrangements for multi-level converters can be divided into three categories:

- Diode clamped multi-level converters.
- Capacitor clamped multi-level converters.
- Cascaded multi-level converters.

The most widely used 3-level converters using these topologies are shown in Figure 8-14. The 3 level diode clamped multi-level converter and the 3 level capacitor clamped multi-level converter are subjected to irregular current stress on the semiconductor components. It was found that the top and bottom switches in the converter leg could be largely affected from those in the middle. On the other hand, the cascaded H-bridge multi-level converter is heavy, bulky and complex. In addition, it is difficult to connect separate DC sources from two back to back converters as there would be a short circuit when two back to back converters do not switch synchronously.

The matrix converter is another type of circuit configuration shown in Figure 8-15. As shown, this converter is a single stage AC to AC converter which is composed of 9 bi-directional switches (semiconductor devices) that link each input phase to its related output phase. The basic principle is that by correctly controlling the switches that link the converter's outputs to their related inputs, the desired output voltage, frequency and input current can be achieved. In order to protect the converter, the following two control rules must be implemented.

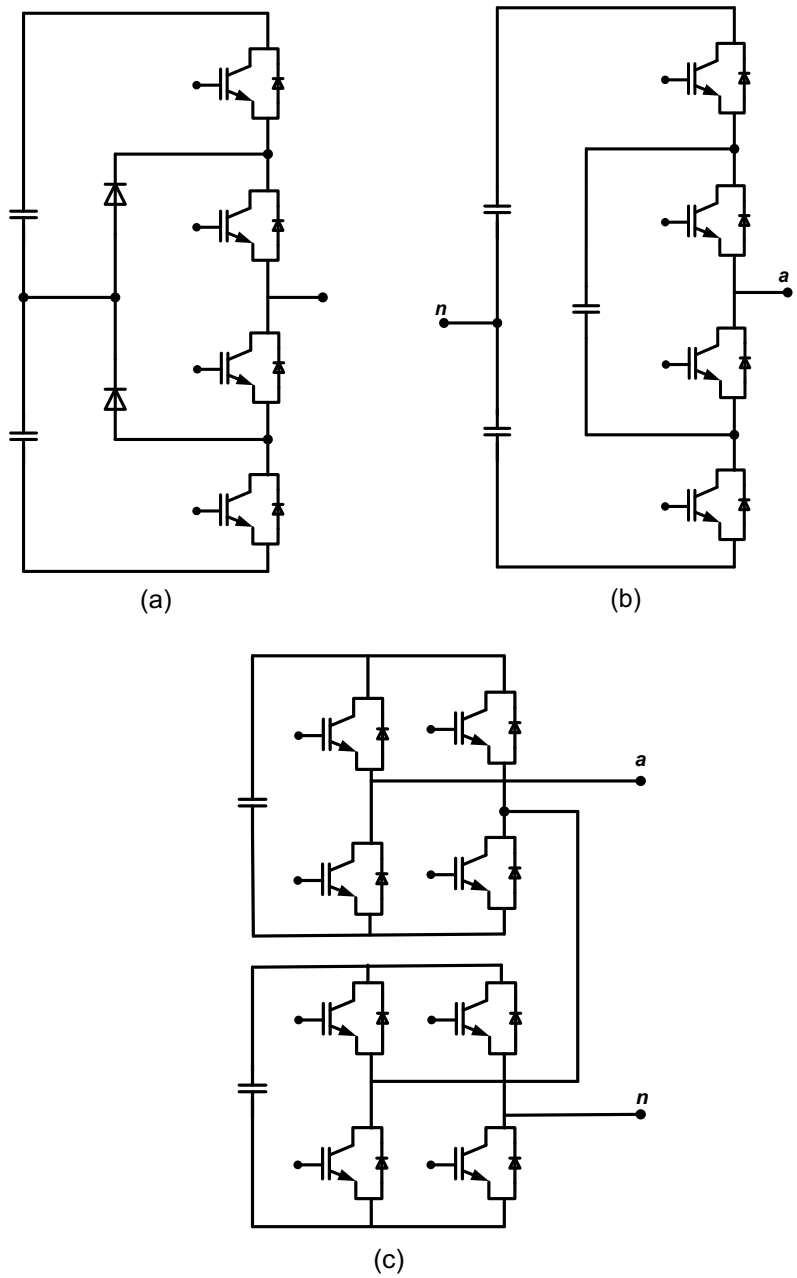

Figure 8-14: Multi level converter arrangements (a) one leg of a diode-clamped 3 level converter (b) one leg of a capacitor clamped 3 level converter (c) one leg of an H-bridge cascaded 3 level converter [172].

In addition, specific control rules must be followed to protect this type of converters.

1. Only 1 switch inside the output leg of the matrix converter can be turned on at any given time.
2. All 3 output phases (A, B, and C) have to be linked to a specific input phase at any point of time.

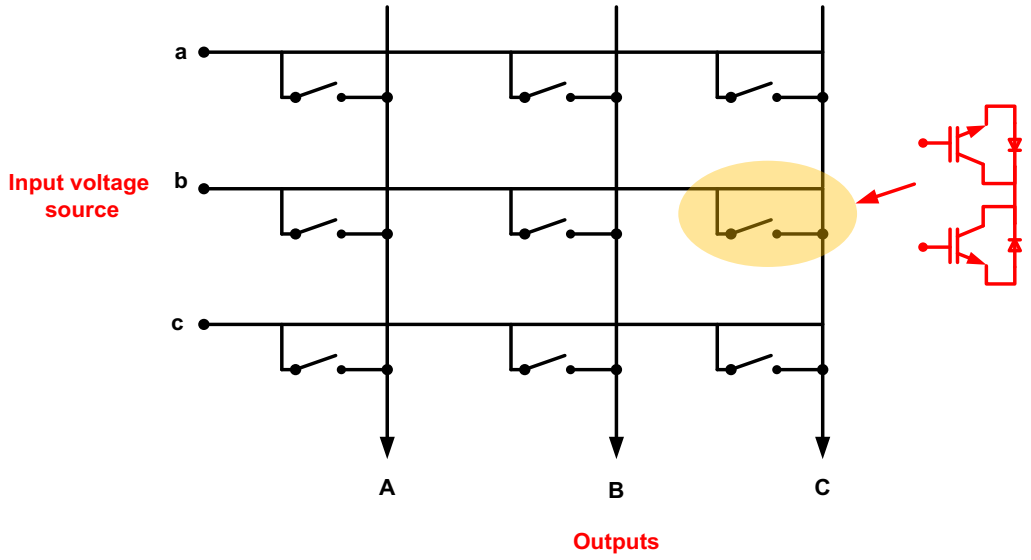

Figure 8-15: Matrix converter [172].

The operation of Type 3 configurations during grid faults could potentially cause voltage sags, leading to over voltage within the DC contact and over-current in the rotor of DFIG and the generator side converter. Ultimately, the generator side converter would be damaged.

In case of a grid fault, a crowbar circuit is often placed between both the DFIG rotor and the generator side converter to short circuit the rotor windings. Subsequently, the generator side converter has become not able to switch, and it also lost its controllability. Consequently, the DFIG starts behaving like a standard SCIG. In specific, produces active power while continuing to consume a limited level of reactive power. Once grid fault is resolved, the generator-side converter is re-launched, and the DFIG rotor is reconnected to the generator side converter after synchronization. Several crowbar circuit topologies are shown in Figure 8-16 including passive and active crowbar configurations. Figure 8-16 (a) depicts the passive crowbar composed of a diode bridge that rectifies rotor phase currents in conjunction with one thyristor connected in series with a resistor. In this circuit, when the DC-link voltage is exceeding its maximum value, or if the rotor current approaches its limit value, the thyristor is activated. The active crowbar configuration, shown in Figure 8-16b, replaces the switching device (i.e., thyristor) in the passive crowbar circuit with a fully controllable semiconductor device such as an IGBT. The short-circuit rotor current can be cut at any point by such type of crowbar. If the DC link voltage or the rotor current approaches their maximum levels, the

switching device (IGBT) of the converter at the generator side is blocked and the active crowbar is enabled. When the crowbar is in operation, the DC-link and the crowbar resistor voltages are also monitored. The crowbar is switched off once the voltages drops under a certain level. The converter at the generator side is reactivated and linked back to the DFIG's rotor circuit after a slight delay (until the rotor currents have fully decayed). The value of crowbar resistance in both topologies has a large influence on the DFIG's dynamic performance, such as the DFIG's overall short-circuit current and ability to regulate reactive power.

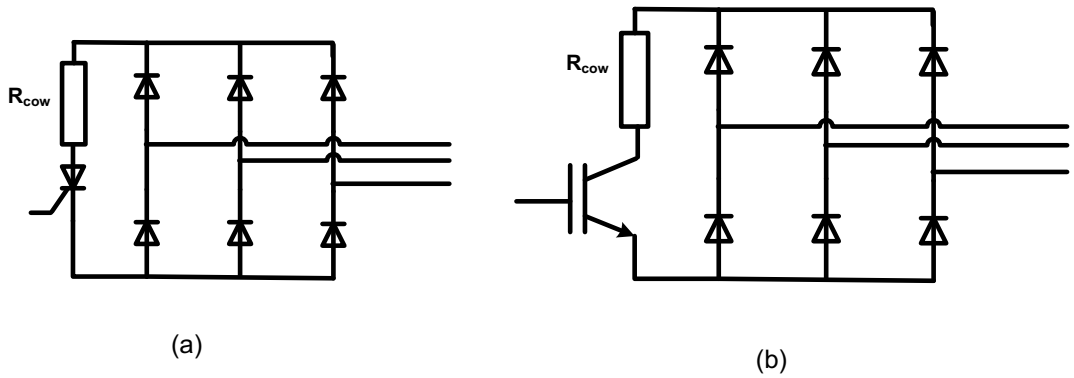

Figure 8-16: Crowbar circuits: (a) passive (b) active [172].

8.4.4 Power Electronics in Wind Turbine Type 4

As shown in Figure 8-17, wind turbine type 4 can be designed in different ways. Squirrel cage induction generator (SCIG) or wound rotor synchronous generator (WRSG) could be adopted and attached to the turbine shaft via a gearbox system as illustrated in Figure 8-17 a and b. The generators such as PMSG and WRSG can also be connected directly to the turbine shaft without the need of using a gearbox as shown in Figure 8-17c and d. Furthermore, as shown in Figure 8-17 b and c, the wound rotor synchronous generator (WRSG) requires an additional small AC to DC converter in order to supply the excitation winding for field excitation. The generator is connected to the power grid using an AC-DC-AC power electronic converter, with the same rating as the electric generator. Since the generator is disconnected from the grid, it can work in a wide frequency range for optimum performance. The PWM converter can be used on the grid side for independent control of the active and reactive power supplied to

the grid and also for providing the grid some supporting features such as power factor and voltage regulation. Consequently, the dynamic response of wind turbines of type 4 is improved as compared to other types of wind turbines. The AC -DC -AC converters illustrated in Figure 8-13 can be utilized to obtain full control over the active and reactive power of the generators through the bidirectional back to back PWM VSC. The WRSG and PMSG types require only a basic bridge rectifier in the generator side converter, as shown in Figure 8-18. For a three-phase network, the required rectifier requires only 6 diodes. Despite the rectifier circuit is simple and inexpensive, the active and the reactive power components cannot be controlled. The wind turbine with an SG must also be configured with a boost DC-DC converter integrated between the bridge rectifier and the DC link for variable speed operation, as depicted in Figure 8-18. Additionally, it is worth noting that the matrix based converter like the one shown in Figure 8-15 can be used to instead of the AC–DC–AC converter type 4 wind turbine systems.

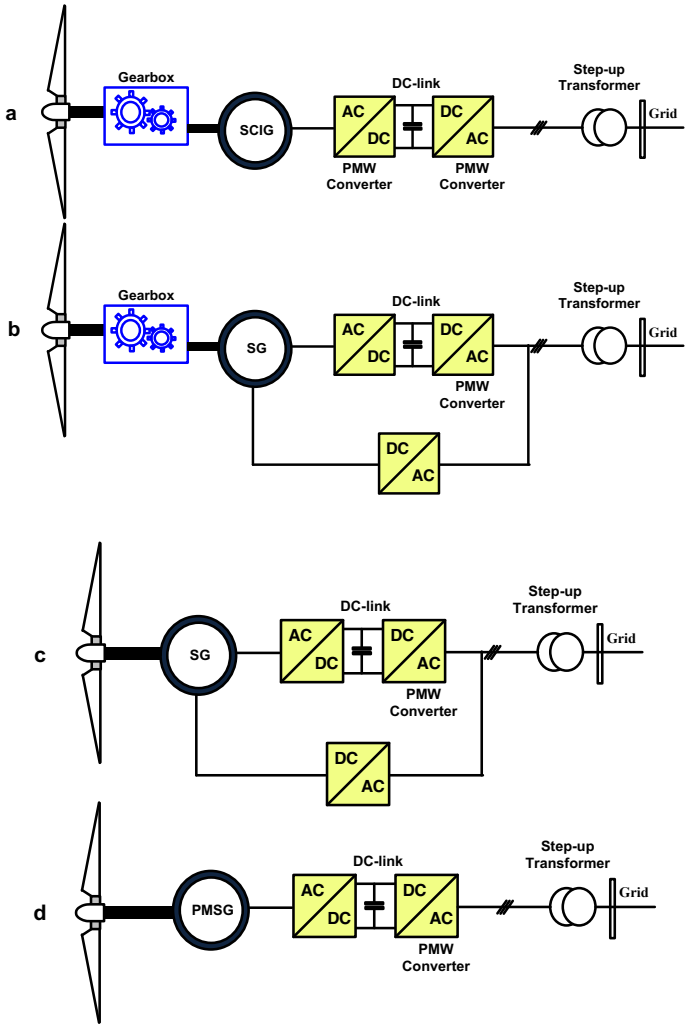

Figure 8-17: Various arrangements of wind turbine type 4 using : (a) SCIG with gearbox; (b) wound-rotor SG with gearbox; (c) wound-rotor SG using large number of poles; (d) PMSG without gearbox [172].

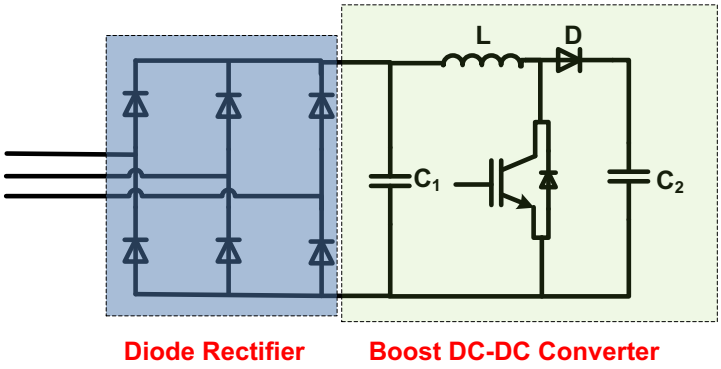

Figure 8-18: Schematic diagram of power electronic system used in wind turbine type 4 [172].

9 Wind Turbines operation and Control

Author(s): Dr Efterpi Nikitidou
Dr Andreas Kazantzidis

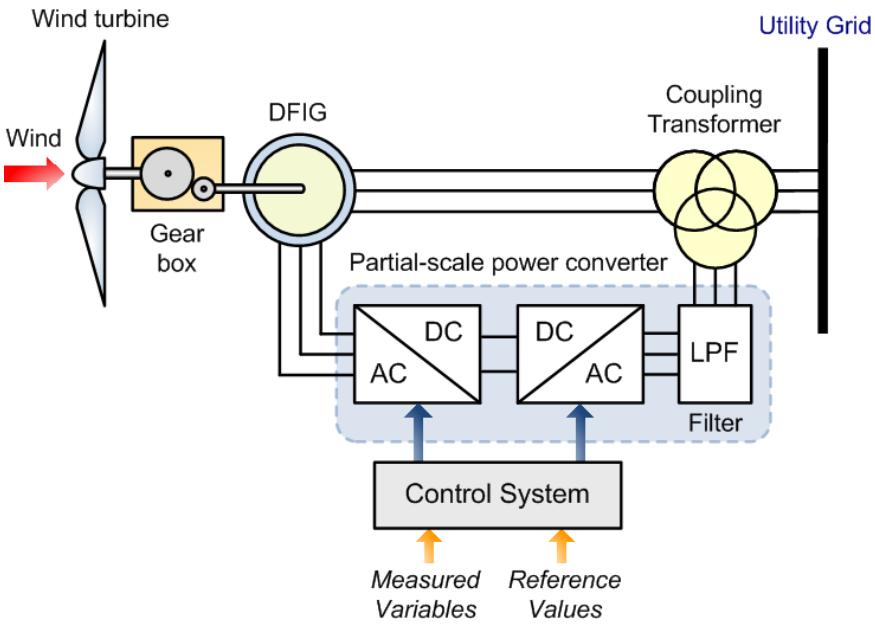

9.1 Wind resource

The source of the wind's energy is the Sun since the formation of winds is a result of pressure differences in the surface of the Earth from its uneven heating by the Sun. Locations near the equator of the Earth absorb more solar energy than areas in the Earth's poles. As a result, convective cells are formed in the troposphere and air rises from the hotter area of the equator, travels in the atmosphere and sinks in the cooler areas of the poles. This air circulation is affected by the Earth's rotation as well as seasonal variations in solar energy.

The heat transfer to the troposphere presents spatial variations that cause pressure variations, forcing the air to move from high pressure areas to low pressure areas. In the vertical direction, a pressure gradient force exists but it's mainly neutralized by the gravitational force directed downward. As a result, the winds appear mainly in the horizontal plane, caused by horizontal pressure gradients. The wind is also affected by other forces that try to mix air masses of different temperature and pressure, the air's inertia as well as friction in the surface which causes turbulence. Figure 9-1 shows the main horizontal surface wind patterns that take place in our planet, as air moves from high pressure areas to low pressure areas. These winds are deflected to the right and to the left, in the Northern and Southern Hemisphere, respectively, due to Earth's rotation. Tropical easterly trade winds are evident in latitudes between 0° and 30°, prevailing westerlies are found in latitudes between 30° and 60° and polar easterlies take place in high latitudes above 60°.

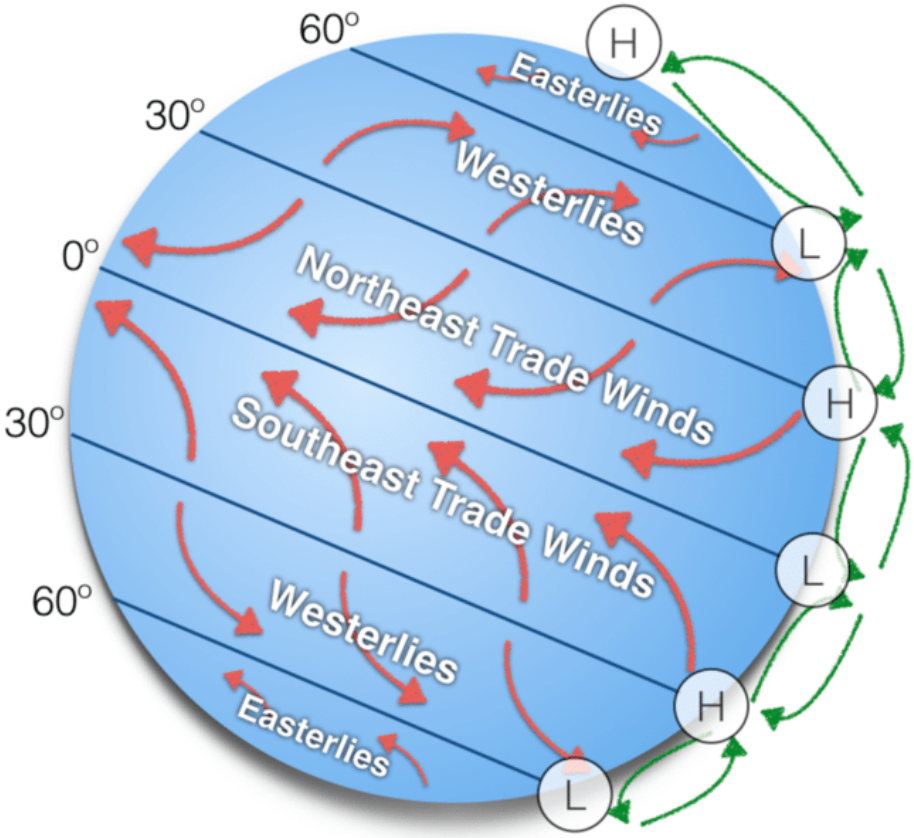

Figure 9-1: Horizontal surface wind circulation patterns. [173]

Atmospheric motions and wind speeds present variations in time and space that affect the amount of available wind power. These variations should be taken into account when calculating the wind resource and the suitability of a location for wind power applications. Wind speed varies with time and these variations can be of different scales. Inter-annual variations describe changes in wind speed that are observed in time periods greater than a year. These variations are very important when calculating long term wind production, therefore they need to be taken into account. This is usually achieved by studying wind data at a given location, going back two or three decades, in order to have reliable calculations of average annual wind speeds at the location of the wind power installation.

Annual variations include changes in the seasonal and monthly values of wind speed that are very common in the majority of locations around the world. Different locations present maximum wind speeds at different times during the year and these may change from year to

year. Figure 9-2 presents the seasonal variations in wind speed and direction in two locations of the Aegean and Ionian Seas in Greece, which were derived from monthly mean data of several years. Karpathian Sea in the Aegean shows winds prevailing in the directions between 270° and 305° that have maximum speeds during summer, while the location in Ionian Sea have winds in the directions between 200° and 360° that have minimum speeds during late spring-early autumn. Another example is shown in Figure 9-3, which presents the monthly median wind plant capacity factors in areas of the USA (only facilities with net summer capacity of 1 MW and above are included), from the years 2001-2013, which are related to the available wind resource or the average wind speed of the location. It is obvious that the seasonal patterns can vary between different locations and regions.

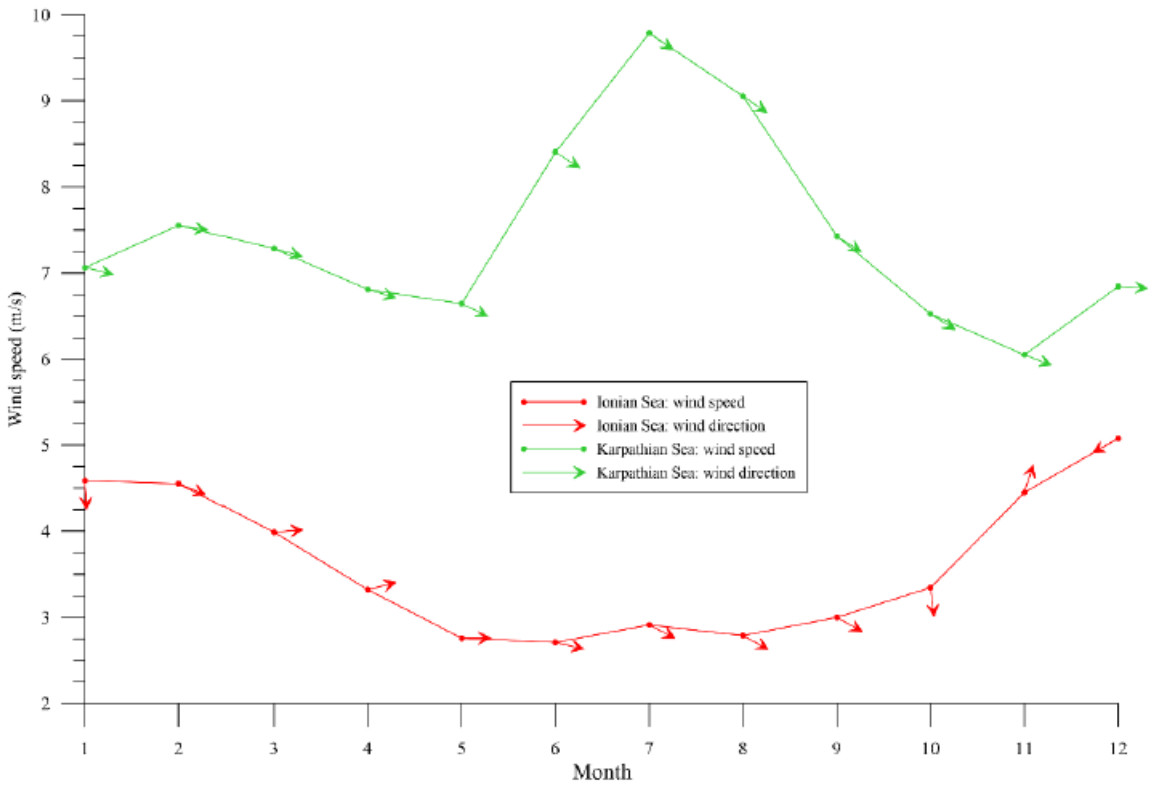

Figure 9-2: Seasonal variations of wind speed and wind direction in locations of the Aegean and Ionian Seas. [174] Licensed under CC BY 4.0

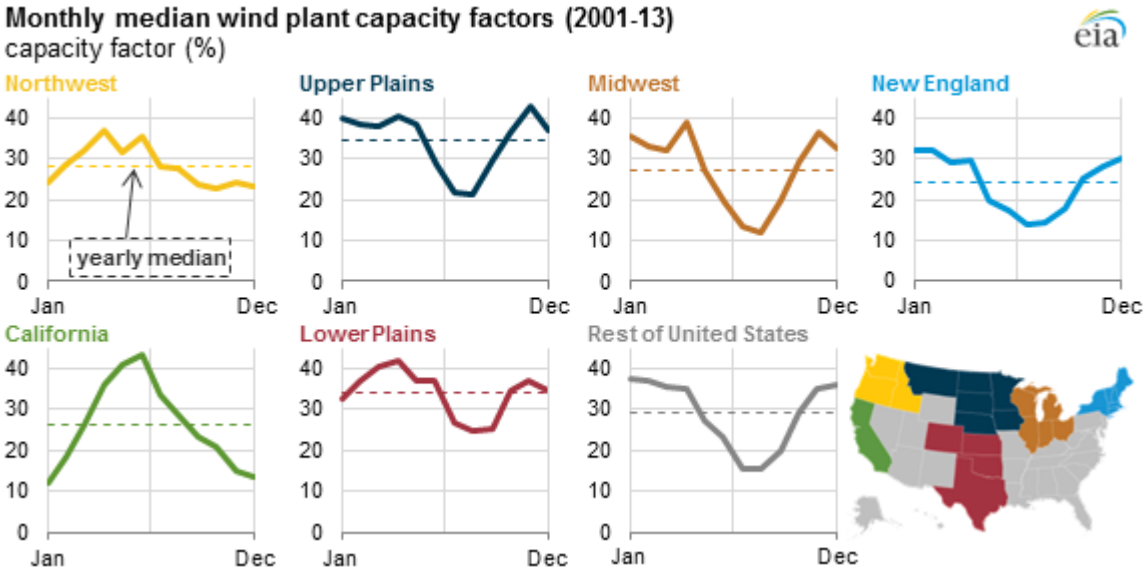

Figure 9-3: Monthly median wind plant capacity factors, for 2001-2013. [175]

Other variations of different time scale on the wind speed are the diurnal variations, those that occur during the course of a day. These are caused by the difference in surface heating by the Sun during the day. Typically the wind speed increases during the day and is decreased when the Sun is absent. Short-term variations in wind speed are another type of variations that include turbulence and gusts. Short-term variations mean that the speed of wind can change in time intervals of minutes. Turbulence involves variations that occur in time intervals of less than a second up to ten minutes and have a stochastic nature. A gust is an event that occurs within a turbulent wind field and is described by the amplitude, the rise time, the maximum gust variation and the lapse time.

Wind speed also presents spatial variations, due to the different topographical and surface characteristics that each location has. Figure 9-4 shows the map of the USA, where the annual average wind speed at 80 meters above surface level is depicted. Central continental areas present higher values than areas in the east and western parts of the country.

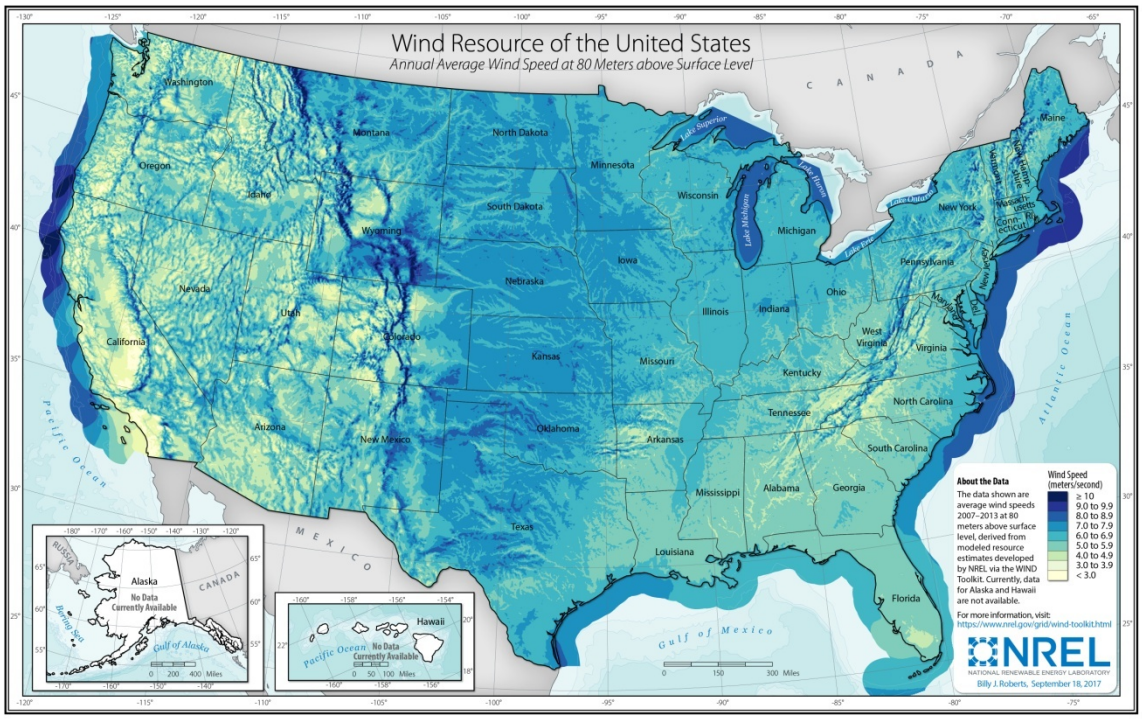

Figure 9-4: Annual average wind speed at 80m above surface level in the USA. [176]

Apart from wind speed, wind direction also changes in the same time scales that wind speed does. These changes need to be taken into account as well, since they affect the rotation of wind turbines and thus the available wind power.

9.1.1 Wind resource estimations

The mass flow rate of air is given by Equation 6-3 as a function of the area A through which the air flows, the air density ρ and the wind speed u.

$$\frac{dm}{dt} = \rho * A * u \qquad \textit{Equation 9-1}$$

The kinetic energy per unit of time (power P), of the air flowing through the surface A is given as:

$$P = \frac{1}{2} * \frac{dm}{dt} * u^2 = \frac{1}{2} * \rho * A * u^3$$ *Equation 9-2*

The wind power density is therefore equal to:

$$\frac{P}{A} = \frac{1}{2} * \rho * u^3$$ *Equation 9-3*

So as it can be seen, the wind power is proportional to the third power of the wind speed. Knowledge of annual average values of wind speed in an area can be used to provide wind power density maps for that area. Based on wind speed data and the efficiency of different types of wind turbines, maps of the wind power density potential can be provided for regions or countries. Figure 9-5 presents a global map of wind power density potential at 100m, which has been developed by the Technical University of Denmark in partnership with the World Bank. These maps can help identify the areas where wind power installations could prove efficient, before taking more precise and detailed measurements of the desired site. Apart from the wind atlas method, the wind resource assessment for an area can be produced based on data taken from measurements only, data derived from mesoscale/microscale modelling or combinations of the above.

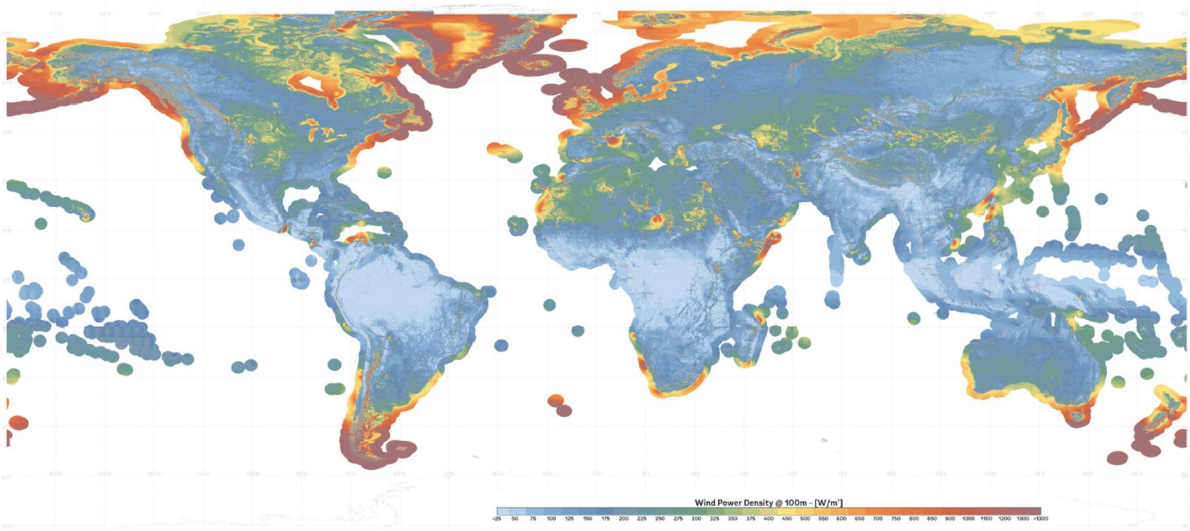

Figure 9-5: Wind power density potential. [25] Licensed under CC BY 4.0

9.1.2 Wind forecasting

Wind power plays an important part in the renewable energy production and its integration with the electricity supply system is vital. This integration however needs to take into account the specific characteristics of wind power which is an intermittent source. Wind power generation depends on the availability of wind and it can't be supplied depending on demand, like power generated from fossil fuels for example. The wind power output presents fluctuations depending on the wind. That is the reason why wind forecasting is so important if one is to integrate wind power to the utility grid.

Wind power forecasting can be achieved with various methods and for various time-scales. The categories for the time horizon of the forecast are four. Ultra-short-term forecasting usually includes forecasts from a few minutes up to one hour ahead. Short-term forecasting is from one hour to several hours ahead. Medium-term forecasting covers several hours up to around one week ahead and long-term forecasting includes forecasts from one week up to several months or longer ahead.

One of the forecasting methods used is the persistence method. The persistence method assumes that the wind speed or power at a certain time in the future will be the same as the speed or power in the present time. So measuring the wind speed and calculating wind power from the measurements will also provide the data for the desired time in the future. This method is most accurate when used for ultra-short-term forecasting and as expected it degrades as the time horizon of the forecast increases. It is the simplest forecasting method and the one with the lowest cost.

The physical approach is another method for forecasting. Physical methods use parameterizations based on a detailed atmospheric physical description with the purpose of converting wind to power. This approach includes various models describing the different physical processes that take place, like the wind conditions and the shading effects at the location of the wind farm, the power curve of the turbine and others. Numerical Weather Prediction (NWP) models provide weather forecasts that are used as input in physical wind power forecast models. Meteorological measurements and observations provided by weather stations, meteorologists and satellites are used as input in the NWP model, which

then calculates the future state of the atmosphere based on weather physical laws. NWP models are run on supercomputers due to the amount of computations they require and as a result they are only run once or twice a day. Existing physical systems for wind power forecasting, use NWP wind forecasts as input data. This type of forecast is useful for medium to long-term forecasts.

Statistical methods make use of previous wind data to perform forecast for the next few hours. They use the difference between the predicted and the measured data for wind speeds in the immediate past to adjust model parameters and make accurate future predictions. The advantages of this approach are that it's easy to model and inexpensive. It is suitable for short-term forecasts and prediction error increases with forecasting time. Statistical methods include time-series based models and neural network (NN) methods. Popular types of time-series based models are the Auto-Regressive Moving Average (ARMA) models and the Auto-Regressive Integrated Moving Average (ARIMA) models. NNs use past data covering long time periods, for training, in order to learn the relationships between input and output data, e.g. wind speeds. They include an input layer, where historical data are used for training, a hidden layer and an output layer that provides the forecasts.

Apart from these forecasting methods, combinations of different approaches can also be used for wind power forecasting. Physical approaches can be combined with statistical approaches for example or short-term and medium-term models can be combined etc. These are referred to as hybrid forecasting methods. Hybrid methods can maximize the information that is available by integrating individual model information and thus exploit the advantages of several forecasting methods to improve the accuracy of predictions.

Attention needs to be given to the relationship of wind power with wind speed. As it can be seen from Equation 9-3, the wind power P and the wind speed u through the area A that is swept by the turbine, have a cubic relationship. That means that any error in the forecast of wind speed will give a much larger error (cubic) in the forecast of wind power. This is even more complicated in a wind farm, where various types of turbines may operate, each of which may use various wind directions and speeds. All this information needs to be taken account to achieve an accurate wind power forecast.

9.2 Wind turbine monitoring systems

Wind turbine systems have considerable costs, an important part of which is the regular maintenance that is being done for the proper operation of the turbine. Apart from that though, various malfunctions that occur occasionally can add up important amounts to the overall cost of the system. Depending on the nature of the malfunction and the turbine component that it affects, the expenses can be high and the wind power production can be compromised. For that reason, it is vital to have a systematic checking of the system components.

There are different types of maintenance strategies, as it can be seen in Figure 9-6. Corrective maintenance is implemented after the component failure. Preventive maintenance can be pre-determined or condition-based. Pre-determined maintenance or time-based maintenance refers to maintenance in fixed time intervals, although this type may also not be able to catch the failure in its beginning and thus save costs. Condition-based maintenance (CBM), or else predictive maintenance, is based on data that is collected by condition monitoring systems (CMS).

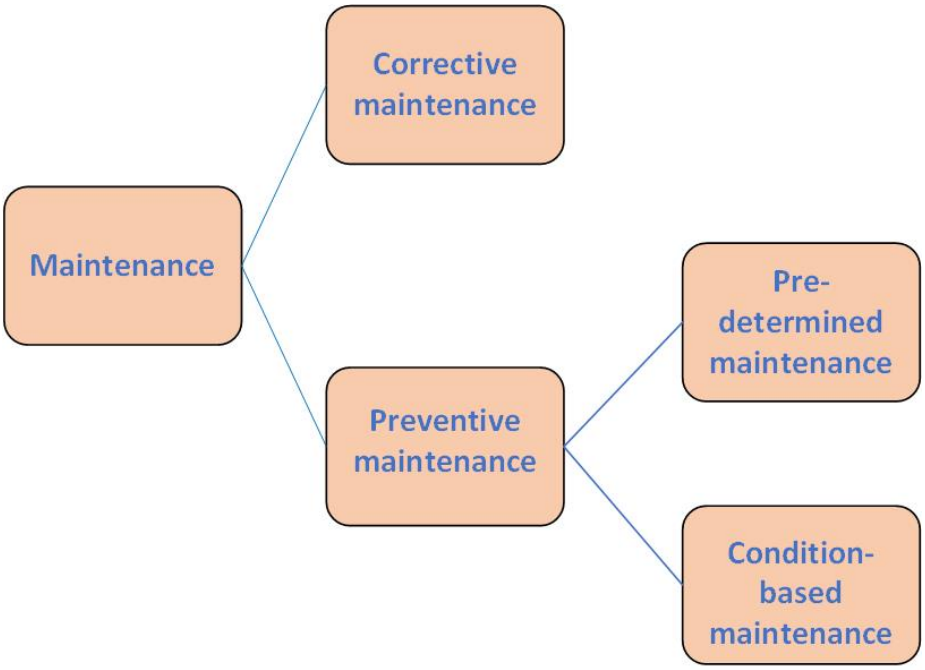

Figure 9-6: The maintenance strategies based on the European Standard EN 13306. [177]

A CMS can provide information regarding the condition of a turbine component and can detect a component failure that is on the verge of occurring. The implementation of a CMS aids in the detection of any degradations and faults in advance, by using condition monitoring (CM) techniques. CM can be achieved offline, in which case it is based on regular measurements and inspections, as well as online, which involves the installation of monitoring equipment. Figure 9-7 shows the main components of a wind turbine. CM can be used for most of the turbine components and when involving the monitoring of structural components, like support structure or blades, it is usually called structural health monitoring (SHM).

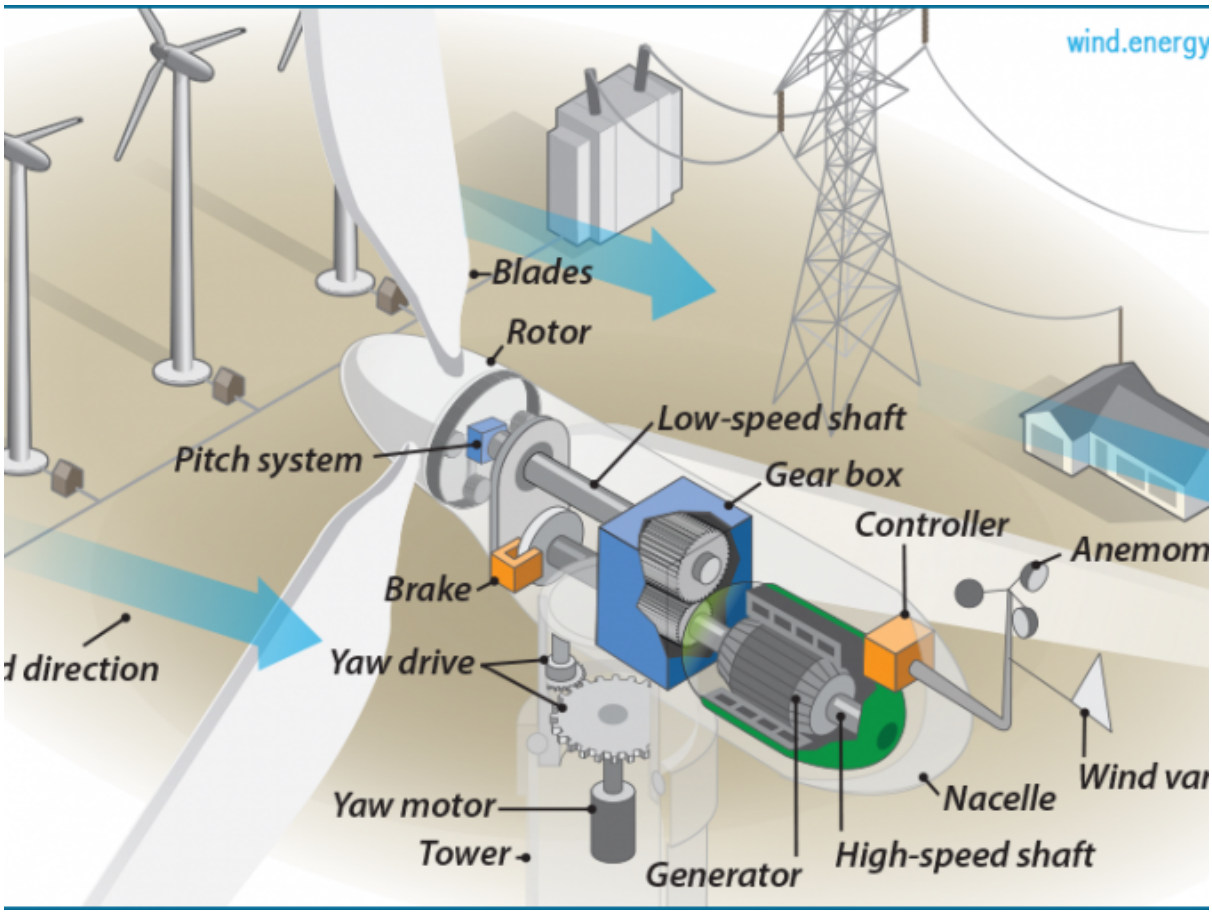

Figure 9-7: Main components of a wind turbine. [178] License: Public Domain

9.2.1 Monitoring techniques

Commercial CMS for wind turbines are usually vibration-based systems. These systems monitor the rotating drivetrain components, which include the main bearing, gearbox, generator bearings and sometimes the tower oscillations. Vibration-based CMS is the standard equipment for a wind turbine system. However as the technology of installations progresses, wind turbines grow larger and locations are more remote, more component monitoring is required. Other monitoring systems that are available on a commercial basis are particle-counting systems for the gearbox oil, as well as SHM systems for the rotor blades and support structures.

9.2.1.1 Vibration analysis

Vibration-based monitoring systems rely on the fact that the majority of failures in rotating components results in vibration effects that can be detected. Depending on each mechanical component problem, a different vibration pattern emerges. To find the turbine component that corresponds to the vibration detected, the time waveform of the vibration signal is decomposed to its spectral components and the characteristic frequencies that are produced in the resulting spectrum are associated with the corresponding faulty component. The sensors used in a vibration-based CMS are position transducers, velocity sensors, accelerometers and spectral emission energy sensors, which are used in low, middle, high and very high frequency ranges, respectively.

The signal can be processed with various methods, which can be time-domain or frequency-domain analysis methods. Time-domain analysis methods include statistical methods and time-synchronous averaging among others and frequency-domain analysis methods include for example Fast-Fourier Transform and spectrum analysis. Figure 9-8 shows an example of the progress of a mechanical failure and how vibration analysis can detect it months before the actual breakdown of the component. Vibration analysis can be applied to turbine components such as gearboxes, bearings, shafts and blades.

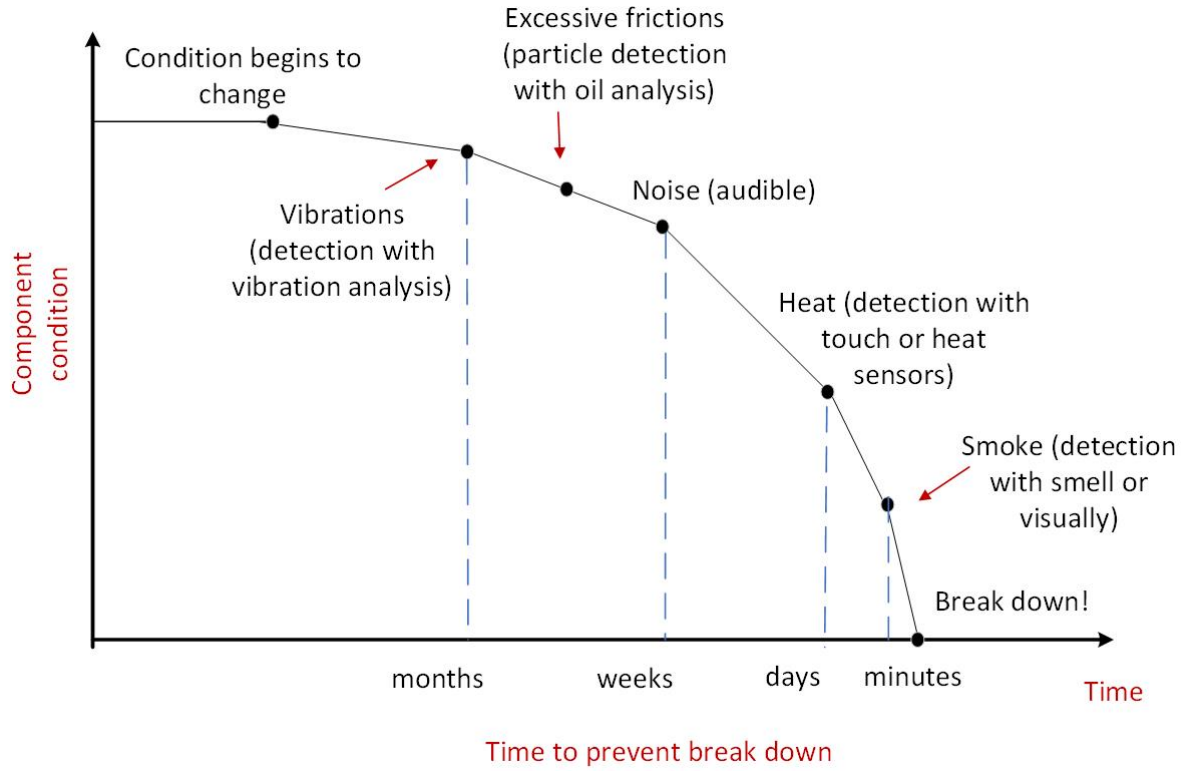

Figure 9-8: Depiction of the progress of a mechanical failure. [179]

9.2.1.2 Oil analysis

The monitoring of the oil condition is performed on the gearboxes of the wind turbine. The oil properties are monitored so that the lubricant quality is assessed and the filter system is checked in terms of its effectiveness. This ensures that a need for an oil change can be detected and performed on time. Apart from that, monitoring of the oil condition can give information regarding, for example, the wear debris, so that faults in the components of the gearbox can be detected. Oil is usually pumped through the component in a system that is characterized as a closed-loop and a filter is used to catch the metal debris from cracks in the gearbox components. Testing the amount of that debris and its type provides information regarding the condition of the component.

There are several tests performed in an oil analysis. These include analysis of the viscosity and oxidation, the water or acid content, temperature, machine wear and particle count analysis. The sensor for particle counting can monitor the wear debris production, where large particles (>50µm) are detected that indicate faults in the gearbox, while sensors for particle

concentration can monitor the level of cleanliness of the oil. The oil monitoring techniques can be of two types: online real-time monitoring or offline oil analysis. Offline analysis is performed by taking oil samples, while online monitoring is advised in situations where locations are remote or applications are such that involve the rapid development of failures. For online monitoring, several sensors are installed in the lubrication loop of the gearbox and the analysis can be performed with electromagnetic sensing, pressure-drop sensing or optical debris sensing. Oil analysis is the method used for the detection of cracks in the gearbox but it is rather expensive, when used for online real-time monitoring, so usually the monitoring of the oil condition is performed with oil samples analysis.

9.2.1.3 Structural health monitoring

SHM systems are used for the monitoring of the condition of rotor blades and support structures. Apart from vibration-based techniques, which are commonly used for blade condition monitoring, strain measurement is a technique that becomes increasingly important for load monitoring in rotor blades and damage detection. Strain measurement involves the installation of foil strain gauges or fibre-optical strain gauges in parts of the blade that are critical. The number of sensors that are installed has to be high so that small damages can be detected.

Deflection-based techniques are another way of monitoring the condition of rotor blades, an example of which is laser technology. When other parameters of the turbine are taken into account, like the wind speed, pitch angle and rotor speed, deflection can be used to monitor changes in the bending stiffness of the blade. The behavior of the blade is compared to the one that has been recorded in the past and the behavior of the other blades, in order to detect changes that could be associated with icing or damages.

Optical fiber monitoring is another method for SHM of the wind turbine. It involves the installation of several sensors in the turbine blade. These sensors take measurements of various parameters, like the strain measurement as mentioned above, the temperature to detect cases of over-heating, the acceleration to monitor the pitch angle and position of the motor, measurements for crack detection as well as lighting detection. Optical fiber sensors are expensive though and increase the complexity of the monitoring system since they need

to be mounted on the surface or installed inside the body of the turbine. Future technological improvements are expected to reduce the costs.

Onshore and offshore support structures, like towers and foundations, also incorporate SHM systems to detect damages, which may be rare but have very high costs when they occur. For monitoring of onshore and offshore support structures, various types of sensors can be used, like strain gauges, optical fibre sensors, displacement or temperature sensors, accelerometers etc. The methods for SHM can be of local or global approach. Local approaches present a dependence on the structure that they monitor and they include fatigue monitoring, scour and grouted-joints monitoring, splash-zone and corrosion monitoring. Vibration-based approaches are considered as global approaches and aim to detect faults that cause changes to the modal parameters of the turbine structure. SHS systems for monitoring of onshore and offshore support structures are under continuous research and development work.

9.2.1.4 Acoustic emissions

Acoustic emissions based monitoring can be applied to bearing, gearboxes, blades and shafts. This technique is based on the fact that developing damages in the turbine components, such as cracking or debonding, will release energy, taking the form of transitory elastic waves inside the material. In contrast with vibration-based methods, acoustic emission analysis can be used to detect faults in high-frequency vibrations, from 50 kHz up to 1 MHz. The parameters that are usually measured include the amplitude, root mean square value, energy, kurtosis and crest factor. Acoustic emissions monitoring can be performed by using piezoelectric transducers or optic fiber sensors. The disadvantage of this technique is the high cost and in order for it to detect small damages, a high number of sensors is required.

9.2.1.5 Temperature measurement and thermography

Monitoring the turbine components temperature is a very common method of fault detecting. It can give information regarding the development process of a failure, which can occur due to mechanical friction because of damaged bearings or gears, insufficient lubricant

properties or faulty electrical connections. Temperature monitoring can be applied to the turbine bearings, fluids, generator etc. The sensors that are used for that purpose include resistant thermometers, optical pyrometers and thermocouples. It is a reliable technique, since the components usually have a limited temperature range in which they operate successfully, thus unexpected temperature changes can point to component failure with high certainty. The problem is that the detection of faults can't usually be achieved at an early stage since temperature develops slowly.

Thermography analysis on the other hand monitors changes in the heat emitted by the turbine components to detect developing faults. It uses infrared (IR) temperature emitters and high-resolution IR cameras. It can be applied to gearboxes, bearings, motors, generators etc. Like temperature measurement, it can't detect early faults and the major disadvantage of this technique is the high cost due to the expensive sensors that it requires.

9.2.1.6 Other monitoring techniques

Ultrasonic testing is a potentially effective tool that can detect early faults in a wind turbine blade or tower. It is based on elastic wave propagation and reflection within the material and it can estimate the location of the failure as well as the nature of it. However it requires methods for scanning the individual components.

Other monitoring techniques that are either in a development phase or very expensive to be commercially used, include shaft torque and torsional vibration measurement, radiographic inspection, electromechanical-parameter based monitoring and shock pulse methods.

9.2.2 SCADA

Nearly all wind turbines nowadays incorporate a supervisory control and data acquisition (SCADA) system in order to record the operating and environmental conditions. SCADA collects data from the system and sends them to a central computer for monitoring and control purposes. It collects data with the use of sensors, incorporated in the wind turbine system, like anemometers, thermocouples or switches, in 10-minute intervals. Depending on the type of wind turbine and its manufacture, the data that are recorded can differ between

wind turbine systems but the minimum data that are collected in each case are: wind speed and direction, active and reactive power, ambient temperature, pitch angle and rotational speed. Figure 9-9 shows a basic schematic of a SCADA system incorporated in a wind farm.

Apart from these parameters, in modern wind turbines, the SCADA system can collect a high number of signals, like temperature measurements from various components of the turbine such as the gearbox, the lubrication system, the generator and the nacelle. Turbine and generator shaft speeds and generator currents and voltages can be recorded as well. Apart from the 10-minute average values, other parameters can be included such as minimum and maximum value or standard deviation. All these data are available to the operator to monitor the turbine operation.

There has been investigation into the usage of SCADA for CM of the wind turbines and there are turbine operators using SCADA for such a purpose, as it is a cheap solution and can provide information to the operator regarding the turbine performance. SCADA data can be used for CM with the use of signal trending, artificial neural networks (ANN) or physical models. Signal trending focuses on the comparison of SCADA data with data received from other turbines under similar conditions. ANN and physical models focus on the modeling of normal turbine operation behavior, by using historical data of time periods when the turbine was sure to operate successfully. SCADA data are used as input to predict the values of the desired parameters and identify any deviations. However, SCADA systems used for CM can't replace the professional CM systems for wind turbines, designed for that specific reason. The SCADA system doesn't collect all the necessary signals to fully perform CM and they are also collected at a low sampling frequency. Another issue is the 10-minute time interval, which is too slow to effectively detect the majority of rotating machine faults.

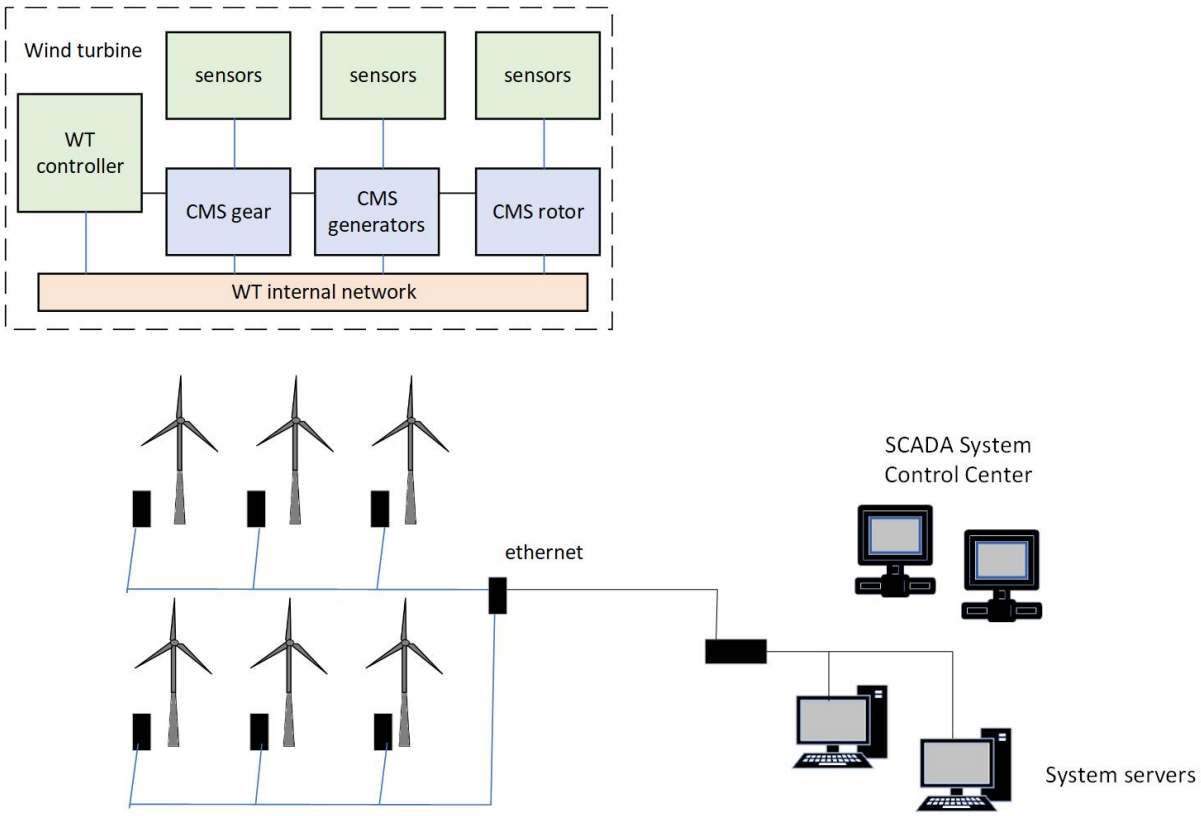

Figure 9-9: Schematic of a SCADA system incorporated in a wind farm. [180]

9.2.3 Future CMS requirements

As technology improves and the number of installations of wind turbines for power production increases, CMS become more vital for their successful and viable operation. CMS need further improvements to address modern issues of wind turbine installations. Many wind turbines are located in remote onshore locations or offshore, making them difficult to access throughout the year for regular monitoring and maintenance. Automated CMS are used for monitoring of the turbine components and detection of any occurring faults. However, due to the difficulty of accessing the turbines location, especially in harsh weather conditions, CMS must be very reliable in their predictions and detections of faults, as the repair or replacement of a component under such conditions can have a great economic cost. CMS therefore must be further improved to increase their accuracy in their predictions.

Another issue is the fact that wind turbines have various technological configurations in their components therefore different CM techniques are required. Commercial CMS are usually based on vibration analysis, due to the high costs that failures in gearboxes can have. However

different types of wind turbines can present faults in other components, which can't be monitored based on vibration analysis. As a result the new CMS should be able to address all wind turbines of various technologies and be able to detect various faults. The size of a wind turbine also plays an important part, since surveys have shown that larger turbines are subject to more faults than smaller ones, most likely due to the higher complexity of their design and the parameters of their operation. These faults would also have higher economical costs. This should also be taken into account in new CMS.

Technological improvements in the design of wind turbines mean that new more complicated control systems will be used. Electrical and electronic components are usually more sensitive and more often susceptible to failures, compared to mechanical components. New CMS should have to improve their predictions regarding electrical and electronic faults, which are now not so successfully monitored as mechanical faults. Last but not least, new CMS should not only be more reliable but also cost-effective, since new wind farm projects become larger and larger, incorporating hundreds of wind turbines, which in turn require higher numbers of CMS, increasing the overall cost of the system significantly.

9.3 Balance of plant

Balance of plant, in a wind turbine infrastructure, refers to the number of all other components, except the turbine, that are required in order to transfer the power from the wind turbine to the electric grid. Balance of plant is used to address all the other aspects of a wind power plant except the turbine itself. The most important of these aspects are described in the following.

Foundations are a key component of a wind turbine infrastructure. Wind turbines are very tall in their design and the foundations are a critical element, both in terms of costs as well as materials, in a wind turbine project. The foundations in a structure have the purpose of transferring the vertical load to the ground. When wind turbines are considered, the main issue is that the wind interacts with force with the turbine rotor, which is located at the top of the tower and there is a danger of knocking the turbine over. In the case of wind turbines, there are large moment loads being applied to the foundations. Therefore it is vital to make sure that the foundations are designed to address this issue. Each wind turbine manufacturer

usually has its own preferred type of foundation but the two types that are most often used are the gravity and the pile reinforced type. A turbine foundation is basically a mass of concrete and reinforcement that is cast in such a way as to connect with the tower of the turbine. It is made of concrete (gravel, sand, cement), reinforcement (steel) and a can or basket assembly. Figure 9-10 shows the gravity based foundation for an onshore wind turbine at Toddleburn wind farm, UK, which is the most common onshore type.

Figure 9-10: Onshore wind turbine foundation at Toddleburn wind farm, UK. [181] Licensed under CC BY-SA 2.0

The turbine foundations must be strong enough to provide the necessary base support for the rest of the turbine components that will be installed above it. The foundation quality is one of the most important aspects in the manufacturing of a wind turbine project and it needs to be done with the outmost care. Cement pouring must be done with extreme cautious so that surface or thermal cracking is avoided and the foundation can meet the quality and standard requirements. Figure 9-11 and Figure 9-12 show the types of foundations for offshore wind turbines, installed into the seabed or floating, respectively, some of which are commercially available and others are designs under development. One of the most common

types of foundations for offshore wind turbines is the monopile, which is a single tubular steel pile, of a large diameter from 4 to 6 meters that is installed into the seabed, in a depth that is 5 to 6 times the pile's diameter. The structural support for the turbine is achieved through the cohesion of the soil and the friction created between the pile and soil.

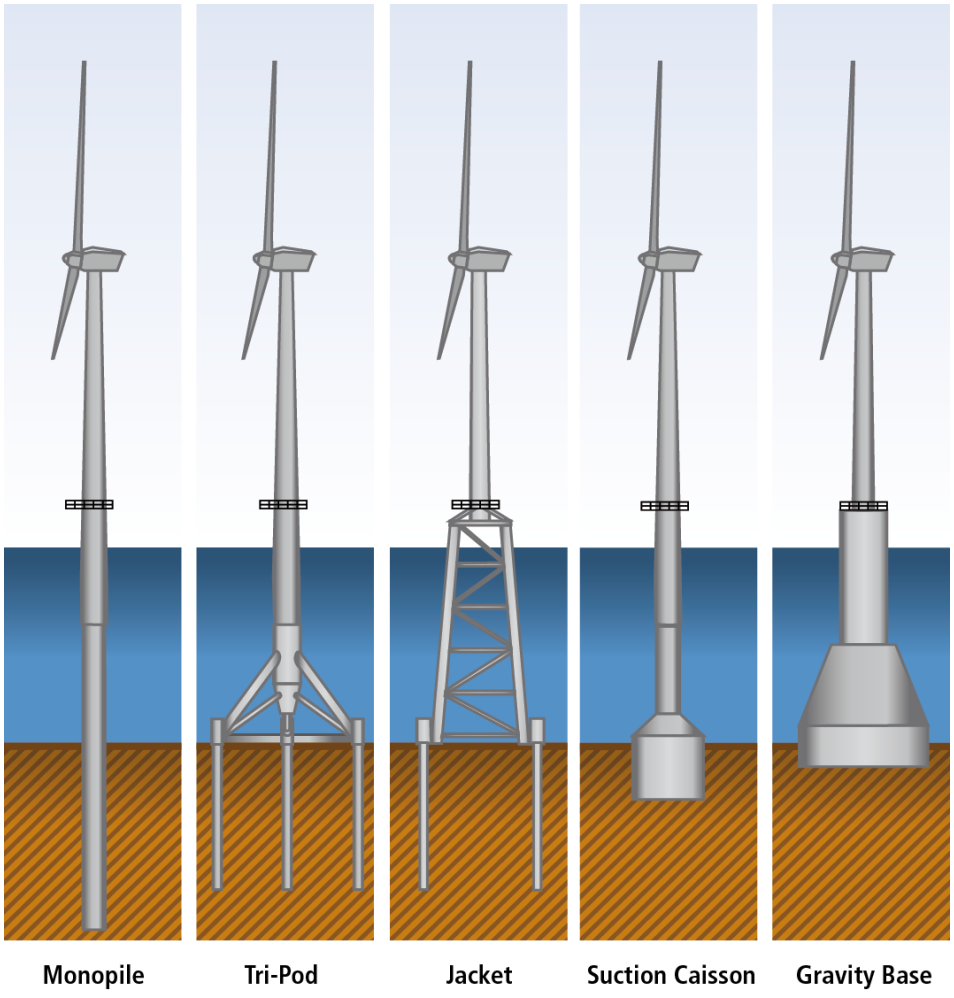

Figure 9-11: Types of offshore wind turbine foundations. [182]

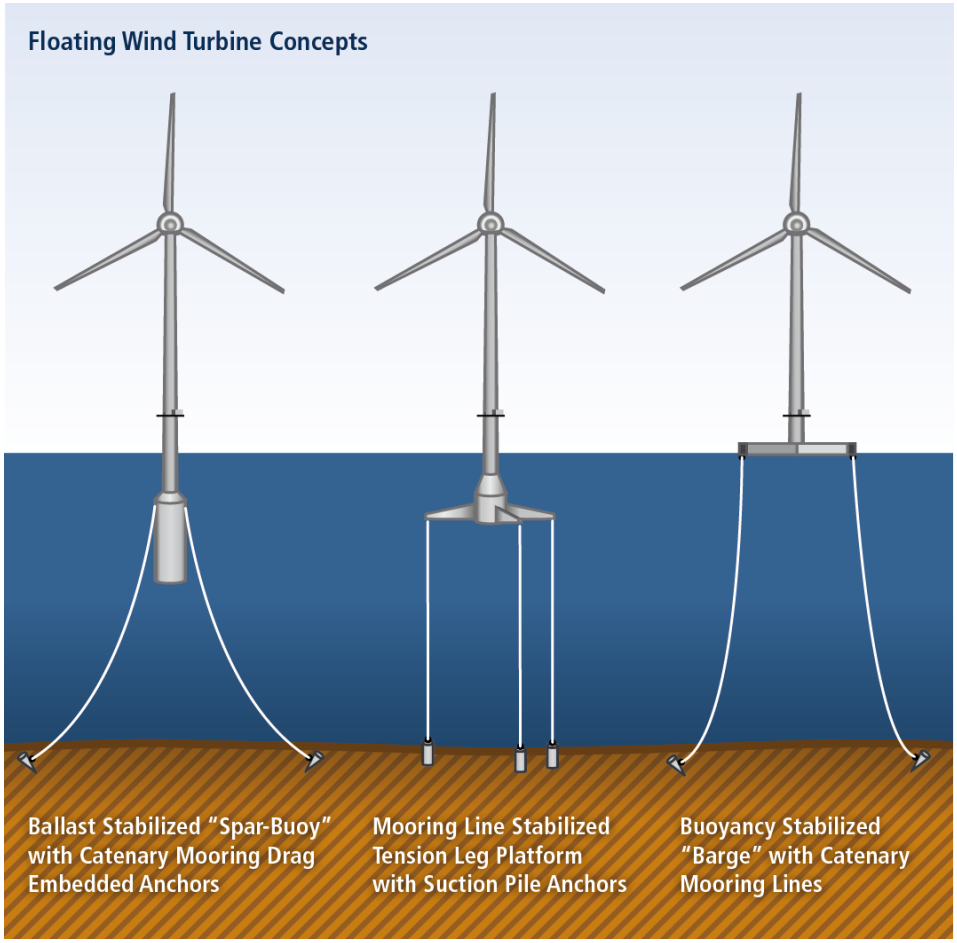

Figure 9-12: Types of offshore wind turbine floating foundations. [182]

Roads and infrastructure are another important aspect in a wind turbine project. Wind turbines are usually constructed in areas that are remote and far away from habitable locations. For that reason it is important for the turbine site to have quality roads that provide access to both people and machinery for the lifetime of the project. The roads should be strong enough to carry the heavy traffic that takes place during the construction of the project and be able to withstand all weather conditions. These roads are usually unpaved and they are made of compacted layers of crushed rock, gravel and a layer of polyethelene geogrid. They include site access roads that connect the site of the wind turbine project with the public road network and wind farm network roads, which are used to connect every turbine location with other structures of the wind farm, so that materials and equipment can be transported around the site at all times. There are general requirements regarding the construction of roads for a wind turbine project to ensure the safety and the efficient operation of the project.

The infrastructure of a wind farm includes a substation, a building for the purpose of housing electrical, safety and other operational equipment. There are required standards regarding the construction of the substation, from its foundations to its walls and roof, as well as the plumbing for cables. The electrical components in the substation usually include power protection systems, switchgear, electric meter etc. There is also usually an external transformer area with an earthed fencing.

The cable network is another important part of the whole wind turbine infrastructure. A cable network is used to transmit the generated power of each turbine to the substation. The cables are usually installed underground. Each cable, from turbine to substation, has a length around half a kilometer. Another set of cables is used to connect the substation with the closest distribution or transmission line. This is usually installed overhead because it's less expensive. The characteristics of the cables depend on the rated power from the wind farm and the transmission voltage on the downstream of the substation. The point of connection includes the commissioning of the required components in order to achieve the connection to the distribution network. These include switches, reinforcements, supports etc. The operation of the various systems at the point of connection can be contestable or non-contestable. The latter regards the security of the distribution line and it is delivered by the operator of the distribution network.

Another component of a wind farm is SCADA. As mentioned before, SCADA is the control system, helping the wind farm operators to monitor and control remote operations of the turbines and other systems in real time. Various parameters can be assessed in real time, like weather data and turbine operation parameters, like temperature and vibration. The cost of a SCADA system varies depending on the complexity of the system and the desired available information.

Transformers are used in wind turbines with the purpose of increasing the voltage of electricity that the turbines generate. Since the generated electricity has a low voltage and in order to limit the losses caused by electricity transmission, transformers are incorporated in the system. They are usually installed at base of the turbine to be more accessible, although when they are installed at the top, close to the generator, the transmission losses are reduced further. Each transformer has characteristics that are fixed depending on the rated power that is produced by the turbine, the level of voltage and the ratio of transformation. If the

transformers are supplied by the manufacturer of the turbines, they are not characterized as part of the balance of plant.

There are other various components of a wind farm that need to be taken into account and contribute to the overall cost of a project. These include transportation, several site facilities, costs for topographic survey and ground investigation and others.

9.4 Standards and technical specifications

Wind turbine standards refer to the design requirements that a turbine must have in order to be operational. These standards cover most of the aspects of the turbine life, which include instructions varying from the conditions that the location of the system must have to requirements regarding the turbine components. Technical specifications are another aspect providing guidelines about the turbine design, although these are characterized more like suggestions and recommendations rather than requirements like the turbine standards.

Wind turbine standards were first developed by each country but now the key body on the subject is the International Electrotechnical Commission (IEC), which began standardizing international certification in 1995. The key standard is IEC 61400, which is a set of design requirements to ensure the longevity and efficient operation of the turbine. These international standards can replace those set by national bodies, therefore helping lead the way to global certification. The most important standard is IEC 61400-1, developed in 2005, which focuses exclusively on the design requirements. It mostly refers to large onshore turbines but it can apply to small turbines or offshore applications also.

IEC 61400-2, first issued in 2005, deals with the safety requirements for small wind turbines. IEC 61400-3 (2008) refers to the design requirements for offshore wind turbines, that are not covered by IEC 61400-1 and involves issues regarding waves, ocean currents etc. IEC 61400-4, which was developed as a revision for the International Standard Organization ISO 81400-4, refers to the design requirements of turbines gearboxes, for turbines from 40kW to 2MW. IEC 61400-6 (2020) is concerned with the design requirements for the turbine tower and foundation. IEC 61400-11 TS is a technical specification from 2006 and refers to measurement techniques for acoustic emissions from turbines. IEC 61400-12 (2005) deals with

measurements of power performance for electricity producing turbines. IEC 61400-13 TS refers to measurements of mechanical loads. IEC 61400-14 refers to the apparent sound power levels and tonality of wind turbines, while IEC 61400-21 covers the power quality measurements, which are important for the electrical and electronic turbine components. IEC 61400-22 TS deals with conformity testing and certification of wind turbines. IEC 61400-23 TS is concerned with the full-scale structural testing of the turbine rotor blades. IEC 61400-24 TR is a technical report that refers to protection from lighting. IEC 61400-25 deals with communications for monitoring and control of the turbines. IEC 61400-26 TS refers to time-based and production-based availability for wind turbines and IEC 61400-27 is concerned with the electrical simulation models for wind turbines.

Other standards, which are used in USA to complement the standards for offshore wind turbines are ISO 19900 with general requirements, ISO 19902/19903 for fixed steel and concrete, respectively, offshore structures, ISO 19904 for floating offshore structures and API RP 2A-WSD (from the American Petroleum Institute) which is concerned with the recommended practice for planning, designing and constructing fixed offshore steel platforms. Figure 9-13 shows an example of the applicability of existing design standards for an offshore wind turbine. IEC standards are used to address the design of the wind turbine and load cases, while ISO and API standards are also needed for the substructure of the system.

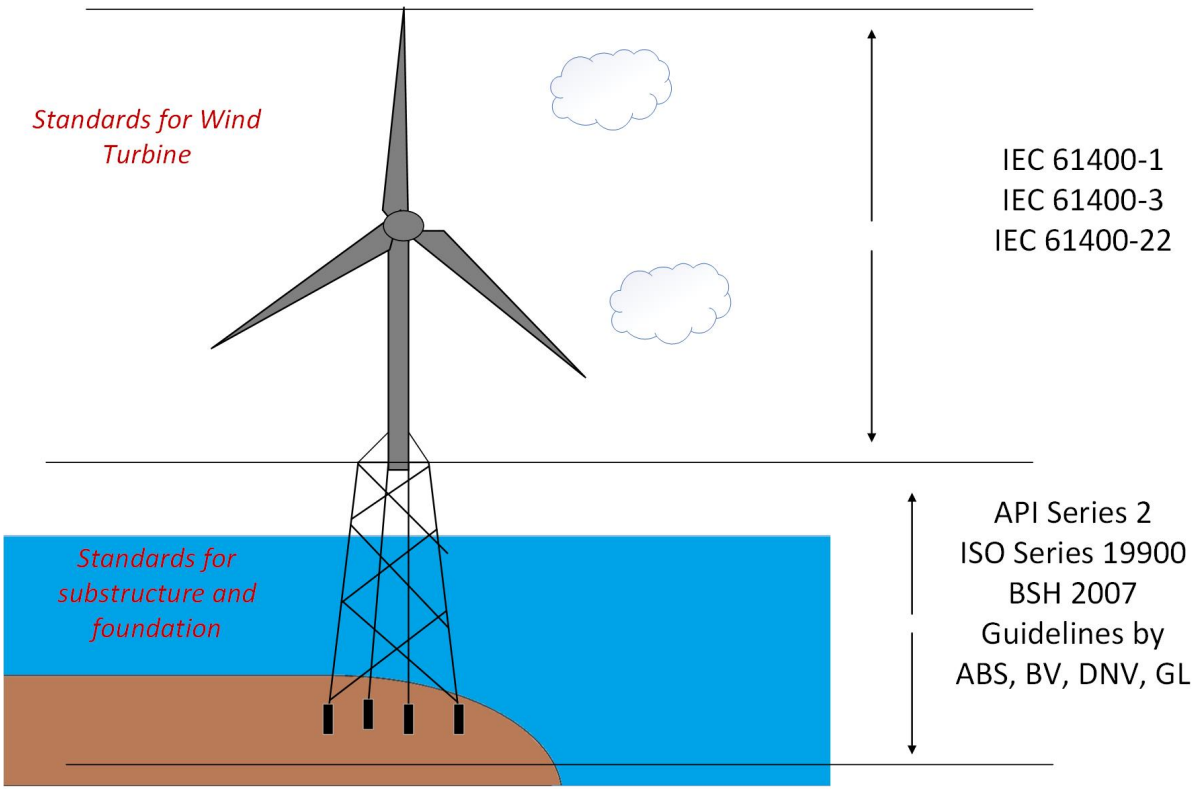

Figure 9-13: Example of the applicability of design standards for offshore wind turbines. [183]

10 Energy storage (1/2)

Author(s): Dr Stelios Ioannou
Dr Marios Raspopoulos

10.1 Abstract

Modern life, the way of living and even the world economies are dependent on electricity and energy. The usage of electricity extends from industrial applications (i.e. manufacturing) to residential (lighting, cooling, heating, etc), to transportation (street lights, electric trains, etc), telecommunications (satellite, wired and wireless), entertainment and the list keeps growing longer. Using layman terms, electricity is the supply of electric current and voltage whereas energy is the supply of electricity over time.

The aim of this work is to introduce the reader to Energy Storage. This work is divided into two main Sections. Section I, includes the main challenges of the electric power industry and shows how energy storage is a feasible solution. Section II on the other hand reviews the various energy storage systems and their technical characteristics.

Section I is divided as follows. It starts with the examination of the role of energy into modern economics followed by the goals of the electric power industry. The impact on the environment is analysed followed with a comparison between conventional and renewable energy sources. For better understanding the reader is introduced to important technical terminology and constraints. Various examples include the cost of electricity, economic dispatch, optimization within constraints and contingency procedures. In addition, the issues (Variability, Uncertainty, Grid Extension and Upgrade, Power Quality and Harmonics, etc) of Renewable Energy Sources (RES) integrated in the grid are analysed and possible solutions (Distributed and Flexible Generation, Extended Geographical Area, Energy Storage, Energy Management, Communications for Remote Data) are discussed. Finally, this work concludes that Energy Storage Systems are of vital importance for the Smart Grid. As presented, Energy Storage could improve the grid's stability and reliability through Energy Management (Peak Shaving, Load Shifting, etc), Optimization and Planning (Economic Dispatch and Minimum Production Cost).

10.2 Understanding the Challenges

10.2.1 Historical Overview

Scientists and historians disagree on the beginning of the history of electricity. Some argue that it dates back to the ancient Greek mathematician Thales of Miletus (624-546BC) who noticed the phenomenon of the fossilized tree resin known as amber which attracted small lightweight objects when rubbed with fur [184], [185]. Others argue that the beginning was given when Benjamin Franklin in 1752 performed the "Kite Experiment" [186] whereas some others also argue that electricity as known today was shaped and evolved in 1831 with Michael Faraday's work on the principles of electricity generation [187]. Additional works, achievements and milestones are also listed by [188] and [189]. The fact that researchers' fascination with electricity has been around for so many years, proves how little it is known and that there is always room for improvements. After all, Faraday's initial handheld device [190]and disk generator [191]as shown on Figure 10-1looks nothing similar compared to today's generators shown on Figure 10-2.

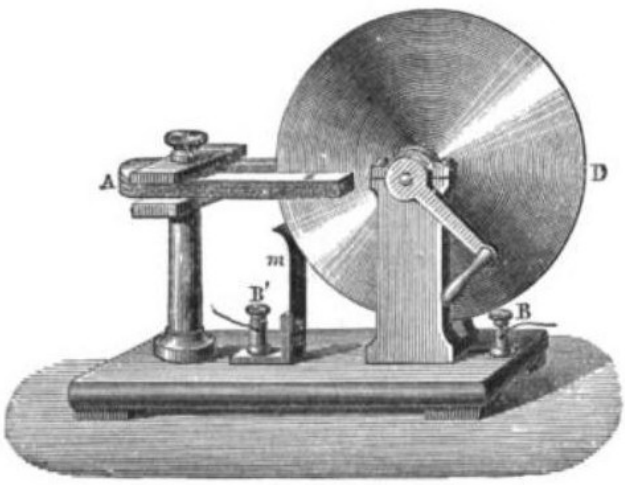

Figure 10-1: Michael Faraday's Disk Generator (Credit: Émile Alglave Wikimedia Commons Author, Public Domain - Published in USA before 1923 [191])

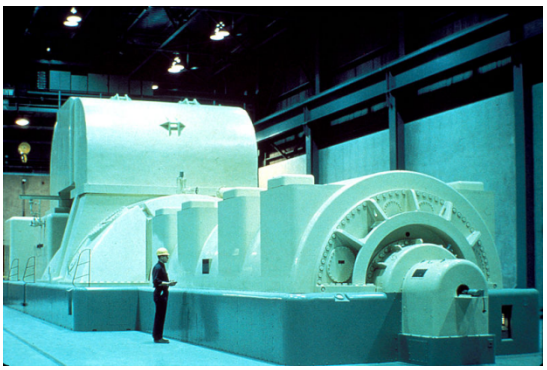

Figure 10-2: Modern Steam Driven Turbine Generator (Credit: www.nrc.gov, USA Public Domain [192])

10.2.2 Global Energy Demand

The historical statistical data of the global energy consumption as reported or directly derived from the International Energy Agency (IEA) [193] , the U.S. Energy Information Administration (EIA) [194], and the European Environment Agency (EEA) [195] is presented on Figure 10-3. As the data shows until late 18th century the need for energy was slowly growing whereas early 19thcentury started increasing rapidly, and the need increased even more rapidly in the 20thand 21stcenturies. This trend is best explained and understood by looking at some historical events and milestones. The First Industrial Revolution (1760-1850) included the transition from hand production to steam engine machines and also introduced the electrical telegraph, whereas the Second Industrial Revolution introduced new technological systems including electrical power and telephones (19thcentury) followed by factory electrification (20thcentury) [188], [189], [196]. Therefore, the second industrial revolution also known as the Technological Revolution introduced energy hungry systems and commodities.

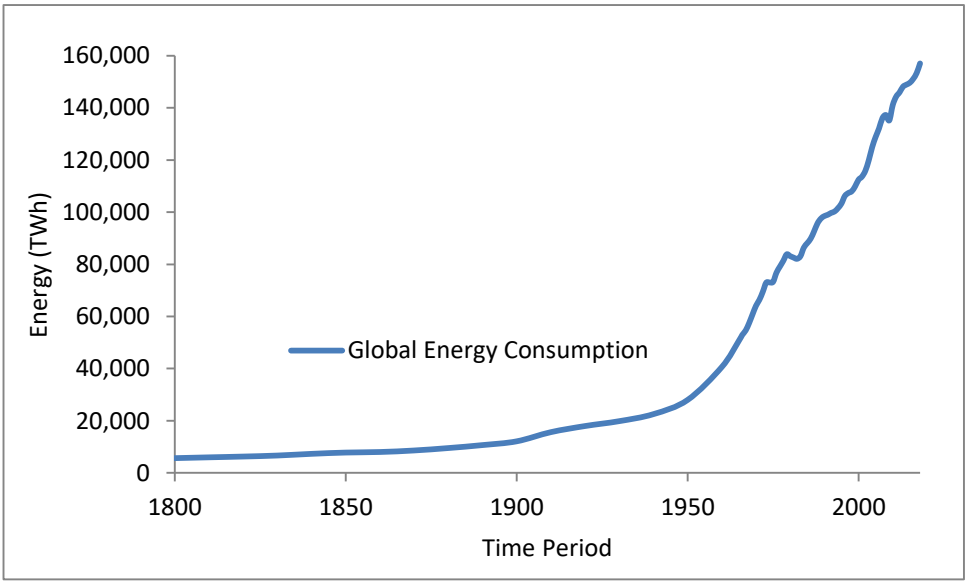

Figure 10-3: Global Energy Consumption

10.2.3 The Role of Energy in Modern Economies

The fascination with energy consumption has opened new areas of non-engineering related studies with an abundance of available literature topics including the role of energy in modern economies, population growth and more. For example, research [197] and [198] demonstrated the positive relationship between economic growth and energy usage whereas [199] quantified the statistical relationships. On the other hand, an in depth review [200] was inconclusive due to the differences among countries and group of countries; heterogeneity in climate conditions, varying energy consumption patterns, the structure and stages of economic development within a country, etc. Furthermore, as concluded in [201]and [202] when the standards of living, energy usage and economic development are increasing then the family size decreases because parents invest more resources in fewer children.

10.2.4 The Electric Power Industry

The increasing energy demand worldwide not only enabled non-engineering areas of study but it has also established an entire new industry which is responsible for the supply of this vital commodity to the society. The electric power industry has been under a continuous transformation, innovation and evolution since day one to meet the challenges. The electric power industry nowadays has three distinctive sectors; generation, transmission and

distribution. Worth noting that as shown on Figure 10-4, transmission lines use ultra-high voltages to minimise the copper losses (I^2R), whereas lower voltages are used at the distribution side to minimise the risk of electric shock and also the cost of equipment; substation customers are using high voltage, primary customers use medium voltage and secondary customers use service voltage which is also known as low voltage.

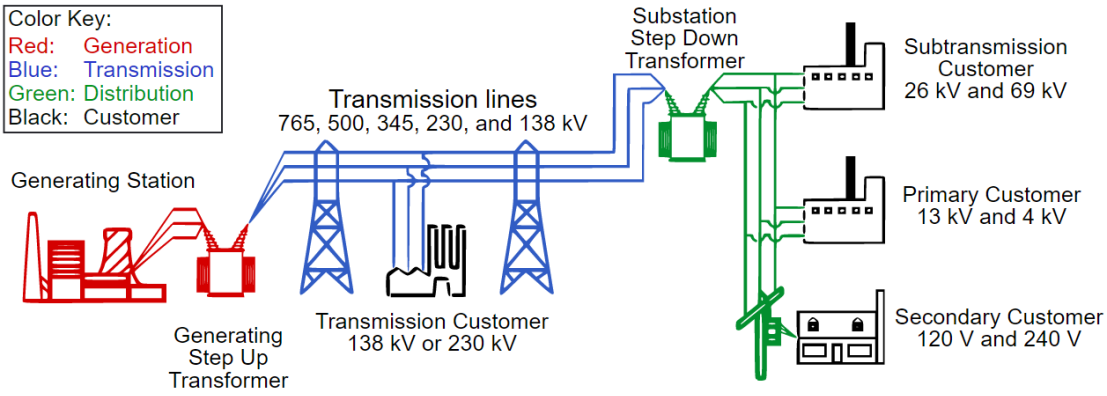

Figure 10-4: Basic Structure of Electric Power System (Credit: United States Department of Energy, Wikimedia Commons author (GNU Free Documentation License - public domain) [203])

10.2.4.1 Goals of the Electric Power Industry

Regardless of the sector, power systems should be operated with the goal of achieving (a) the highest reliability standards, (b) the lowest operation cost and (c) the minimum environmental impacts [204], [205]. System reliability including adequacy and security can be achieved by what is known as the "6 musts";

- Generation capacity must be greater than load
- Transmission must not be overloaded
- Voltages must be within limits
- Must be able to withstand loss of generator
- Must be able to withstand loss of transmission line
- Must not lose stability during short-circuit

Furthermore, this industry to meet the challenges has enabled new specialised job opportunities including but not limited to electricians, line installers and repairers, electrical and electronics engineers, researchers, scientists, construction managers, power plant operators, distributors and dispatchers accountants and more. There areas of research nowadays also include material engineering and manufacturing [206], [207], [208], optimization [209], [210], power quality [211], [212], [213] and more.

10.2.4.2 Visual Landscape and Footprint Issues

As shown on Figures 1 and 2, nowadays generators are increasing in size to meet the new demand. Power plants (generation) and ultra-high voltage transmission lines (transmission) are also increasing in sizes. Because of their enormous sizes usually power plants are built in remote isolated areas [194]. As a result the landscape is affected. These large structures alter the visual landscape as shown on Figure 10-5 to 8. Furthermore, their footprint increases by the need of land clearing, access roads, railroads, and pipelines for fuel delivery, cooling water supplies, etc.

Figure 10-5: Hunter Power Plant, a coal-fired power plant south of Castle Dale, Utah (Credit: Tricia Simpson, Wikimedia Commons author (GNU Free Documentation License - public domain) [214])

Figure 10-6: The two coal-fired power plants of the Crystal River North Steam Complex in Crystal River, Florida, (Credit: John Bradley (Ebyabe), Wikimedia Commons author (GNU Free Documentation License - public domain) [215])

Figure 10-7: High Voltage Transmission Tower and Lines. Auburn WA, (Credit: Ron Clausen, Wikimedia Commons author (GNU Free Documentation License - public domain) [216])

Figure 10-8: Close View of a 500kV Lines, Southern California Edison's Path 26 (Credit: RaumfahrtHauptfokus (Henristosch), Wikimedia Commons author (GNU Free Documentation License - public domain) [217])

10.2.4.3 AC versus DC Systems

At this point, it is worth mentioning a well-known feud between Edison and Tesla to what has been known as the "war of the currents". Edison was an advocate of Direct Current (DC) whereas Tesla of Alternating Current (AC). Alternating systems dominated and became the preferred method and technology for the electric power industry. However, to this day there is a lot of literature examining the economic aspects and comparison between the two systems. Clearly as shown on Figure 10-9, the AC system is the preferred method because it requires half the initial cost/investment and remains cheaper for transmission lines up to 500-600km. For longer transmission lines then the DC systems are more economical [218], [219], [220], [221], [222], [223], [224]. Furthermore, as reported by [223] and [224] DC transmission lines are approximately half the size of AC transmission lines. Therefore, DC transmission lines could offer a lower impact on the environment because of their reduced footprint.

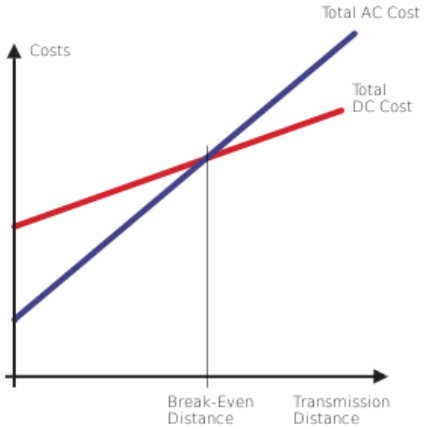

Figure 10-9: Diagram Costs over line Length (Distance) in Comparison HVAC 3-phase Systems versus HVDC Systems (Credit: Wdwd, Wikimedia Commons author (GNU Free Documentation License - public domain) [225])

10.2.4.4 Conventional Power Generation

Conventional power generation as shown on Figure 10-10 is a relatively simple concept. Fuel is burned to heat the water to its boiling point, to create steam which rotates the turbine which produces electricity at the output side. There is also what is known as a combined heat and power setup (Figure 10-11) where an internal combustion engine or a stirling engine are used to produce electricity and heat. With the use of block diagrams the power generation can be easily explained. However, in reality due to continuous research and innovations on reliability, safety and low cost, as shown on Figure 10-12 and **Error! Reference source not found.**, a power station is composed of many more parts; safety valves, governors, feeders, pumps, fans, etc.

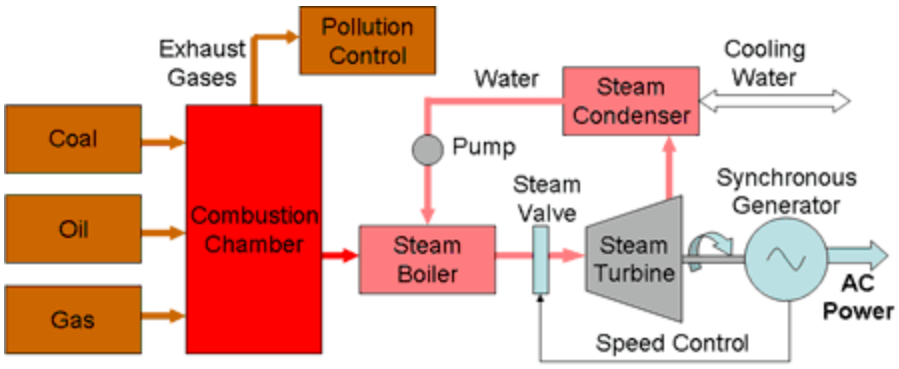

Figure 10-10: Conventional Power Generation Block Diagram(Credit: B. Lawson, Electropaedia and mpoweruk.com [226] using Written License Consent)

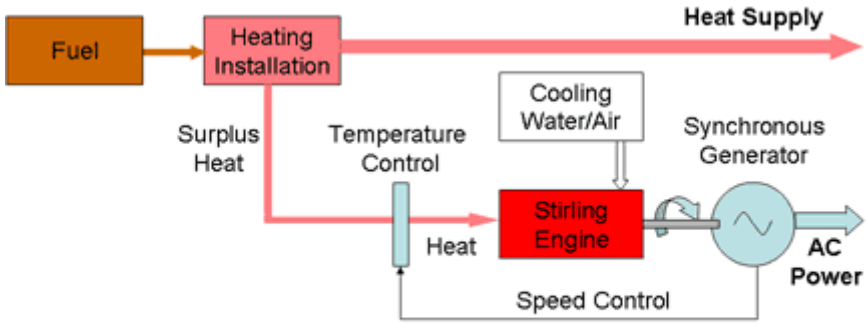

Figure 10-11: Combined Heat and Power (CHP) Block Diagram(Credit: B. Lawson, Electropaedia and mpoweruk.com [226] using Written License Consent)

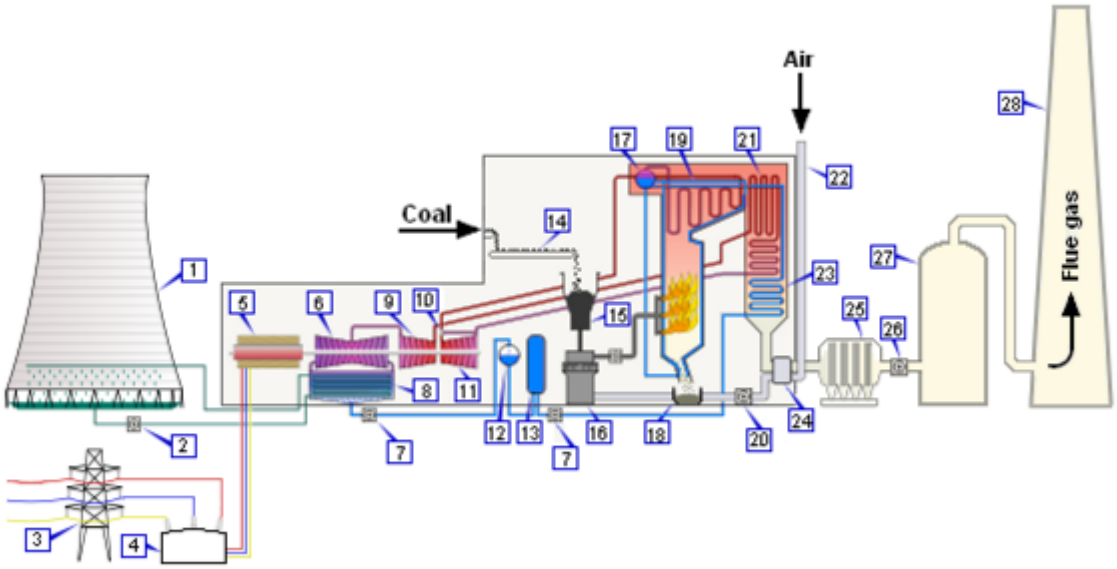

Figure 10-12: Detailed Conventional Power Station Layout (Credit: C. Bill (BillC) Wikimedia Commons author (GNU Free Documentation License - public domain) [227])

Table 10-1: Legend for Figure 10-11 Detailed Conventional Power Station Layout

Index	Description	Index	Description

1	Cooling Tower	15	Coal Hopper
2	Cooling Water Pump	16	Pulverised Fuel Mill
3	Pylon (Termination Tower)	17	Boiler Drum
4	Step-up Transformer	18	Ash Hopper
5	Generator	19	Superheater
6	Low Pressure Turbine	20	Forced Draught Fan
7	Boiler Feed Pump	21	Reheater
8	Condenser	22	Air Intake
9	Intermediate Pressure Turbine	23	Economiser
10	Steam Governor	24	Air Preheater
11	High Pressure Turbine	25	Precipitator
12	Deaerator	26	Induced Draught Fan
13	Feed Heater	27	Chimney Stack
14	Fuel Conveyor		

10.2.4.5 Conventional Power Generation Fuels

Conventional power generation fuel includes Coal, Crude Oil, Natural Gas, traditional Biomass and Nuclear. As shown on Figure 10-13 which was obtained or directly derived from [193], [194], [195] throughout the centuries the use of traditional biomass has been constant. Until 1900s traditional biomass primarily included the use of wood, whereas nowadays biomass includes crops, garbage, landfill gas, alcohol fuels, etc. Furthermore, after 1950 coal has become the primary source of fuel to be replaced by crude oil approximately in the 1970s.

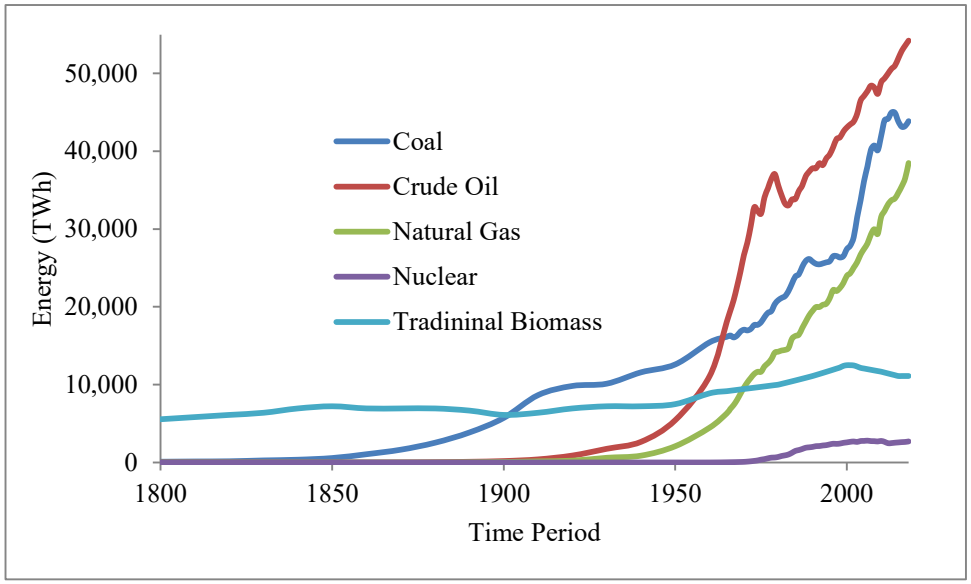

Figure 10-13: Conventional Power Generation Fuels

10.2.5 Emissions and Pollution

The problem with conventional power generation fuels (Fossil fuel, biomass, and waste burning) is the emissions that are released which cause pollution and affect the environment. The by-products when these fuels are burned include carbon dioxide (CO_2), carbon monoxide (CO), sulfur dioxide (SO_2), nitrogen oxides (NO_x), particulate matter (PM) and heavy metals such as mercury. The negative impacts to the environment of all these by-products are as follows:

- CO_2 is a greenhouse gas, which contributes to the greenhouse effect.

- SO_2 causes acid rain, which is harmful to plants and to animals that live in water. SO also worsens respiratory illnesses and heart diseases, particularly in children and the elderly.
- NO_x contribute to ground-level ozone, which irritates and damages the lungs.
- PM results in hazy conditions in cites and scenic areas and coupled with ozone, contributes to asthma and chronic bronchitis, especially in children and the elderly. Very small, or fine PM, is also believed to cause emphysema and lung cancer.
- Heavy metals such as mercury are hazardous to human and animal health.

The realization of all the aforementioned negative impacts on the environment and hazards to human and animal health, introduced in the 1970s the Clean Air Act which regulates air emissions from stationary and mobile sources. In the United States of America (USA) this is undertaken by the US Environmental Protection Agency (EPA) [228] whereas in the European Union by the Environment Directorate General of the European Commission ('DG Environment') [229].

Because of the Clean Air Act, power plants control emission by treating the gases before released to the atmosphere. Some of the control devices:

- Bag-houses: Filters that trap particulates.
- Electrostatic precipitators: Electrically charged plates that attract and remove particulates.
- Wet scrubbers: Liquid solution that removes PM.
- Dry scrubbers: Mix lime in the fuel (i.e. coal) or spray the lime solution into combustion gases to reduce SO_2 emissions.
- Fluidized bed combustion also results in lower SO_2 emissions.
- NO_x emissions controls include low NO_x burners during the combustion phase or selective catalytic and non-catalytic converters during the post combustion phase.

In addition to the control devices there are also controlled processes for treating especially coal to reduce the sulphur content. For example:

- Co-fire wood chips with coal
- Pre-treating and processing coal can also reduce the level of undesirable compounds

10.2.5.1 Emissions Trading System (ETS)

Controlling the amount of emissions released in the atmosphere does not imply their complete elimination (reduced to zero). Therefore, in 2007 an Emissions Trading System (ETS) was discussed by the International Carbon Action Partnership (ICAP) for climate change mitigation [230]. ETS basically created a carbon market, put a price on carbon and enabled trading between countries to avoid the penalties. In the EU as part of the Energy and Climate action reporting showed that ETS works. In 2020 it was reported 21% decrease compared to 2005 whereas the EU 2030 climate and energy framework expects a 43% cut compared to 2005 [231]. Worth reminding that carbon includes both power generation and automobile emissions.

10.2.6 Glossary

10.2.6.1 Terminology, Units and Conversion Factors

In engineering the use of prefixes is a common practice. In electrical engineering for example electric current according to the application can range from nano-amperes (nA) to mega-amperes (MA). For power generation the prefixes most commonly used for power and energy are in the range of kilo (k) to Terra (T).

For electrical engineers parameters such as current (in amperes, A), voltage (in volts, V), power (in watts, W), energy (in joules, J) are straight forward. However, the electric power industry is multi-disciplinary and it involves the conversion from one type of energy to another. For example, the conventional power generation process involves the burning of fuels such as oil, gas, coal, etc. Therefore, it is important to quantify the amount of energy released during combustion. The quantification of the heating value is also known as energy or calorific value. The units for the volumetric and gravimetric calorific values are given by Joules/Litter (J/L) and Jules/kg (J/kg) respectively. For example, the calorific value for crude oil is 38.8MJ/L and 45.3MJ/kg [232], [233].

Table 10-2: Essential Units and Conversion Factors

1 barrel of oil = 158.987294928 L
1 kWh = 3.6 MJ
1 Btu = 1055.056 J
1 therm = 105.5056 MJ
1 calorie = 4.1868 J
1 tonne of oil equivalent (toe) = 41.868 GJ (LHV)
1 barrel of oil (LHV) ≈ 5.70 GJ (IEA def.)
1 barrel of oil (LHV) ≈ 5.86 GJ (global avg.)
1 mechanical hp ≈ 745.7 W
1 PS ≈ 735.5 W
10,000 TWh/y ≈ 1.14 TW (peak power)

Units and conversion factors that are used by the electric power industry are tabulated on

Table 10-2. The data was either obtained or directly derived from [232] and [233]. Worth noting, that LHV and HHV stands for lower heating value and higher heating value respectively.

10.2.6.2 Technical Characteristics and Constraints

In electrical engineering overload and short circuit protection is of paramount importance. Likewise electrical and electronic devices have their nominal characteristics and limitations. For example, nominal characteristics include operating voltage, maximum power, frequency, etc. There is always an allowable tolerance. It is very important to emphasize that nominal values do not only include maximum limits but also lower limits are included. When the tolerance is over or under the limits then the device could suffer catastrophic failures; generator stalling, shaft breaking, etc. In the electric power industry irrelevant to the technology, conventional or renewables, all "generators" or generating sources share the same technical characteristics [204], [205].

- **Capacity or maximum power** - The maximum (P_{max}) output of a plant, in (MW)
- **Minimum Operating Limit** - The minimum (P_{min}) amount of power a plant can generate once it is turned on, in (MW)
- **Start-up and Shut-down Costs** - These are the costs involved in turning the plant on and off, in ($/MWh). Start-up and Shut-down Costs could be different according to the technology used.
- **No-Load Cost** - The cost of turning the plant on, but keeping it in an idle state ready to increase power output, in ($/MWh).
- **Minimum Run Time** - The shortest amount of time a plant can operate once it is turned on, in (h).
- **Start-up or Ramp time** - The amount of time it takes from the moment a generator is turned on to the moment it can start providing energy to the grid at its lower operating limit, in (h).
- **Shut-down time** – The time it takes a generator to stop spinning, in hours (h). If a generator does not stop spinning completely then it cannot be turned back on.

- **Ramp rate** - This variable influences how quickly the plant can increase or decrease power output. This is measured in MW/h or in % of capacity per unit time.

Renewable energy sources offer ramp-times in the range of minutes and they have zero minimum run-time restriction, whereas conventional energy sources ramp in a few hours and their minimum run-time is in the range of hours to days.

10.3 Cost of Power Generation

The cost of power generation is a complex and complicated process which changes from country to country. The cost is composed of fixed and variable costs. The fixed costs include capital (buildings) and land whereas variable costs are proportional to the amount of generated power and include cost of fuel, maintenance, replacement parts, personnel costs, etc. Capital costs are also known as overnight cost. In addition, like any other investment all the costs are analysed using financial methodologies which include the net present value, the time value of money and the discounted cash flow (DCF).

Finally, the breakeven point over the lifetime of the plant is calculated using the Levelized Cost of Energy (LCOE) method shown by Equation 10-1 and Equation 10-2. The breakeven point is regarded as the minimum constant price at which electricity must be sold ($/Wh). The lifetime of the plant is usually considered between 25-35 years. The LCOE method gives a good metric for the plant's performance and it is a good consistent basis for comparison between the various technologies.

$$LCOE = \frac{\text{Total cost of ownership (\$)}}{\text{System production over its lifetime (kWh)}}$$

Equation 10-1

Using financing and discounted rate then Equation 10-1 is rewritten as

$$LCOE = \frac{\sum_{t=1}^{n} \frac{I_t + M_t + F_t}{(1+r)^t}}{\sum_{t=1}^{n} \frac{E_t}{(1+r)^t}}$$

Equation 10-2

where,

I_t is the investment costs in the year t

M_t represents the operations and maintenance costs in the year t

F_t is the fuel cost in the year t

E_t is the electrical generated energy in the year t

r is the discount rate

n is the expected lifetime of system or power station

Example 1: Assume a rooftop solar PV system will be installed on a commercial facility, and the characteristics of the project are the following:

- Project capacity = 100 kilowatts
- Initial investment = $300,000
- Maintenance costs = $3,000/year (1% of initial investment)
- Estimated yearly production = 182,500 kWh
- Project life = 25 years

Over its lifetime, the total kWh production of this PV system will be:

Lifetime output = 182,500 kWh/year x 25 years = 4,562,500 kWh

The total cost of ownership, considering the initial investment and maintenance costs will be:

Total Cost of Ownership = $300,000 + $3,000/year x 25 years = $375,000

Therefore, this project will have the following LCOE:

LCOE = $375,000 / 4,562,500 kWh = $0.0822 / kWh

If electric utility rates at the project's location are higher than this, the net effect will be a reduction in energy expenses.

Example 2: A hypothetical wind turbine takes one year to build and costs $1.5 million. The operating and maintenance costs are $300,000 per year, with an associated growth rate of 2% annually. There are no associated fuel costs. The wind turbine's lifespan is 10 years, and it is estimated to produce 3 million kWh each year. Finally, the associated discount rate for the project is 8%.

The following image shows the calculation of the LCOE for this project. In a comparative analysis, the figure would be calculated for numerous energy sources to be compared against one another.

Levelized Cost of Energy Template (LCOE)

Assumptions (in '000s)	
Initial Investment Cost ($)	1,500
Operations and Maintenance Costs ($)	100
O&M Growth Rate (%)	2.00%
Annual Fuel Costs ($)	-
Annual Electricity Output (kWH)	3,000
Project Lifespan (years)	10
Discount Rate (%)	8.00%

Total Costs	Entry	1	2	3	4	5	6	7	8	9	10
Initial Investment	1,500										
O&M Costs		-	100	102	104	106	108	110	113	115	117
Fuel Costs		-	-	-	-	-	-	-	-	-	-
Discount Factor		92.6%	85.7%	79.4%	73.5%	68.1%	63.0%	58.3%	54.0%	50.0%	46.3%
Present Value of Costs	1,500	-	86	81	76	72	68	64	61	57	54
NPV of Total Costs	**$2,121**										

Total Energy Output	Entry	1	2	3	4	5	6	7	8	9	10
Yearly Output	-	-	3,000	3,000	3,000	3,000	3,000	3,000	3,000	3,000	3,000
Discount Factor	-	92.6%	85.7%	79.4%	73.5%	68.1%	63.0%	58.3%	54.0%	50.0%	46.3%
Present Value of Costs	-	-	2,572	2,381	2,205	2,042	1,891	1,750	1,621	1,501	1,390
NPV of Total Output	**17,352 kWH**										

LCOE	$0.12/kWH

This file is for educational purposes only. E&OE

CFI

Corporate Finance Institute®
https://corporatefinanceinstitute.com/

Cover Page | LCOE

Figure 10-14: LCOE Analysis for Example 2 [234]

The capital and operating costs of various conventional and renewable energy sources are tabulated on Table 10-3. The data was either obtained or directly derived from [234], [235],

[236], [237], [238], [239], [240], [241]. The tabulated data is indicative and does not include LCOE because as mentioned earlier from there is a big deviation among countries and regions regarding financing, labour and personnel costs, and fuel costs. As shown from the tabulated data the higher the capital costs then operating costs are lower. Renewable energy sources offer the lowest operating cost of less than 0.01 $/kW.

Table 10-3: Capital and Operating Costs

Technology		**Capital Cost ($/kW)**	**Operating Cost ($/kW)**
Conventional Sources	Natural Gas Combustion Turbine	400 – 1,000	0.04-0.10
	Natural gas combined-cycle	600 - 1,200	0.04-0.10
	Coal-fired Combustion Turbine	500 - 1,000	0.02-0.04
	Coal Gasification Combined-Cycle (IGCC)	1,000 - 1,500	0.04-0.08
	Coal (with SO_2 and NO_x controls)	3,500 - 3,800	0.04-0.08
	Nuclear	1,200 - 6,000	0.02-0.05
Renewable Sources	Wind (on-shore)	1,600	<0.01
	Wind (off-shore)	6,500	<0.01
	Solar PV (fixed)	1,060 - 1,800	<0.01
	Solar PV (Tracking)	1,130 - 2,000	<0.01

	Geothermal	2,800	<0.01
	Hydro-electric	1,200 - 5,000	<0.01
	Fuel Cells	7,200	N/A
Storage	Batteries	2,000	N/A

It is very important to emphasize at this point that capital and operating cost do not represent the customer price. As shown on Figure 10-15, customer price for energy consumption includes taxes such as Value Added Tax (VAT) which differ from country to country. For example, the country of Denmark has the lowest price of approximately 0.11€/kWh. However, after adding all the additional taxes then Denmark has the highest price among all EU countries of 0.29€/kWh.

The customer pricing is an even more complex and complicated process. It involves knowledge of the available sources connected to the grid and their characteristics and constraints (see Section: Important Technical Characteristics and Constraints), and then it becomes an economic dispatch optimization problem. Economic dispatch optimization problems include demand forecast, scheduling, unit commitments, fuel prices, constraints and require optimization techniques such as linear and dynamic programming [204], [205]. Such methodologies are usually covered in modules such as Power System Operation and Control.

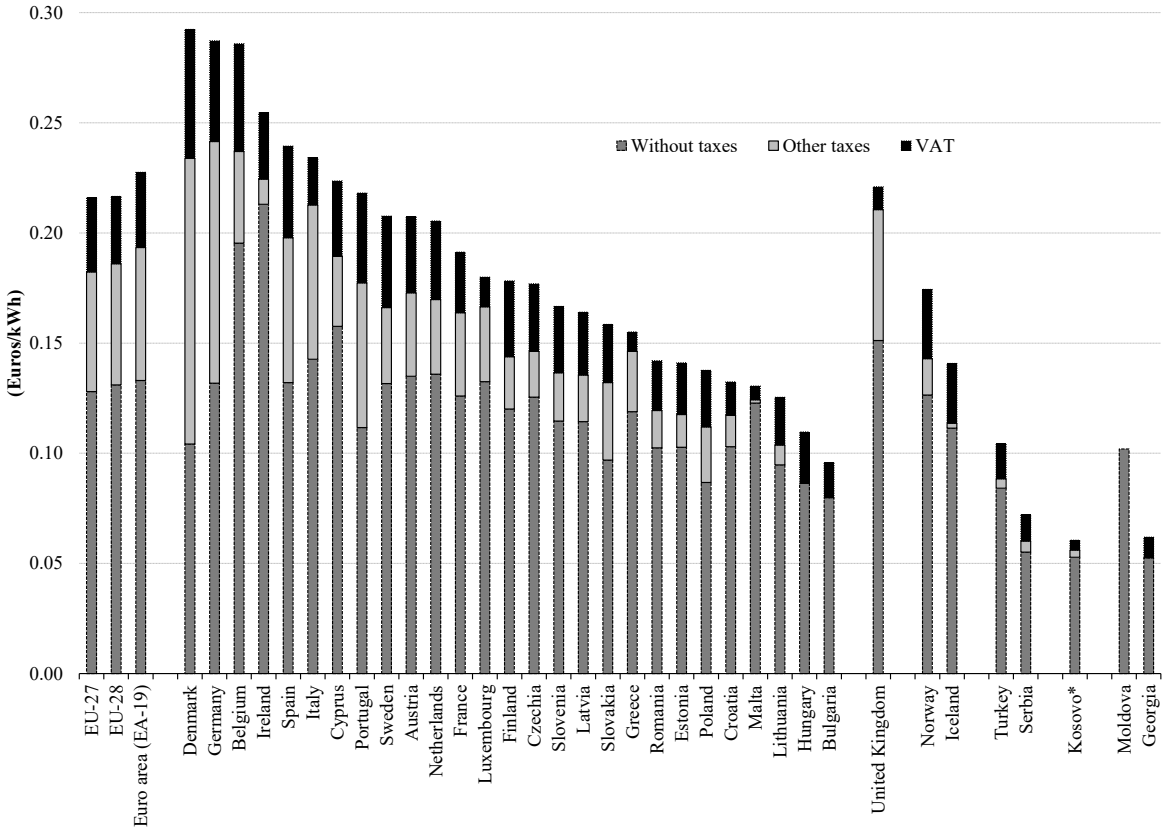

Figure 10-15: Electricity Prices for Household Consumers, Second Half 2019 [242], [243]

Example 3: Given the following generation unit characteristics and costs, determine what combination of online units should be used to supply 550 MW?

Unit 1: Is a coal-fired steam unit. The minimum output power is 150 MW whereas the maximum output power is 600 MW. The unit's fuel cost is 1.1$/MBtu whereas the Input-Output curve is described by:

$$H_1\left(\frac{MBtu}{h}\right) = 510 + 7.2P_1 + 0.00142(P_1)^2$$

Unit 2: Is an oil-fired steam unit. The minimum output power is 100 MW whereas the maximum output power is 400 MW. The unit's fuel cost is 1.0$/MBtu whereas the Input-Output curve is described by:

$$H_2\left(\frac{MBtu}{h}\right) = 310 + 7.85P_2 + 0.00194(P_2)^2$$

Unit 3: Is an oil-fired steam unit. The minimum output power is 50 MW whereas the maximum output power is 200 MW. The unit's fuel cost is 1.2$/MBtu whereas the Input-Output curve is described by:

$$H_3\left(\frac{MBtu}{h}\right) = 78 + 7.97P_3 + 0.00482(P_3)^2$$

Following the methodologies presented in [204], [205]:

1. Test all combinations of the three units
2. Do not violate the power limitations (constraints) of each generator; P_{min} and P_{max}
3. Identify feasible and infeasible combinations
    a. Infeasible
        i. The sum of all maximum MW for the units committed is less than the load or
        ii. The sum of all minimum MW for the units committed is greater than the load
4. For each feasible combination
    a. The units will be dispatched using the Economic Dispatch techniques

The complete solution is shown on Figure 10-16. As shown, for a load of 550 MW then the optimum solution would be when only unit 1 is ON.

Unit 1	Unit 2	Unit 3	Max Generation	Min Generation	P_1	P_2	P_3	F_1	F_2	F_3	Total Generation Cost $F_1 + F_2 + F_3$
Off	Off	Off	0	0					Infeasible		
Off	Off	On	200	50					Infeasible		
Off	On	Off	400	100					Infeasible		
Off	On	On	600	150	0	400	150	0	3760	1658	5418
On	Off	Off	600	150	550	0	0	5389	0	0	5389
On	Off	On	800	200	500	0	50	4911	0	586	5497
On	On	Off	1000	250	295	255	0	3030	2440	0	5471
On	On	On	1200	300	267	233	50	2787	2244	586	5617

Figure 10-16: Solution to Economic Dispatch Example

Example 4: Given the following word problem then formulate the profit and constraint equations.

A factory produces 3 products (A, B and C). Product A requires 2 hours of fabrication, 1 hour of assembly and gives the company a profit of 7. Product B requires 3 hours of fabrication, 1 hour of assembly and gives the company a profit of 8. Product C requires 2 hours of fabrication, 2 hours of assembly and gives the company a profit of 10. The company has 1000

labour hours for fabrication and 800 for assembly. How many products of each type, does the company have to sell to maximise profits?

Following the aforementioned methodologies:

1. Assign variables: A → x_1, B → x_2 and C → x_3 (note that variables x_1, x_2.. x_n are preferred in the power electric industry)
2. Profit, $P = 7x_1 + 8x_2 + 10x_3$
3. Inequality $x_1, x_2, x_3 \geq 0$ (variables such as goods/products, power generation, fuel consumption are either zero or positive)
4. Constraints
    a. Fabrication: $2x_1 + 3x_2 + 2x_3 \leq 1000$
    b. Assembly: $x_1 + x_2 + 2x_3 \leq 800$

Using the simplex method (Linear Programming) the first step requires that inequality equations are converted to equality with the use of slack variables.

For example, inequality equations for fabrication (1) and assembly (2) using slack variables S1 and S2 can be rewritten as (3) and (4) respectively:

$$2x_1 + 3x_2 + 2x_3 \leq 1000 \quad (1)$$

$$x_1 + x_2 + 2x_3 \leq 800 \quad (2)$$

$$2x_1 + 3x_2 + 2x_3 + S_1 = 1000 \quad (3)$$

$$x_1 + x_2 + 2x_3 + S_2 = 800 \quad (4)$$

Using the simplex system method, the system of equations is shown on Figure 10-17.

$$\begin{array}{c} \\ S_1 \\ S_2 \\ P \end{array} \left[\begin{array}{cccccc|c} x_1 & x_2 & x_3 & S_1 & S_2 & P & \\ 2 & 3 & 2 & 1 & 0 & 0 & 1000 \\ 1 & 1 & 2 & 0 & 1 & 0 & 800 \\ -7 & -8 & -10 & 0 & 0 & 1 & 0 \end{array}\right]$$

Figure 10-17: System of Equations using the Simplex Method

Finally, as shown on Figure 10-18, the maximum possible profit could be $4,400 when the company sells 200 and 300 pieces of product A (x_1) and product C (x_3) respectively. Product B (x_2) should not be produced.

$$\begin{array}{c|cccccc|c} & x_1 & x_2 & x_3 & S_1 & S_2 & P & \\ x_1 & 1 & 2 & 0 & 1 & -1 & 0 & 200 \\ x_3 & 0 & -1/2 & 1 & -1/2 & 1 & 0 & 300 \\ P & 0 & 1 & 0 & 2 & 3 & 1 & 4400 \end{array}$$

Figure 10-18: Solution using the Simplex Method

This simple optimization can also be performed using Matlab.

Example 5: Using Matlab implement Linear Programming to maximise the objective function subject to constraints and calculate the values for x_1, x_2, and x_3.

Objective function: $f(x_1, x_2, x_3) = 4x_1 + 2x_2 + x_3$

Subject to Constraints: $x_1 + x_2 + 2x_3 \leq 6$

$2x_2 + 3x_3 \leq 8$

$2x_1 + 3x_2 + x_3 \leq 10$

$x_1, x_2, x_3 \geq 0$

Using Matlab:

```
>> A = [1 1 2; 0 2 3; 2 3 1];
>> b = [6 8 10]';
>> f = [-4 -2 -1]';
>>Aeq = [];
>>beq = [];
>>lb = [0 0 0]';
>>ub = []';
>>
>> [x fval] = linprog(f, A, b, Aeq, beq, lb, ub)

Optimal solution found.


x =

    5
    0
    0


fval =

  -20.0000
```

Listing 10-1: Linear Programming Matlab Code

Therefore, using the Matlab code, it can be acknowledged that the answers are for (x_1, x_2, x_3) = (5,0,0) and f (fval) = -20. The value of f using the theoretical approach was found to be 20 and Matlab to be -20. This is due to the fact that Matlab is minimizing the objective as opposed to the required maximization, hence the difference in sign.

10.4 Worldwide Usage of Renewable Energy Sources

Environmental concerns and penalties forced countries and policy makers to turn to alternative methods of power generation which are friendly to the environment; Green Energy or Renewable Sources of Energy (RES) which have zero emissions. Renewable Energy Sources include Solar (Photovoltaics (PV), Solar Thermal, Concentrated Solar Thermal (CSP) and Solar Heating), Wind, Hydro, Biomass (organic material that comes from plants and animals), Geothermal, Waves, Ocean Currents and Tidal [244], [245], [246], [247], [248], [249], [250], [251]. As shown from Figure 10-19 (obtained or directly derived from [193], [194], [195]) after the 1900s hydro power has been producing more power compared to all other RES combined. However, as discussed in [245], [250], [251], it is controversial whether hydro power should be included in the RES family because mega-dams affect the environment and ecosystem; divert and reduce natural river flows, thus restricting access for animal and human populations. On the other hand, small hydroelectric plants divert only a fraction of the river flow hence they are considered as less harmful to the environment.

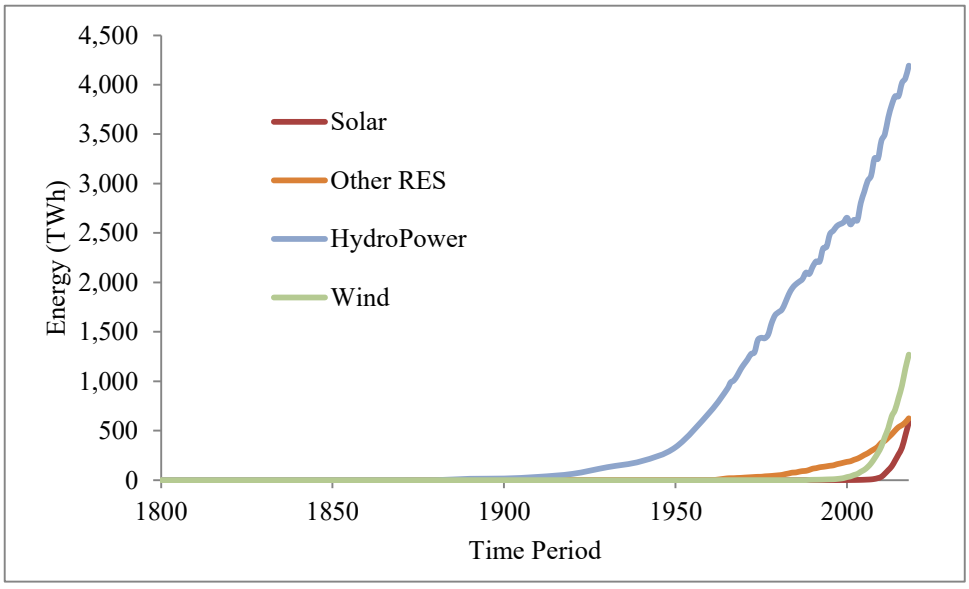

Figure 10-19: Worldwide Energy from RES

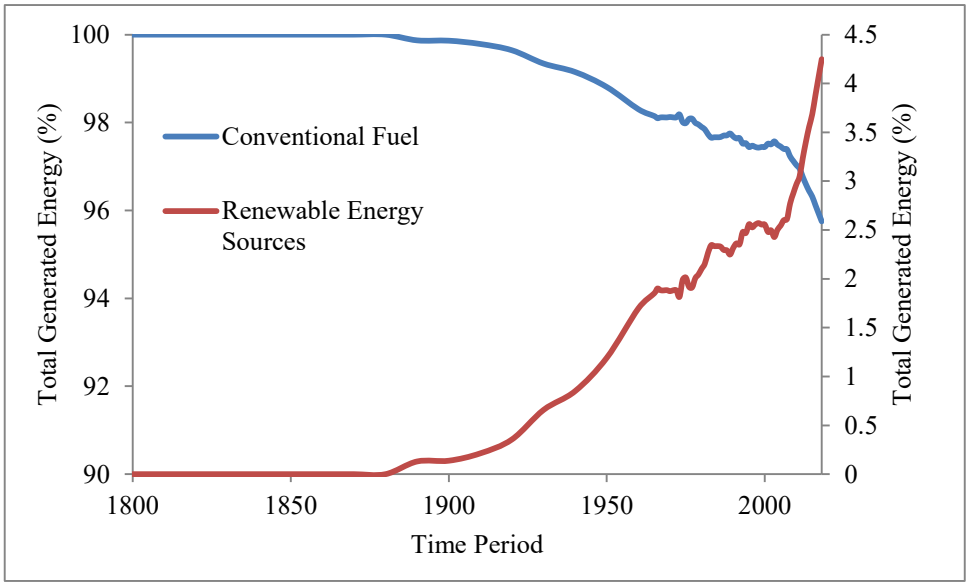

Figure 10-20: Percentage of Worldwide Generated Power

Despite the environmental and climate change concerns as shown on Figure 10-20 (obtained or directly derived from [193], [194], [195]) the penetration of RES into the total worldwide energy production is very slow with a total percentage of 5%. Worth noting however, that after 2000 there is a more rapid increase in the percentage reaching to nearly 4.5% from 2.5%.

10.5 RES Integration Issues and Solutions

Power demand worldwide is variable; it changes hourly, daily, weekly, monthly. It depends on weather conditions, people's habits and comfort levels. It changes from country to country. The patterns presented on Figure 10-21 to Figure 10-23 were either obtain or directly derived from [252]. However, as shown the aforementioned patterns change in a predictable manner.

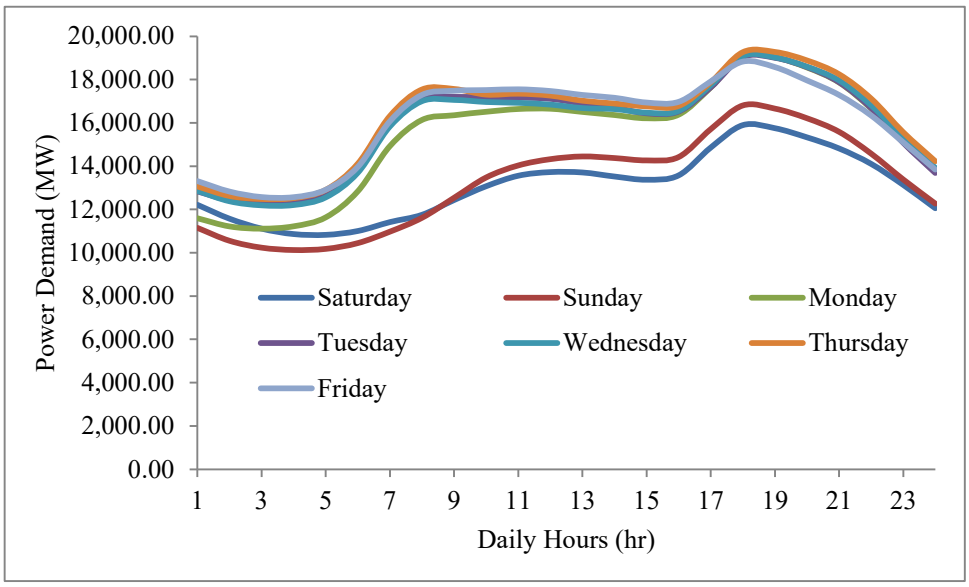

Figure 10-21: Daily Power Demand Pattern

The daily pattern presented on Figure 10-21 show that the "on-peak" hours are from 7am to 10pm whereas the off-peak hours are from 10pm to 7am. Also, the demand during weekends is lower as compared to the rest of the week. The predictability due to repetition is also identified from the data presented on Figure 10-22.

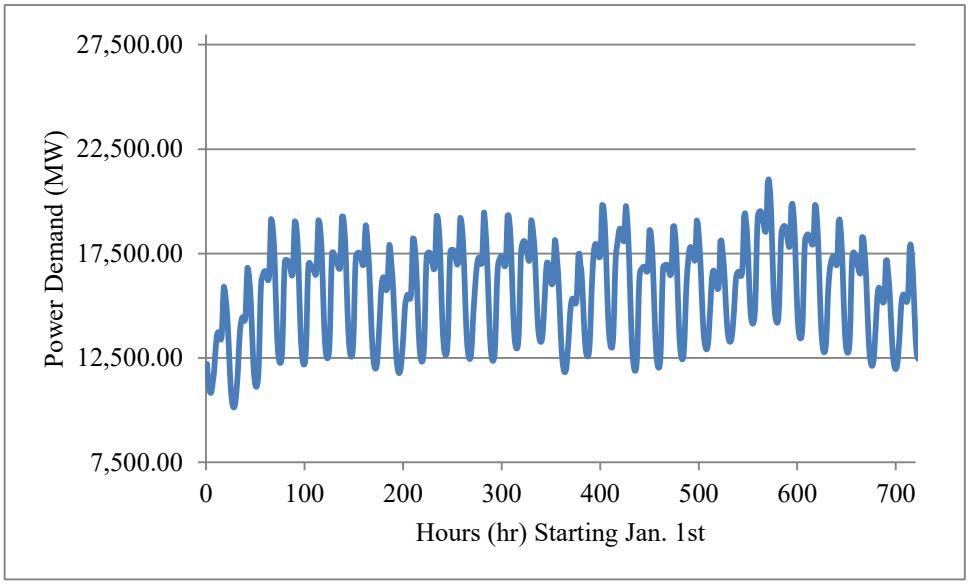

Figure 10-22: Weekly Power Demand Pattern

The seasonal pattern is presented of Figure 10-23. During the seasons of summer and winter the power demand is higher because of cooling and heating respectively whereas during fall and spring the demand is lower. The yearly peak demand is always during summer or winter time. However, for countries like Cyprus where heating is primarily using conventional fuels then peak demand is during summer for cooling purposes.

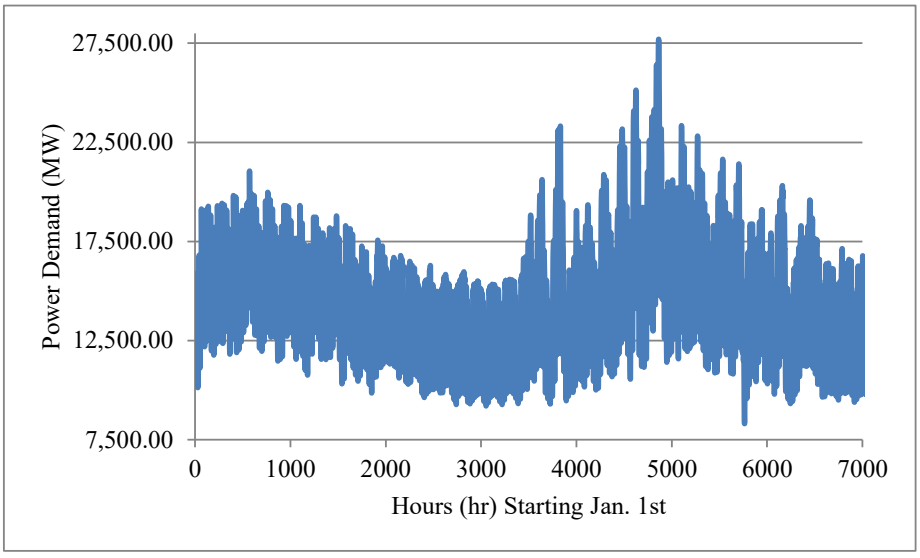

Figure 10-23: Seasonal Power Demand Pattern

The study of historical data is imperative for reliable forecasting to maintain system stability and reliability. In addition, reliable forecasting could provide energy at lower prices to the consumers and higher profits to the producers through techniques such as scheduling and unit commitment, and economic dispatch. The typical daily example shown on Figure 10-24 is directly obtained or derived from Cyprus Transmission System Operator (CTSO) [253]. As can be seen the forecast and actual generation curves are very similar with a very small deviation. Furthermore, worth noting that the system available generation capacity is around 1,100 MW whereas the generation from wind farms totals approximately 200 MW. The total available generation capacity provides the "reserves" required to compensate for the RES variability and uncertainty.

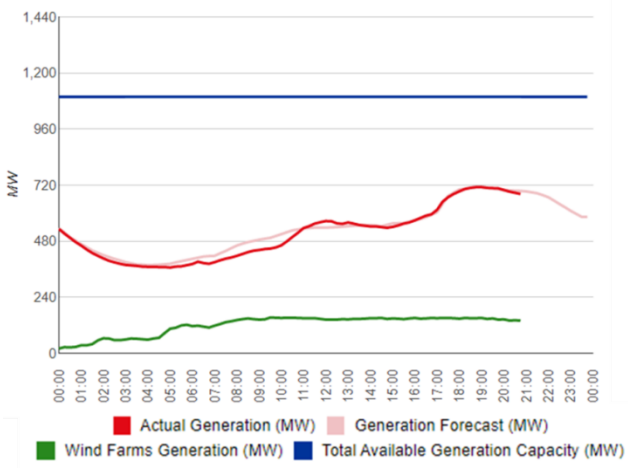

Figure 10-24: Cyprus System Generation

10.5.1 Issues

The purpose of the electric grid is to transfer power from one location to another. The grid's major constraints are maximum temperature and loading (maximum power). Equilibrium is kept when energy is conserved; generated power equals to the sum of power demand and losses, as shown on equation (3):

$$\sum P_{Gen} = \sum P_{demand} + \sum P_{Loss}$$

Equation 10-3

Power losses include the copper losses (I^2R) of transmission and distribution lines, inefficiencies of all equipment (transformers, switchgear, etc) and auxiliary power required for the operation of power plans and substations. When the equilibrium is disturbed then system becomes unstable resulting in blackouts also known as loss of service. Instability could be transient (portion of the cycle) and long term (several cycles).

The two most commonly used words within the electric power industry are reliability and stability. Both have become major areas of study. Reliability involves the "compromise" of the equipment including the electric grid. Reliability is the study of sustained outages, switchgear lockout, blown fuses and loss of service, access and integrity. Stability on the other hand involves the study of maintaining the power system's (generation, transmission and

distribution) harmonization with stable frequency, voltage and rotor angles. Research [254], [255], [256] provides detailed information on reliability recovery techniques such as FLISR (Fault Location, Isolation and Service Restoration) whereas [257] provides a very elaborate definition and classification of Power System Stability.

As has already been mentioned the penetration of RES into the grid presents several challenges that can affect the systems stability and reliability. For this reason the integration has been implemented in a controlled manner. Over the last several years extensive research [258], [259], [260], [261], [262], [263], [264], [265], [266], [267] has identified the following issues associated with RES integration into the grid.

- Variability and Uncertainty
- Grid Extension and Upgrade
- Power Quality / Harmonics

10.5.1.1 Variability and Uncertainty

The generation from photovoltaic systems is very predictable because the sun path throughout the year is well understood and documented. In addition, according to the location the optimal tilt angles are available [268]. An advantage of PV systems is that maximum generation coincides with maximum demand. The problem with PV generation is the shading caused by clouds which is not predictable since clouds might be passing by at different speeds. This PV variability is shown on Figure 10-25.

Wind turbines on the other hand are not as predictable as PV systems. Wind turbines are subject to seasonal patterns such as winter when wind blows stronger. However, their daily patterns are an issue when at night when wind picks-up and the load demand is minimal. Furthermore, the uncertainty is exacerbated by wind gusts available throughout the year. A typical example of wind turbines' performance is shown on Figure 10-26.

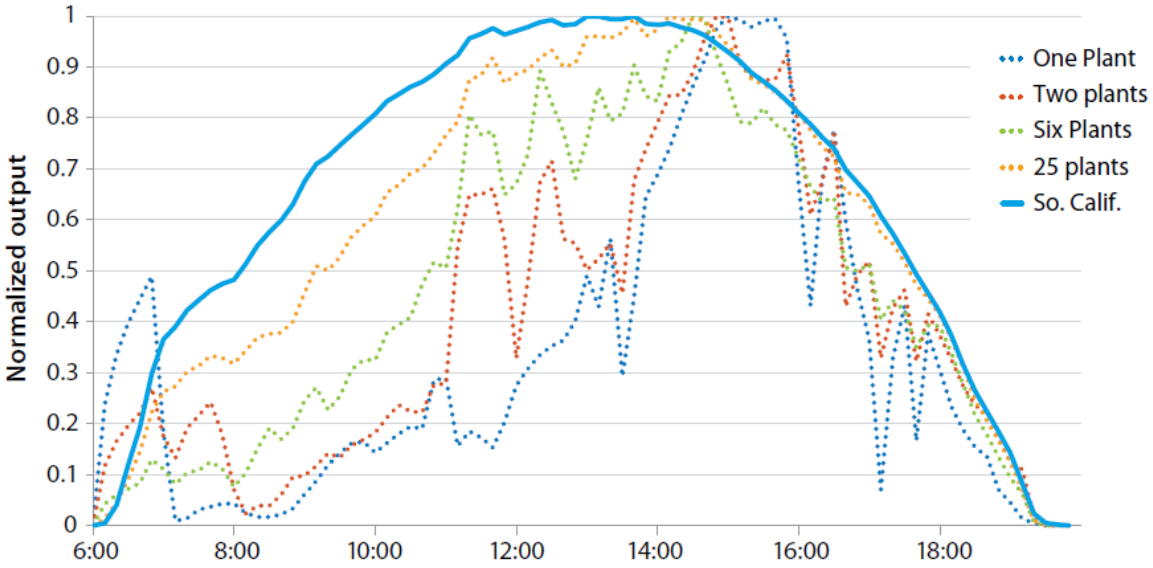

Figure 10-25: Normalized power output for increasing aggregation of PV in Southern California for a partly cloudy day [260], [261]

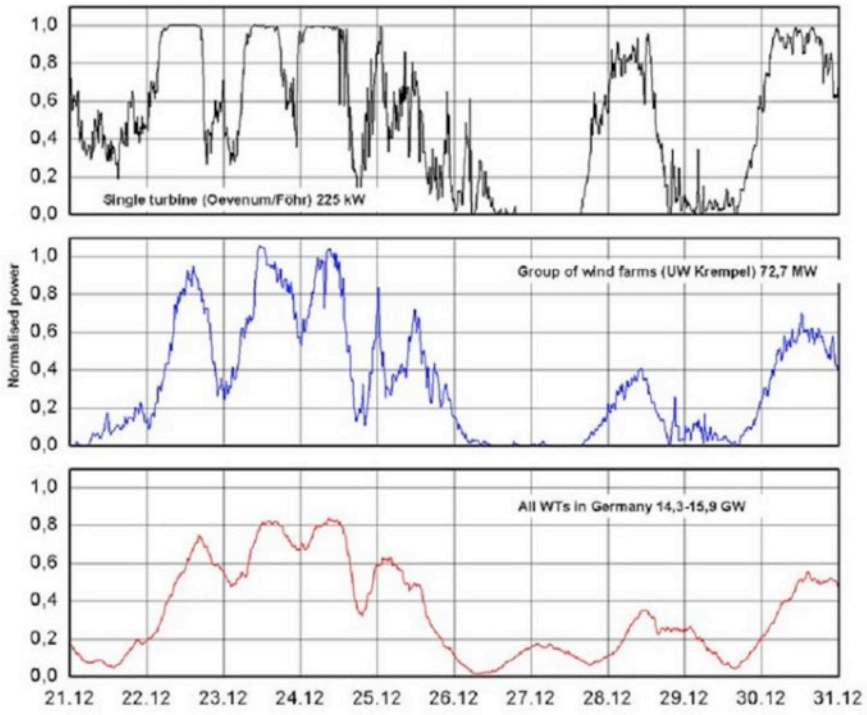

Figure 10-26: Time series of normalized power output from a single wind generator, a group of wind generators and all wind generators in Germany [21]

According to the aforementioned research [258], [259], [260], [261], [262], [263], [264], [265], [266], [267] large wind and PV plants can affect severely the stability of the grid. Hence, it is suggested that smaller plants are spread on a bigger geographical area to smooth out the performance and limit the impact on the grid. However, this solution imposes another problem related to the grid and will be discussed at section “Grid Extension and Upgrade”.

10.5.1.2 Grid Extension and Upgrade

Spreading the RES (wind and solar) to a wider geographical area allows for smoother generated power curves as shown on Figure 10-25 and Figure 10-26. However, this imposes an issue with the grid which might need to extend or upgraded. Metropolitan areas have adequate power lines. However, building new RES plants within metropolitan areas is rarely feasible due to the availability and high cost of the land. In addition, in developed countries metropolitan areas include adequate rooftop PV systems and permits for additional generation might be impossible. On the other hand the grid might not reach on remote available areas hence an extension is required. Furthermore, even if the grid is available at the location it might still require upgrades to accommodate the added generation at the required voltage level.

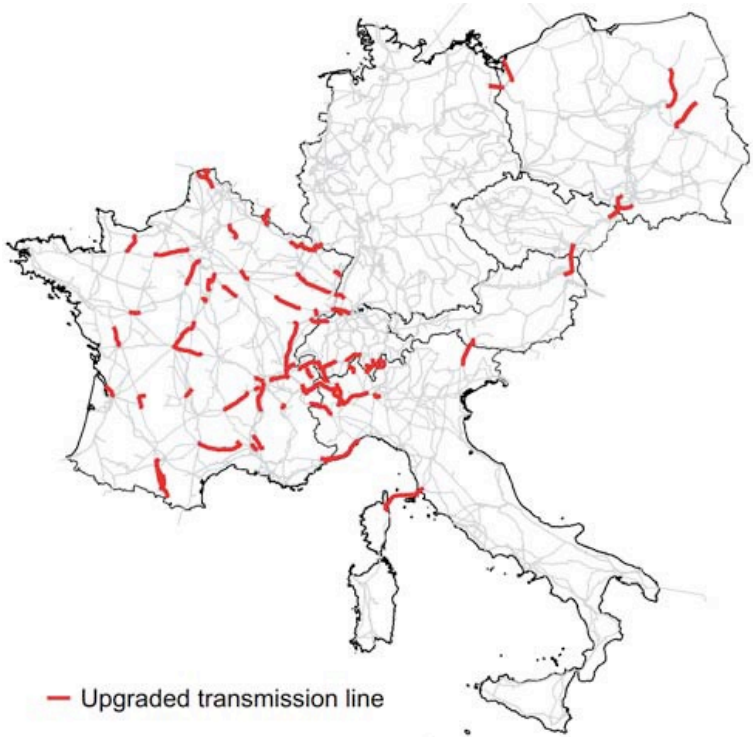

Figure 10-27: Required Upgraded Transmission Lines (Credit: Dr. Reza Abhari and Energy Science Center (ESC), ETH Zurich [269])

A recent study [269] examined the optimal RES portfolio to achieve 45% renewable electricity in central Europe (France, Italy, Switzerland, Austria, Germany, Poland and the Czech Republic) by 2030. The results also shown on Figure 10-27concluded that among the seven countries 116 transmission lines with a total length of 5000 km require reinforcement. However, in the case of the aforementioned developed countries this only equates to only 4% of the total length of the transmission system which might be considered insignificant. This might not be the case for other countries.

10.5.1.3 Power Quality / Harmonics

The integration of RES to the grid requires the use of power electronics and power converters which generate a lot of harmonics at the mains AC [270] and at the point of common coupling (PCC) [263]. Power electronic converters fall in four categories: AC-DC, AC-AC, DC-DC and DC-AC. Using the two-port network representation, the power of converters can flow in either direction. When the power flows from the AC side towards the DC side, then the converter is

said to work in the rectification-mode, whereas from DC to AC it is said that is in inverter-mode [271].

Nowadays, the area of power electronics includes electric power, electronics and control theory. By controlling the switching of the electronic devices the output of the converters can be controlled at the desired voltage and current levels, frequency and quality (distortion and harmonics). The most efficient switching process is the Pulse Width Modulation (PWM). Modulation techniques are divided according to the switching frequency; low and high. Low switching frequency modulation includes the Selective Harmonic Elimination (SHE) and the Space Vector Control, whereas high switching frequency modulation includes Sinusoidal PWM and the Space Vector PWM. More control techniques are also discussed in [272] and [273]. Additionally as discussed in [263], [274], [275] filters such as LC and LCL are also used. The main aim of these techniques is to improve the output waveforms; the amplitude of the fundamental component, the harmonic content, the effect of harmonics on the source, the switching losses and controllability.

The inherent modulation processes in power converters relating input and output parameters to a switching function are analysed and identified in [270]. The timing of the switching instances and duration of the on/off periods applied to the semiconductor power switches constitutes a Switching Function. Two popular power converters are investigated the AC to DC Controlled Rectifier and the PWM sinusoidally modulated 3-Level H-Bridge inverter. Both share the same power circuit configuration, namely the H-Bridge. Figure 10-28shows the Input-Output Waveforms of the AC to DC Converters whereas Figure 27 presents the frequency spectrum of modulation function. As seen on Figure 10-29, the switching function contains a strong fundamental component at ω and harmonics centred at the switching frequency mω and its multiples.

Using LC filtering in combination with control techniques as shown on Figure 10-30and Figure 10-31 the THD at the output current is reduced to 0.5%. Research [270], [274], [275] provide and in-depth analysis and comparison between theoretical and simulated results.

Additional power quality issues with RES integration to the grid mainly due to the RES variability and uncertainty as discussed in additional literature [213], [276], [277] include voltage sags and swells, frequency deviations and spikes.

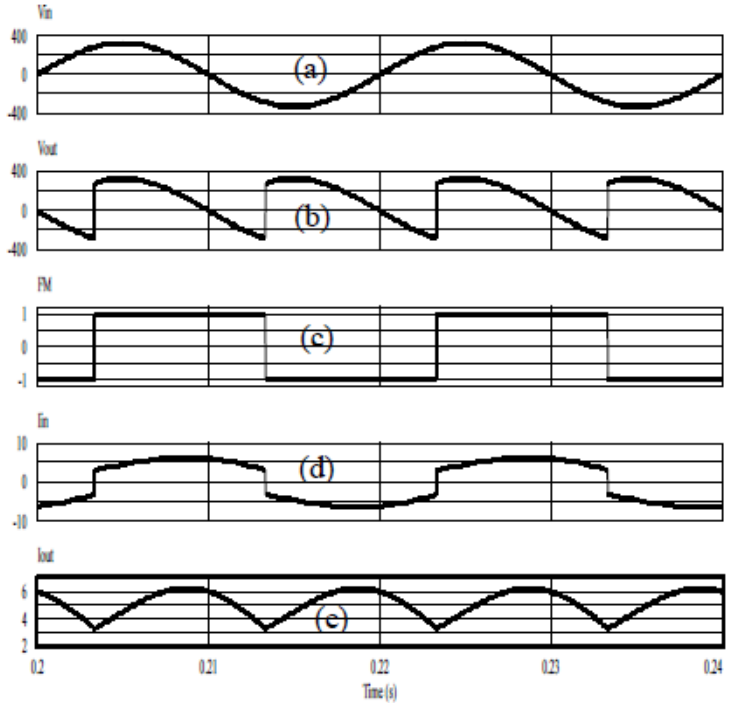

Figure 10-28: Input-Output Waveforms of the AC to DC Converters (a) Input Voltage, Vin(t), (b) Output Voltage, Vo(t), (c) Switching Function, FM(t), (d) Input Current, Iin(t) and (e) Output Current, Io(t)

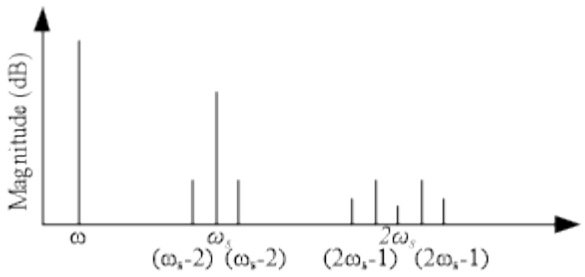

Figure 10-29: Frequency Spectrum of Modulation Function

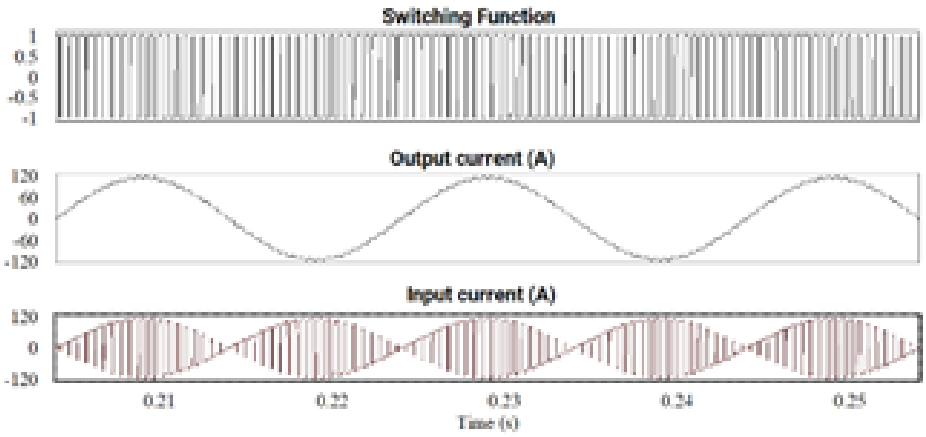

Figure 10-30: Switching Function output (peak 110A) and input (peak 110A) current waveforms of the sinusoidally modulated H-Bridge 3-Level inverter

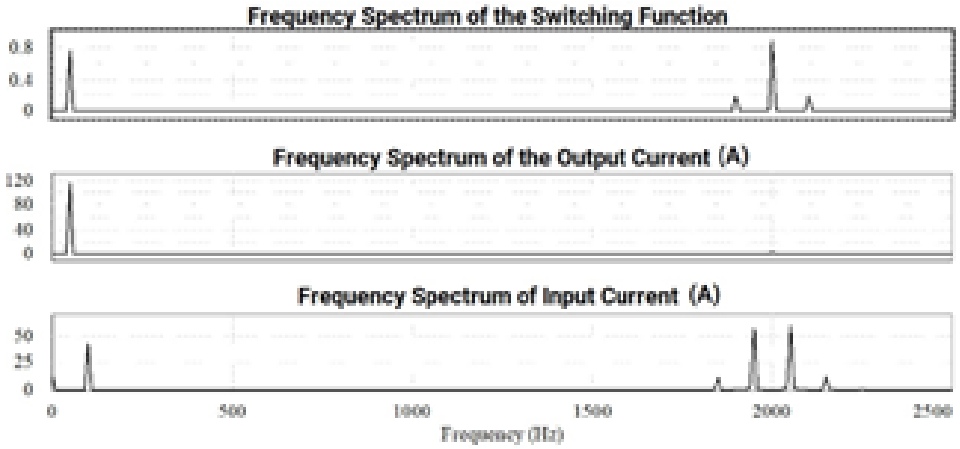

Figure 10-31: Frequency Spectrum of the Sinusoidally Modulated H-Bridge 3-Level Inverter

10.5.2 Solutions

Research [258], [259], [260], [261], [262], [263], [264], [265], [266], [267] has identified several issues associated with RES integration into the grid and also proposed the following solutions:

- Distributed and Flexible Generation
- Extended Geographical Area
- Energy Storage
- Energy Management

- Communications for Remote Data

10.5.2.1 Distributed and Flexible Generation

Distributed Generation (DG) is a proposed technique to address the aforementioned discussed issues associated with the integration of RES to the grid. Distributed generation brings smaller generation technologies closer to the customer. These DG technologies from literature are also referred to as Distributed Generators (DG) or Distributed Energy Resources (DER) [278]. DG technologies include small PV and wind farms (<100kWp), roof-top PV systems, small wind turbines, fuel-cell, internal combustion engines, etc. DGs are connected to the distribution network [279] which is also illustrated by Figure 10-32. Being connected on the distribution network offers the advantages of lower voltages and in addition being closer to the customer requires shorter power lines and limited grid extension and upgrades. Furthermore, small generation capacities minimise the impact due to variability and uncertainty whereas many generators increase redundancy, stability and reliability.

However, as discussed in [261] and [280], using only RES, DG is not enough to overcome the limitations and constraints (ramp up and down) of steam power plants and offer the required system flexibility and stability at low cost. Therefore, it is proposed that flexible generation is added to the mix. Flexible generators are characterised by their start-up time and cycling costs. Internal combustion engines are the most flexible generators offering start-up time of less than 60 seconds, ramp-up time to full power in less than 5 minutes and negligible cycling costs.

Some scholars [281], [282], [283] suggest that policy makers promoted free market competition by deregulation, privatization and liberalization of electricity markets. This free market competition gave incentives to promote and expand distributed generation. Different types of DG are also included in the IEEE 123 Node Test Feeder [284].

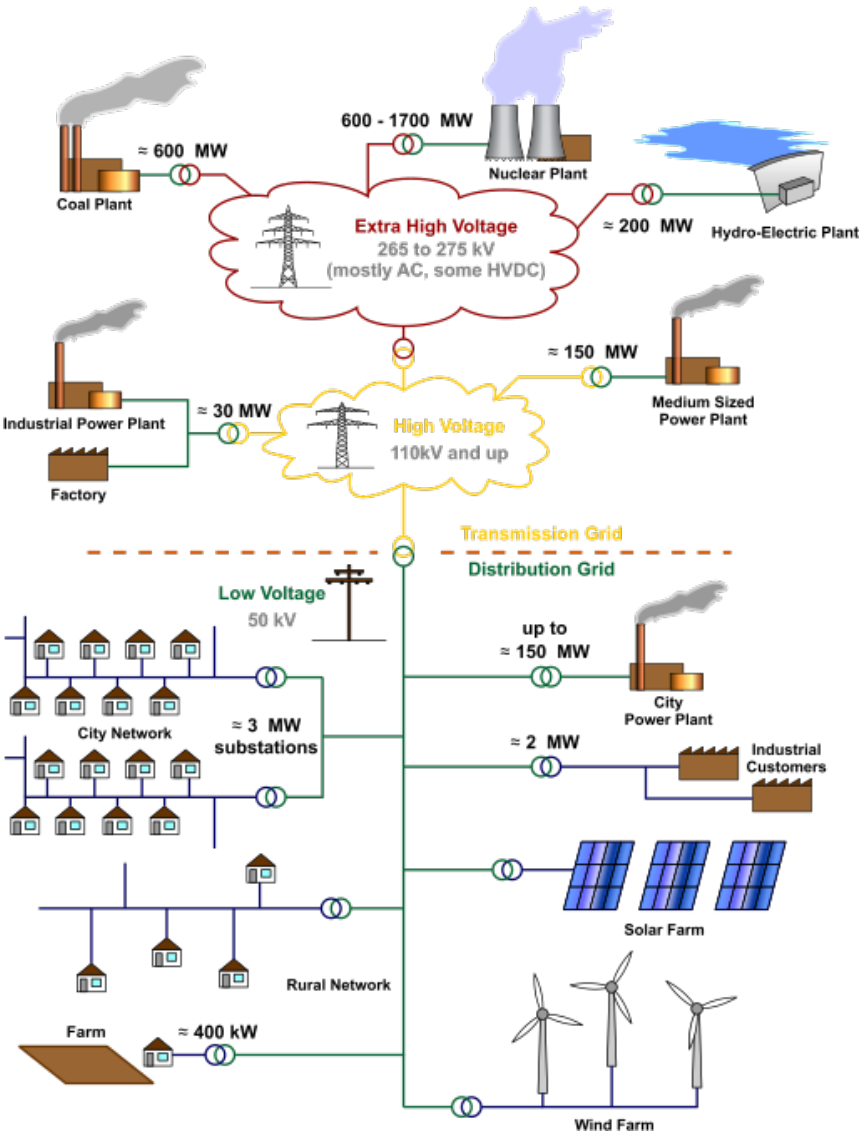

Figure 10-32: Electricity Grid Schematic (Credit: M. Bison, Creative Commons Attribution 3.0 License [285]

10.5.2.2 Extend Geographical Area

As it has already been discussed by dispersing the wind and solar generation to a wider geographical area minimizes the impact on the grid due to variability and uncertainty. This is because clouds and wind fluctuations affect only portions of the plats' capacity. An example is illustrated on Figure 10-33which represents the solar and wind generation on a typical day in Cyprus. It is evident that solar and wind dispersed around the island provide a smooth power generation curve. Also, evident is the fact that solar peak is around noon whereas wind peak is in the afternoon and evening hours. The data was derived from [253].

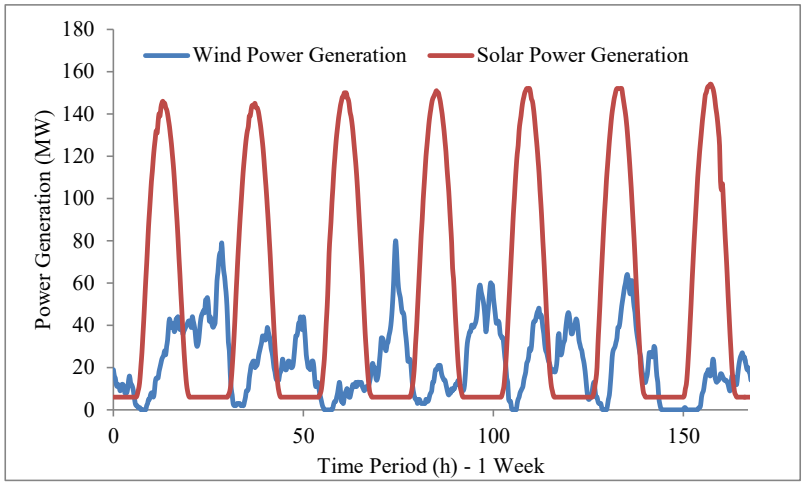

Figure 10-33: Distributed Wind and Solar Power Generation in Cyprus

A recent study [269]and [286] examined the possibility of an optimal RES portfolio to achieve 45% renewable electricity in central Europe (France, Italy, Switzerland, Austria, Germany, Poland and the Czech Republic) by 2030. As it was suggested and presented on Figure 10-34, this is feasible by spreading the wind and solar generation to the identified locations.

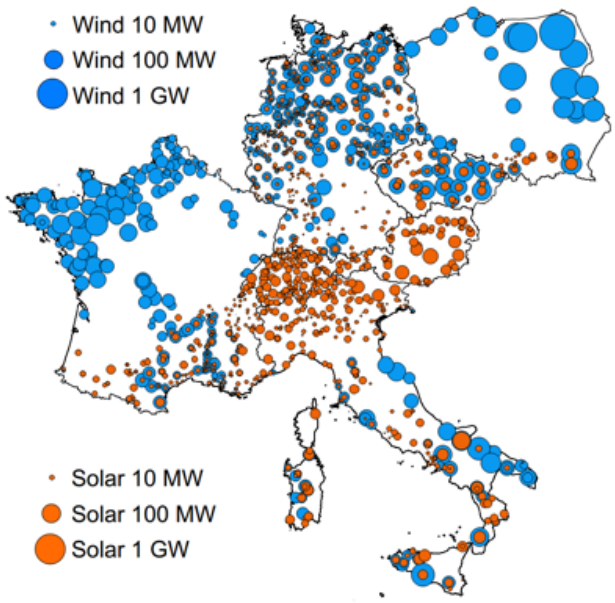

Figure 10-34: Optimal RES portfolio to achieve 45% renewable electricity in central Europe by 2030 (Credit: Dr. Reza Abhari and Energy Science Center (ESC), ETH Zurich [286])

10.5.2.3 Energy Storage

The concept of energy storage is simple and has been very well visualised by research [287], [288], [289] [290], [291], [292]as illustrated on Figure 10-35. Energy is stored when is least needed (off-peak hours) and then it is used needed the most (peak hours). As illustrated storage helps to reduce the peak generation power while at the same time it helps maintain the frequency and voltage. The integration of energy storage to the grid requires the use of power electrics and energy management techniques and algorithms which are discussed on the next section. Traditionally, the first form of stored energy was available through pumped hydro dams whereas recent advancements in material manufacturing and technology nowadays the list of technologies includes batteries, fly-wheels, super-capacitors, compressed air and hydrogen. All energy storage devices will be examined and analysed at a later section.

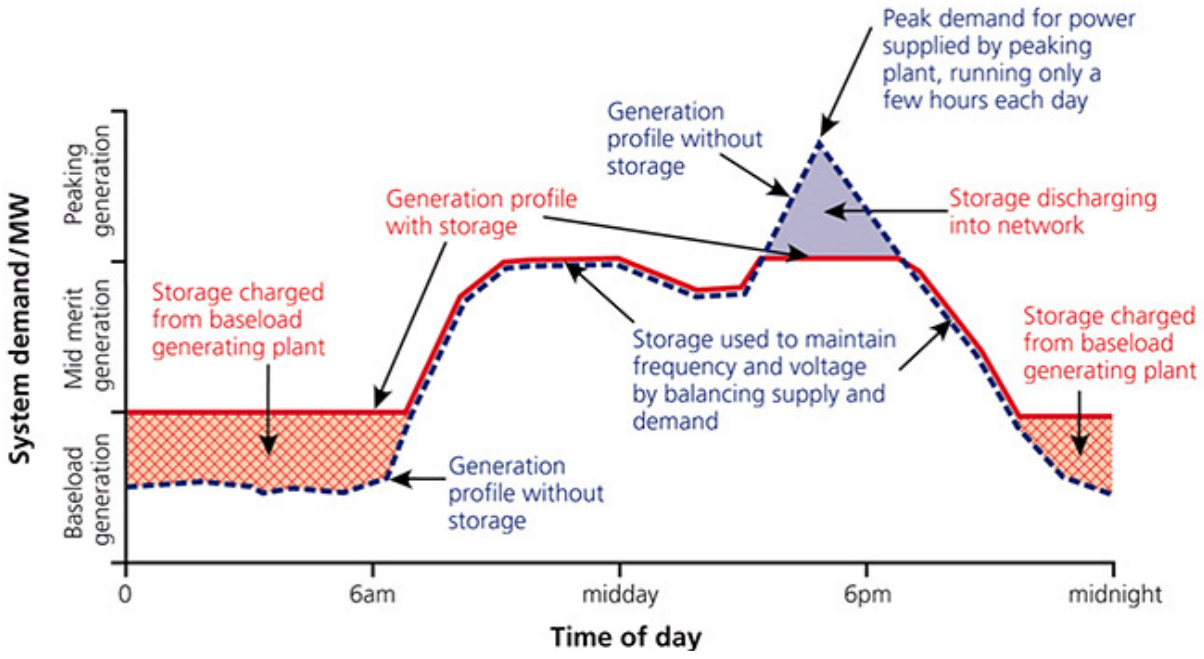

Figure 10-35: Fundamental Idea of Energy Storage [287], [288], [289] [290], [291], [292]

10.5.2.4 Energy Management

Early energy management systems (EMS) developed in the 1970s were simple because the electric power industry was centralised and monopolised. The distribution network was a passive system because power flowed only in one direction; from generation to the customers. Therefore, EMS was required only on Transmission side. However, nowadays, with the penetration of DG the distribution network is bidirectional, allowing power to flow from customers to the network, hence more advanced EMS are required.

An EMS is a computerised system that helps the Transmission and Distribution System Operators (TSO and DSO respectively) to monitor, control, and optimize the network. The concepts for both transmission and distribution networks are the same. However, because the characteristics of transmission and distribution lines are completely different (construction, X/R ratio, phase imbalance, etc.) then an "all-purpose" EMS is not feasible.

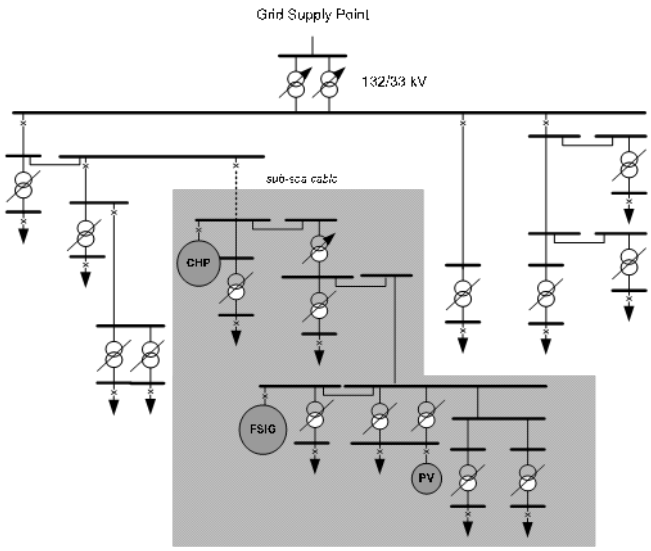

Figure 10-36: Single-line diagram of the 33 kV distribution network with different types of distributed generation

The Single-line diagram of the 33 kV distribution network with different types of distributed generation is presented on Figure 10-36. The system operators (TSO and DSO) are interested for the state of the system. The "state" includes all the bus voltages and power angles also known as the "static state vector", as well as all the currents, power magnitudes (MW and MVAR) and directions, power line loading, etc. The theoretical system's state can be

calculated starting with the power line impedances, then forming the network's admittance matrix also known as the "Jacobian Matrix", and finally using techniques such as the Newton-Raphson solve for the parameters of the power flow equations [204], [205]. However, this process is very time consuming.

Computers are used for faster and accurate results using simulation software such as the PowerWorld Simulator [293]. Using simulation software, the operators can study the systems performance and also design contingency procedures. Contingency procedures are counter measures to be taken to avoid line overloading, frequency and voltage collapse in the events of loss of transmission lines, generation etc. To illustrate a contingency situation a simple 3 bus system is analysed. Figure 10-37 shows the initial performance of the 3 bus system with two generators and one load. As shown the load demand of 200MW (real power) and 100MVAR (reactive power) is met with generator 1 supplying 200MW, 71MVAR and generator 2 only 64MVAR. However, as shown from the simulation results when this scenario is implemented an overload (24%) is created on the line connecting buses 1 and 2. Arrows represent the power directions. When the arrows are green then the power is within limits whereas red arrows indicate a constraint violation.

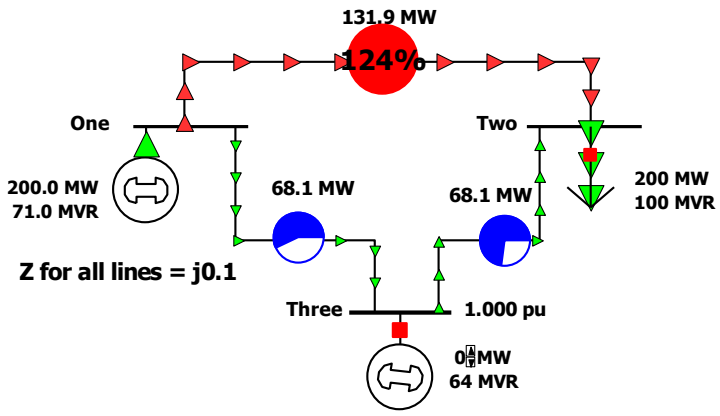

Figure 10-37: Contingency Example of a 3 Bus System using Power World Simulator (Before)

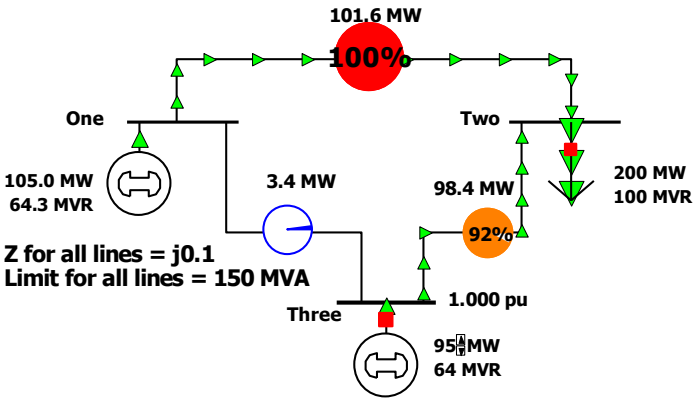

Figure 10-38: Contingency Example of a 3 Bus System using Power World Simulator (After)

The contingency solution to the line overload as shown from Figure 10-38 is to minimise the real power supplied by generator 1 from 200MW to 105MW and increase the real power supplied by generator 2 from zero to 95MW. The proposed solution is not unique and it depends on the experience and skills of the operators. Furthermore, using the simulation software for the specific 3 bus system the simulation time to converge is less than a second.

Figure 10-39 represents a bigger network with numerous busses, transformers, generators and loads using Power World Simulator. The initial input of the network in the software according to experience could take up to 2 hours. However, after that the convergence time is less than 20 seconds.

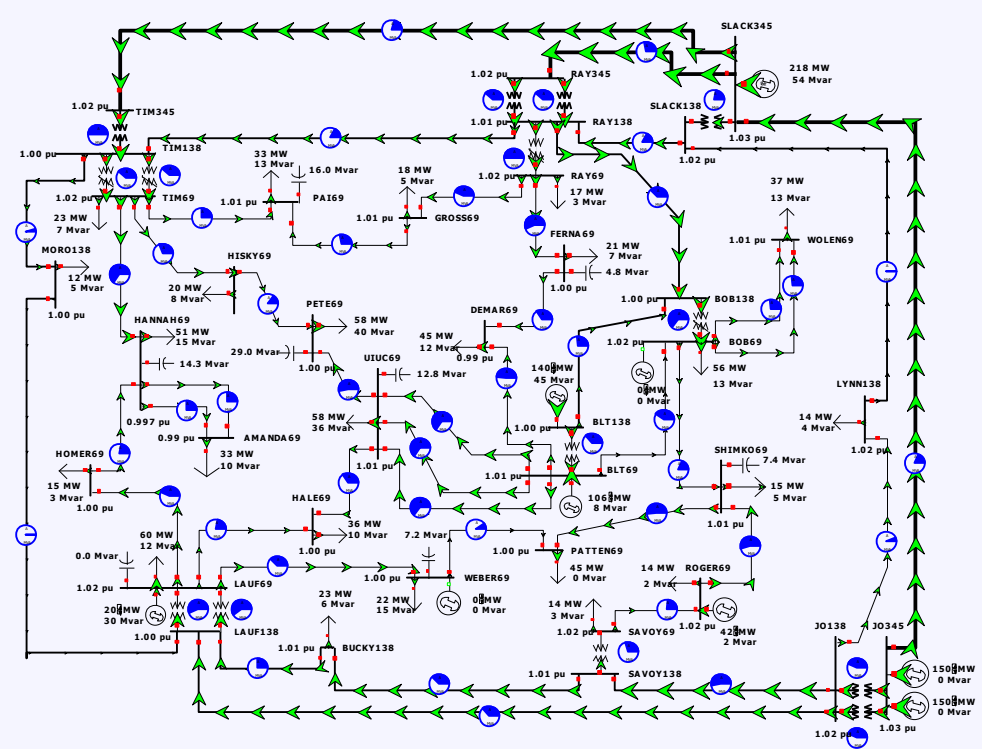

Figure 10-39: Power Flow Simulation using the Power World Simulator

Simulation results enable the operators to have an overview of the system's theoretical state. The actual state on the other hand requires access to system measurements which are affected by tolerance, errors, missing and corrupted data due to noise and interference; Supervisory Control and Data Acquisition (SCADA) is discussed on the next section.

Nowadays, the mitigation of missing and corrupted network data is handled with the use of "State Estimation (SE)". First introduced in 1968 by Fred Schweppe, SE was defined as a data processing algorithm offering better analysis of the electric power system with an estimate of the state by converting redundant meter readings and other available information [294], [295], [296].

Hayes and Prodanovics [297], [298] with the use of a block diagram (Figure 10-40) summarised the functions of ES as described in literature. Inputs include the network parameters obtained from the construction of the network (i.e. busses, line and transformer admittances, constraints, etc), pseudo-measurements obtained from forecasting (i.e. weather conditions, load demand, RES generation, etc) and actual system measurements (i.e. dispatched power, loss of lines or generation, etc) [297], [298].

The first function identified as the Network Topology Processing is responsible for the verification and validation of the given network parameters (i.e. ensuring that the network model is update). The second identified function is the Observability Analysis which determines that there is enough data (measurements) for the SE. In the event that data is inadequate then pseudo-measurements are provided. Data adequacy depends on the Jacobian Matrix [299]. The third proposed SE algorithm uses the verified and validated data from the previous functions and identifies the solution for the system's state that best fits the systems criteria and constraints. The fourth and last identified function is the Bad Data Processing (BDP) which identified and removes data affected by errors and noise. The works of [297], [298], [299], [300], [301] give comprehensive literature reviews for various SE and BDP algorithms.

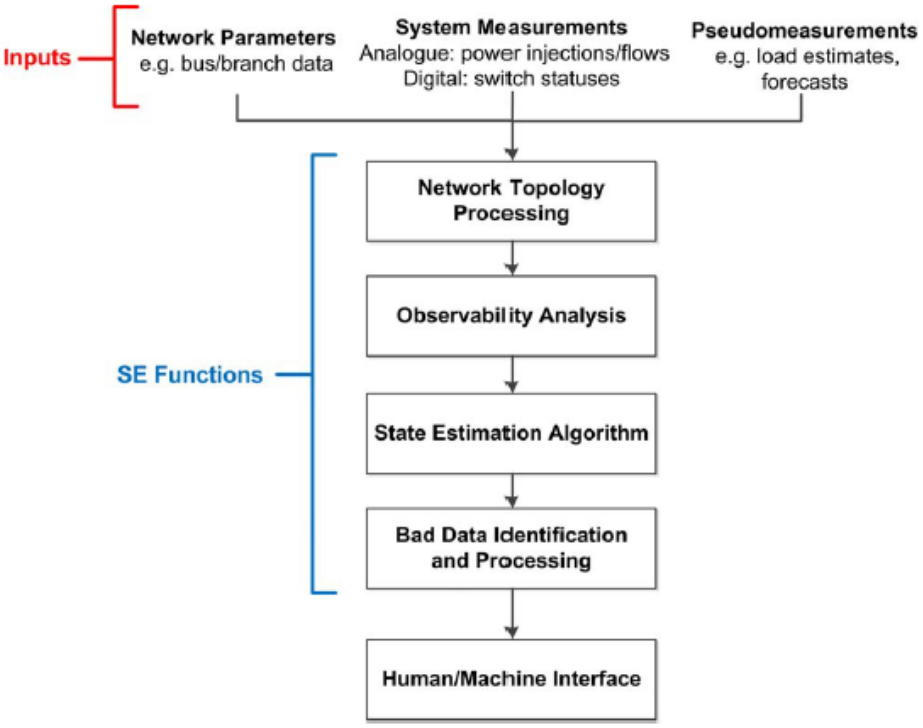

Figure 10-40: Summarised the ES Functions of ES [298]

Energy management can also be applied on the demand side providing flexibility to the electric power system. Flexibility is defined by the industry as the ability to adapt to dynamic and changing conditions such as the ability to balance the supply and demand by time periods ranging from hours to seconds. Demand side energy management aims at smoothing of the steep slopes of instantaneous demand as presented on Figure 39; i.e. load shifting, valley shifting and peak shaving are some of the techniques used to provide system flexibility. A lot of research focuses on residential buildings to shift loads (heating, cooling, energy storage charging, etc) from on-peak hours towards off-peak hours using economic benefits and incentives [302], [303]. Additional areas of study includes planning and scheduling by employing conventional [304], [305] and computational [306], [307] optimization techniques as well as load shedding and peak shaving techniques [308], [309], [310].

Worth mentioning at this point some new network technologies, Flexible AC Transmission Systems (FACTS), Distributed FACTS (D-Facts) and shunt-connected FACTS (STATCOM), which are able to accommodate increased power transfers on the grid including voltage regulation, system damping and power flow control [311], [312], [313], [314].

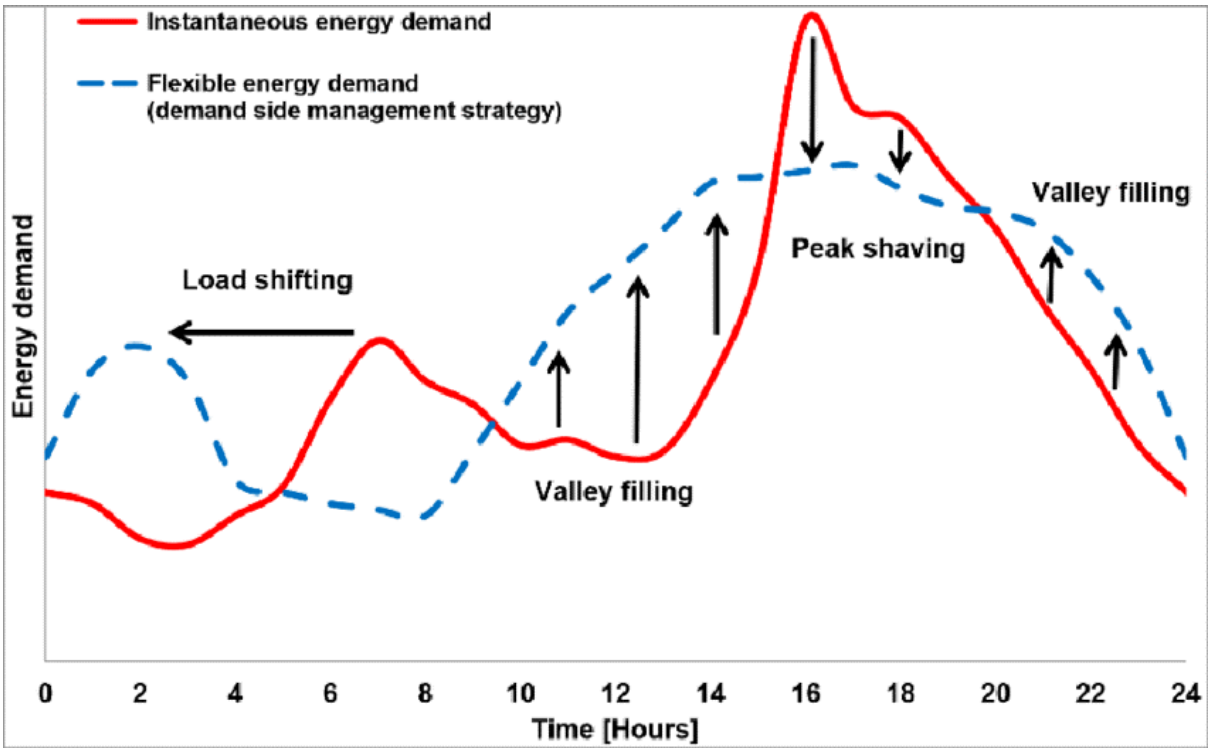

Figure 10-41: Demand Side Management and Energy Flexibility (Available via license CC BY 3.0 [302])

10.5.2.5 Supervisory Control and Data Acquisition (SCADA)

The grid has been evolved to a bidirectional network which includes DG, RES, smart meters, net-metering, EMS and more. The heart of all these is composed of the Supervisory Control and Data Acquisition (SCADA) systems. SCADA has two major functions. First is to retrieve data and alarms from remote sites and second is to enable control of devices or machines at remote sites [315].

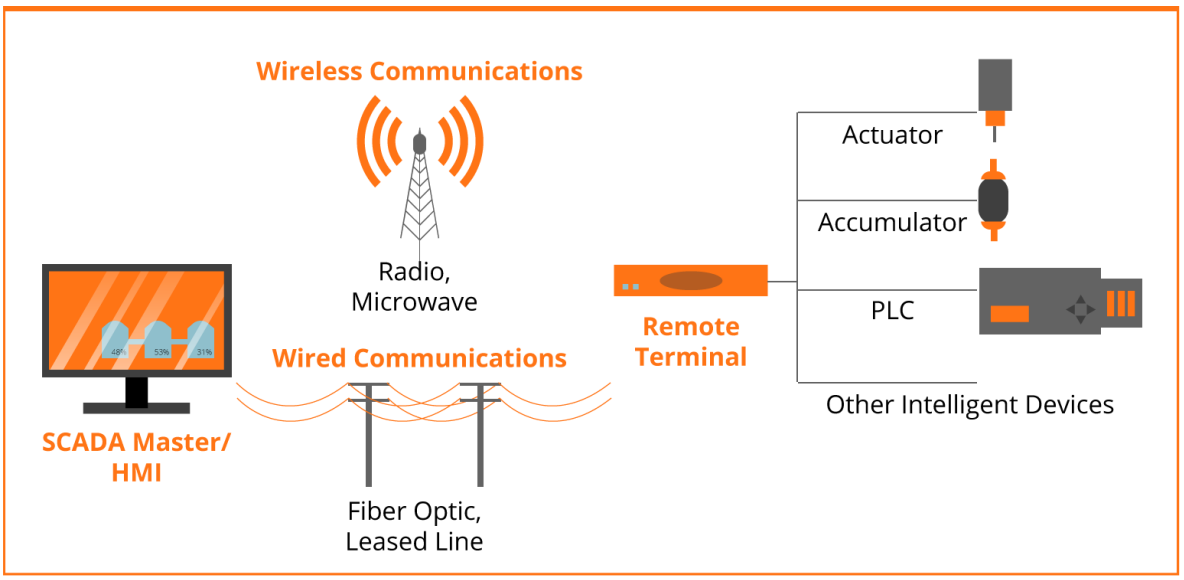

Figure 10-42: General SCADA Layout (Credit: Deramsey, Wikimedia Commons author (GNU Free Documentation License - public domain) [316])

The general SCADA layout is presented on Figure 10-42. The human machine interface (HMI) is connected to the remote terminal via wireless and wired communication methods. Wired technologies include Power Line Communications (PLC), fiber-optics and Digital Subscriber Line (DSL). Wireless technologies on the other hand include but are not limited to World Wide Interoperability for Microwave Access (WiMAX), Universal Mobile Telecommunications System (UMTS), Long-Term Evolution (LTE), Wi-Fi and Wireless Personal Area Network (WPAN). Literature [317], [318], [319], [320], [321] includes elaborate system characteristics and comparisons including the standards and protocols used for each technology.

The remote terminal connects to actuators, accumulators, programmable logic controllers and other intelligent devices. Intelligent devices include volt meters, current transducers, thermometers, mano-meters required for the system measurements as presented on Figure 38 and Distributed Load Shedding Relays (DLSR) required for the system flexibility as presented on Figure 39. Additional sensors and applications are discussed in [322], [323], [324], [325].

10.6 The Smart Grid

The electric power grid has been around for more than 100 years and has been evolving ever since. It is delivering electric power to the connected users, always aiming and striving at the highest reliability and efficiency possible. Innovation and advancements in manufacturing and engineering offered an abundance of sensors [322], [323], [324], [325] whereas Information Communications Technology (ICT) provided the connectivity [317], [318], [319], [320], [321]required to enable the grid to be transformed to an active intelligent network [326], [327] also known as the "smart grid". Today's grid is considered as one of the biggest and most complex man-made system [327].

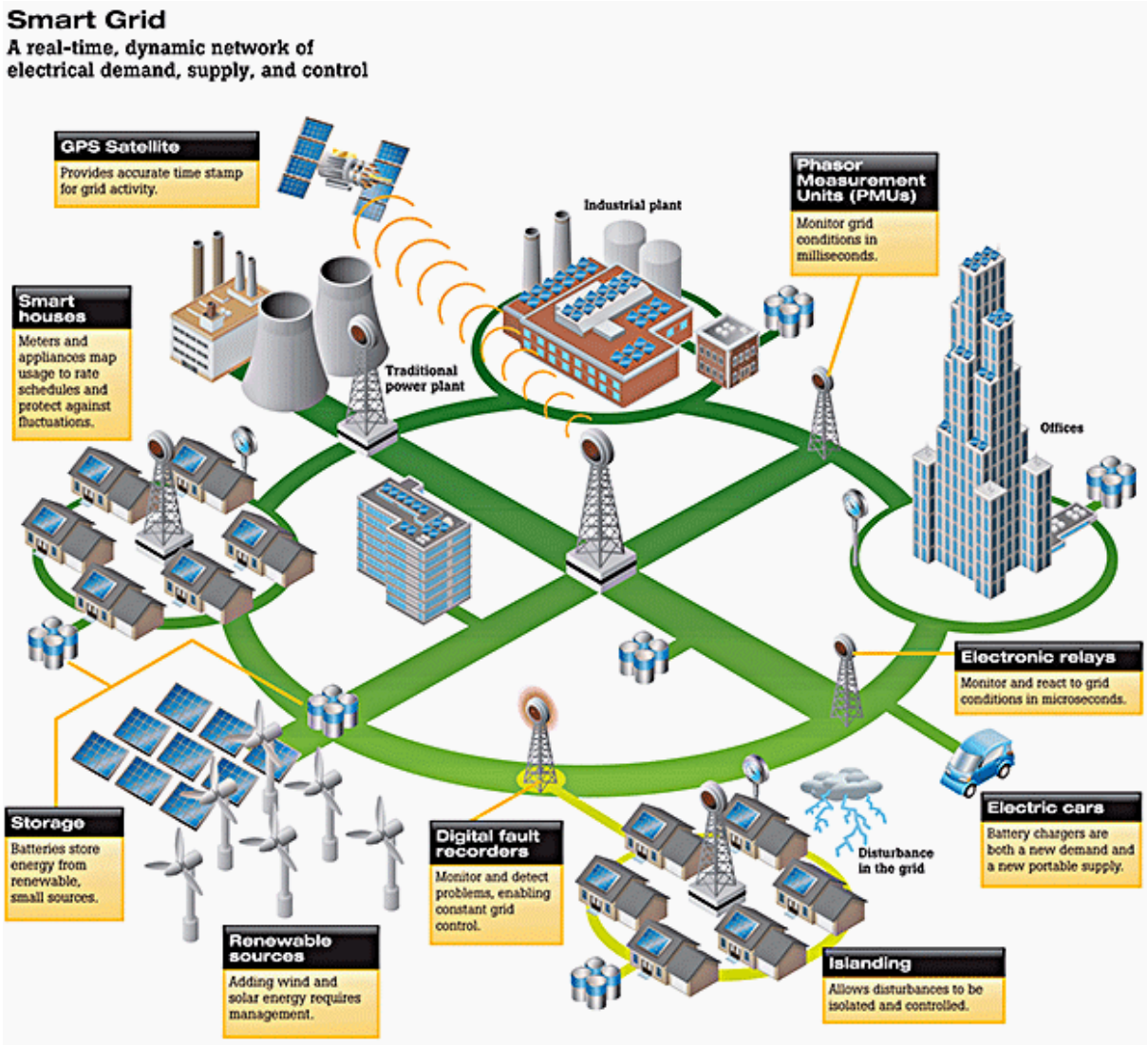

Figure 10-43: SMART GRID – A real-time dynamic network of electrical demand, supply and control (Photo Credit: David Blaza and utilityproducts.com [328] using Written License Consent)

Utility products and Mr Blaza [328] nicely summarise today's smart grid as "a real-time dynamic network of electrical demand, supply and control" and visualise it as presented on Figure 10-43. DG and RES closer to the customer and multiple storage systems for higher flexibility (i.e. load shifting and peak shaving), smart houses with small pv roof top systems and electric cars. Furthermore, the presence of digital fault recorders to monitor and detect problems and islanding for isolating the disturbances on smaller geographical areas thus affecting smaller number of customers. Finally, GPS for more accurate time stamp so that devices such as Phasor Measurement Units (PMU) are able to monitor the grid's state in milli-second time intervals.

10.7 Conclusions

The aim of this work is to introduce the reader to the main challenges of the electric power industry and shows how energy storage is a feasible solution. After an elaborate analysis through exhaustive literature review, this work concludes that Energy Storage Systems are of vital importance for the Smart Grid. As presented, Energy Storage could improve the grid's stability and reliability through Energy Management (Supply and demand, Peak shaving, Load shifting, etc) and through Optimization and Planning (Economic Dispatch and Minimum Production Cost).

11 Energy storage (2/2)

Author(s): Dr Stelios Ioannou
Dr Marios Raspopoulos

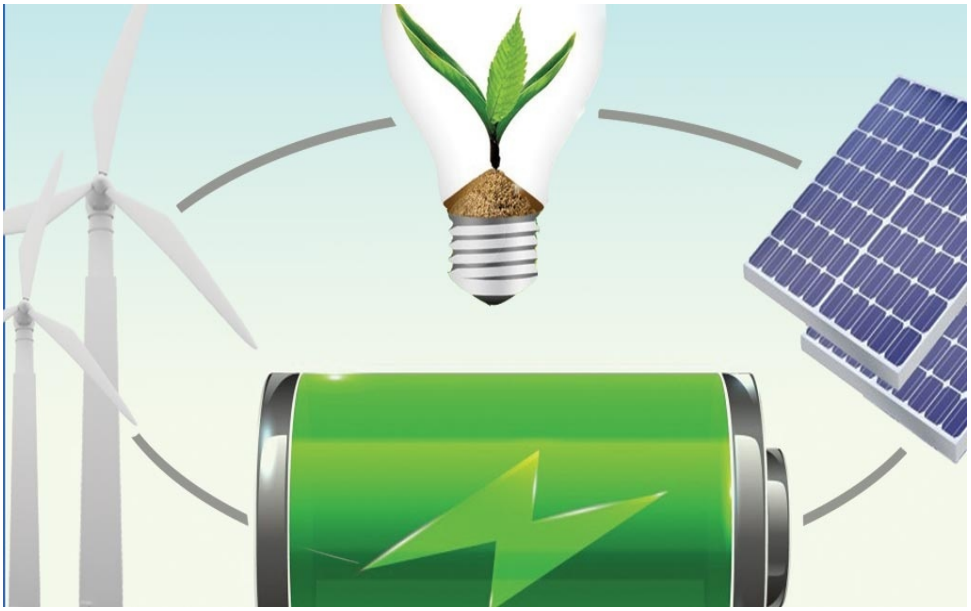

11.1 Abstract

The aim of this two sections work is to introduce the reader to Energy Storage. Section I, included the main challenges of the electric power industry and showed how energy storage is a feasible solution. After an elaborate analysis through exhaustive literature review, this work concludes that Energy Storage Systems are of vital importance for the Smart Grid. As presented, Energy Storage could improve the grid's stability and reliability through Energy Management (Supply and demand, Peak shaving, Load shifting, etc) and through Optimization and Planning (Economic Dispatch and Minimum Production Cost).

Section II reviews the various energy storage systems and their technical characteristics. The technologies under investigation include batteries, fuel-cells, super capacitors, hybrid (battery and super-capacitor), compressed air and flywheels. An overview of each technology is presented followed by the performance metrics. Finally, the technologies are compared and discussed followed by conclusions.

11.2 Introduction

Energy storage applications and examples are summarised on Figure 11-1. The block diagram of Figure 11-1 was derived from literature [55], [329], [330], [331], [332], [333], [334], [335], [336].Energy storage applications are categorized to short-term, intermediate and long-term. Short term applications have duration between milli-seconds to few seconds and require high power whereas long term applications have duration of hours and require high energy. On the other hand the intermediate term have duration between seconds to minutes and require a combination of high power and energy.

Short term applications deal with power quality issues ranging from voltage spikes and sags, momentary outages and harmonics. Energy storage systems for such applications require a combination of fast response and high peak power capabilities. Commercially available systems that meet the criteria include technologies like batteries, fly-wheels, capacitors and super-capacitors, and hybrids.

Hybrid systems are a combination of super-capacitors and batteries. Super-capacitors offer very fast response and high power density whereas the battery offers the energy required for

the application. Research [337]has shown that hybrids are feasible energy storage systems and offer higher efficiency when serving pulsating load currents [338]. However, even though passive systems are simple and cheap yet they lack flexibility and controllability. Hence, research [339], [340], [341], [342], [343], [344], [345] is directed towards active hybrid systems for power enhancement, energy management and optimization. An extensive literature review on active hybrid systems is provided by [329].

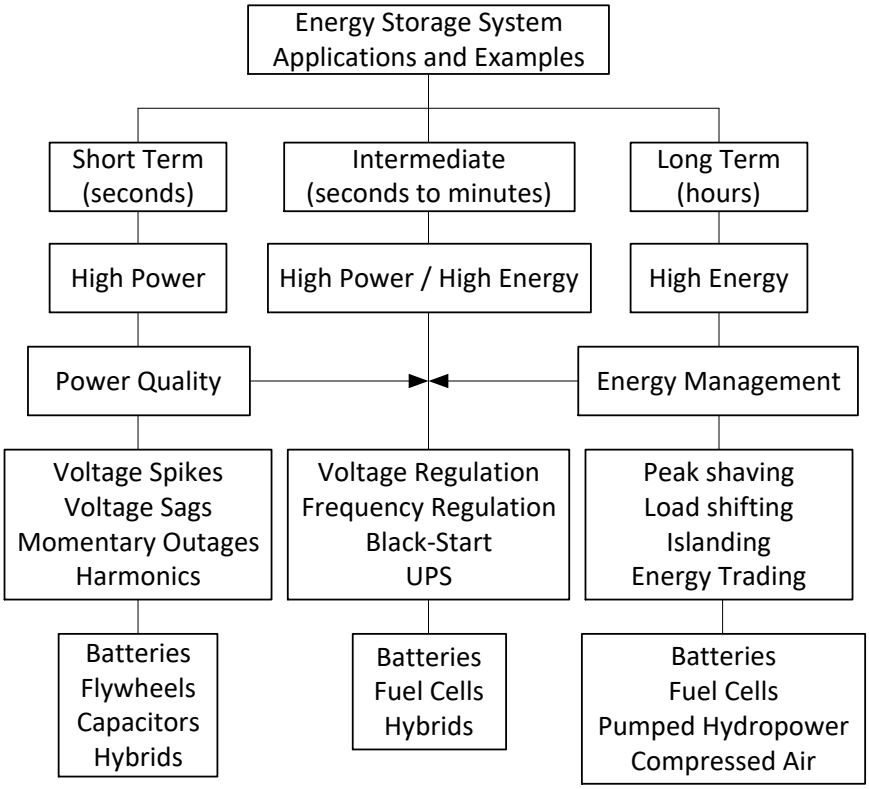

Figure 11-1: Energy Storage Applications and Examples

Intermediate term applications are a combination between power quality and energy management. Such applications deal with issues including voltage and frequency regulation, uninterruptable power supply (UPS) and black-start; black-start is the process of recovering from a total or partial outage. Commercially available technologies that meet the criteria include batteries, fuel cells and hybrids.

Long term applications deal with energy management issues which include peak shaving, load shifting, islanding and energy trading. Commercially available technologies which meet the criteria include the batteries, fuel cells, pumped hydropower and compressed air (CAES).

An important term worth mentioning at this point regarding energy storage systems is that their efficiency is measured and referred to as the Round-trip efficiency which is also known as the AC/AC efficiency. Round trip efficiency takes into consideration the amount of energy stored in the storage system and amount of delivered or retrieved energy. Some indicative efficiencies for the energy storage technologies under investigation are derived from literature [55], [329], [330], [331], [332], [333], [334], [335], [336] and tabulated on Table 11-1.

Table 11-1: Reported Round-Trip Efficiency for Energy Storage Systems

Energy Storage Technology	**Efficiency (%)**
Pumped Hydropower	65-80
Flywheels	80-90
Batteries	75-90
Compressed Air (CAES)	65-75

As shown from the tabulated round-trip efficiencies, batteries and fly-wheels offer the highest efficiencies. However, because batteries offer a combination of high power and high energy then it is the preferred technology for all aforementioned applications.

Energy storage systems are classified to mechanical, chemical and electromagnetic as shown on Figure 11-2.

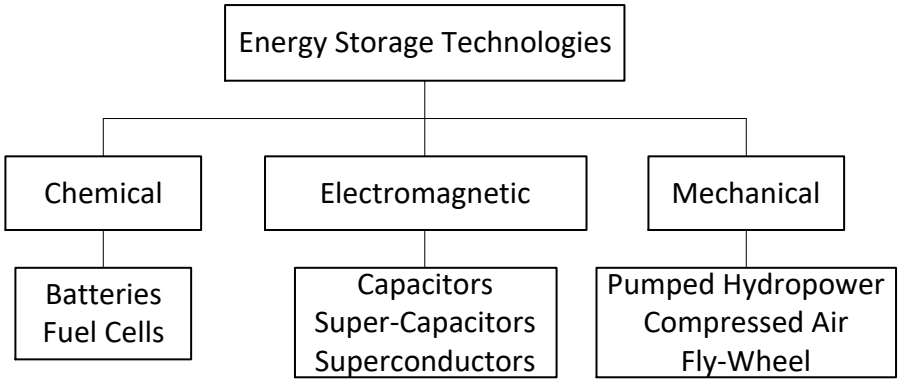

Figure 11-2: Classification of Energy Storage Systems and Technologies

11.3 Batteries

11.3.1 Technology Overview

Battery technologies are electrochemical devices that store energy. When a load is connected across the cathode and anode terminals then the chemical energy is converted to electrical. The process involves oxidation (loss of electrons) and reduction (gain of electrons) of the anode and cathode terminals respectively. The rate of change of charge is known as electric current, and it is proportional to the chemical energy stored in the battery.

Batteries are categorised to rechargeable (secondary) and non-rechargeable (primary) technologies. As the names imply, rechargeable batteries can be used multiple times (reusable) by recharging them when discharged, whereas non-rechargeable batteries are non-reusable and should be replaced when discharged. The process of charging/recharging a battery is achieved via an electronic device known as a "charger" and involves the reversing of the oxidation and the reduction reactions which occur during the discharging activity. Hence, it can be said that the charger can force current into the battery.

As shown in Table 11-2, battery technologies have been around since the 1950s. The technologies compared include Nickel-Cadmium (NiCad), Nickel Metal Hydride (NiMH), Sealed Lead Acid (SLA), Lithium Ion (Li-Ion), Alkaline, and more. There is always a trade-off when choosing a battery technology, hence engineers should study and understand the various characteristics:

- **Technology age:** Shows the maturity of the technology. The oldest technology (NiCad) shows that it has been excessively studied and it is well understood.
- **Energy Density (Wh/kg):** Indicates the amount of energy with respect to the battery's weight. For example, Li-Ion offers the highest energy density which means that it can store 3 times more energy than SLA and twice as much as the rest of the other technologies. High energy density makes Li-Ion the preferred technology for mobile applications such as cellphones, laptops etc.
- **Internal Resistance:** Represents the technology's opposition (resistance) to the flow of electrons (electrical current). High resistance indicates high internal losses (low efficiency). Technologies such as alkaline with the highest internal resistance are limited to low power applications.

- **Load Current:** Battery technologies have limited load current capabilities which are determined by the chemistry and manufacturing processes. Engineers should take into consideration the load's required current and batteries highest current capability. The load current should be less than the battery's current.

Therefore, taking into consideration the characteristics and trade-off some examples of the market trends are as follows:

- **NiCad**: its high life cycle, low internal resistance, and high load current characteristics make it an attractive choice for power tools, two way radios and biomedical instruments.
- **Reusable alkaline**: are very cheap, but their high internal resistance limits their use to only very low current applications.
- **SLA**: despite the low energy density, low price makes sealed lead acid (SLA) batteries attractive for applications where volume and weight is not a problem.
- **Lithium ion**: are the most expensive technology. However, with their high energy density and cell voltage, lithium technology is the most attractive choice for electronic devices where dimensions and weight are critical such as unmanned aerial vehicles (UAVs) also known as unmanned aerial systems (UAS). Market trends and new research show that Lithium batteries have dominated not only mobile applications but also the RE applications. Hence, lithium batteries will be primarily investigated in this study.

Table 11-2: Overview of Various Battery Technologies [346], [347]

	NiCad	NiMH	SLA	Li-Ion	Reusable Alkaline
Energy Density (Wh/Kg)	40-60	60-80	30	165	80 (initial)
Internal Resistance (mΩ)	100-300	200-800	<100	300-500	200-2000
Cycle Life	1500	500	200-300	500-1000	10000
Cell Voltage	1.2	1.2	2	3.6	1.5
Load Current	>2C	0.5-1C	0.2C	2C	0.2C
Operating Temperature (°C)	-40 to +60	-20 to +60	-20 to +60	-20 to +60	0 to 65
Cost	$50	$70	$25	$100	$5
In Commercial Use Since	1950	1990	1970	1991	1992

11.3.2 Lithium Batteries

Lithium technology batteries offer the highest cell voltage and the highest energy density as compared to other technologies hence they are the preferred choice for applications where constraints such as weight and volume are major issues. Compared to other technologies, lithium solutions offer one-third of the weight and one-half of the volume than SLA technology and one-half of the weight and two-thirds of the volume than NiMH [346], [347], [348], [349].

11.3.2.1 Technology Overview

Specific Energy Density is a metric for comparing the amount of energy a battery technology offers with respect to the package weight. The units of specific energy density are given in Ah/kg. Literature [350] lists the specific energy of lithium metal in the range of 3800Ah/Kg (1727Ah/lb), whereas for lead is listed at 260Ah/Kg, and cadmium at 480Ah/Kg. On the other hand, lithium technology is vulnerable and highly susceptible to catastrophic failures which result in fire. Hence, the use of electronic safety designs is a must. The safety circuitry controls the battery's vital parameters such as the operating temperature range and cell voltage during both processes of charging and discharging [347], [351], [348].

Advancements in material and manufacturing enabled the use additional cathode compositions such as Li-MnO2 [352], [353].Nowadays, lithium battery technologies (lithium ion and polymer) offer cell voltages in the range of 3.85 and 4.2V at improved stability compared to their predecessors. In addition to the higher cell voltage they provide discharge currents and discharge rates (C-rate) as high as 50 and 100 times their rated capacities. For, example a battery with capacity of 1Ah at 50C will give a discharge current of 50A and will discharge in 0.02 hours or 1.2 minutes.

The price of the materials used is the major bottleneck for lithium batteries [352]. For example, lithium polymer is more expensive than lithium-ion. Hence, lithium polymer batteries are limited to applications of mass production such as cell-phones and aeromodelling that come in a "credit card" like shape [347] because the volume is also an important constraint and limitation for these applications.

11.3.2.2 Charging Process

The charging process of lithium battery technologies is represented in Figure 11-3. The charging is a 3-stage process also known as the constant voltage/constant current method (CV/CC). During the first stage a constant current is applied by the charger to the battery until the battery reaches a voltage of 4.2v per cell. During the second stage, the voltage is kept constant while the charging current is slowly decreased to 3% of rated current. At this point the battery is considered fully charged reaching its rated capacity. Finally, the third stage compensates for the battery's self-discharge.

The open circuit voltage (OCV) for most of lithium-ion cells is in the range of 4.2v. However, some commercially available products such as Panasonic – CGP30486 OCV are 4.1V [354]. Specified chargers should be used for lithium technologies for safety and performance purposes. For example, the charger for the Panasonic battery (CGP30486) will limit the voltage to 4.1v for safety reasons. However, if the same charger is used for a battery designed for 4.2v and it is only charged to 4.1V then its capacity is reduced by 10% [347]. In addition to the cell voltage, various lithium technologies have different charging currents. Smaller cell phone batteries are charged at approximately 1C (1 hour), whereas larger 18650 type cells are charged slower, for example 0.8C which is equivalent to 1.25 hours. As mentioned already, the charger is responsible for the monitor and control of important battery parameters including to but not limited to overcharge, over-discharge, and operating temperatures.

Usually, the charging process for lithium ion and polymer batteries is in the range of 1 to 3 hours. However, some companies release new rechargeable lithium ion batteries which can be recharged to 80% of their capacity in a few minutes [355].

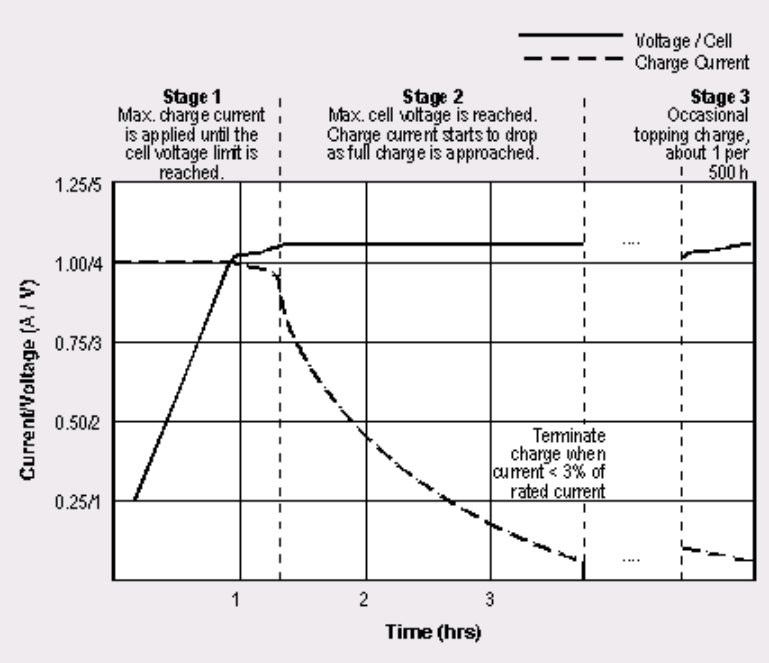

Figure 11-3: Charging of Lithium Technologies (Credit: Isidor Buchmann and CADEX Electronics Inc., [347], [352], [351]).

11.3.2.3 Performance Characteristics

The performance metrics for battery technologies include the discharge current, voltage and temperature as presented on Figure 11-4. At lower temperatures, -10°C compared to 60°C, the battery shows lower cell voltage. The performance of lithium batteries is significantly affected when operated at temperatures below 0°C and above 65°C [356], [357], [358]. This battery behaviour with respect temperature variations is attributed to variations in internal resistances [356], [359]. Battery internal resistance is inversely proportional to the operating temperature. Therefore, at lower temperatures, the internal resistance increases causing a higher voltage drops. The battery performance (capacity and voltage) with respect to operating temperatures is presented in Figure 11-4 at a constant discharge rate of 1C (1 discharge hour). The lithium-ion cell under consideration was the 18650 which indicates a cylindrical shape with diameter 18mm and length 65mm. As presented at -10°C cell capacity is less than 1400mAh whereas at operating temperatures between 20°C and 60°C, the capacity is approximately 1500mAh. The increased internal resistance affects the battery efficiency and capacity. Similar performance behaviour is observed at the results presented on Figure 11-5 at higher discharge rates (~5C).

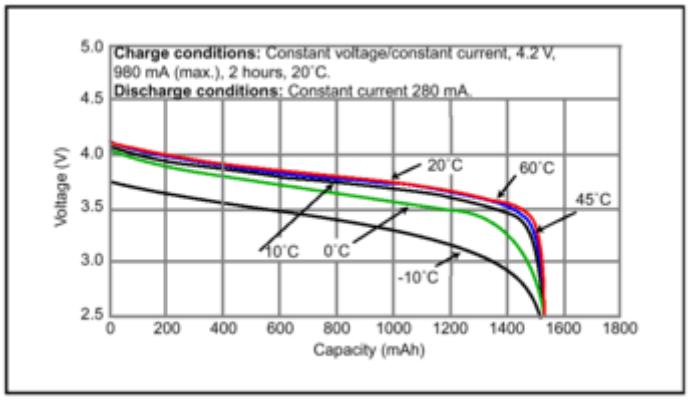

Figure 11-4: Lithium-Ion Performance Characteristics at Various Operating Temperatures [360].

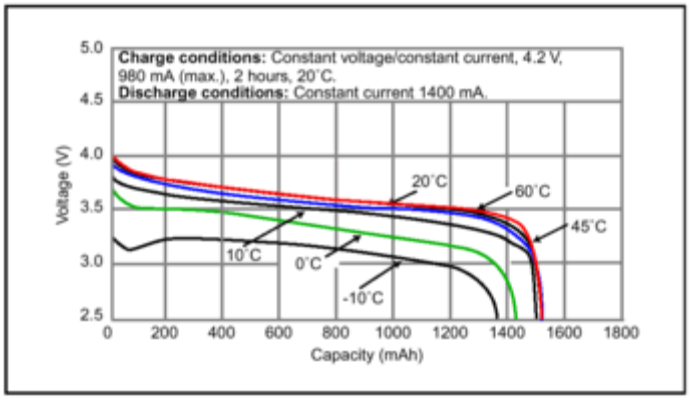

Figure 11-5: Lithium-Ion High Rate (~5C) Performance Characteristics at Various Operating Temperatures [360].

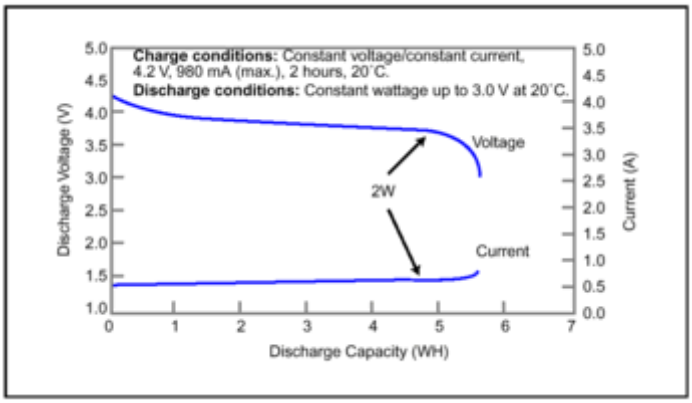

Figure 11-6: Typical Lithium-Ion Constant Power Discharge Performance [360].

The constant power discharge performance presented on Figure 11-6 is very important for RE applications. Notice how the discharge current increases as the voltage decreases to maintain the required constant power. The manufacturer determines the end voltage of each product with the aim to prolong the battery life and avoid and catastrophic failures.

To sum up, Lithium technologies offer the following advantages:

- high energy densities
- no need prolonged priming when new
- low self-discharge (less than 10% per month)
- low maintenance
- No memory effect

The disadvantages of lithium technologies are as follows:

- Expensive material
- Added costs and complexity due to the required protection circuitry to control and monitor the voltage, current and temperature.
- Aging starts from the date of manufacture and it is also affected by low temperatures which leads an increased internal impedance and power loss [348].
- High discharge currents are available at the expense of higher weights and volumes.

On the other hand, lithium polymer (Li-Po) batteries offer higher safety and stability compared to Li-Ion due to the gelled electrolytes which are more resistant to overcharge and electrolyte leakage. Furthermore, Li-Po are easier to manufacture in any shape and size than Li-ion batteries. However, Li-Po compared to Li-Ion are more expensive, offer decreased cycle count and lower efficiency due to the higher internal impedance (lower electrolyte ionic conductivity) [361].

11.3.3 Primary Lithium Batteries

Primary lithium batteries do not have any recharging capabilities; they only have one time use. Compared to secondary batteries primary are more expensive and are limited to low power applications which leads to higher service life. Commercially available products

according to an extensive literature review [360], [362], [363], [364], [365], [366], [367], [368], [369] include cathode and anode material compositions composed of Lithium/Poly-Carbon Monofluoride, Lithium/Manganese Dioxide, Lithium Thionyl Chloride, Lithium/ Sulphur Dioxide, etc.

The discharge characteristics presented on Figure 11-7 and Figure 11-8 are obtained are directly derived from the manufacturer datasheet for the Toshiba (ER6VP) Thionyl Chloride Lithium Battery. This primary lithium battery offers a nominal voltage of 3.6V, a capacity of 2000mAh and a weight of only 16gr. As observed, from the aforementioned figures the battery voltage is constant (zero slope) and the service life is in the range of hundreds of hours. To an untrained eye and non-experienced engineer the discharge characteristics of the primary batteries could be seen superior compared to the previously analysed characteristics of secondary batteries. However, this is not true. As mentioned, primary batteries are expensive and are limited to low power applications.

Using Ohm's law, from Figure 11-7, with a given cell voltage of 3.6V and load resistances in the range of 300, 1K, 3.6K and 36KΩ, then the discharge currents are calculated to 12mA, 3.6mA, 1mA and 100μA, respectively. Therefore, for a given rated capacity in the range of 2000mAh, then the discharge rates (C-rate) are calculated for the equivalent discharged currents of 12mA and 3.6mA discharge currents as 0.006C or 167 hours discharge time and 0.0018C or 556 hours, respectively. Using similar methodology for the Li-Ion 18650 cell with given rated capacity in the range of 1400mAh, then at a discharge current of 12mA, then the calculated discharge rate is 0.0086C or 117 hours discharge time, which is not an identical performance but comparable. In addition to the discharge time, at load currents in the range of a few milli-amperes, the voltage drop due to the internal resistance would be very small, yielding to a constant and stable voltage.

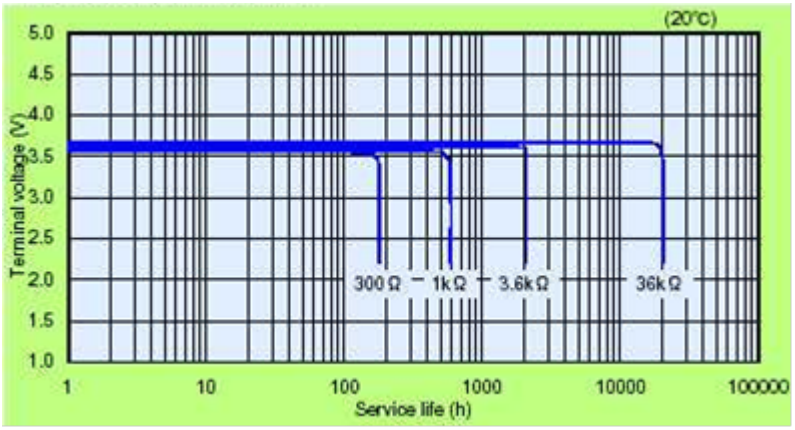

Figure 11-7: Primary Lithium Battery Discharge Characteristics [354].

Figure 11-8: Primary Lithium Battery Discharge Versus Temperature [354].

Finally, primary batteries similar to secondary batteries are also susceptible to increased internal resistance and power loss.

11.3.4 Scaled Up Secondary Lithium Ion Batteries

Scaled up secondary batteries are composed of multiple cells connected in series to achieve the desired voltage and connected in parallel to achieve the desired increased current that is required for high power applications. High power applications include satellites, automobiles, and Renewable Energy.

Satellite applications include the geo-synchronous orbit (GEO) which requires the batteries to sustain a lifespan of 15 years and 1200-2400 cycles at 60% depth-of-discharge (DOD), and the low earth orbit (LEO) which requires a lifespan of 7 years and 35,000 cycles at 25% DOD [348]. According to literature [348] the Ni-H2 (INTELSAT V) required a total weight of 24kg because of the 1.2v cell voltage and energy density in the range of 40-50Wh/Kg whereas for the same application using lithium ion batteries the weight was reduced to half (12kg), with the 3.6V cell voltage and energy density in the range of 90-140Wh/Kg.

For application involving Electric and Hybrid Electric Vehicles (EV and HEV) the required battery pack voltage ranges from 148V for order models and 330-500V for newer models [347], [370].Higher voltages have minimal copper losses and also minimal strain on switches.

Using a lithium cell with a 3.7v operating voltage then to achieve a desired voltage in the range of 450V, requires the use of 90 Lithium Ion cells to be connected in series (also known as string connection). More than two series cells form a module and more than two modules in parallel form a battery pack. All chemistries and battery technologies are vulnerable to failures. When the failure includes a short-circuited module it results in a reduced voltage drop whereas in the event of an open circuit results in zero electrical current (cut-off).The higher the number of modules connected increases the possibility of failures. However, as already mentioned the matrix formation (series and parallel) cannot be avoided because it is the only way to achieve the voltage and capacity requirements. Parallel connected (battery pack) increases the battery capacity. On the downside, parallel connected cells should be almost identical cells of the same rated capacity and voltage. An advantage of parallel connected packs is that an open circuit failure does not affect the voltage and normal operation of the battery pack. An open circuit failure will only result on reduced runtime. An example of matrix formation, using Ni-MH cells, 1.2V, 6.5Ah to meet the Toyota Prius battery specifications of terminal voltage of 273.6V and energy of 1,779Wh. To achieve the design

specifications mandates the uses of 38 modules with six cells per module. Furthermore, with the module weight in the range of 1.04Kg then the total battery weight would be in the range of 53.3Kg [356]. On the other hand, as proposed in [356] the battery pack voltage would be lower at 259V (70 modules with 4 cells per module), but on the other hand the battery capacity would be increased to 20,072Whand the weight would be decreased to 20kg (0.24Kg/module).

As always in engineering, Utopia does not exist. The battery pack matrix (series and parallel connections) suffers from increased internal temperature which results to reduced battery life and can also potentially lead to thermal runaway [6]. In the case of lithium technology uneven heat transfer may result in fire. Heat variations lead to different internal resistances for different cells [347], [357] and even when identical cells are charged in parallel, the cell with the lowest impedance will receive higher charging current [348]. Hence, the charging process is controlled by temperature and voltage safety circuitry. Furthermore, improved battery performance may result from controlling the temperature which is also known as Thermal management. Thermal management includes the process of cooling to prevent overheating of the battery pack whereas at low temperature losses are overcome by heating the pack. Commercially available cars such as the Toyota Prius use parallel-flow air-cooling [357]whereas the Nissan Tino uses passenger air to cool down the batteries [348]. Leading companies in Li-Ion cells and battery packs for electric vehicle applications are Shin-Kobe Electric Machinery Co., Ltd., Japan Storage Battery Co., Ltd., and Saft.

11.3.5 Performance Metrics

Batteries have 2 important performance metrics: the capacity and the energy density. Battery capacity is measured in ampere hours (Ah), whereas energy density is measured with respect to weight (Ah/kg) and with respect to volume (Ah/m^3). With respect to weight is known as gravimetric or specific energy density whereas with respect to volume it is known as volumetric. Capacity and energy density are two parameters that engineers should use to compare the performance between various products.

Battery capacity is depended on the discharge current which is usually expressed as a fraction of the numerical value of the capacity. At higher discharge currents (high discharge rate) the

battery efficiency decreases and as a result less energy is delivered. The first mathematical model that captures this effect also known as Peukert's equation is given by:

$$C_p = I^p t$$

Equation 11-1

where C_p is the Peukert's battery capacity, I the discharge current, t the time and p Peukert's exponent usually between 1.1 and 1.4 dependent on the battery [371], [372].Unfortunately, battery manufacturers use different discharge currents to calculate their battery capacities making straightforward comparison troublesome. This problem affects the other performance measures since they are derived from battery capacity. More details on how to use the Peukert's equation are presented in [371], [372].

Energy density (volumetric or gravimetric) is a commonly used performance metric for battery sizing because the weight and volume is always available on the datasheet. For accurate battery run time then loss of capacity at higher discharge currents should be taken into consideration as shown in the literature [371], [372].

11.4 Fuel Cells

11.4.1 Technology Overview

Electrolysis involves the process of breaking down the water molecules to hydrogen and oxygen with the aid of electricity. Fuel-cells on the other hand produce electricity and water by combining hydrogen and oxygen. For as long as the fuel is available then the fuel cells are producing electricity. The re-fueling process takes less than a few minutes, which is significantly faster compared to the charging process of battery technologies which takes a couple of hours. As research [370] suggests Fuel Cells (FCs) and batteries share the same principle of operation. However, batteries are devices that store energy whereas fuel-cells are devices that provide on-site energy production.

Table 11-3: Fuel Cell Technology Profile from [370]

	PAFC	AFC	MCFC	SOFC	SPFC	DMFC

Operating Temperature (°C)	150-210	60-100	600-700	900-1000	50-100	50-100
Power Density (W/ cm^2)	0.2-0.25	0.2-0.3	0.1-0.2	0.24-0.3	0.35-0.6	0.04-0.23
Projected Life (hrs)	40,000	10,000	40,000	40,000	40,000	10,000
Projected Cost (US$/KW)	1000	200	1000	1500	200	200

The characteristics of some commercially available fuel cell technologies are tabulated on Table 11-3. Commercially available fuel cells include the Proton Exchange Membrane Fuel Cell (PEMFC), the Alkaline Fuel Cell (AFC), the Direct Methanol Fuel Cell (DMFC), the Solid Oxide Fuel Cell (SOFC), the Molten Carbonate Fuel Cell (MCFC) and the Phosphoric Acid Fuel Cell (PAFC). The electrolyte or the fuel used determines the name of each fuel cell type.

The storage and handling of hydrogen which is the primary fuel used in PEMFCs is an added complexity [373]. On the other hand, the Direct Methanol Fuel Cells (DMFCs) which is a subset of PEMFCs, uses methanol as a fuel which is simple to store and handle even though it is considered as toxic. Furthermore, DMFCs have lower efficiencies compared to PEMFCs. On the other hand, DMFCs offer higher energy densities which makes them the preferred energy and power system for portable applications in the sub-kilowatt range [374], [375], [376], [377], [378], [379].

The basic operation of hydrogen fuel cells is best described by two reactions that occur concurrently. At the anode of an acid electrolyte, hydrogen gas ionizes releasing two electrons, two mobile protons (H^+) and energy.

$$2H_2 \rightarrow 4H^+ + 4e^-$$

Equation 11-2

The mobile protons will travel through the acid electrolyte to the cathode, whereas the electrons cannot go through and are forced to travel through an external connection provided by the load. At the cathode, oxygen reacts with the proton taken from the electrolyte and electrons arriving externally, to form water.

$$O_2 + 4e^- + 4H^+ \rightarrow 2H_2O$$

Equation11-3

In the meantime, the electron flow between the electrodes is defined as electrical current, which provides electrical power the load.

Different fuel cell types/chemistries experience different anode and cathode reactions. However, the principle of operation remains the same. According to the fuel cell type, the cell operating voltage is in the range of 0.6 to 0.875V [380]. Higher cell voltages can be achieved with the use of different anode/cathode reactants. The required voltage is achieved by connecting cells in series which then form the stack.

Pressure and temperature play an important role on the performance of fuel cells [380]. The current and voltage characteristics and the losses of a PEMFC presented on Figure 11-9were directly obtained from [381] and [382].The ideal voltage also known as theoretical or no-loss voltage is approximately 1.2V. However, the actual open circuit voltage is drops to approximately 1V because of fuel cross-over [383]. The I-V characteristic curve of fuel-cells is like batteries. However, in the case of fuel cells it is called a polarization curve.

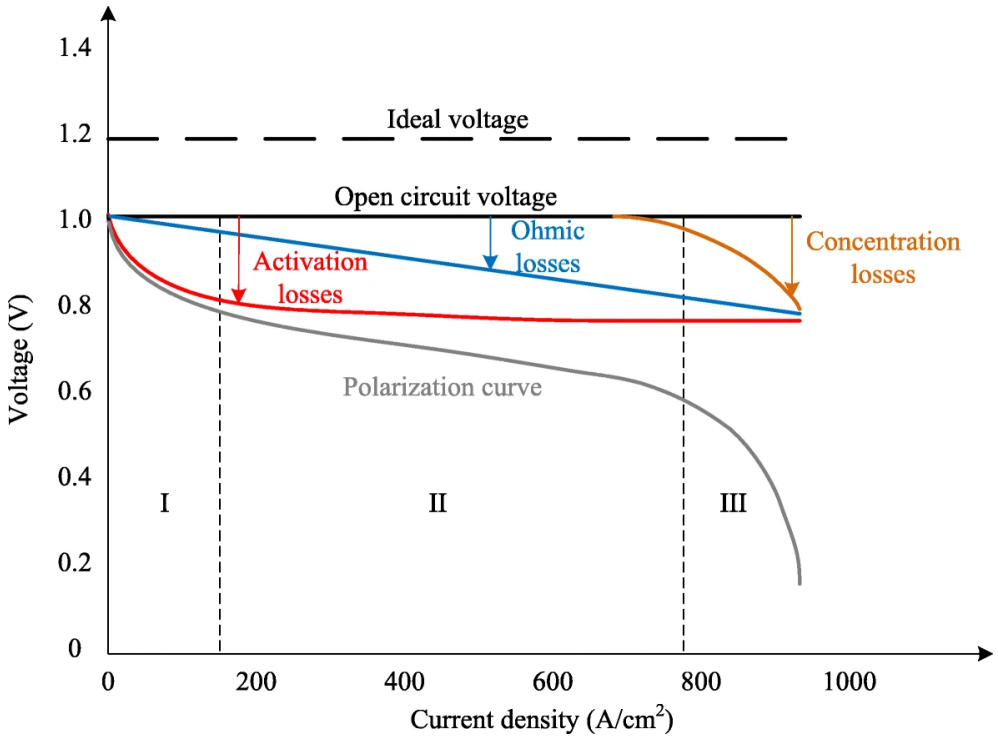

Figure 11-9: I-V Characteristics and Losses of PEMFC (Credit: Zhongliang Li, Open Access Creative Commons Attribution 4.0 International License, [381] and [382]).

As shown the fuel cell polarization curve has three distinctive regions when a load is connected. In the first region, at low load currents, the voltage drops by 20% due to the activation losses. In the second region, the cell voltage decreases linearly with the load current because of the ohmic-losses. Finally, in the third region, the cell voltage decreases rapidly due to the concentration losses.

11.4.2 Performance Metrics

Like batteries the performance metrics of Fuel-cells include the measure of gravimetric and volumetric energy densities. However, in the case of fuel-cells the calculation of energy density is not a straightforward process. The total fuel-cell system weight is proportional to the number of stacks used to achieve the required system voltage. On the other hand, the system's total energy depends on the type of fuel and containers holding the fuel. For example, canisters holding hydrogen under high pressure are much heavier than a plastic container containing alcohol. Therefore, the energy density calculation includes the apparent fuel to energy conversion. For example, as shown on Figure 11-10the SOFC under investigation could provide a fuel energy density of approximately 3,000 Wh/kg, whereas the DMFCs are in the range of approximately 1,500 Wh/kg. Worth noting that hydrogen fuel-cells as presented provide an energy density of approximately 100 times smaller than DMFC which may lead to the conclusion that they are inferior, which is not the case.

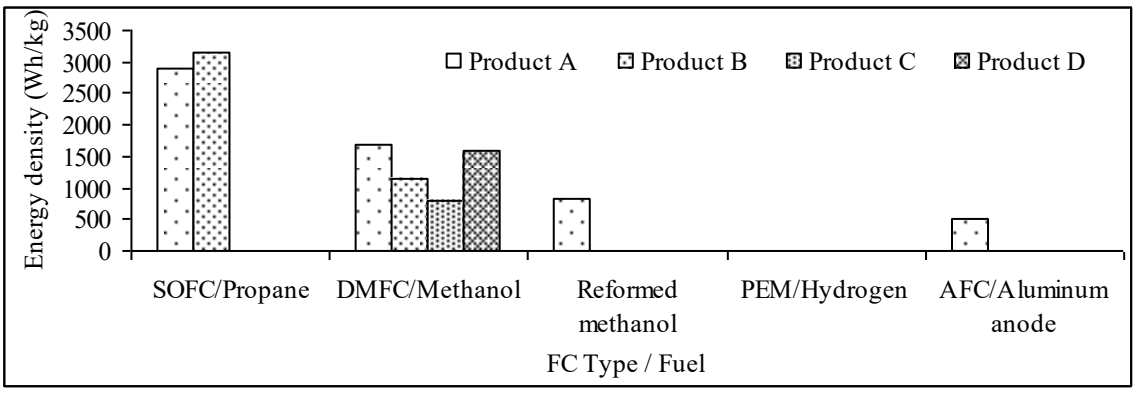

Figure 11-10: Fuel Energy Density for Various Fuel Cell Technologies.

Fuel-cell system selection depends on the application. The confusion with the fuel cells energy density calculations and avoidance of premature conclusions are overcome by evaluating the performance over continuous operation at rated power, for durations of 1, 3 and 10 days. Furthermore, the system weight is composed of the required fuel and its container for the application scenarios.

11.5 Super-Capacitors

11.5.1 Technology Overview

Super-Capacitors are also known as ultra-capacitors. They are a relatively new category of energy storage devices resulted from advancements in manufacturing and material engineering. As literature [384], [385], [386], [387], [388], [389], [390] shows compared to other energy and power systems such as batteries and fuel-cells, super-capacitors offer faster response time due to lower RC time constants, higher power densities due to lightweight construction, higher efficiencies due to lower effective series resistance (ESR) and finally they exhibit limited performance dependency due to temperature. However, ultra-capacitors are more expensive and have lower energy densities compared to other technologies. On the other hand, when super-capacitors are connected in parallel with other systems (high energy) then the best of both worlds can be achieved. The ultra-capacitors could deliver the short-term instantaneous power demand which exceeds the average forecasted demand. As research [391] and [392] report, the paralleling of ultra-capacitors and batteries, prevents battery over-sizing and results in battery improved efficiency and longer lifetime.

Super-capacitors are part of the capacitor family (electrolytic, ceramic, etc). Their structure includes two electrodes separated by an electrolyte. As shown by Equation 11-4 their capacitance is directly proportional to electrode surface area denoted by *A* and measured in squared meters (m^2) and it is inversely proportional to the separation distance between the electrodes denoted by *d* and measured in meters (m).

$$C = \frac{A\varepsilon}{d}$$

Equation 11-4

On the other hand, as research [385], [386], [387], [388], [389], [390], [391], [392], [393] shows super-capacitors offer capacitance in the range of farads as compared to the remaining capacitor family which are in the range of milli-farads and picofarads. As a result of the higher capacitance as shown by Equation 11-5, super-capacitors store more energy.

$$E_C = \frac{1}{2}CV^2$$

Equation 11-5

Super-capacitors exhibit higher capacitance because of higher surface area and lower electrode separation. As research [384], [385], [386], [387], [388], [389], [390] reports, the surface area is attributed to the electrode composition which includes porous activated carbon material whereas the electrode separation is attributed to the proper electrolyte selection and pore-size optimization [384], [385], [386].

Electrode composition, electrolyte selection and pore-size optimization are also known as the energy storage mechanisms which further separate ultra-capacitors to the categories of double layer and redox. In the case of double layer, capacitance is electrostatic, and energy is stored between the electrode double layer interface and the electrolyte whereas in the case of redox energy is available through the chemical reaction (redox). The redox reaction is like the battery chemical reaction process and as research [386] and [392] explains capacitance is known as pseudo-capacitance because the redox reaction is a reversible process between the oxidation states in the electrode material.

11.5.1.1 Redox Super-Capacitors

Redox super-capacitors are named after the reversible reaction processes of reduction and oxidation which are formed within the electrode material. These electrode oxidation layers, form what is known as a pseudo-capacitance which enables energy storage through the redox reaction. In this respect batteries are very similar to redox-super-capacitors. Conducting polymers and metal oxides are the most commonly used and research materials for pseudo-capacitance.

11.5.1.2 Double Layer Super-Capacitors

Double layer super-capacitors are named after the double layer interface formation between the electrodes and electrolyte as presented on Figure 11-11. They are the most used commercially available super-capacitors.

The double layer super-capacitor structure is represented on Figure 11-11. The electrodes are surrounded by the electrolyte and the electrolyte ions. The electrodes are composed of porous activated carbon material that allows the electrolyte to flow through and around. As

shown two separate capacitors are formed between the electrolyte/electrode interface. The electrolyte is considered as an effective conductive plate between the two capacitors and provides the conductive linking path.

The two capacitors in series with the electrolyte resistance are represented by the DC electrical model of the double layer super-capacitor as shown on Figure 11-12. It should be noted that in the case of super-capacitors the series resistance is much lower than the effective internal resistance of batteries.

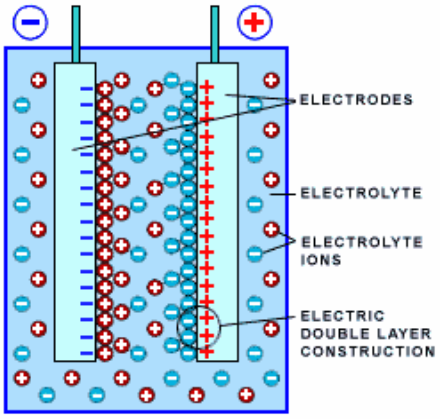

Figure 11-11: Double Layer Super-Capacitor Structure [385], [387].

The electrodes are usually composed of carbon whereas the electrolytes are organic or aqueous [385], [388]. The advantages of using carbon include low price, availability, non-toxic, and easy to process. On the other hand, the electrical conductivity depends on the carbon preparation. Carbon electrodes have been available as active powders, felts and cloths, xerogels, aerogels, and nanotubes.

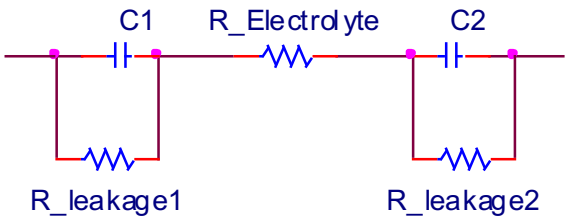

Figure 11-12: DC Electrical Model of a Double Layer Super-Capacitor from [384], [385].

Electrolytes are divided to the categories of organic and aqueous. Organic electrolytes offer higher cell voltage, in the range of 2.5V, as compared to aqueous which in the range of 1.2V [387], [388]. On the other hand, organic electrolytes exhibit lower capacitance than the aqueous counterparts. However, as shown by Equation 11-5 organic electrolytes store higher energy as compared to aqueous. On the other hand, aqueous electrolytes offer lower electrical series resistance (ESR) as compared to the organic electrolytes. Low ESR makes aqueous electrolytes an attractive choice for high power applications as shown by the following equation,

$$P = \frac{V^2}{R}$$

Equation 11-6

where R equals ESR [386], [388].

Table 11-4: Commercially Available Double Layer Super-Capacitors and their Characteristics

Brand	Voltage (Volts)	Capacitance (Farads)	ESR (mΩ) DC	ESR (mΩ) AC	Energy Wh/Kg	Power W/Kg	Weight (gram)	RC Time Const. (Sec.)
Single Cell								
EPCOS	2.5	1800	0.6	0.3	2.9	2300	540	1.08
EPCOS	2.3	5	330	200	0.7	1200	5.5	1.65
NESS	2.3	20	55	40	3.7	6600	4	1.10
NESS	2.3	120	30	20	5.2	2600	17	3.60
Maxwell	2.7	2600	0.4	0.28	5.6	10400	470	1.04
Maxwell	2.5	2700	1	0.7	3.2	2.2	725	2.70
Skeleton	3	47	5.5	-	11.5	9600	5	0.26
MODULES								
EPCOS	14	200	5	2.6	1.9	1700	2800	2.50
EPCOS	42	67	15	8	2	1700	8200	1.01
NESS	5.4	1.5	200	150	1.74	10410	3.5	0.30
NESS	90	2.8	500	400	2.1	2800	1700	1.40
Maxwell	16.2	430	3.5	2.5	3.1	5200	5000	1.51

Commercially available double layer ultra-capacitors are manufactured by companies including but not limited to Maxwell, Skeleton, EPCOS, NESS, Matsushita etc. Ultra-capacitors come in single cells and using the series and parallel connectivity as presented in the section of batteries then the design specifications regarding operating voltage and energy can be

achieved. In addition, it is worth noting that specific energy and power densities are measures of comparison for double layer super-capacitors.

Commercially available double-layer super-capacitors and their characteristics are tabulated on Table 11-4. As shown, commercial availability includes multiple options in operating voltages, capacitance, weight, and electrical characteristics. The ultra-capacitor applications include primary and back-up power supplies for consumer electronic devices (LED displays, toys, electric buzzers, hand-held scanners, etc), peak power supplies for automobiles, voltage compensators, and car audio systems. For example, as reported by [394] the NESS ultra-capacitor is intended for consumer electronic applications hence its operating voltage is limited to 2.3V and its capacitance to 120F whereas as reported by [388] the MAXWELL ultra-capacitor is intended for automotive subsystems, power quality and rail system power applications and while its operating voltage is only 2.5V its capacitance is 20 times higher (2700F). Worth noting that power quality includes filtering.

As mentioned, capacitors can be connected in the matrix series and parallel configuration to achieve the desired operating voltage and capacitance. However, remember that when capacitors are connected in series then the capacitance decreases whereas when connected in parallel the total capacitance increases. For example, the module (NESS 90V, 2.8F)required the series connection of 36 cells with voltage 2.7V and capacitance 100F. As a result, the module voltage increased by a factor of 36 whereas the module capacitance decreased by the same factor. Similarly, a 7x4 matrix of the ultra-capacitor (2.7V, 100F) will results in a module voltage increased by 7 times to 17.5V whereas the capacitance will decrease by 7 times (100/7=14.3F) and increase by a factor of 4 thus yielding a total capacitance of 57F as presented by [394].

Worth noting that a super-capacitor with operating voltage of 3V and capacitance of 47F exhibit specific energy in the range of 41,400J/Kg whereas another one rated at 5.4V and 1.5 exhibits specific power density in the range of 10,410W/Kg. It is always a trade-off according to the application.

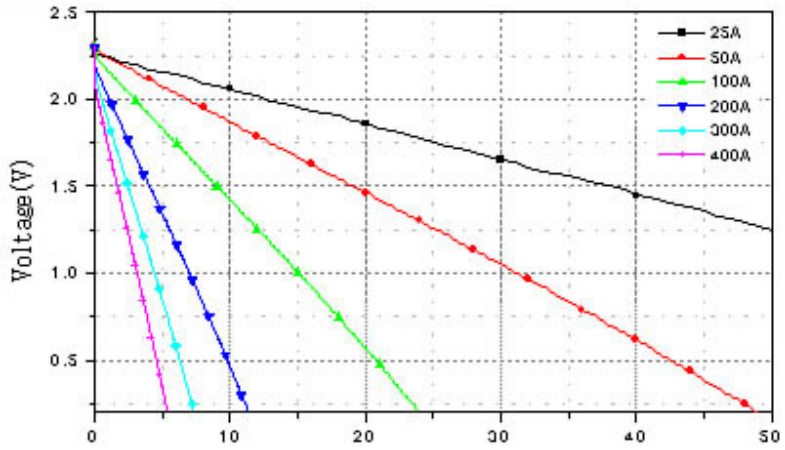

Figure 11-13: I-V Characteristics for Double Layer Super-Capacitor under Constant Discharge Current (Credit: NESSCAP1200P Datasheet [394]).

As shown from Figure 11-13 the higher the discharge current the faster the stored energy is released. The capacitor current is proportional to the rate of change of voltage as shown by Equation 11-7.

$$I_C = C\frac{dV_C}{dt}$$

Equation 11-7

11.6 Battery and Super-Capacitor Combination

Batteries and fuel-cells offer high energy densities, but they are limited to their reaction time (high time constant). On the other hand, super-capacitors offer very high-power densities and very fast reaction time (low time constant). Therefore, when super-capacitors are connected in parallel with other systems (high energy) then the best of both worlds can be achieved. The ultra-capacitors could deliver the short-term instantaneous power demand which exceeds the average forecasted demand whereas the battery or fuel-cell could provide the required runtime. Additional benefits as reported by research [391] and [392], the paralleling of ultra-capacitors and batteries, prevents battery over-sizing and results in battery improved efficiency and longer lifetime.

Worth remembering as electrical engineers that the inability to deliver the required instantaneous (short period of time; milli-seconds to seconds) power demand which exceeds the average power demand, creates a power quality issued which may cause the reset of computers to reset and stalling of motors. Over-sizing the energy and power system would mitigate the issue at the expense of cost, weight and volume.

Initial research included applications with similar profiles, low average power and high pulse power demands. These areas included portable electronic devices, telecommunications, and electric vehicles [36], [391]. The battery-supercapacitor combination has been extensively studies by literature [386], [387], [389], [390]. The combination was named as a hybrid-system and was separated into passive and active systems.

A passive system is simple and cheap because it involves the direct parallel connection between the two devices. Research [392] involving GSM telecom applications (0.5ms pulses), compared the passive hybrid and the battery only solutions. The results showed a voltage sag in the range on 0.1V with the hybrid-system whereas with the previously used only battery powered system the voltage sag was in the range of 1.1V.In addition, the same research reported a battery average discharge current of 0.2A with the hybrid system whereas with the battery only the discharge current was in the range of 2A. The higher discharge current results in higher losses and internal heating (I^2R). In addition, the hybrid system delivered 40% higher power (5-8W with pulses of 35W) whereas the battery alone system was limited to

3.5-4W with pulses of 15W.Additional research [395], reported that higher pulsed power resulted in higher system efficiency, longer runtime and battery life.

The battery and super-capacitor passive hybrid system suffer from two major disadvantages. First, due to the capacitor charging and discharging then the battery current could show high ripple which could potentially activate the lithium battery protection schemes and turn-off the battery. Second, the output voltage is not regulated. The output voltage is proportional to the battery terminal voltage which decreases as the battery discharges.

An active system on the other hand, includes a bidirectional DC to DC converter connected between the two devices. The converter minimises the ripple on the battery current and in addition it offers a regulated output voltage to the load. Furthermore, the active system offers design flexibility since the ultra-capacitor and battery voltages can be different [395]. Furthermore, the same research [395] concludes that the active hybrid system under investigation offered higher peak (x3.2) and specific energy (x2.7) than the passive system. Finally, the bidirectional DC-DC converter can serve a dual purpose, load voltage regulator and a battery charging regulator. On the other hand, the converter losses due to internal power electronics, increases the system's temperature and minimizes the overall runtime.

11.7 Pumped Storage Hydropower

The power of water (hydro derived from the Greek wordὕδωρ) has been one of the main RES since 1900s as shown on Figure 10-19. However, the power derived from the energy of falling or fast-running water has been harnessed since the ancient times using different kinds of watermills for useful purposes including irrigation and the operation of various mechanical devices, such as gristmills, sawmills, textile mills, trip hammers, dock cranes, domestic lifts, and ore mills. Such an example, is the 12th century mill in Belgium illustrated in Figure 11-14.

Figure 11-14: Moulin Banal in Braine-le-Chateau, Belgium Dating from the 12th Century (Credit: Pierre (Pierre79) , Wikimedia Commons author (GNU Free Documentation License - public domain) [396])

The hydro electric technology is now matured and well understood. Advancements in engineering and manufacturing have led to the development of mega-dams capable with reservoirs big enough to power entire cities and countries. Such an example shown on Figure

11-15 is the Itaipu dam located on the borders between Brazil and Paraguay. However, as discussed in [245], [250], [251] mega-dams affect the environment and ecosystem; divert and reduce natural river flows, thus restricting access for animal and human populations.

Figure 11-15: Itaipu Hydro Electric Dam (Credit: Jonas de Carvalho – Flickr licenced under CC BY-SA 2.0, [397])

Figure 11-16: Three Gorges Hydro Electric Dam in China (Credit: Le Grand Portage licenced under CC BY 2.0, [52])

Furthermore, some of the mega-dams significantly affect the visual landscape as shown on Figure 11-16 whereas smaller hydro electric dams as shown on Figure 11-17 do not affect the landscape in such a great extend. Pumped storage hydro electric dams are usually smaller in size.

Figure 11-17: Goldisthal Pumped Storage Hydro Electric Dam in Germany (Credit: Voith under Written Permission, [398])

11.7.1 Technology Overview

Hydropower is the most stable and predictable RES compared to wind and solar. Due to the storage capabilities, dams, reservoirs and lakes, hydropower offers high controllability and dispatchability. According to research [399] in 2019, 12% of European Union's electricity was generated by hydropower. This percentage is equivalent to a 36% of the total RES combined generated power.

The process of generating electricity using hydropower is simple. Because of elevation difference then water flows downhill thus converting potential energy to kinetic. Then the kinetic energy is converted to mechanical by rotating the turbine which in turn rotates a generator producing electricity. This process is best described by the mathematical Equation 11-8.

$$P = n\rho gQH$$

Equation 11-8

where

P is the power in watts

η is the efficiency (micro – 50-60%, small > 80%)

ρ is the density of water (1000 kg/m^3)

g is the acceleration due to gravity (9.81 m/s^2)

Q is the flow passing thru the turbine (m^3/s)

H is the head or drop of water (m)

Worth mentioning that hydropower dams are classified according to their output power generation. Micro generally generates less than 100 kW, micro between 0.1 to 1 MW and small between 1 to 50 MW. The efficiency of micro hydropower is between 50 and 60% whereas for small it exceeds 80% [400], [401].

The power generation is a function of water discharge and the size of the head. As research shows and presented on Figure 11-18 these two parameters are critical in the selection of the turbine to be used. The range of turbines includes the Francis, Crossflow, Kaplan and Pelton or Turgo wheel. These turbines fall in two categories; reaction and impulse.

Impulse turbines such as Pelton, Turgo and cross flow turbines, are driven by high-velocity water jets. On the other hand, reaction turbines such as Kaplan and Franscis, have their rotors fully immersed in water and enclosed in pressure casings which creates pressure differences and lift forces which enables the runner blades to rotate very fast. Research has shown that the runner blades of reaction turbines are able to rotate faster than their counterparts used in aircraft jets.

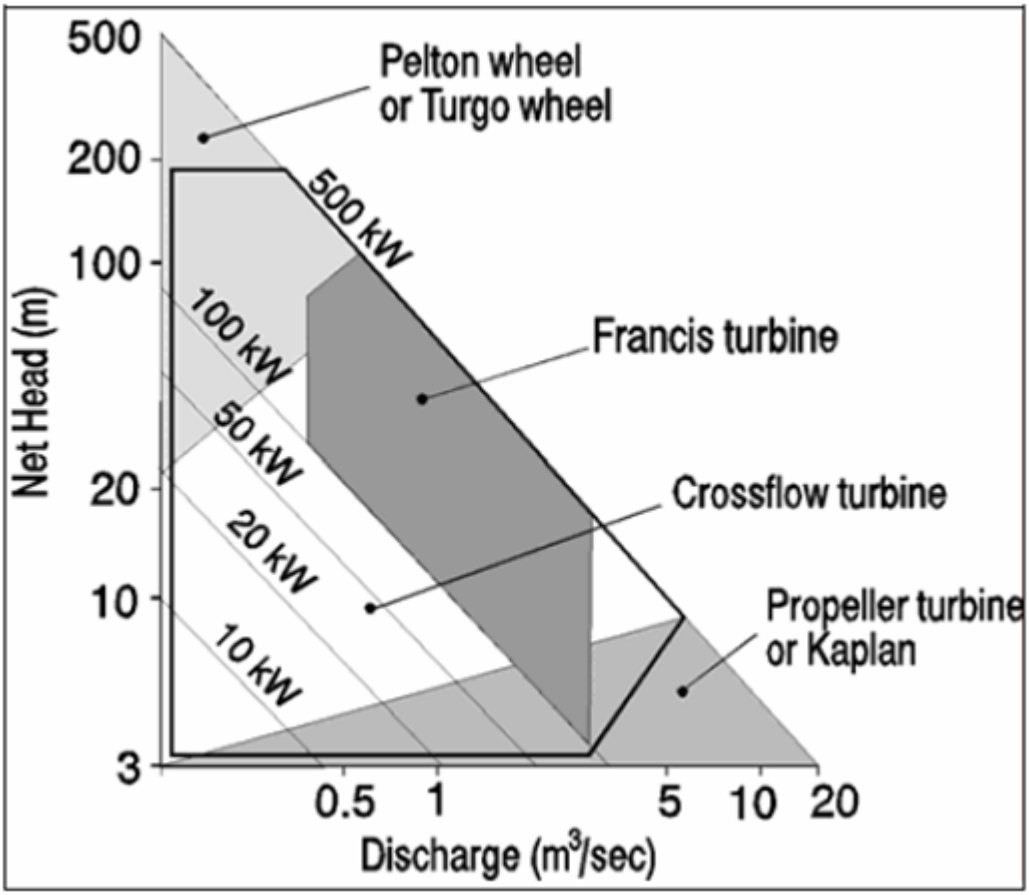

Figure 11-18: Head-flow Range of Small Hydro Turbines [400], [401].

The process of pumped storage hydropower is very similar to ordinary hydropower with the difference of the presence of a second reservoir as shown on Figure 11-19. During peak hours, water flows from the upper reservoir to the lower thus producing electricity whereas during off-peak hours water from the lower reservoir is pumped back up to the upper reservoir. The water channel is also known as conductor and penstock.

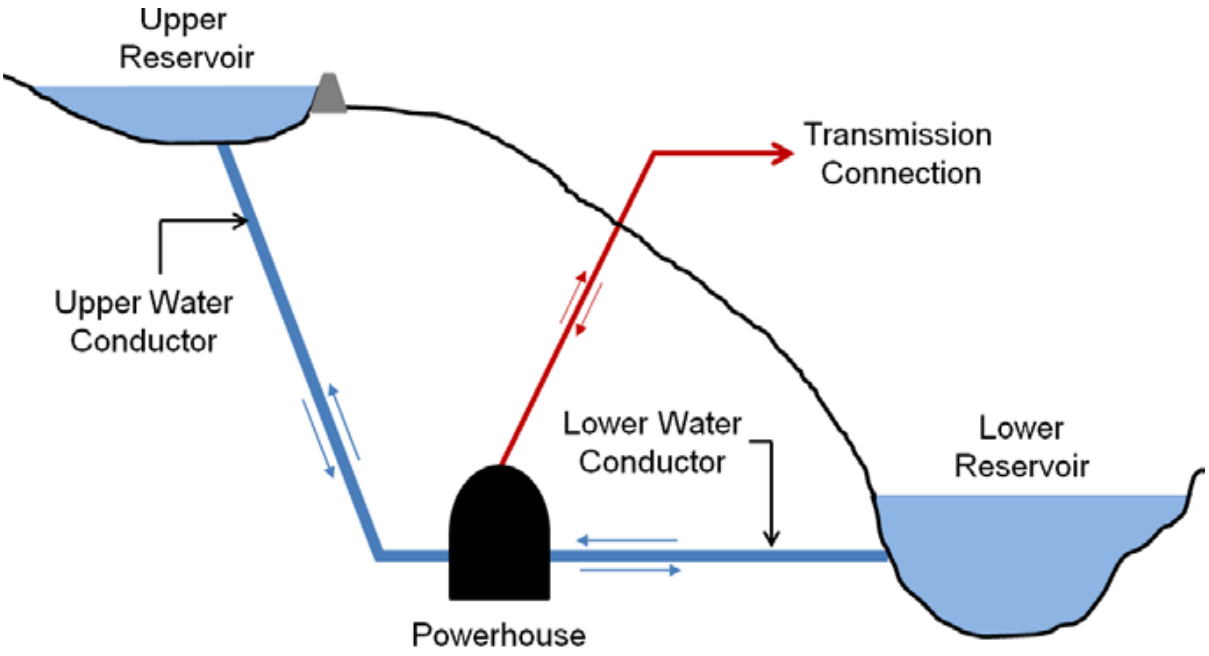

Figure 11-19: Typical Pumped Storage Configuration [402].

The power generation from pumped storage hydropower is controlled by controlling the water flow. Some useful industry terminology includes the flow and power duration curves which are depended on the percentage exceedance. The % exceedance represents the water flow variability and probability. The minimum flow is shown as 100% exceedance whereas maximum with 0%.

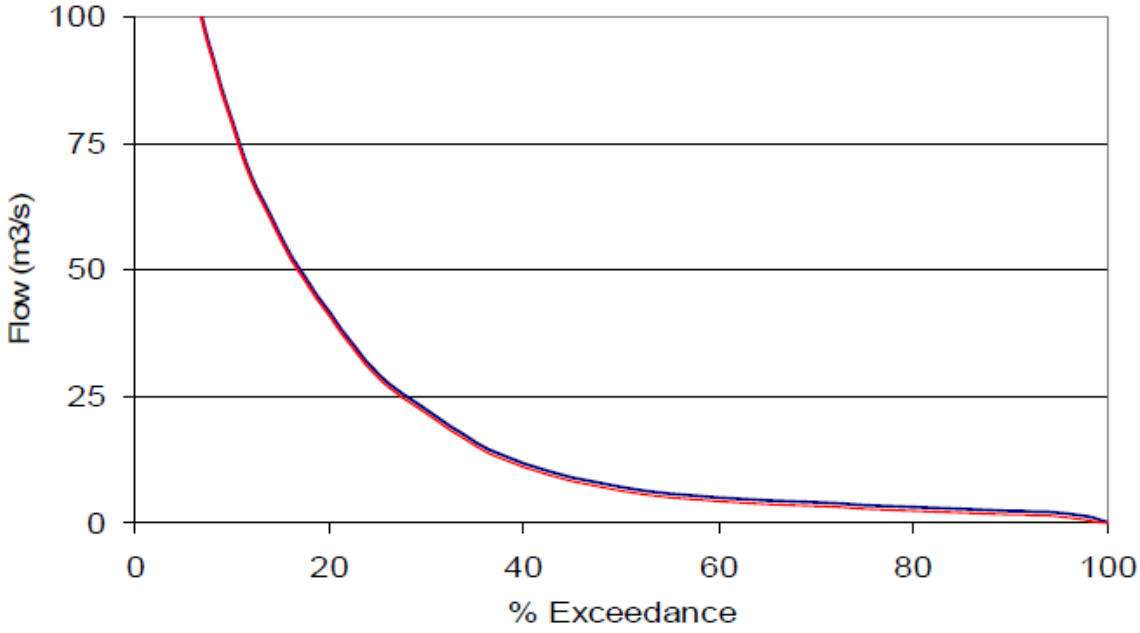

Figure 11-20: Flow Duration Curve [400], [401].

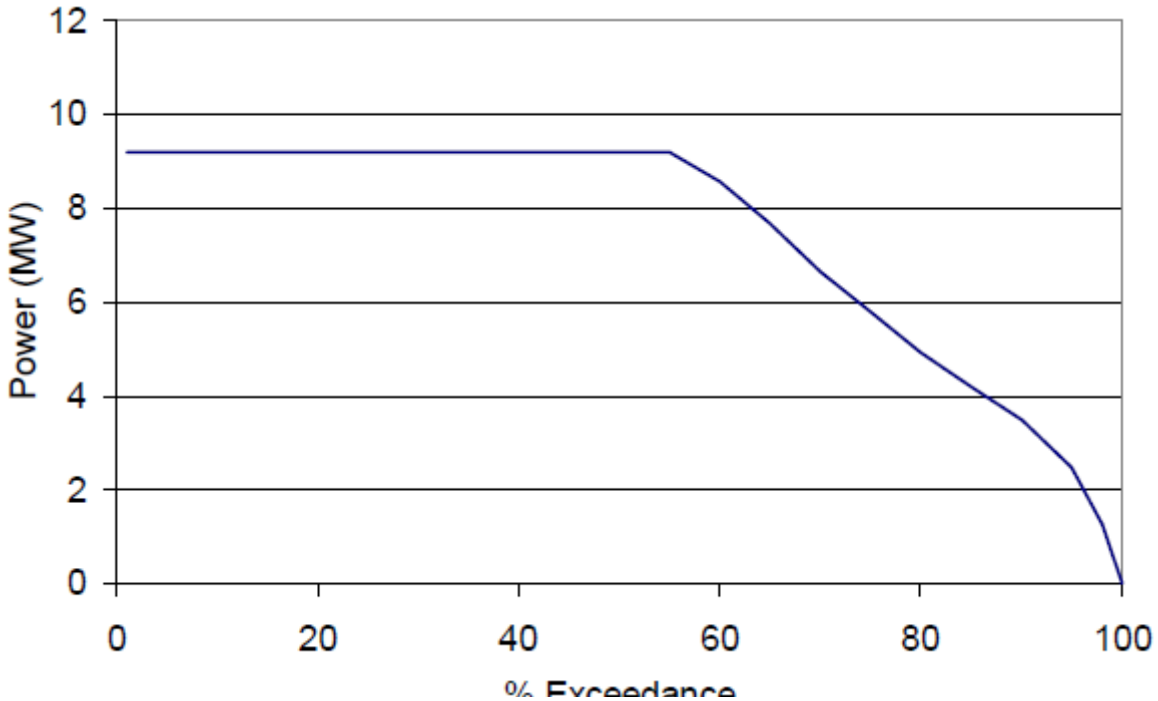

Figure 11-21: Power Duration Curve [400], [401].

11.8 Flywheel Energy Storage Systems

Flywheels are mechanical systems which store energy in the form of kinetic energy. This energy is proportional to the moment of inertia and angular velocity of the rotating wheel. Flywheels come in all circular shapes and sizes. Applications of flywheel systems range from traditional locomotion, industrial size energy storage, automotive and racing. In 1802 the British inventor Richard Trevithick as shown on Figure 11-22 used a flywheel to evenly distribute the power of its single cylinder steam locomotive.

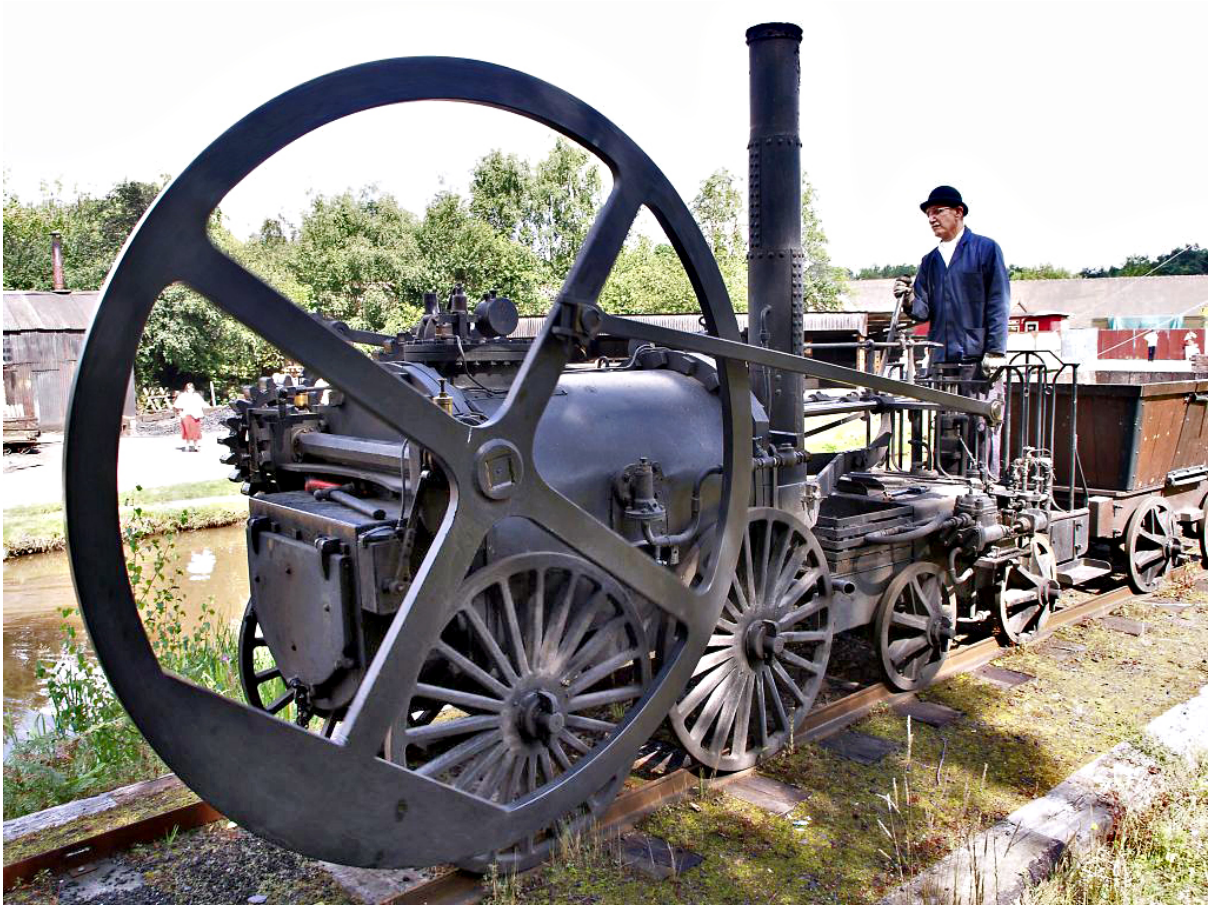

Figure 11-22: Trevithick's 1802 steam locomotive (Credit: Birmingham Museums Trust licenced under CC BY-SA 4.0, [403])

On the other hand, Figure 11-23 presents an industrial size, commercially available flywheel energy storage system which is used for wind farms and public transportation applications. Finally, Figure 11-24 presents an example of regenerative energy used in formula 1 racing,

where the flywheel stores energy when the car is braked, allowing it to be recycled to accelerate the car later.

Figure 11-23: Flywheel system for wind farms and public transport (Credit: STORNETIC GmbH [404])

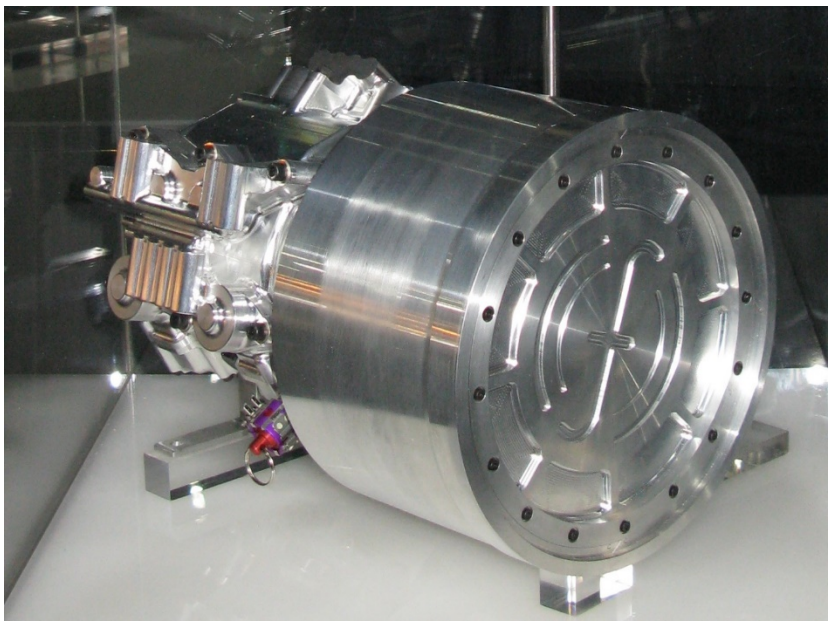

Figure 11-24: A Flybrid Systems Kinetic Energy Recovery System built for use in Formula One (Credit: Genilicensed under GFDL CC-BY-SA [405])

11.8.1 Technology Overview

As presented on Figure 11-25 a flywheel is composed of the rotor which provides and mass and moment of inertia, the hub or shaft that connects the rotational movement to the motor or generator. All these are enclosed in vacuum to eliminate the losses due to air resistance and for higher efficiency magnetic bearings are used that eliminate the friction losses.

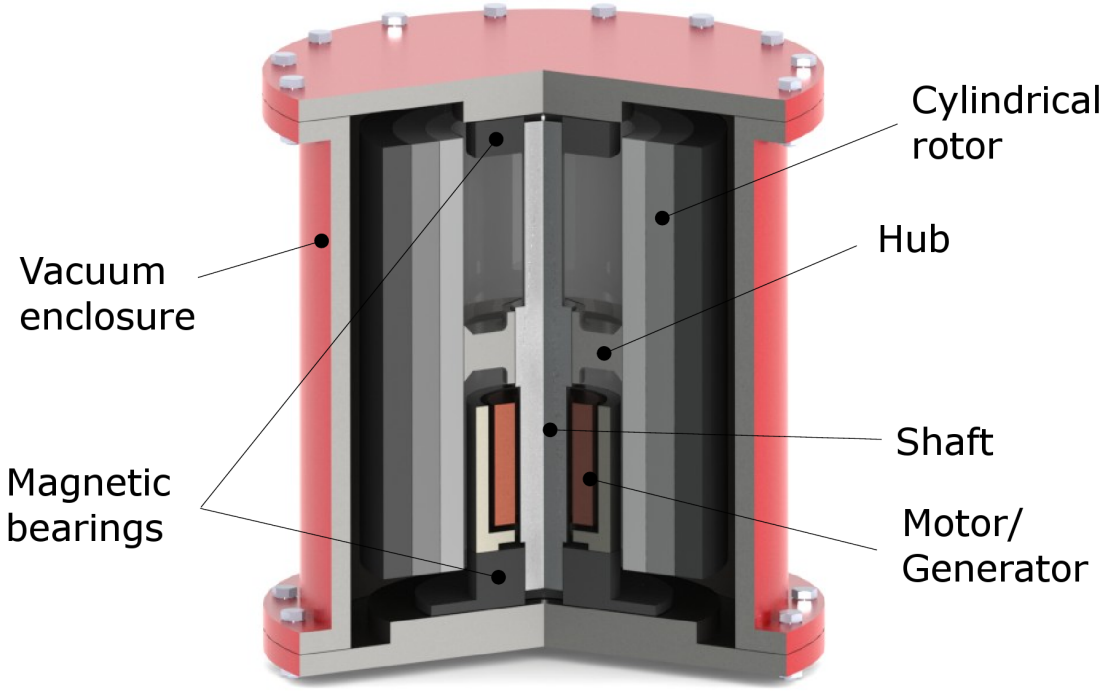

Figure 11-25: The main components of a typical cylindrical flywheel rotor assembly (Credit: Pjrensburg under GNU Free Documentation License [72].

The moment of inertia of the cylindrical rotos is calculated given the Equation 11-9

$$J = mr^2$$

Equation 11-9

Where *J* is the moment of inertial measured in kgm^2, *m* is the mass in kg and *r* is the radius in m.

The stored kinetic energy is best described by Equation 11-10

$$E_k = \frac{1}{2} J\omega^2$$

Equation 11-10

Where E_k is the kinetic energy in Joules (*J*) and $\omega$is the angular velocity in rad/s.

The faster the rotor spins then the higher amount of energy is stored in the flywheel. The maximum theoretical stored energy depends on the material used. When the maximum

energy is exceeded then the device shutters. This is because of the tensile strength of materials.

$$\sigma_t = \rho r^2 \omega^2$$

Equation 11-11

Where σ_t is the tensile stress on the rim of the cylinder in joules, ρ is the density of the cylinder, r is the radius of the cylinder and$\omega$is the angular velocity of the cylinder.

According to the handbook of mechanical alloy design [406] ceramics offer the highest specific tensile stress of approximately 2000kJ/kg but they are weak and brittle hence cannot be used for this application. On the other hand, cast iron is very strong but its specific tensile stress is only 8kJ/kg. The composite carbon-fibre (500kJ/kg) provides the best performance with respect to strength and cost thus offering the highest flywheel efficiency.

The output power of the flywheel equals to the output power of the connected machine. For example, in the case of a synchronous machine

$$P = V_i V_t \left(\frac{\sin(\delta)}{X_s}\right)$$

Equation 11-12

Where V_i is the voltage of rotor winding which is produced by field interacting with the stator winding, V_t is the stator voltage, δ is the torque angle also known as the angle between two voltages, and X_s is the stator reactance.

Flywheel storage systems are typically small with peak power capability is the range of 20 MW. Hence, they are used to serve as a short-term compensation storage, to aid in the power grid stability and frequency regulation. Flywheels can be connected directly on the grid as shown on Figure 11-26 or connected on a DC link as shown on Figure 11-27. In both cases back to back bidirectional converters are required.

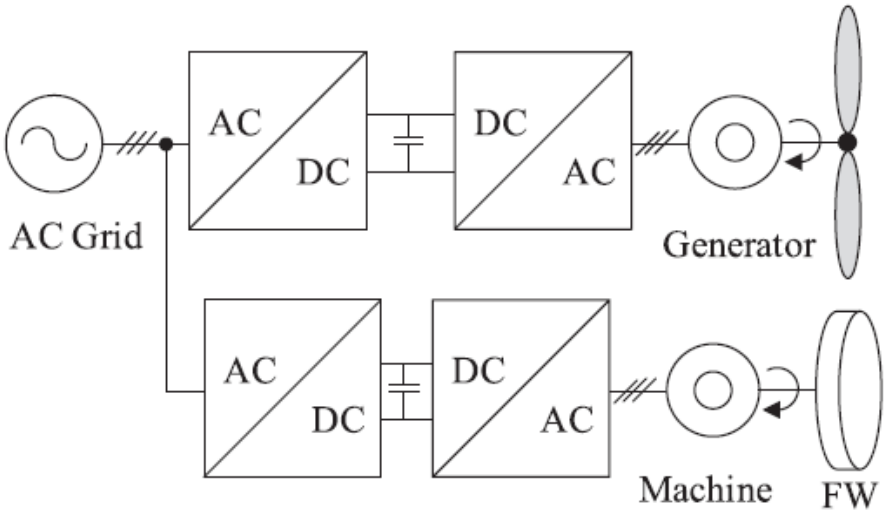

Figure 11-26: Back to Back DC-AC connected directly to the grid

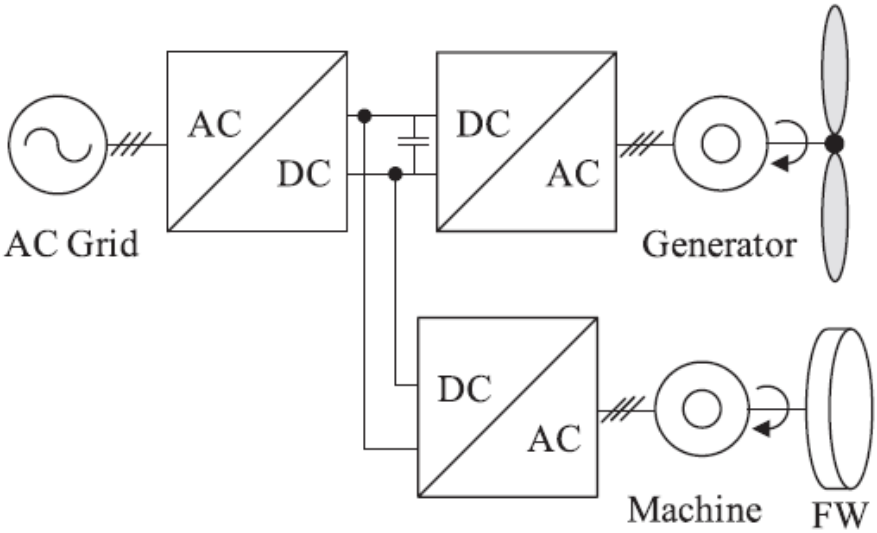

Figure 11-27: Back to Back DC-AC converter connected in DC-link.

Additional information on detail recent advancements including materials, components, machines, and technical characteristics can be found on [407], [408], [409] which provide elaborate critical reviews.

11.9 Compressed Air Energy Systems

Compressed air energy systems (CAES) like all other energy storage systems convert electrical energy during off-peak hours to other forms of energy. In the case of CAES electrical energy is converted to pressurised gas which is stored in compressed air reservoirs. When the gas is in small quantities as shown on Figure 11-28then it is stored in metal containers whereas when it is in bigger quantities then it is stored in underground salt cavern as shown on Figure 11-29. During peak hours, the pressurised air is released (expand / decompressed) through a generator which produces electricity.

Figure 11-28: A pressurized air tank used to start a diesel generator set in Paris Metro (Credit: F1jmm under licence CC BY-SA 3.0 [410]).

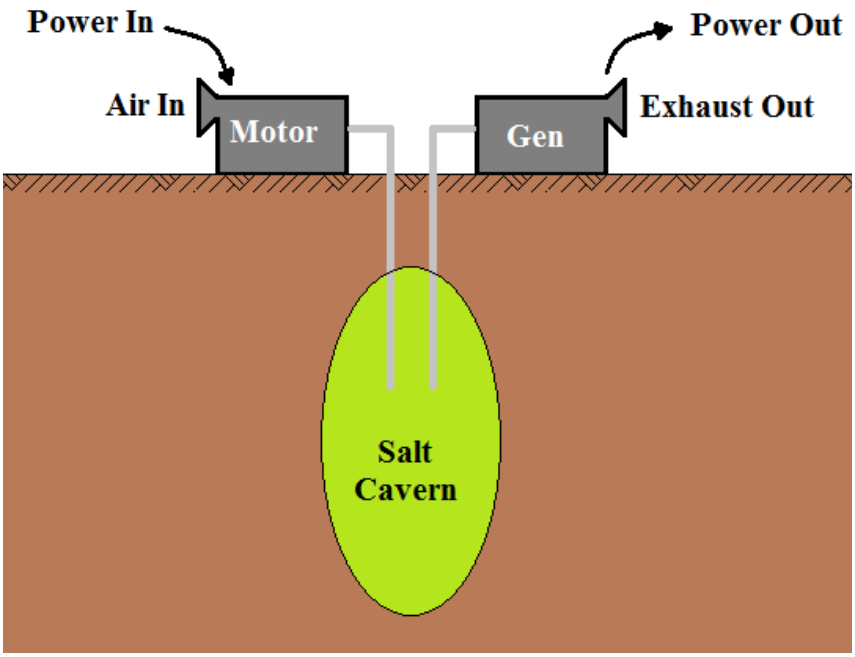

Figure 11-29: CAES using underground salt cavern (Credit: Lee Clayton, PE, and www.PhDOnline.com, under Written Permission [411]).

The process of compressing and decompressing the air introduces a lot of losses (heating and cooling of the gases) resulting in round trip efficiencies of 65 to 75%. Large CAES have higher losses hence lower efficiency compared to smaller scale CAES.

According to literature [411], [412], [413], CAES date back to the 1870s in big European and Latin America cities for the purpose of powering machinery. Furthermore, in 1896 a 2.2 MW CAES system served the industry in Paris. The system's air pipes were distributed over 50 km at an operating pressure of 550 kPa.

Furthermore, more recently, in 1978 a 290 MW plant was build in Huntorf, Germany whereas in 1991 a plant of 110 MW peak power and 26 hoursduration was built in McIntosh, Alabama, USA. Both plants are operational to this day. An aerial photo of the Huntorf plant is presented on Figure 11-30.

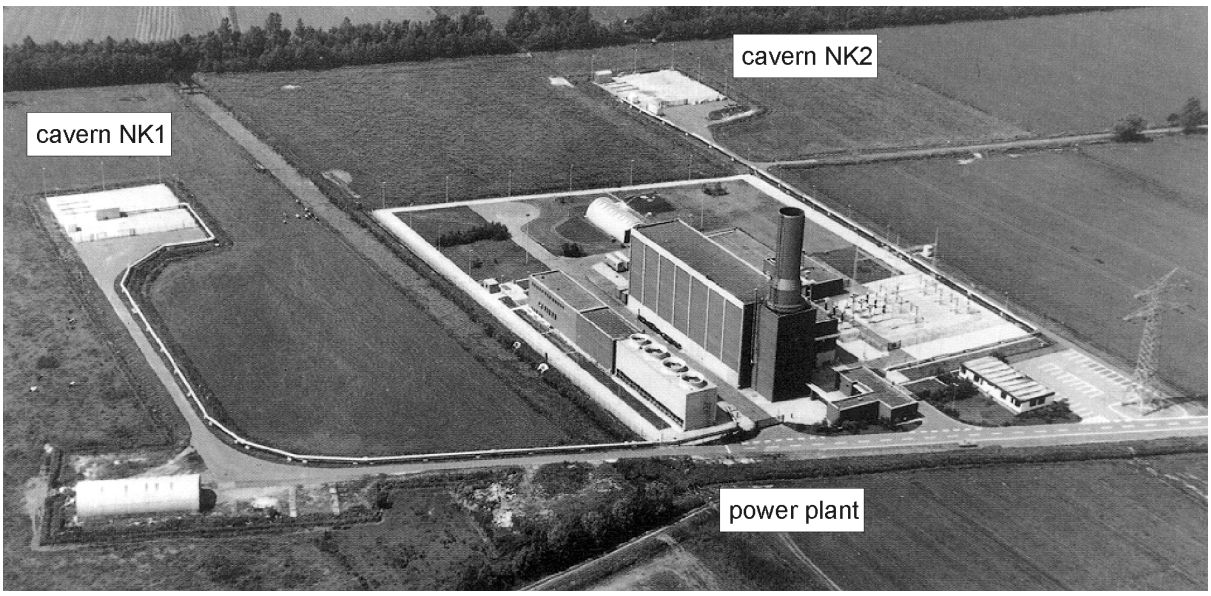

Figure 11-30: Aerial picture of Huntorf plant (Credit: F. Crotogino, et.al, and Solution Mining Research Institute (SMRI), under Written Premission [414], [415]).

11.9.1 Technology Overview

Compressed Air Energy System refers to the process of compressing and storing air under high pressures in containers. The compressing of the air can be achieved using compressors or turbines whereas the generation of electricity is with the use of generators.

The storage containers fall under two categories: constant volume and constant pressure. Mine caverns, aquifers and automotive are examples of constant volume storage whereas Underwater pressure vessels and Hybrid Pumped Hydro - Compressed Air Storage are examples of constant pressure.

The process of compression creates heat which causes the compressed air to be warmer, whereas expansion removes heat causing the expanded air to be colder. CAES handle these issues by varying the thermodynamic conditions of the storage technologies. The three main thermodynamic processes used are adiabatic, diabatic and isothermal (or near-isothermal).

The amount of energy stored is best described using the isothermal (also known as reversible) process under the assumptions that the compressed air obeys the ideal gas law and that the temperature remains constant.

$$pV = nRT$$

Equation 11-13

Where *p* is measured in pascals, *V* is measured in cubic metres, *n* is measured in moles, and *T*is the absolute temperature in kelvins. The ideal gas constant, *R*, is the product of the Boltzmann's constant and the Avogadro's constant which yields a value of 8.314 J/(K·mol). The absolute temperature is 0 K which is equivalent to -273°C. Therefore, it can be said that for the isothermal process

$$pV = nRT = constant$$

Equation 11-14

The amount of work from an initial state A to a final state B is calculated

$$W_{AB} = \int_{V_A}^{V_B} pdV = \int_{V_A}^{V_B} \frac{nRT}{V} dV$$

Equation 11-15

Which can be rewritten as

$$W_{AB} = p_B V_B ln\frac{p_A}{p_B} + (p_B - p_A)V_B = p_A V_A ln\frac{p_A}{p_B} + (V_A - V_B)p_A$$

Equation 11-16

For example, in a storage vessel of 1 m^3 at a pressure of 70 bars (7.0 MPa) and an ambient pressure is 1 bar (0.10 MPa) using Equation 11-16 it is calculated that the stored energy comes to -22.8MJ. The negative sign indicates that work is done on the gas by the surroundings. This amount of energy distributed over a period of 1 hour or 3600 seconds is equivalent to 6.33 kWh.

During the charging process, the compressor consumed electric power is given by:

$$P = \frac{kQR_{gas}T_{in}}{(k-1)\eta_c}\left(\beta^{\frac{\kappa-1}{\kappa}} - 1\right)$$

Equation 11-17

Where *P* is the compressor's consumed power, *k* is the adiabatic exponent, η_c is the compressor efficiency, *Q* is the mass flow rate of air, R_{gas} is the air gas constant, T_{in} is the air temperature entering the compressor's inlet and *β* is the compression ratio.

In addition, the air temperature exiting the outlet can be expressed as:

$$T_{out} = T_{in}\left(\frac{\beta^{\frac{\kappa-1}{\kappa}} - 1}{\eta_c} + 1\right)$$

Equation 11-18

Additional explanations regarding the mechanics and thermodynamic processes related to CAES are presented in research [416], [417], [418].

11.10 Discussion and Conclusions

This work included an elaborate literature review and presentation of the major energy storage technologies for applications involving RES integration to the grid. The presentation and analysis included the technical characteristics and terminologies used in the industry. This final section attempts to summarize and compare the important characteristics of all the technologies under investigation.

The tabulated comparison data of Table 11-5and Table 11-6were either derived or directly obtained from literature [55], [329], [419], [420], [421], [422], [423], [424], [425], [426].

Table 11-5: Summary of Energy Storage Technology Characteristics

Technology	Peak Power	Energy	Round Trip Efficiency	Discharge Time	Lifetime / Cycles	Cost
	(MW)	(MWh)	(%)			(€/kWh)
PHPS	100-4,000	10,000	65-80	1-24 h	30-40 years	35-70
CAES	50-300	5,000	65-75	1-24 h	30 years	10-70
Battery	50	500	75-90	s - h	10^3-10^4 cycles	70-4,000
Hydrogen	50	N/A	20-50	14-24 h	10^4 hours	2,000-15,000
SMES	0.1-10	1,000	80-90	ms - s	10^6 cycles	200-500
Flywheel	0.75-10	5	80-90	ms - s	10^6 cycles	140-350
Supercapacitors	0.1-10	3	90-95	ms - m	10^6 cycles	70-400

Legend: h – hours, s – seconds, ms – milli-seconds, m - minutes

As can be seen from Table 11-5 energy storage technologies can serve a wide range of needs, ranging from peak power, to energy, to response time from milli-seconds to hours. According to the required specifications then the selected technology will have the equivalent cost.

Table 11-6: Summary of Battery Technology

Technology	Toxic material	Flammable	Rare Metal	Moving part
Flow Battery	Yes	No	No	Yes
Liquid Metal	No	Yes	No	No
Sodium ion	No	Yes	No	No
Lead-Acid	Yes	No	No	No
Na-S Battery	Yes	No	No	No
Ni-Cd	Yes	No	Yes	No
Lithium-Ion	No	Yes	No	No

As seen from Table 11-6 the Lithium battery chemistry has become the preferred choice because it offers high power and energy density, and also it is non-toxic, lithium is not a rare material, has no moving parts which entitles minimal running costs. The only drawback that lithium batteries have is that they are flammable. However, using the correct safety electronics then this is overcome.

12 OFF-grid/ Stand-alone systems

Author: Dr. Abdallah Altahan Alnauimi
Dr. Mohammad Zakariya Siam

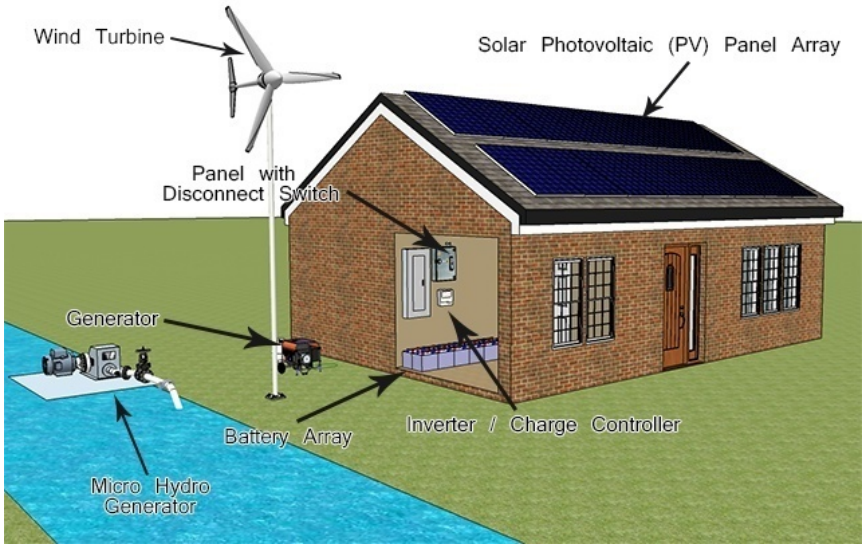

12.1 Preface

Providing electricity access has two general approaches: the former is by extending the public electricity grid and the latter is by implementing a new out of system grid [427]. Normally, governments and its utilities extend the electricity grid to serve population if it is possible. About 99% of electricity infrastructures investments used in extending the normal electrical grid. On the other hand, investments on electrical systems that are out of normal grid are only taking into consideration when there many out-of-solving reasons to extend the grid to certain community [427]. Some obvious reasons are seen below:

- Off-grid electrical systems are low-cost on the basis of per-unit or per-connection.
- The wait for installing off-grid system is less than extending the normal grid.
- The extending of the normal grid is not enough for the community needs.

The cost of grid extension electrification is directly proportional to the distance between the desired place and the grid. The off-grid cost does not depend on the distance. This is a good reason to use off-grid solutions.

Off-grid -as might be seen in [428] and [429]-is a system that is designed to help population and community without the need of faraway supplying. In electricity, off-grid includes stand-alone systems and mini-grid systems. Electrification that depends on off-grid system depends on accessing and using electricity locally without the need to use the public utility grid. This makes certain communities live in a self-sufficient style regarding the usage of utility grids [428] and [429].

Figure 12-1: Overview of off-grid system

12.2 Off-grid Systems

In civilian societies, most important needs for people reach them using utility grids. The most important needs recently are water and electricity, but there are several hard-to-reach sites that have many difficulties to obtain the services of utility grids [430]. Many rural areas and islands are far away from the utility grids and the electrification for these areas is costly and has many technical difficulties.

The optimum solution is to use a local source of renewable energy to electrify the private and community buildings. [427]. About 14% of the planet population has no access to electricity source and the off-grid systems represent one choice of the realistic solutions to solve this problem.

Figure 12-2: House solar system

12.2.1 Stand-alone systems

When the electrical power is generated and used in the same site, this system is called stand-alone system (SAPS, SPSor RAPS) which is out of the normal grid. SAPS is one type of off-grid system which is used for far away locations [431]. The generated electrical power may be transmitted directly to the load or it may be stored in batteries to be then used to function

the loads later on. The generation of electrical power may be obtained using two main types of electricity generation, namely the power generation using the conventional sources and the power generation of renewable sources. The first type includes the usage of the well-known fuel generators. The second type includes solar, wind and hydro generators among others [428].

Most of stand-alone power systems use battery banks to store power. The direct output power that is directly used from batteries is DC which is used for lighting and for house appliances that use DC power. Usually, an inverter is used to convert DC to AC power that is used mostly in normal appliances. The stand-alone system may be divided into three types: the Pico system, the home system and the productive system.

Figure 12-3: Roof-mounted system

12.2.1.1 Pico System

This type of power systems is the smallest among the others mentioned. It is used for function individual appliances like light bulbs, televisions and radios. Pico system is very cheap and very easy to install. Also, it does not take big area or long time to install [430].

12.2.1.2 Home System

This type of power systems is medium in power, size and cost. It can be used to supply power to certain household. All the home appliances could be powered and work normally using this

system of supplying power. All appliances used for civilian needs that are dependent on electrical power will have sufficient power to work [430].

12.2.1.3 Productive System

This type of power systems is the largest in power, size and cost among all types of stand-alone systems. It can be used to supply power to certain big independent stand-alone single unit like factory, hotel, clinic or farm [430].

Figure 12-4: Farm solar panel

12.2.1.4 Stand-alone System Applications

Any place that is far away from the electrical utility grid and need to be supplied by electricity can use the stand-alone systems. Many applications can use this type of power providing which generate the power locally. Some of the most well-known applications are [432]:

- Villages in faraway areas.
- Normal houses and offices.
- Telephony stations.
- Rural areas facilities.

- Communications of emergency stations.
- Monitoring stations of drinking water.
- Pumping of drinking water.
- Pumping for Irrigation and livestock.
- Monitoring stations of weather data.
- Lighting of streets.
- Water desalination stations.

12.2.1.5 Stand-alone Solar System Components

There are several types of components that altogether implement the stand-alone solar systems. The main components are [432]:

- Inverters.
- Transformers.
- Metering devices.
- Batteries.
- Distribution panels.
- Solar modules.
- Controllers.

Solar panel or module produces DC electricity which is charging the storage batteries using controller of solar charge. All appliances that are charged with DC power which connected to the battery must be fused (using fuses to protect its). The lights that are operated by DC are connected directly to the controller of charge. To operate the AC appliances, they are connected to the inverter which is directly connected to the battery. Usually, the voltages of stand-alone systems are in the range from 12V DC to 48 V DC. For larger systems, the voltages are from 400 V DC to 800 VDC [432].

The generated DC voltage of the solar panel must be higher than 12 V DC to charge the battery of 12 VDC. Normally, a voltage of 14.4 V DC generated using solar panel can charge the battery of 12 V DC. In the case of high temperature weather, the solar panel must provide a voltage of more than 20 V DC to charge the battery properly.

Charge controller is used for battery protection and for ensuring high quality performance. For battery protection from over-discharge, the charge controller disconnects the battery from the load. This operation is called low-voltage disconnection (LVD). Similarly, for battery protection from over-charge, the charge controller disconnects the battery from the charger. This operation is called high voltage disconnect (HVD). Furthermore, the charge control protect the solar panel from the flowing back current (reverse current) that might be flow back during night.

12.2.1.6 Design Procedure for Stand-alone System

There are several effective steps to design a high quality stand-alone power system. The design procedure contains the following steps:

- Determining how much electricity is needed by calculating the load in daily or weekly basis.
- Determining the battery type regarding the storage capacity in Ah that is enough to the real needs.
- Calculating the amount sun rays the desired site receives monthly taking into consideration the month of least sun rays and more demand.
- Approximating the array size depending on the worst month regarding sun shining.

12.2.2 Mini-grid System

A mini-grid is an off-grid system that is isolated from the public utility grid. This system has a small distribution grid that supplies power to a limited numbers of consumers. This type of systems has additional names like micro-grid and isolated grid. The wattage generated normally in this type ranged from 10 KW to 10 MW.The mini-grid may provide power to small residential villages, small technical workstations and group of shops [430].

Mini-grids that depend on renewable energy are called clean energy mini-grids (CEMGs). It depends on one or more types of renewable energy sources like solar, wind and hydro. The mini-grid electrification system is to produce electricity and distribute it to population in a limited geographical area [427]. Mini-grids could be divided into the following sub- systems:

- Production.
- Distribution.
- Consuming.

Most of the components related to production operation are located inside the power house. The components of the distribution operation are connecting the energy production sub-system to the users using over-headlines or under-ground lines.

12.3 Electricity Generation

There are many ways of generating electricity. Some of them are [430]:

- Solar system.
- Micro-hydro system.
- Geo-thermal Source.
- Wind turbine.
- Thermoelectric generator.
- Diesel or biofuel generator.

These sources are used in the different countries depending on the abundance of it in each country. For example, in the sunny countries most of the time, the solar source of electricity is preferable. On the other hand, in the countries that have rivers and seas or adjacent to oceans, it is best to use hydro source, and so on.

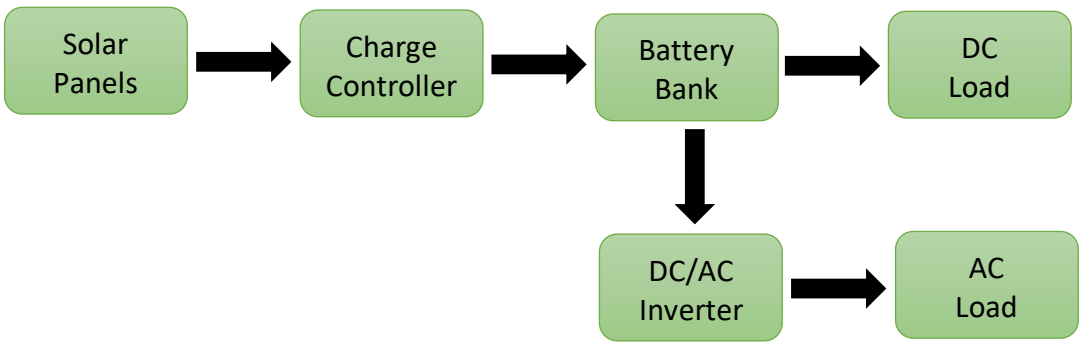

Figure 12-5: Diagram of house solar system

12.4 Hybrid Power System

The hybrid-power system is the system of power that uses more than one power system of renewable energy. The hybrid system may use two, three or more renewable energy sources [431]. The criteria of choosing the accredited sources of the hybrid system depending upon the abundance of the source in the desired area.If the hybrid system use more than one abundant source, it becomes more reliable to serve the desired area in high efficiency and it ensures the service sustainability.

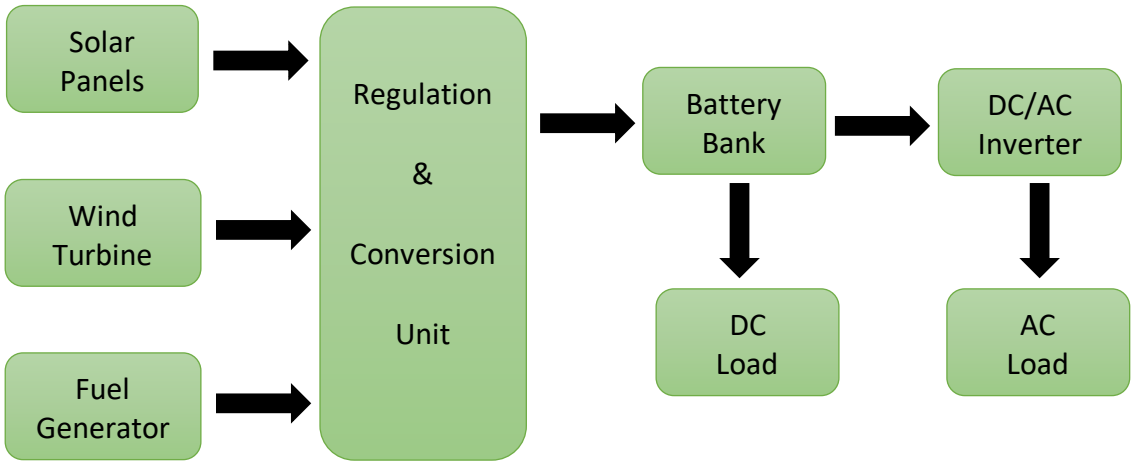

Figure 12-6: Diagram of hybrid system

12.5 Advantages of Off-grid System

There are many advantages of the off-grid system over the public utility grid extension to the rural and the faraway places, some of them are *[427]* and *[430]*:

- It is cheaper than using the public utility grid.
- It is adaptable to local needs and conditions in contrast of the public utility grid.
- It could be operated by local technicians which leads to local employment.
- It is easier to be implemented than the installation of transmission lines of the public utility grid.

- It takes less time to be implemented which reduces the waiting time for the population to use it.
- It can use the local renewable energy sources to provide electricity.
- It is more reliable and there are no sudden interruptions in the electrical current.
- There are no bills or running costs.
- It has full local control.

12.6 Load Related Problems

There are many problems that may be occurred from different types of loads that might be connected to the stand-alone systems [431]. Some of them are:

- The wrong load selection that is used.
- Bad wiring and Low-quality protection devices.
- Loads with low efficiency affect the power consumption.
- Mode of stand-y in certain loads consumes power.
- High start-up currents for certain loads may overload the system.
- The difference between the circulating current and the consumed current in the case of inductive or capacitive loads.
- Harmonic distortion for the inverter waveform due to non-linear loads.
- The efficiency reduction due to mismatching between the inverter and the load.

12.7 Solar Home System

Solar home system (SHS) is one type of stand-alone photovoltaic solar systems [433]. Each solar system is unique and should be designed to achieve the user needs taking into account the geographic location. Each system should be designed to reflect the user energy consumption [434].

SHS is cheap and effective supplier of power for lighting and home appliances. So, it may be used in rural areas to supply households by electricity for all human needs [434]. Stand-alone solar power system is independent from utility electric grid [432]. Recently, hundreds of thousands of households were provided with electricity via SHS in faraway locations. SHS

provides usually 12V DC which could be connected directly to DC appliances. Through using inverters, SHS can provide the households with effective AC electricity for the normal household's appliances. Solar energy system is more reliable source because it does not involve moving parts [434]. Typically, SHS includes the following modules and components beside others:

- One or more photovoltaic (PV) modules, each of them consists of solar cells.
- Charge controller to distribute power and protect the batteries and appliances from damage.
- One or more battery to store energy for use in night and rainy or cloudy days.

12.7.1 Standard of Living Improvement using SHS

There are many contributions resulted from using SHS which improve the standard living of human. Some of them are [427] and [433]:

- Improving population health.
- Lighting for home study.
- Lighting for house work.
- Access to information and communication.
- Avoiding greenhouse gas.
- Providing cooling for medicines.

12.7.2 Technical Standards for SHS

SHS has many technical standards to ensure functionality, reliability and safety [434]. Some of these technical standards will be mentioned in the following sub sub-sections depending on the different parts that the SHS contains [435] and [436].

Figure 12-7: Residential complexes with solar panels

12.7.2.1 Module Installation of SHS Photovoltaic

The quality of the solar home system that provides electricity to households depends mainly on the module installation of the photovoltaic modules. Some of the criteria related to this matter are mentioned below:

- Identical modules should be used if more than one is required, and all should be connected in parallel.
- Solar cells must be waterproof.
- The mounting structure must hold the photovoltaic modules properly.
- The structure of photovoltaic array must withstand wind gusts up to 160 km/hour.
- The structure orientation angle must be specified and fixed to provide maximum energy during the year.
- All external connections in the structure must be corrosion resistant.
- The modules could be mounted on roof or mounted on ground. In both cases, extensive care must be taken to install the modules in a solid and robust way.

12.7.2.2 Circuit Protection and Charge Controls

There are many criteria to protect users and system components. Also, the criteria must ensure the sustainability of the electrification providing service. Some of the main criteria are mentioned below:

- Preventing battery overcharge.
- Preventing battery from under-charging and excessive discharging.
- Protection against load short-circuit.
- Protection against shorts circuits in controller, inverter or any other device.
- Protection against damage resulted from high photovoltaic voltage of the open circuit when it is connected to the controller with no battery.
- Preventing battery discharging resulted from reverse current.
- The charge controller must protect the system against high voltage and low voltage by automatic circuit disconnection.

Figure 12-8: Mega solar system to supply main grid

12.7.2.3 Batteries

Batteries are responsible about storing energy generated by the photovoltaic and use it to supply the loads when required. There are technical specifications that must be taken into consideration when designing the SHS system [432], [435] and [436]. Some of them are:

- Useful life of the selected batteries must be five years or more.
- Electrical size of each battery must exceed 50Ah at 10-hours.
- Batteries must be supplied in a dry-charged condition.
- Batteries enclosures must be designed to be highly protective.
- Batteries must have high efficiency of charging.
- Batteries must have low charging currents.
- Batteries must have low-self discharge.

Figure 12-9: Micro solar system to supply danger horn to alert citizens during disasters

There are many advantages for using battery bank when using solar home system [437], some of them are:

- The availability of electricity in night and in cloudy days.
- Money saving if the system is connected with local or normal grid.
- More independence, since you can store the energy that you generate.

In spite of the obvious advantages, there are some disadvantages for using batteries to store the solar energy, some of them are:

- Raising the total price of the solar system.
- Increasing the system complexity because of the additional equipment needed.
- The system needs additional space to install the battery bank.

The cost of ordinary home battery system depends on the capacity (electrical size) of the battery in kWh, installation location, backup power requirements, and the brand of the inverter used. Normally, the range of the cost is between $4000 and $12000.

In general, a battery system for solar home system may cost between $800 and $1200 for each kWh stored.

Figure 12-10: Micro stand-alone solar system for highway emergency station

Introducing Recent Electrical Engineering
Developments into undErgraduate cuRriculum

13 Integrating of Renewable Energy into electrical grid (Challenges, Solutions and Grid Code)

Author(s): Dr. Eyad Almaita
Dr. Ahmad Aljaafreh

13.1 Introduction

While electrical power grids have been designed to deal with predictable generation and variable load patterns, the increasing number of renewable energy projects introduces new problems for operators and electric utilities because of its uncontrollable nature uncertainty. Fortunately, a wide range of technical and operational practices exist to facilitate integration of higher share of renewable energy generation. This section focuses on renewable energy (solar and wind) integration challenges and solutions.

The integrated RE is the process of incorporating renewable energy into the existing electrical grids (distribution and transmission). The AC grid could have distributed generation, renewable energy plants, energy storage, thermally activated technologies [438], [439]. The integration of Renewable energy aims to help utilities to:

1. Lower carbon emissions by increasing the share of wind and solar energy and other clean and low carbon footprint technologies.
2. Better asset management through coordination between distributed generation and customer loads which leads to peak load levelling and avoid peak-time tariff.
3. boost reliability, adaptability and, security in highly stressed spots of the electric network.
4. Cut fossil fuel use by support operations and energy exchange between the grid and plug-in electric vehicle.

13.2 Challenges

The intermittent and variable nature of renewable power generators accompanied with the topological modifications have increased the annoys about power systems control, dynamics, and automation. Consequently, it is a challenge task to merge RE power into existing electric grid. There are several challenges of this merge and Figure 13-1 shows the main challenges that will be reviewed later in this section.

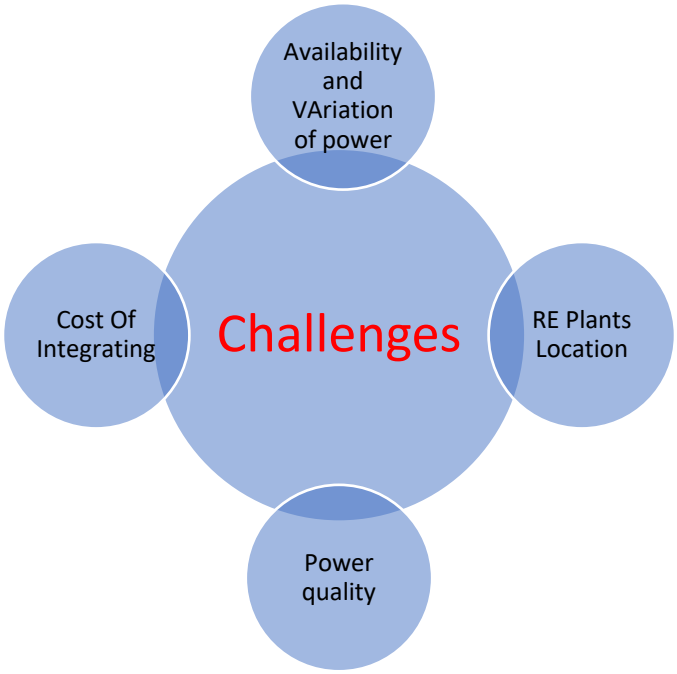

Figure 13-1: RE Integration Challenges

13.2.1 Availability and Variation of Power generation

One of the major challenges in RE-Grid integration is the power generation comes from RE rely on natural resources that cannot be controlled. In PV-solar energy delivering power stand up on during the day and off at evening time, and furthermore wind vitality depends on the availability of wind, so if the wind speed is around zero below the minimum level, the turbine will stop, and as a result zero power will flow to the grid. This uncertainty of solar and wind generation may present difficulties for network administrators. The uncertainty and variability in renewable energy sources require further actions to adjust the system. Extra flexibility in the system can help grids to deal with supply-side uncertainty and maintain healthy relationship between loads and generation levels. The variability in wind generation can affect system operations in terms of lead to deeper turn downs, steeper ramps, and shorter peaks. In Ramps operation - changes in demand dominate the rate of decrease or increase dispatchable generation. For example, if demand rises accompanied with wind generation decreasing Ramps can be steep. On the other hand, if demand decreases accompanied with high wind generation the must be turned down. All these conditions create the need for flexible dispatchable generators that can be ready for steep rise or quick turn-down. The use of renewable energy along with conventional generators will result in Shorter

peaks periods which will reduce the operating hours for conventional generators, impacting security of supply and cost recovery [440].

13.2.2 Location of RE Plants

Most of RE power plants that fed their energy generation into the grid usually have large capacity, which lead to need of large area of such RE power plant. The location of RE plant is not arbitrary and several factors, related to each RE technology, can dictate the chosen location. Choosing a location to run one of RE technology includes many factors that affect RE-Grid integration. First, not each RE technology can be operate in each region. Second, how far is RE plant from the grid is a crucial factor that can affect efficiency and cost. Third, geographical location and climate conditions are essential for picking RE source. For example, PV solar technology in sunny locations is more efficient than foggy or cold locations because of the large amount of sun radiation per day in these locations. Also, ocean wave and tidal energy are another example can show the uncontrolled nature of selecting location of RE power plant. Another point regarding location selection is choosing the right location in grid structure (Transmission or distribution network). The electric grid could have different types of power generators such as conventional power generators and RE sources (wind, solar, etc). The nature of output power from RE source should be an AC power so power can be transferred to the substation. After that, the power can transfer to transmission lines, or directly to distribution system [438], [441].

13.2.3 Cost of integration

The adequate assessment of renewable energy integration costs is vital for system planning and policy making. Any fiscal assessment of the transition from conventional electric grid towards renewables-based electric grid, must take into consideration all different factors that affect the cost of integration. Not all these costs are credited to RE, especially when the electrical system is flexible enough to manage fluctuation.

The extra cost of integration of renewable energy into the existing electric grid can be broke down into **grid infrastructure** and **operation costs**. The smart grid technologies extra costs

are approximately estimated to be same with the value financial savings due to decreased top masses and expanded energy efficiency.

A. **Grid infrastructure costs** cover:

1. **Grid connection costs** consist of the cost of installing a new cable from the new RE power plant to the operating power grid. The distance between the new RE plant and the existing grid is the main factor of this cost. Also, the voltage level (high or low) of the connection line. This cost is related to the isolation type, and the availability of appropriate tools. The connection costs have significant economic for renewables projects located in remote areas. Several studies have shown that grid connection costs for majority of new renewable projects in urban regions can range between 0% and 5% of the total cost. Principally, this type of cost is the influential financial part in infrastructure costs for wind projects. In most projects, these costs are considered as part of the initial investment cost.
2. **Grid upgrading costs** cover the cost of new grid equipment and tools needed to integrate renewable project into the current grids. These costs are highly related to the capacity of the renewable energy project, Renewable power plant location, and the structure of the current grid. Based on load flow analyses, many studies carried out in different countries suggest a strong correlation between the cost of grid upgrading and the level of renewable electricity share, i.e., costs are around EUR 0.5–3/MWh for twenty to thirty percent renewable share.

B. **System operation costs** cover the extra costs related to the power system conventional part caused by the integration of renewable projects. It can be divided into:

1. **Profile costs** include costs related to the mismatch between load profile and RE generation and cover three types: reduced utilization of conventional power plants, capacity costs, and curtailed RE generation when demand is less than power supply. The utilization effect is considered the dominant single

integration cost part and can reach up to more than half of the total integration costs at 30%-40% renewable penetration level (EUR 15–25/MWh). At low penetration levels, the profile costs are negligible or can result in savings.

2. **Short-term system balancing costs**. Secure and stable power grid operation needs continuous balance between demand and generation (supply). Because of uncertain and variable nature RE generators, the reserve capacity required for power grid regulation is higher comparing to a power grid has only conventional power generator. This will have a modest to negligible impact for second-to-minute scale power variability and will have significant grid operation impact for minute-to-hour scale power variability. The extra needs for reserve capacity correspond to the increased costs for the conventional power plant units. These additional costs are necessary to ensure adequate reserve power capacity.

13.2.4 Power quality

The power quality definition according to IEEE is “The measure, analysis and improvement of the bus voltage to maintain a sinusoidal waveform at rated voltage and frequency”. There are two major categories of power disturbances:

1. Continuous or long-lasting disturbances
2. Random or transient disturbances

Each main category comprises several power quality problems. In the following a more detailed description about these power quality problems can be provided: [442], [443], [444].

13.2.4.1 Flicker

Flicker can be defined as visual variation of input voltage in the specific duration, the flicker may be stated as the change in voltage over nominal expressed as a percent. Or Impression of unsteadiness of visual sensation induced by a light stimulus whose spectral or luminance distribution fluctuates with time or the flicker is the repaid change in fluctuating loads which result in visual sensation as induced

by a light stimulus whose spectral or luminance distribution fluctuates with time the IEC standard provides total flicker levels for HV system must not exceed certain value.

In flicker definitions there are two concepts the first concept is the short-term flicker for 10 minutes (Pst) the other one is the long-term flicker (Plt). Table 13-1 shows the acceptable flicker limits for both types.

Table 13-1 Flicker Limits

Flicker	Acceptable limits
Pst	3%
Plt	1%

13.2.4.2 Power Frequency:

Power frequency is the nominal frequency of the oscillation of A C Current in an electric power network transmitted from power generation plant to the end–user and the frequency in the range used for alternating currents supplying power (usually 50 or 60 Hz). Table 13-2 shows the frequency limits under different operating conditions.

Table 13-2 Frequency variation *limits*

Under **normal operation** and introconnected with other systems	49.95Hz to 50.05 Hz
Under **normaloperation** but not interconnected with other systems	49.95Hz to 50.05Hz
Under **system stress**	48.75Hz to 51.25Hz
Under extreme system fauult conditions all **generating units** should have disconnected by these (high or low) frequencies unless agreed otherwise in writing with the TSO	By a frequency greater than or equal to 51.5Hz By a frequency less than or equal to 47.5Hz

13.2.4.3 Crest Factor:

Can be defined as the ratio of peak value of voltage or current waveform to its RMS value it is a numerical value without any units, the Crest Factor for normal sinusoidal wave is 1.414.

$$CF = \frac{peak\ amplitude}{root\ mean\ square} \qquad \textit{Equation 13-1}$$

13.2.4.4 Voltage Unbalance (imbalance)

Can be defined as the ratio of the negative (V_n) sequence component or zero(V_z) sequence component to the positive sequence component, the unbalanced load, such as large single-phase loads, and Incorrect distribution of loads by the three phases of the system are the cause of these components. In voltage unbalance the three voltage magnitudes or the phase-angle differences between them are not equal. The maximum limit of the voltage unbalance according to the American National Standard for Electric Power Systems and Equipment ANSI C84.1 should not exceed 3 percent. The Voltage unbalance can be calculated as:

$$Voltage\ unbalance\ = \frac{max\ deviation\ from\ average\ voltage}{average\ voltage} \qquad \textit{Equation 13-2}$$

Where the $max deviation from average voltage = max value - average value$

13.2.4.5 Sag

Sag is an event causes RMS reduction in AC voltage at power frequency in short period (few seconds) like heavy loads such as motor or arc furnaces. There are many definitions that identify voltage sag according to the duration and magnitude of the event. According to the IEEE standard, voltage sag is defined as a reduction of rms voltage magnitude from 0.1 to 0.9pu, and the duration can span from 0.5 cycle to 1 minute. The causes of Voltage sag are system faults, energizing of transformer, or switching of heavy load.

13.2.4.6 Swell:

It is an increase in magnitude of AC voltage at power nominal frequency in short period (few seconds).Or, it is a Rapid increase of the Ac voltage magnitude, at the nominal frequency, beyond the predefined limits, for period of more than one cycle to less than a few seconds.

Causes:

- Switching of heavy loads.
- Ill design of power sources.
- Inadequate transformers sizing and regulating.

13.2.4.7 POWER SYSTEM HARMONICS

13.2.4.7.1 Harmonics Definitions:

Voltage or current periodic sinusoidal waveforms have frequency that is multiple integer of the fundamental frequency.

The conventional generation system is normally produced constant voltage and frequency 50 Hz or 60Hz (determined by the countries around the world). When a nonlinear loads, like the power electronics and switching devises loads, is connected to a sinusoidal voltage source, it will draw a distorted current and not perfectly sinusoidal. As a result, a non-sinusoidal voltage drop will be occurred because of system impedance, which will cause a voltage distortion at the point of common coupling.

Harmonics are not only produced by renewable energy sources but also loads that draw a nonlinear current like a transformer operated at higher flux density during an overvoltage will operate in the saturation region producing current a non-sinusoidal waveform and not only produce odd harmonics but also produced even harmonic and theses harmonic not be taken in consideration in the steady sate , and in fact all electrical equipment that contains power electronics produces harmonics and converter is similar .

13.2.4.7.2 General harmonic expressions and indices:

There are many indices to expression for harmonics distortions, the common one is the total harmonic distortion (THD), which is identified as the RMS of all harmonics expressed as a ratio to the fundamental component. The voltage THD and the current THD can be calculated as

Equation 13-3 and Equation 13-4 respectively. Most common standards recommend measuring the harmonics up to 50th.

$$THD_V = \frac{\sqrt{\sum_{n=2}^{N} V_n^2}}{V_1} \quad \textit{Equation 13-3}$$

$$THD_i = \frac{\sqrt{\sum_{n=2}^{N} I_n^2}}{I_1} \quad \textit{Equation 13-4}$$

THD index may be misleading, at certain conditions, for measuring current distortion as above mention in Equation 13-4. When the fundamental component of load current is low and when the load is light, a high THD magnitude for input current will not have significant impact. So to avoid ambiguity and mismatch the Total Demand Distortion (TDD) factor is used and defined as:

$$TDD = \frac{\sqrt{\sum_{n=2}^{N} I_n^2}}{I_R} \quad \textit{Equation 13-5}$$

Where: I_R is rated load current magnitude.

13.3 Solutions

Several solutions are accessible to mitigate integration effects. Key factors in selecting approaches are the cost-effectiveness of the method and the nature of the current grid. Generally, Flexible grids are required to accommodate the extra uncertainty of renewables. Flexibility may include regulation changes, operational practices, energy storage, demand-side management, adaptable generators, and other courses. Several of these courses are discussed below [441], [445], [446].

13.3.1 Advanced Forecasting

Advance forecasting for Wind and solar power can mitigate the uncertainty of intermittent renewable sources. Advance forecasting can help advanced and efficient planning for generating unit dispatch. This will help grid to adapt with the variability in wind and solar

generation and to be ready for any for radical events. Forecasting can lead to reduction in the operating reserves required for the grid and balancing costs. Short-term forecasting can range from one hour ahead to one week ahead. One hour ahead forecast errors commonly span from 3% to 6% of rated capacity and a day ahead forecast error range from 6% to 8% on a regional basis. In comparison, load forecasting errors commonly span from 1% to 3%.

13.3.2 Fast Dispatch and Larger Balancing Authority Areas

Quick dispatch mitigates the intermittent nature and variability of renewable generation, since it mitigates the necessity for regulating resources, enhances efficiency, and gives access to a more extensive arrangement of assets to balance the system. When using fast dispatch techniques, generation can track load level more precisely which will reduce the need for more costly regulating reserves. This enhances the utilization of the most cost-efficient resources and boost extra environment friendly balancing approach. Five-minute dispatch is most common method used nowadays.

13.3.3 Reserves Management

Practices change in Reserve management can assist to cope with the variability of wind and photo voltaic power generators. Practices that decrease average reserve limits can result in widespread value savings. Possible ways for managing variability consist of putting boundaries for wind electricity ramps to mitigate the need for reserves and allow different renewables to grant reserves or different ancillary services. Ramp incidents that impact plants across a balancing authority vicinity result from huge weather activities that can be extra without difficulty predicted than nearby climate events. By setting ramping boundaries on windmills, when substantial climate events are forecasted, levelling reserve requirements may also be drastically reduced.

13.3.4 Demand Side Management

Demand-side management can contribute to the integration process of intermittent renewable generation, especially in extreme events or in cases of fast ramps. Demand response can comprise of peak reduction, ancillary services, and Supply reserves. The

employment of demand side management to balance the system at some stage in infrequent occasions in which there is tremendous over-, or undersupply of generation can result in value financial savings in contrast to always keeping extra reserves.

13.3.5 Energy Storage

Advances in energy storage technologies ought to notably alternate how variability and uncertainty are managed by way of the grid. The energy storage market has been increased dramatically in the last few years. As energy storage choice seen as cost-effective approach and more players entered the market. Energy storage will become more widely affordable within the coming few years. Energy storage will facilitate renewable integration and provides the grid with needed flexibility by shifting load and generation peaks. It also can help to maintain grid reliability and stability. Although strength storage is not quintessential to integrate renewable energy, lower priced storage may want to minimize integration challenges. In particular, as countries try to meet excessive renewable power targets. New battery applied sciences ought to appreciably enlarge the price of wind, which frequently produces electricity at some stage in the evening when demand is low. In areas where solar manufacturing may also peak a few hours earlier than demand is highest, energy storage ought to enable photo voltaic electricity to be used in the times of peak demand when electrical energy is most highly priced.

13.3.6 Microgrids

With the proliferation of Distributed Generation (DG), Microgrid concept has been adopted as an effective scheme to coordinate the operation of these multiple and parallel DGs. Microgrid scheme can have several benefits for customers and utilities. For customers it can improve the power quality and reduce the cost of the power. For the utilities it can minimize the power exchange between the distribution and transmission networks, which will reduce the losses on the grid and mitigate the impact of integration of renewable energy sources. It usually connected to low voltage distribution network, has several distributed generators, and storge elements, and can operate as stand-alone grid (off grid/ Islanded mode) or

connected to the grid (on-grid). The microgrid is connected to the grid at the point of common coupling (PCC) through the static transfer switch (STS) [447], [448], [449].

13.4 Renewable Resources Grid Code

All Generators connecting to the electrical grid must comply with the grid Code governing the electric network. The grid Code was originally covering conventional synchronous generators. With the increase number of Intermittent (wind and solar photovoltaic) Renewable Resources this code was revised to contain these types of resources. The following set comprises of common grid codes technical connection requirements [450], [451], [452].

13.4.1 LVRT requirements

Low Voltage Ride Through (LVRT) capability considers one of the most important requirements in modern grid codes, which means that the renewable energy conversion system must endure dip in grid voltage (during grid faults) to a predetermined limit of the nominal voltage for a specific duration and operate normally. After clearance of fault, renewable energy must swiftly recover supply of active and reactive power to the prefault value. In some regulations, the renewable generator is obligated to supply reactive power during the fault and operate like conventional synchronous generators to help maintain voltage stability.

LVRT requirements are usually defined by a voltage versus time curve as shown in Figure 13-2, which demonstrate general grid code for LVRT requirements. The renewable energy plants should have the ability to operate continuously in normal operation area (A), which represents the nominal voltage at PCC. If the voltage is in the blue region (B), the renewable energy plant has to remain connected to the system and with stand voltage dip for a duration span from (t0 → t1). Otherwise, it must be decoupled. If the voltage at the Point of Common Coupling in area C is restored to V1 during time t2 after fault occurrence, it is obligatory for renewable plant to remain work continuously without any disconnection.

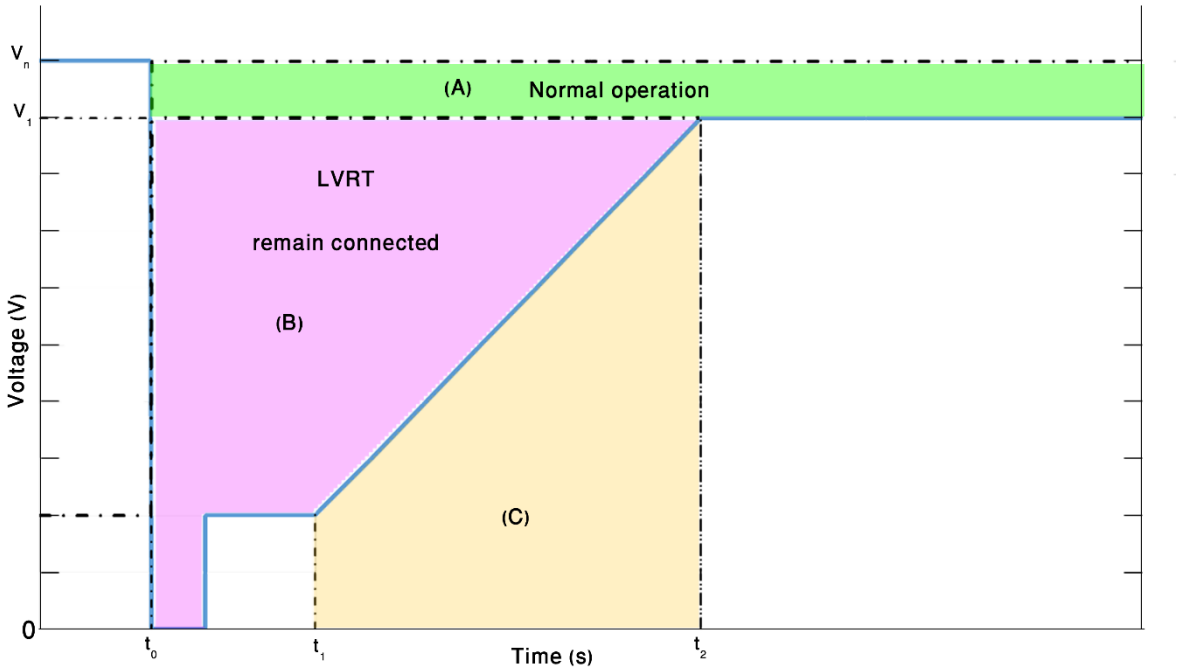

Figure 13-2: Curve limits for low-voltage ride-through requirements

13.4.2 HVRT requirements

Like the grid code for LVRT requirements, some modern Grid codes insist that renewable plants must remain coupled to the system when the voltage swell (overvoltage) take place for a predefined period. This requirement is defined as HVRT capability, which aims to maintain the overall stability of grid voltage and avoid catastrophic situations induced by overvoltage. Nowadays, most grid codes require the HVRT functionality to be applied, in spite of overvoltage event is less frequent event compared to under voltage event (voltage sag).The HVRT requirements depending on specific characteristics (RE penetration level and operational policy) of each power system differ from each other.

13.4.3 Reactive power requirements

To ensure grid voltage stability which is related to the reactive power, therefore, to curb the instability of electric grid, in case of high penetration of renewable energy, modern Grid codes require renewable energy generators to be part of grid stability scheme by providing reactive

support during and after disturbances, like traditional power plants. Reactive support can be in form of reactive power control and reactive current injection.

13.4.4 Voltage and frequency range

Modern Grid codes require large-scale renewable energy plants to continuously maintain the voltage and frequency within predefined boundaries throughout steady-state operation of the electric grid. These voltage and frequency boundaries must be kept under variable operating circumstances. Therefore, modern Grid codes define the voltage and frequency limits for continuous operation of the renewable plant. Many nations such as Japan, Germany, and China adopt a grid code for voltage limits at the point of common coupling by±10% of the nominal voltage. The frequency operational limit, for most international Grid codes, has limits between 47 and 52.0 to 53.0 Hz.

Bibliography

[1] "Martinburo/Wikimedia Commons. Bp_world_energy_consumption. By Martinburo - Own work, CC BY-SA 4.0, https://commons.wikimedia.org/w/index.php?curid=53803246," 2016, December.

[2] R. Vooradi, S. Anne, A. Tula, M. Eden and R. Gani, "Energy and CO2 management for chemical and related industries: issues, opportunities and challenges," *BMC Chemical Engineering,* vol. 1 (7), 2019. https://doi.org/10.1186/s42480-019-0008-6.

[3] IEA, "World Energy balances: overview. World Energy balances. International Energy Agency. 2017a. https://webstore.iea.org/world-energy-balances-2018. Accessed 5 Aug 2018".

[4] H. Ritchie and M. Roser, ""Energy". Published online at OurWorldInData.org. Retrieved from: 'https://ourworldindata.org/energy' [Online Resource]. Source: BP Statistical Review of World Energy (2019). OurWorldInData.org/energy/ CC BY," 2020.

[5] "BP: Statistical Review of World Energy," 2019.

[6] H. Ritchie and M. Roser, "Retrieved from: 'https://ourworldindata.org/fossil-fuels' [Online Resource]. Source: Vaclav Smil (2017). Energy Transitions: Global and National Perspective & BP Statistical Review of World Energy. OurWorldInData.org/fossil-fuels/ CC BY," 2017. "Fossil Fuels". Published online at OurWorldInData.org.

[7] "IPCC 2014: Summary for Policymakers. In Climate Change 2014: Mitigation of Climate Change. Contribution of Working Group III to the Fifth Assessment Report of the Intergovernmental Panel on Climate Change," Cambridge University Press, Cambridge, United Kingdom and New York, NY, USA, [Edenhofer, O., R. Pichs-Madruga, Y. Sokona, E. Farahani, S. Kadner, K. Seyboth, A. Adler, I. Baum, S. Brunner, P. Eickemeier, B. Kriemann, J. Savolainen, S. Schlömer, C. von Stechow, T. Zwickel and J.C. Minx (eds.)].

[8] M. K. Hubbert, "Energy resources. In: Resources and man. National Academy of Sciences - National Research Council, Report of Committee on Resources and Man, Freeman, San Francisco, pp. 157-242; also in Energy resources of the Earth, Sci Am, 60, 1971.," 1969.

[9] G. Maggio and G. Cacciola, "When oil, natural gas and coal peak?," *Fuel,* vol. 98, pp. 111-123, 2012.

[10] "U.S. Energy Information Administration. https://www.eia.gov/dnav/pet/hist/LeafHandler.ashx?n=PET&s=MCRFPUS2&f=A, https://www.eia.gov/dnav/pet/hist/LeafHandler.ashx?n=PET&s=MCRNTUS2&f=A.".

[11] "Hubbert peak theory. By Own work - US Energy Information Administration. CC BY-SA 3.0, https://commons.wikimedia.org/w/index.php?curid=24951796, 19 September 2020".

[12] "Tim Starling/Wikimedia Commons. Semiconductor_band_structure_(lots_of_bands). By Drawn by Tim Starling - Own work, CC BY-SA 3.0, https://commons.wikimedia.org/w/index.php?curid=342033," 2005, September.

[13] "U.S. Energy Information Administration. https://www.eia.gov/energyexplained/solar/photovoltaics-and-electricity.php (Last updated: August 25, 2020)".

[14] "Rfassbind/Wikimedia Commons. From a solar cell to a PV system. Diagram of the possible components of a photovoltaic system. By Rfassbind - Own work, Public Domain, https://commons.wikimedia.org/w/index.php?curid=34961018," 2014, August.

[15] "IRENA (2020), Renewable capacity statistics 2020 International Renewable Energy Agency (IRENA), Abu Dhabi".

[16] "European Commission. Smart Specialisation Platform. https://s3platform.jrc.ec.europa.eu/concentrated-solar-power," Last updated: 10/05/2020 (version: 1.0).

[17] "Nsttf/Wikimedia Commons. SandiaNSTTF fieldimage. By Nsttf - This is the view from the control room of the NSTTFPreviously published: 2012-10-03, CC BY-SA 3.0, https://commons.wikimedia.org/w/index.php?curid=21895271," 2012, October 3.

[18] "U.S. Department of Energy. https://www.energy.gov/eere/solar/linear-concentrator-system-concentrating-solar-thermal-power-basics".

[19] "An array of solar panels. By USA.Gov - BLM - BUREAU OF LAND MANAGEMENT - http://www.ca.blm.gov/cdd/alternative_energy.html, Public Domain, https://commons.wikimedia.org/w/index.php?curid=15957890," 2020, February 14.

[20] "NOVATEC BIOSOL. Solar power plant PE 1 based on linear Fresnel technology. By NOVATEC BIOSOL - http://www.novatec-biosol.com/index.php?article_id=48&clang=4, FAL, https://commons.wikimedia.org/w/index.php?curid=7583488," 2009, April 1.

[21] "Photo by Plataforma Solar de Almería / CIEMAT. http://www.psa.es/en/facilities/dishes/eurodish.php".

[22] A. Greco, E. Gundabattini, D. Gnanaraj and C. Masseli, "A comparative study on the performances of flat plate and evacuated tube collectors deployable in domestic solar water heating systems in different climate areas," *Climate,* vol. 8, no. 6:78, 2020. https://doi.org/10.3390/cli8060078.

[23] S. Raza, S. Ahmad, T. Ratlamwala, G. Hussain and M. Alkahtani, "Techno-Economic Analysis of Glazed, Unglazed and Evacuated Tube Solar Water Heaters," *Energies,* vol. 13, no. 23:6261, 2020. https://doi.org/10.3390/en13236261.

[24] T. Özbalta and S. Kartal, "Heat gain through Trombe wall using solar energy in a cold region of Turkey," *Scientific Research and Essays,* vol. 5(18), pp. 2768-2778, September 2010. Article Number - 40112C319953. https://doi.org/10.5897/SRE.9000542.

[25] GlobalWindAtlas, "Map obtained from the "Global Wind Atlas 3.0, a free, web-based application developed, owned and operated by the Technical University of Denmark (DTU)," The Global Wind Atlas 3.0 is released in partnership with the World Bank

Group, utilizing data provided by Vortex, using funding provided by the Energy Sector Management Assistance Program (ESMAP). For additional information: https://globalwindatlas.info.

[26] "Zavijava/Wikimedia Commons. Wind turbine of REpower MD 70 type near Boehmenkirch. By Zavijava - Own work, CC BY-SA 3.0, https://commons.wikimedia.org/w/index.php?curid=14783648," 2011, April 3.

[27] "Guillom/Wikimedia Commons. World highest Darrieus wind generator Éole, Gaspé peninsula, Quebec, Canada. By guillom - Own work, CC BY-SA 3.0, https://commons.wikimedia.org/w/index.php?curid=466915," 2005, December 18.

[28] "Savonius Wind Turbine. By Toshihiro Oimatsu - Flickr, CC BY 2.0, https://commons.wikimedia.org/w/index.php?curid=3178843," 2006, March 21.

[29] "Stahlkocher/Wikimedia Commons. H-Darrieus-Rotor. By Stahlkocher - photo taken by Stahlkocher, CC BY-SA 3.0, https://commons.wikimedia.org/w/index.php?curid=38639," 2007, June 21.

[30] "Fred Hsu/Wikimedia Commons. Wind turbines at Jinguashi. By Fred Hsu on en.wikipedia - Own work, CC BY-SA 3.0, https://commons.wikimedia.org/w/index.php?curid=9536672," 2009, November.

[31] "Popolon/Wikimedia Commons. Sunset on more than 2000 Windturbines at Guanzhou wind farm, Gansu province, China. By Popolon - Own work, CC BY-SA 3.0, https://commons.wikimedia.org/w/index.php?curid=28073693," 2013, May.

[32] "The joy of all things/Wikimedia Commons. Hornsea wind farm from Barmston beach. By The joy of all things - Own work, CC BY-SA 4.0, https://commons.wikimedia.org/w/index.php?curid=81516269," 2019, August 13.

[33] "World Bioenergy Association. Global bioenergy statistics 2019. https://worldbioenergy.org/".

[34] "D-Kuru/Wikimedia Commons. A huddle of wood pellets. By D-Kuru - Own work, CC BY-SA 3.0 at, https://commons.wikimedia.org/w/index.php?curid=6187400," 2009, March.

[35] "Britta Gustafson/Wikimedia Commons. Aerial photo of the Puente Hill Landfill. By Britta Gustafson - Flickr: IMG_1097, CC BY-SA 2.0, https://commons.wikimedia.org/w/index.php?curid=22615319," 2012, July 9.

[36] "Ian Zammit/Wikimedia Commons. Flow chart showing the production of ethanol from plant material. By Ian Zammit - Own work, CC BY-SA 3.0, https://commons.wikimedia.org/w/index.php?curid=29794212," Elsevier, 2013, November 23.

[37] "Alternative Fuels Data Center. Energy Efficiency & Renewable Energy, U.S. Department of Energy. https://afdc.energy.gov/fuels/biodiesel_production.html".

[38] "Dake/Wikimedia Commons. Schematic section through the Earth. By Dake - Own work (Software: Inkscape), CC BY-SA 2.5, https://commons.wikimedia.org/w/index.php?curid=809709," 2006, May.

[39] "USGS. Tectonic plates. By Map:USGS Description:Scott Nash - This file was derived from: Tectonic plates.png, Public Domain, https://commons.wikimedia.org/w/index.php?curid=535201," 1996, February 1.

[40] "Eruption of Strokkur close by. By Andreas Tille - Own work - see http://fam-tille.de/sparetime.htmlImage with Information in EnglishBild mit Informationen auf Deutsch, CC BY-SA 3.0, https://commons.wikimedia.org/w/index.php?curid=43874," 1996, July.

[41] "Brocken Inaglory/Wikimedia Commons. Grand Prismatic Spring and Midway Geyser Basin. By Brocken Inaglory, CC BY-SA 3.0, https://commons.wikimedia.org/w/index.php?curid=6051164," 2008, July.

[42] "Alexander Grebenkov/Wikimedia Commons. Mudpots at Hverarönd. By Alexander Grebenkov - Own work, CC BY 3.0, https://commons.wikimedia.org/w/index.php?curid=83641265," 2019, July.

[43] "Chmee2/Valtameri/Wikimedia Commons. Geothermal area Námafjall near Mývatn Lake, Iceland. Smoking fumarole. By Chmee2/Valtameri - Own work, CC BY 3.0, https://commons.wikimedia.org/w/index.php?curid=11306541," 2009, August.

[44] E. Barbier, "Geothermal energy technology and current status: an overview," *Renewable and Sustainable Energy Reviews,* vol. 6, no. 1-2, pp. 3-65, 2002. https://doi.org/10.1016/S1364-0321(02)00002-3.

[45] I. Johnston, G. Narsilio and S. Colls, "Emerging Geothermal Energy Technologies," *KSCE Journal of Civil Enginnering,* vol. 15(4), pp. 643-653, 2011.

[46] Y. He and X. Bu, "Performance of Hybrid Single Well Enhanced Geothermal System and Solar Energy for Buildings Heating," *Energies,* vol. 13, no. 10:2473, 2020. https://doi.org/10.3390/en13102473 .

[47] "U.S. Department of Energy. https://www.energy.gov/energysaver/heat-and-cool/heat-pump-systems/geothermal-heat-pumps".

[48] J. Lund and A. Toth, "Direct Utilization of Geothermal Energy 2020 Worldwide Review," in *Proceedings World Geothermal Congress 2020*, Reykjavik, Iceland, April 26 - May 2, 2020.

[49] "Goran tek-en/Wikimedia Commons. Diagram showing how electricity is generated in a vapor-dominated hydrothermal system. By Goran tek-en, CC BY-SA 4.0, https://commons.wikimedia.org/w/index.php?curid=31077637," 2014, February.

[50] "Goran tek-en/Wikimedia Commons. Diagram showing how electricity is generated from a hot-water hydrothermal system. By Goran tek-en, CC BY-SA 4.0, https://commons.wikimedia.org/w/index.php?curid=31077638," 2014, February.

[51] "Geothermal Binary System. By Rehman Abubakr - Own workThis file was derived from:Diagram HotWaterGeothermal inturperated version.svgGeothermal Binary

System.svgPower line.svg, CC BY-SA 4.0, https://commons.wikimedia.org/w/index.php?curid=73221609," 2018, September.

[52] "The Three Gorges Dam on the Yangtze River, China. By Source file: Le Grand Portage Derivative work: Rehman - File:Three_Gorges_Dam,_Yangtze_River,_China.jpg, CC BY 2.0, https://commons.wikimedia.org/w/index.php?curid=11425004," 2009, September 20.

[53] "Schematic diagram of Hydroelectric power plant. By Tennessee Valley Authority; SVG version by Tomia - This file was derived from: Hydroelectric dam.png, CC BY-SA 3.0, https://commons.wikimedia.org/w/index.php?curid=3302749," 2000, August 18.

[54] "Bureau of Reclamation. https://www.usbr.gov/lc/hooverdam/".

[55] P. Nikolaidis and A. Poullikkas, "A comparative review of electrical energy storage systems for better sustainability," *Journal of Power Technologies, [S.I.],* vol. 97, no. 3, pp. 220-245, November 2017. ISSN 2083-4195. Available at: https://papers.itc.pw.edu.pl/index.php/JPT/article/view/1096. Date accessed: 07 apr. 2021.

[56] "Sirbatch/Wikimedia Commons. Castaic Power Plant Front. By Sirbatch at English Wikipedia, CC BY-SA 3.0, https://commons.wikimedia.org/w/index.php?curid=86486796," 2011, April 12.

[57] A. Ali, S. Algburi and M. Aljaradin, "Design Optimization of A Hybrid Hydro-Wind Micropower System for Rural Communities," *Journal of Engineering and Sustainable Development,* vol. 22, no. 2 (Part-5), March 2018. ISSN 2520-0917. doi:10.31272/jeasd.2018.2.62.

[58] "By U.S. Army Corps of Engineers, photographer unknown - U.S. Army Corps of Engineers Digital Visual LibraryImage pageImage description pageDigital Visual Library home page, Public Domain, https://commons.wikimedia.org/w/index.php?curid=1896635".

[59] "Emoscopes/Wikimedia Commons. Schematic diagram summarising the differences between impulse and reaction turbines. By Emoscopes - Own work, drawn using XaraX, CC BY-SA 3.0, https://commons.wikimedia.org/w/index.php?curid=595228," 2006, February.

[60] "Zedh/Wikimedia Commons. 40kW pelton turbine - wheel. By Zedh - Own work, CC BY-SA 3.0, https://commons.wikimedia.org/w/index.php?curid=4951423," 2008, October 8.

[61] "Stahlkocher/Wikimedia Commons. Francis Turbine with Generator. By Original uploader was Stahlkocher - Originally from the English Wikipedia, CC BY-SA 3.0, https://commons.wikimedia.org/w/index.php?curid=939928," 2004, March.

[62] M. Pidwirny, "Surface and Subsurface Ocean Currents: Ocean Current Map. Fundamentals of Physical Geography, 2nd Edition. Date viewed: 8 April 2021. http://www.physicalgeography.net/fundamentals/8q_1.html," 2006.

[63] "Ingvald Straume/Wikimedia Commons. World map showing wave energy flux in kW per meter wave front. By Ingvald Straume - Own work, CC0, https://commons.wikimedia.org/w/index.php?curid=31768763," 2014, March.

[64] "Aquatic Renewable Energy Technologies (Aqua-RET). www.aquaret.com".

[65] "P123/Wikimedia Commons. Pelamis Wave Energy Converter on site at the European Marine Energy Test Centre (EMEC). By P123 - Own work, Public Domain, https://commons.wikimedia.org/w/index.php?curid=4859717," 2008, September 25.

[66] "Arne Müseler/Wikimedia Commons. Photo: Arne Müseler / arne-mueseler.com / CC-BY-SA-3.0 / https://creativecommons.org/licenses/by-sa/3.0/de/deed.de. https://commons.wikimedia.org/w/index.php?curid=89012888".

[67] "Tswgb/Wikimedia Commons. Aerial view of the tidal barrage on the Rance and of Saint Malo. By Tswgb - Own work, Public Domain, https://commons.wikimedia.org/w/index.php?curid=3182853," 2007, June.

[68] "U.S. Energy Information Administration. Source: Adapted from National Energy Education Development Project (Public Domain). https://www.eia.gov/energyexplained/hydropower/tidal-power.php".

[69] "Alternative Energy Tutorials. https://www.alternative-energy-tutorials.com/tidal-energy/tidal-barrage.html".

[70] "By Original uploaded by StefKa81 (Transfered by Obersachse) - Original uploaded on de.wikipedia; http://www.nrel.gov/otec/, Public Domain, https://commons.wikimedia.org/w/index.php?curid=12766111".

[71] M. Cusano, Q. Li, A. Obisesan, J. Urrego-Blanco and T. Wong, "Coastal City and Ocean Renewable Energy: Pathway to an Eco-San Andres," in *LRF Collegium 2013 Series, Volume 3, University of Southampton 2013*.

[72] "Sectional view of a flywheel storage. By Pjrensburg - a rendering from a solid-works model, edited to include labels, in png formatPreviously published: 2012-04-29, CC BY-SA 3.0, https://commons.wikimedia.org/w/index.php?curid=19258681," 2012, July.

[73] Z. Qi and G. M. J. Koening, "Review Article: Flow Battery Systems with Solid Electroactive Materials," *Journal of Vacuum Science & Technology B,* Vols. 35, 040801, 2017. https://doi.org/10.1116/1.4983210.

[74] "Kelvinsong/Wikimedia Commons. Diagram of the Sun. By Kelvinsong - Own work, CC BY-SA 3.0, https://commons.wikimedia.org/w/index.php?curid=23371669," Astrophysics and Space Science Library, Vol.294 (Dordrecht: Kluwer), 2012, December 27.

[75] "Nick84/Wikimedia Commons. Spectrum of solar radiation at sea level (red) and out of the atmosphere (yellow). By Nick84 - File:Solar_spectrum_ita.svg, CC BY-SA 3.0, https://commons.wikimedia.org/w/index.php?curid=24648395," 2013, February 14.

[76] J. Fieducik, "The use of solar radiation for generating heat in a solar air collector in northern Poland," in *E3S Web of Conferences 100, 00016. doi:10.1051/e3sconf/201910000016*, 2019.

[77] M. Hassane Babikir, D. Njomo, M. Barka, M. Khayal, D. Goron, V. Chara-Dackou, T. Martial, D. Kamta Legue and J. E. N. Gram-shou, "Modeling the Incident Solar Radiation of the City of N'Djamena (Chad) by the Capderou Method," *International Journal of Photoenergy,* Vols. 2020. Article ID 6292147, 10 pages, 2020. https://doi.org/10.1155/2020/6292147.

[78] "ITACA. https://www.itacanet.org/the-sun-as-a-source-of-energy/part-1-solar-astronomy/," http://www.powerfromthesun.net/book.html.

[79] M. Cengiz and M. Mamiş, "A research on determining the panel inclination angle in terms of the place and seasons," *Journal of Multidisciplinary Engineering Science and Technology (JMEST),* vol. 2(8), 2015.

[80] H. Ennaceri and K. Loudiyi, "Modeling the variation of optimum tilt angles for flat-plate solar collectors in Ifrane, Morocco," in *International Renewable and Sustainable Energy Conference (IRSEC)*, 2013, pp. 106-111.

[81] K. Mertens, Photovoltaics. Fundamentals, Technology and Practice, Wiley, 2014.

[82] "JabberWok at English Wikipedia. A vector graphic similar of an image originally created by User:PAR, of the Bohr model. By JabberWok, CC BY-SA 3.0, https://commons.wikimedia.org/w/index.php?curid=2639910," 2007, February 23.

[83] S. Mitridis, "Determination of lattice site location of impurities in compound semiconductors, by transmission electron microscopy. Physics of Advanced Materials Winter School 2008," 2011.

[84] "TheNoise/Wikimedia Commons. A p-n junction in thermal equilibrium with zero voltage applied. By TheNoise at English Wikipedia, CC BY-SA 3.0, https://commons.wikimedia.org/w/index.php?curid=3833411," 2007, August.

[85] S. Greg, "Intersubband approach to silicon based lasers-circumventing the indirect bandgap limitation," *Advances in Optics and Photonics,* vol. 3, no. 1, pp. 53-87, 2011. https://doi.org/10.1364/AOP.3.000053.

[86] G. Fisher, M. Seacrist and R. Standley, "Silicon Crystal Growth and Wafer Technologies," in *Proceedings of the IEEE. 100. 1454-1474. 10.1109/JPROC.2012.2189786*, 2012.

[87] "Twisp/Wikimedia Commons. Czochralski process, silicon monocrystal fabrication. By Twisp - Own work, This W3C-unspecified vector image was created with Inkscape ., Public Domain, https://commons.wikimedia.org/w/index.php?curid=3416042," 2008, January 18.

[88] Siltronic, "https://www.siltronic.com/en/products.html".

[89] N. Drouiche, P. Cuellar, F. Kerkar, S. Medjahed, N. Boutouchent-Guerfi and M. Hamou, "Recovery of solar grade silicon from kerf loss slurry waste," *Renewable and Sustainable Energy Reviews,* vol. 32, pp. 936-943, 2014.

[90] "OSAKA FUJI Corporation. https://www.ofic.co.jp/en/r_and_d/slicing/".

[91] G. Gaspar, A. Autruffe and J. Pó, "Silicon Growth Technologies for PV Applications," in *New Research on Silicon - Structure, Properties, Technology. Ch 9*, Talanin, Vitalyi Igorevich, Ed.: doi:10.5772/intechopen.68351, 2017.

[92] G. Hahn, S. Seren, M. Kaes, A. Schonecker, J. Kalejs, C. Dube, A. Grenko and C. Belouet, "Review on Ribbon Silicon Techniques for Cost Reduction in PV," in *2006 IEEE 4th World Conference on Photovoltaic Energy Conference*, Waikoloa, HI, USA, 2006. pp. 972-975. doi: 10.1109/WCPEC.2006.279280.

[93] "Klaus Mueller/Wikimedia Commons. Comparison of crystalline solar cells. By Klaus Mueller - This image is a cutout of an image by Klaus Mueller, CC BY-SA 3.0, https://commons.wikimedia.org/w/index.php?curid=34948067," 2014, August 25.

[94] "Intelligent Solar. http://intelligentsolar.eu/tailored-modules/".

[95] I. Benigno and D. Darminto, "Effect of intrinsic layer energy gap and thicknesses optimization on the efficiency of p-i-n amorphous silicon solar cell," *IPTEK, Journal of Science,* vol. 2 (3), 2017.

[96] M. Fraga, R. Pessoa, H. Maciel and M. Massi, "Recent developments on silicon carbide thin films for piezoresistive sensors applications," in *Silicon Carbide - Materials, Processing and Applications in Electronic Devices*, Intech, 2011, pp. 369-388.

[97] V. Avrutin, N. Izyumskaya and Morkoç, "Amorphous and micromorph Si solar cells: current status and outlook," *Turkish Journal of Physics,* vol. 38, pp. 526-542, 2014.

[98] Mse395chris, "Cross-section of a CdTe thin film solar cell. Based on Chopra et al., Progress in Photovoltaics 2004, 12, 69-92. By Mse395chris - Own work, CC BY-SA 3.0, https://commons.wikimedia.org/w/index.php?curid=6877299," 2009, May 27.

[99] "DS New Energy. https://www.dsneg.com/info/cigs-solar-cell-technology-32692187.html".

[100] "Tem5psu/Wikimedia Commons. Schematic cross-section of a HIT solar cell. By Tem5psu, CC BY-SA 4.0, https://commons.wikimedia.org/w/index.php?curid=38904169," BS Publications, 2015, March 13.

[101] I. Mathews, D. O'Mahony, K. Thomas, E. Pelucchi, B. Corbett and A. Morrison, "Adhesive bonding for mechanically stacked solar cells," *Progress in Photovoltaics: Research and Applications,* vol. 23, pp. 1080-1090, 2015.

[102] "Wavelength Electronics. https://www.teamwavelength.com/photodiode-basics/".

[103] J. Cubas, S. Pindado and C. de Manuel, "Explicit Expressions for Solar Panel Equivalent Circuit Parameters Based on Analytical Formulation and the Lambert W-Function," *Energies,* vol. 7, pp. 4098-4115, 2014.

[104] J. Kadhum, "Design and Construction of a Tracking Devide for Solar Electrical Systems," *Journal of Scientific and Engineering Research,* vol. 5(7), pp. 225-236, 2018.

[105] M.-H. Wang and M.-J. Chen, "Two-Stage Fault Diagnosis Method Based on the Extension Theory for PV Power Systems," *International Journal of Photoenergy,* Vols. 2012, Article ID 892690, 10 pages, 2012. https://doi.org/10.1155/2012/892690.

[106] V. Franzitta, A. Orioli and A. Di Gangi, "Assessment of the usability and accuracy of the simplified one-diode models for photovoltaic modules," *Energies,* Vols. 9,1019, 2016.

[107] "Squirmymcphee/Wikimedia Commons. Solar cell I-V curve as a function of specific shunt resistance. By Squirmymcphee - Own work, CC BY-SA 3.0, https://commons.wikimedia.org/w/index.php?curid=5025975," 2008, October.

[108] C. Honsberg and S. Bowden, "Photovoltaics Education Website. www.pveducation.org," 2019.

[109] C. Chellaswamy and R. Ramesh, "An optimal parameter extraction and crack identification method for solar photovoltaic modules," *ARPN Journal of Engineering and Applied Sciences,* vol. 11(24), 2016.

[110] Y. Atia, "Photovoltaic maximum power point tracking using SEPIC converter," *Engineering Research Journal. Faculty of Engineering, Minoufiya University,* vol. 32(4), 2009.

[111] A. Smets, K. Jäger, O. Isabella, R. Van Swaaij and M. Zeman, Solar Energy - The physics and engineering of photovoltaic conversion, technologies and systems, UIT Cambridge, 2016.

[112] E. Kabalci, A. Boyar and Y. Kabalci, "Design and analysis of a micro inverter for PV plants," in *9th International Conference on Electronics, Computers and Artificial Intelligence (ECAI)*, Targoviste, Romania, 29 June-01 July, 2017.

[113] H. Luo, H. Wen, X. Li and Y. Hu, "Synchronous buck converter based low-cost and high-efficiency sub-module DMPPT PV system under partial shading conditions," *Energy Conversion and Management,* vol. 126, pp. 473-487, 2016.

[114] "Electrical Equipment. http://engineering.electrical-equipment.org/electrical-distribution/cascaded-h-bridge-multilevel-inverters.html".

[115] S. Frame, S. Dubovsky, Q. Li, D. Katsis, C. Cuadros, D. Borojevic and F. Lee, "Three-phase soft-switching inverters for electric vehicle applications. 1995 VPEC seminar proceedings".

[116] M. Hannan, M. Hoque, A. Mohamed and A. Ayob, "Review of energy storage systems for electric vehicle applications: Issues and challenges," *Renewable and Sustainable Energy Reviews,* vol. 69, pp. 771-789, 2017.

[117] H. Ullah, Implementation of charge controller & inverter for a solar panel, Lambert Academic Publishing, 2012.

[118] "Alternative Energy Tutorials. https://www.alternative-energy-tutorials.com/category/solar-power".

[119] "International Energy Agency. A user guide to simple monitoring and sustainable operation of PV-diesel hybrid systems. Report IEA-PVPS T9-16: 2015".

[120] M. El-Raouf, M. Mosaad, M. Al-Ahmar and F. El Bendary, "MPPT of hybrid solar-wind-grid power generation system," *International Journal of Industrial Electronics and Drives,* vol. 2(40), 2015.

[121] Energypedia, "SHS Cuzco. https://energypedia.info/wiki/File:SHSCuzco.jpg," 2013, November 11.

[122] M. Rhaman, "A remarkable cost-effective solar home system in rural area of Bangladesh," *Current Alternative Energy,* vol. 2, pp. 37-41, 2018.

[123] N. Pearsall, The Performance of Photovoltaic (PV) Systems: Modelling, Measurement and Assessment, Woodhead Publishing Series in Energy, 2016.

[124] M. Abu-Aligah, "Design of photovoltaic water pumping system and compare it with diesel powered pump," *Jordan Journal of Mechanical and Industrial Engineering,* vol. 5(3), pp. 273-280, 2011.

[125] NASA, "Solar-Powered Refrigeration System. https://www.nasa.gov/centers/johnson/techtransfer/technology/MSC-22970-1_Solar-Refrigerator-TOP.html," 2011, August 2.

[126] "IRENA (2020), Renewable Power Generation Costs in 2019. International Renewable Energy Agency, Abu Dhabi".

[127] "Fraka/Wikimedia Commons. Levelized cost of electricity generation for Germany in EuroCent/kWh, source: Fraunhofer ISE, March 2018. By FraKa - Own work, CC BY-SA 4.0, https://commons.wikimedia.org/w/index.php?curid=68116717," 2018, April 7.

[128] K. Chumpolrat, V. Sangsuwan, N. Udomdachanut, S. Kittisontirak, S. Songtrai, P. Chinnavornrungsee, A. Limmanee, J. Sritharathikhun and K. Sriprapha, "Effect of Ambient Temperature on Performance of Grid- Connected Inverter Installed in Thailand," *International Journal of Photoenergy,* Vols. 2014, Article ID 502628, 6 pages, 2014. https://doi.org/10.1155/2014/502628.

[129] "Homer Energy. https://www.homerenergy.com/products/pro/docs/latest/pv_temperature_coefficient_of_power.html".

[130] B. Elias, S. AlSadoon and S. Abdulgafar, "Modeling and Simulation of Photovoltaic Module Considering and Ideal Solar Cell," *International Journal of Advanced Research in Physical Science (IJARPS),* vol. 1, no. 3, pp. 9-18, 2014. ISSN 2349-7874 (Print) & ISSN 2349-7882 (Online). www.arcjournals.org.

[131] B. Pannebakker, A. de Waal and W. van Sark, "Photovoltaics in the shade: one bypass diode per solar cell revisited," *Progress in Photovoltaics: Research and Applications,* vol. 25, pp. 836-849, 2017.

[132] B. Alsayid, S. Alsadi, J. Jallad and M. Dradi, "Partial Shading of PV System Simulation with Experimental Results," *Smart Grid and Renewable Energy,* vol. 4, no. 6, pp. 429-435, 2013. doi: 10.4236/sgre.2013.46049.

[133] M. El-Shobokshy and F. Husein, "Effect of the dust with different physical properties on the performance of photovoltaic cells," *Solar Energy,* vol. 51(6), pp. 505-511, 1993.

[134] N. Al-Rousan, N. Mat Isa and M. Mat Desa, "Advances in solar photovoltaic tracking systems: A review," *Renewable and Sustainable Energy Reviews,* vol. 82, no. 3, pp. 2548-2569, 2018. https://doi.org/10.1016/j.rser.2017.09.077.

[135] S. Seme, B. Štumberger, M. Hadžiselimovic and K. Sredenšek, "Solar photovoltaic tracking systems for electricity generation: a review," *Energies,* vol. 13, p. 4224, 2020.

[136] K. Jeong, T. Hong, C. Koo, J. Oh, M. Lee and J. Kim, "A prototype design and development of the smart photovoltaic system blind considering the photovoltaic panel, tracking system, and monitoring system," *Applied Sciences,* vol. 7, p. 1077, 2017.

[137] K. Lovegrove and J. Pye, "Fundamental principles of concentrating solar power systems," in *Concentrating Solar Power Technology, Principles, Developments, and Applications. Second edition. Ch 2*, Lovegrove, K; Stein, W, Eds., 2020.

[138] D. Mills and G. Morrison, "Compact linear Fresnel reflector solar thermal powerplants," *Solar Energy,* vol. 68, no. 3, pp. 263-283, 2000.

[139] D. Baharoon, H. Rahman, W. Wan Omar and S. Fadhl, "Historical development of concentrating solar power technologies to generate clean electricity efficiently - A review," *Renewable and Sustainable Energy Reviews,* vol. 41, pp. 996-1027, 2015.

[140] Y. Yohanis, O. Popel, S. Frid and B. Norton, "Geographic variation of solar water heater performance in Europe," *Proceedings of the Institution of Mechanical Engineers, Part A, Journal of Power and Energy,* vol. 220, pp. 395-407, 2006.

[141] A. Adeyanju, "Thermal energy storage techniques," *Sci-Afric Journal of Scientific Issues, Research and Essays,* vol. 3(5), pp. 726-736, 2015.

[142] I. Sarbu and C. Sebarchievici, "Thermal Energy Storage," in *Solar Heating and Cooling Systems. Ch 4*, 2017, pp. 99-138.

[143] S. Kuravi, Y. Goswami, E. Stefanakos, M. Ram, C. Jotshi, S. Pendyala, J. Trahan, P. Sridharan, M. Rahman and B. Krakow, "Thermal energy storage for concentrating solar power plants," *Technology and Innovation,* vol. 14, pp. 81-91, 2012.

[144] U. Herrmann, B. Kelly and H. Price, "Two-tank molten salt storage for parabolic trough solar power plants," *Energy,* vol. 29, no. 5-6, pp. 883-893, 2004. https://doi.org/10.1016/S0360-5442(03)00193-2.

[145] G. Angelini, A. Lucchini and G. Manzolini, "Comparison of thermocline molten salt storage performances to commercial two-tank configuration," *Energy Procedia,* vol. 49, pp. 694-704, 2014.

[146] Z. Wang, Z. Huang, S. Zheng and X. Zhao, "Solar Water Heaters," in *A comprehensive guide to solar energy systems, with special focus on photovoltaic systems. Ch 6*, 2018, pp. 111-125.

[147] "U.S. Department of Energy. Batch solar thermal collectorColour. By USA Dept Energy - Existing graphics on Creative Commons, Public Domain, https://commons.wikimedia.org/w/index.php?curid=10513563," 2010, February 6.

[148] GreenRiverside, "http://www.energydepot.com/RPUres/library/Swaterheater.asp".

[149] "Sustainable Sources LLC. https://sustainablesources.com/energy/solar-hot-water-heating-and-cooling-systems/#ACTIVEDHW".

[150] M. Abdunnabi, I. Rohuma, E. Endya and E. Belal, "Review on solar water heating in Libya," *Solar Energy and Sustainable Development,* vol. 7, pp. 1-28, 2018.

[151] "Alternative Energy Tutorials. https://www.alternative-energy-tutorials.com/solar-hot-water/evacuated-tube-collector.html".

[152] "Centralamerica/Wikimedia Commons. Comparison between a Solar Parabolic Concentrator and a Non-imaging Compound Parabolic Concentrator. By

Centralamerica - Own work, CC BY-SA 3.0, https://commons.wikimedia.org/w/index.php?curid=9092820," 2010, January 27.

[153] "The World Bank, Source: Global Solar Atlas 2.0, Solar resource data: Solargis. https://solargis.com/maps-and-gis-data/download/world," 2019.

[154] "Solar Energy Industries Association (SEIA). http://www.seia.org/policy/power-plant-development/utility-scale-solar-power/water-use-management".

[155] O. Behar, D. Sbarbado and L. Moran, "Which is the most competitive solar power technology for integration into the existing copper mining plants: Phtovoltaic (PV), Concentrating Solar Power (CSP), or hybrid PV-CSP?," *Journal of Cleaner Production,* vol. 287, 2021. https://doi.org/10.1016/j.jclepro.2020.125455.

[156] REN21, "Renewables 2020 Global Status Report," REN21 Secretariat, Paris, 2020.

[157] NationalElectricPowerCompany_(NEPCO), "Annual Reports," http://www.nepco.com.jo, 2018.

[158] "Ministry of Energy and Mineral Resources (MEMR). Renewable Energy & Energy Efficiency Law," 2018. [Online].

[159] J. Jaber, E. Fawwaz, A. Emil and K. Anagnostopoulos, "Employment of renewable energy in Jordan: Current status, SWOT and problem analysis," *Renewable and Sustainable Energy Reviews,* vol. 49, pp. 490-499, 2015.

[160] M. A. El-Sharkawi, Wind Energy: An Introduction, CRC Press, 2016.

[161] S. R. Joshua Earnest, Wind Power Technology, PHI Learning, 2019.

[162] K. Mertens, Photovoltaics: fundamentals, technology, and practice, John Wiley & Sons, 2018.

[163] Electrical4U, "Electrical4U," 2020. [Online]. Available: https://www.electrical4u.com/basic-construction-of-wind-turbine/. [Accessed 9 3 2021].

[164] GE, "GE Renewable Energy," GE , 2021. [Online]. Available: https://www.ge.com/renewableenergy/wind-energy/offshore-wind/haliade-x-offshore-turbine. [Accessed 09 03 2021].

[165] M. A. El-Sharkawi, Electric Energy: An Introduction, Third Edition, CRC Press, 2012.

[166] J. F. Manwell, J. G. McGowan and A. L. Rogers, Wind Energy Explained: Theory, Design and Application, Wiley, 2010.

[167] S. N. Singh, Non Conventional Energy Resources, Pearson Education India, 2017.

[168] M. P. Kazmierkowski, R. Krishnan, F. Blaabjerg and J. D. Irwin, Control in Power Electronics_ Selected Problems, Academic Press Series in Engineering, 2002.

[169] J. O. A.K. Wallace, "Variable-Speed Generation Controlled by Passive Elements," in *Proc. of ICEM 98*, 1998.

[170] L. Hansen, P. Madsen, F. Blaabjerg, H. Christensen, U.Lindhard and K. Eskildsen, "Generators and power electronics technology for wind turbines," in *Proc. of IECON '01*, 2001.

[171] D. C. Aliprantis, "Fundamentals of Wind Energy Conversion for Electrical Engineers," 2014. [Online]. Available: https://engineering.purdue.edu/~dionysis/EE452/Lab9/Wind_Energy_Conversion.pdf. [Accessed 25 8 2020].

[172] L. L. Grigsby, The Electric Power Engineering Handbook, 3 ed., vol. 5, CRC Press, 2012.

[173] M. Grossi, M. Monim and A. Gangopadhyay, "Global Climate Patterns: An overview of Arctic oscillation, Pacific decadal oscillation, Pacific/North American pattern, and El Nino Southern oscillation," School for Marine Science & Technology, University of Massachusetts Dartmouth. Technical Report SMAST-17-0401, April 2017. doi:10.13140/RG.2.2.34586.44480.

[174] T. Soukissian, A. Papadopoulos, P. Skrimizeas, F. Karathanasi, P. Axaopoulos, E. Avgoustoglou, H. Kyriakidou, C. Tsalis, A. Voudouri, F. Gofa and P. Katsafados, "Assessment of offshore wind power potential in the Aegean and Ionian Seas based on high-resolution hindcast model results," *AIMS Energy,* vol. 5, no. 2, pp. 268-289, 2017. doi:10.3934/energy.2017.2.268.

[175] "U.S. Energy Information Administration. Forms EIA-860 and EIA-923. https://www.eia.gov/todayinenergy/detail.php?id=20112 (February 25, 2015)".

[176] "National Renewable Energy Laboratory. Golden, Colorado. https://www.nrel.gov/gis/wind.html".

[177] K. Fischer and D. Coronado, "Condition monitoring of wind turbines: State of the art, user experience and recommendations," *VGB PowerTech,* vol. 7, 2015.

[178] "Office of Energy Efficiency & Renewable Energy. U.S. Department of Energy. The inside of a Wind Turbine. https://www.energy.gov/eere/wind/inside-wind-turbine".

[179] P. Tchakoua, R. Wamkeue, M. Ouhrouche, F. Slaoui-Hasnaoui and T. E. G. Tameghe, "Win Turbine Condition Monitoring: State-of-the-Art Review, New Trends, and Future Challenges," *Energies,* vol. 7, no. 4, pp. 2595-2630, 2014. https://doi.org/10.3390/en7042595.

[180] M. Ahmed and Y.-C. Kim, "Hybrid Communication Network Architectures for Monitoring Large-Scale Wind Turbine," *Journal of Electrical Engineering and Technology,* vol. 8, no. 6, pp. 1626-1636, 2013. http://dx.doi.org/10.5370/JEET.2013.8.6.1626 .

[181] "Walter Baxter/Wikimedia Commons. A turbine foundation at Toddleburn Wind Farm. By Walter Baxter, CC BY-SA 2.0, https://commons.wikimedia.org/w/index.php?curid=13961201," 2009, April 5.

[182] R. Wiser, Z. Yang, M. Hand, O. Hohmeyer, D. Infield, P. Jensen, V. Nikolaev, M. O'Malley, G. Sinden and A. Zervos, "Wind Energy. In IPCC Special Report on Renewable Energy Sources and Climate Change Mitigation. [O. Edenhofer, R. Pichs-Madruga, Y. Sokona, K. Seyboth, P. Matschoss, S. Kadner, T. Zwickel, P. Eickemeier, G. Hansen, S. Schlömer, C. von Stechow (eds)]," Cambridge University Press, Cambridge, United Kingdom and New York, NY, USA, 2011.

[183] W. Musial, R. Sheppard, D. Dolan and B. Naughton, "Development of offshore wind recommended practice for U.S. waters," in *Conference paper NREL/CP-5000-57880. Offshore Technology Conference, Houston, Texas, May 6-9, 2013*.

[184] Duane Emerson Roller and Duane H.D. Roller, The Development of the Concept of Electric Charge: Electricity from the Greeks to Coulomb, Cambridge: Harvard University Press, 1954.

[185] P. F. O'Grady, Thales of Miletus: The Beginnings of Western Science and Philosophy, 1 ed., Ashgate Publishing, 2002, p. 8.

[186] "Institute of Energy Research (IER)," 7 2020. [Online]. Available: https://www.instituteforenergyresearch.org/history-electricity/. [Accessed 27 7 2020].

[187] "Engineering Time Lines," 7 2020. [Online]. Available: http://www.engineering-timelines.com/how/electricity/electricity_05.asp. [Accessed 27 7 2020].

[188] R. E. Leposky, 7 2020. [Online]. Available: https://www.ecmag.com/section/your-business/brief-history-electricity. [Accessed 27 7 2020].

[189] A. Energy, 1 2020. [Online]. Available: https://www.aepenergy.com/2020/01/10/the-history-of-electricity/. [Accessed 27 7 2020].

[190] P. Wilkinson, 7 2020. [Online]. Available: https://www.rigb.org/our-history/iconic-objects/iconic-objects-list/faraday-generator. [Accessed 27 7 2020].

[191] É. Alglave, "Wikimedia Commons," 1884. [Online]. Available: https://commons.wikimedia.org/wiki/File:Faraday_disk_generator.jpg. [Accessed 17 4 2021].

[192] "US Nuclear Regulatory Commission (NRC.gov)," 7 2020. [Online]. Available: https://commons.wikimedia.org/wiki/File:Modern_Steam_Turbine_Generator.jpg. [Accessed 27 7 2020].

[193] "International Energy Agency (IEA)," 7 2020. [Online]. Available: https://www.iea.org/data-and-statistics?country=WORLD&fuel=Energy%20supply&indicator=Total%20primary%20energy%20supply%20(TPES)%20by%20source. [Accessed 27 7 2020].

[194] "U.S. Energy Information Administration (EIA)," 7 2020. [Online]. Available: https://www.eia.gov/. [Accessed 27 7 2020].

[195] "European Environment Agency (EEA)," 7 2020. [Online]. Available: https://www.eea.europa.eu/. [Accessed 27 7 2020].

[196] H. Editors, 7 2020. [Online]. Available: https://www.history.com/topics/industrial-revolution/industrial-revolution. [Accessed 27 7 2020].

[197] E. Topal and S. Shafiee, "An econometrics view of worldwide fossil fuel consumption and the role of US," *Energy Policy,* no. 36, p. 775–786, 2008.

[198] V. Smil, Energy in Nature and Society: General Energetics of Complex Systems, vol. 89, MIT Press, 2008.

[199] J. H. Brown and e. al, Energetic Limits to Economic Growth, vol. 61, 2011, pp. 19-26.

[200] J. E. Payne, "Survey of the international evidence on the causal relationship between energy consumption and growth," *Journal of Economic Studies,* vol. 37, no. 1, pp. 53-95, 2010.

[201] J. Brown and M. Moses, "Allometry of human fertility and energy use," *Blackwell Publishing Ltd; Ecology Letters,* no. 6, pp. 295-300, 2003.

[202] W. S. Thompson, "Population," *American Journal of Sociology,* no. 34, p. 959–975, 1929.

[203] "United States Department of Energy," 28 12 2008. [Online]. Available: https://en.wikipedia.org/wiki/File:Electricity_grid_simple-_North_America.svg. [Accessed 27 7 2020].

[204] Sivanagaraju, Power Systems Operation and Control, Pearson Education, 2009.

[205] A. J. Wood and B. F. Wollenberg, Power Generation, Operation and Control, John Wiley & Sons, 2012.

[206] E. Commission, 7 2020. [Online]. Available: https://ec.europa.eu/research/industrial_technologies/pdf/novel-materials-for-energy-applications_en.pdf. [Accessed 27 7 2020].

[207] "US Department of Energy," 2015. [Online]. Available: https://www.energy.gov/sites/prod/files/2016/04/f30/QTR2015-6B-Advanced-Materials-Manufacturing.pdf. [Accessed 27 7 2020].

[208] T. Gutowski and J. D. a. A. Thiriez, "Electrical Energy Requirements for Manufacturing Processes," in *13th CIRP International Conference of Life Cycle Engineering*, 2006.

[209] R. C. Bansal, "Optimization Methods for Electric Power Systems: An Overview," *International Journal of Emerging Electric Power Systems,* vol. 2, no. 1, 2020.

[210] H. Dong and T. Xiao-Jiao, "Review of Mathematical Methodology for Electric Power Optimization Problems," *Journal of the Operations Research Society of China,* vol. 8, p. 295–309, 2020.

[211] F. G. Montoya, A. G. Cruz, M. G. Montoya and F. M. Agugliaro, "Power quality techniques research worldwide: A review," *Renewable and Sustainable Energy Reviews,* no. 54, p. 846–856, 2016.

[212] A. Luo, Q. Xu, F. Ma and Y. Chen, "Overview of power quality analysis and control technology for the smart grid," *J. Mod. Power Syst. Clean Energy,* vol. 4, no. 1, pp. 1-9, 2016.

[213] S. Ioannou, E. K. Stefanakos and P. H. Wiley, "New MOV Failure Mode Identification Invention," *IEEE Transactions on Consumer Electronics,* vol. 53, no. 3, pp. 1068-1075, 2007.

[214] T. Simpson, 26 4 2008. [Online]. Available: https://commons.wikimedia.org/wiki/File:HunterPowerPlant.jpeg. [Accessed 27 7 2020].

[215] J. B. (Ebyabe), 18 2 2007. [Online]. Available: https://commons.wikimedia.org/wiki/File:Crystal_River_NPP02.jpg. [Accessed 27 7 2020].

[216] R. Clausen, 29 7 2017. [Online]. Available: https://commons.wikimedia.org/wiki/File:High_voltage_transmission_tower_and_lines._Auburn_WA.jpg. [Accessed 27 7 2020].

[217] R. H. (Henristosch), 3 7 2005. [Online]. Available: https://commons.wikimedia.org/wiki/File:Img0289SCE_500kV_lines_close.JPG. [Accessed 27 7 2020].

[218] G. Samorodov, S. Kandakov, S. Zilberman, T. Krasilnikova, M. C. Tavares, C. M. Jr. and Q. Li, "Technical and economic comparison between direct current and half-

wavelength transmission systems for very long distances," *IET Gener. Transm. Distrib.,* vol. 11, no. 11, pp. 2871-2878, 2017.

[219] L. M. Castroa, J. Tovar-Hernándezb, N. González-Cabrerac and J. Rodríguez-Rodrígueza, "Real-power economic dispatch of AC/DC power transmission systems comprising multiple VSC-HVDC equipment," *Elsevier Electrical Power and Energy Systems,* no. 107, pp. 140-148, 2019.

[220] D. Larruskain, I. Zamora, A. Mazón, O. Abarrategui and J. Monasterio, "Transmission and Distribution Networks: AC versus DC," 2005.

[221] H. E. Gelani, F. Dastgeer, K. Siraj, M. Nasir, K. A. K. Niazi and Y. Yang, "Efficiency Comparison of AC and DC Distribution Networks for Modern Residential Localities," *Appl. Sci.,* vol. 9, no. 582, 2019.

[222] H. Guo, "Survey of Three Gorges Power Grid (TGPG)," *Proc. 2000 IEEE Power Eng. Soc. Winter Meeting,* vol. 1, no. 3, 2000.

[223] M. P. Bahrman and B. K. Johnson, "The ABCs of HVDC Transmission Technologies," *IEEE Power and Energy Magazine 5,* vol. 1, no. 2, 2007.

[224] R. Rudervall, J. P. Charpentier and R. Sharma, "High Voltage Direct Current (HVDC) Transmission Systems," in *Energy Week 2000*, Washington D.C., 2000.

[225] Wdwd, 31 3 2011. [Online]. Available: https://commons.wikimedia.org/wiki/File:HVDC_HVAC_Diagram_Costs_over_Distance.svg. [Accessed 28 7 2020].

[226] Electropaedia, 2020. [Online]. Available: https://www.mpoweruk.com/fossil_fuels.htm. [Accessed 28 7 2020].

[227] C. Bill, 24 6 2004. [Online]. Available: https://commons.wikimedia.org/wiki/File:PowerStation3.svg. [Accessed 28 7 2020].

[228] "US Environmental Protection Agency," 2020. [Online]. Available: https://www.epa.gov/. [Accessed 28 7 2020].

[229] " Environment Directorate General of the European Commission ('DG Environment'),” 2020. [Online]. Available: https://ec.europa.eu/environment/basics/home_en.htm. [Accessed 28 7 2020].

[230] “International Carbon Action Partnership (ICAP),” 2007. [Online]. Available: https://icapcarbonaction.com/en/partnership/about. [Accessed 28 7 2020].

[231] E. Commission, “Climate Action – EU Emissions Trading System,” 2020. [Online]. Available: https://ec.europa.eu/clima/policies/ets_en. [Accessed 28 7 2020].

[232] “Bureau of Energy and Efficiency. Fuels and Combustion,” 2020. [Online]. Available: https://beeindia.gov.in/sites/default/files/2Ch1.pdf. [Accessed 28 7 2020].

[233] “Claverton Energy Research Group. The Energy and Fuel Data Sheet,” 2020. [Online]. Available: https://www.claverton-energy.com/wordpress/wp-content/uploads/2012/08/the_energy_and_fuel_data_sheet1.pdf. [Accessed 28 7 2020].

[234] “Corporate Finance Institute,” 7 2020. [Online]. Available: https://corporatefinanceinstitute.com/. [Accessed 28 7 2020].

[235] K. Branker, M. J. Pathak and J. M. Pearce, “A Review of Solar Photovoltaic Levelized Cost of Electricity,” *Renewable and Sustainable Energy Reviews,* no. 15, p. 4470–4482, 2011.

[236] R. Fu, D. Feldman and R. Margolis, 2018. [Online]. Available: https://www.nrel.gov/docs/fy19osti/72399.pdf. [Accessed 28 7 2020].

[237] “US Energy Information Administration,” 2020. [Online]. Available: https://www.eia.gov/outlooks/aeo/assumptions/pdf/table_8.2.pdf. [Accessed 28 7 2020].

[238] “Bloomberg New Energy Finance (BNEF),” 2020. [Online]. Available: https://about.bnef.com/. [Accessed 28 7 2020].

[239] "International Renewable Energy Agency (IRENA)," 2020. [Online]. Available: https://www.irena.org/. [Accessed 28 7 2020].

[240] Lazard, 2020. [Online]. Available: https://www.lazard.com/. [Accessed 28 7 2020].

[241] P. Breeze, "The Cost of Power Generation - The current and future competitiveness of renewable and traditional technologies," 2010.

[242] Eurostats, 7 2020. [Online]. Available: https://ec.europa.eu/eurostat/statistics-explained/index.php?title=File:Electricity_prices_for_household_consumers,_second_half_2. [Accessed 28 7 2020].

[243] E. Commission, 2020. [Online]. Available: https://ec.europa.eu/energy/sites/ener/files/epc_report_final_1.pdf. [Accessed 28 7 2020].

[244] P. A. Owusu and S. Asumadu-Sarkodie, "A review of renewable energy sources, sustainability issues and climate change mitigation," *Cogent Engineering,* no. 3, 2016.

[245] A. Qazi, F. Hussain, N. A. Rahim and e. al, "Towards Sustainable Energy: A Systematic Review of Renewable Energy Sources, Technologies, and Public Opinions," *IEEE Access,* vol. 7, p. 63837 – 63851, 2019.

[246] Y. Kuang, Y. Zhang, B. Zhou, C. Li, Y. Cao, L. Li and L. Zeng, "A review of renewable energy utilization in islands," *Renewable and Sustainable Energy Reviews,* vol. 59, p. 504–513, 2016.

[247] A. K. Aliyu, B. Modu and C. W. Tan, "A review of renewable energy development in Africa: A focus in South Africa, Egypt and Nigeria," *Renewable and Sustainable Energy Reviews,* 2020.

[248] M. A. Eltawi, Z. Zhengming and L. Yuan, "A review of renewable energy technologies integrated with desalination systems," *Renewable and Sustainable Energy Reviews,* vol. 13, p. 2245–2262, 2009.

[249] N. T. Raja, S. Iniyanb and R. Goic, "A review of renewable energy based cogeneration technologies," *Renewable and Sustainable Energy Reviews,* vol. 15, p. 3640–3648, 2011.

[250] J. Shen and C. Luo, "Overall review of renewable energy subsidy policies in China – Contradictions of intentions and effects," *Renewable and Sustainable Energy Reviews,* vol. 41, p. 1478–1488, 2015.

[251] W. Wilknson, "Environmental impact of electricity generation," *Trans. Roy. Soc. S. Afr.,* vol. 56, no. 2, pp. 131-133, 2001.

[252] U. E. I. Administration, 2018. [Online]. Available: https://www.eia.gov/todayinenergy/detail.php?id=4190. [Accessed 28 7 2020].

[253] C. T. S. Operator, 2020. [Online]. Available: https://tsoc.org.cy/general/. [Accessed 28 7 2020].

[254] D. P. Le, D. M. Bui, C. C. Ngo and A. M. T. Le, "FLISR Approach for Smart Distribution Networks Using E-Terra Software—A Case Study," *Energies,* vol. 11, no. 3333, 2018.

[255] R. A. Spalding and e. al, "Fault Location, Isolation and Service Restoration (FLISR) Functionalities Tests in a Smart Grids Laboratory for Evaluation of the Quality of Service," in *IEEE 17th International Conference on Harmonics and Quality of Power (ICHQP)*, 2016.

[256] J. D. Taft, "Electric Grid Resilience and Reliability for Grid Architecture," 2017.

[257] P. Kundur and e. al, "Definition and Classification of Power System Stability," *IEEE Transactions on Power Systems,* vol. 19, no. 2, pp. 1387-1401, 2004.

[258] Q. Wu, Z. Xu and J. Østergaard, "Grid Integration Issues for Large Scale Wind Power Plants (WPPs)," *IEEE Power and Energy Society General Meeting,* vol. 10, no. 109, 2010.

[259] R. Leão, T. Degner and F. Antunes, "An Overview on the Integration of Large-Scale Wind Power, Into the Electric Power System," *Renewable Energies and Power Quality Journal (REPQJ),* vol. 1, no. 5, pp. 572-579, 2007.

[260] D. Lew and e. al, "The Western Wind and Solar Integration Study Phase 2," 2010.

[261] L. Bird, M. Milligan and D. Lew, "Integrating Variable Renewable Energy: Challenges and Solutions," 2013.

[262] A. S. Anees, "Grid Integration of Renewable Energy Sources: Challenges, Issues and Possible Solutions," in *IEEE 5th India International Conference on Power Electronics (IICPE)*, 2012.

[263] X. Liang and C. A. B. Karim, "Harmonics and Mitigation Techniques through Advanced Control in Grid-Connected Renewable Energy Sources: A Review," *IEEE Transactions on Industry Applications,* vol. 54, no. 4, pp. 3100-3111, 2018.

[264] A. Chidurala, T. K. Saha, N. Mithulananthan and R. C. Bansal, "Harmonic emissions in grid PV systems: A case study on a large scale rooftop PV site," in *IEEE PES General Meeting, Conference & Exposition*, 2014.

[265] X. Liang, "Emerging power quality challenges due to integration of renewable energy sources," *IEEE Trans. Industry Applications,* vol. 53, no. 2, pp. 855-866, 2017.

[266] D. Ronanki, P. H. Sang, V. Sood and S. S. Williamson, "Comparative assessment of three-phase transformerless grid-connected solar inverters," in *IEEE International Conference on Industrial Technology (ICIT)*, 2017.

[267] IEEE and I. S. 519-2014, *IEEE Recommended Practice and Requirements for Harmonic Control in Electric Power Systems,* 2014.

[268] M. Z. Jacobson and V. Jadhav, "World estimates of PV optimal tilt angles and ratios of sunlight incident upon tilted and tracked PV panels relative to horizontal panels," *Solar Energy,* vol. 169, pp. 55-66, 2018.

[269] P. Eser, N. Chokani and R. S. Abhari, "Optimal RES portfolio to achieve 45% renewable electricity in central Europe by 2030," *IEEE Power & Energy Society General Meeting (PESGM),* 2017.

[270] S. Ioannou, M. C. Argyrou, M. Darwish and C. C. Marouchos, "Modulation Processes in Power Electronic Converters," in *55th International Universities Power Engineering Conference (UPEC 2020)*, 2020.

[271] I. Colak, E. Kabalci and R. Bayindir, "Review of multilevel voltage inverter topologies and control schemes," *Energy Conversion And Management,* vol. 52, pp. 1114-1128, 2011.

[272] A. Aktaibi, M. A. Rahman and A. Razali, "A Critical Review of Modulation Techniques," in *IEEE 19th Annual Newfoundland Electrical and Computer Eng. Conference (NECEC 2010)*, 2010.

[273] M. U.Bopche and P. V. Kapoor, "Comparative Analysis of Modulating Technique in Three Level Cascaded H-Bridge Inverter," in *International Conference on Smart Electric Drives & Power System*, 2018.

[274] S. Ioannou, M. C. Argyrou, C. Marouchos and M. Darwish, "Efficiency Investigation of a Grid Connected PV System with Power Smoothing," in *54th International Universities Power Engineering Conference (UPEC19)*, Romania, 2019.

[275] S. Ioannou, C. Marouchos, M. Darwish and G. A. Putrus, "Efficiency Investigation of A Protection and Correction Solid State Device for Low-Voltage Distribution Networks," in *54th International Universities Power Engineering Conference (UPEC19)*, Romania, 2019.

[276] M. AlMuhaini, "Impact of Distributed Generation Integration on the Reliability of Power Distribution Systems," in *Distributed Generation Systems*, Butterworth-Heinemann, 2017, pp. 453-508.

[277] Y. Menchafou, H. E. Markhi, M. Zahri and M. Habibi, “Impact of distributed generation integration in electric power distribution systems on fault location methods,” in *IEEE 3rd International Renewable and Sustainable Energy Conference (IRSEC)*, 2015.

[278] A. Tsikalakis and N. Hatziargyriou, “Environmental benefits of distributed generation with and without emissions trading,” *Energy Policy,* vol. 35, p. 3395–3409, 2007.

[279] R. Lasseter and e. al, “White Paper on Integration of Distributed Energy Resources - The MicroGrid Concept,” CA, 2002.

[280] N. Puga and e. al, “The Importance of Combined Cycle Generating Plants in Integrating Large Levels of Wind Power Generation,” *The Electricity Journal,* vol. 23, no. 7, pp. 33-44, 2010.

[281] G. Bakos, “Distributed power generation: A case study of small scale PV power plant in Greece,” *Applied Energy,* vol. 86, p. 1757–1766, 2009.

[282] N. I. Meyer, “Distributed generation and the problematic deregulation of energy markets in Europe,” *International Journal of Sustainable Energy,* vol. 23, no. 4, pp. 217-221, 2003.

[283] M. Dicorato, G. Forte and M. Trovato, “Environmental-constrained energy planning using energy-efficiency and distributed-generation facilities,” *Renewable Energy,* vol. 33, p. 1297–1313, 2008.

[284] I. Power and E. S. Resources. [Online]. Available: https://site.ieee.org/pes-testfeeders/resources/. [Accessed 28 7 2020].

[285] M. Bison, 7 3 2010. [Online]. Available: https://commons.wikimedia.org/wiki/File:Electricity_Grid_Schematic_English.svg . [Accessed 28 7 2020].

[286] R. Abhari and E. S. C. (.-E. Zurich, 2020. [Online]. Available: https://www.spotlight-esc.ethz.ch/2017/11/17/optimal-renewables-portfolio-to-achieve-45-renewable-electricity-in-central-europe-by-2030/. [Accessed 29 7 2020].

[287] C. J. Bennett, R. A. Stewart and J. Lu, "Development of a three phase battery energy storage scheduling and operation system for low voltage distribution networks," *Applied Energy,* vol. 146, pp. 122-134, 2015.

[288] S. V. Giannoutsos and S. N. Manias, " cascade control scheme for a grid connected Battery," in *IEEE International Energy Conference and Exhibition (ENERGYCON)*, 2012.

[289] T. H. Mehr, M. A. Masoum and N. Jabalameli, "Grid-Connected Lithium-Ion Battery Energy Storage System for Load Leveling and Peak Shaving," in *Australasian Universities Power Engineering Conference (AUPEC13)*, Australia, 2013.

[290] H. Ibrahim and A. Ilinca, "Techno-Economic Analysis of Different Energy Storage Technologies," in *Energy Storage*, Intech Open Science/Open Minds, 2013.

[291] E. S. Association, 2020. [Online]. Available: www.electricitystorage.org. [Accessed 29 7 2020].

[292] L.Rosen and 2. c. Tech, 2020. [Online]. Available: https://www.21stcentech.com/australian-university-develops-battery-energy-storage-system-microgrids/. [Accessed 29 7 2020].

[293] P. W. Corporation, 2020. [Online]. Available: https://www.powerworld.com/. [Accessed 29 7 2020].

[294] F. Schweppe, "Sensor-Array Data Processing for Multiple-Signal Sources," *IEEE Transactions on Information Theory,* vol. 14, no. 2, pp. 294-305, 1968.

[295] F. F. Wu, "Power system state estimation: a survey," *International Journal of Electrical Power and Energy Systems,* vol. 12, no. 2, pp. 80-87, 4 1990.

[296] F. Schweppe and D. Rom, "Power system static-state estimation: Parts I, II, & III," *IEEE Trans. Power & Sys.,* vol. 89, no. 1, pp. 125-130, 1 1970.

[297] B. P. Hayes and M. Prodanovic, "State Forecasting and Operational Planning for Distribution Network Energy Management Systems," *IEEE Transactions on Smart Grid,* 2015.

[298] B. P. Hayes and M. Prodanovic, "State Estimation Techniques for Electric Power Distribution Systems," in *IEEE Computer Society UKSim-AMSS 8th European Modelling Symposium*, 2014.

[299] E. Castillo, A. Conejo, R. Pruneda and C. Solares, "State estimation observability based on the null space of the measurement jacobian matrix," *IEEE Trans. Power Sys.,* vol. 20, no. 3, p. 1656–1668, 2005.

[300] A. P. S. Meliopoulos, E. Polymeneas, Z. Tan, R. Huang and D. Zhao, "Advanced Distribution Management System," *IEEE Transaction on Smart Grid,* vol. 4, no. 4, pp. 2109-2117, 2013.

[301] A. Saint-Pierre and P. Mancarella, "Active Distribution System Management: A Dual-Horizon Scheduling Framework for DSO/TSO Interface Under Uncertainty," *IEEE Transaction on Smart Grid,* vol. 8, no. 5, pp. 2186-2197, 2017.

[302] P. V. K. Andersen and e. al, "Using residential buildings to manage flexibility in the district heating network: perspectives and future visions from sector professionals," in *IOP Conf. Series: Earth and Environmental Science 352*, 2019.

[303] Y. Chen, P. Xu, J. Gu, F. Schmidt and W. Li, "Measures to improve energy demand flexibility in buildings for demand response (DR): A review," *Energy & Buildings,* 2018.

[304] A. M. Zin, H. M. Hafiz and W. Wong, "Static and dynamic under-frequency load shedding: a comparison," in *IEEE International Conference on Power System Technology*, Singapore, 2004.

[305] R. M. Larik and e. al, "An improved algorithm for optimal load shedding in power systems," *Energies,* vol. 11, no. 7, pp. 1-16, 2018.

[306] A. M. Haidar, A. Mohamed and A. Hussain, "Vulnerability control of large scale interconnected power system using neuro-fuzzy load shedding approach," *Expert Syst Appl,* vol. 37, no. 4, p. 3171-3176, 2010.

[307] P. Acharjee, "Identification of maximum loadability limit and weak buses using security constraint genetic algorithm," *Int J Electr Power Energ Syst,* vol. 36, no. 1, p. 40-50, 2012.

[308] J. Laghari, H. Mokhlis, A. Bakar and H. Mohamad, "Application of computational intelligence techniques for load shedding in power systems: a review," *Energ Conver Manage,* vol. 75, pp. 130-140, 2013.

[309] M. L. Raja, W. M. Mohd and N. A. Muhammad, "A critical review of the state-of-art schemes for under voltage load shedding," *Int Trans Electr Energ Syst,* vol. 29, no. 2828, pp. 1-26, 2019.

[310] M. Uddina and e. al, "A review on peak load shaving strategies," *Renewable and Sustainable Energy Reviews,* vol. 82, p. 3323–3332, 2018.

[311] V. Salehi, S. Afsharnia and S. Kahrobaee, "Improvement of Voltage Stability in Wind Farm Connection to distribution Network Using FACTS Devices," in *32nd Annual Conference of the IEEE Industrial Electronics Society (IECON2006)*, Paris, 2006.

[312] Z. Chen, F. Blaabjerg and Y. Hu, "Stability Improvement of Wind Turbine Systems by STATCOM," in *32nd Annual Conference of the IEEE Industrial Electronics Society (IECON2006)*, Paris, 2006.

[313] S. Bozhko, R. Li, R. Blasco-Gimenez, G. M. Asher, J. C. Clare, L.Yao and C. Sasse, "STATCOM-controlled HVDC Power Transmission for Large Offshore Wind Farms: Engineering Issues," in *32nd Annual Conference of the IEEE Industrial Electronics Society (IECON2006)*, Paris, 2006.

[314] D. Divan and H. Johal, "Distributed FACTS - A New Concept for Realizing Grid Power Flow Control," in *36th IEEE Power Electronics Specialists Conference (PESC05)*, 2005.

[315] D. V. Slyke, 2020. [Online]. Available: http://site.ieee.org/sas-pesias/files/2016/03/SCADA_20150316_Slides.pdf. [Accessed 30 7 2020].

[316] Deramsey, 24 2 2015. [Online]. Available: https://commons.wikimedia.org/wiki/File:SCADA_Systems_Layout.png. [Accessed 30 7 2020].

[317] F. R. Yu, P. Zhang, W. Xiao and P. Choudhury, "Communication Systems for Grid Integration of Renewable Energy Resources," *IEEE Network,* pp. 22-29, 2011.

[318] T. Cruz and e. al, "A Cybersecurity Detection Framework for Supervisory Control and Data Acquisition Systems," *IEEE Transactions on Industrial Informatics,* vol. 12, no. 6, pp. 2236-2246, 12 2016.

[319] M. M. Rana and L. Li, "Controlling the Distributed Energy Resources Using Smart Grid Communications," in *IEEE Computer Society 12th International Conference on Information Technology - New Generations*, 2015.

[320] Y. Kabalci, "A survey on smart metering and smart grid communication," *Renewable and Sustainable Energy Reviews,* vol. 57, p. 302–318, 2015.

[321] D. Baimel, S. Tapuchi and N. Baimel, "Smart Grid Communication Technologies," *Journal of Power and Energy Engineering,* vol. 4, pp. 1-8, 2016.

[322] X. Wang, J. .. Guerrero, F. Blaabjerg and A. Chen, "A review of power electronics based microgrids," *J. Power Electr,* vol. 12, no. 1, p. 181–192, 2012.

[323] V. C. Gungor, B. Lu and G. P. Hancke, "Opportunities and challenges of wireless sensor networks in smart grid," *IEEE Trans. Ind. Electron,* vol. 57, no. 10, p. 3557–3564, 2010.

[324] M. Alonso, H. Amaris, D. Alcala and D. M. R. Florez, "Smart Sensors for Smart Grid Reliability," *Sensors,* vol. 20, no. 8, pp. 2187-2210, 2020.

[325] J. D. Taft, "Sensor Network Issues for Advanced Power Grids," 2017.

[326] J. Jackson, "Smart Grids-An Optimised Electric Power System," in *Future Energy Improved, Sustainable and Clean Options for our Planet*, 2 ed., 2014, pp. 633-651.

[327] M. Shengwei, Z. Xuemin and C. Ming, Power Grid Complexity, Springer, 2011.

[328] U. Products, 2020. [Online]. Available: https://www.utilityproducts.com/. [Accessed 30 7 2020].

[329] V. M. Miñambres-Marcos, M. A. Guerrero-Martínez, F. Barrero-González and M. I. Milanés-Montero, "Grid Connected Photovoltaic Inverter with Battery-Supercapacitor Hybrid Energy Storage," *Sensors,* vol. 17, no. 1856, 8 2017.

[330] P. Denholm, E. Ela, B. Kirby and M. Milligan, "The Role of Energy Storage with Renewable Electricity Generation," 2010.

[331] J. G. N. Barath, H. Oleksandr and N. Manonmani, "Overview of Energy Storage Technologies For Renewable Energy," *International Journal of Innovative Science, Engineering & Technology,* vol. 2, no. 9, pp. 749-754, 2015.

[332] S. Faias, P. Santos, J. Sousa and R. Castro, "An Overview on Short and Long-Term Response Energy Storage Devices for Power Systems Applications," *Renewable Energies and Power Quality Journal,* vol. 1, no. 6, pp. 442-447, 2008.

[333] B. Zakeri and S. Syri, "Electrical energystoragesystems:Acomparativelifecyclecostanalysis," *RenewableandSustainableEnergyReviews,* vol. 42, p. 569–596, 2015.

[334] R. Caldon, F. Rossetto and A. Scala, "Reactive power control in distribution networks with dispersed generators: a cost based method," *Electric Power Systems Research,* vol. 64, pp. 209-217, 2003.

[335] S. Meshram, G. Agnihotri and S. Gupta, "Performance Analysis of Grid Integrated Hydro and Solar Based Hybrid Systems," *Advances in Power Electronics,* pp. 1-7, 2013.

[336] A. K. Srivastava, A. A. Kumar and N. N. Schulz, "Impact of Distributed Generations with Energy Storage Devices on the Electric Grid," *IEEE Systems Journal,* vol. 6, no. 1, pp. 110-117, 2012.

[337] M. A. Guerrero-Martínez, E. Romero-Cadaval, F. B. González, M. Montero and E. G. Romera, "Supercapacitors: Alternative Energy Storage Systems," *Przegl ˛ad Elektrotechniczny,* vol. 85, pp. 188-195, 209.

[338] A. Kuperman and I. Aharon, "Battery–ultracapacitor hybrids for pulsed current loads: A review," *Renew. Sustain. Energy Rev.,* vol. 15, pp. 981-992, 2011.

[339] L. Gao, R. Dougal and S. Liu, "Power enhancement of an actively controlled battery/ultracapacitor hybrid," *IEEE Trans. Power Electr.,* vol. 20, p. 236–243, 2005.

[340] M. Choi, S. Kim and S. Seo, "Energy Management Optimization in a Battery/Supercapacitor Hybrid Energy," *IEEE Trans. Smart Grid,* vol. 3, p. 463–472, 2012.

[341] F. Ongaro, S. Saggini and P. Mattavelli, "Li-Ion Battery-Supercapacitor Hybrid Storage System for a Long," *IEEE Transac. Power Electr.,* vol. 27, p. 3944–3952, 2012.

[342] B. Hredzak, V. Agelidis and M. A. Jang, "Model Predictive Control System for a Hybrid Battery-Ultracapacitor," *IEEE Trans. Power Electr.,* vol. 29, p. 1469–1479, 2014.

[343] S. Kollimalla, M. Mishra and N. Narasamma, "Design and Analysis of Novel Control Strategy for Battery and Supercapacitor Storage System," *IEEE Trans. Sustain. Energy,* vol. 5, p. 1137–1144, 2014.

[344] X. Feng, H. Gooi and S. Chen, "Hybrid Energy Storage with Multimode Fuzzy Power Allocator for PV Systems," *IEEE Trans. Sustain. Energy,* vol. 5, p. 389–397, 2014.

[345] M. Glavin and W. Hurley, "Optimisation of a photovoltaic battery ultracapacitor hybrid energy storage system," *Sol. Energy,* vol. 86, p. 3009–3020, 2012.

[346] I. Buchmann, "Understanding your Batteries in a Portable World," in *IEEE Proc. of the Fourteenth Annual Battery Conference on Applications and Advances*, 1999.

[347] I. Buchmann, Batteries in Portable World, Second ed., 2001.

[348] W. A. V. Schalkwijk and B. Scrosati, Advances in Lithium-Ion Batteries, Boston: Springer, 2002.

[349] M. Broussely, M. Perelle, J. McDowall, G. Sarre and J. Martaeng, "Lithium Ion: The Next Generation of Long Life Batteries – Characteristics, Life Predictions and Integration into Telecom Systems," in *NTELEC. Twenty-Second International Telecommunications Energy Conference (Cat. No.00CH37131)*, Phoenix, AZ, 2000.

[350] C. Robillard, A. Vallee and H. Wilkinson, "The impact of lithium-metal-polymer battery characteristics on telecom power system design," in *INTELEC 2004. 26th Annual International Telecommunications Energy Conference*, Chicago, IL, USA, 2004.

[351] "CADEX ELECTRONICS INC," 2021. [Online]. Available: https://www.cadex.com/en. [Accessed 17 4 2021].

[352] E. Humbert, "Lithium Rechargeable Batteries in Standby but not for Power," 2005.

[353] N. Hideyuki, "Alternative Cathode Material for Cobalt," in *Portable Power Conference and Expo*, 2004.

[354] Panasonic, "Lithium Ion Application Notes – Overcharge/ Over Discharge/ Over Current Safety Circuits," 2000.

[355] T. Battery, "Press Release, 29 March, 2005 – Toshiba's New Rechargeable Lithium-Ion Battery Recharges in only 1 Minute," 2005.

[356] S. M. Lukic, S. A. Khateeb, S. Al-Hallaj, J. R. Selman and A. Emadi, "On the Suitability of a New High Power Lithium Ion Battery for Hybrid Electric Vehicle Applications," 2003.

[357] "Sony Co. US18650 Lithium Ion Battery Manual," 1993.

[358] S. Al-Hallaj, J. Prakash and J. R. Selman, "Charatcerization of Commercial Li-Ion Batteries Using Electrochemical-Calometric Measurement," *IEEE Journal on Power Sources,* vol. 87, no. 1, pp. 186-194, 2000.

[359] S. Al-Hallaj and J. R. Selman, "Thermal Modelling of Secondary Lithium Batteries for Electric Vehicle/Hybrid Electric Vehicle Applications," *Journal on Power Sources,* vol. 110, no. 2, pp. 341-348, 2002.

[360] H. O. Batteries, "Design Assistance- How to Select the Right Kind of Battery for your Application," 2007.

[361] D. Morrison, "Batteries Seek Higher Capacity, Power and Safety," 1 10 2004. [Online]. Available: https://www.powerelectronics.com/markets/mobile/article/21856321/batteries-seek-higher-capacity-power-and-safety. [Accessed 2020].

[362] "Battery Design LLC. Battery Companies," 9 2020. [Online]. Available: http://www.batdesign.com/links.html#Battery_Companies. [Accessed 10 2020].

[363] "Matsushita Battery Industrial Co. Ltd," 9 2020. [Online]. Available: http://industrial.panasonic.com/www-ctlg/ctlg/qACA4000_WW.html. [Accessed 9 2020].

[364] "Sanyo Electric Co Ltd. Lithium-Ion and Lithium-Polymer Batteries," 2007.

[365] Samsung, "Rechargeable Battery Products – Lithium Polymer," 2005.

[366] S. Batteries, "Saft Battery Products," 9 2020. [Online]. Available: https://www.saftbatteries.com/products-solutions/products. [Accessed 9 2020].

[367] J. S. Battery, "Major Products – Lithium Ion," 2007.

[368] S. K. E. Machinery, "Automotive and Industrial Batteries- Lithium-Ion batteries for Hybrdi Electric Vehicles," 2007.

[369] T. Battery, "List of Primary Batteries – Ultra Lithium," 2007.

[370] C. C. Chan, "The State of the Art of Electric Vehicles," *Journal of Asian Electric Vehicles,* vol. 2, no. 2, 12 2004.

[371] S. Ioannou, K. Dalamagkidis, E. K. Stefanakos, K. P. Valavanis and P. H. Wiley, "Runtime, capacity and discharge current relationship for lead acid and lithium batteries," in *IEEE 24th Mediterranean Conference on Control and Automation (MED2016)*, Athens, 2016.

[372] S. G. Ioannou, "Discrete Linear Constrained Multivariate Optimization for Power Sources of Mobile Systems," Florida, 2008.

[373] M. Ni, K. Sumathy, M. Leung and Y. Leung, "Feasibility study on renewable hydrogen for Hong Kong," in *Business, Environmental Science*, 2004.

[374] M. Lange, A. Teller, C. Keleshis, S. Ioannou, P. Philimis, J. Lelieveld and Z. Levin, "Autonomous Flying Platforms for Atmospheric and Earth Surface Observations (APAESO)-A pioneering research facility in Cyprus," in *EGU General Assembly Conference*, Vienna, 2010.

[375] M. Lange, M. Argyrides, S. Ioannou, C. Keleshis and Z. Levin, "Unmanned Aerial Systems as Versatile Tools for Atmospheric and Environmental Research," in *EGU General Assembly Conference*, Vienna, 2013.

[376] G. Demetriou, S. Ioannou, A. Hadjipieri, I. Panayidou, A. Papasavva and A. Savva, "ERON: A flexible autonomous surface vessel," in *24th Mediterranean Conference on Control and Automation (MED)*, Athens, 2016.

[377] C. Keleshis, S. Ioannou, M. Vrekoussis, Z. Levin and M. Lange, "Data Acquisition (DAQ) system dedicated for remote sensing applications on Unmanned Aerial Vehicles (UAV)," in *Second International Conference on Remote Sensing and Geoinformation of the Environment (RSCy2014)*, Paphos, 2014.

[378] S. Ioannou, K. Dalamagkidis, K. P. Valavanis, E. K. Stefanakos and P. H. Wiley, "On improving endurance of unmanned ground vehicles: The ATRV-Jr case study," in *14th Mediterranean Conference on Control and Automation*, Ancona, 2006.

[379] S. Ioannou, K. Dalamagkidis, K. P. Valavanis and E. K. Stefanakos, "Improving Endurance and Range of a UGV with Gimballed Landing Platform for Launching Small Unmanned Helicopters," *Journal of Intelligent and Robotic Systems,* vol. 53, no. 4, pp. 399-416, 2008.

[380] J. Larminie and A. Dicks, Fuel Cell Systems Explained, 2nd ed., Wiley, 2003.

[381] Z. Li, Z. Zheng, L. Xu and X. Lu, "A review of the applications of fuel cells," *BMC Energy,* vol. 1, no. 8, pp. 1-24, 2019.

[382] Z. LI, Data-driven fault diagnosis for PEMFC systems, UNIVERSITE D'AIXMARSEILLE, 2014.

[383] C. Spiegel, "Fuel Cell Store," 20 6 2017. [Online]. Available: https://www.fuelcellstore.com/blog-section/polarization-curves. [Accessed 18 4 2021].

[384] P. P. Barker, "Ultracapacitors for use in power quality and distributed resource applications," in *IEEE Power Engineering Society Summer Meeting*, Chicago, IL, 2002.

[385] S. Technologies, "Breakthrough in Super-Capacitors," 2003.

[386] W. V. Schalkwijk and B. Scrosati, "Electrochemical Supercapacitors," in *Advances in Lithium Ion Batteries*, Kluwer Academic/Plenum, 2002.

[387] EPCOS, "General Technical Information – Ultra-Capacitor Technology," 2005.

[388] "Ultra-Capacitor Application Notes," 2005.

[389] B. E. Conway, Electrochemical Super-Capacitors: Scientific Fundamentals and Technological Applications, New York: Plenum, 1999.

[390] G. L. Bullard, H. B. Sierra-Alcazar, H. L. Lee and J. L. Morris, "Operating principles of the ultracapacitor," *IEEE Transactions on Magnetics,* vol. 25, no. 1, pp. 102-106, 1989.

[391] i. Gao, R. A. Dougal and S. Liu, "Power enhancement of an actively controlled battery/ultracapacitor hybrid," *IEEE Transactions on Power Electronics,* vol. 20, no. 1, pp. 236-243, 1 2005.

[392] H. W. Brandhorst and Z. Chen, "Achieving a high pulse power system through engineering the battery-capacitor combination," in *IEEE Sixteenth Annual Battery Conference on Applications and Advances. Proceedings of the Conference (Cat. No.01TH8533)*, Long Beach, CA, 2001.

[393] J. R. Miller, "Fundamentals and Applications of Electrochemical Capacitors," 2008.

[394] I. P. Systems, "Electrochemical Capacitors," 2008.

[395] R. A. Dougal, S. Liu and R. E. White, "Power and life extension of battery-ultracapacitor hybrids," *IEEE Transactions on Components and Packaging Technologies,* vol. 25, no. 1, pp. 120-131, 3 2002.

[396] Pierre, "Wikimedia Commons," 14 11 2004. [Online]. Available: https://commons.wikimedia.org/wiki/File:Braine_le_Chateau,Belgium,moulin_banal.JPG. [Accessed 15 9 2020].

[397] J. d. Carvalho and Flickr, "Wikipedia," 31 12 2011. [Online]. Available: https://en.wikipedia.org/wiki/Itaipu_Dam#/media/File:Itaipu_geral.jpg. [Accessed 15 9 2020].

[398] Voith, "Goldisthal Pumped Hydro Electric Dam," [Online]. Available: http://voith.com/us-en/industry-solutions/hydropower/pumped-storage-plants/goldisthal-germany.html. [Accessed 15 9 2020].

[399] E. Cora, J. J. Fry, M. Bachhiesl and A. Schleiss, “Hydropower Technologies The State-of-the-Art,” EU, 2020.

[400] D. Basnyat, “Financing Cogeneration and Small-Hydro projects in the Sugar and tea Industry in East and Southern Africa Training,” ADB FINESSE Training Course on Renewable Energy & Energy Efficiency for Poverty Reduction, Nairobi; Kenya;, 2006.

[401] B. H. Association, “A Guide to UK mini-hydro development,” 2012.

[402] V. Koritarov and e. al, “Modeling and Analysis of Value of Advanced Pumped Storage Hydropower in the United States,” Argonne National Lab. (ANL), Argonne; IL (United States);, 2014.

[403] B. M. Trust, “Wikipedia Commons,” 11 8 2005. [Online]. Available: https://commons.wikimedia.org/wiki/File:Thinktank_Birmingham_-_Trevithick_Locomotive(1).jpg. [Accessed 20 9 2020].

[404] S. GmbH, “Stornetic The Energy Storage Company,” 2020. [Online]. Available: https://stornetic.com/. [Accessed 20 9 2020].

[405] Geni, “Wikipedia Commons,” Flybrid Systems Kinetic Energy Recovery System, 2009. [Online]. Available: https://commons.wikimedia.org/wiki/File:Flybrid_Systems_Kinetic_Energy_Recovery_System.jpg. [Accessed 20 9 2020].

[406] G. E. Totten, L. Xie and K. Funatani, Handbook of Mechanical Alloy Design, New York: Marcel Dekker, 2004.

[407] S. Mousavi, F. Faraji, A. Majazi and K. Al-Haddad, “A comprehensive review of Flywheel Energy Storage System,” *Renewable and Sustainable Energy Reviews,* vol. 67, pp. 477-490, 2017.

[408] A. Ojha, P. K. Chaturvedi, A. Mittal and S. K. Jain, "Back to Back Connected Multilevel Converters: A Review," *IOSR Journal of Electrical and Electronics Engineering (IOSR-JEEE),* vol. 5, no. 5, pp. 57-67, 2013.

[409] M. E. Amiryar and K. R. Pullen, "A Review of Flywheel Energy Storage System Technologies and Their Applications," *Applied Sciences,* vol. 7, no. 286, pp. 1-21, 2017.

[410] F1jmm, "Wikipedia Commons," 7 10 2009. [Online]. Available: https://commons.wikimedia.org/wiki/File:Bouteille_air_d%C3%A9marrage.JPG. [Accessed 22 9 2020].

[411] L. Layton, "PDHonline Course E365 (4 PDH)," 2012. [Online]. Available: https://www.pdhonline.com/index.cgi. [Accessed 23 9 2020].

[412] R. E. Storage, "CAES Technology: History," [Online]. Available: http://www.ridgeenergystorage.com/caes_history.htm. [Accessed 23 9 2020].

[413] W. and R. Chambers, "Chambers's Encyclopaedia: A Dictionary of Universal Knowledge," W. & R. Chambers LTD;, 7 1 2009. [Online]. Available: https://archive.org/details/bub_gb_4pwMAAAAYAAJ. [Accessed 23 9 2020].

[414] F. Crotogino, K. U. Mohmeyer and R. Scharf, "Huntorf CAES: More than 20 Years of Successful Operation," in *CAES Meeting*, Orlando; Florida;, 2001.

[415] "Solution Mining Research Institute (SMRI)," [Online]. Available: https://www.solutionmining.org/. [Accessed 18 4 2021].

[416] H. Chen, X. Zhang, J. Liu and C. Tan, "Compressed Air Energy Storage," in *Energy Storage - Technologies and Applications*, IntechOpen, 2013.

[417] L. Chen, T. Zheng, S. Mei, X. Xue, B. Liu and Q. Lu, "Review and prospect of compressed air energy storage system," *J. Mod. Power Syst. Clean Energy,* pp. 1-13, 2016.

[418] J. Wang and e. al., "Overview of Compressed Air Energy Storage and Technology Development," *Energies,* pp. 1-22, 2017.

[419] A. Chauhan and R. Saini, "A review on Integrated Renewable Energy System based power generation for stand-alone applications: Configurations, storage options, sizing methodologies and control," *Renewable and Sustainable Energy Reviews,* vol. 38, 2014.

[420] "Variability of Wind Power and other Renewables:Management Options and Strategies," International Energy Agency Publications, 2005.

[421] N. Hamsic, A. Schmelter, A. Mohd, E. Ortjohann, E. Schultze, A. Tuckey and J. Zimmermann, "Increasing Renewable Energy Penetration in Isolated Grids Using a Flywheel Energy Storage System," in *Proceedings of Powereng 2007 - International Conference on Power Engineering, Energy and Electrical Drives*, Sebutal, 2007.

[422] T. Mito, "Development of UPS-SMES as a Protection From Momentary Voltage Drop," *IEEE Transactions on Applied Superconductivity,* vol. 14, no. 2, pp. 721-726, 2004.

[423] T. Sels, C. Dragu, T. V. Craenenbroeck and R. Belmans, "Overview of new energy storage systems for an improved power quality and load managing on distribution level," in *16th International Conference and Exhibition on Electricity Distribution*, Amsterdam, 2001.

[424] G. L. Hunt, "The Great Battery Search," *IEEE Spectrum,* vol. 35, no. 11, 1998.

[425] J. M. Ogden, "Prospects for Building a Hydrogen Infrastructure," *Annual Review of Energy and the Environment,* vol. 24, pp. 227-279, 1999.

[426] S. M. Schoenung, J. M. Eyer, J. J.Iannucci and S. A. Horgan, "Energy Storage for a Competitive Power Market," *Annual Review of Energy and the Environment,* vol. 21, no. 1, 1996.

[427] H. Louie, "Off-Grid Electrical Systems in Developing Countries".

[428] "https://en.wikipedia.org/wiki/off-the-grid," [Online].

[429] "https://outbackpower.com/applications/off-grid," [Online].

[430] "https://ruralelec.org/grid-electricity-systems," [Online].

[431] "https://en.wikipedia.org/wiki/Stand-alone_Power_System," [Online].

[432] "http://www.go-pure.en/off-grid," [Online].

[433] "https://www.rpc.com.au/Solar-Systems/off-grid-solar-power.html," [Online].

[434] "https://energypedia.info/wiki/Solar_Home_Systems (SHS)," [Online].

[435] "https://energypedia.info/wiki/Portal i Solar," [Online].

[436] "https://www.sciencedirect.com/topics/engineering/mini-grids," [Online].

[437] "https://www.cleanenergyreviews.info/blog/home-solar-battery-systems," [Online].

[438] B. Everett and G. Boyle, "Integrating Renewable Energy," *Renew. Energy Power a Sustain. Futur.,* vol. 2016, no. Figure 1, pp. 461-522, 2012.

[439] A. Keyhani, M. Marwali and M. Dai, "Integration of Green and Renewable Energy in Electric Power Systems," 2009.

[440] J. Cochran and e. al., "Flexibility in 21st Century Power Systems," *21st Century Power Partnership,* vol. May, p. 14, 2014. doi:10.2172/1130630.

[441] X. Xu, Z. Wei, Q. Ji, C. Wang and G. Gao, “Global renewable energy development: Influencing factors, trend predictions and countermeasures,” *Resour. Policy,* vol. 63, no. June, 2019. doi:10.1016/j.resourpol.2019.101470.

[442] “IEEE Std 1159, IEEE Recommended Practice for Monitoring Electric Power Quality,” vol. 2019, 2019.

[443] M. Ramachandran, A. Mary, M. Muthukumaran, J. Ganesan, A. Krishnaveni and D. Selvaraj, “A Review on Basic Concepts and Important Standards of Power Quality in Power System,” *Int. J. Sci. Eng. Appl.,* vol. 4, no. 5, pp. 299-303, 2015. doi:10.7753/ijsea0405.1013.

[444] A. Apostolov, “IEC 61850 and power-quality monitoring and recording,” *Power Syst.,* vol. 23, pp. 379-415, 2007. doi:10.1007/978-1-84628-772-5_13.

[445] P. Skills and e. al., “Course guides 320162 - IXESER - Grid Integration of Renewable Energy Teaching unit : Degree : Others :,,” pp. 1-5, 2020.

[446] R. Sataloff, M. Johns and K. Kost, “No 主観的健康感を中心とした在宅高齢者における健康関連指標に関する共分散構造分析Title,” pp. 4-6.

[447] T. Hoang and H. Lee, “Accurate Power Sharing with Harmonic Power for Islanded Multibus Microgrids,” *IEEE J. Emerg. Sel. Top. Power Electron,* vol. 7, no. 2, pp. 1286-1299, 2019. doi:10.1109/JESTPE.2018.2865207.

[448] H. Abdelgawad and V. Sood, “A comprehensive review on microgrid architectures for distributed generation,” *2019 IEEE Electr. Power Energy Conf. EPEC 2019,* vol. 3, 2019. doi:10.1109/EPEC47565.2019.9074800.

[449] B. Hartono, Budiyanto and R. Setiabudy, “Review of microgrid technology,” *2013 Int. Conf. Qual. Res. QiR 2013 - Conjunction with ICCS 2013 2nd Int. Conf. Civ. Sp.,* pp. 127-132, 2013. doi:10.1109/QiR.2013.6632550.

[450] M. Tsili and S. Papathanassiou, “A review of grid code technical requirements for wind farms,” *IET Renew. Power Gener.,* vol. 3, no. 3, pp. 308-332, 2009. doi:10.1049/iet-rpg.2008.0070.

[451] I. Erlich and F. Shewarega, “Grid Codes in Power Systems with Significant Renewable-Based Generation,” *Smart Grid Handb.,* pp. 1-12, 2016. doi:10.1002/9781118755471.sgd073.

[452] H. Khairy, M. El-Shimy and G. Hashem, “Overview of Grid Code and Operational Requirements of Grid-connected Solar PV Power Plants,” *Ind. Acad. Collab. Conf. 2015, Energy Sustain. Dev. Track,* 2015.